Department of
Industry and Resources

REPORT
90

GOLD MINERALIZATION IN THE EDJUDINA–KANOWNA REGION EASTERN GOLDFIELDS WESTERN AUSTRALIA

by F. I. Roberts, W. K. Witt, and J. Westaway

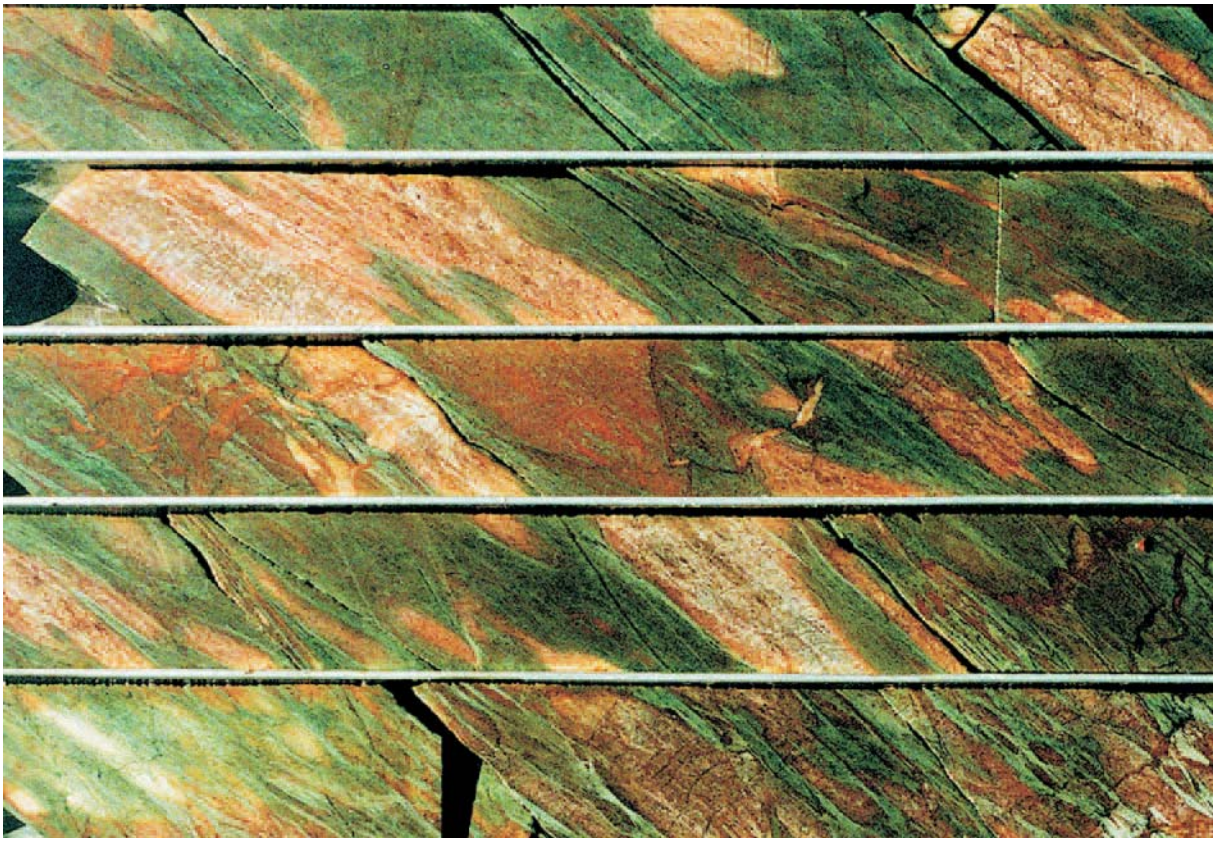

Geological Survey of Western Australia

GEOLOGICAL SURVEY OF WESTERN AUSTRALIA

REPORT 90

GOLD MINERALIZATION IN THE EDJUDINA–KANOWNA REGION, EASTERN GOLDFIELDS, WESTERN AUSTRALIA

by
F. I. Roberts, W. K. Witt[1], and J. Westaway[1]

[1] Sons of Gwalia Ltd, 16 Parliament Place, West Perth, W.A. 6005

Perth 2004

MINISTER FOR STATE DEVELOPMENT
Hon. Clive Brown MLA

DIRECTOR GENERAL, DEPARTMENT OF INDUSTRY AND RESOURCES
Jim Limerick

DIRECTOR, GEOLOGICAL SURVEY OF WESTERN AUSTRALIA
Tim Griffin

REFERENCE
The recommended reference for this publication is:
ROBERTS, F. I., WITT, W. K., and WESTAWAY, J., 2004, Gold mineralization in the Edjudina–Kanowna region, Eastern Goldfields, Western Australia: Western Australia Geological Survey, Report 90, 263p.

National Library of Australia
Cataloguing-in-publication entry

Roberts, F. Ivor.
Gold mineralization in the Edjudina–Kanowna region, Eastern Goldfields, Western Australia.

Bibliography.
ISBN 0 7307 8938 1

1. Gold ores — Western Australia — Yilgarn Craton.
2. Greenstone belts — Western Australia — Yilgarn Craton.
3. Gold mines and mining — Western Australia — Yilgarn Craton.
4. Geology, Stratigraphy — Archaean.
I. Witt, W. K.
II. Westaway, Jane.
III. Geological Survey of Western Australia
IV. Title. (Series: Report (Geological Survey of Western Australia); 90).

553.41099416

ISSN 0508–4741

Grid references in this publication refer to the Geocentric Datum of Australia 1994 (GDA94). Locations mentioned in the text are referenced using Map Grid Australia (MGA) coordinates, Zone 51. All locations are quoted to at least the nearest 100 m.

Copy editor: K. Blundell
Cartography: S. Dowsett
Desktop Publishing: A. Lockwood

Published 2004 by Geological Survey of Western Australia
This report is published in digital format (PDF), as part of a digital dataset on CD, and is available online at www.doir.wa.gov.au/gswa. Laser-printed copies can be ordered from the Information Centre for the cost of printing and binding.

Further details of geological publications and maps produced by the Geological Survey of Western Australia can be obtained by contacting:
Information Centre
Department of Industry and Resources
100 Plain Street
EAST PERTH, WESTERN AUSTRALIA 6004
Telephone: +61 8 9222 3459 Facsimile: +61 8 9222 3444

Cover photograph:
Drillcore from CMBD-15, Butcher Well North deposit, showing the strong alteration and foliation in the intermediate to mafic pseudo-fragmental volcanic rock overlying the ore zone. The rock is altered to a non-pyritic carbonate–sericite(–quartz–plagioclase–chlorite) assemblage

Contents

Appendices

Figures

Introduction and Geological setting

1. Gordon–Mulgarrie

2. Pennyweight Point – Yundamindera

3. Yarri

4. Yerilla – Mount Remarkable

5. Yilgangi

6. Karonie–Roe

7. Eucalyptus – Pykes Hollow

8. Jubilee–Kurnalpi

9. Mulgabbie – Old Plough Dam

10. Porphyry

11. Randalls

12. Balagundi–Bulong–Taurus

13. Trans Find–Juglah and Majestic

14. Morelands Find – Black Hills – Wombola

15. Sudden Jerk – Mount Monger

16. Linden

17. Butcher Well and Tin Dog Flats

18. Mount Celia

19. Edjudina

20. Pinjin

21 Kalpini and Mayday

22. Gindalbie

23 Kanowna

Tables

Gold mineralization in the Edjudina–Kanowna region, Eastern Goldfields, Western Australia

by

F. I. Roberts, W. K. Witt*, and J. Westaway*

Abstract

The Edjudina–Kanowna region covers an area of over 50 000 km^2 within the Eastern Goldfields Granite–Greenstone Terrane of the Yilgarn Craton, and includes parts of the Kalgoorlie, Gindalbie, Kurnalpi, Edjudina, and Linden Terranes. These terranes represent elongate structural entities separated by regional north-northwesterly trending faults, and all terranes host gold mineralization. About 145 t of gold has been produced from about 220 deposits in the region, with the bulk of current resources restricted to a few major deposits — in particular, Kanowna Belle and Carosue Dam. Historically, the region has not been a significant producer of gold compared to the Kalgoorlie region to the west. Gold was discovered in the region in the late 1890s and early 1900s, and small quantities were produced intermittently until the discovery of major deposits, such as Kanowna Belle and Carosue Dam, in the mid-1980s to late 1990s.

Gold mineralization is widespread in the Edjudina–Kanowna region, and is hosted by a variety of rock types. The Kanowna Belle deposit, the largest in the region, is within metamorphosed Archaean sedimentary and felsic volcanic rocks. Most of the gold mineralization in the region is structurally hosted lode style, typically developed within shear zones that display structural regimes varying from low strain to high strain. The gold is typically the only ore mineral present and is associated with quartz veining. Pyrite is a common accompanying sulfide mineral, and to a lesser extent pyrrhotite and arsenopyrite.

Silicification, carbonation, and potassic alteration are commonly associated with the auriferous structures, with many of the deposits showing an enrichment of SiO_2 and to a lesser extent K_2O and S. Typically, CO_2 is also added to the mineralized shear zones. Some deposits have an increase in the Fe_2O_3/FeO ratio that accompanies late-stage hematization.

There is potential for further discoveries of gold mineralization in the region. Structural settings that have areas of local heterogeneity of stress distribution, with accompanying brittle and brittle–ductile structures, are potential exploration targets.

KEYWORDS: gold mineralization, Archaean, Edjudina, Kanowna, Eastern Goldfields Granite–Greenstone Terrane, Yilgarn Craton, alteration.

Introduction

This Report presents information on gold deposits in the Edjudina–Kanowna region, and is the third in a series of publications describing gold mineralization in regions of the Yilgarn Craton. The first of the series (Keats, 1991) covered the Southern Cross region, and the second (Witt, 1993a,b,c and accompanying publications Witt, 1993d,e) described the Menzies–Kambalda region. The purpose of this series is to systematically document gold mines in densely mineralized parts of the Yilgarn Craton.

The Edjudina–Kanowna region (Fig. I.1) covers an area of over 50 000 km^2 approximately bound by latitudes 29°S and 31°15'S and longitudes 121°30' and 123°E. The area includes parts of the EDJUDINA† (SH 51-6), KURNALPI (SH 51-10), and WIDGIEMOOLTHA (SH 51-14) 1:250 000 map sheets and numerous 1:100 000 sheets (Fig. I.2). The gazetted townsites are all abandoned mining settlements, such as Kanowna, Kurnalpi, and Bulong, but the pastoral stations of Cowarna Downs, Hampton Hill, Yindi, Pinjin, Yarri, Menangina, and Gindalbie are inhabited (Fig. I.3). Good-quality gravel roads, together with pastoral tracks and fence lines, provide access to most of the region. The

* Sons of Gwalia Ltd, 16 Parliament Place, West Perth, W.A. 6005.

† Capitalized names refer to standard 1:250 000 map sheets, unless otherwise indicated.

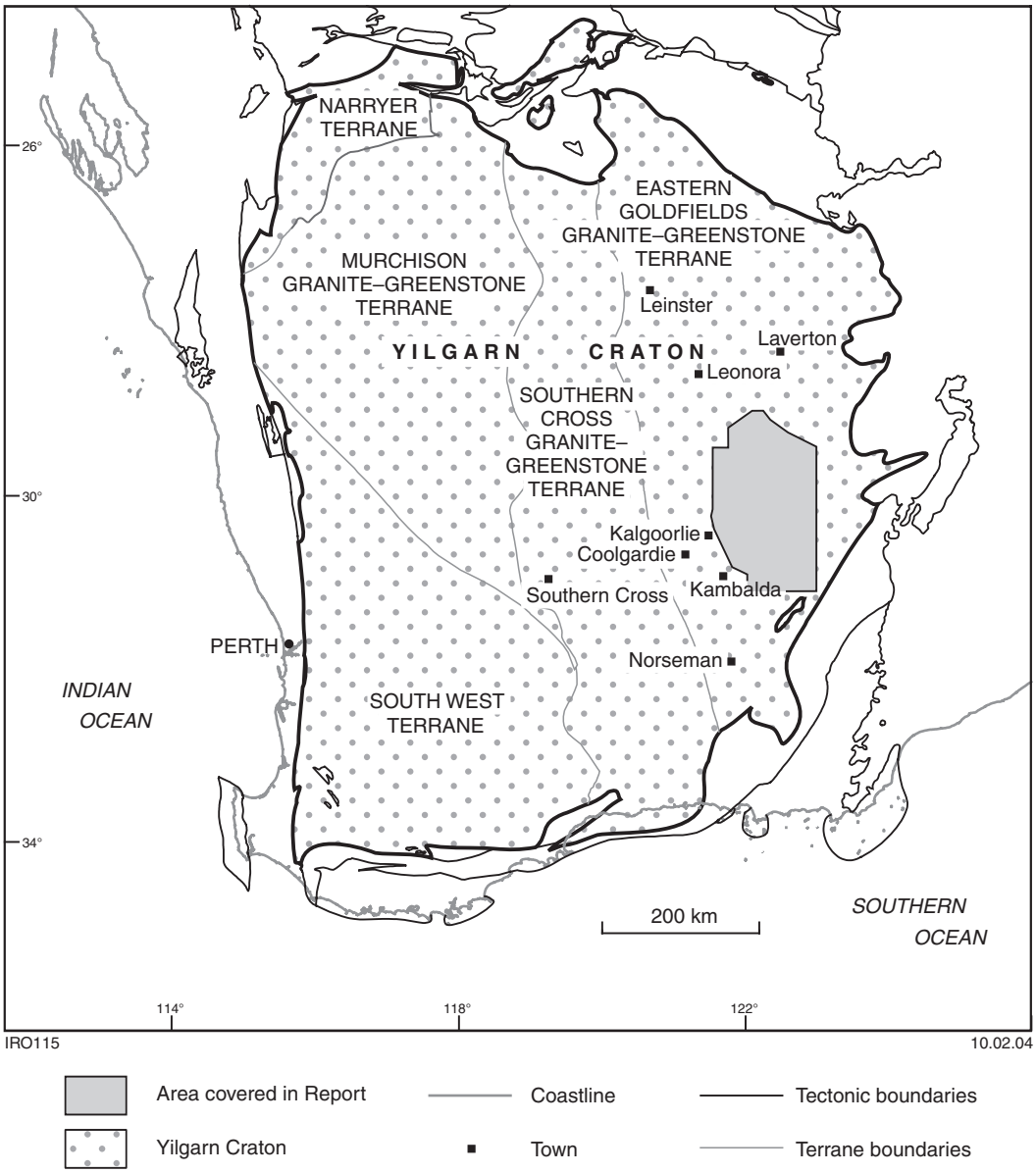

Figure I.1. Location diagram of the Edjudina–Kanowna region

Trans Australia Railway extends east across the region from Kalgoorlie (Fig. I.3).

The region can be subdivided into three main land components: a series of large playa lakes, including Lake Carey, Lake Raeside, Lake Rebecca, Lake Roe, and Lake Yindarlgooda; undulating plains underlain mainly by granitic rocks; and ridges, plateaus, and deeply weathered rocks over the greenstone belts.

This Report summarizes the geology and main characteristics of gold mineralization in each of 23 mining areas in the Edjudina–Kanowna region (Fig. I.4). For each mining area, deposits that produced more than 5 kg of gold are described, including details on production, host rock, structure, and alteration. Most of these deposits were visited in the course of the study by W. Witt and J. Westaway. Samples were collected from exposed workings, mine dumps, and drillcore. Because of the large amount of research already conducted at Kanowna (the most significant mining centre in the region), no fieldwork was carried out at Kanowna for this study, but details have been summarized from published accounts.

There has been extensive exploration for gold in the region from the 1980s onwards, especially from the mid-1980s to the late 1990s. Company exploration reports are available from the Department of Industry and Resources' (DoIR's) Western Australian mineral exploration (WAMEX) open-file database. Reports released after Item 9000 (1996) are available on DoIR's Internet site <http//:www.doir.wa.gov.au>. Reports prior to Item 9000 are available for viewing at the DoIR Library, Mineral House, 100 Plain St, East Perth, and at the Geological Survey of Western Australia's (GSWA's) Kalgoorlie regional office.

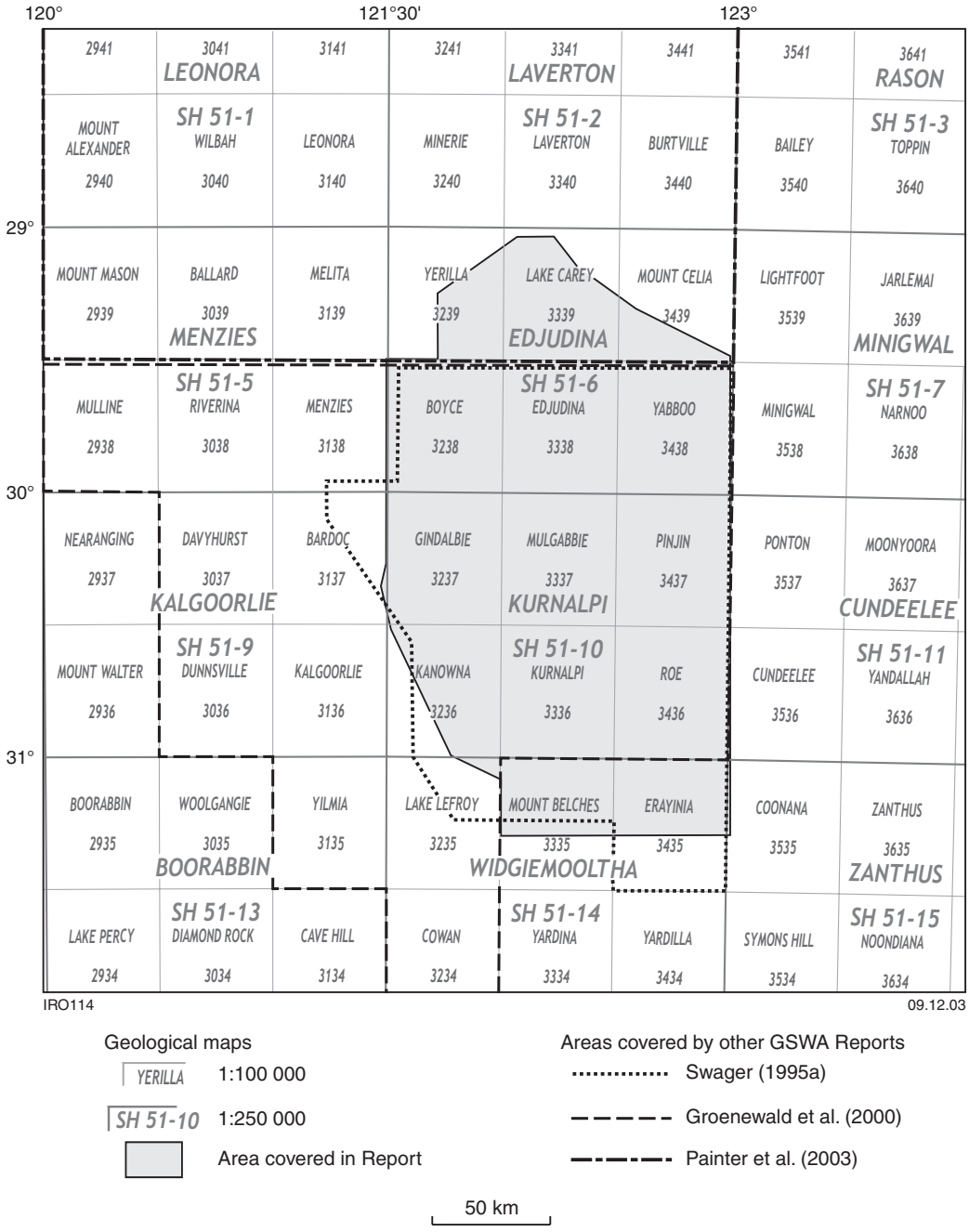

Figure I.2. Index map showing geological sheets and other maps and databases that cover the Edjudina–Kanowna region

The emphasis of this Report is the presentation of field-related data, and the integration of these data with other geological information. The development of genetic models has not been attempted.

Geological setting

The region covered by this Report forms part of the Eastern Goldfields Granite–Greenstone Terrane of the Archaean Yilgarn Craton (Tyler, 2001). The region is characterized by granites that intrude or are in faulted contact with Archaean supracrustal rocks, including metamorphosed sedimentary and felsic and mafic volcanic rocks (Fig. I.5). The supracrustal rocks are folded and metamorphosed to greenschist–amphibolite facies, and are dissected by regional-scale faults (Fig. I.5).

Limited outcrop necessitates interpretation of the regional geology using both airborne-magnetic and field-mapping data. Details of the regional geology are given by Swager (1995a, 1997), Groenewald et al. (2000), and Painter et al. (2003), as well as 1:100 000 and 1:250 000 map sheets and Explanatory Notes for the region (see Table I.1).

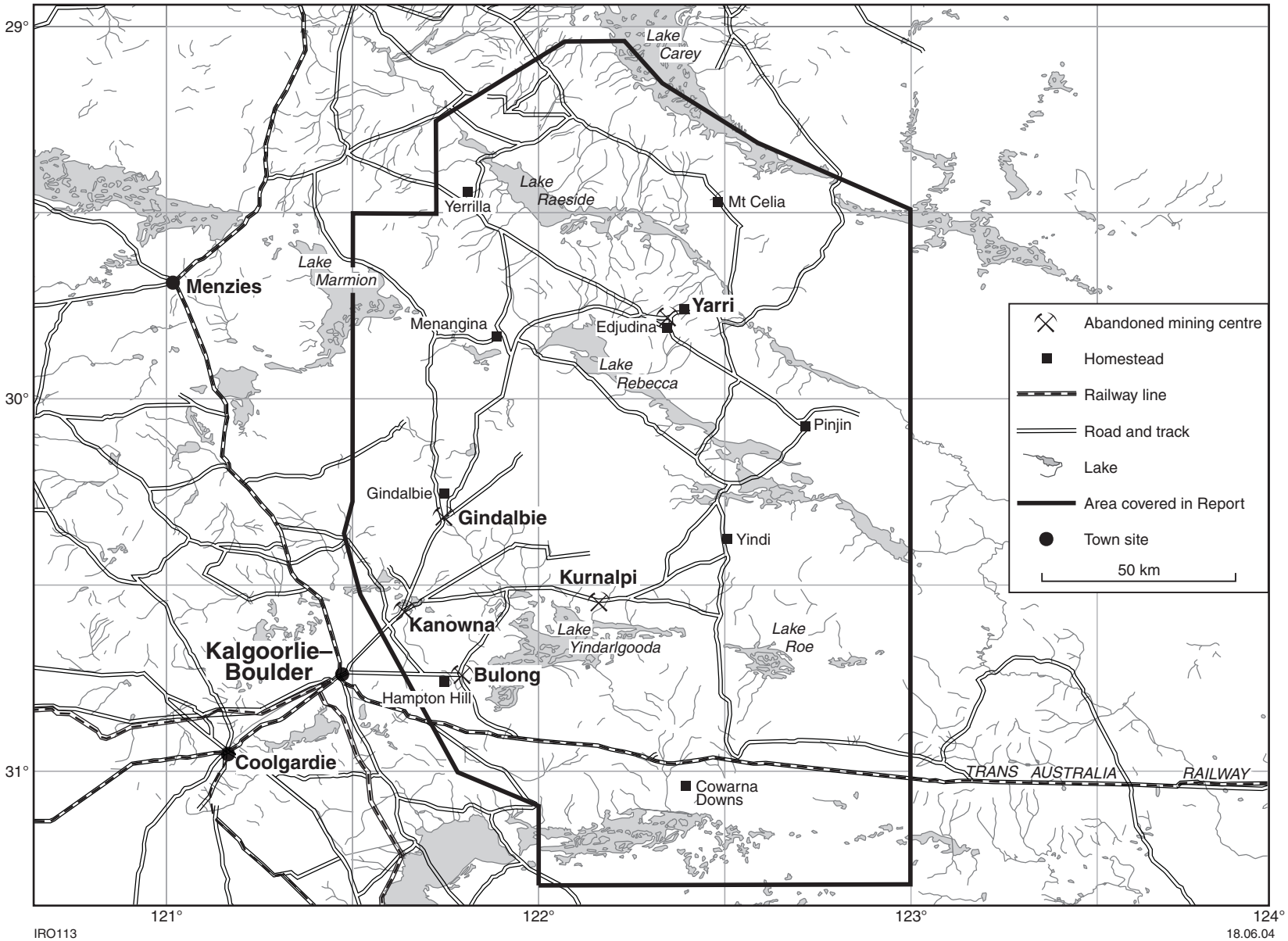

Figure I.3. Topographical features of the Edjudina–Kanowna region

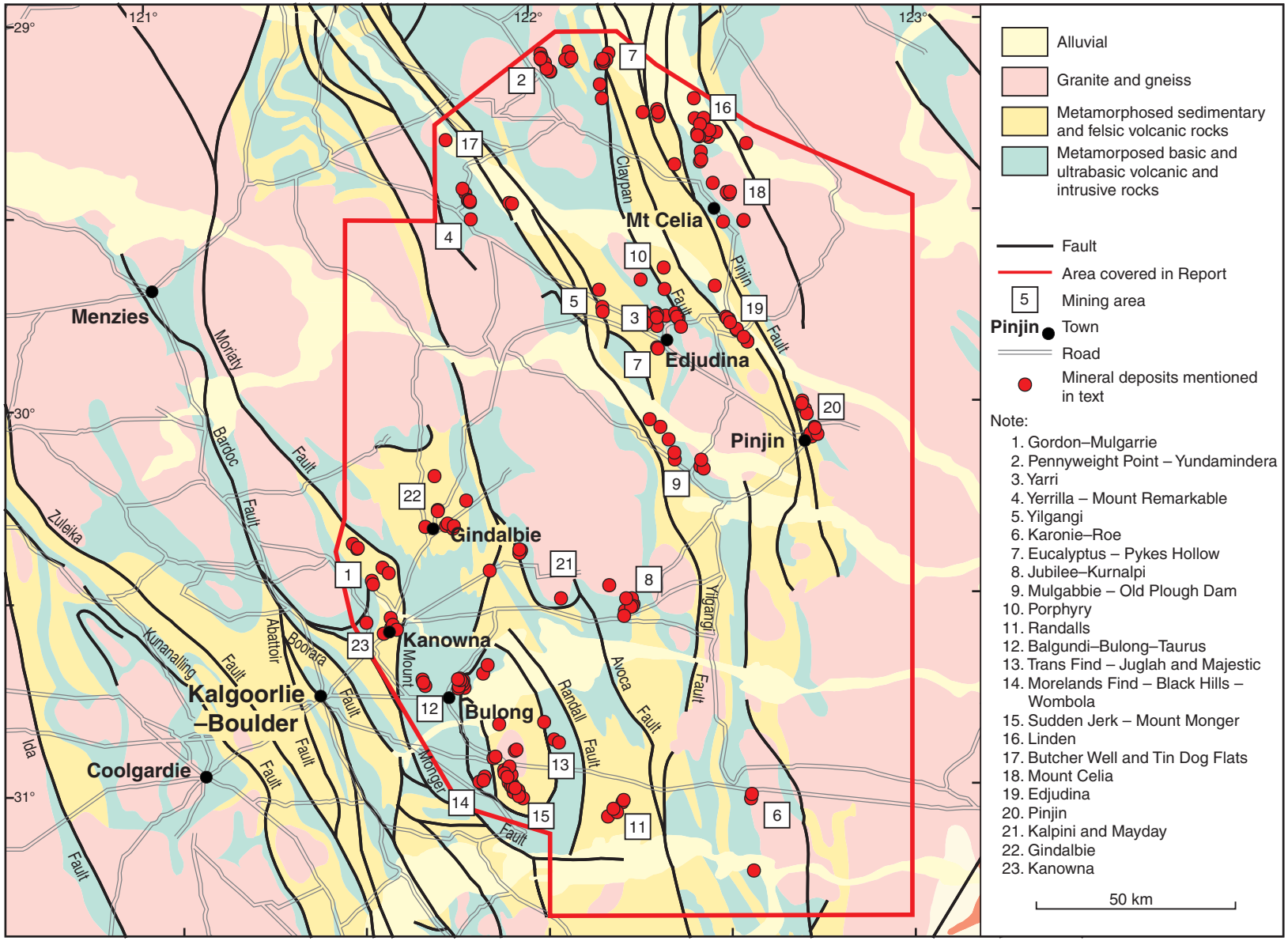

Figure I.4. Mining areas in the Edjudina–Kanowna region

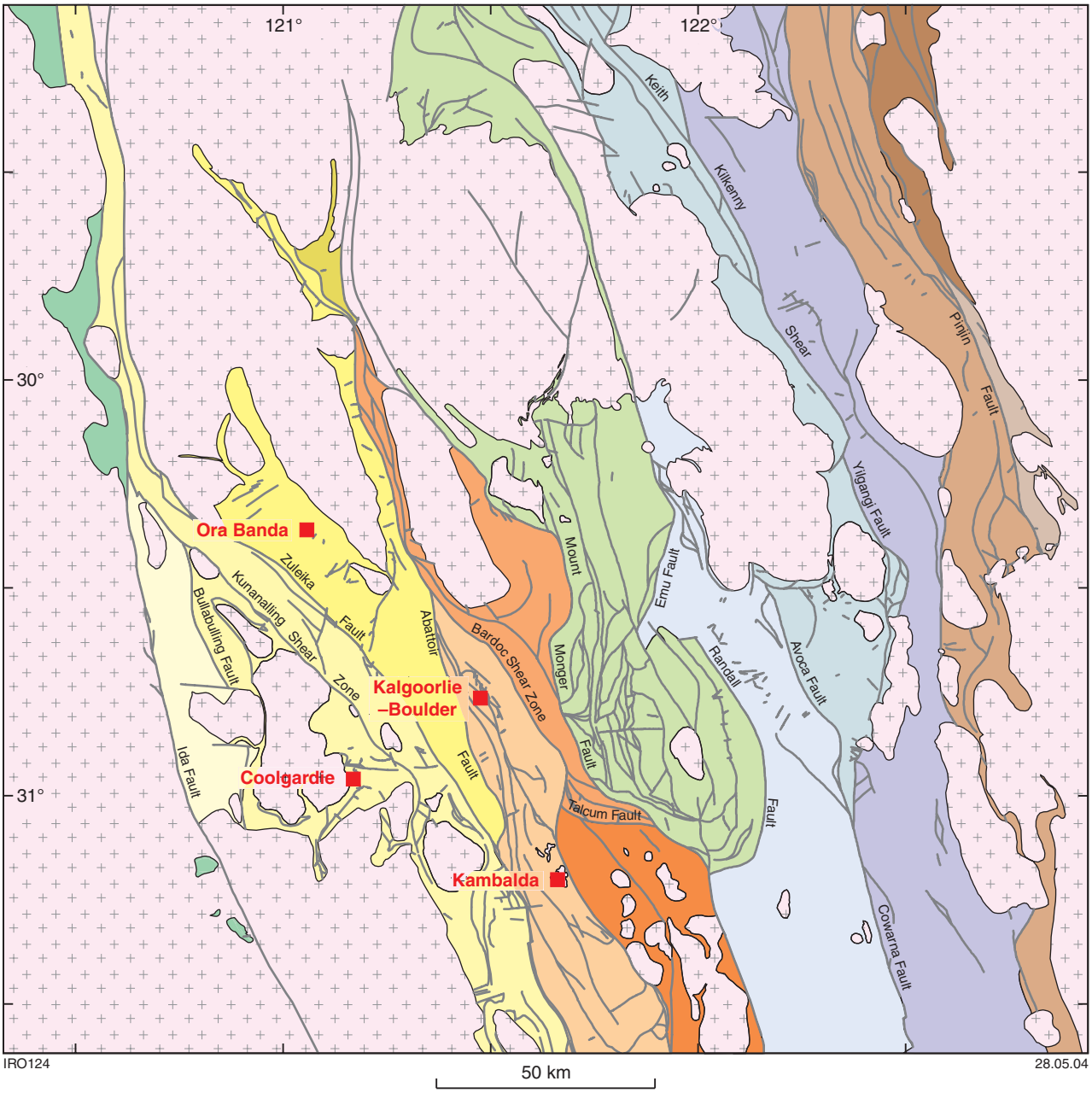

Figure I.5. Subdivision of the Edjudina–Kanowna region into greenstone terranes and domains (after Swager, 1997)

Table I.1. Map sheets that cover the area of this Report

Sheet	*Index*	*Map reference*	*Explanatory Notes reference*
1:100 000 scale			
Lake Lefroy	3225	Griffin and Hickman (1988a)	Griffin (1990)
Kanowna	3236	Ahmat (1995b)	Ahmat (1995a)
Gindalbie	3237	Ahmat (1995c)	–
Boyce	3238	Chen and Witt (1997)	–
Yerilla	3239	Oversby and Vanderhor (1995)	–
Mount Belches	3335	Painter and Groenewald (2000)	Painter and Groenewald (2001)
Kurnalpi	3336	Swager (1993)	Swager (1994a)
Mulgabbie	3337	Morris (1994a)	Morris (1994b)
Edjudina	3338	Swager and Rattenbury (1994)	Swager (1995b)
Lake Carey	3339	Rattenbury and Swager (1994)	–
Erayinia	3435	–	–
Roe	3436	Smithies (1994a)	Smithies (1994b)
Pinjin	3437	Swager (1994b)	Swager (1994c)
Yabboo	3438	Swager (1994d)	Swager (1995b)
Mount Celia	3439	Duggan (1992)	–
1:250 000 scale			
Widgiemooltha	SH51-14	Griffin and Hickman (1988b)	Griffin (1989)
Kurnalpi	SH51-10	Swager (1996)	–
Edjudina	SH51-6	Williams et al. (1976), Chen (1998)	Chen (1999)

Myers 1990, Swager et al. (1990, 1995), and Swager (1995a, 1997) divided the greenstone succession of the southern part of the Eastern Goldfields Granite–Greenstone Terrane into a number of elongate structural entities, called greenstone terranes, separated by regional north-northwesterly trending faults. These greenstone terranes do not include intrusive granites or upper metaconglomerate sequences, and are further subdivided into fault-bound domains (Swager, 1997). Except for the northern half of Edjudina, the subdivision of Swager (1997) has been used in this Report. A comparison between the schemes of Swager (1995a), Swager (1997), Chen (1999), and Groenewald et al. (2000) is given in Table I.2.

Terranes

Kalgoorlie Terrane

The Kalgoorlie Terrane (Myers, 1990) is divided into a number of domains bound by major shear zones. The Boorara domain is situated in the southwestern corner of the study area (Fig. I.5). Despite poor outcrop and a complex deformational history, a simple stratigraphy has been interpreted for the Kalgoorlie Terrane: a lower metabasalt overlain by metakomatiite, in turn overlain by an upper metabasalt, and followed by metamorphosed felsic volcanic and sedimentary rocks, including a late metaconglomerate (Swager et al., 1990, 1995). Intrusions

Table I.2. Tectonic subdivisions of the Edjudina–Kanowna region

Swager (1995a)	*Swager (1997)*	*Chen (1999)*	*Groenewald et al. (2000)*
Kalgoorlie Terrane Boorara domain	Kalgoorlie Terrane Boorara domain	–	Kalgoorlie Greenstones Boorara domain
Gindalbie Terrane	Gindalbie Terrane	Malcolm greenstones	Kalgoorlie Greenstones Gindalbie domain
Jubilee Terrane	Kurnalpi Terrane Jubilee domain	Malcolm greenstones	Edjudina–Laverton Greenstones Jubilee domain
Kurnalpi Terrane	Kurnalpi Terrane Steeple Hill domain	Malcolm greenstones	Edjudina–Laverton Greenstones Kurnalpi domain
Mulgabbie Terrane	Kurnalpi Terrane Mulgabbie domain	Murrin greenstones	Edjudina–Laverton Greenstones Mulgabbie domain
Edjudina Terrane	Edjudina Terrane Yabboo domain	Laverton greenstones	Edjudina–Laverton Greenstones Edjudina domain
Pinjin Terrane	Edjudina Terrane Pinjin domain	–	Edjudina–Laverton Greenstones Pinjin domain
Linden Terrane	Linden Terrane	Laverton greenstones	Edjudina–Laverton Greenstones Linden domain

of layered and differentiated mafic sills, as well as felsic porphyry dykes are present in the sequence. Within the Boorara Domain the upper metabasalt is absent, and the metamorphosed felsic volcanic and sedimentary rocks typically directly overlie metakomatiite (Witt, 1994).

Gindalbie Terrane

The Gindalbie Terrane lies between the Mount Monger Fault to the west and the Emu and Randall Faults to the east (Fig. I.5). The northern part of the terrane is dominated by bimodal metabasalt–metarhyolite, and the southern part by metamorphosed komatiitic basalt and calc-alkaline volcanic rocks (Swager, 1997).

Kurnalpi Terrane

The Kurnalpi Terrane lies between the Emu Fault to the west and Claypan Fault to the east, and consists of three fault-bound domains: the Jubilee, Steeple Hill, and Mulgabbie domains (Swager, 1997). The terrane contains metamorphosed mafic to felsic volcanic rock sequences and intercalated metakomatiite (Swager, 1995a, 1997). Metamorphosed andesitic volcanic and epiclastic rocks are a minor component, and banded iron-formations (BIFs) are present locally (Swager, 1995a, 1997). The Mount Belches Formation may represent a southern extension of the Kurnalpi Terrane, as it does not appear to be a lateral equivalent of the overlying Penny Dam Conglomerate (Painter and Groenewald, 2001).

The Jubilee domain is bound to the west by the Randall Fault and overlying metaconglomerate, and to the east by the Avoca Fault (Fig. I.5). Based on seismic reflection work (Goleby et al., 1993), Swager (1997) interpreted the Jubilee domain as a west-dipping homoclinal greenstone package on a domal structure. It is characterized by substantial volumes of contemporaneous metamorphosed basalt and felsic volcanic rocks, with thin metakomatiite lenses (Swager, 1997).

The Steeple Hill domain of Swager (1997) is bound by the Avoca Fault and granites to the west, and the Yilgangi Fault to the east. The Steeple Hill syncline is the principal structure in the south, whereas in the north, there is a complex east-dipping greenstone sequence (Swager, 1995b).

The Mulgabbie domain of Swager (1997) lies between the Yilgangi and Claypan Faults and comprises a large volume of metamorphosed ultramafic rocks, komatiitic basalt, and mafic intrusive rocks, as well as substantial andesitic (calc-alkaline) and felsic volcanic rocks (Chen, 1999).

Edjudina Terrane

The Edjudina Terrane of Swager (1997) consists of the western Yabboo domain and the southeastern Pinjin domain (Fig. I.5). The Yabboo domain is bound by the Claypan Fault to the west and the Pinjin Fault to the east. It differs from domains to the west, with minor volumes of metabasalt and metakomatiite, and a large number of calc-alkaline andesitic complexes and their epiclastic debris, together with abundant BIF, metachert and metasedimentary rocks intruded by metadolerite (Swager, 1995a, 1997).

The Pinjin domain is bound to the east by granite gneiss (Fig. I.5) and contains a metabasalt and BIF association and a meta-andesite and metadacite sequence that have been metamorphosed to middle–upper amphibolite facies (Swager, 1997).

Linden Terrane

The southern part of the Linden Terrane (Swager, 1997) is bound to the west by the Safari Fault, and granites mark the eastern boundary (Fig. I.5). Extrapolation of the Linden Terrane to the north, however, is ambiguous and its northern limits are unclear. Swager (1997) reported that the Linden Terrane contains metamorphosed basalts, komatiites, and felsic volcanic rocks in a sequence that youngs to the west.

Deformation and metamorphism

The deformational history of the region is similar to that proposed for the Eastern Goldfields Granite–Greenstone Terrane, and a summary, based on Groenewald et al. (2000), is presented in Table I.3. The regional deformational history is also described by Griffin (1989, 1990), Ahmat (1995a), Painter and Groenewald (2001), Swager (1994a,c), Swager (1995a,b), Swager (1997), Swager et al. (1995), Morris (1994b), Smithies (1994b), and Chen (1999).

The principal deformational phases (Chen, 1999; Groenewald et al., 2000) are:

- D_1 — a north–south thrusting accompanied by isoclinal and recumbent folding;
- D_2 — a regional east-northeast to west-southwest shortening event that resulted in upright north-northwesterly trending folds with steeply dipping axial-planar foliation;
- D_3 — transpressional deformation with strike-slip sinistral movement in ductile shear zones and along well-defined brittle faults, with associated en echelon folds;
- D_4 — a shortening event that produced northwest to west-northwest oblique sinistral faults and northeast to east-northeast oblique dextral/reverse faults with associated kink folds and a local crenulation cleavage.

Table I.3 summarizes these deformational compressional phases, as well as some controversial extensional phases.

The regional distribution of metamorphic zones in the Eastern Goldfields Granite–Greenstone Terrane was described by Binns et al. (1976), and for parts of the

Edjudina–Kanowna region by Swager (1995a, 1997), Groenewald et al. (2000), and Mikucki and Roberts (2004). The generalized regional metamorphic pattern is lower grade zones (greenschist facies) in the central part of the greenstone belts, and higher grade zones (amphibolite facies) typically marginal to granite bodies (Swager, 1995a; 1997). Mikucki and Roberts (2004) concluded that the metamorphic zonation is controlled by the distribution of post-regional folding granites, while Swager (1995a) also considered that a subsequent extensional event has juxtaposed rocks from different crustal levels and P–T conditions.

Table I.3. Summary of deformational events in the Eastern Goldfields Granite–Greenstone Terrane

Event		*Structures*	*Locality or example*	*Age*
?De		Low-angle shear on granite–greenstone contacts; N–S movement; synvolcanic granites[a]; polydirectional extension, local recumbent folding[b]	Lawlers; Mount Malcolm (central Eastern Goldfields)	c. 2705[n] – c. 2680 Ma
D_1	D_{1c}	Low-angle thrust faults and recumbent folds[c,d,j]; ?shear on early granite–greenstone contacts; late synvolcanic slides caused by uplift[a,b]	Between Kalgoorlie and Democrat (south of Kambalda)	Maximum age constraint: 2681 ± 5 Ma, 2675 ± 3 Ma[n]
	D_{1e}	Deformed contacts between early granite complexes and greenstones; N–S lineations in contact zone; recumbent folds in overlying greenstones[e]	Jeedamy–Kookynie area	
De		Roll-over anticlines and E–W extension leading to clastic infill of synclinal basins[f,g]	Kurrawang, Penny Dam, Merougil metaconglomerates	2674 ± 6 Ma[q]
D_2		Upright folds with shallowly plunging, NNW fold axes[c,e,h]	Kambalda Anticline, Goongarrie – Mount Pleasant anticline, Kurrawang syncline	Minimum: 2660 ± 3 Ma
D_e		Local extension in final uplift of granite domes[i]	Barret Well (Yabboo)	Maximum: 2675 ± 2 Ma
D_3		Tightening of F_2 folds[k,l]; NW to NNW sinistral strike-slip faults and shear zones; N to NNE dextral strike-slip faults and shear zones	Boorara–Menzies Fault[e,k] Boulder–Lefroy Fault Butchers Flat Fault	Minimum: 2658 ± 13 Ma; 2640 ± 8 Ma
		Transpression on NNW faults, with compressional jogs and fold axes trending N to NNE[m]	Laverton, Yandal (central and northeast Eastern Goldfields)	
Late D_3		Steeply plunging lineations on strike-slip faults	Goongarrie, Bardoc Tectonic Zone[e]	
		Steeply dipping reverse faults	Melita, Niagara [e]	
D_e		Post-metamorphic orogenic collapse[r]	Ida Fault	c. 2640 Ma
D_4		NW to WNW oblique sinistral[e] faults; NE to ENE oblique dextral–reverse faults[e,j]	Paddington area; Mount Charlotte (Kalgoorlie); Black Flag Fault (Mount Pleasant)	2638 ± 26 Ma[o]; 2651 ± 5 Ma[p]

NOTE: modified from Groenewald et al. (2000)

SOURCES:
(a) Hammond and Nisbet (1992)
(b) Passchier (1994)
(c) Swager and Griffin (1990)
(d) Gresham and Loftus-Hills (1981)
(e) Witt (1994)
(f) Williams (1993)
(g) Swager (1997)
(h) Hunter (1993)
(i) Swager and Nelson (1997)
(j) Archibald et al. (1981)
(k) Swager et al. (1995)
(l) Swager (1989)
(m) Chen et al. (2001)
(n) Nelson (1997)
(o) Hill et al. (1992)
(p) Nelson (1995)
(q) Kent and McDougall (1996)
(r) Goleby et al. (1993)

References

AHMAT, A. L., 1995a, Geology of the Kanowna 1:100 000 sheet: Western Australia Geological Survey, 1:100 000 Geological Series Explanatory Notes, 28p.

AHMAT, A. L., 1995b, Kanowna, W.A. Sheet 3236: Western Australia Geological Survey, 1:100 000 Geological Series.

AHMAT, A. L., 1995c, Gindalbie, W.A. Sheet 3237: Western Australia Geological Survey, 1:100 000 Geological Series.

ARCHIBALD, N. J., BETTENAY, L. F., BICKLE, M. J., and GROVES, D. I., 1981, Evolution of Archaean crust in the Eastern Goldfields Province of the Yilgarn Block: Geological Society of Australia, Special Publication, no. 7, p. 491–504.

BINNS, R. A., GUNTHORPE, R. J., and GROVES, D. I., 1976, Metamorphic patterns and development of greenstone belts in the eastern Yilgarn Block, *in* The early history of the Earth *edited by* B. F. WINDLEY: New York, John Wiley and Sons, p. 303–316.

CHEN, S. F., 1998, Edjudina, W.A. (2nd edition): Western Australia Geological Survey, 1:250 000 Geological Series.

CHEN, S. F., 1999, Edjudina, W.A. (2nd edition): Western Australia Geological Survey, 1:250 000 Geological Series Explanatory Notes, 32p.

CHEN, S. F., and WITT, W. K., 1997, Boyce, W.A. Sheet 3238 (1st edition): Western Australia Geological Survey, 1:100 000 Geological Series.

CHEN, S. F., WITT, W. K., and LIU, S., 2001, Transpressional and restraining jogs in the northeastern Yilgarn Craton, Western Australia: Precambrian Research, v. 106, p. 309–311.

DUGGAN, M. B., 1992, Mount Celia, W.A. Sheet 3439 (preliminary edition): Australian Geological Survey Organisation, 1:100 000 Geological Series.

GOLEBY, B. R., RATTENBURY, M. S., SWAGER, C. P., DRUMMOND, B. J., WILLIAMS, P. R., SHERATON, J. E., and HEINRICH, C. A., 1993, Archaean crustal structure from seismic reflection profiling, Eastern Goldfields, Western Australia: Australian Geological Survey Organisation, Record 1993/15, 54p.

GRESHAM, J. J., and LOFTUS-HILLS, G. D., 1981, The geology of the Kambalda nickel field, Western Australia: Economic Geology, v. 76, p. 1373–1416.

GRIFFIN, T. J., 1989, Widgiemooltha, W.A. (2nd edition): Western Australia Geological Survey, 1:250 000 Geological Series Explanatory Notes, 43p.

GRIFFIN, T. J., 1990, Geology of the granite–greenstone terrane of the Lake Lefroy and Cowan 1:100 000 sheets, Western Australia: Western Australian, Report 32, 53p.

GRIFFIN, T. J., and HICKMAN, A. H., 1988a, Lake Lefroy, W.A. Sheet 3235: Western Australia Geological Survey, 1:100 000 Geological Series.

GRIFFIN, T. J., and HICKMAN, A. H., 1988b, Widgiemooltha, W.A. (2nd edition): Western Australia Geological Survey, 1:250 000 Geological Series.

GROENEWALD, P. B., PAINTER, M. G. M., ROBERTS, F. I., McCABE, M., and FOX, A., 2000, East Yilgarn Geoscience Database, 1:100 000 geology Menzies to Norseman — an explanatory note: Western Australian Geological Survey, Report 78, 53p.

HAMMOND, R. L., and NISBET, B. W., 1992, Towards a structural and tectonic framework for the Norseman–Wiluna greenstone belt, Western Australia, *in* The Archaean: Terrains, processes and metallogeny *edited by* J. E. GLOVER and S. E. HO: University of Western Australia, Geology Department and University Extension, Publication no. 22, p. 39–50.

HILL, R. I., CHAPPELL, B. W., and CAMPBELL, I. H., 1992, Late Archaean granites of the southeastern Yilgarn Block, Western Australia: age, geochemistry and origin: Transactions of the Royal Society of Edinburgh, v. 83, p. 211–226.

HUNTER, W. M., 1993, The geology of the granite–greenstone terrane of the Kalgoorlie and Yilmia 1:100 000 sheets, Western Australia: Western Australia Geological Survey, Report 35, 80p.

KEATS, W., 1991, Geology and gold mines of the Bullfinch–Parker Range region, Southern Cross Province, Western Australia: Western Australia Geological Survey, Report 28, 44p.

KENT, A. J. R., and McDOUGALL, I., 1996, ^{40}Ar–^{39}Ar and U–Pb age constraints on the timing of gold mineralization in the Kalgoorlie Gold Field, Western Australia — a reply: Economic Geology, v. 91, p. 795–799.

MIKUCKI, E. J., and ROBERTS, F. I., 2004, Metamorphic petrography of the Kalgoorlie region, Eastern Goldfields Granite Greenstone Terrane: METPET database: Western Australian Geological Survey, Record 2003/12, 40p.

MORRIS, P. A., 1994a, Mulgabbie, W.A. Sheet 3337: Western Australia Geological Survey, 1:100 000 Geological Series.

MORRIS, P. A., 1994b, Geology of the Mulgabbie 1:100 000 sheet: Western Australia Geological Survey, 1:100 000 Geological Series Explanatory Notes, 18p.

MYERS, J. S., 1990, Precambrian tectonic evolution of part of Gondwana, southwestern Australia, Geology, v. 18, p. 537–540.

NELSON, D. R., 1995, Compilation of SHRIMP U–Pb zircon dates, 1994: Western Australia Geological Survey, Record 1995/03, 244p.

NELSON, D. R., 1997, Compilation of SHRIMP U–Pb zircon geochronology data 1996: Western Australia Geological Survey, Record 1997/2, 189p.

OVERSBY, B. S., and VANDERHOR, F., 1995, Yerilla, W. A. Sheet 3239: Australian Geological Survey Organisation, 1:100 000 Geological Series.

PAINTER, M. G. M., and GROENEWALD, P. B., 2000, Mount Belches, W.A. Sheet 3335: Western Australia Geological Survey, 1:100 000 Geological Series.

PAINTER, M. G. M., and GROENEWALD, P. B., 2001, Geology of the Mount Belches 1:100 000 sheet: Western Australia Geological Survey, 1:100 000 Geological Series Explanatory Notes, 38p.

PAINTER, M. G. M, GROENEWALD, P. B., and McCABE, M., 2003, East Yilgarn Geoscience Database, 1:100 000 geology of the Leonora–Laverton region, Eastern Goldfields Granite–Greenstone Terrane — an explanatory note: Western Australia Geological Survey, Report 84, 45p.

PASSCHIER, C. W., 1994, Structural geology across a proposed Archaean terrane boundary in the eastern Yilgarn craton, Western Australia: Precambrian Research, v. 68, p. 43–64.

RATTENBURY, M. S., and SWAGER, C. P., 1994, Lake Carey, W.A. Sheet 3339: Australian Geological Survey Organisation, 1:100 000 Geological Series.

SMITHIES, R. H., 1994a, Roe, W.A. Sheet 3436: Western Australia Geological Survey. 1:000 000 Geological Series.

SMITHIES, R. H., 1994b, Geology of the Roe 1:100 000 sheet: Western Australia Geological Survey: 1:100 000 Geological Series Explanatory Notes, 15p.

SWAGER, C. P., 1989, Structure of the Kalgoorlie greenstones — regional deformation history and implications for the structural setting of the Golden Mile gold deposits: Western Australia Geological Survey, Report 25, Professional Papers, p. 59–84.

SWAGER, C. P., 1993, Kurnalpi, W.A. Sheet 3336: Western Australia Geological Survey, 1:100 000 Geological Series.

SWAGER, C. P., 1994a, Geology of the Kurnalpi 1:100 000 sheet: Western Australia Geological Survey, 1:100 000 Geological Series Explanatory Notes, 19p.

SWAGER, C. P., 1994b, Pinjin, W.A. Sheet 3437: Western Australia Geological Survey, 1:100 000 Geological Series.

SWAGER, C. P., 1994c, Geology of the Pinjin 1:100 000 sheet: Western Australia Geological Survey, 1:100 000 Geological Series Explanatory Notes, 22p.

SWAGER, C. P., 1994d, Yabboo, W.A. Sheet 3438: Western Australia Geological Survey, 1:100 000 Geological Series.

SWAGER, C. P., 1995a, Geology of the greenstone terranes in the Kurnalpi–Edjudina region, southeastern Yilgarn Craton: Western Australia Geological Survey, Report 47, 31p.

SWAGER, C. P., 1995b, Geology of the Edjudina and Yabboo 1:100 000 sheets: Western Australia Geological Survey, 1:100 000 Geological Series Explanatory Notes, 43p.

SWAGER, C. P., 1996, Kurnalpi, W.A. (2nd edition): Western Australia Geological Survey, 1:250 000 Geological Series.

SWAGER, C. P., 1997, Tectono-stratigraphy of late Archaean greenstone terranes in the southern Eastern Goldfields, Western Australia: Precambrian Research, v. 83, p. 11–42.

SWAGER, C. P., and GRIFFIN, T. J., 1990, An early thrust duplex in the Kalgoorlie–Kambalda greenstone belt, Eastern Goldfields Province, Western Australia: Precambrian Research, v. 48, p. 63–73.

SWAGER, C. P., GRIFFIN, T. J., WITT, W. K., WYCHE, S., AHMAT, A. L., HUNTER, W. M., and McGOLDRICK, P. J., 1990, Geology of the Archaean Kalgoorlie Terrane — an explanatory note: Western Australian Geological Survey, Record 1990/12, 54p.

SWAGER, C. P., GRIFFIN, T. J., WITT, W. K., WYCHE, S., AHMAT, A. L., HUNTER, W. M., and McGOLDRICK, P. J., 1995, Geology of the Archaean Kalgoorlie Terrane — an explanatory note: Western Australian Geological Survey, Report 48, 26p.

SWAGER, C. P., and NELSON, D. R., 1997, Extensional emplacement of a high-grade granite gneiss complex into low-grade greenstones, Eastern Goldfields, Yilgarn Craton, Western Australia: Precambrian Research, v. 83, p. 203–219.

SWAGER, C. P., and RATTENBURY, M. S., 1994, Edjudina, W.A. Sheet 3338: Western Australia Geological Survey, 1:100 000 Geological Series.

TYLER, I. M., 2001, Tectonic units map of Western Australia: Western Australia Geological Survey, 1:2 500 000 Geological Series.

WILLIAMS, I. R., GOWER, C. F., and THOM, R., 1976, Edjudina, W.A.: Western Australia Geological Survey, 1:250 000 Geological Series Explanatory Notes, 29p.

WILLIAMS, P. R., 1993, A new hypothesis for the evolution of the Eastern Goldfields Province, *in* Kalgoorlie 93 — an international conference on crustal evolution, metallogeny, and exploration in the Eastern Goldfields *compiled by* P. R. WILLIAMS and J. A. HALDANE: Australian Geological Survey Organisation, Record 1993/54, p. 77–83.

WITT, W. K., 1993a, Gold deposits of the Mt Pleasant–Ora Banda areas, Western Australia — Part 1 of a systematic study of the gold mines of the Menzies–Kamblada region: Western Australia Geological Survey, Record 1992/13, 158p.

WITT, W. K., 1993b, Gold deposits of the Mt Pleasant–Ora Banda areas, Western Australia — Part 2 of a systematic study of the gold mines of the Menzies–Kamblada region: Western Australia Geological Survey, Record 1992/14, 104p.

WITT, W. K., 1993c, Gold mineralization in the Menzies–Kambalda–St Ives area, Western Australia — Part 3 of a systematic study of the gold deposits of the Menzies–Kambalda region: Western Australia Geological Survey, Record 1992/15, 108p.

WITT, W. K., 1993d, Gold mineralization in the Menzies–Kambalda region, Eastern Goldfields, Western Australia: Western Australia Geological Survey, Report 39, 165p.

WITT, W. K., 1993e, Lithological and structural controls on gold mineralization in the Archaean Menzies–Kambalda area, Western Australia: Australian Journal of Earth Sciences, v. 40, p. 65–86.

WITT, W. K., 1994, Geology of the Bardoc 1:100 000 sheet: Western Australia Geological Survey, 1:100 000 Geological Series Explanatory Notes, 50p.

Mineralization

1. Gordon–Mulgarrie

The Gordon and Mulgarrie mining areas lie in a northwest-striking greenstone belt on the eastern limb of the D_2 Scotia–Kanowna anticline. The belt lies within the eastern part (Boorara domain) of the Kalgoorlie Terrane (Swager, 1997). The stratigraphy in the western part of this domain was described by Witt (1990). Felsic volcanic rocks in the eastern part of the Boorara domain are interbedded with mafic to ultramafic rocks in the lower part of the greenstone sequence, forming a bimodal volcanic succession in the Gordon–Mulgarrie area. Gold is present throughout the greenstone sequence, but the largest deposit (Sirdar at Gordon) is hosted by the upper felsic unit. This upper felsic unit has been thrust over the lower ultramafic unit and bimodal volcanic succession (Swager and Griffin, 1990). Graded bedding in volcaniclastic metasedimentary rocks suggests this upper felsic unit is overturned (younging towards the west). The mineralized parts of the greenstone sequence have been metamorphosed at greenschist facies conditions.

Up until the 1990s, the Gordon area had produced about 500 kg of gold, mainly from the Sirdar mine, and the Mulgarrie centre had produced about 160 kg of gold, mainly from the Palm deposit. Both of these deposits have seen a revival of mining in recent years, as openpit operations. The Sirdar deposit produced 185 kg Au and the Palm deposit produced 450 kg Au in the 1990s.

Although the upper contact of the ultramafic unit at Mulgarrie may be a D_1 fault, the ultramafic host rocks at Palm are foliated but not strongly sheared. They are, however, very strongly carbonated, and this carbonation has imparted a brittle character to the ultramafic rocks. Late-tectonic fracturing produced sheeted east–west-oriented quartz veins in the brittle, carbonated units. Other deposits in the Mulgarrie area (e.g. Gem and Lady Clara) appear to be related to the contact between ultramafic and mafic units. Mineralization at Mount Eba (Gordon) lies on a northwest-trending contact between mafic and felsic units and is probably related to the competency contrast between adjacent units during late-tectonic east–west compression. The contacts at Mount Eba and Mulgarrie would have been zones of high shear strain in response to east–west compression, and mineralized quartz veins may have formed where the contact changed strike and was bent around local irregularities. The arrangement of deposits at Mulgarrie along lineaments interpreted from airborne magnetic data suggests that mineralization may also be related to one or more late, north-trending (D_4) faults.

Deposits that lie within the bimodal volcanic sequence to the west of Gordon Sirdar (e.g. North Kanowna Star and Koh-I-Nor Leases) display some features that suggest an early (epithermal or subsea-floor) origin. The mineralized units, which have been deformed by D_2, are interpreted as metamorphosed thin, interflow chert and silicified, pyritic black shale horizons within a metamorphosed basaltic flow sequence, and could be examples of the mixed chemical–clastic horizons that may form in a subsea-floor environment along strike from volcanogenic massive sulfide (VMS) deposits (Galley, 1995). Transgressive pyrite-rich veins that probably formed in synvolcanic faults are also mineralized. The banded, crustiform nature of veins typically found in epithermal deposits (Larsen and Hutchinson, 1993) have not been observed, but such textures may have been destroyed by metamorphic recrystallization.

As for Mount Eba, gold in metamorphosed felsic volcaniclastic rocks at Sirdar is associated with the deformed, northwest-striking contacts of a metamorphosed felsic hyaloclastite unit, but the mineralized structures do not appear to be typical late-orogenic brittle–ductile shear zones. Late, shear-related quartz veins are only locally developed and are not consistently associated with gold. Instead, the ore zones contain strongly deformed, sulfide-rich quartz–pyrite veins and veinlets. Deep drilling beneath the Sirdar pit has intersected stockwork pyrite veining in the undeformed interior of the hyaloclastite unit. These veins become increasingly deformed with the host rock towards the margins of the unit. Drilling also intersected a thick sequence of metamorphosed felsic volcaniclastic rocks that overlie the hyaloclastite. These are interpreted as having been deposited in a subaqueous setting, either directly from a (possibly subaerial) volcanic eruption, or more probably from slumping of earlier pyroclastic deposits. Widespread silica–pyrite alteration and strongly deformed quartz–pyrite(–chlorite) veinlets are exhibited in some of the metavolcaniclastic units, but are unmineralized (Fig. 1.1). The early timing of this alteration is evident from the overprinting nature of the regional sericitic fabric. Pyrite is absent from the silicified metavolcaniclastic rocks where overprinted by regional deformation and sericitization. Metamorphic recrystallization of the deformed metavolcaniclastic units has produced andalusite and chloritoid in some sections of the silica–pyrite alteration facies (Fig. 1.2). Garner (1996) suggested that the presence of andalusite and chloritoid in immature metavolcaniclastic rocks at Sirdar indicates that the early silica–pyrite alteration was associated with (subsea-floor) alkali (K and Na) leaching.

Deep drilling beneath Sirdar also revealed the presence of metamorphosed coarse, pyritic, polymictic conglomerate containing clasts of altered, metamorphosed, pyritic ultramafic, mafic, and felsic volcanic rocks, as well as metamorphosed pyritic chert and black shale, and massive to bedded pyrite. Gold is not present in significant amounts in the silica–pyrite-facies metavolcaniclastic rocks in the deep drillhole below Sirdar (GSD-1), but the metamorphosed polymictic conglomerate unit contains some (locally very rich) ore zones (Fig. 1.3). These units do not contain quartz veins or quartz–pyrite veinlets. They do contain pyrite-rich clasts, but there does not seem to be a correlation between gold abundance and sulfide-rich clasts in GSD-1. Instead, gold-bearing sections contain irregular, carbonate-rich domains that seem to be partly veins and partly primary interclast porosity infill (Fig. 1.4). These carbonate-rich domains contain minor pyrite, sphalerite, and chalcopyrite. The ratio of pyrite to base-metal sulfides in these carbonate-rich domains is much lower than in typical mesothermal quartz veins.

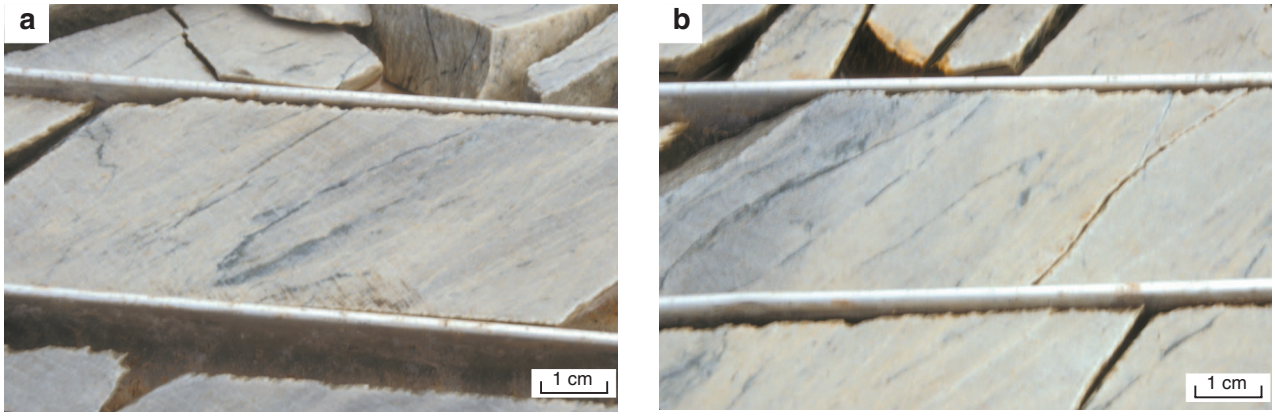

IRO131 15.12.03

Figure 1.1. Deformed quartz–pyrite–chlorite veinlets in a silicified, metamorphosed, fine-grained, felsic volcaniclastic unit, Gordon Sirdar deposit: a) oriented sericite in zones of later, barren, deformation-related alteration (cream) overprint the silicified metavolcaniclastic rock (grey); b) the contact between the pyritic, silicified, metamorphosed felsic volcaniclastic rock and quartz–pyrite–chlorite veinlets (grey, left) and later, deformation-related sericitization (cream, right). Note the relict deformed quartz–pyrite–chlorite veinlet in the sericitized zone

The origin of the gold at Sirdar is enigmatic. The location of the deposit, on a contact between units of contrasting competency (the hyaloclastite unit is brittle compared to adjacent hangingwall schists), and the proximity of the deposit to a late, crosscutting fault, is consistent with a late-orogenic origin. However, gold is also associated with the footwall contact against a massive felsic unit, and the competency contrast between this unit and the hyaloclastite is probably quite small. Several features at Sirdar contrast with the typical characteristics of late-orogenic gold deposits, and are more compatible with an early (synvolcanic) origin for the gold mineralization. The pyrite-rich nature of the vein system contrasts strikingly with the quartz-rich nature of most late-orogenic deposits. The consistent deformation of veins with the host rock indicates a much earlier formation of the veins and related mineralization. The concentration of gold at the margins of the hyaloclastite unit may not reflect competency contrasts, but could be attributed to the increased synvolcanic porosity (brecciation) of the contact zones. The widespread silicification in the hangingwall metavolcaniclastic rocks suggests that the mineralization formed part of a larger hydrothermal system. Silica–pyrite alteration is commonly associated with epithermal styles of gold mineralization (e.g. Hedenquist et al., 1994), but stratabound zones of silicification have also been documented in some subsea-floor (VMS) alteration systems (Skirrow and Franklin, 1994; Galley, 1995). The association of mineralization with synvolcanic faults is another feature that is common to subsea-floor environments (Large, 1992; Kerr and Gibson, 1993). Gold in the metamorphosed polymictic conglomerate unit in GSD-1 is unrelated to veins or shearing and is most likely synvolcanic in origin. Sea-floor fluids percolating through the unconsolidated pebbles and cobbles deposited carbonate and sulfides in intraclast spaces.

IRO33 15.12.03

Figure 1.2. Randomly oriented, bladed kyanite in metamorphosed, altered felsic volcaniclastic rock, Gordon Sirdar mine area

Deposits of the Gordon–Mulgarrie area

Sirdar

Other names: Pride of the Morning

Coordinates: 30°27'01"S, 121°35'40"E

Production: 46 703.3 t of ore for 510.67 kg Au (10.9 g/t Au) between 1899 and 1981. Modern production (post-1988) from the Sirdar openpit mine has amounted to 129 535 t of ore for 185.16 kg Au (1.43 g/t Au).

The indicated resource (openpit) at the time of writing was 1.39 Mt of ore at 1.65 g/t Au (2307 kg Au; MINEDEX* site code S03946).

* MINEDEX is the Department of Industry and Resources' (DoIR's) mines and mineral deposits information database for Western Australia, and can be accessed through the Online Databases link on the DoIR homepage at <http//:www.doir.wa.gov.au>. Resource estimates detailed in MINEDEX are figures submitted by mining companies, and have not been verified by the Department.

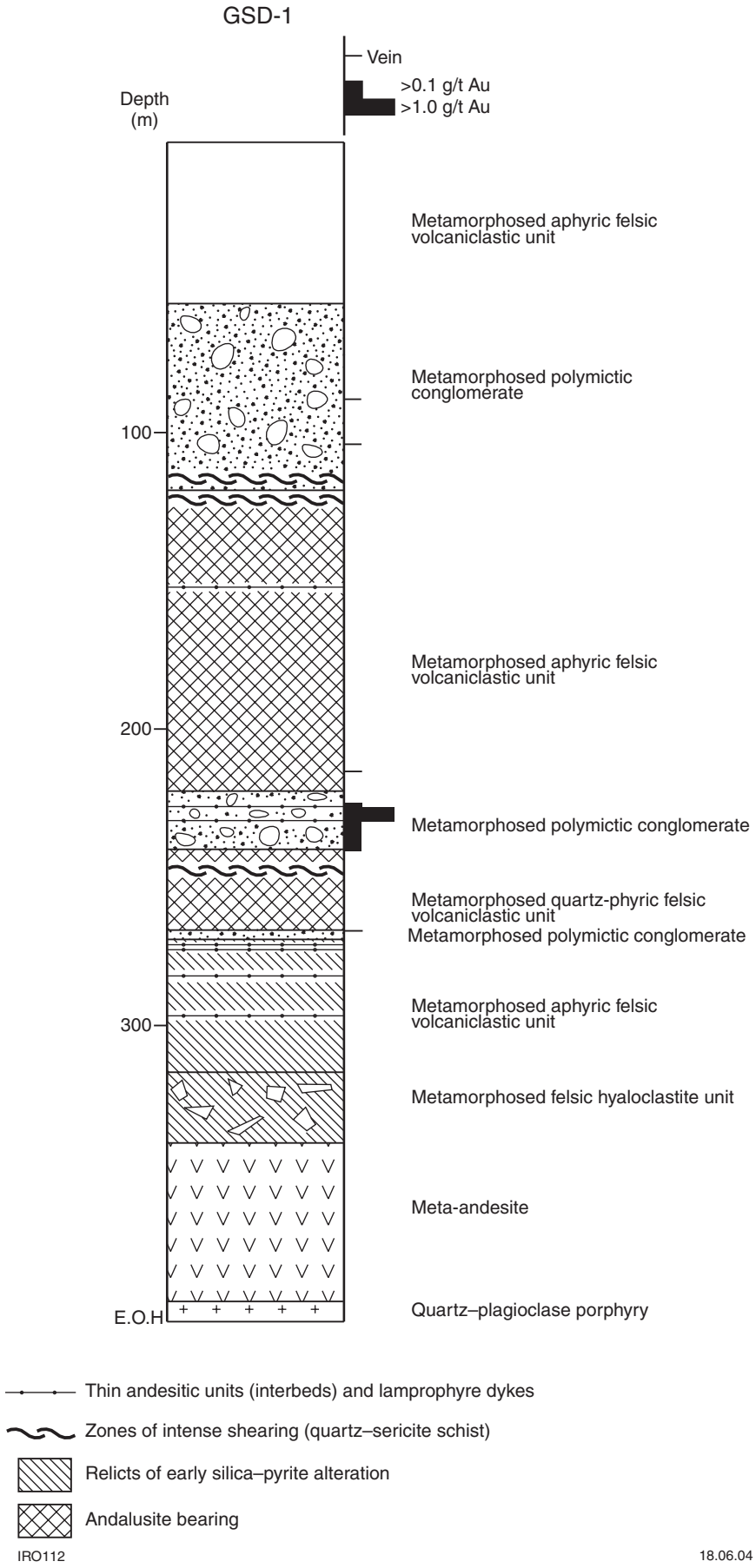

Figure 1.3. Summary log of diamond drillhole GSD-1, Gordon Sirdar mine

IRO34 15.12.03

Figure 1.4. Irregular carbonate-rich domains (?primary porosity infill) between clasts in metamorphosed polymictic conglomerate, GSD-1, Gordon Sirdar mine

Host rock: The main rock types encountered in diamond drillhole GSD-1 and the Sirdar openpit mine are described in Table 1.1. The host rock is a massive to brecciated siliceous unit (Fig. 1.5), which is interpreted to be a felsic hyaloclastite — a lava that has shattered upon contact with cold seawater following submarine eruption. The host unit is underlain by metamorphosed felsic to intermediate volcaniclastic sedimentary rock to the west, and massive quartz–plagioclase porphyry to the east. Thin lenses of polymictic, volcaniclastic metaconglomerate lie within the hangingwall metavolcaniclastic rocks and are locally mineralized. Several late, unmineralized lamprophyre dykes cut the sequence.

Structure: A small, recent openpit has targeted mineralization associated with the deformed contacts of a metamorphosed intermediate volcaniclastic rock (Fig. 1.6). These contacts and the shear zones strike 140° and dip subvertically. Gold mineralization is developed over a strike length of about 200 m. The best grades exist where the sheared contacts are cut by a north-trending dextral fault.

Gold is associated with a stockwork system of pyrite-rich veins that are consistently deformed with the host rock (Fig. 1.7). Although mining was focused on the margins of the hyaloclastite unit, deep drilling indicates that the pyrite-vein stockwork persists towards the less-deformed interior of the unit (Fig. 1.8). The mineralized, sheared contact zones are 1–15 m wide and characterized by anastomosing sericite-rich bands that define a shear fabric and overprint the earlier pyrite-rich veins, with lineations plunging 20–40°S. This linear fabric is most likely an intersection lineation. Late, quartz-rich veins related to shear strain on the deformed contact zones are only at the northern end of the western contact.

Alteration: The deformed contact zones of the hyaloclastite unit are also zones of intense silicification and pyritization, and contain up to 5% deformed, sulfide-rich quartz–pyrite veins (≤7 mm). Selective chloritization of vitric clasts is apparent in zones within the hyaloclastite unit. The sericitic shear fabric associated with regional deformation overprints this earlier silica–pyrite alteration. Extensive silicification of the hangingwall metamorphosed volcaniclastic sedimentary unit, and the implications for this, are described in the overview.

Whole-rock analyses of some mineralized and unmineralized metamorphosed polymictic conglomerate samples are presented in Appendix 5.

References: Feldtmann (1917), Garner (1996), Roberts and Witt (2002).

Mount Eba

Coordinates: 30°26'10"S, 121°34'45"E

Production: 679.4 t of ore for 7.66 kg Au (11.3 g/t Au) between 1898 and 1910.

Host rock: The mafic host rocks form a thin unit between ultramafic rock to the west and felsic schist after volcaniclastic rock to the east.

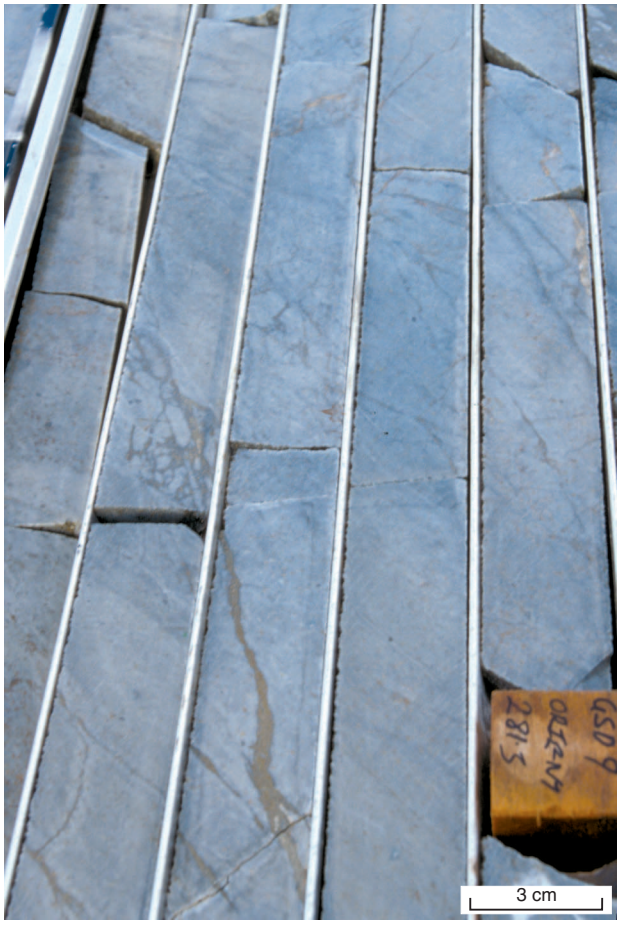

IRO36 15.12.03

Figure 1.5 Fine-grained metamorphosed felsic hyaloclastite unit, Gordon Sirdar mine area, showing zones of jigsaw-fit breccia and local pyrite infill between breccia clasts

Table 1.1. Petrographic descriptions of rock units in diamond drillhole GSD-1, Gordon mining centre

Rock unit	*Lithology and petrography*	*Interpretation*	*Alteration*
Metamorphosed polymictic conglomerate	This metamorphosed, poorly sorted, matrix-supported conglomerate contains a diverse range of subangular to subrounded lithic clasts, up to a maximum size of about 5 cm, in a matrix of fine to coarse volcaniclastic sand. Clasts are mainly of felsic volcanic (?dacitic, ?rhyolitic) and sedimentary origin, but include intensely silicified mafic to intermediate volcanic clasts and locally abundant ß-quartz crystal fragments. Sedimentary clasts are mainly pyritic metamorphosed chert and black shale and bedded to massive pyrite. Bedding is absent, or poorly defined by variations in clast population and average clast size on a scale of several metres. Disseminated pyrite is abundant in all volcanic clasts	This unit is interpreted as a subaqueous, immature mass-flow deposit derived from a mixed volcanic source, and includes syngenetic pyrite mineralization. The lowermost part of this unit has a chloritic matrix that suggests a relatively mafic source region	The matrix contains up to 30% carbonate in the form of disseminations and irregular aggregates. There is only minor disseminated pyrite in the groundmass. An irregular fabric is defined by discontinuous, anastomosing sericitic seams, which appear to post-date carbonation
Metamorphosed aphyric felsic volcaniclastic unit	This fine-grained quartz–feldspar–muscovite schist has a local fragmental structure defined by flattened, angular to subangular felsic volcanic clasts up to about 3 mm in length. Equant quartz crystal fragments up to about 1.5 mm across are a minor component or absent. Fine-grained rutile is an accessory phase. Bedding is poorly developed or absent. In the section between 118 and 267 m, andalusite porphyroblasts up to 4 mm across overgrow the muscovite fabric, and fine-grained, randomly oriented prisms of chloritoid are present in some sections	The schist is interpreted as variably deformed, subaqueous, volcaniclastic siltstone, metasandstone, and minor breccia, and may include some subaqueously deposited pyroclastic flows	The schist contains relict lenses of dense, grey, silicified volcanic rock with abundant disseminated pyrite. Pyrite is present only in minor or trace amounts in the sericitic schist. The schist also encloses some elongate quartz–chlorite–pyrite aggregates that are interpreted as deformed veinlets. The presence of andalusite and chloritoid in the section between 118 and 267 m suggests an early phase of alkali leaching, possibly associated with the quartz–pyrite alteration. There is little or no carbonate in this unit
Felsic schist after quartz-phyric volcaniclastic rock	This unit is similar to the schistose aphyric felsic volcaniclastic unit, but contains unflattened, angular crystal fragments of ß-quartz up to 3 mm across. Some of these crystal fragments appear to be incorporated within elongate rhyolitic or dacitic clasts	The schist is interpreted as variably deformed, subaqueous, volcaniclastic siltstone, metasandstone, and minor breccia	This unit displays the same alteration characteristics as the metamorphosed aphyric felsic volcaniclastic unit
Metamorphosed felsic hyaloclastite unit	This unit is a massive to brecciated, siliceous rock in which angular to subangular clasts of felsic volcanic rock (≤3 mm) commonly display a jig-saw fit structure and grade into massive but fractured felsic volcanic rock (?dacite). Prismatic pseudomorphs (≤1 mm) of quartz, chlorite, and carbonate (?after hornblende) constitute up to 5% of the rock. The unit is unbedded	This unit is a subaqueous lava, with extensive brecciation attributed to the shattering effect of contact with cold seawater	The unit contains several percent disseminated pyrite and deformed quartz–pyrite veinlets, except where subsequent sericitization has remobilized the sulfides. Between 296 and 314 m, a later generation of quartz-rich quartz–pyrite veinlets cuts the earlier generation of veinlets and the sericitic schist. These veinlets are accompanied by thin (1–3 mm) selvages of bleaching and up to 10% disseminated carbonate

All of the above units are variably deformed. A deformation fabric is defined by oriented and flattened lithic clasts and the preferred orientation of muscovite in discontinuous, anastomosing seams. Intensely deformed sections are altered to quartz–sericite schist

Table 1.1 (continued)

Rock unit	*Lithology and petrography*	*Interpretation*	*Alteration*
Meta-andesite	This unit is a fine- to medium-grained, mesocratic to melanocratic rock with a poorly preserved volcaniclastic structure, with lithic clasts (≤1 mm) and minor quartz-crystal fragments within a quartz–plagioclase–chlorite matrix. The matrix contains about 40% chlorite and accessory leucoxene. Most of this unit is unbedded, but the deepest, thickest part grades uphole (?upwards) from a massive, crystalline rock, through a section that contains 5–10% lithic clasts (≤3 mm) and rare quartz-crystal fragments, to a very fine grained sediment at 339 m	The meta-andesite is interpreted as a subaqueous mass-flow deposit from pyroclastic eruptions of an andesitic volcanic vent. The rock may have been deposited directly, or by slumping of earlier pyroclastic deposits derived from a shallower or subaerial eruptive centre	The meta-andesite contains 30–40% secondary carbonate in the form of disseminations and irregular aggregates. Discontinuous chloritic foliae define a weak foliation. There is little or no sericite and only minor pyrite. The thick unit between 319 and 394 m is cut by several late-tectonic quartz–carbonate(–chlorite) veins (≤4 cm wide) with 'bleached' (?carbonated, silicified) alteration selvages up to 2 cm wide. Veins are especially common between 367 and 368 m and between 384 and 388 m
Metaporphyry	This metamorphosed massive, pink quartz–plagioclase porphyry comprises 25% subhedral plagioclase (≤2 mm), 5% rounded phenocrysts of quartz (≤3 mm), and minor (altered) biotite phenocrysts (~1 mm) in a very fine grained quartzofeldspathic groundmass. Minor muscovite and biotite form a weak fabric defined by fine-scale, anastomosing seams. Ilmenite is an accessory phase	This metaporphyry is interpreted as a subvolcanic intrusion	Approximately 15% secondary carbonate forms irregular disseminations and larger aggregates. Trace pyrite is present throughout the unit, and there are some irregularly distributed quartz–carbonate veins

IRO37 15.12.03

Figure 1.6. Gordon Sirdar openpit mine, looking south. The dark unit in the centre of the pit wall is the mineralized metamorphosed hyaloclastite unit. Gold associated with disseminated and veinlet pyrite was mined mainly from the contact zones of this unit

Structure: Moderately deep, historic workings have been developed over about 750 m, on a subvertical, north-northwesterly striking (140–145°) brittle–ductile shear zone. This mineralized shear is not well exposed, but most mine dumps contain mafic to felsic schist and abundant vein quartz. Veins in the chloritic schist range from less than 1 mm to about 30 cm in width. They are boudinaged and ptygmatically folded. Mine-dump samples therefore suggest that mineralization is in a brittle–ductile shear zone located on or near a contact between metamorphosed felsic volcaniclastic rock and mafic rock. The northernmost workings on this line have focused on a north-trending fault.

Alteration: The mafic host rock is deformed and altered to chlorite–carbonate–plagioclase schist. Mineralization is associated with veined and hydraulically fractured, 'bleached' rock containing sericite and pyrite in addition to chlorite, carbonate, and plagioclase. Quartz veins contain minor ankerite and pyrite.

Kanowna North Star

Other names: Sulphide Monster Lode, Advance Australia Prospectors Ltd

Coordinates: 30°28'14"S, 121°33'09"E

Production: 345.4 t of ore for 9.12 kg Au (26.4 g/t Au) between 1900 and 1903.

Host rock: Mine workings are within a mafic volcanic sequence that contains metamorphosed thin interflow sedimentary units and has been intruded by felsic porphyry dykes. The main host rock appears to be felsic (?volcaniclastic) rock.

Structure: Shallow workings are developed over an area of about 300 × 500 m. Mineralized veins within this area have a wide range of orientations, but most strike between 140° and 220° and dip steeply to about 60°E. Stockwork veining is exposed in a small, exploratory pit and on mine dumps. The veins are up to about 1 m wide, but are mostly less than 20 cm. They include white buck quartz and massive to banded, fine-grained, grey veins with a cherty appearance. The latter may include interflow sedimentary units (?exhalites). Cherty, grey, banded rocks exposed at the surface display minor D_2 folds that plunge 20–30°S (Fig. 1.9). Many veins contain massive to banded pyrite or limonite after sulfides. Veins exposed in exploratory costeans are strongly deformed in isolated zones of ductile deformation.

Alteration: Samples from deeper workings indicate the widespread presence of disseminated pyrite in felsic units. More-restricted, centimetre-scale selvages of 'bleaching' (?silicification) are adjacent to quartz veins. Banded quartz–pyrite rocks may be strongly silicified volcanogenic exhalites. The one sample that was examined in polished thin section contained abundant fine-grained tourmaline.

Koh-I-Nor Leases

Other names: Golden Rainbow

Coordinates: 30°28'52"S, 121°33'14"E

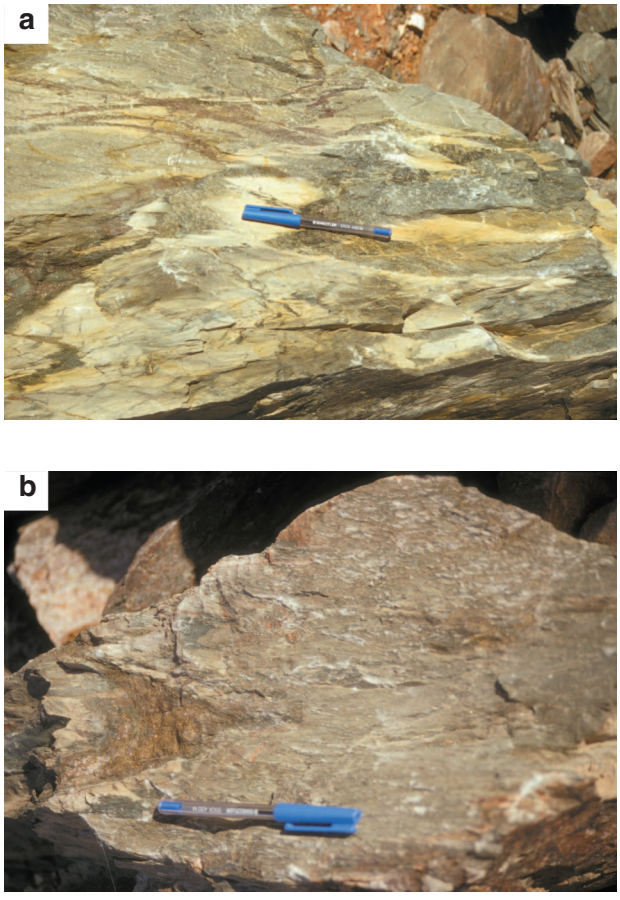

IRO38 15.12.03

Figure 1.7 Metamorphosed felsic hyaloclastite unit, Gordon Sirdar mine, showing: a) stockwork of deformed pyrite-rich veinlets; b) a folded pyrite-rich vein

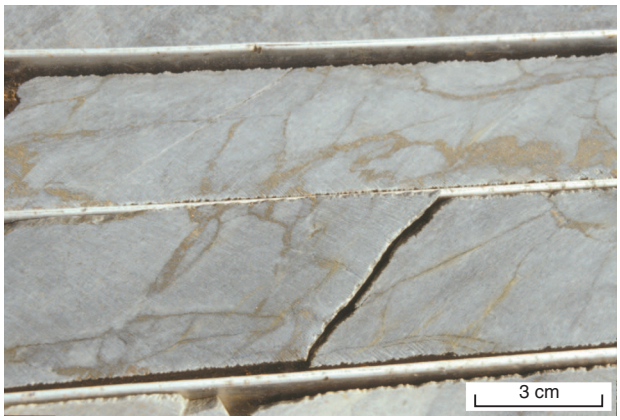

IRO40 15.12.03

Figure 1.8. Stockwork of pyrite-rich veinlets in the undeformed interior of the metamorphosed felsic hyaloclastite unit, Gordon Sirdar mine area

Production: 349.3 t of ore for 6.65 kg Au (19.0 g/t Au) between 1898 and 1903.

Host rock: The original nature of the host rock is unclear, but mine-dump samples suggest a deformed and altered meta-andesite or metamorphosed basaltic andesite.

Structure: Shallow workings on a metre-wide brittle–ductile shear zone extend over about 150 m strike length. The shear zone strikes 320° and dips 70°SW, but is not well exposed.

Alteration: Mine dumps are dominated by chloritic schist with quartz–sericite–pyrite veins.

Palm

Other names: Edith, Moorilla, Phoenix Gold Mines Ltd, Band of Hope North-West, Lady Pratt, Hit or Miss South, Mount Jewell

Coordinates: 30°22'55"S, 121°31'02"E

Production: 6367.0 t of ore for 108.23 kg Au (17.0 g/t Au) between 1897 and 1923. An additional 34.95 kg Au was produced from dollied and alluvial sources. Modern production (post-1988) from the Palm openpit mine amounts to 452.80 kg Au from 142 225 t of ore (3.2 g/t Au).

Host rock: Gold is related to quartz veins that are more or less confined to a strongly carbonated ultramafic rock (metakomatiite). This host unit contains about 80% carbonate in contrast to adjacent units of talc–carbonate–chlorite schist, which contain only 20–30% carbonate. A 1 m-wide albitite dyke within the carbonated unit strikes about 150°, parallel to primary layering (S_0), but does not appear to be a major host rock.

Structure: The openpit mine exposes a carbonate-rich unit that contains sheeted, steeply dipping to vertical quartz veins, up to 10 cm thick, that strike 060–080°. They are offset by several faults and fractures that dip about 40°N. The drag of the quartz veins indicates reverse movement across these structures. The sheeted veins are in packages up to about 10 m wide with a vein density of about one per metre. A second, minor set of quartz veins, striking 135° and dipping 70°NE, is exposed near the albitite dyke in the eastern wall of the openpit.

Alteration: No visible alteration was observed adjacent to the quartz veins, other than the widespread, intense carbonation that probably pre-dated vein formation.

Gem

Other names: Valentine

Coordinates: 30°23'05"S, 121°30'35"E

Production: 386.6 t of ore for 13.12 kg Au (33.9 g/t Au) between 1912 and 1915.

Host rock: Metabasalt.

Structure: Some moderately deep stopes and a deep shaft access a poorly exposed structure that strikes 150° and dips 50°W. Quartz veining is common in mine-dump samples, but there is little evidence of ductile deformation. The orebody is probably a tabular zone of veining and brecciation on or close to the contact between mafic and ultramafic rocks. Veins exposed in the hangingwall strike 210° and dip 55°W, suggesting dextral movement on the main structure.

Alteration: Altered mine-dump samples are 'bleached' and contain chlorite–carbonate–sericite with minor quartz and disseminated pyrite. The altered samples contain numerous quartz–ankerite–pyrite veins and veinlets.

Lady Clara

Other names: Dickens Custer Mines Ltd

Coordinates: 30°22'20"S, 121°29'54"E

Production: 203.2 t of ore for 8.89 kg Au (43.7 g/t Au) between 1901 and 1912.

IRO41 15.12.03

Figure 1.9. Folded metamorphosed cherty sedimentary unit (?volcanogenic exhalite) from the North Kanowna Star mine area

Host rock: Strongly carbonated mafic rock and schist.

Structure: There are several shafts and historic shallow opencuts over an area of about 300 × 50 m. The workings expose thick, subvertical quartz veins (one to several metres wide) that strike 290° and 130°. The thick quartz veins are associated with sheeted quartz veins in zones up to about 50 m wide. The 290°-striking vein exposed in the main historic pit dips about 70°N. Slickensides on this vein plunge 60°N. Sheeted quartz veins in the hangingwall strike 210° and dip 70°NW. Rotation of these veins near their junction with the 290°-striking veins suggest they formed as a result of sinistral displacement across the latter.

Alteration: The mafic rock that contains the quartz veins is altered to chlorite–carbonate rock and schist. More-intense alteration selvages adjacent to quartz veins have not been recognized.

References

FELDTMANN, F. R., 1917, Contribution to the study of the geology and ore deposits of Kalgoorlie, East Coolgardie Goldfield, Part III. The north end of Kalgoorlie: Western Australia Geological Survey, Bulletin 69, p. 92–95.

GALLEY, A. G., 1995, Target vectoring using lithogeochemistry: applications to the exploration for volcanic-hosted massive sulphide deposits: Canadian Institute of Mining and Metallurgy, Bulletin, v. 88, p. 15–27.

GARNER, T. A., 1996, Geological study of the felsic volcaniclastic rocks of the Gordon–Sirdar project area, Western Australia: United Kingdom, Camborne School of Mines, University of Exeter, MSc thesis (unpublished).

HEDENQUIST, J. W., MATSUHISA, Y., IZAWA, E., WHITE, N. C., GIGGENBACH, W. F., and OAKI, M., 1994, Geology, geochemistry, and origin of high sulfidation Cu-Au mineralization in the Nansatsu district, Japan: Economic Geology, v. 89, p. 1–30.

KERR, D. J., and GIBSON, H. L., 1993, A comparison of the Horne volcanogenic massive sulfide deposit and intracauldron deposits on the mine sequence, Noranda, Quebec: Economic Geology, v. 88, p. 1419–1442.

LARGE, R. R., 1992, Australian volcanic-hosted massive sulphide deposits: features, styles and genetic models: Economic Geology, v. 87, p. 471–510.

LARSEN, J. E., and HUTCHINSON, R. W., 1993, The Selbaie Zn–Cu–Ag deposits, Quebec, Canada: an example of evolution from subaqeous to subaerial volcanism and mineralization in an Archean caldera environment: Economic Geology, v. 88, p. 1460–1482.

ROBERTS, F. I., and WITT, W. K., 2002, Compilation of whole-rock geochemical data for the Gordon area, Eastern Goldfields: Western Australia Geological Survey, Record 2002/13, 28p.

SKIRROW, R. G., and FRANKLIN, J. M., 1994, Silicification and metal leaching in semiconformable alteration beneath the Chisel Lake massive sulfide deposit, Manitoba: Economic Geology, v. 89, p. 31–50.

SWAGER, C. P., 1997, Tectono-stratigraphy of late Archaean greenstone terranes in the southern Eastern Goldfields, Western Australia: Precambrian Research, v. 83, p. 11–42.

SWAGER, C. P., and GRIFFIN, T. J., 1990, An early thrust duplex in the Kalgoorlie–Kambalda greenstone belt, Eastern Goldfields Province, Western Australia: Precambrian Research, v. 48, p. 63–73.

WITT, W. K., 1990, The geology of the Bardoc 1:100 000 sheet, Western Australia: Western Australia Geological Survey, Record 1990/14, 111p.

2. Pennyweight Point – Yundamindera

The Pennyweight Point – Yundamindera mining area lies within the Mulgabbie domain of the Kurnalpi Terrane of Swager (1997). Geologically, the area is dominated by two granite intrusions, which include two or more petrographically distinct phases. The earliest granite intrusion is poorly exposed, but was described by Hallberg (1985) as a hornblende granodiorite containing minor biotite. This unit hosts the gold mineralization in the Yundamindera mining area, but most samples collected from mine dumps contain very little K-feldspar and are here referred to as metatonalite. Samples from the southern part of the mining area contain less quartz, and the host rock at Boer is classified as a diorite or quartz diorite. The metatonalite body has a very irregular shape and the northern part of the unit displays a striking aeromagnetic pattern, which suggests multiple phases. The metatonalite is intruded by a circular to ovoid porphyritic biotite–hornblende monzogranite to the west. A thin screen of amphibolite enclaves remains between the two intrusions in the Yundamindera mining area. The western margin of the metatonalite intrusion has been offset dextrally by late, north-northeasterly trending faults (Fig. 2.1).

The Pennyweight Point mining area has produced a little over 100 kg of gold, mainly from the AWA and Highland Chief mines (68 kg Au), but the greater production has come from the Yundamindera mining area, which has produced over 1500 kg Au. Most of this production took place in the early 1900s at Potosi, Maori Queen, and Queen of the May.

Host rocks in the Pennyweight Point mining area are metabasalt and amphibolite, with only some of the smaller mines hosted by the metatonalite. Most of the larger mines (Problem, AWA, Highland Chief), and some of the smaller ones, appear to be spatially related to a curvilinear fault that is subparallel to the contact between greenstones and metatonalite to the north. The attitude of this fault is unknown, but to the west, minimal displacement on the contact between the mafic units and the metatonalite suggests mainly subvertical displacement. The fault cuts and offsets numerous porphyry dykes that are genetically related to the metatonalite intrusion (Hallberg and Wilson, 1983). A series of late, north-northwesterly trending faults, interpreted from aeromagnetic data, cut the metatonalite and project towards the main mining area. The main mines are near where these fault projections intersect the curvilinear fault, which suggests these faults may be another element of structural control.

Tonalitic and dioritic rocks of the earlier intrusion host gold in the Yundamindera mining area. The mine workings extend for about 7 km along the western margin of the unit (Fig. 2.1). Most of the orebodies are in a series of northwesterly to north-northwesterly trending shear zones that dip 40–60°NE. North-northwesterly trending structures are mainly in the southern part of the mining area and are not well exposed, but where in situ observations could be made, linear fabrics plunge steeply, either down-dip or steeply to the north-northeast on north-northwesterly trending shears. Microstructural observations on oriented samples from Landed at Last North Extended, and S–C fabrics at Boer, indicate reverse movement, consistent with east–west compression. Moderate to intense ductile deformation in the shear zones has converted the tonalitic and dioritic rocks to a fine- to medium-grained quartzofeldspathic gneiss, and associated veins are variably folded and disrupted by the shear fabric. Additionally, there are some relatively late, transgressive veins and veinlets.

Alteration assemblages in both mining areas indicate high-temperature hydrothermal activity. Representative mineral analyses are shown in Tables 2.1 to 2.6 and are plotted in Figures 2.2 and 2.3. Altered mafic rocks at AWA and Highland Chief contain clinopyroxene, plagioclase, amphibole, titanite, and minor K-feldspar. These assemblages indicate alteration temperatures in excess of 550°C (Witt, 1991). However, there has been extensive retrograde alteration to epidote, sericite, chlorite, carbonate, and prehnite. In the Yundamindera deposits, calc-silicate alteration, evident from quartz–plagioclase–titanite(– calcic amphibole –epidote–biotite–carbonate–K-feldspar) assemblage, in mineralized shears is associated with deformed quartz–clinopyroxene veins. A typical alteration-zoning scheme is summarized in Table 2.7. Compared to the least-altered and undeformed metatonalite host rock at Maori Queen, calc-silicate alteration assemblages at Maori Queen and Boer contain amphiboles that have higher alkali contents, higher Mg/Mg+Fe ratios and lower amounts of SiO_2 (Fig. 2.2). Compositional differences between least-altered metatonalite and altered metatonalite for plagioclase and biotite are not as clear. Plagioclase in least-altered metatonalite is strongly zoned, whereas metasomatic plagioclase appears to display a more limited compositional range (Table 2.1).

The main chemical changes in mineralized calc-silicate shears are the addition of SiO_2 and, to a lesser extent, S. Na_2O, CaO, Fe_2O_3, MgO, and K_2O are commonly added to the calc-silicate lodes, but most chemical components are depleted in very intensely deformed shear centres, which are zones of extreme SiO_2 enrichment. Although minor calcite is a common component of the lode systems, addition of CO_2 to the host rocks is much less significant than in most Archaean lode-gold deposits (Barley et al., 1990; Witt, 1993).

Late-stage veinlets and fractures are associated with retrograde prehnite, carbonate, K-feldspar (adularia), and hematite. The main sulfide mineral in both mining areas is pyrite. Pyrite is closely associated with calc-silicate alteration and veins, but less consistently associated with retrograde hydrothermal activity.

The calc-silicate alteration assemblages at Pennyweight Point and Yundamindera are somewhat unusual for Archaean lode-gold deposits, but have possible analogues at Three Mile Hill, Coolgardie (Knight et al., 1997), and Karonie (this Report). Similar assemblages

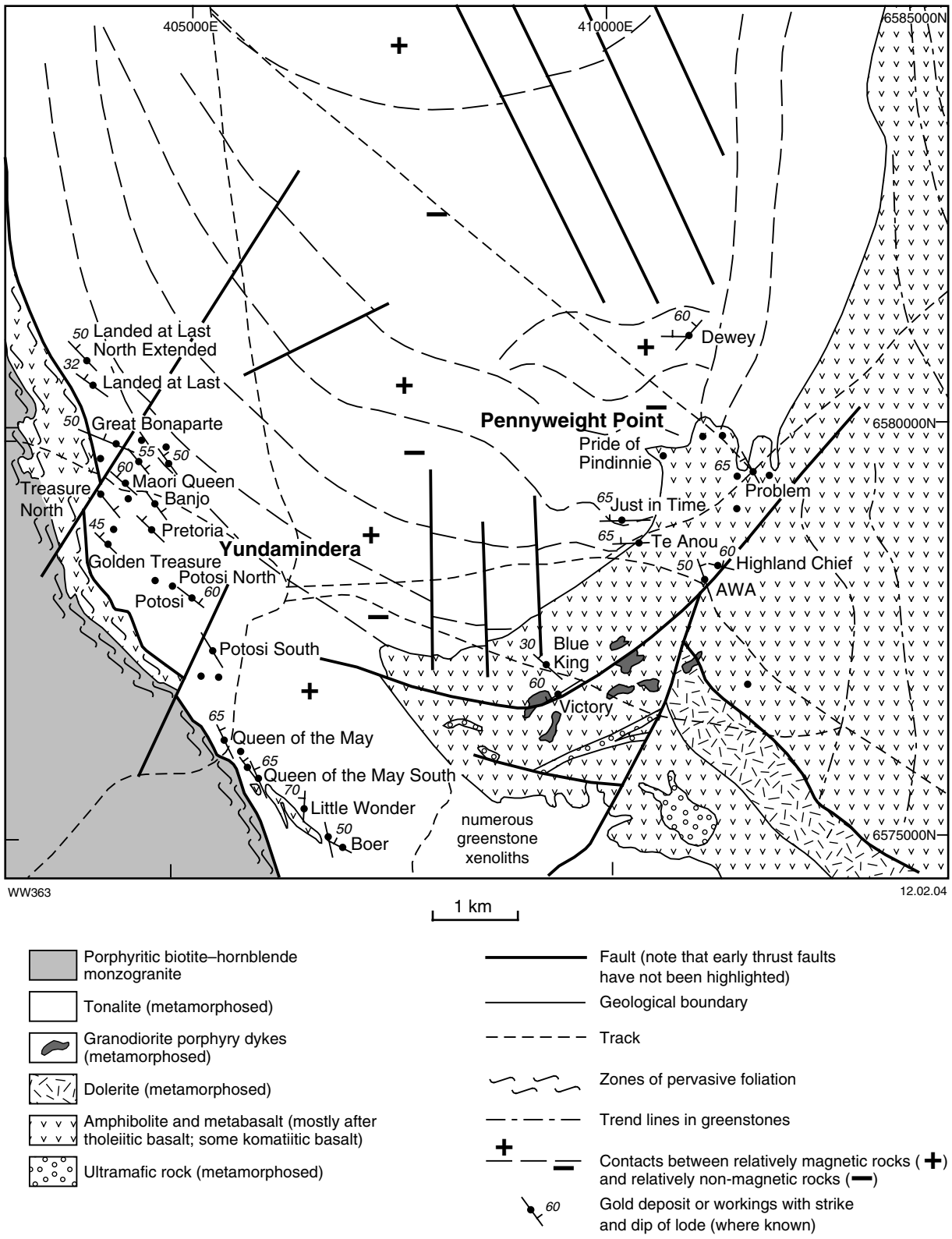

Figure 2.1. Geological map of the Pennyweight Point and Yundamindera mining areas, showing the location and nature of gold deposits (based on regional maps and aeromagnetic data)

Table 2.1. Analyses of plagioclase, Yundamindera mining centre

	GSWA 119978								*GSWA 119984*						*GSWA 132907*								
	least-altered metatonalite, Maori Queen								*calc-silicate lode, Maori Queen*						*calc-silicate lode, Boer*								
	core	*intermediate*			*margin*			*rim*	*margin of qtz–cpx vein*		*altered wallrock (qtz–pl–amp–bt)*				*margin of complex calc-silicate vein*				*altered wallrock (pl–amp–ep)*				
	P3	*P5*	*P12*	*P13*	*P6*	*P17*	*P15*	*P8*	*P23*	*P24*	*P26*	*P27*	*P28*	*P30*	*FP2*	*FP3*	*FP5*	*FP7*	*FP8*	*FP9*	*FP10*	*FP12*	*FP13*
SiO_2	59.23	59.95	61.50	61.86	61.83	59.50	66.32	60.11	63.30	61.58	61.98	62.02	63.80	63.41	62.91	61.86	60.38	59.21	58.71	62.44	60.57	62.99	62.14
Al_2O_3	24.60	25.90	24.41	24.57	25.08	25.99	20.84	25.32	23.15	23.87	23.15	24.17	23.05	22.32	23.02	24.22	24.73	24.99	25.55	23.43	23.38	22.92	23.34
CaO	6.92	8.06	6.19	6.01	1.81	8.20	1.64	7.34	4.69	5.65	5.09	5.83	4.38	4.17	4.49	5.77	6.85	7.26	7.88	5.16	6.30	4.73	5.29
Na_2O	7.42	7.17	8.38	7.99	7.48	7.17	10.44	7.42	8.85	8.37	8.52	8.32	9.06	9.13	9.37	8.25	7.58	7.09	7.00	8.78	8.30	8.90	8.42
K_2O	–	–	0.18	–	2.66	–	0.15	0.08	–	–	0.15	0.09	0.09	–	0.07	–	0.08	0.18	0.13	0.16	0.12	0.09	0.16
Total	**98.16**	**101.08**	**100.67**	**100.43**	**98.96**	**100.85**	**99.38**	**100.28**	**100.00**	**99.47**	**98.90**	**100.58**	**100.38**	**99.03**	**99.87**	**100.09**	**99.62**	**98.73**	**99.28**	**99.98**	**98.67**	**99.63**	**99.35**
An	34.0	38.3	28.7	29.4	9.8	38.7	7.9	35.2	22.7	27.2	24.6	27.8	21.0	20.1	20.9	27.9	33.1	35.8	38.1	24.3	29.3	22.6	25.5
Ab	66.0	61.7	70.3	70.6	73.1	61.3	91.2	64.3	77.3	72.8	74.8	71.7	78.5	79.9	78.7	72.1	66.4	63.2	61.1	74.8	70.0	76.9	73.6
Or	–	–	1.0	–	17.1	–	0.9	0.5	–	–	0.9	0.5	0.5	–	0.4	–	0.5	1.0	0.8	0.9	0.6	0.5	0.9

NOTES: Analyses of mineral phases were carried out using a JEOL 6400 scanning electron microscope (SEM) at the Centre of Electron Microscopy, University of Western Australia. Analytical conditions are described in Appendix 7
Analyses with K_2O have probably been influenced by minor sericitization of the plagioclase
qtz: quartz cpx: clinopyroxene pl: plagioclaise
amp: amphibole bt: biotite ep: epidote

Table 2.2. Analyses of amphiboles, Yundamindera mining centre

	GSWA 119978					*GSWA 119984*		*GSWA 119984*				*GSWA 132907*			
	least-altered metatonalite, MaoriQueen					*calc-silicate lode, Maori Queen*		*calc-silicate lode, Maori Queen*				*calc-silicate lode, Boer*			
				hornblende clot		*adjacent to complex calc-silicate vein*		*altered wallrock (qtz–pl–amp–bt)*				*thin amphibole selvage to clinopyroxene band in complex calc-silicate vein*		*altered wallrock (pl–amp–ep)*	
	AM2	AM4	AM6	AM7	AM8	AM11	AM12	AM14	AM15	AM18	AM19	HB1	HB4	HB6	HB9
SiO_2	48.49	47.78	47.65	52.93	52.59	53.64	44.69	46.99	40.75	46.18	49.32	45.45	39.42	44.64	40.7
TiO_2	0.87	1.23	0.40	–	0.15	0.14	0.45	0.23	0.89	0.51	0.24	0.26	1.14	0.75	1.34
Al_2O_3	6.14	6.60	7.22	2.28	2.95	2.21	8.94	7.46	12.00	8.60	5.66	8.17	13.21	9.75	11.32
Cr_2O_3	–	–	–	0.13	0.23	–	0.16	0.13	0.45	–	–	–	–	–	–
FeO	17.25	17.37	17.56	14.29	14.48	13.97	19.15	16.29	19.60	15.45	13.07	20.29	20.76	18.80	20.18
MnO	0.29	0.44	0.25	0.46	0.37	0.47	0.37	0.53	0.44	0.59	0.43	0.48	0.46	0.50	0.45
MgO	11.86	11.81	11.46	14.91	14.47	15.03	10.54	12.12	8.52	12.22	14.31	9.65	7.44	9.51	8.13
CaO	11.79	11.32	12.16	12.17	11.97	12.98	12.22	12.50	11.76	12.45	12.36	12.15	12.01	12.14	11.90
Na_2O	1.03	1.07	1.16	0.62	0.62	0.37	1.11	0.91	1.31	1.16	0.76	0.99	1.41	1.03	1.19
K_2O	0.26	0.26	0.37	0.07	–	0.07	0.89	0.69	1.61	0.78	0.44	0.66	1.83	1.06	1.52
Total	**97.98**	**97.88**	**98.24**	**97.87**	**97.82**	**98.88**	**98.52**	**97.86**	**97.33**	**97.93**	**96.59**	**98.11**	**97.68**	**98.18**	**96.72**
Fe/Fe+Mg	44.9	45.2	46.2	35.0	36.0	34.3	50.5	43.0	56.3	41.5	33.9	54.1	61.0	52.6	58.2
Si/Al	6.70	6.14	5.60	19.7	15.14	20.64	4.24	5.34	2.88	4.56	7.39	4.72	2.53	3.88	3.05

NOTES: Amphiboles in sample GSWA 119978 are optically zoned, perhaps reflecting the presence of both igneous and metamorphic amphibole, but consistent compositional differences between margins and cores of amphibole grains could not be detected. The hornblende clot (an aggregate, about 5 mm across, of amphibole grains) appears to contain some chemically anomalous amphibole (high SiO_2, low FeO and Al_2O_3)

qtz: quartz pl: plagioclaise ep: epidote
amp: amphibole bt: biotite

Table 2.3. Analyses of micas and related phyllosilicates, Yundamindera mining centre

	GSWA 119978					*GSWA 119984*			*GSWA 132907*				
	least-altered metatonalite, Maori Queen					*calc-silicate lode, Maori Queen*			*calc-silicate lode, Boer*				
						altered wallrock (qtz–pl–amp–bt)			*ms–ep aggregates after pl in margin of complex calc-silicate vein*		*ms–ep aggregates after pl in altered wallrock (pl–amp–ep)*		
	BI1	*BI2*	*BI5*	*BI6*	*BI8*	*BI9*	*BI11*	*BI12*	*MS2*	*MS3*	*MS9*	*MS10*	*MS11*
SiO_2	35.22	33.61	35.40	33.66	30.37	36.43	31.39	37.54	47.61	49.80	45.50	45.99	46.60
TiO_2	2.22	1.96	2.18	3.65	1.55	1.07	0.74	1.00	0.18	–	–	0.61	0.13
Al_2O_3	16.50	16.57	16.36	16.19	17.13	16.40	16.37	16.60	32.05	28.40	31.38	30.34	31.81
Cr_2O_3	–	–	–	–	–	–	–	0.13	–	–	–	–	–
FeO	21.08	22.13	21.97	21.64	24.78	17.61	25.52	16.41	0.67	1.28	2.79	3.53	2.72
MnO	–	–		0.19	0.26	0.27	0.26	0.24	–	–	–	–	–
MgO	10.83	11.77	10.95	11.40	13.43	13.08	12.12	13.54	2.33	3.28	1.30	1.90	1.38
CaO	–	–	–	0.44	0.35	–	–	0.11					
K_2O	8.06	6.62	7.88	6.46	2.20	9.02	3.71	9.65	11.37	11.29	10.93	11.22	11.02
Total	**93.92**	**92.67**	**94.75**	**93.63**	**90.08**	**93.89**	**90.12**	**95.23**	**94.21**	**94.06**	**91.88**	**93.59**	**93.65**
Fe/Fe+Mg	58.0	51.3	53.0	51.6	50.9	43.0	54.1	40.5	–	–	–	–	–

NOTES: Samples designated BI are optically biotite, and those designated MS are optically muscovite, although some analyses indicate the minerals are partially altered to chlorite, illite, and other clay minerals
qtz: quartz cpx: clinopyroxene pl: plagioclaise ms: muscovite
amp: amphibole bt: biotite ep: epidote

Table 2.4. Clinopyroxene analyses, Yundamindera mining centre

	GSWA 119984 calc-silicate lode, Maori Queen					*GSWA 132907 calc-silicate lode, Boer*	
	margin of quartz–clinopyroxene vein					*cpx band in complex calc-silicate vein*	
	PX3	*PX4*	*PX5*	*PX6*	*PX8*	*DI3*	*DI4*
SiO_2	51.94	52.22	52.76	51.36	52.62	52.24	52.10
Al_2O_3	1.19	0.27	0.37	1.41	0.36	0.51	0.35
FeO	13.45	11.51	9.95	12.33	11.78	11.77	11.24
MnO	0.33	0.30	0.38	0.28	0.24	0.54	0.51
MgO	9.87	11.21	12.37	10.27	11.11	11.15	11.08
CaO	23.53	24.03	24.13	23.68	23.84	23.54	23.98
Na_2O	–	0.27	0.56	0.67	0.38	0.45	0.47
Total	**101.07**	**100.24**	**100.51**	**100.01**	**100.33**	**100.20**	**99.73**
Fs	22.0	18.5	15.8	20.2	19.0	19.0	18.2
En	28.7	32.1	35.0	30.0	31.9	32.1	32.0
Wo	49.3	49.4	49.1	49.8	49.2	48.8	49.8

NOTE: cpx: clinopyroxene

Table 2.5. Carbonate mineral analyses, Yundamindera mining centre

	GSWA 119984 calc-silicate lode, Maori Queen		*GSWA 132907 calc-silicate lode, Boer*	
	quartz–clinopyroxene vein		*carbonate veinlet in complex calc-silicate vein*	
	CB1	*CB2*	*CB1*	*CB3*
FeO	–	0.35	–	–
MnO	–	0.20	0.14	–
MgO	–	0.27	–	–
CaO	56.54	56.56	55.21	55.46
Total	**56.54**	**57.38**	**55.35**	**55.46**
$FeCO_3$	–	0.5	–	–
$MnCO_3$	–	0.3	0.2	–
$MgCO_3$	–	0.7	–	–
$CaCO_3$	100	98.6	99.8	100
Nomenclature	Calcite	Calcite	Calcite	Calcite

Table 2.6. Epidote mineral analyses, Yundamindera mining centre

	GSWA 132907 calc-silicate lode, Boer					
	replaces plagioclase in margin of complex calc-silicate vein				*replaces plagioclase*	
	EP2^m	*EP4*^{m}	*EP6*^{b}	*EP7*^{b}	*EP8*^{m}	*EP9*^{m}
SiO_2	39.01	38.54	43.16	43.51	38.23	38.33
TiO_2	–	0.15	1.58	–	–	–
Al_2O_3	27.77	27.13	22.60	24.23	25.11	27.98
FeO	6.81	7.59	0.53	0.19	9.98	6.22
MnO	0.15	–	–	–	–	–
MgO	0.22	–	–	–	–	–
CaO	24.36	24.41	27.24	27.46	24.25	24.20
Total	**98.40**	**98.38**	**95.11**	**95.39**	**97.56**	**96.72**

NOTES: m: associated with muscovite
b: associated with biotite

elsewhere, referred to as sodic–calcic alteration, have been ascribed to up-temperature flow of hydrothermal fluids in close proximity to granitoid intrusions (Dilles and Einaudi, 1992; DeJong and Williams, 1995). Phase-equilibria and fluid-inclusion studies have been used to estimate temperatures of 400–600°C for sodic–calcic alteration at Cloncurry, Coolgardie, and Nevada.

A full appreciation of the structural controls on gold mineralization in the Pennyweight Point and Yundamindera mining areas requires some discussion of the enigmatic aeromagnetic patterns in the metatonalite body (Fig. 2.1). They could be interpreted as a northward-migrating sequence of roughly circular intrusions. An alternative interpretation is that the overlapping magnetic patterns are caused by a series of low-angle thrust faults that have cut a circular pluton into several circular discs (Fig. 2.4). The direction of overlap suggests that thrusting displaced successively higher parts of the original pluton to the north. Weakly magnetic domains are interpreted as thrust faults that dip gently to the south and which are associated with hydrothermal alteration of igneous magnetite. The southern portion of the metatonalite unit represents a deeper part of the original intrusive body, and the re-entrant domain of greenstones that host mineralization in the Pennyweight Point area was structurally emplaced by normal-oblique faulting of the south-plunging intrusion. Isolated bodies of ultramafic rock within the greenstones south of the Pennyweight Point mining area may represent tectonic slices exposed where gently dipping thrust faults intersect the erosion surface.

Although north-directed thrusting presumably predated mineralization (which formed during late-tectonic east–west compression), one or more of these gently south dipping thrust faults may have played a role in localizing gold mineralization in both mining areas. In the Pennyweight Point mining area, the thrust faults could have provided a 'capping surface' that impeded upward flow of hydrothermal fluids through subvertical fractures related to the north-northwesterly trending faults and the curvilinear fault, leading to high fluid pressures

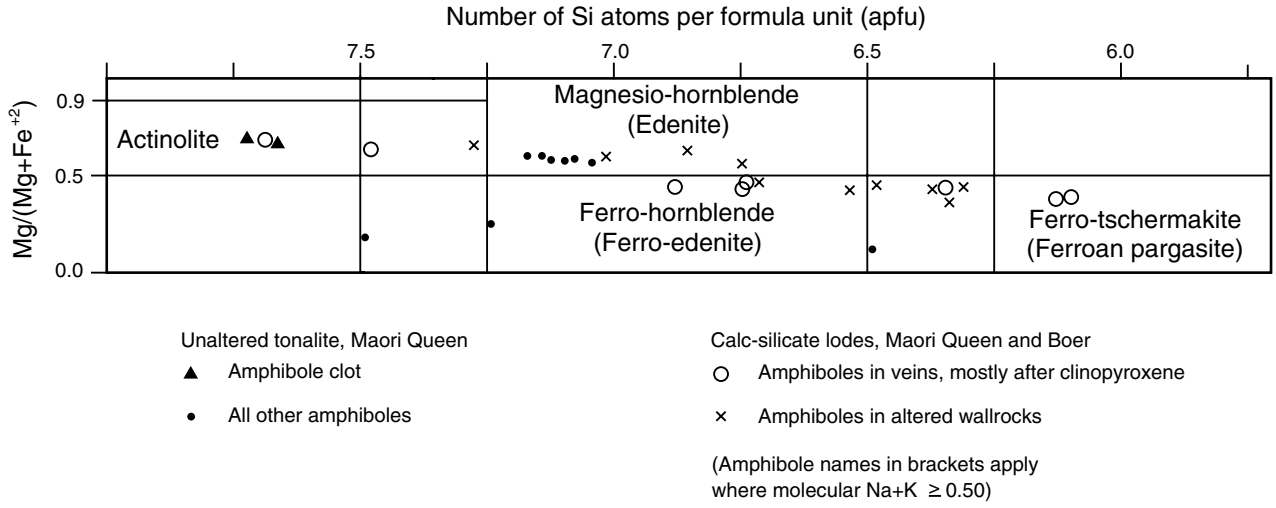

Figure 2.2. Composition of amphiboles in unaltered metatonalite and calc-silicate alteration assemblages, Yundamindera mining area (after Leake, 1978)

and hydraulic fracture of the mafic host rocks. At Yundamindera, the amphibolite screen and the margins of the porphyritic biotite–hornblende monzogranite both contain a strong and pervasive foliation oriented parallel to the contact with the metatonalite intrusion, and dipping about 70°ENE. Stretching lineations in the monzogranite are steep. These relationships suggest that the amphibolite screen and the metatonalite–monzogranite contact acted as a zone of reverse shear movement in response to east–west compression. Slightly less steep mineralized shears in the hangingwall metatonalite intrusion are second-order splays related to reverse movement on the contact zone. Low-angle thrust faults in the tonalitic intrusion could have acted as 'capping surfaces' and helped localize high fluid pressures, fluid flow, and mineralization within second-order shears.

The north–south contact zone in the Yundamindera mining area is oriented normal to the interpreted east–west far-field stress vector and is therefore ideally oriented for brittle failure in relatively competent bodies (Ridley, 1993). The competency contrast between amphibolite and

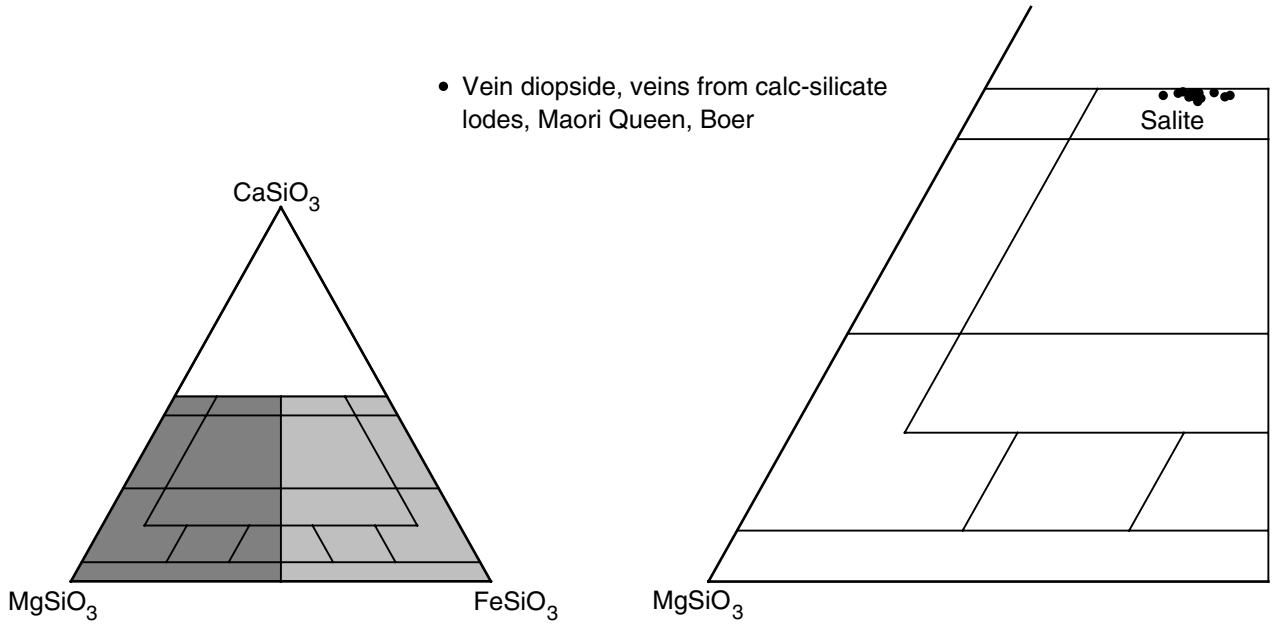

Figure 2.3. Composition of clinopyroxene in calc-silicate alteration assemblages, Yundamindera mining area

Table 2.7. Alteration zoning in mineralized dioritic rocks at Boer mine, Yundamindera mining area

Least-altered diorite	*Deformed diorite*	*Strong alteration (bleaching)*	*Pervasive alteration (bright white)*	*Calc-silicate veins*
QUARTZ	QUARTZ	QUARTZ	QUARTZ	QUARTZ
PLAGIOCLASE	PLAGIOCLASE	PLAGIOCLASE	PLAGIOCLASE	CPX (SALITE)
BIOTITE	BIOTITE	amphibole	microcline	AMPHIBOLE
AMPHIBOLE	AMPHIBOLE	biotite	epidote	epidote
ilmenite	titanite	epidote	pyrite	plagioclase
magnetite	pyrite	titanite	–	titanite
–	–	carbonate	–	rutile
–	–	pyrite	–	pyrite

NOTES: Minerals shown in upper case are essential minerals that commonly form more than 10% of the rock
Minerals shown in lower case are minor to accessory phases
CPX: clinopyroxene

metatonalite may have been a crucial factor in the localization of gold mineralization at Yundamindera (cf. Granny Smith; Ojala et al., 1993). The contact zone between metatonalite and greenstones changes orientation to the north and south of Yundamindera and is therefore less prospective. However, the eastern margin of the metatonalite intrusion is similarly oriented north–south and therefore offers a further exploration target.

The high temperatures during hydrothermal activity and gold deposition cannot be related to the tonalitic intrusion, which was deformed prior to mineralization, but are very likely related to late-tectonic emplacement of the porphyritic biotite–hornblende monzogranite. Contemporaneous fluids would have been drawn towards this hot body at depth and subsequently focused upwards along its contact zones (Furlong et al., 1991). Thus, the

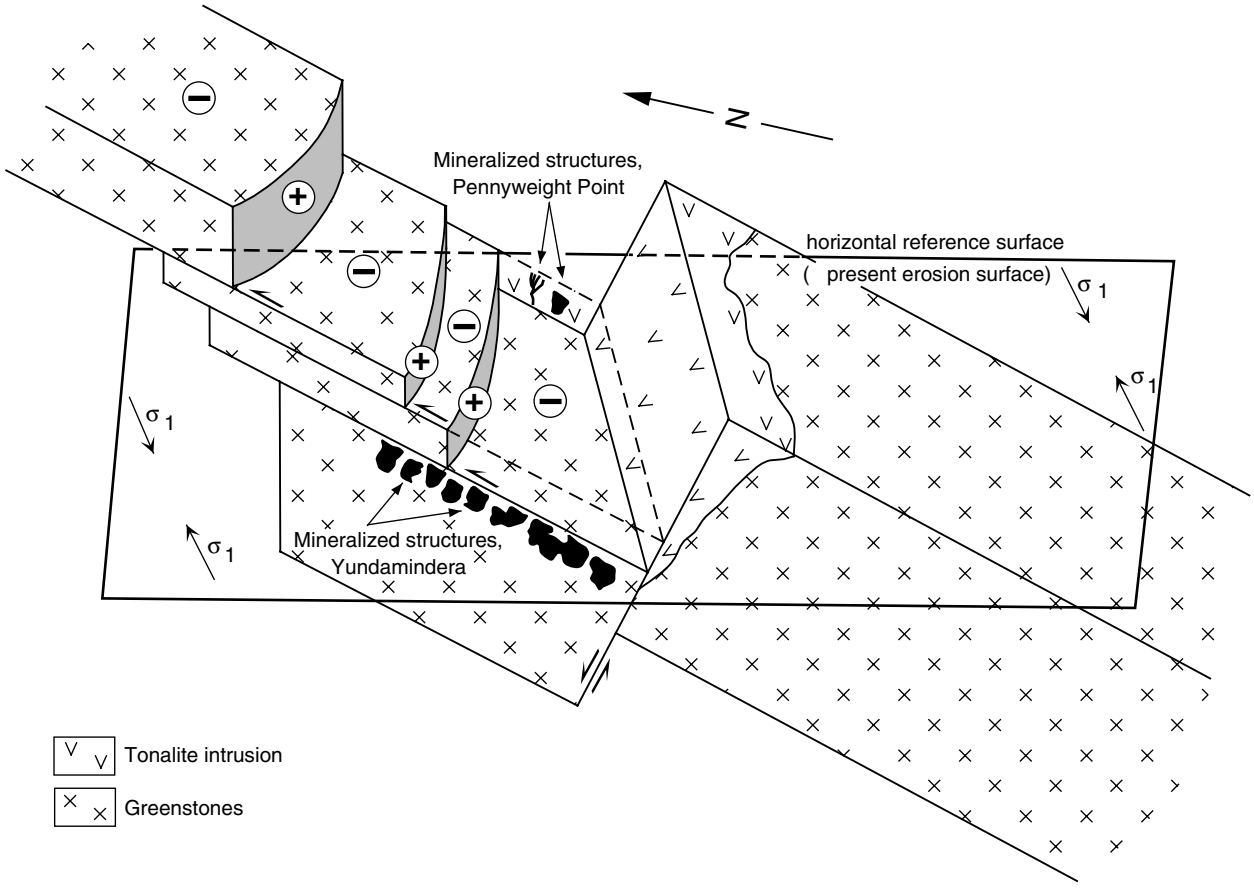

Figure 2.4. Interpreted geometry of the mineralized metatonalite intrusion at the Yundamindera mining area

Yundamindera gold deposits appear to have formed at a location where fluids were thermally, as well as structurally, focused.

There are two smaller mining centres (Larkins Find and Gardners Find) on or close to the north- to northwest-trending contacts of a third granite intrusion, which appears to have been emplaced after the tonalitic intrusion but before the porphyritic biotite–hornblende monzogranite to the west of Yundamindera. The deposits are hosted by mafic rocks, including amphibolite and metadolerite, and are mainly quartz veins in shear zones. Lamprophyre samples are present on some mine dumps at Larkins Find. The mineralized shears are mostly oriented parallel or subparallel to the granite contact and dip moderately to steeply east and northeast. Structural controls on gold mineralization at these localities are not clear, but mineralized structures may be related to brittle failure of competent units in and adjacent to a zone of high shear strain defined by closely spaced, north-trending faults. Foliation-controlled biotitization of the mafic host rocks characterizes altered wallrocks adjacent to veins in the Larkins Find area, whereas sericite and ankerite are more typical alteration minerals at Gardners Find. Numerous small garnet porphyroblasts are associated with biotitization of mafic rocks in one of the mines at Larkins Find.

Deposits of the Pennyweight Point – Yundamindera area

Dewey

Other names: George Washington, Washington

Coordinates: 29°26'30"S, 122°27'31"E

Production: 243.0 t of ore for 13.04 kg Au (53.7 g/t Au) between 1897 and 1900.

Host rock: Weathered granitoid rock.

Structure: Shallow workings are located on quartz veins that strike 040–050° and dip 50–70°NW, and easterly trending quartz veins that dip north. The veins are 20–50 cm wide and cut 120–150°-trending shear zones, which may be related to the north-northwesterly trending faults identified from aeromagnetic images (Fig. 2.1).

Alteration: Alteration is obscured by weathering.

References: Maitland (1903), Honman (1917), Mt Burgess Gold Mining Co. NL (1984).

Problem

Other names: Tucker Bag, Straight Mates Tucker Bag

Coordinates: 29°06'31"S, 122°05'34"E

Production: 280.4 t of ore for 4.70 kg Au, and 1.61 kg dollied gold, between 1900 and 1905.

Host rock: Mainly metabasalt with possible minor mineralization in porphyry dykes. Most workings are less than 15 m deep and do not penetrate the oxidized zone. There is some gold mineralization in the lateritic duricrust (to a depth of 15 m) and a further zone of gold enrichment (10–15 m thick) at the base of the weathering profile (up to 70 m below the surface). The intervening, kaolinitic saprolite is a zone of gold depletion. There are extensive alluvial workings in the vicinity of the pits and shafts.

Structure: Most workings are aligned on short (<50 m strike length), 330°-trending structures that dip 60–75°W and are up to 4 m wide. Several of these structures form an en echelon series that extends for about 120 m on a trend of about 050°. Linear fabrics within 330°-trending structures plunge 60° toward 248°, and ore shoots are steep. Relative proportions of weathered mafic schist and vein quartz on mine dumps suggest that the 330°-trending lodes are veined brittle–ductile shears. Several of these structures appear to be localized by contacts between porphyry dykes and metabasaltic country rocks. Quartz veins, up to 0.5 m wide, are mostly subparallel to shear-zone margins, but north-trending quartz-vein splays are present at the margins of some shear zones. Combined with a locally developed shear fabric (strike of 310°), the quartz-vein splays indicate a component of dextral movement on the 330°-trending structures, although steep linear fabrics imply predominantly reverse displacement.

A second style of mineralization is associated with a metre-wide quartz vein that strikes 030° and dips 30–35°W, located about 40 m south of the 330°-trending structures. The orientation of mineralized structures and related kinematic indicators at Problem are not consistent with formation during east–west compression.

Alteration: Weathered chlorite–carbonate schist is common on most mine dumps. Alteration includes silicification, potassic alteration (muscovite, biotite), and epidotization. Mineralization is associated with pyrite, quartz, and ankerite, but there are also minor amounts of pyrrhotite, chalcopyrite, arsenopyrite, ilmenite, rutile, sphalerite, molybdenite, native tellurium, and various unidentified Pb and Bi tellurides.

Just In Time

Other names: Queen of Sheba

Coordinates: 29°06'48"S, 121°04'39"E

Production: 749.8 t of ore for 16.33 kg Au (21.7 g/t Au) between 1901 and 1909.

Host rock: Coarse-grained amphibolite (?after leuco-gabbro).

Structure: Shallow to moderately deep pits and shafts trend easterly over a strike length of about 300 m. The mineralized structure is a 1–2 m-wide, veined brittle–ductile shear zone that dips 60–70°N and crosses the contact between metabasalt and granite. S–C fabrics identified locally within the mineralized shear suggest oblique sinistral-normal movement, but no linear fabrics have been recognized.

Alteration: Alteration is obscured by weathering.

References: Honman (1917).

AWA

Other names: Battles Ville, Bound-to-Rise, Highland Chief, General Cadorna, Wauchope

Coordinates: 29°07'08"S, 122°05'13"E

Production: 3319.2 t of ore for 68.62 kg Au (20.7 g/t Au) between 1897 and 1918.

Host rock: Metabasalt.

Structure: Moderately deep stopes and shafts in the AWA mine area lie on a 075° trend, but appear to access two or more subparallel, veined brittle–ductile shear zones that strike 330–350° and dip 40–60°E. These structures are several metres wide and are oriented at a large angle to the district-wide foliation (030–045°). The shear fabric is defined by a pervasive millimetre- to centimetre-scale banding in the central part of the shear zones, which, locally, is tightly folded. Locally observed S–C fabrics suggest a normal component (east side down) of movement. Quartz veins within the mineralized shears are up to 0.5 m wide and there has been some hydraulic brecciation. Mylonitization of some breccia samples attest to alternating periods of brittle and ductile deformation.

The Highland Chief deposit, about 250 m northeast of AWA, is on a structure that strikes 100° and dips 50–70°N. The mineralized structure is poorly exposed, but mine-dump samples suggest a similar type of lode to those at AWA.

Alteration: Gold is found mainly in quartz veins within 0.5 to 1 m-wide zones of bleaching in the central parts of the mineralized shears. These central zones of alteration contain a finely banded calc-silicate assemblage with several percent of disseminated and veinlet sulfides (pyrite and pyrrhotite). Individual bands consist of: subhedral prisms of clinopyroxene (0.5 – 1.0 mm) with interstitial chlorite and compositionally zoned plagioclase; fine-grained (≤0.1 mm) granoblastic quartz and plagioclase with coarser grained subhedral clinopyroxene; or massive, matted, medium-grained (about 0.5 mm) amphibole with up to about 20% plagioclase. All bands contain accessory titanite, and minor microcline K-feldspar has been observed in some samples. Chlorite exhibits anomalous brown interference colours, suggesting an iron-rich composition. Hydraulic breccias consist of amphibole-rich clasts in a matrix of quartz, plagioclase, and calcite. Mineralized shear centres are enveloped in a broader zone of foliated amphibolite with minor carbonate and disseminated pyrrhotite. Plagioclase is extensively replaced by epidote in this outer zone of amphibolite.

Mass-balance calculations, based on whole-rock geochemical data, indicate that the mineralized shear centre is characterized by extreme enrichment of SiO_2 and moderate enrichment of K_2O and S. CO_2 has not been added to the mineralized shear in significant amounts. FeO, CaO, and MgO display marked depletion (Fig. 2.5).

There is extensive, micro-scale, retrograde alteration of calc-silicate lodes, including sericitization of plagioclase, amphibolitization of clinopyroxene, and widespread epidotization. Some larger samples of quartz–muscovite–

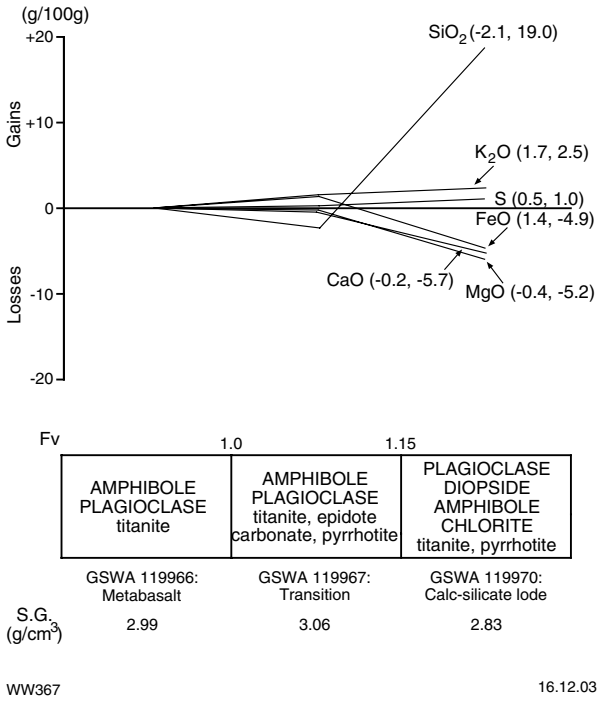

Figure 2.5. Mass-balance changes (calculated using the method of Gresens, 1967) associated with development of mineralized calc-silicate lode in metabasalt host rock, AWA mine, Pennyweight Point. Mineral components of alteration assemblages are listed in approximate order of abundance, with main mineral components in upper case and minor mineral components in lower case

chlorite–epidote schist and rock with disseminated and veinlet pyrite suggest that shearing and fracturing (with associated mineralization) persisted to lower temperatures than those at which calc-silicate alteration occurred. Late-stage chloritic microshears and veinlets of prehnite–chlorite–carbonate represent a further stage of retrograde alteration.

References: Maitland (1903), Honman (1917), Mt Burgess Gold Mining Co. NL (1984).

Landed at Last

Other names: Landed at Last Extended

Coordinates: 29°05'56"S, 122°00'56"E

Production: 4689.6 t of ore for 24.99 kg Au (5.3 g/t Au) between 1905 and 1943.

Host rock: Massive to weakly deformed, coarse-grained, metamorphosed biotite–hornblende tonalite.

Structure: The Landed at Last deposit is marked by shallow workings, which extend over about 50 m on a trend of 250°. The mineralized structure is poorly exposed, but was described by Maitland (1903) as a 1–2 m-wide, laminated quartz reef that strikes 305° and dips about

32°NE. Comparison with the similarly oriented structure at Landed at Last North Extended (see below) suggests that this may be a banded brittle–ductile shear zone (Witt, 1993).

More-substantial excavations have been carried out at Landed at Last North Extended, where a shear zone is exposed in an open stope. The shear zone strikes 315° and dips 40–60°N. The exposed shear zone is 1–2 m wide, but Mt Burgess Gold Mining Co. NL (1984) reported drill intersections of up to 7 m. Quartz veins are up to about 0.5 m wide and constitute about 50% by volume of the exposed shear. The veins and all planar fabrics are rotated parallel to the margins of the shear zone, and the structure is equivalent to the banded brittle–ductile shear zones of Witt (1993). Linear fabrics (?stretching lineation) plunge steeply. At the northwestern end of the stope, the shear zone offsets a steep 315°-trending fault zone, and associated drag indicates reverse movement on the mineralized shear. Reverse movement is supported, at a micro-scale, by asymmetric tails on feldspar porphyroclasts and extensional shear bands observed in oriented thin sections.

Alteration: The mineralized shear centre is a 1–2 m-wide, finely banded, medium-grained quartzofeldspathic gneiss with thin folia of muscovite. Primary ferromagnesian minerals in the host metatonalite are unstable and there is minor dusty hematite and trace tourmaline. This central zone of alteration is enveloped in a broader zone of quartz–sericite–chlorite schist.

References: Maitland (1903), Mt Burgess Gold Mining Co. NL (1984).

Great Bonaparte

Coordinates: 29°06'19"S, 122°00'59"E

Production: 499.9 t of ore for 7.10 kg Au (14.2 g/t Au) between 1908 and 1922.

Host rock: Massive to weakly deformed, coarse-grained, metamorphosed biotite–hornblende tonalite. Workings appear to be confined to the oxidized zone.

Structure: Shallow workings over 150–200 m access a shear zone that strikes 295° and dips 40–60°N. The exposed shear zone is 0.5 to 1 m wide, but exploration drilling has intersected widths of up to 3 m. The shear zone is not well exposed but appears to be a less ductile structure than that at Landed at Last, comprising quartz veins (≤10 cm wide) and anastomosing zones of strongly foliated and altered metatonalite. It is probably comparable to the veined brittle–ductile shear zones of Witt (1993).

There are also some smaller workings on associated structures (025°, 30–40°NW; and 335°, 30–40°NE).

Alteration: Alteration is obscured by weathering, but strongly foliated wallrocks are probably oxidized quartz(–feldspar)–muscovite schist.

References: Maitland (1903), Mt Burgess Gold Mining Co. NL (1984).

Treasure North

Other names: Big Stone, Kingfisher

Coordinates: 29°06'44"S, 122°00'46"E

Production: 2308.3 t of ore for 58.75 kg Au (25.4 g/t Au) between 1902 and 1924.

Host rock: Massive to weakly deformed, coarse-grained, metamorphosed biotite–hornblende tonalite.

Structure: Shallow to moderately deep workings trend 320° over a strike length of about 100 m. The mineralized structure is not well exposed, but the location of the main shaft indicates dip to the northeast. Mine dumps contain moderately to strongly foliated metatonalite and vein quartz.

Alteration: Alteration is unclear but mine-dump samples include weathered schist and quartzofeldspathic gneiss.

Maori Queen

Other names: Treasure East

Coordinates: 29°06'30"S, 122°00'54"E

Production: 2218.9 t of ore for 76.02 kg Au (34.3 g/t Au) between 1901 and 1910.

Host rock: Massive to weakly deformed, metamorphosed biotite–hornblende tonalite. Mine dumps contain two varieties: the coarse-grained metatonalite that is mineralized in other mines to the north, and a medium-grained variety that is the main host rock at this deposit.

Structure: Deep shafts and a collapsed stope access a veined shear zone that strikes 310° and dips 60°N. Maitland (1903) described the mineralized 'reef' as extending for more than 800 m in strike and having a width of up to almost 1 m. There are no good exposures of the mineralized structure, but mine dumps contain a mix of strongly foliated metatonalite and massive metatonalite with brittle fracturing and veining. Deformation in strongly foliated metatonalite samples is accompanied by dramatic grain-size reduction, and a pervasive fabric is defined by fine-scale mineral banding and oriented aggregates of biotite and amphibole. Veins in these samples are variably deformed. The pervasive foliation is axial planar to the open to tight folds defined by early veins. Late veins are markedly transgressive to the foliation. Breccia samples on mine dumps imply a small component of hydraulic brecciation. These observations suggest that the mineralized structure is a veined or banded brittle–ductile shear zone (Witt, 1993).

Alteration: Strongly foliated samples from the centre of the mineralized shear are fine- to medium-grained quartzofeldspathic gneiss after metatonalite. Amphibole and biotite are completely recrystallized and oriented parallel to the shear fabric, and ilmenite is altered to titanite. Deformation is accompanied by the introduction of minor amounts of epidote (up to 10%), carbonate, and pyrite. The amphibole in these strongly deformed (calc-silicate) rocks is characterized by higher Fe/Mg ratios and

alkali (Na_2O and K_2O) concentrations, and lower amounts of SiO_2, compared to the magnesiohornblende present in undeformed metatonalite (Fig. 2.2). Amphibole is replaced by biotite or colourless amphibole (?cummingtonite) in some strongly deformed and recrystallized samples. Pyrite is present as discontinuous veinlets (with biotite and/or chlorite) and fine, anhedral disseminations commonly arranged in elongate trails parallel to the shear fabric. Pyrite is the overwhelmingly dominant sulfide, but is accompanied by trace pyrrhotite (commonly as inclusions in pyrite) and chalcopyrite.

Early deformed veins and some later transgressive veins (up to several centimetres wide but generally thinner) contain quartz, clinopyroxene (salite), amphibole, pyrite, epidote, carbonate, and plagioclase. Most of these veins have quartz-rich cores and margins containing coarse (1–4 mm), subhedral prisms of clinopyroxene (Fig. 2.6). The green amphibole (ferro-edenite) generally appears to be secondary after clinopyroxene. The ferromagnesian minerals may be aligned in elongate aggregates, which are continuous with the foliation in the adjacent wallrocks. Many such veins have narrow (≤3 mm) halos of bleached wallrock in which amphibole is unstable. There is a strong correlation between the presence of quartz–clinopyroxene veins and the abundance of disseminated pyrite.

Late-stage veinlets with associated retrograde alteration are prehnite–carbonate and hematite-rich, untwinned feldspar (?adularia). Adjacent wallrocks may be hematitized for up to 1 cm from the adularia veinlets, with wider halos displaying patchy hematitization of feldspars. There is no apparent association of pyrite with these late-stage veins.

Mass-balance calculations, based on whole-rock geochemical data, indicate that the mineralized shear centres are characterized by large additions of SiO_2, and relatively minor Na_2O and S enrichment. These changes are accompanied by an increase in the Fe_2O_3/FeO ratio (Fig. 2.7). An increase in the Fe_2O_3/FeO ratio also accompanies late-stage hematitization, but this change in oxidation state is apparently not accompanied by other changes in the mass balance of chemical components (Fig. 2.8).

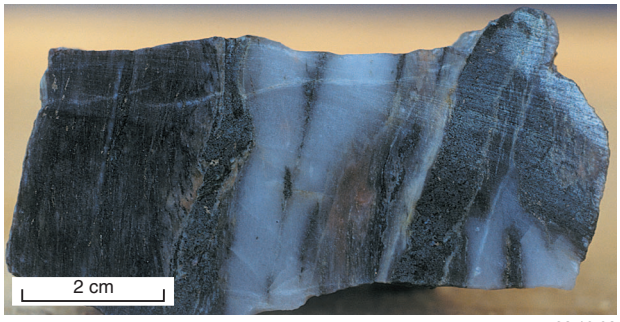

IRO67 23.10.03

Figure 2.6. Banded quartz–clinopyroxene vein (white and dark green, left) in deformed, altered tonalite (dark brown, right), Maori Queen mine, Yundamindera mining area

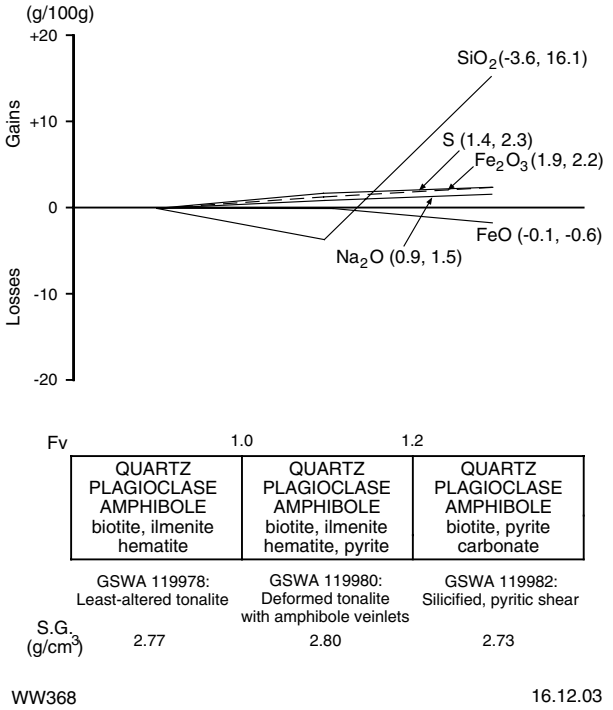

Figure 2.7. Mass-balance changes (calculated using the method of Gresens, 1967) associated with a silicified pyritic shear in metatonalite, Maori Queen mine, Yundamindera mining area. Mineral components of alteration assemblages are listed in approximate order of abundance, with main mineral components in upper case and minor mineral components in lower case

References: Maitland (1903), Honman (1917), Mt Burgess Gold Mining Co. NL (1984).

Golden Treasure

Other names: New Golden Treasure, Golden Treasure New Leases, Mahalah

Coordinates: 29°06'34"S, 122°01'16"E

Production: 2095.2 t of ore for 27.49 kg Au (13.1 g/t Au) between 1908 and 1945.

Host rock: Massive to weakly deformed, coarse-grained, metamorphosed biotite–hornblende tonalite.

Structure: Widespread workings are distributed on several associated structures. The main mineralized structure is oriented 315° and dips 40–50°NE. It is a 1–2 m-wide zone of strong ductile deformation containing 30–40% quartz veins (≤30 cm wide) that are all more or less parallel to the shear-zone margins. Stretching lineations plunge down-dip. To the southeast, the shear zone changes strike to 095° (dip 60°N) before resuming a 315° trend. This inflection, or 'dog-leg', plunges to the northeast, and the main production shaft lies on a bearing of 050° from where the point of inflection intersects the present erosion surface.

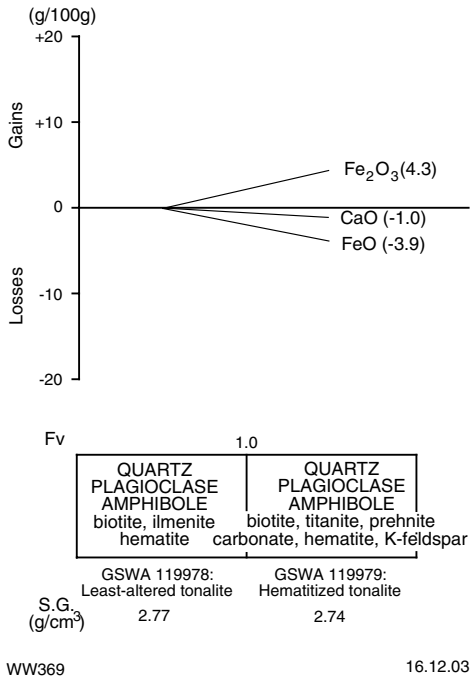

Figure 2.8. Mass-balance changes (calculated using the method of Gresens, 1967) associated with late-stage hematitization in metatonalite, Maori Queen mine, Yundamindera mining area. Mineral components of alteration assemblages are listed in approximate order of abundance, with main mineral components in upper case and minor mineral components in lower case

Other, smaller mineralized structures include a quartz vein (250° strike, 40°N dip) that lies north and a shear zone (010° strike, 70°E dip) that lies south of the point of inflection in the main structure.

Alteration: Alteration styles in samples from the main shaft area are very similar to those described above (Maori Queen), although hematitization was not recognized.

References: Honman (1917), Mt Burgess Gold Mining Co. NL (1984).

Potosi

Other names: Potosi North Extended

Coordinates: 29°07'12"S, 122°01'18"E

Production: 55 983.5 t of ore for 998.84 kg Au (17.8 g/t Au) between 1899 and 1912.

Host rock: Massive to weakly deformed, medium-grained, metamorphosed biotite–hornblende tonalite.

Structure: Several deep workings are distributed over a strike length of about 150 m on a structure that strikes 310° and dips 50–70°NE. The structure is poorly exposed, but samples from mine dumps suggest a similar style of structure to that at Maori Queen.

In combination with extensions or similar subparallel structures to the north and south, the total strike length of workings is in excess of 500 m.

Alteration: Similar styles of alteration to those described for Maori Queen are present, including quartz veining (Fig. 2.9) and potassic alteration, as indicated by pervasive sericitization of plagioclase. Retrograde alteration of high-temperature alteration assemblages may be more widespread than at Maori Queen, with retrograde alteration of biotite and amphibole to chlorite, carbonate, and epidote. Patchy microcline in some plagioclase grains may represent retrograde alteration, but may alternatively reflect potassic alteration or a relatively potassic rich host rock. Fine-grained pyrite is associated with some late-stage adularia veinlets, suggesting that some gold may have been deposited during this lower temperature hydrothermal activity. Pyrite is associated with minor disseminated secondary magnetite in one of the samples examined.

Mass-balance calculations, based on whole-rock geochemical data, indicate massive addition of SiO_2 to the mineralized shear zone, accompanied by smaller additions of CaO, K_2O, and S (Fig. 2.10). Na_2O is also added to the most strongly deformed sample (GSWA 119989), but is depleted in other samples of sheared metatonalite (?the outer parts of the mineralized shear zone).

References: Honman (1917), Mt Burgess Gold Mining Co. NL (1984).

Queen of the May

Other names: East Reef, West Reef, Queen of the May South

Coordinates: 29°08'15"S, 122°01'46"E

Production: 10 696.4 t of ore for 239.13 kg Au (22.4 g/t Au) between 1899 and 1959.

Host rock: Massive to weakly deformed, medium-grained, metamorphosed biotite–hornblende tonalite. There is also a medium- to coarse-grained biotite monzogranite exposed on the mine dumps, but this does not appear to be mineralized.

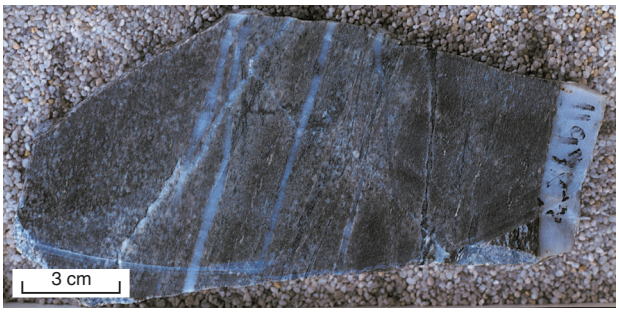

IRO68 23.10.03

Figure 2.9. Quartz–amphibole veins in strongly deformed, weakly altered (paler) metatonalite, Potosi mine, Yundamindera mining area

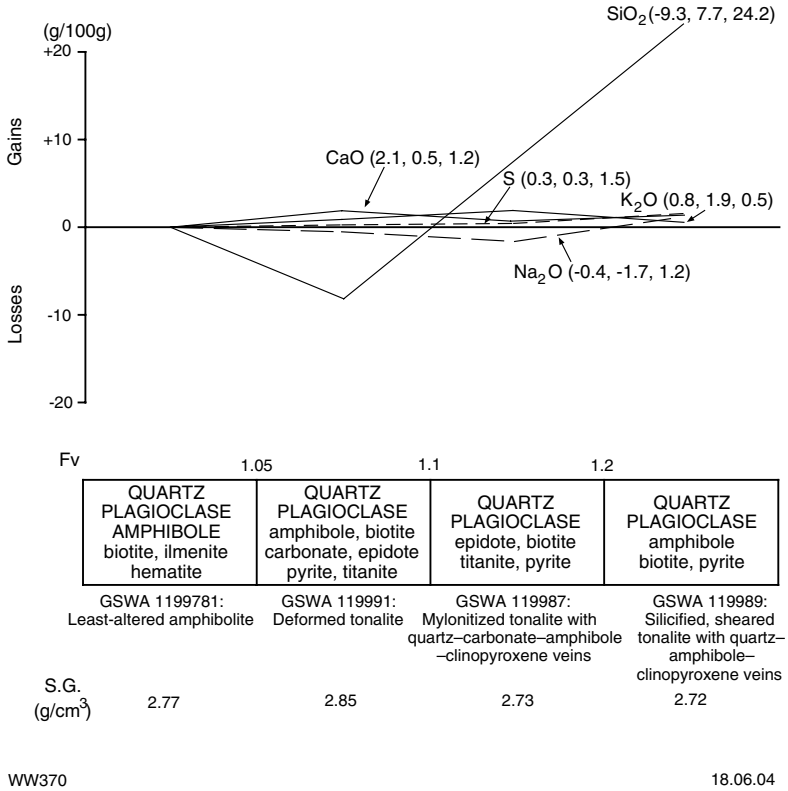

Figure 2.10. Mass-balance changes (calculated using the method of Gresens, 1967) associated with a mineralized shear in metatonalite, Potosi mine, Yundamindera mining area. Mineral components of alteration assemblages are listed in approximate order of abundance, with main mineral components in upper case and minor mineral components in lower case

Structure: There is an almost continuous line of workings, trending southeast from Queen of the May to Queen of the May South, that extends for about 700 m. The deepest workings are at Queen of the May.

Workings lie on a 330–340°-trending zone of strong ductile deformation that dips 60–70°NE. The ore zone appears to be about 1–2 m wide, but lies within a much broader envelope of strongly foliated metatonalite. This zone has been offset across several dextral faults. The broad envelope of foliated metatonalite is characterized by millimetre-scale banding, oriented biotite, and grain-size reduction as a result of dynamic recrystallization. The ore zone displays evidence for intense ductile deformation, including further grain-size reduction, S–C fabrics, and asymmetric quartz lenses ('fish'). Veins of quartz and calc-silicate minerals are strongly deformed. They are boudinaged and crenulated or tightly folded with the pervasive shear fabric axial planar to folds. Veins that are markedly transgressive to the shear fabric are not common. These features suggest that the mineralized structure is a banded brittle–ductile shear zone (Witt, 1993). Quartz in the veins is strongly recrystallized and displays preferred orientation of c-axes, locally in two directions: one parallel to banding and the other at an angle of 30–40° to banding (S–C fabric). An absence of accessible in situ exposures prevented collection of oriented samples.

Alteration: Strongly foliated samples from the mineralized shear are fine- to medium-grained quartzofeldspathic gneiss. In metatonalite that has undergone strong ductile deformation and calc-silicate alteration, hornblende and biotite are commonly stable but completely recrystallized and oriented parallel to the shear fabric, with ilmenite altered to titanite. Deformation is accompanied by the introduction of minor amounts (up to 10%) of epidote, carbonate, and pyrite. The 'bleached' (silicified) ore zone is characterized by the instability of amphibole and biotite and a relative increase in the modal abundance of quartz, epidote, and disseminated pyrite. Trace pyrrhotite is present as small inclusions in pyrite. Strongly deformed calc-silicate veins of quartz–clinopyroxene–amphibole(–plagioclase) have been observed in the ore zone and surrounding envelope of strong ductile deformation.

Mass-balance calculations, based on whole-rock geochemical data, indicate extreme mobility of SiO_2, with different samples from the mineralized shear zone showing enrichment or depletion (Fig. 2.11). In the most-intensely altered sample (GSWA 120000), most elements (including Al_2O_3) are depleted, leaving a SiO_2-rich rock. Addition of S is accompanied by an increase in the Fe_2O_3/FeO ratio.

References: Maitland (1903).

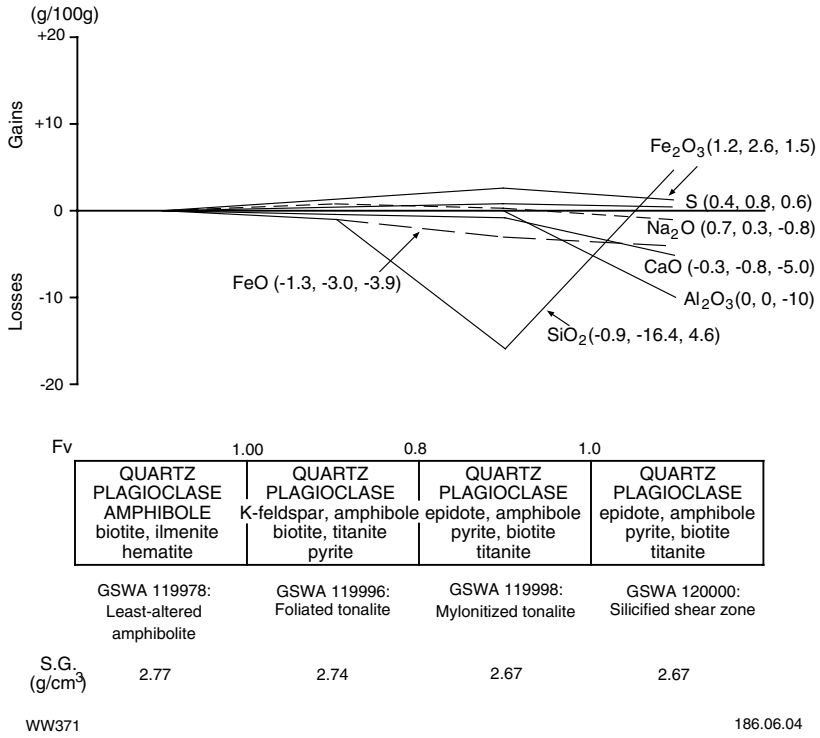

Figure 2.11. Mass-balance changes (calculated using the method of Gresens, 1967) associated with a mineralized shear in metatonalite, Queen of the May mine, Yundamindera mining area. Mineral components of alteration assemblages are listed in approximate order of abundance, with main mineral components in upper case and minor mineral components in lower case

Little Wonder

Other names: Woomera, E.J.C.

Coordinates: 30°02'36"S, 122°42'22"E

Production: 559.7 t of ore for 43.77 kg Au (78.2 g/t Au) between 1899 and 1907.

Host rock: Massive to weakly deformed, medium-grained, metamorphosed biotite–hornblende tonalite.

Structure: Shallow to moderately deep workings extend over about 50 m on a north–south trend. The mineralized structure is not well exposed, but appears to dip about 70°W. Foliated metatonalite and vein quartz are both common on mine dumps.

Alteration: Similar to that at Queen of the May.

References: Maitland (1903).

Boer

Other names: Boomerang, Rich View, Emu

Coordinates: 29°08'47"S, 122°02'24"E

Production: 630.9 t of ore for 36.85 kg Au (58.4 g/t Au) between 1900 and 1904.

Host rock: Medium-grained, equigranular biotite–amphibole (quartz) diorite. A medium-grained, seriate to porphyritic biotite granodiorite is also on some mine dumps, but does not appear to carry significant mineralization.

Structure: Moderately deep workings access a structure that is oriented about 300° and dips 40–60°NE, but deviates to about 345° and 60°NE at its northern end. The structure appears to be a zone of moderately to strongly foliated (quartz) diorite with abundant fractures and veins (up to 30 cm wide). The larger veins are mostly subparallel to the foliation, but are also locally deformed by the foliation-forming event. Many of the smaller veinlets are markedly transgressive to the foliation and variably deformed. Possible S–C fabrics, observed locally in open stopes, suggest reverse movement. The foliation is defined by the preferred orientation of biotite and aggregates of amphibole and, in some cases, a weak mineral banding. Many of the strongly altered and veined samples taken from mine dumps do not have a strong ductile fabric. However, they do have a fine- to medium-grained, granoblastic fabric, suggesting recovery of a deformed rock in a high-temperature, low-strain environment. Although the wallrocks are relatively unstrained, vein quartz is highly strained and displays a preferred c-axis orientation fabric, which is variously oriented parallel, or at an angle of 30–40°, to the vein margins.

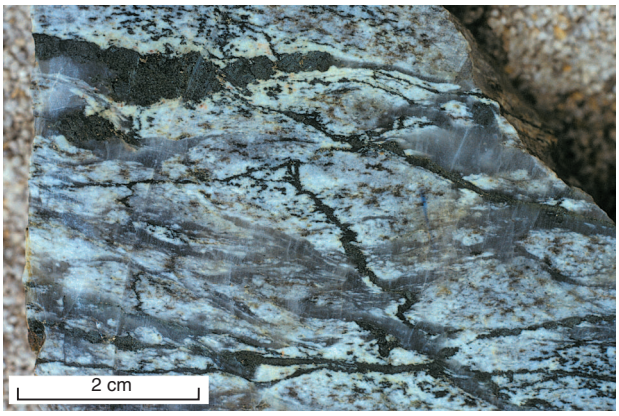

Figure 2.12. Mineralized breccia, showing clasts of calc-silicate altered metatonalite (quartz–plagioclase–amphibole) in quartz, Boer mine, Yundamindera mining area

Figure 2.13. Narrow selvage of weak bleaching adjacent to a quartz–clinopyroxene–pyrrhotite vein, Boer mine, Yundamindera mining area

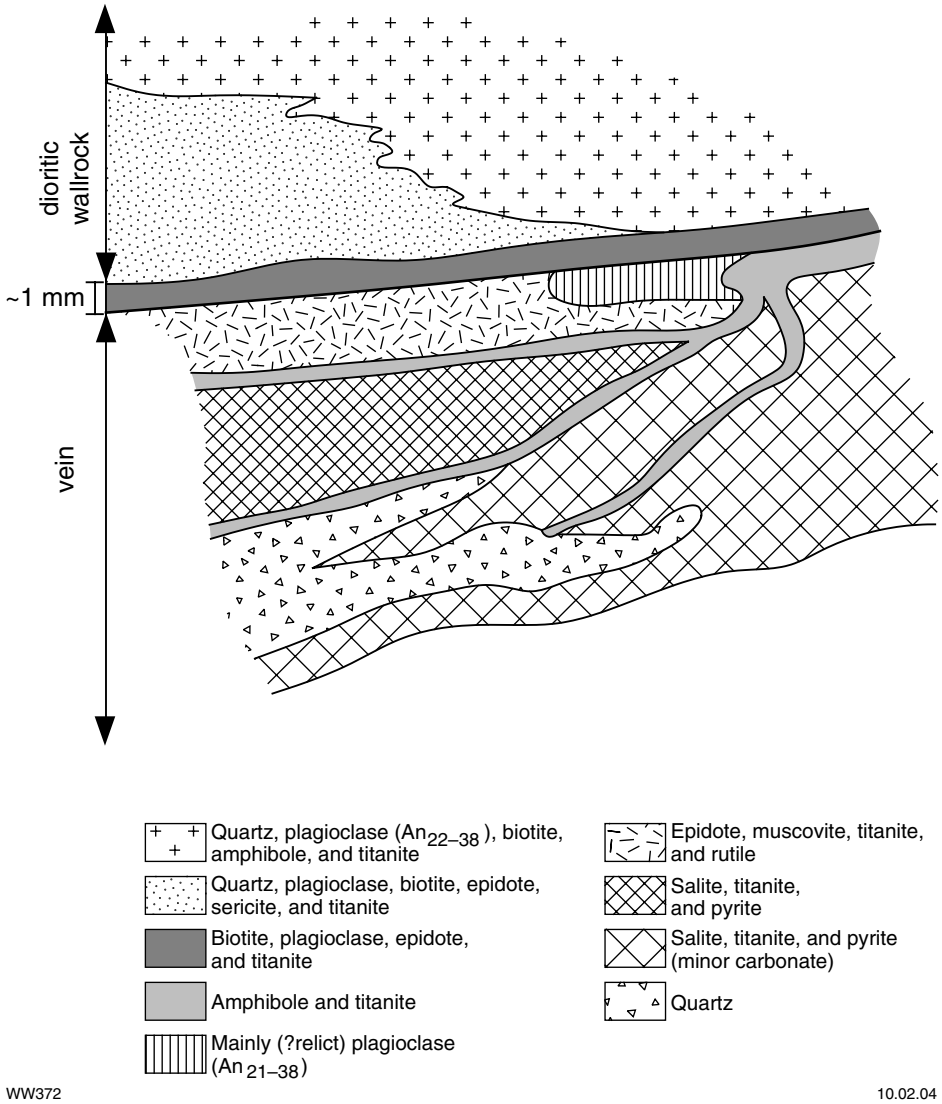

Figure 2.14. Sketch of sample GSWA 132907, showing relationships between various alteration assemblages and a quartz–clinopyroxene vein, Boer mine, Yundamindera mining area

A second structure, a few tens of metres north of the first, is poorly exposed but trends 005°, deviating to 270° at its northern end. This structure supports smaller and fewer workings.

Alteration: Interpreted alteration zoning is summarized in Table 2.7. Most mine-dump samples appear to be deformed, fractured, and veined (Fig. 2.12), but not strongly altered, except in the immediate vein and veinlet margins (Fig. 2.2). Vein and veinlet wallrock margins may be bleached for 1–3 mm (Fig. 2.13). The bleaching reflects destruction of amphibole and is normally accompanied by the introduction of epidote and disseminated pyrite.

More-intensely altered samples are characterized by broader zones of bleaching (calc-silicate alteration) with some relict domains in which amphibole remains stable (Fig. 2.2). Both amphibole (magnesio- to ferro-hornblende and ferro-edenite) and biotite are unstable in bright-white zones of very intensely altered diorite adjacent to veins. These assemblages are predominantly quartz and plagioclase ($An_{22–38}$), as well as minor microcline.

The main veins are quartz or calc-silicate veins that are zoned from quartz-rich cores, to margins consisting predominantly of green, calcic amphibole (ferro-edenite and ferroan pargasite) or clinopyroxene (salite), or both, with minor carbonate, epidote, plagioclase, titanite, pyrite, and rutile (Fig. 2.14). Some thinner veinlets contain predominantly amphibole(–relict clinopyroxene). In some cases, these smaller veinlets are also zoned, from relatively pale-green amphibole(–relict clinopyroxene) cores to darker green amphibole margins. In general, the smaller veinlets overprint larger quartz and calc-silicate veins.

Pyrite (and presumably gold) is enriched in and adjacent to the veins and veinlets, particularly the larger veins, and there is a common association between pyrite and clinopyroxene. Amphibole appears to replace clinopyroxene and pyrite, to varying degrees, in many veins.

Mass-balance calculations, based on whole-rock geochemical data, indicate addition of large amounts of SiO_2 to altered, mineralized metatonalite (Fig. 2.15). Silicification is accompanied by minor additions of Na_2O and S. Fe_2O_3, CaO, and MgO are also added to sample GSWA 132907.

References: Maitland (1903).

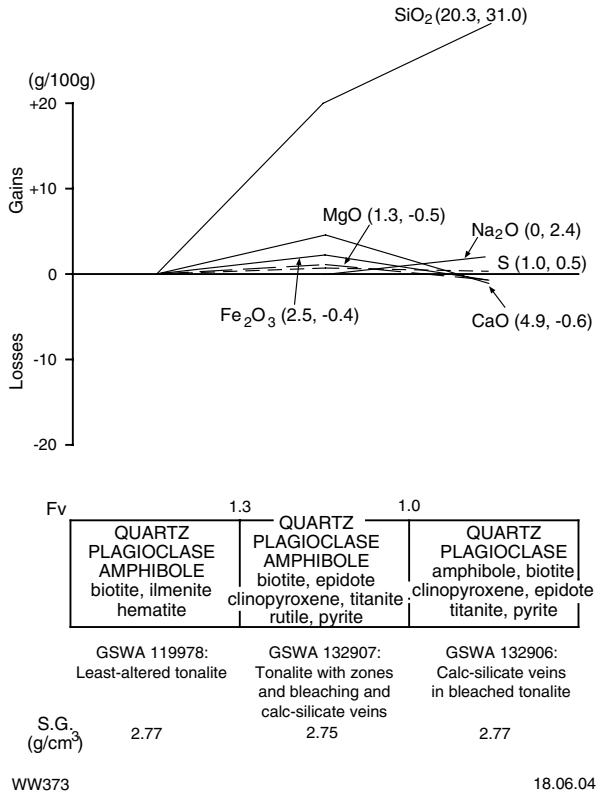

Figure 2.15. Mass-balance changes (calculated using the method of Gresens, 1967) associated with calc-silicate alteration of metatonalite, Boer, Yundamindera mining area. Mineral components of alteration assemblages are listed in approximate order of abundance, with main mineral components in upper case and minor mineral components in lower case

References

BARLEY, M. E., CASSIDY, K. F., GOLDING, S. D., GROVES, D. I., and McNAUGHTON, N. J., 1990, Alteration haloes, *in* Gold deposits of the Archaean Yilgarn Block, Western Australia: nature, genesis and exploration guides *edited by* S. E. HO, D. I. GROVES, and J. M. BENNETT: University of Western Australia, Geology Department (Key Centre) and University Extension, Publication no. 20, p. 317–327.

DeJONG, G., and WILLIAMS, P. J., 1995, Giant metasomatic system formed during exhumation of mid-crustal Proterozoic rocks in the vicinity of the Cloncurry Fault, northwest Queensland: Australian Journal of Earth Sciences, v. 42, p. 281–290.

DILLES, J. H., and EINAUDI, M. T., 1992, Wall-rock alteration and hydrothermal flow paths about the Ann-Mason porphyry copper deposit, Nevada — a 6 km vertical reconstruction: Economic Geology, v. 87, p. 1963–2001.

FURLONG, K. P., HANSON, R. B., and BOWERS, J. R., 1991, Modelling thermal regimes, *in* Contact metamorphism *edited by* D. M. KERRICK: Reviews in Mineralogy, v. 26, p. 437–506.

GRESENS, R. L., 1967, Composition–volume relationships of metasomatism: Chemical Geology, v. 2, p. 47–65.

HALLBERG, J. A., 1985, Geology and mineral deposits of the Leonora–Laverton area, northeastern Yilgarn Block, Western Australia: Perth, Western Australia, Hesperian Press, 140p.

HALLBERG, J. A., and WILSON, P., 1983, Relative timing of igneous intrusion in the Eucalyptus area, northeastern Yilgarn Block, Western Australia: Journal of the Geological Society of Australia, v. 30, p. 383–392.

HONMAN, C. S., 1917, The Geology of the North Coolgardie Goldfield — Part I. The Yerilla District: Western Australia Geological Survey, Bulletin 73, 98p.

KNIGHT, J. T., RIDLEY, J. R., GROVES, D. I., and McCALL, C., 1997, Syn-peak metamorphic gold mineralization in the amphibolite-facies, metagabbro-hosted Three Mile Hill deposit, Coolgardie Goldfield, Western Australia: a high-temperature analogue of mesothermal metagabbro-hosted gold deposits: Australasian Institute of Mining and Metallurgy, Transactions, Section B, v. 105, p. 175–199.

LEAKE, B. E., 1978, Nomenclature of amphiboles: American Mineralogist, v. 63, p. 1023–1053.

MAITLAND, A. G., 1903, Notes on the country between Edjudina and Yundamindera, North Coolgardie Goldfield: Western Australia Geological Survey, Bulletin 11, 58p.

MT BURGESS GOLD MINING CO. NL, 1984, Report on Yundamindera leases: Western Australia Geological Survey, Statutory mineral exploration report, Item 11646 A34254 (confidential)*.

OJALA, V. J., RIDLEY, J. R., GROVES, D. I., and HALL, G. C., 1993, The Granny Smith gold deposit: the role of hetergeneous stress distribution at an irregular granitoid contact in a greenschist facies terrane: Mineralium Deposita, v. 28, p. 409–419.

RIDLEY, J. R., 1993, The relations between mean rock stress and fluid flow in the crust: with reference to vein- and lode-style gold deposits: Ore Geology Reviews, v. 8, p. 23–27.

SWAGER, C. P., 1997, Tectono-stratigraphy of late Archaean greenstone terranes in the southern Eastern Goldfields, Western Australia: Precambrian Research, v. 83, p. 11–42.

WITT, W. K., 1991, Regional metamorphic controls on alteration associated with gold mineralization in the Eastern Goldfields Province, Western Australia: implications for the timing and origin of Archaean lode-gold deposits: Geology, v. 19, p. 982–985.

WITT, W. K., 1993, Gold mineralization in the Menzies–Kamblada region, Eastern Goldfields, Western Australia: Western Australia Geological Survey, Report 39, 165p.

---

* Confidential references are used with permission of companies.

3. Yarri

The Yarri deposits lie within biotite monzogranite and mafic country rocks (amphibolite and metabasalt) of the Mulgabbie domain of the Kurnalpi Terrane (Swager, 1997). In this terrane, greenstone units form a west-dipping homoclinal sequence that has been dissected by late, north-trending faults. The coarse-grained, locally porphyritic biotite monzogranite (Yarri Monzogranite) is a pervasively foliated, elongate pluton (about 20 km long and 0.75 – 2.5 km wide). The shape is atypical of intrusions in the Eastern Goldfields Granite–Greenstone Terrane, but lies within a north-northwesterly trending zone of elongate, pervasively deformed plutons, which includes the Outcamp Bore Tonalite, 20 km north of Yarri. The timing of emplacement of the Yarri Monzogranite is uncertain. The pervasive foliation, which is parallel to the regional foliation in the surrounding country rocks, suggests a relatively early emplacement, and it must certainly pre-date intrusion of the Galvalley Monzogranite, which appears to have pushed the southern part of the Yarri Monzogranite aside. Swager (1995) interpreted the intrusion to have been emplaced prior to D_2 regional folding. Recent SHRIMP dating of zircons from the Outcamp Bore Tonalite has yielded an age (2719 ± 5 Ma; Nelson, 1997) equivalent to or older than the volcanic component of the greenstones in the Eastern Goldfields Granite–Greenstone Terrane, suggesting that these elongate, deformed plutons may be synvolcanic intrusions.

The Yarri Monzogranite has produced about 460 kg of gold, mainly from the Wallaby Central and Yarri Proprietary mines. Smaller amounts of gold have come from mafic-hosted deposits in the country rocks. The main contributor was the amphibolite-hosted Yarri South mine (40 kg Au).

The main line of workings, almost 1500 m long, encompasses the more or less contiguous workings at Wallaby North, Wallaby Central, and Yarri Proprietary. These deposits lie several kilometres west of the regional-scale Claypan Fault, which forms the eastern boundary of the Mulgabbie domain. The workings have exposed a 330–340°-trending, subvertical to steeply west dipping shear zone that is more or less conformable within the regional foliation. The mineralized shears are commonly located at the margins of prominent quartz veins of similar orientation. They represent zones of relatively high strain that may have been localized by the contrast in competency between the veins and the wallrocks.

The mineralized shears are up to several metres wide and record a greater strain intensity than the veined brittle–ductile shears described by Witt (1993). A pervasive foliation, defined by oriented phyllosilicates and a fine-scale mineral banding, is uniformly parallel to shear-zone margins. Quartz veins have been rotated into the plane of the shear fabric and locally show evidence of isoclinal folding and boudinage. A subhorizontal lineation is widely preserved, and Swager (1995) noted left-lateral movement indicators. Some subhorizontal quartz veins overprint the shear fabric and related steep veins.

Farther south, the mafic-hosted workings at Star of Yarri and Queens Birthday are poorly exposed due to recent surface prospecting, but appear to lie on different trends to that defined by the monzogranite-hosted deposits. Swager (1995) noted quartz veins and shear zones, interpreted as sinistral shear bands, with similar trends to those at Star of Yarri and Queens Birthday, over a much wider area of the Yarri Monzogranite. The structure at Yarri South is a steeply east dipping, banded brittle–ductile shear zone (Witt, 1993).

There are several small deposits and workings in the Yarri Monzogranite south of the main mining area. The main area of interest is near Byer Well, where mineralized shears have been interpreted by Swager (1995) as sinistral shear bands. Relatively small deposits are also in mafic rocks west (Dostmund) and north of Yarri. The area between Gibberts and Great Banjo contains numerous quartz blows and widespread quartz float. Mineralization in this area appears to be associated mainly with a more brittle style of deformation, involving small shears, quartz veins, and fault gouge. At Great Banjo, a recent shallow pit that has fed a heap-leaching operation is located on the contact between mafic rock and a thin felsic schist unit.

Mineralization at Yarri is within a zone of sinistral shear that appears to have caused several kilometres of lateral displacement on intrusive contacts of the Yarri Monzogranite. The main area of mineralization also coincides with the intersection of this mineralized shear with a late, north-trending fault, and is at the narrowest (and therefore weakest) section of the Yarri pluton. The orientation of the mineralized shear zone at Yarri, and the faulted granite–greenstone contact, is approximately normal to the principal axis of regional compression (east–west). The potential for brittle failure of the more competent granite unit under these circumstances is high. All north–south contacts between granites and less-competent greenstone units are potentially associated with brittle quartz-vein arrays in the more competent unit. Late, north-trending faults also deserve investigation, especially where they juxtapose units of contrasting competency.

The pervasive foliation of the Yarri Monzogranite has been accompanied by quartz veining, carbonation, and sericitization. Disseminated pyrite is also widespread (Swager, 1995). Increased strain in mineralized shears, including the main 'Yarri line', is accompanied by increased hydration of feldspars and an increase in modal disseminated pyrite, ultimately producing a pyritic quartz–sericite schist. Epidote and fine, dusty hematite is locally abundant. This alteration is accompanied by enrichment of SiO_2 and K_2O, and depletion of CaO and Na_2O. Late, coarse, randomly oriented muscovite, commonly associated with brittle fracture, overprints the shear fabric in some samples from Wallaby Central and the Byer Well area, but is not associated with sulfides.

Mafic-hosted mineralization is associated with carbonation and quartz–muscovite assemblages, except at South Yarri. Tourmaline is commonly present in minor

amounts and is locally abundant (e.g. at Gibberts). At South Yarri, banded calc-silicate alteration assemblages indicate higher temperature alteration and probably reflect the higher grade amphibolitic wallrocks (cf. Witt, 1991, 1993). SiO_2, K_2O, and S have been added to the calc-silicate lodes, whereas MgO has been depleted. The calc-silicate alteration contrasts with lower temperature, quartz–muscovite-dominated alteration assemblages in other deposits close to the margin of the Yarri Monzogranite. Two interpretations are possible:

i) Mineralization at South Yarri formed relatively early in the history of the greenstone belt, contemporaneous with emplacement of the Yarri Monzogranite and contact metamorphism of the surrounding host rocks. Mineralization at Star of Yarri and Queens Birthday formed at a later stage when temperatures in the contact aureole had fallen to less than 350°C;
ii) Mineralization at all deposits was more or less contemporaneous and late in the tectonic history of the greenstone belt. High-temperature alteration assemblages in amphibolite at South Yarri are related to contact metamorphism in the thermal aureoles of one or more poorly exposed late-tectonic granites restricted to the immediate South Yarri area.

Deposits of the Yarri area

Great Banjo

Other names: Welcome

Coordinates: 29°42'53"S, 122°20'13"E

Production: 129.0 t of ore for 2.62 kg Au (20.3 g/t Au) between 1903 and 1905. The present inferred in situ resource is 17 000 t at 2.93 g/t Au (50 kg Au). There is evidence of a recent heap-leach operation at this site.

Host rock: Metabasalt and felsic schist after volcaniclastic rock.

Structure: A small, recent opencut exposes a sheared contact between metabasalt (in the hangingwall) and felsic schist (in the footwall) 15 m wide, over a strike length of about 150 m. This shear zone, which appears to have yielded the main feed for the heap-leaching operation, trends about 305° and dips 70°NE. Mineralization is associated with quartz veins (up to 20 cm thick), which are mostly parallel to bedding and the main schistosity (shear fabric). Quartz veining is particularly developed in Z-shaped changes in the strike of the mineralized shear zone, and in 'rollovers' where the dip of the shear zone flattens.

Historic workings a short distance to the south of the recent opencut are focused on a large, laminated quartz(–?tourmaline) vein and associated fault gouge, which strikes 320° and dips 50°NE within felsic schist. Slickensides exposed on the surface of the quartz vein plunge 10°S. The vein is several metres wide and outcrops intermittently over about 500 m.

Alteration: Alteration is obscured by weathering. Exploration drilling suggests quartz–muscovite alteration of deformed metabasalt.

References: Lynas Gold NL (1993).

Wallaby North

Coordinates: 29°46'41"S, 122°21'51"E

Production: 3875.5 t of ore for 37.86 kg Au (9.8 g/t Au) between 1903 and 1912.

Host rock: Coarse-grained biotite monzogranite (Yarri Monzogranite).

Structure: Open stopes, shafts, and pits are located on a shear zone, about 2 m wide, that trends 330°and dips 70°NE. Workings extend over about 100 m, but are essentially continuous with the Wallaby Central workings. A prominent subhorizontal mineral lineation is defined within the shear zone by elongate biotite aggregates and quartz ribbons. Quartz veins up to about 40 cm thick are mostly parallel or subparallel to the pervasive shear fabric, but locally display evidence of having been isoclinally folded.

Alteration: Within the shear zone, the monzogranite host rock is altered to quartz(–feldspar)–muscovite schist with disseminated pyrite.

References: Swager (1995).

Wallaby Central

Other names: Wallaby

Coordinates: 29°46'51"S, 122°21'56"E

Production: 18 795.2 t of ore for 259.14 kg Au (13.8 g/t Au) between 1903 and 1985.

Host rock: Coarse-grained biotite monzogranite (Yarri Monzogranite).

Structure: Open stopes and several deep shafts are distributed over a strike length of several hundred metres on the margins of a prominent quartz vein. The quartz vein, which is several metres wide, strikes 340° and dips subvertically to 70°E (i.e. subparallel to the regional foliation). Workings at the northern end of the lode system are mainly in the hangingwall of the quartz vein, whereas to the south, workings are on both sides of the vein.

Mineralization is present in a 1–4 m-wide shear zone, consisting of intensely and pervasively foliated (locally mylonitized) and altered monzogranite and quartz veins (Fig. 3.1). A prominent subhorizontal mineral lineation is defined by elongate biotite aggregates and quartz ribbons. There are numerous quartz veins, mostly less than 5 mm wide, but up to about 1 m wide and subparallel to the pervasive shear fabric. The veins display evidence of isoclinal folding and boudinage. Boudinage is especially evident in roof and floor exposures, suggesting steeply plunging quartz boudins. The orientation of the mineral lineation and quartz-vein boudins indicates dominantly strike-slip movement on the mineralized shear zone.

Late-stage, subhorizontal quartz veins, which overprint the steep shear fabric and quartz veins, are locally exposed (Fig. 3.2).

Alteration: Within the mineralized shear zone, the monzogranite host rock is altered to quartz(–feldspar)–

IRO69 23.10.03

Figure 3.1. Deformed quartz veins in a mineralized, tight, brittle–ductile shear zone along the margin of a large quartz vein (left of the shear), Wallaby Central deposit, Yarri mining area

muscovite schist with disseminated pyrite. Pyrite is fine to medium grained (up to about 2 mm) with coarser grains tending toward idioblastic. Fine, dusty hematite is common in some samples. Feldspars are unstable in quartz–muscovite schist in very high strain zones near the centre of the shear zone. Thin (≤1 mm), discontinuous veinlets of K-feldspar (?adularia) oblique to the shear fabric were observed in one sample of quartz(–feldspar)–muscovite schist. Mass-balance calculations, based on whole-rock geochemical data, indicate that SiO_2 is depleted from the margins of the mineralized shear zone and enriched in the shear centre (Fig. 3.3). K_2O is enriched within the shear zone, whereas CaO and Na_2O are depleted. Coarse (up to several millimetres), undeformed muscovite locally overprints the shear fabric in strongly deformed zones.

References: Swager (1995).

Yarri Proprietary

Other names: Wild Dog, Hidden Treasure, Wallaby

Coordinates: 129°46'46"S, 22°21'52"E

Production: 13 688.0 t of ore for 147.17 kg Au (10.7 g/t Au) between 1903 and 1917. The inferred resource (MINEDEX site code S05677) at Yarri–Wallaby is 84 000 t of ore at 1.75 g/t Au for 147 kg Au.

Host rock: Coarse-grained biotite monzogranite (Yarri Monzogranite).

Structure: The historic workings lie 50–100 m west of the contact between the monzogranitic host rock and metabasaltic wallrocks to the east. A small openpit has been sunk on this site, along strike from the Wallaby Central lode. The pit is about 100 m long by 10 m deep and is oriented about 345°. The dominant foliation exposed in the pit dips 65°E, but the mineralized shear zone is not well exposed. Mine-dump samples adjacent to the pit suggest a similar structure to that described for Wallaby Central.

Alteration: Mine-dump samples are foliated biotite monzogranite and quartz–muscovite schist with limonitic pits after idioblastic pyrite. Quartz veins are up to about 1 m wide.

References: Swager (1995).

Star of Yarri

Other names: Record

Coordinates: 29°47'28"S, 122°22'18"E

Production: 276.3 t of ore for 4.14 kg Au (15.0 g/t Au) between 1902 and 1907.

Host rocks: Metamorphosed tholeiitic basalt.

Structure: Shallow workings and a moderately deep shaft define a mineralized zone that extends over a strike length of about 50 m. The mineralized structure is poorly exposed, but the workings trend about 315° and expose quartz veins up to 1 m thick. Mine dumps contain abundant fragments of vein quartz and weathered mafic schist. Based on this information, the mineralized structure is probably a veined brittle–ductile shear zone (terminology of Witt, 1993).

IRO70 23.10.03

Figure 3.2. Late-stage, subhorizontal quartz veins cutting the foliation in a mineralized brittle–ductile shear, Wallaby Central deposit, Yarri mining area

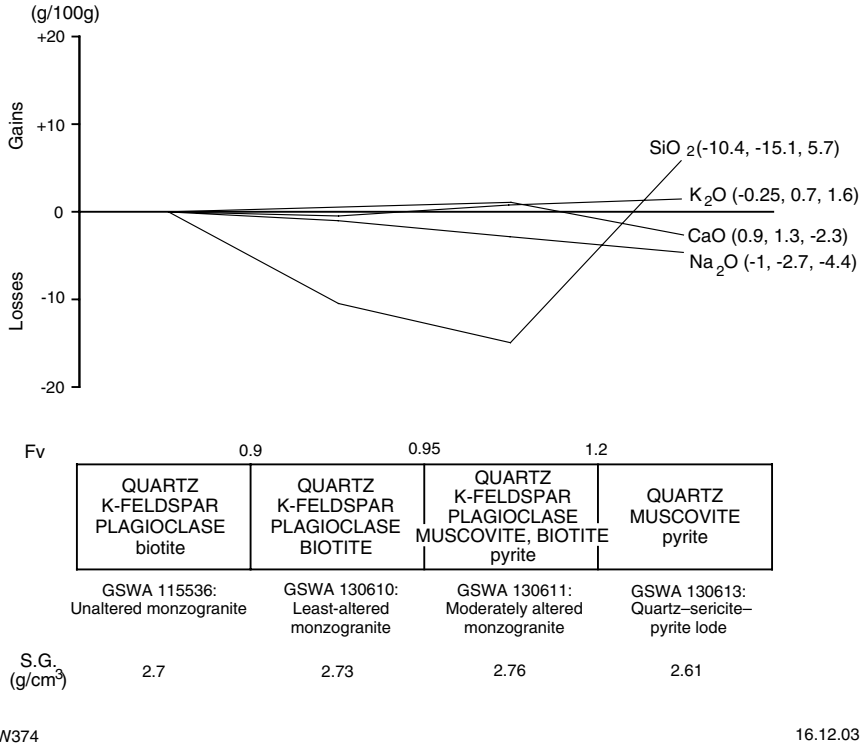

Figure 3.3. Mass-balance changes (calculated using the method of Gresens, 1967) associated with quartz–sericite–pyrite alteration in a mineralized brittle–ductile shear zone, Wallaby Central, Yarri mining area. Mineral components of alteration assemblages are listed in approximate order of abundance, with main mineral components in upper case and minor mineral components in lower case

Alteration: Only the main shaft has penetrated the oxidized zone. Although weathered mine-dump samples appear to be mostly (?carbonated) mafic schist with minor quartz–muscovite schist. The latter contains small quartz veins and veinlets and limonite after idioblastic pyrite (≤1 mm).

References: Swager (1995).

Queens Birthday

Coordinates: 29°47'34"S, 122°22'24"E

Production: 499.9 t of ore for 24.83 kg Au (49.7 g/t Au) between 1902 and 1907.

Host rock: Metamorphosed tholeiitic basalt.

Structure: Shallow stoping over a strike length of about 50 m defines a 290°-trending structure. The workings expose a 1–2 m-thick quartz vein that dips about 70°N, and an approximately 1 m-wide zone of strongly foliated and altered metabasalt on the hangingwall of the vein.

Alteration: Most workings do not penetrate the oxidized zone. Mine dumps adjacent to the deeper workings contain mafic (?carbonated) schist, quartz–muscovite schist (altered ?metabasalt) and abundant vein quartz with carbonate(–tourmaline).

References: Swager (1995).

Yarri South

Other names: Beatrice

Coordinates: 29°48'49"S, 122°22'46"E

Production: 1120.7 t of ore for 39.14 kg Au (34.9 g/t Au) between 1902 and 1911.

Host rock: Amphibolite after metamorphosed tholeiitic basalt.

Structure: An open stope and several moderately deep shafts have been sunk over about 100 m strike length on a shear zone that trends 355° and dips 70–80°E. The mineralized shear is an approximately 1 m-wide zone of pervasive, ductile strain and consists of banded quartz and altered amphibolite. Quartz(–diopside) veins, mostly conformable and variably deformed within the pervasive shear fabric, are up to about 30 cm wide.

There is a smaller group of workings on a similar, subparallel structure, about 50 m west of the main line of workings.

Alteration: Altered rocks are banded calc-silicate rocks (Fig. 3.4) with variable amounts of biotite and microcline K-feldspar. Typical assemblages contain at least 10% calcic amphibole, plagioclase, epidote, diopside, biotite, and K-feldspar. In most samples, there are also smaller amounts of quartz, calcite, titanite, and pyrrhotite. Minor

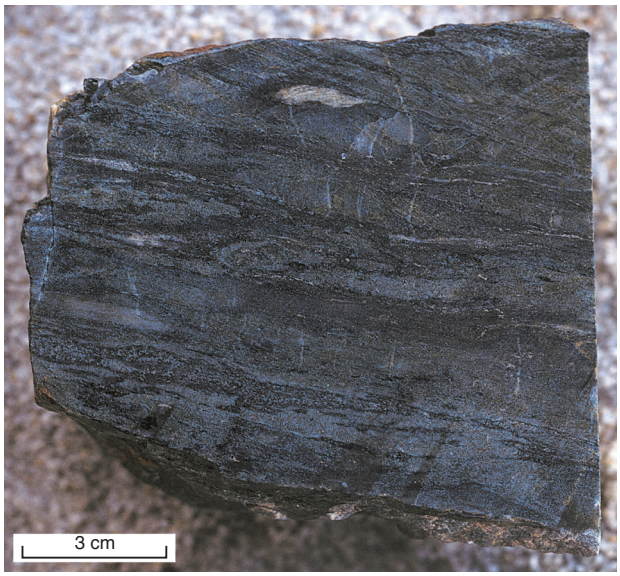

IRO71 23.10.03

Figure 3.4. Banded calc-silicate alteration assemblage, Yarri South, Yarri mining area

cummingtonite replaces calcic amphibole in one sample. Banding is defined by variable mineral proportions, especially amphibole–plagioclase, epidote, biotite, and diopside–K-feldspar. Amphibole and biotite are oriented parallel to the banding. K-feldspar (subequant grains) and diopside (stubby prisms) are relatively coarse grained (up to 3 mm across); quartz and feldspars tend towards a fine-grained, granoblastic habit, and pyrrhotite and titanite are finely disseminated in trails and aggregates, parallel to banding. Minor K-feldspar, diopside, quartz, calcite, epidote, and pyrrhotite are also in fine veinlets subparallel to, and crosscutting, the pervasive banding. Pyrrhotite in these veins is relatively coarse grained and undeformed.

As with many other Archaean lode gold deposits, mass-balance calculations, based on whole-rock geochemical data, indicate addition of SiO_2, K_2O, and S to the mineralized shear zone (Fig. 3.5). CaO and MgO are depleted and enrichment of CO_2 is not significant, which is consistent with other high-temperature Archaean lode gold deposits (Witt, 1993).

References: Swager (1995).

Dostmund

Other names: Dostmund West

Coordinates: 29°47'04"S, 122°13'44"E

Production: 1325.9 t of ore for 71.93 kg Au (54.2 g/t Au) between 1905 and 1915.

Host rock: Amphibolite after dolerite and tholeiitic basalt.

Structure: Several moderately deep shafts lie on a trend of about 280°, over a strike length of 70–80 m, on a structure that dips about 70°N. The mineralized structure is not well exposed, but mine dumps contain fine-grained amphibolite and metadolerite with small (<3 mm) quartz veinlets and chloritic fractures, and some more-strongly deformed (sheared) samples.

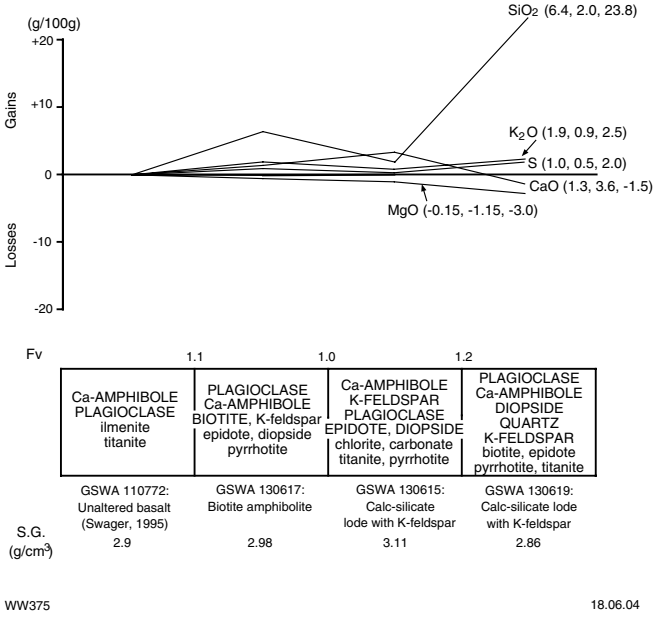

Figure 3.5. Mass-balance changes (calculated using the method of Gresens, 1967) associated with calc-silicate lode, Yarri South, Yarri mining area. Mineral components of alteration assemblages are listed in approximate order of abundance, with main mineral components in upper case and minor mineral components in lower case

Minor mineralization is also present in a subvertical, 340–350°-trending brittle–ductile shear zone.

Alteration: Narrow (1–2 mm), bleached selvages are adjacent to chloritic fractures. More-intensely deformed rocks display foliation-controlled sericitization and silicification. Strongly deformed, fine-grained siliceous rocks may be altered mafic rocks or derived from lenses of felsic porphyry (or ?metatuff), which are common within this mafic unit (Swager, 1995).

References: Enterprise Gold Mines NL (1992a,b), Consolidated Resources NL (1994), Swager (1995).

References

CONSOLIDATED RESOURCES NL, 1994, Annual report, Dec 1992 to Dec 1993, on Edjudina gold exploration: Western Australia Geological Survey, Statutory mineral exploration report, Item 11652 A40259 (unpublished).

ENTERPRISE GOLD MINES NL, 1992a, Report on P31/113, P31/1417–1418, M31/99, M31/76 and M30/30: Western Australia Geological Survey, Statutory mineral exploration report, Item 11655 A37396 (unpublished).

ENTERPRISE GOLD MINES NL, 1992b, Report on P31/1417–1418, M31/99, M31/76 and M31/30: Western Australia Geological Survey, Statutory mineral exploration report, Item 11655 A37397 (unpublished).

LYNAS GOLD NL, 1993, Report on M31/14: Western Australia Geological Survey, Statutory mineral exploration report, Item 11659 A39251 (unpublished).

GRESENS, R. L., 1967, Composition–volume relationships of metasomatism: Chemical Geology, v. 2, p. 47–65.

NELSON, D. R., 1997, Compilation of SHRIMP U–Pb zircon geochronology data 1996: Western Australia Geological Survey, Record 1997/2, 189p.

SWAGER, C. P., 1995, Geology of the Edjudina and Yabboo 1:100 000 sheets: Western Australia Geological Survey, 1:100 000 Geological Series Explanatory Notes, 43p.

SWAGER, C. P., 1997, Tectono-stratigraphy of late Archaean greenstone terranes in the southern Eastern Goldfields, Western Australia: Precambrian Research, v. 83, p. 11–42.

WITT, W. K., 1991, Regional metamorphic controls on alteration associated with gold mineralization in the Eastern Goldfields Province, Western Australia: implications for the timing and origin of Archaean lode-gold deposits: Geology, v. 19, p. 982–985.

WITT, W. K., 1993, Gold mineralization in the Menzies–Kambalda region, Eastern Goldfields, Western Australia: Western Australia Geological Survey, Report 39, 165p.

4. Yerilla – Mount Remarkable

The mining areas of Yerilla and Mount Remarkable lie within the Kurnalpi Terrane (Swager, 1997), with the majority of deposits lying in the Steeple Hill domain (western part of the terrane). Gold mineralization is in a steeply east dipping and east-younging, northerly to north-northwesterly striking sequence of mafic rocks dominated by metamorphosed tholeiitic basalt (including minor amounts of metamorphosed coarsely plagioclase-phyric basalt) with lesser amounts of metadolerite. A north-northwesterly striking, east-dipping fault lies about 1 km east of the main mine workings at Yerilla. Witt and Davy (1997) interpreted this fault as the eastern boundary of the Jubilee domain. South of Yerilla, this fault (termed here the Yerilla Fault) truncates regional fold structures in the greenstones to the west and east. Historic mine workings are distributed intermittently in the footwall of the Yerilla Fault, from Westward Ho in the south, to Friday Well in the north — a distance of almost 35 km. However, the main centre of production was near Yerilla Homestead, where about 350 kg of gold has been produced, mainly from within the oxidized zone. There was also some deep-lead activity in the vicinity of the Yerilla King deposit. There are no recent commercial operations (other than small-scale alluvial mining) in the Yerilla and Mount Remarkable mining areas, but a combined resource of almost 1000 kg of gold has been identified at Bull Terrier and Dingo. These deposits, which are east of the Yerilla Fault, are especially significant because they lie within the McAuliffe Well Syenite. Syenitic granites are traditionally thought to have been emplaced well after the main orogenic event in the Eastern Goldfields Granite–Greenstone Terrane (c. 2550 Ma; Libby, 1989), whereas gold mineralization is generally regarded as late-orogenic (Groves et al., 1989; Perring et al., 1989; Witt 1993; Witt et al., 1996). However, recent U–Pb zircon data (Nelson, 1997) have established an age of 2651 ± 5 Ma for the McAuliffe Well Syenite.

The main centre of gold production at Yerilla coincides with a small granite intrusion that is unexposed at the surface, but documented in underground workings by Jutson (1915). Weathered granite samples can also be observed on mine dumps at Melba Consols. The subsurface form of this granite is unknown, but the pluton was probably important in creating local stress inhomogeneities that promoted hydraulic fracture in domains of low mean stress. The nature, location, and orientation of mineralized structures in this area are consistent with formation during late-tectonic, east–west regional compression (Fig. 4.1). Under these conditions, the Yerilla Fault would have accommodated a mainly reverse sense of movement. The Viola and Yerilla Central deposits are in country rocks at the southern end of the pluton. This site would have been in the pressure shadow of the pluton during east–west regional deformation, and would therefore have been a domain of low mean stress. Other brittle host structures that dip 45° west and east within the pluton (Melba and West Melba) probably formed as complimentary fractures within the same stress regime. The Yerilla King deposit is a shear zone that dips 45°W, within mafic rocks adjacent to the western margin of the pluton. This may be a similar structure to that at Melba Reef, which has projected upwards into the country rocks. The Queen of the Earth deposit is a steep, brittle–ductile shear zone oriented subparallel to the north-trending margin of the northwestern corner of the granite intrusion. This would have been a site of high shear strain during east–west compression.

Other, smaller deposits west of the Yerilla Fault, including La Tosca in the Mount Remarkable mining centre, are in subvertical, northerly to north-northwesterly striking veined shear zones that are conformable or subconformable with the strike of the greenstones. At Mount Catherine, east of the Yerilla Fault, a prominent quartz blow is oriented 335° and dips steeply northeast within metabasalt. Mining was concentrated along a zone of strong ductile deformation, several metres wide, adjacent to the vein, and in the margins of the vein itself. The main workings appear to be in the hangingwall of the quartz vein.

Alteration in the Yerilla and Mount Remarkable centres is generally obscured by the effects of weathering. However, oxidized mine-dump samples suggest that low-temperature (<400°C) alteration of mafic rocks produced chlorite–carbonate schist and quartz–sericite schist. Limonite after small (<1 mm), idioblastic pyrite crystals is associated with some quartz–sericite schist samples. No visible alteration could be recognized adjacent to granite-hosted veins.

The Bull Terrier deposit is a subvertical, north-northeasterly striking, dextral, brittle fault zone in the McAuliffe Well Syenite (Fig. 4.2). The granite pluton probably acted in a similar fashion to the one at Yerilla in creating a local domain of stress heterogeneity with low mean stress in the syenite. Dextral movement on the fault zone is consistent with an east–west compressional regime. Syenite in and adjacent to the mineralized fault is characterized by a deep, brick-red colour that reflects hematitization. Ore zones are further characterized by the destruction of amphibole, and the addition of hematite, biotite, calcite, and pyrite.

Despite the failure of the Yerilla and Mount Remarkable areas to generate any significant commercial activity, there is some potential for undiscovered mineralization. Mineralization at Yerilla does not appear to be directly related to movement on nearby regional faults or shear zones such as the Yerilla Fault. Instead, gold is in a variety of brittle and brittle–ductile structures that were probably developed in domains of low mean stress in proximity to a small granite intrusion. Other granite plutons northeast of McAuliffe Well and north of Mount Remarkable would have caused local heterogeneity of stress distribution, with implications for brittle failure and fluid focusing (Oliver et al., 1990). In particular, contacts that are oriented north–south, normal to the principal, far-field stress vector, offer attractive exploration targets.

Deposits of the Yerilla – Mount Remarkable area

Bull Terrier

Coordinates: 29°29'17"S, 120°55'34"E

Production: No previous production or resource figures are available. Core from diamond drillhole YBD-9 records grades of 0.46 g/t Au over 46 m (Fig. 4.3).

Host rock: Massive, coarse-grained amphibole syenite (Fig. 4.4). The amphibole is actinolite and actinolitic hornblende (Table 4.1).

Structure: Mineralization is associated with a fault that trends 030° and dips 80°SE to subvertical. Displacement of the contact between felsic syenite and more-mafic monzogabbroic rocks indicates 180 m of dextral movement on the mineralized fault (Fig. 4.5).

At the surface, the fault is exposed as a 1–3 m-wide zone of fracturing and alteration. Diamond drilling from the east intersected zones of quartz veining and micro-fracturing over widths of at least 50 m (Figs 4.3 and 4.6). Individual zones of veining and microfracturing are up to several metres wide and become more closely spaced towards the fault. Microfractured sections are associated with anastomosing zones of cataclasis defined by marked grain-size reduction (≤0.01 mm) and angular to subangular relicts of feldspar grains up to about 1 mm across. A weak foliation, where present, is defined by the grain size and abundance of feldspar porphyroclasts, the orientation of long axes of feldspar porphyroclasts, and opaque mineral trails. To the northeast, the fault deviates towards 060° and opens out into a broad but diffuse zone of fracturing and alteration (Fig. 4.5).

The fault becomes a relatively ductile structure, characterized by a more pervasive foliation, where it traverses the monzogabbroic rocks. The faulted contact between felsic syenite and monzogabbro consists of several centimetres of intensely foliated chloritic schist and reddish clay. Monzogabbroic to pyroxenitic rocks west of the fault are brecciated, fractured, and locally foliated (Fig. 4.3). Jigsaw-fit breccia is common, with angular clasts of altered monzogabbro and pyroxenite up to about 10 cm across.

Alteration: Alteration halos adjacent to quartz(–chlorite–carbonate–pyrite) veins are up to several centimetres wide,

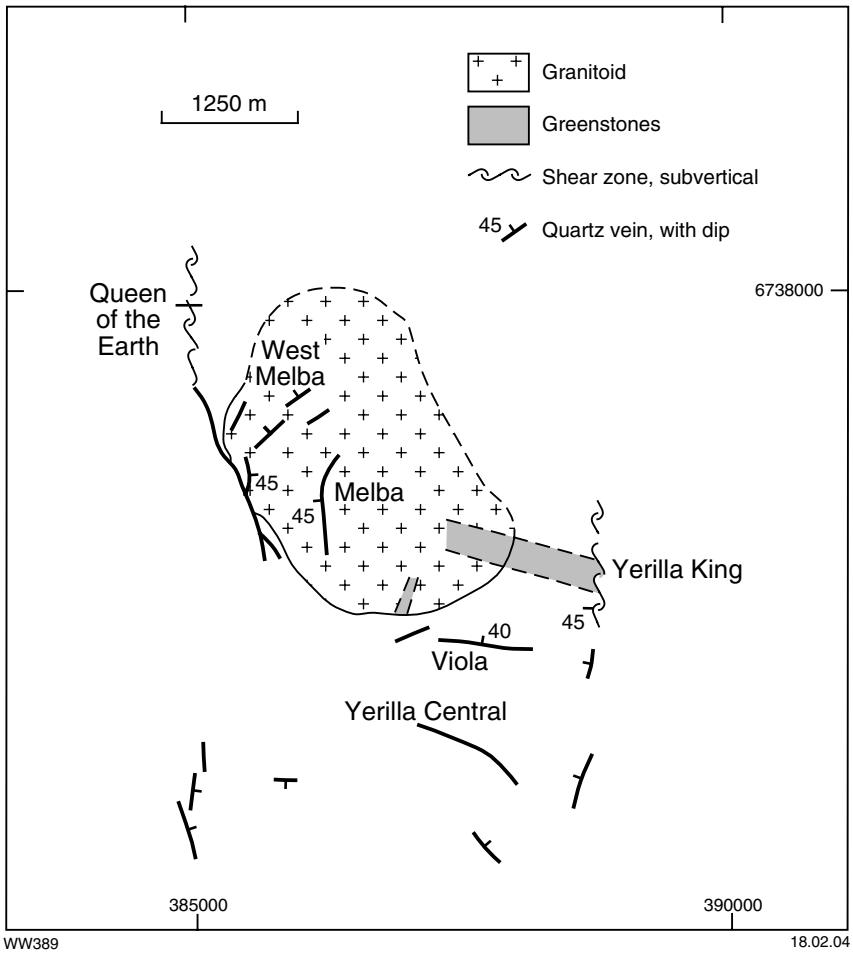

Figure 4.1. Geological map of the Yerilla mining area, showing the location and nature of gold deposits (after Jutson, 1915)

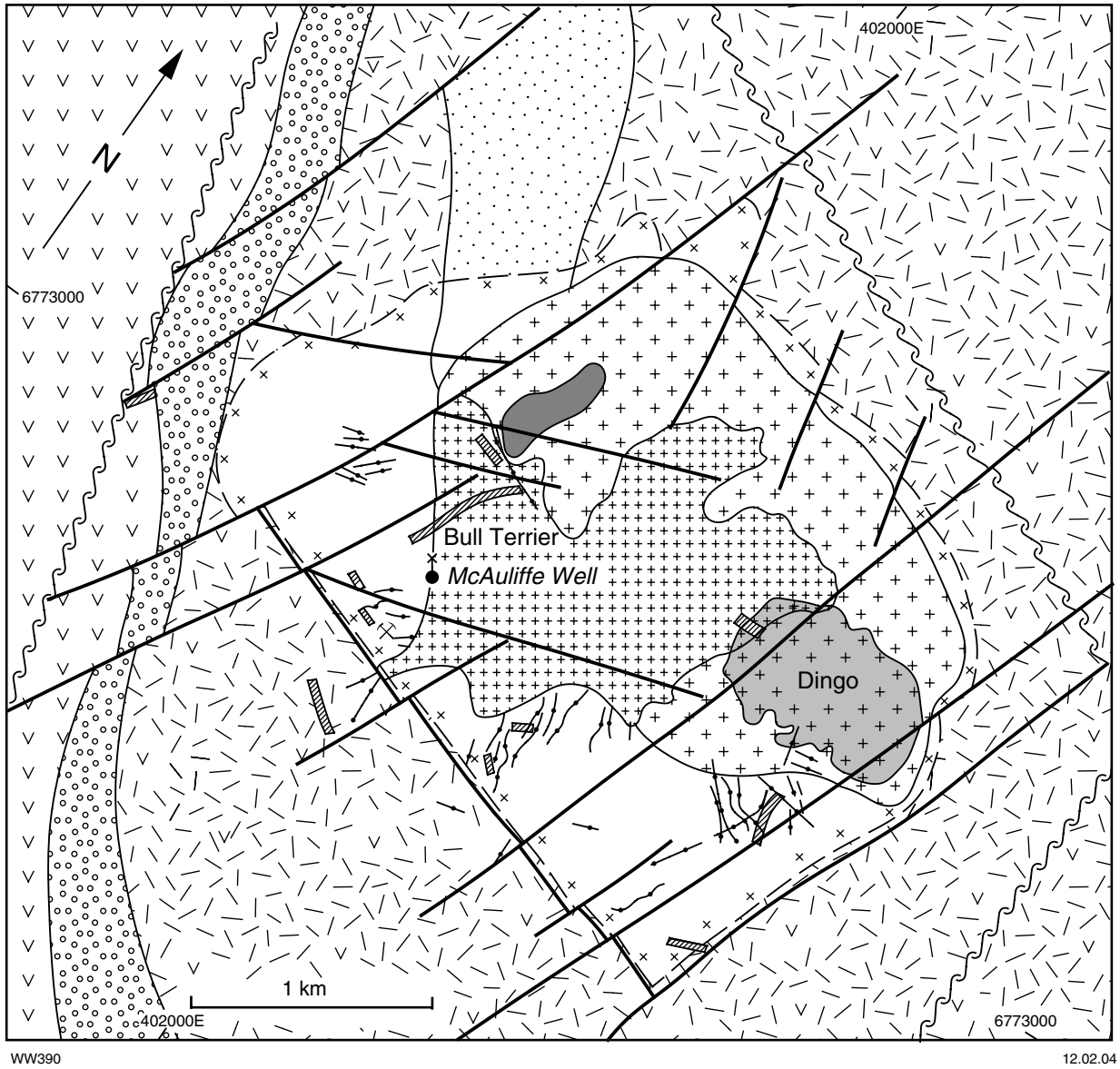

Mineralization

- Superficial mineralization in the regolith
- Skarn
- Zones of quartz veining and microfracturing with associated mineralization
- Historic workings

Structures

- Fault
- Shear zone

Rock types

- Syenite dykes and apophyses
- Subsurface syenite and related rocks (interpreted from aeromagnetic data)
- Syenite subcrop
- Syenite outcrop
- Metasedimentary rocks
- Metabasalt
- Metamorphosed dolerite
- Metamorphosed ultramafic rocks

Figure 4.2. Geological map of the McAuliffe Well area, showing the location of the Bull Terrier and Dingo gold deposits

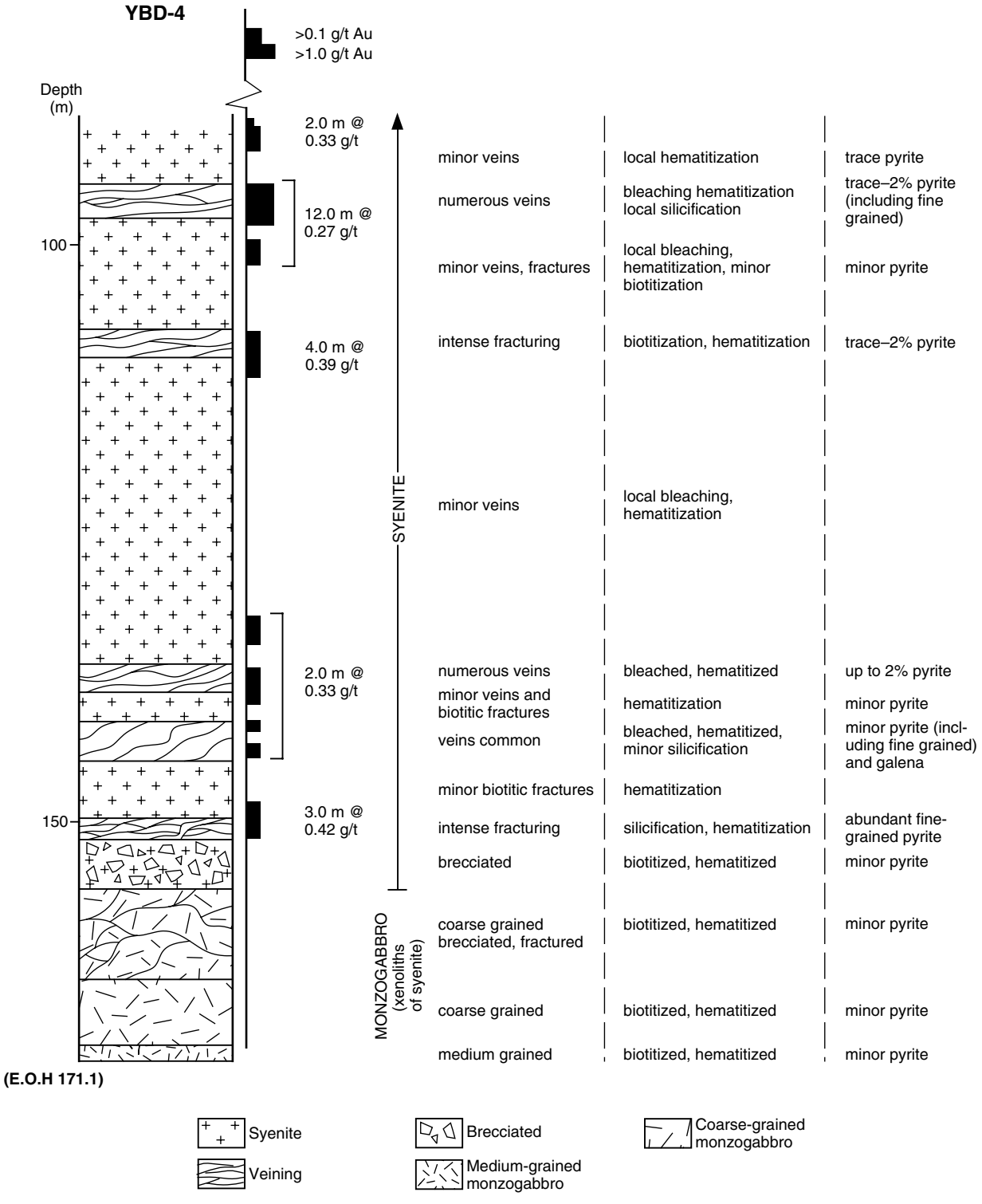

Figure 4.3. Summary log, diamond drillhole YBD-4, Bull Terrier

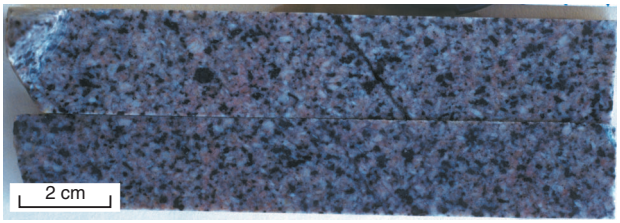

Figure 4.4 McAuliffe Well Syenite, host rock to the Bull Terrier gold deposit, Yerilla mining area

and more pervasive in zones of microfracturing. Hematitization is ubiquitous, producing a deep, brick-red-coloured syenite (Fig. 4.7). Hematitization is commonly associated with alteration of primary amphibole to biotite or chlorite and calcite. Secondary biotite (brown and green varieties) and carbonate have commonly been introduced along fractures. Trace pyrite is present throughout most of the syenite intrusion, but commonly forms 2–3% idioblastic grains (≤2 mm) in zones of veining, fracturing, and hematitization.

More-intense alteration is characterized by destruction of amphiboles (replacement by calcite, minor quartz, biotite, and chlorite), hematitization, carbonation, and pyritization. The best gold grades tend to be in fine-grained, intensely hematitized sections characterized by complete destruction of primary texture, 30–40% calcite, and several percent finely disseminated pyrite. Titanite breaks down to ilmenite and leucoxene. Primary magnetite commonly displays only minor replacement by hematite despite the abundance of fine, dusty, disseminated hematite. Apatite remains stable throughout the alteration halo. No change in the proportions of microcline and albite with increasing intensity of alteration could be recognized.

Representative mineral analyses from sample GSWA 130663B — a syenite with crosscutting microfractures and alteration — are shown in Tables 4.1 – 4.5. Site 1 is relatively unaltered syenite, and the degree of alteration increases through sites 2 and 3 to site 4, which lies within the zone of microfracturing. Microcline is a nearly pure K-feldspar phase with little or no anorthite or albite component. Albite in unaltered, and weakly altered syenite contains minor anorthite but becomes a relatively pure sodium feldspar with increasing intensity of alteration. Mass-balance calculations, based on whole-rock geochemical data, indicate addition of K_2O, Fe_2O_3, and S, and depletion of Na_2O and SiO_2 in mineralized zones (Fig. 4.8).

Mafic rocks (monzogabbro and pyroxenite) contain abundant (probably primary) biotite. Where deformed and altered, ferromagnesian minerals (pyroxene and amphibole) are altered to biotite, chlorite, and carbonate. Feldspars and syenitic xenoliths are strongly hematitized. Brecciated sections are infilled with chlorite and biotite.

References: Metana Minerals NL (1992a,b).

Dingo

Coordinates: 29°29'20"S, 121°56'06"E

Production: No historic production or resource figures are available.

Host rock: Ferruginous, cemented rock (‘protolaterite’) and saprolite developed over syenite.

Structure: This shallow, surficial deposit is possibly underlain by weakly mineralized primary mineralization in syenite. The deposit occupies an area of about 400 × 300 m to a depth of about 10 m.

Alteration: Not applicable.

Westward Ho

Other names: Yerilla G.M. Co. NL, New Westward Ho

Coordinates: 29°31'46"S, 121°49'36"E

Production: 903.7 t of ore for 14.61 kg Au (16.2 g/t Au) between 1897 and 1914.

Host rock: Mafic rock; possibly metamorphosed gabbro or dolerite.

Structure: Several moderately deep shafts and one deeper shaft extend over about 150 m on a subvertical, veined shear zone that trends 010°. The shear zone is up to about 1.5 m wide and contains quartz veins that are up to 20 cm wide, but most are thinner.

Alteration: Altered mine-dump samples are mainly chlorite–carbonate schist.

References: Jutson (1915).

Yerilla Central

Other names: Yerilla Claims Ltd, Lady Florence

Coordinates: 29°28'58"S, 121°49'14"E

Production: 2926.3 t of ore for 101.36 kg Au (34.6 g/t Au) between 1897 and 1911.

Host rock: Mafic greenstones (metamorphosed ?dolerite and plagioclase-phyric dolerite).

Structure: Moderately deep to shallow workings extend over about 300 m on a trend of 315°. The deeper shafts are at the eastern end of the line of workings.

Alteration: Few workings have penetrated the oxidized zone, and weathering largely obscures alteration. However, most dumps contain weathered chlorite–carbonate schist and quartz–sericite schist, in addition to vein quartz.

References: Jutson (1915).

Viola

Other names: Central East, Roscommon

Coordinates: 29°28'56"S, 121°49'18"E

Production: 2954.5 t of ore for 66.53 kg Au (22.5 g/t Au) between 1905 and 1914.

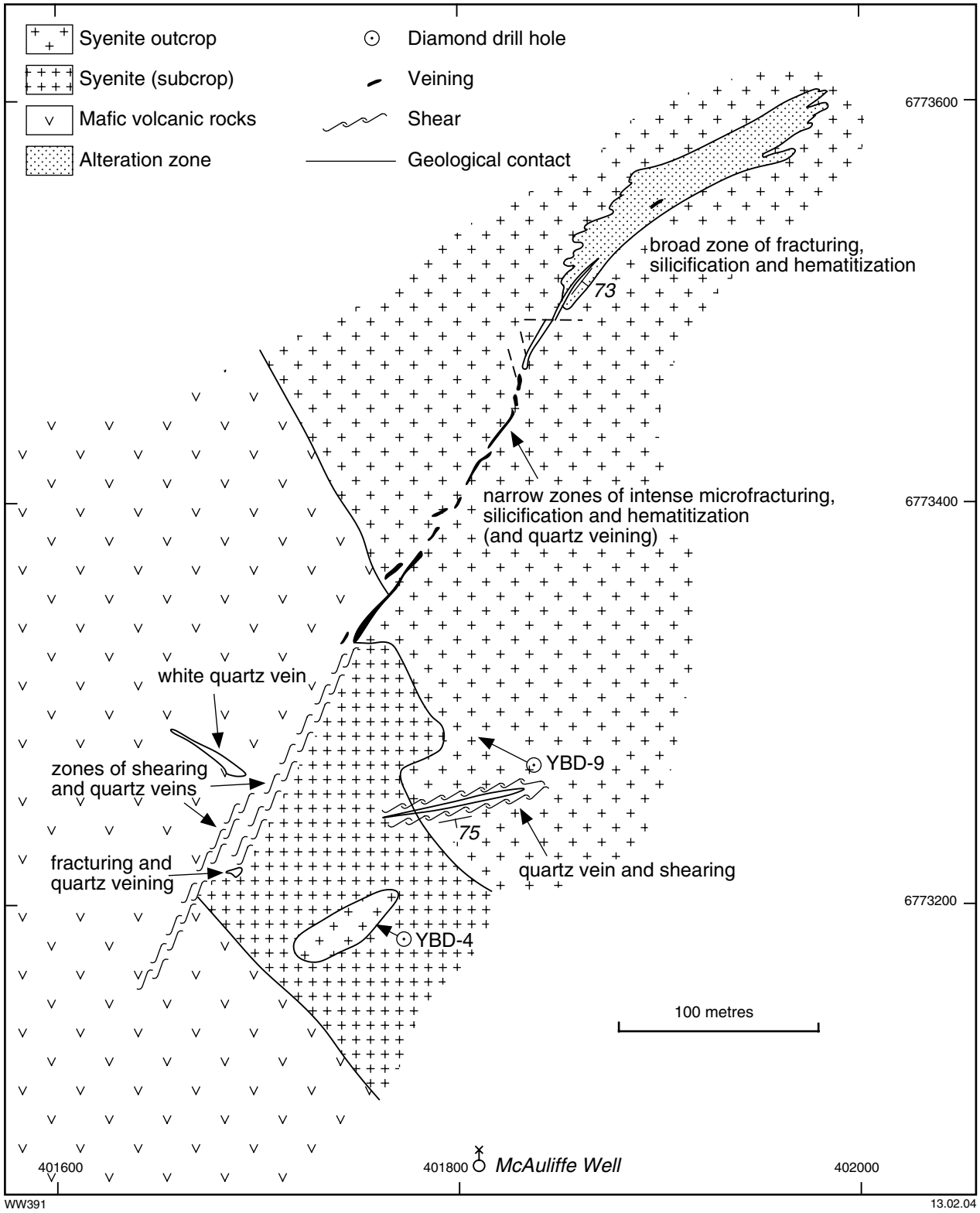

Figure 4.5. Geological map of the Bull Terrier deposit (modified from Metana Minerals NL, 1992b)

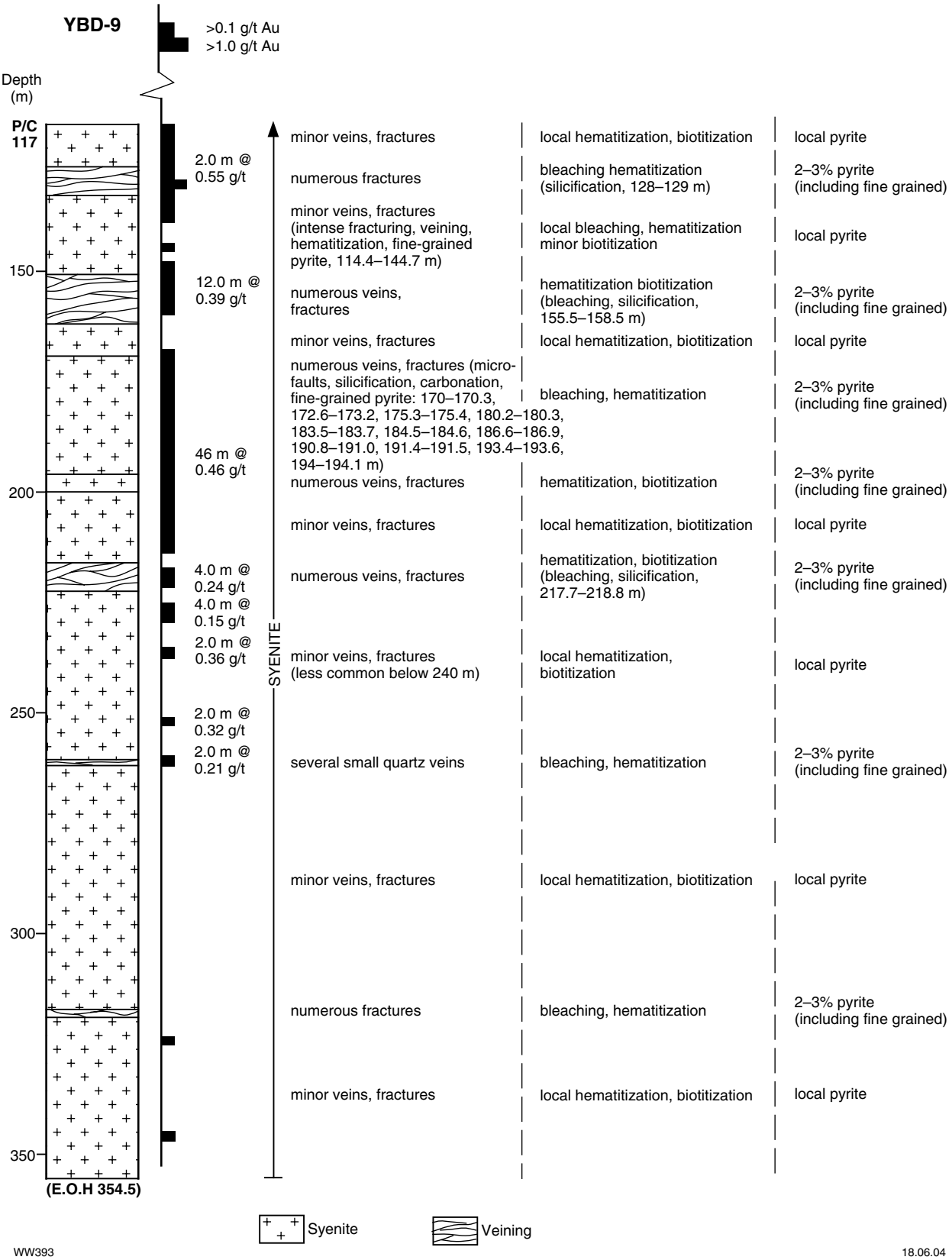

Figure 4.6. Summary log, diamond drillhole YBD-9, Bull Terrier

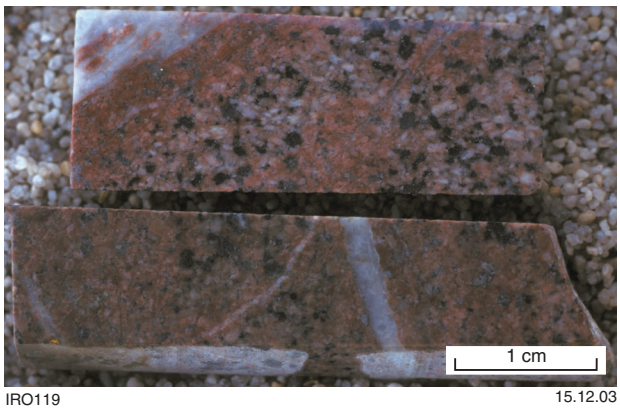

Figure 4.7. Quartz veins and zones of hematitic alteration in McAuliffe Well Syenite

Host rock: Mafic greenstones (metamorphosed ?dolerite and plagioclase-phyric dolerite).

Structure: Shallow to moderately deep workings on a poorly exposed quartz reef that is oriented east–west and dips 35–40°N. Jutson (1915) described the reef as about 1 m thick. Vein quartz is common on mine dumps.

Alteration: Few workings have penetrated the oxidized zone, and weathering largely obscures alteration. However, most dumps contain weathered chlorite–carbonate schist and quartz–sericite schist, in addition to vein quartz. Jutson (1915) reported that gold from this deposit was silver rich, but did not quantify this statement.

References: Jutson (1915).

Yerilla King

Coordinates: 29°29'20"S, 121°49'24"E

Production: 5991.4 t of ore for 142.08 kg Au (23.7 g/t Au) between 1906 and 1947.

Host rock: Mafic rocks of uncertain origin (metamorphosed ?basalt). Jutson (1915) noted the presence of associated granitic dykes.

Structure: A line of workings that includes one deep, timbered shaft and several moderately deep shafts lies on a 170° trend and extends over about 300 m. The structure is not well exposed, but was described by Jutson (1915) as a zone of highly schistose greenstones around and between quartz veins, and is probably a veined brittle–ductile shear in the terminology of Witt (1993). The mineralized shear dips about 45°W and its width varies up to a maximum of about 1 m. The hangingwall contact is described as smooth and regular in contrast to the irregular footwall. There are a number of 'rolls' (flexures associated with steeper dips or dip reversal, and thinning of the 'reef') that pitch to the north. Ore shoots also pitch north, but at a different angle to the flexures reported to be associated with low gold values.

Table 4.1. SEM analyses of amphibole in syenite, sample GSWA 130663B, Bull Terrier deposit

	Primary amphiboles in least-altered syenite host rock (Site 1)		
	AM1	*AM2*	*AM3*
SiO_2	51.11	49.43	49.40
TiO_2	0.15	0.43	0.57
Al_2O_3	2.91	4.29	4.33
FeO	12.39	11.90	12.20
MnO	0.63	0.45	0.68
MgO	15.67	15.19	15.51
CaO	11.15	11.20	11.44
Na_2O	1.29	1.74	1.28
K_2O	0.36	0.38	0.45
Total	**95.66**	**95.0**	**95.83**
Fe/Fe+Mg	0.31	0.30	0.31
Nomenclature	actinolitic hornblende	actinolite	actinolite

NOTE: Nomenclature after Leake (1978)
Site 1 represents the stage of alteration where amphibole is stable, and there is minor relict pyroxene

Table 4.2. SEM analyses of chlorite in altered syenite, sample GSWA 130663B, Bull Terrier deposit

	Chlorite in pseudomorphs after primary amphibole (Site 2)	
	CH1	*CH3*
SiO_2	31.30	31.52
Al_2O_3	13.94	13.66
FeO	16.83	18.37
MgO	22.85	21.91
Total	**84.91**	**85.47**
Fe/Fe+Mg	0.29	0.32

NOTE: Site 2 represents the stage of alteration where amphibole is altered to chlorite and calcite

Alteration: Chlorite–carbonate schist and quartz–sericite schist are on the deeper mine dumps. Jutson (1915) reported the presence of pyrite and galena.

References: Jutson (1915).

Melba Consols

Other names: Melba Consols G.M. Co., Melba, Melba Proprietary, Lady Ailsa

Coordinates: 29°28'52"S, 121°49'09"E

Production: 1260.9 t of ore for 17.98 kg Au (14.3 g/t Au) between 1903 and 1915. A second group of workings, 60–70 m west of the main Melba workings, was called West Melba by Jutson (1915), but no separate production against this name was recorded in the Cancelled Gold Mining Leases report of 1954 (Department of Mines Western Australia, 1954).

Table 4.3. SEM analyses of carbonate minerals in altered syenite, sample GSWA 130663B, Bull Terrier deposit

	Calcite (finely intergrown with quartz) in pseudomorphs after primary amphibole			*Calcite (finely intergrown with quartz) in pseudomorphs after primary amphibole*		*Coarse dissemination or deformed band of calcite*	
	Site 2			*Site 3*		*Site 4*	
	CB2	*CB5*	*CB6*	*CB8*	*CB10*	*CB13*	*CB15*
SiO_2	–	0.34	0.29	0.83	2.45	–	0.37
FeO	0.20	0.63	0.25	0.39	2.65	0.17	0.46
MnO	1.49	1.49	1.07	1.02	0.79	1.66	0.62
MgO	–	0.39	–	–	1.80	–	–
CaO	52.65	54.36	54.91	56.90	48.69	57.77	53.71
Total	**54.34**	**57.21**	**56.52**	**59.13**	**56.38**	**59.60**	**55.16**
$FeCO_3$	0.3	0.9	0.3	0.5	3.8	0.2	0.7
$MnCO_3$	2.2	2.1	1.5	1.4	1.2	2.2	0.9
$MgCO_3$	–	1.0	–	–	4.6	–	
$CaCO_3$	97.5	96.1	98.1	98.1	90.4	97.6	98.4

NOTE: Sites 2 to 4 represent progressive stages of alteration, as follows:
Site 2. Amphibole altered to chlorite and calcite
Site 3. Amphibole altered to quartz, sericite, and calcite
Site 4. Destruction of primary texture; intense hematitization and pyritization

Table 4.4. SEM analyses of K-feldspar in syenite and altered syenite, sample GSWA 130663B, Bull Terrier deposit

	Site 1		*Site 2*		*Site 3*		*Site 4*	
	KF2	*KF4*	*KF5*	*KF7*	*KF8*	*KF9*	*KF11*	*KF13*
SiO_2	63.91	64.02	63.62	63.52	64.08	63.57	63.78	63.93
Al_2O_3	17.96	17.54	17.52	17.99	17.56	17.78	18.01	18.03
Na_2O	0.30	–	–	–	–	–	–	–
K_2O	16.99	16.88	16.87	16.79	16.93	16.76	16.76	16.81
Total	**99.17**	**98.45**	**98.01**	**98.30**	**98.56**	**98.11**	**98.56**	**98.78**
An	–	–	–	–	–	–	–	–
Ab	2.6	–	–	–	–	–	–	–
Or	97.3	100	100	100	100	100	100	100

NOTE: Sites 1 to 4 represent progressive stages of alteration, as follows:
Site 1. Amphibole stable, minor relict pyroxene
Site 2. Amphibole altered to chlorite and calcite
Site 3. Amphibole altered to quartz, sericite, and calcite
Site 4. Destruction of primary texture; intense hematitization and pyritization

Table 4.5. SEM analyses of albite in syenite and altered syenite, sample GSWA 130663B, Bull Terrier deposit

	Site 1		*Site 2*		*Site 3*		*Site 4*	
	AB2	*AB3*	*AB4*	*AB5*	*AB8*	*AB9*	*AB11*	*AB12*
SiO_2	67.81	67.76	65.81	66.73	68.27	67.96	68.28	68.56
Al_2O_3	19.62	19.85	20.06	20.60	19.27	19.12	19.18	19.20
CaO	–	0.59	0.82	1.05	–	–	–	–
Na_2O	10.83	10.77	10.32	10.40	10.96	11.09	11.23	11.30
K_2O	–	–	0.16	0.11	0.07	–	0.07	–
Total	**98.26**	**98.96**	**97.18**	**98.89**	**98.58**	**98.18**	**98.76**	**99.05**
An	–	2.9	4.2	5.3	–	–	–	–
Ab	100	97.1	94.9	94.1	99.5	100	99.6	100
Or	–	–	1.0	0.7	0.4	–	0.4	–

NOTE: Sites 1 to 4 represent progressive stages of alteration, as follows:
Site 1. Amphibole stable, minor relict pyroxene
Site 2. Amphibole altered to chlorite and calcite
Site 3. Amphibole altered to quartz, sericite, and calcite
Site 4. Destruction of primary texture; intense hematitization and pyritization

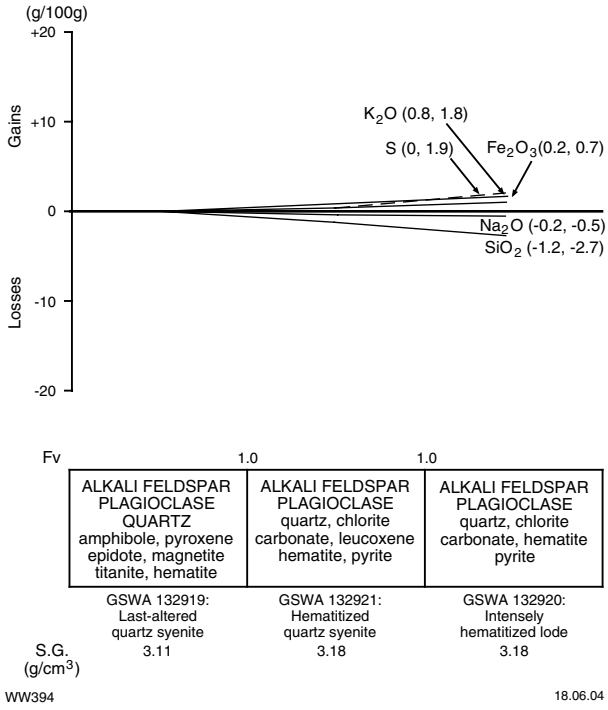

Figure 4.8. Mass-balance changes (calculated using the method of Gresens, 1967) associated with an intensely hematitized ore zone in the McAuliffe Well Syenite, Bull Terrier deposit, Yerilla mining area. Mineral components of alteration assemblages are listed in approximate order of abundance, with main mineral components in upper case and minor mineral components in lower case

Host rock: Massive, coarse-grained, equigranular granite.

Structure: Shallow workings are distributed over about 200 m on a north–south trend, deviating to a northeasterly trend at its northern end. A reef, about 0.2 – 0.5 m thick and consisting of up to four quartz veins, dips 45°W and is accessed by several deep, timbered shafts. The deepest workings are in the vicinity of the change in trend of the reef from north to northeast. The quartz veins are brittle structures with little associated ductile deformation of the granite wallrocks.

The West Melba deposit is another north–south reef that dips to the east.

Alteration: Samples from mine dumps and surface exposures give no visible evidence of alteration adjacent to mineralized quartz veins.

References: Jutson (1915).

Queen of the Earth

Other names: King-of-the-Earth, Queen-of-the-Earth

Coordinates: 29°28'41"S, 121°49'02"E

Production: 515.2 t of ore for 14.49 kg Au (28.1 g/t Au) between 1897 and 1907.

Host rock: Metamorphosed fine-grained, aphyric basalt and plagioclase-phyric basalt.

Structure: Moderately deep shafts and shallow workings are focused on two subvertical, brittle–ductile shear zones with quartz veins. The main workings follow a 340–350°-trending shear zone and are conformable within the regional foliation. The second shear zone, to the west, is oriented about 020°. The workings extend over 300 m. The shear zones are up to 7 m wide, and the veins within the shear zones are up to 3 m wide, but average 60–70 cm.

Alteration: Mine-dump samples include chlorite–carbonate schist and quartz–sericite schist with limonitic pseudomorphs after idioblastic pyrite.

References: Montgomery (1906), Jutson (1915).

Lady Gertrude

Other names: Gertrude, Lady Gertrude South

Coordinates: 29°27'39"S, 120°48'35"E

Production: 280.9 t of ore for 8.43 kg Au (30.0 g/t Au) between 1897 and 1899.

Host rock: Weathered mafic rock and felsic schist after volcaniclastic sedimentary rock.

Structure: Two subparallel lines of workings, separated by about 300 m, lie on 320–330° trends. The deeper workings lie on the western line, which extends over about 100 m, whereas shallow to moderately deep workings on the eastern line extend over almost 400 m. Both structures are poorly exposed, but vein quartz and weathered schist are common on most mine dumps, suggesting that mineralization is within veined, brittle–ductile shear zones that are more or less conformable with the regional foliation.

Alteration: Alteration is obscured by weathering.

McGregor North

Other names: McGregor, Queen of the Earth No. 9 North

Coordinates: 29°26'55"S, 121°48'13"E

Production: 264.1 t of ore for 4.88 kg Au (18.5 g/t Au) between 1897 and 1906.

Host rock: Mafic rock (?metadolerite).

Structure: Shallow to moderately deep workings extend for about 100 m on a subvertical, north-trending shear zone. Vein quartz is moderately common on most mine dumps.

Alteration: Mine dumps are dominated by chlorite–carbonate schist.

References: Montgomery (1906).

La Tosca

Other names: La Tosca Gold Mines

Coordinates: 29°19'20"S, 121°45'44"E

Production: 389.3 t of ore for 10.16 kg Au (26.1 g/t Au) between 1897 and 1901.

Host rock: Felsic schist after volcaniclastic sedimentary rocks. Unpublished petrographic descriptions (Hannans Gold Ltd, 1987) suggest that the schist is a metamorphosed plagioclase-phyric, andesitic to dacitic tuff or epiclastic sedimentary rock.

Structure: Numerous workings, including a deep shaft and open stopes, expose a 300 m-long, 0.5–1.0 m-wide shear zone. The shear zone strikes 005° and dips subvertically to 80°E. It consists of foliation-parallel quartz veins (10–50 cm wide) within a broader zone of ductile deformation.

Alteration: Alteration is obscured by weathering, but weathered, carbonated, sericitic schist can be recognized on several mine dumps.

References: Hannans Gold Ltd (1987).

References

DEPARTMENT OF MINES WESTERN AUSTRALIA, 1954, List of cancelled gold mining leases which have produced gold: Western Australia Department of Mines, 271p.

GRESENS, R. L., 1967, Composition–volume relationships of metasomatism: Chemical Geology, v. 2, p. 47–65.

GROVES, D. I., BARLEY, M. E., and HO, S. E., 1989, The nature, genesis and tectonic setting of mesothermal gold mineralization in the Yilgarn Block, Western Australia, *in* The geology of gold deposits: The perspective in 1988 *edited by* R. R. KEAYES, W. R. H. RAMSAY, and D. I. GROVES: Economic Geology, Monograph 6, p. 71–85.

HANNANS GOLD LTD, 1987, Annual report on P31/00695 and P31/00200–00201 La Tosca: Western Australia Geological Survey, Statutory mineral exploration report, Item 4271 A23318 (unpublished).

JUTSON, J. T., 1915, The mining geology of Yerilla, North Coolgardie Goldfield: Western Australia Geological Survey, Bulletin 64, p. 13–45.

LEAKE, B. E., 1978, Nomenclature of amphiboles: American Mineralogist, v. 63, p. 1023–1053.

LIBBY, W. G., 1989, Chemistry of plutonic felsic rocks in the Eastern Goldfields, Western Australia: Western Australia Geological Survey, Report 26, p. 83–104.

METANA MINERALS NL, 1992a, Report, Jul 1991 to Mar 1992 on E31/58, P31/1412–1413, and M31/107: Western Australia Geological Survey, Statutory mineral exploration report, Item 11660 A35792 (unpublished).

METANA MINERALS NL, 1992b, Annual report, Jan 1992 to Dec 1992 on E31/58, E31/84, P31/1412–1413, M31/112, M31/105, M31/110 and M31/107: Western Australia Geological Survey, Statutory mineral exploration report, Item 11660 A37013 (unpublished).

MONTGOMERY, A., 1906, Report on the state of mining progress in the Kurnalpi, Mulgabbie, Pinjin, Edjudina, Yarri, and Yerilla Districts: Western Australia Department of Mines, Annual Report for 1905, p. 82–97.

NELSON, D. R., 1997, Compilation of SHRIMP U–Pb zircon geochronology data 1996: Western Australia Geological Survey, Record 1997/2, 189p.

OLIVER, N. H. S., VALENTA, R. K., and WALL, V. J., 1990, The effect of heterogeneous stress and strain on metamorphic fluid flow, Mary Kathleen, Australia, and a model for large-scale fluid circulation: Journal of Metamorphic Geology, v. 8, p. 311–331.

PERRING, C. S., ROCK, N. M. S., GOLDING, S. D., and ROBERTS, D. E., 1989, Criteria for the recognition of metamorphosed or altered lamprophyres: a case study from the Archaean of Kambalda, Western Australia: Precambrian Research, v. 43, p. 215–237.

SWAGER, C. P., 1997, Tectono-stratigraphy of late Archaean greenstone terranes in the southern Eastern Goldfields, Western Australia: Precambrian Research, v. 83, p. 11–42.

WITT, W. K., 1993, Gold mineralization in the Menzies–Kambalda region, Eastern Goldfields, Western Australia: Western Australia Geological Survey, Report 39, 165p.

WITT, W. K., and DAVY, R., 1997, Geology and geochemistry of granitoids in the southwest Eastern Goldfields Province, Western Australia: Western Australia Geological Survey, Report 49, 137p.

WITT, W. K., SWAGER, C. P., and NELSON, D. R., 1996, 40Ar/39Ar and U–Pb constraints on the timing of gold mineralization in the Kalgoorlie gold field, Western Australia: a discussion: Economic Geology, v. 91, p. 792–795.

5. Yilgangi

The Yilgangi Fault forms the western boundary of the Mulgabbie domain of the Kurnalpi Terrane (Swager, 1997). A sedimentary basin containing coarse clastic rocks lies immediately east of the Yilgangi Fault and unconformably overlies greenstones of the Mulgabbie Terrane. Metamorphosed polymictic conglomerate, wacke, and quartzofeldspathic sandstone and siltstone in the sedimentary basin are tightly folded. Swager (1995) interpreted the basin to have formed during an extensional episode that post-dates D_1 but pre-dates D_2. The sedimentary units have been intruded by plugs and discordant sheets of monzodiorite porphyry dated at 2662 ± 5 Ma (Nelson, 1995).

The main producing mines in this sedimentary basin are hosted by metamorphosed quartzofeldspathic sandstone and siltstone (e.g. Yilgangi Queen — 1 t Au), with some mineralization also within the monzodiorite (e.g. Yilgangi King — 11 kg Au). At the southern end of the mining camp there is a small mine (Quondong) located in a small syenitic intrusion.

Gold is associated with quartz veining in brittle faults that trend 330–350° and dip steeply to 70°W. Reverse movement on these faults is implied by the gently plunging ore shoots at Yilgangi Queen, which have formed where the fault flattens as it cuts relatively competent sedimentary units. The main zone of gold deposits lies where bedding and contacts between monzodiorite and sedimentary rocks are oriented north–south. Brittle fracture and mineralization appear to have formed where contacts between units of contrasting competency were oriented approximately normal to the east–west regional σ_1. Altered metasedimentary rocks adjacent to mineralized quartz veins are altered to quartz–muscovite–carbonate assemblages with idioblastic pyrite and arsenopyrite. Alteration involves addition of SiO_2 and K_2O to the metasedimentary host rocks.

Deposits of the Yilgangi area

Yilgangi Queen

Other names: Melody, Heppingstone, Bradfords, Golden Hill, Lynas Gold NL

Coordinates: 29°42'51"S, 122°09'45"E

Production: 42 350.9 t of ore for 1095.06 kg Au (25.9 g/t Au) between 1935 and 1982. The indicated resource (MINEDEX site code S00790) is 22 000 t at 10.1 g/t Au (222.2 kg Au).

Host rock: Metamorphosed fine-grained wacke and feldspathic siltstone. Mineralization is localized near the contact with a relatively mafic metasedimentary unit to the east.

Structure: Several deep shafts and numerous shallower pits and shafts extend over about 1 km, and are located on four subparallel, 340–360°-trending quartz reefs (Fig. 5.1). The deeper shafts are located on the Yilgangi–Melody reef system. All reefs are offset by about 55 m across a subvertical, west-northwesterly trending dextral fault. The reefs are 1–2 m-wide faults that dip about 70°W. They consist of quartz veins (mostly 20–30 cm, but up to 1 m wide) and interspersed zones of fractured and altered wallrock. Mineralization is present where the reefs flatten as they refract across relatively competent units in a steeply dipping metasedimentary sequence. These sites would be dilational during reverse movements on the mineralized faults. Asymmetric, quartz-fibre-filled pressure shadows against idioblastic arsenopyrite in altered wallrocks indicate that the mineralized reefs were associated with some fault movement. Gently south plunging ore shoots are probably controlled by the intersection between the mineralized faults and relatively competent sedimentary units.

Alteration: Alteration halos associated with the mineralized reefs are up to 20 m wide. A broad zone of muscovite–chlorite–dolomite(–pyrite) envelopes a narrower mineralized zone dominated by quartz, calcite, muscovite, and albite with idioblastic pyrite and arsenopyrite and minor chalcopyrite (Fig. 5.2). Tourmaline is a common accessory in some samples. Mass-balance calculations, based on whole-rock geochemical data, indicate addition of SiO_2 and K_2O to the altered metasedimentary host rock (Fig. 5.3). CO_2 is also added to strongly altered and mineralized wallrocks; less-intensely altered metasedimentary rocks show addition of FeO and depletion of Na_2O.

The unmineralized, relatively mafic metasedimentary unit to the east is altered to chlorite-rich schist and hosts quartz–calcite veins.

References: Lynas Gold NL (1993), Swager (1995).

Yilgangi

Coordinates: 29°45'43"S, 122°10'17"E

Production: 1094.0 t of ore for 18.83 kg Au (17.2 g/t Au) between 1903 and 1905.

Host rock: Well-sorted, metamorphosed quartzofeldspathic sandstone. Tourmaline is locally abundant. Monzodiorite is also in the mine environment and may be a less important host to mineralization.

Structure: Deep shafts and open stopes have been sunk over about 200 m strike length on a 350°-trending lode in metasedimentary rocks. The lode is a 0.5 to 1 m-wide zone of fracturing, quartz veins (≤10 cm), and minor ductile deformation. The zone and some of the veins within it dip 70–80°W. Other sets of veins, oriented 340° (45°SW dip) and 050° (25°NW dip), extend beyond the margins of the central zone of fracturing.

Alteration: Sedimentary rocks within the central zone of fracturing are altered to quartz(–feldspar)–muscovite–carbonate schist with idioblastic pyrite and arsenopyrite.

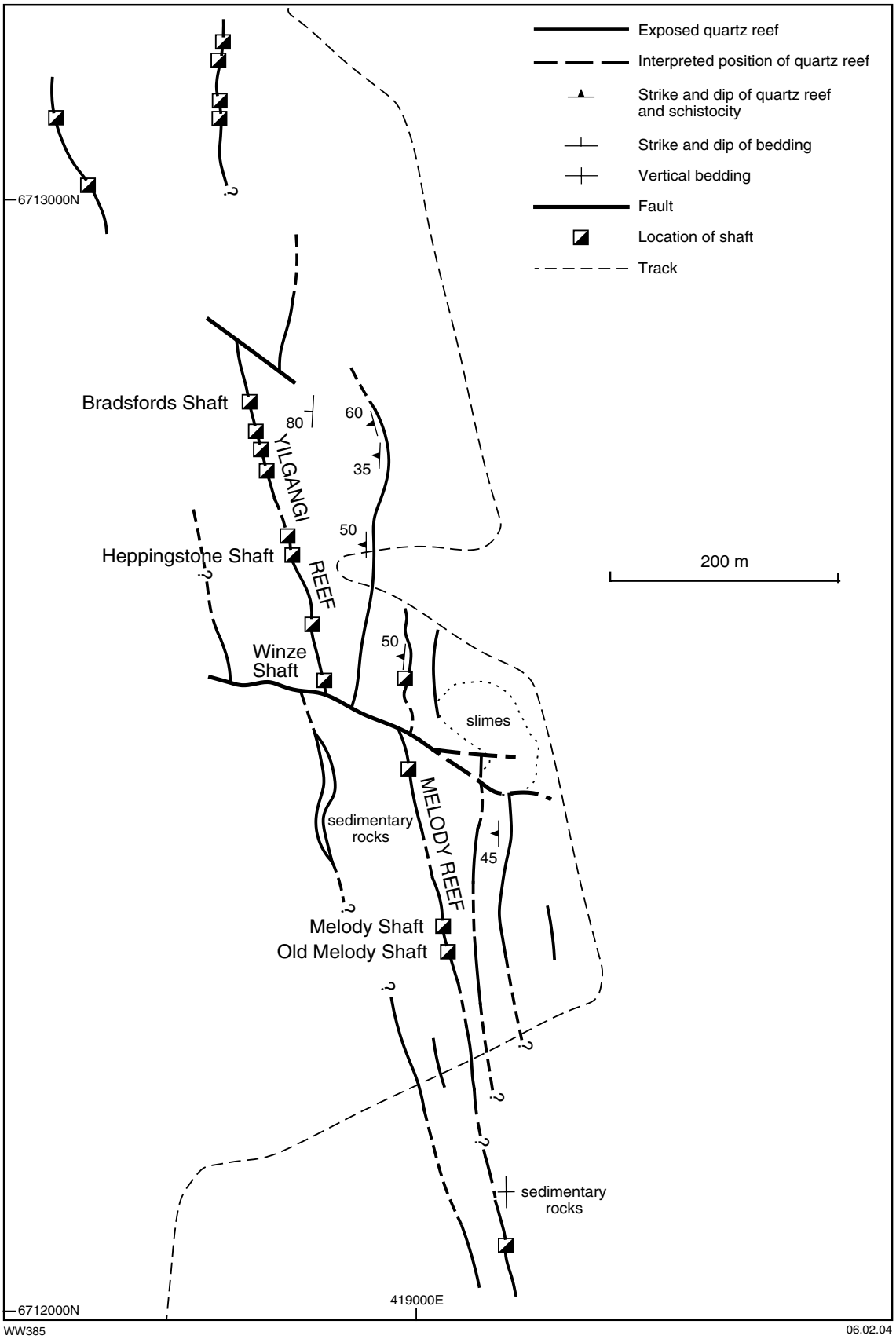

Figure 5.1. Geological map of the Yilgangi Queen mine area (after Lynas Gold NL, 1993)

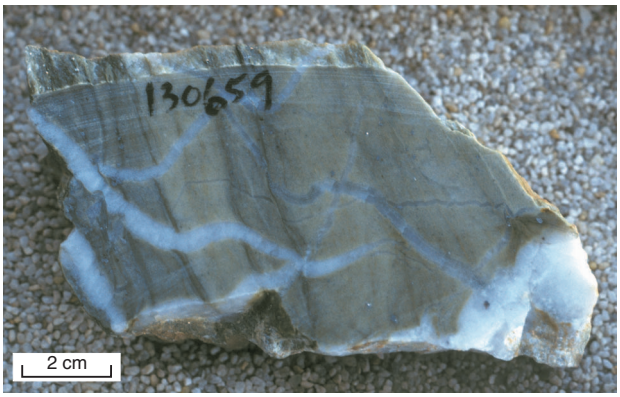

Figure 5.2. Quartz veins and idioblastic sulfides in quartz–calcite–muscovite–albite rock (altered sedimentary rock), Yilgangi Queen deposit, Yilgangi mining area

Quartz veins contain smaller amounts of carbonate and pyrite. Wallrocks that host veins outside this central zone contain minor muscovite and pyrite. Mass-balance calculations, based on whole-rock geochemical data, indicate addition of SiO_2, CO_2, CaO, and K_2O to altered, mineralized host rocks; these changes are accompanied by minor depletion of Na_2O (Fig. 5.4).

Altered monzodiorite contains secondary carbonate and muscovite and disseminated, idioblastic arsenopyrite. Quartz veins contain minor albite where hosted by monzodiorite.

References: Swager (1995).

Yilgangi King

Coordinates: 29°46'26"S, 122°43'04"E

Production: 636.00 t of ore for 11.36 kg Au (17.9 g/t Au) between 1924 and 1974.

Host rock: Massive monzodiorite porphyry.

Structure: Two moderately deep shafts and several shallow pits have been sunk over about 100 m strike length on a 330° trend. A small (historic) openpit at one end of the workings exposes a 330°-trending quartz vein (10–20 cm wide) that dips about 70°SW. A stacked series of quartz veins and subparallel fractures in the footwall of this vein dips 15–45°NW. Individual quartz veins are up to 1 m thick. Arching (?rotation) of these footwall veins adjacent to the 330°-trending quartz vein suggests that they formed as a result of reverse movement on a 330°-trending fault.

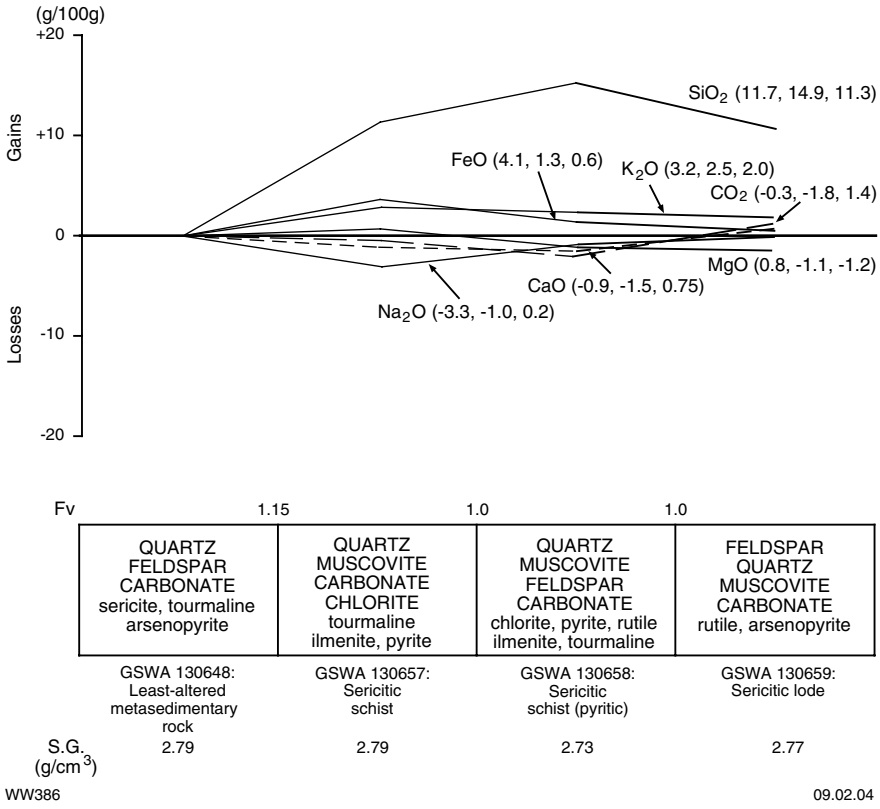

Figure 5.3. Mass-balance changes (calculated using the method of Gresens, 1967) associated with alteration of mineralized sedimentary rock, Yilgangi Queen deposit, Yilgangi mining area. Mineral components of alteration assemblages are listed in approximate order of abundance, with main mineral components in upper case and minor mineral components in lower case

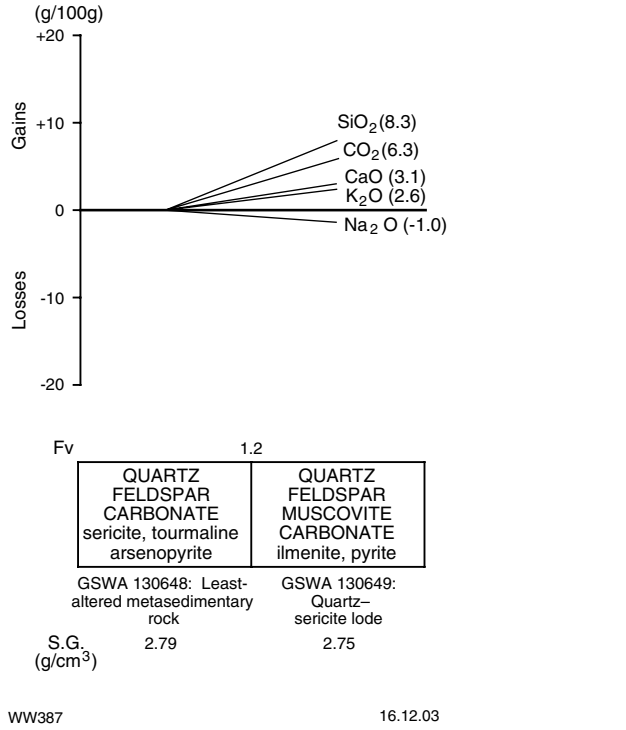

Figure 5.4. Mass-balance changes (calculated using the method of Gresens, 1967) associated with alteration of mineralized sedimentary rock, Yilgangi deposit, Yilgangi mining area. Mineral components of alteration assemblages are listed in approximate order of abundance, with main mineral components in upper case and minor mineral components in lower case

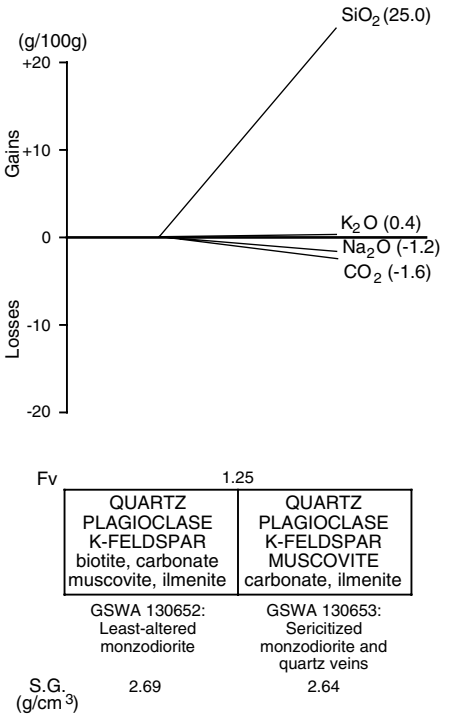

Figure 5.5. Mass-balance changes (calculated using the method of Gresens, 1967) associated with alteration of mineralized monzodiorite, Yilgangi King deposit, Yilgangi mining area. Mineral components of alteration assemblages are listed in approximate order of abundance, with main mineral components in upper case and minor mineral components in lower case

Alteration: Visible alteration selvages adjacent to stacked quartz–carbonate(–albite) veins could not be identified. Examination of thin sections revealed widespread sericitization of feldspars and minor carbonate. Chemical changes accompanying alteration of mineralized monzodiorite are minimal, apart from the addition of SiO_2 (Fig. 5.5).

References: Swager (1995).

References

GRESENS, R. L., 1967, Composition–volume relationships of metasomatism: Chemical Geology, v. 2, p. 47–65.

LYNAS GOLD NL, 1993, Report on M31/14: Western Australia Geological Survey, Statutory mineral exploration report, Item 11659 A39251 (unpublished).

NELSON, D. R., 1995, Compilation of SHRIMP U–Pb zircon dates, 1994: Western Australia Geological Survey, Record 1995/03, 244p.

SWAGER, C. P., 1995b, Geology of the Edjudina and Yabboo 1:100 000 sheets: Western Australia Geological Survey, 1:100 000 Geological Series Explanatory Notes, 43p.

SWAGER, C. P., 1997, Tectono-stratigraphy of late Archaean greenstone terranes in the southern Eastern Goldfields, Western Australia: Precambrian Research, v. 83, p. 11–42.

6. Karonie–Roe

The Karonie area (including Roes Find) saw little historic gold production, but came to notice in the 1990s through mining developments at the Main and West Zones and Harrys Hill openpit mines at Karonie, which have a combined resource (production plus reserves) of 6.7 t of gold. These deposits are in a north-trending, steeply west dipping belt of rocks (mainly amphibolite and felsic metasedimentary rocks) near the eastern margin of the greenstones of the Eastern Goldfields Granite–Greenstone Terrane. There are a number of granitoids in the area, the most significant being the Erayinia Granitoid Complex (Smithies, 1994) and the Cardunia Rocks Monzogranite. The former has been dated at about 2636 Ma by the conventional U–Pb zircon method (de Luca, 1995) and the latter at 2638 ± 26 Ma by SHRIMP (Hill et al., 1992). The Cardunia Rocks Monzogranite is a fractionated, hornblende-bearing, leucocratic body with accessory fluorite and cassiterite (de Luca, 1995). The Karonie greenstone belt is cut by several late, northeast-trending cross-faults. These show apparent sinistral offset of contacts between greenstones and the Erayinia Granitoid Complex, but apparent dextral displacement of steeply dipping greenstones is evident east of Karonie railway siding (see **Main and West Zones**).

The host rocks at Karonie are medium- to coarse-grained amphibolites (after ?dolerite), locally containing quartz, within finer grained amphibolite (?metabasalt). The high ilmenite content and whole-rock geochemistry indicate tholeiitic precursors for the amphibolites (de Luca, 1995). There are also minor, thin interbeds of quartz–biotite(–plagioclase–K-feldspar–almandine–garnet) metasedimentary rock and more rarely, metamorphosed black shale. The quartz–biotite metasedimentary rock is a dense, fine- to medium-grained rock with a granoblastic fabric, but cross-bedding and flame structures are locally preserved. One of the metasedimentary units is prominently exposed in the Main Zone pit, and defines a tight, shallowly north plunging ($?F_2$) fold at the northern end of the pit (see **Main and West Zones**).

In the Main and West Zones mine area, metamorphic grade is estimated to be mid- to upper amphibolite facies, based on the presence of hornblende, calcic plagioclase (andesine), and less commonly cummingtonite and almandine garnet in mafic rocks. These high-grade assemblages were described by de Luca (1995) as being confined between strike-parallel faults, with lower grade, actinolite-bearing mafic rocks to the east and west, suggesting late (post-metamorphic) differential uplift.

The deposits at Karonie are located in a broad zone of ductile shear and hydrothermal alteration (Fig. 6.1). Asymmetric folds that imply dextral movement are widely developed in pyroxene-bearing calc-silicate assemblages on the eastern margin of the Main and West Zones pit. The quartz–biotite metasedimentary unit in this pit may have been a relatively competent unit at the high temperatures accompanying ductile deformation. If shear strain developed during dextral movement, ore-grade zones lie within the pressure shadow of this unit, consistent with their formation in domains of low mean stress. However, the interpretation is equivocal because the asymmetric folds may be related to a nearby anticline instead of simple shear.

North-trending brittle–ductile faults (‘marker units’ in local mine terminology) produce sinistral offset of metasedimentary units in the Main and West Zones pit. The right-stepping, en echelon geometry of the ore lenses, especially notable in the Harrys Hill pit, may be due to sinistral displacement on brittle–ductile faults. Associated quartz(–amphibole–biotite–carbonate–pyrrhotite, and even, in rare cases, pyroxene) veins indicate moderately high temperatures during this later phase of faulting. Sinistral movement on these late, brittle–ductile faults implies a north–south axis of compression, which is anomalous with respect to the far-field stress regime (east–west) during regional deformation throughout most of the Eastern Goldfields Granite–Greenstone Terrane. The anomalous late stress regime at Karonie may be related to accretion of Mesoproterozoic rocks to the south during the Albany–Fraser Orogeny (Myers, 1995). However, this interpretation appears to be inconsistent with the relatively high temperature alteration assemblages that were stable during activity on late brittle–ductile faults.

Within the shear zone, there are four types of alteration (Table 6.1), characterized by biotite-rich assemblages, mafic gneiss, calc-silicate assemblages, and late alteration related to discrete brittle–ductile faults (‘marker units’). Alternating bands of these assemblages are present throughout the zone of ductile shear and are oriented approximately parallel to the margins of the shear zone. However, local crosscutting relationships allow relative timing of events to be determined and indicate that calc-silicate alteration post-dated formation of biotite-rich assemblages. Fabric relationships indicate contemporaneity of ductile deformation and hydrothermal alteration, with metamorphic recrystallization and strain recovery outlasting ductile deformation. Mass-balance

IRO81 15.12.03

Figure 6.1. South face of Karonie Main Zone pit, showing the broad zone of ductile shear that constitutes the orebody. Late quartz and carbonate veins are in the left hand corner of the pit

Table 6.1. Mineral assemblages in amphibolite and altered amphibolite, Karonie Main and West Zones deposits

'Unaltered' amphibolite	*Mafic gneiss*	*Biotite alteration*	*Calc-silicate alteration*	*'Marker units'*
HORNBLENDE	HORNBLENDE	BIOTITE	DIOPSIDE	BIOTITE
CALCIC PLAGIOCLASE	CALCIC PLAGIOCLASE	CALCIC PLAGIOCLASE	CALCIC PLAGIOCLASE	CALCIC PLAGIOCLASE
			EPIDOTE	K-FELDSPAR
				(in 'marker units')
Quartz	Quartz	QUARTZ	Quartz	QUARTZ
		Hornblende	Hornblende	Hornblende
	Carbonate	Carbonate	Carbonate	Carbonate
Ilmenite	Ilmenite	Ilmenite	Titanite	Ilmenite
	Titanite	Titanite	Rutile	Titanite
	Pyrrhotite	Pyrrhotite	Pyrrhotite	Pyrrhotite
	Pyrite	Pyrite	Pyrite	Pyrite

NOTES: Minerals shown in upper case are essential minerals and commonly form >10% of the rock
Minerals shown in lower case are minor to accessory phases

calculations, indicate addition of CaO, Na_2O, and SiO_2 in the development of clinopyroxene-bearing calc-silicate alteration and mafic gneiss (sodic–calcic alteration). This style of alteration is similar to that at Yundamindera and potentially has similar implications for up-temperature fluid flow.

As with other amphibolite-facies-hosted deposits (Ridley, 1990; McCuaig et al., 1993), alteration zoning is complex and poorly defined on the larger scale, but is well defined around smaller scale structures (e.g. individual bands or veins). Thus, the units shown in representative drill logs only portray the dominant rock type in each interval of drillcore. For example, intervals of mafic gneiss commonly contain bands of calc-silicate altered rock, and altered rock units typically contain bands of mafic gneiss.

In other amphibolite-facies-hosted deposits (Ridley, 1990; McCuaig et al., 1993), an outer, biotite amphibolite passes into a diopside-dominated calc-silicate assemblage at the centre of the mineralized shear. The inner, calc-silicate zone hosts the greater part of gold mineralization in these high-temperature orebodies. The Karonie deposits are different in that the main ore zones tend to be flanked by ferrosalite-bearing calc-silicate alteration assemblages, and mineralization tends to be associated with mafic gneiss (± bands of biotite) and bands of amphibole that may represent selvages between mafic gneiss and calc-silicate alteration. Although the two styles of alteration at Karonie are associated with one another on the scale of the regional shear zone, bands of biotitization and clinopyroxene-bearing calc-silicate alteration are independent of one another. Crosscutting and overprinting relationships, although rare, suggest that two distinct hydrothermal fluids were present and that biotitization pre-dated pyroxene-bearing calc-silicate alteration. Given the larger scale relationships between the two alteration types, it is considered likely that the two alteration styles reflect a temporal evolution of the same fluids, rather than two distinct fluid sources.

Phase diagrams published by Mikucki and Ridley (1993) and Ridley (1990) provide some insight into the hydrothermal environment at Karonie. These diagrams (Figs 6.2 and 6.3) are constructed for the system K_2O–CaO–MgO–Al_2O_3–SiO_2–H_2O–CO_2. The addition of Fe to the system will modify mineral compositions and change the positions of the equilibria to some extent, but the overall geometries of the phase boundaries should remain similar. The diagrams show that the biotite-rich and clinopyroxene-bearing calc-silicate alteration at

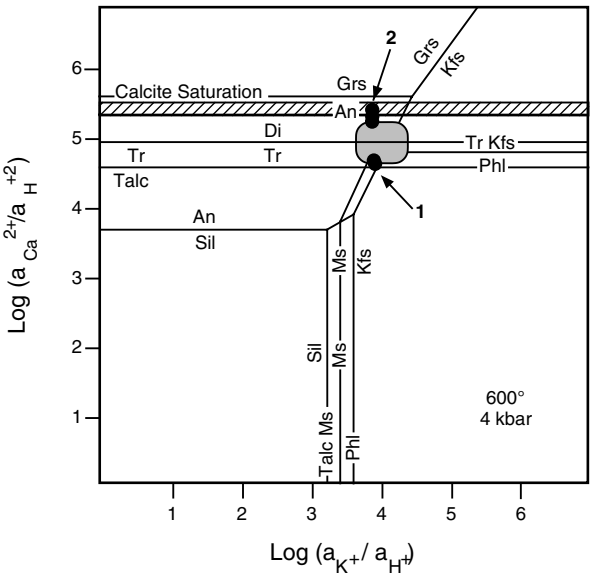

1 Fluids in equilibrium with biotite alteration

2 Fluids in equilibrium with calc-silicate alteration

WW346 22.06.04

Figure 6.2. Log ($a_{Ca^{2+}}/a_{H^{+2}}$) versus log (a_{K^+}/a_{H^+}) diagram showing mineral stability relations at 600°C and 4 kbar (after Mikucki and Ridley, 1993). Calcite saturation is shown for a fluid with X_{CO_2} = 0.1. Abbreviations: anorthite (An), diopside (Di), grossularite (Grs), K-feldspar (Kfs), muscovite (Ms), phlogopite (Phl), sillimanite (Sil), talc, tremolite (Tr)

Karonie can be produced by only small changes in fluid composition, mainly involving $a_{Ca^{2+}}/a_{H^+}$ (Fig. 6.2). Small-scale zoning around individual veins can also be explained in terms of decreasing $a_{Ca^{2+}}/a_{H^{+2}}$ (for pyroxene-bearing calc-silicate alteration) or decreasing a_{K^+}/a_{H^+} (for biotitization) away from fluid conduits, but is less readily explained in terms of variable X_{CO_2} (Fig. 6.3). The assemblage plagioclase–amphibole is stable in the presence of fluids with compositions intermediate between fluids that produce biotite and those that produce pyroxene, accounting for the widespread presence of mafic gneiss in the ore environment.

The timing of high-temperature gold mineralization compared to regional deformation and metamorphism is problematic. De Luca (1995) noted the association of gold with low-temperature minerals such as tellurides, epidote, and prehnite, and concluded that mineralization at Karonie post-dated the high-temperature ductile-deformation event represented by the regional shear that hosts the deposits. She also determined a conventional U–Pb age of 2618 ± 4 Ma for titanite in a 'marker unit'. However, the habit of this titanite defines a strong shear fabric analogous to regional metamorphism and ductile deformation (D_3), which elsewhere in the Eastern Goldfields Granite–Greenstone Terrane appears not to have lasted much beyond 2660 Ma (Witt et al., 1996; Swager and Nelson, 1997). The 2636 Ma age of the undeformed Cardunia Rocks Monzogranite suggests a similar history at Karonie. Bogacz (1995) emphasized the role of relatively late veins associated with brittle–ductile deformation. However, mineralization is more widespread than in the late, brittle–ductile faults. The association between ore lenses and pyroxene-bearing calc-silicate alteration suggests high-temperature mineralization, although this mineralization may well have been remobilized to some extent during the later faulting. In most cases, amphibolite-facies-hosted mineralization is considered to be contemporaneous with peak regional metamorphism late in the tectonic evolution of the greenstone belts (Ridley, 1990; Knight et al., 1993; McCuaig et al., 1993; Witt, 1991, 1993). Randomly oriented amphiboles and other alteration silicates do not necessarily imply pre-peak metamorphic ore formation since these fabrics can reflect heterogeneous partitioning of strain or fluids, or both, during synmetamorphic ore formation (Witt, 1993). It is considered most likely that gold was deposited at Karonie during late-tectonic regional metamorphism, similar to most other deposits in the Eastern Goldfields Granite–Greenstone Terrane. Alternatively, it is possible that the gold mineralization formed during relatively early (?D_1) ductile deformation and metamorphism, and was subsequently tilted into an upright attitude during D_2 folding, and finally remobilized, in part, at slightly lower temperatures during D_3 or D_4 brittle–ductile faulting. Further work is required to establish the local tectonothermal evolution of the Karonie area before the genesis of the gold deposits can be assessed with more confidence.

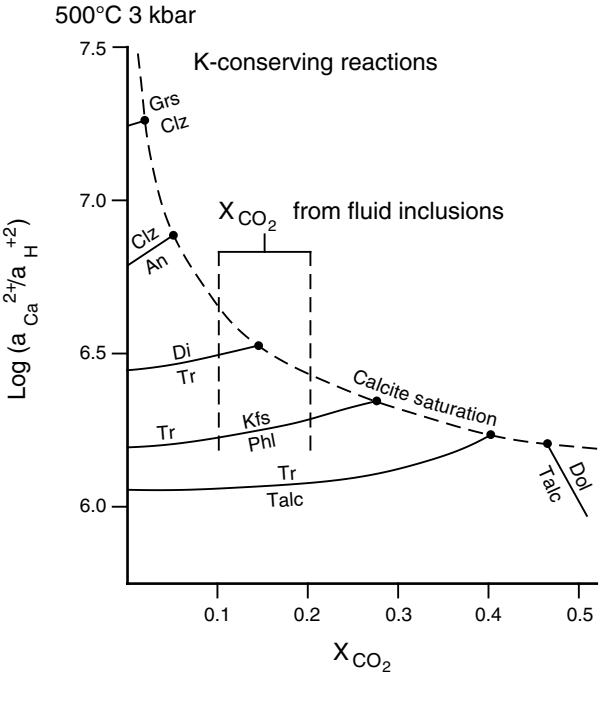

Figure 6.3. Log ($a_{Ca^{2+}}/a_{H^{+2}}$) versus X_{CO_2} diagram showing mineral stability relations at 500°C and 3 kbar (after Ridley, 1990). Abbreviations: anorthite (An), clinozoisite (Clz), diopside (Di), dolomite (Dol), grossularite (Grs), K-feldspar (Kfs), muscovite (Ms), phlogopite (Phl), sillimanite (Sil), talc, tremolite (Tr)

Although it has produced less than 5 kg of gold, one of the more important deposits (from a geoscientific point of view) outside the Karonie area is Roes New Find, about 40 km northeast of Karonie, within an area of poorly exposed granitoids east of the greenstones. Advanced weathering makes recognition of rock types difficult, but the workings have been sunk on an east-northeasterly trending zone of mineralization that deviates to a north-northeasterly orientation at its northern end. The ore zone appears to be located on the lower contact of a migmatitic zone within granitoid gneiss. This zone dips 50–60°NW but flattens to 30–40°NW at around 5 m depth. The migmatite zone consists of irregular bands of granitoid gneiss with coarse, unoriented grains of neoblastic muscovite, quartz–muscovite schist, and granitic pegmatite with pods (?boudins) of vein quartz. Banding is isoclinally folded with fold axes plunging 40–50°N, but no other linear fabrics are preserved. The upper contact of the migmatitic zone is not exposed, so the thickness of the zone is unknown. No visible alteration in the adjacent granitoid gneiss could be recognized and no sulfide minerals were observed. The available evidence suggests that gold was deposited during the high-temperature migmatitization event from fluids that were in equilibrium with the migmatitic assemblage.

There are several groups of shallow workings, most of which are hosted by medium-grade metamorphosed mafic rocks, in a zone stretching north from Lake Roe to east of Yindi Woolshed. These deposits have produced little, if any, gold.

Deposits of the Karonie–Roe area

Karonie Main and West Zones

Coordinates: 31°02'02"S, 122°33'36"E

Production: No historic production. The openpit mine accounts for the bulk of a total combined production from the Main and West Zones and Harrys Hill openpit mines of 4960.349 kg Au during the period 1987–92. Separate figures for these deposits are not available. Probable reserves are 9000 t of ore at 1.7 g/t Au (15.3 kg Au) and the indicated resource is 520 000 t of ore at 3.66 g/t Au (1903.2 kg Au; MINEDEX site code S00390).

Host rock: Medium to coarse-grained (quartz) amphibolite, possibly a deformed and metamorphosed, fractionated dolerite. Quartz–biotite metasedimentary rock (Fig. 6.4) is a minor host to gold mineralization.

Structure: The orebodies are within a broad zone of strong ductile deformation interpreted as a regional shear zone (Fig. 6.1). This zone of deformation is parallel to the regional foliation and the main lithological trends in the area (i.e. north–south and steeply west dipping; Fig. 6.5). The width of the deformation zone is unknown but is greater than the width of the Main Zone pit (about 100 m). Within the ductile shear zone, millimetre- to metre-scale mineral banding defines a foliation that is parallel–subparallel to the shear-zone margins. Tight, isoclinal (including intrafolial) folding of this banding is common. Mesoscopic folds with Z-shaped asymmetry are well developed in calc-silicate assemblages along the eastern side of the pit, suggesting dextral movement. However, the asymmetry of these folds may not record the main movement on the ductile shear zone, and they may have alternatively formed as a result of flexural slip on the west side of a north-plunging anticline (Fig. 6.5).

Logging of representative drillcores indicates that quartz veins are uncommon and do not correlate well with mineralization (Figs 6.6 – 6.8). However, some quartz and calcite veins are present in relatively thin, strike-subparallel 'marker units' (local mine terminology). These 'marker units' probably represent a number of discrete

IRO83 15.12.03

Figure 6.4. Dense, fine-grained quartz–biotite metasedimentary rock in the north face of Karonie Main Zone pit

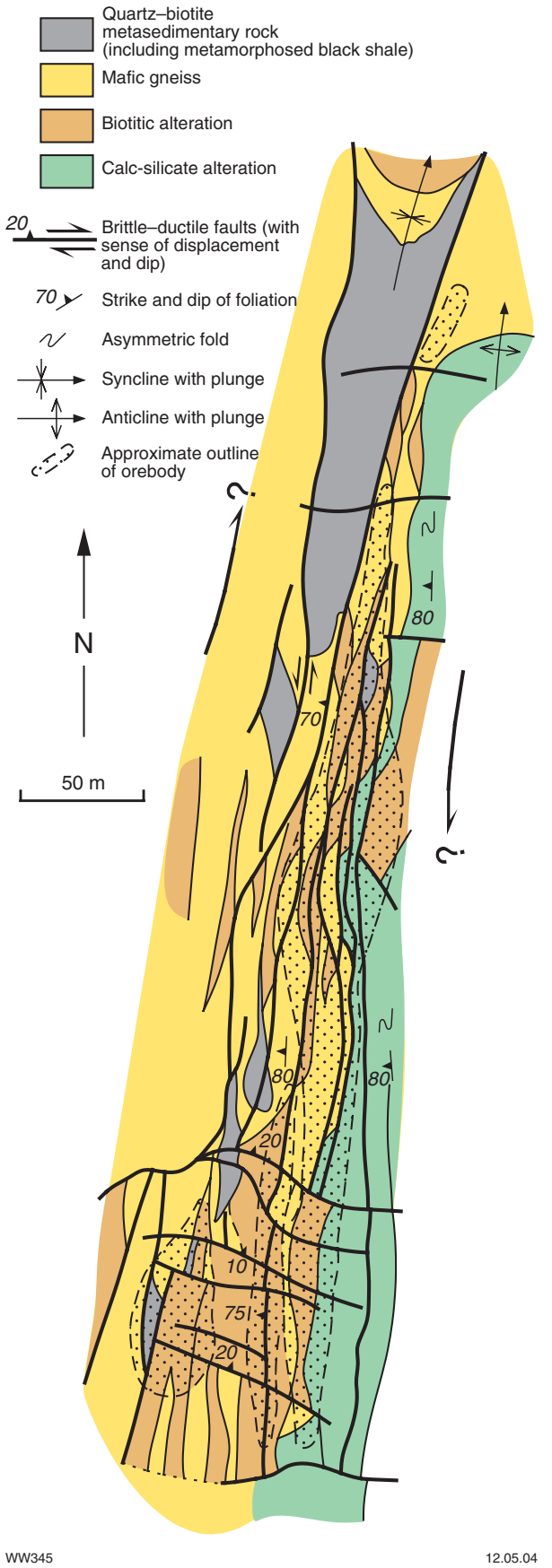

Figure 6.5. Geological plan of the Main and West Zone orebodies at the 275-m level, Karonie mining area (after Poseiden Exploration Ltd, 1992)

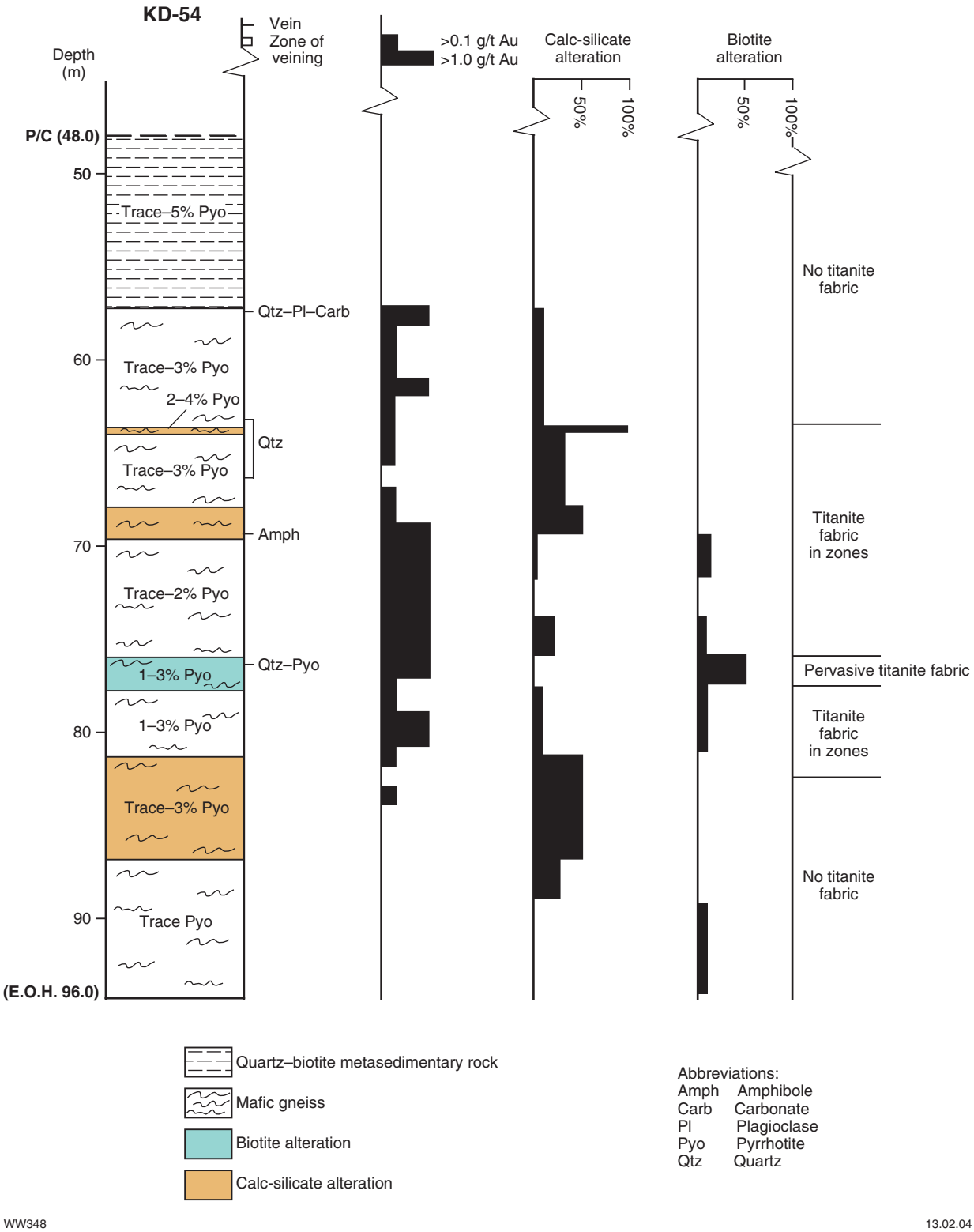

Figure 6.6. Summary log, diamond drillhole KD-54, Karonie Main Zone deposit

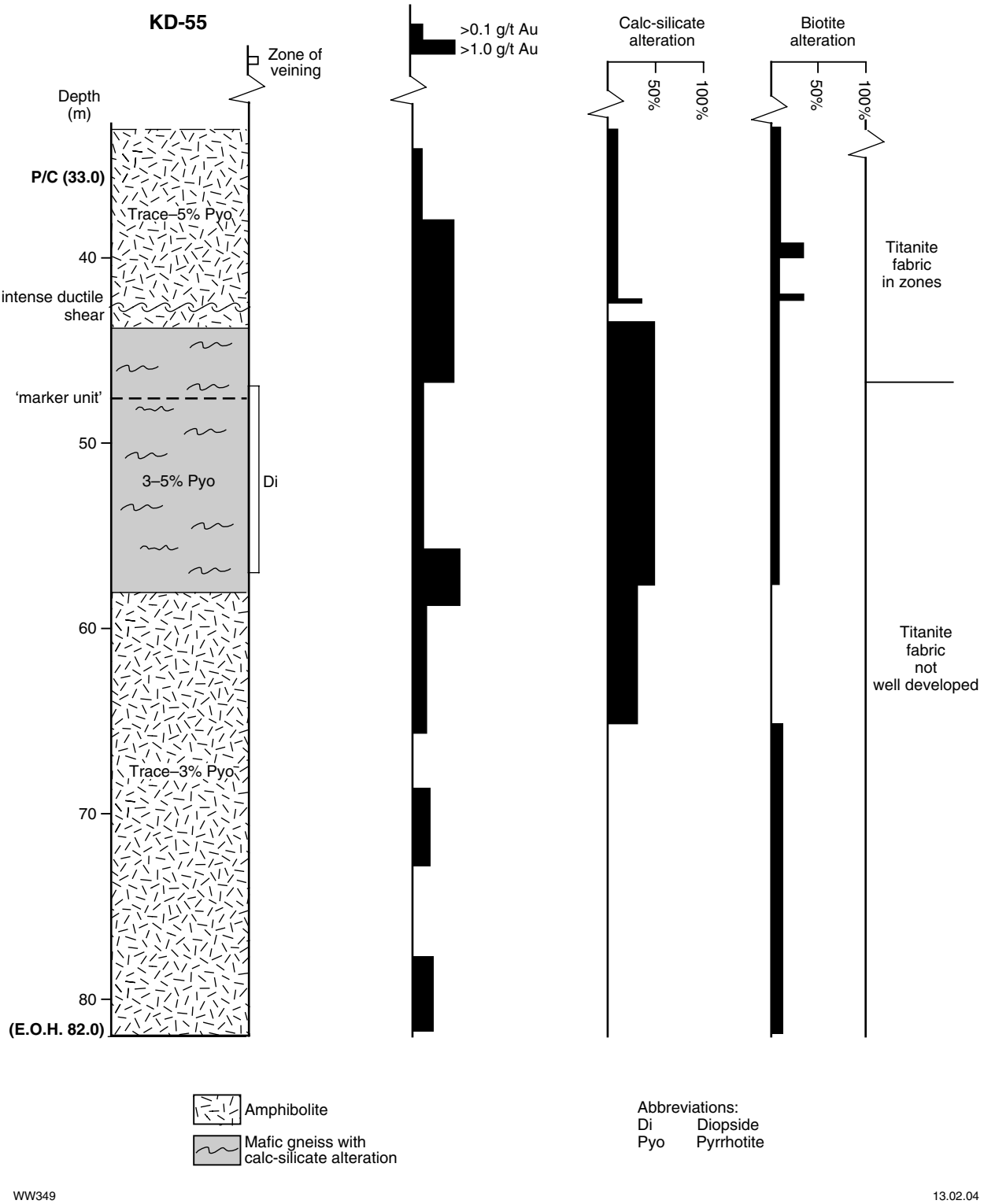

Figure 6.7. Summary log, diamond drillhole KD-55, Karonie Main Zone deposit

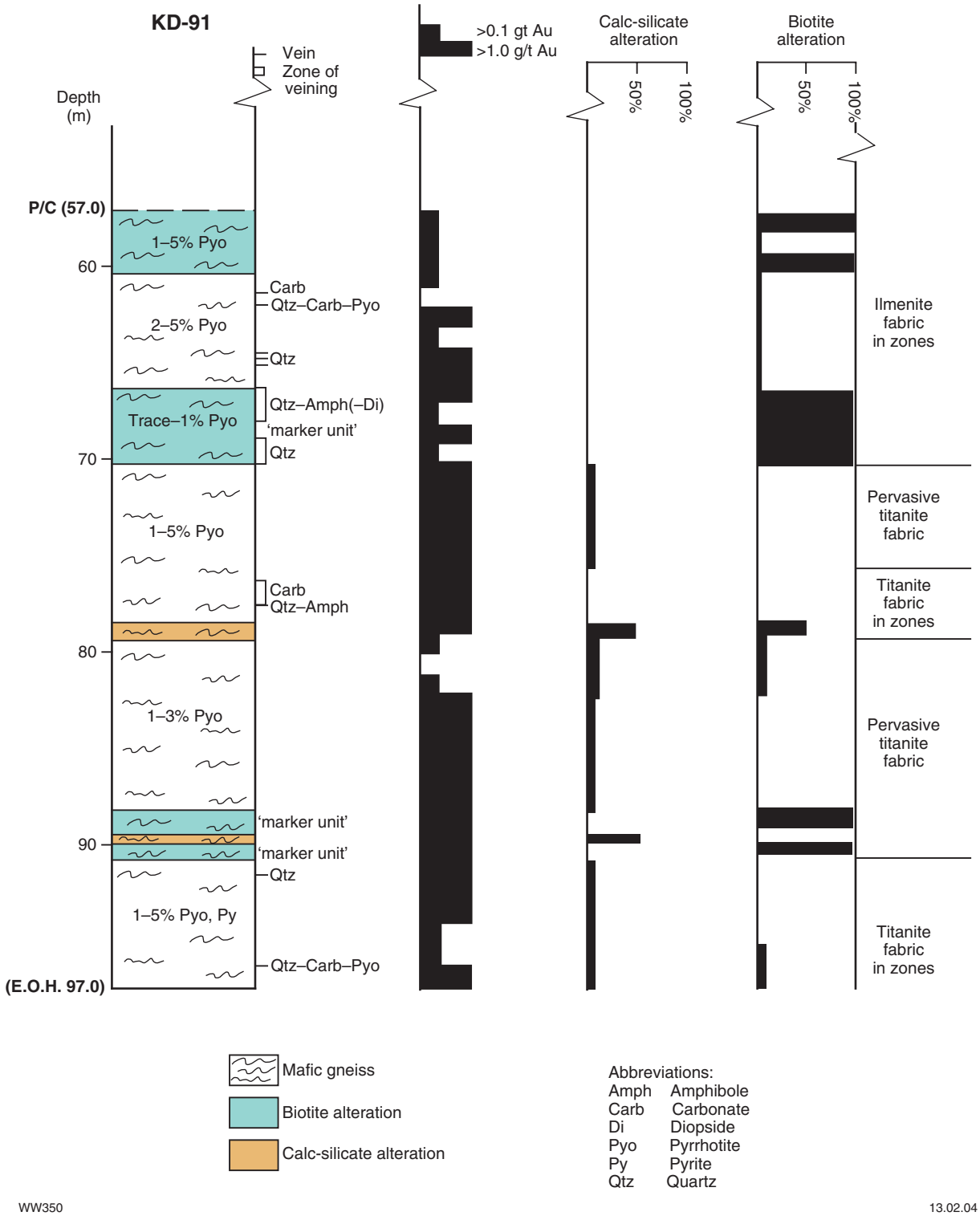

Figure 6.8. Summary log, diamond drillhole KD-91, Karonie Main Zone deposit

zones of brittle–ductile deformation that have been superimposed upon the ductile deformation. Examples of these faults, consisting of cataclasis and quartz veining, can be observed overprinting the lithological banding of the ductile shear zone in the southern face of the Main Zone pit. Offset of the quartz–biotite metasedimentary unit in the northern part of the pit indicates sinistral movement on this set of faults, consistent with the orientation of en echelon quartz veins (tension gashes) observed along the western side of the pit (Fig. 6.9). Late, crosscutting, gently north dipping faults and fractures post-date ductile deformation and strike-parallel brittle–ductile faults (Fig. 6.5).

The Main Zone orebody has a strike length of about 600 m and a width of up to 40 m (Fig. 6.5). It consists of several lenses that are more or less conformable with the strike of the shear zone. The West Zone orebody is smaller (about 120 m long and 4–12 m wide).

Alteration: The ductile shear zone is characterized by an increase in the scale of metamorphic banding and by several alteration styles that can be recognized in the Main and West Zones openpit as well as in drillcore (Table 6.1). Unaltered amphibolite is exposed only locally along the western margin of the pit. The following alteration types, in their interpreted chronological order, are recognized. Representative analyses of minerals from amphibolite and the various alteration assemblages are presented in Tables 6.2 – 6.6 and Figures 6.10 – 6.12.

1. Biotite alteration: foliation-parallel bands of biotite-rich rock form bands and relict lenses within mafic gneiss and calc-silicate alteration (Fig. 6.13). The assemblage is similar to that of a biotite amphibolite (Table 6.1). A few biotite-rich bands are separated from mafic gneiss by an intervening selvage of amphibole-rich rock (Fig. 6.14b), and locally these banded assemblages define intrafolial folds. These biotite-rich bands may be metasedimentary units or products of an early period of hydrothermal alteration.
2. Mafic gneiss: Coarsely banded (centimetre- to metre-scale) mafic gneiss (Figs 6.13a and 6.15) contains bands that range from melanocratic (80% hornblende) to leucocratic (<50% hornblende). Some quartz in the mafic gneiss may be primary but most is probably secondary. The mafic gneiss probably did not form simply by metamorphic segregation and grain-size coarsening. A partly metasomatic origin for the mafic gneiss is supported by the relatively calcic-plagioclase compositions and differences in amphibole compositions (higher Fe/Mg, K_2O/Na_2O) compared to similar minerals in least-altered amphibolite (Table 6.1, Figs 6.10 and 6.11). The mafic gneiss is thus thought to have resulted from a form of calc-silicate alteration. Mass-balance calculations, based on whole-rock geochemical data, indicate CaO and Na_2O enrichment, and lesser addition of Fe_2O_3, compared with unaltered amphibolite (Fig. 6.16). During this process, MgO and K_2O are lost from the amphibolite.
3. Calc-silicate alteration: Most calc-silicate zones consist of one or more thin (1–3 mm) pyroxene-rich veins within alteration selvages in which hornblende has been replaced by porphyroblasts of pyroxene (Figs 6.14a,d–h, and 6.16). Plagioclase is commonly replaced by epidote, and titanite replaces ilmenite. Pyroxene compositions consistently indicate the presence of ferrosalite (Table 6.1, Fig. 6.12). As with biotite alteration, many calc-silicate bands are separated from mafic gneiss by a selvage of amphibole-rich rock (Figs 6.14c,g,h, and 6.17) and locally define intrafolial folds (Figs 6.14c and 6.17). An amphibole-rich assemblage that forms a prominent part of the Main Zone orebody (Fig. 6.18) may be a large-scale version of one of these selvages between mafic gneiss and calc-silicate alteration. Mass-balance calculations, based on whole-rock geochemical data, indicate some similarities to the qualitative changes associated with formation of mafic gneiss (Figs 6.16 and 6.19). CaO (± Na_2O, SiO_2) are added to the altered rock. MgO and Fe_2O_3 depleted from the calc-silicate alteration zones are added to the amphibole-rich selvage (Fig. 6.16).
4. Brittle–ductile faults: 'marker units' are quartz–feldspar–biotite rocks with porphyroclasts of feldspar, including K-feldspar. They have diffuse contacts with adjacent units and differ from other biotitized mafic gneiss zones in that they are relatively late and cut all other alteration assemblages. The biotite is well oriented parallel to the margins of the faults. These units have been interpreted as deformed porphyries by Hopwood (1991), but are here interpreted as alteration zones associated with late brittle–ductile structures in mafic gneiss.

IRO84 15.12.03

Figure 6.9. Late, sheeted quartz(–carbonate) veins related to a brittle–ductile shear, western wall of Karonie Main Zone pit

Fabric relationships involving metasomatic minerals indicate that ductile deformation was contemporaneous with hydrothermal alteration. A strong shear fabric is defined by oriented trails of titanite (in calc-silicate zones; Fig. 6.14c) or ilmenite (in biotitized zones and locally in mafic gneiss; Fig. 6.14b). This fabric is parallel to metamorphic banding and axial planar to intrafolial folds, but amphiboles, biotite, and diopside are commonly randomly oriented and overgrow the shear fabric. Intrafolial folds are defined by metasomatic assemblages

Table 6.2. Selected SEM analyses of plagioclase, Karonie Main Zone deposit

	GSWA 132813 amphibolite				*GSWA 132802 mafic gneiss*				*GSWA 132802 mafic gneiss*		*GSWA 132808 calc-silicate alteration*				*GSWA 132812 calc-silicate alteration*		*GSWA 132810 biotitized mafic gneiss*	
					amphibole–plagioclase band				*diopside–plagioclase band*		*wallrock*				*very coarse grained plagioclase in diopside–plagioclase band*		*amphibole–plagioclase band*	
	PLAG 1	*PLAG 2*	*PLAG 3*	*PLAG 5*	*PLAG 6*	*PLAG 7*	*PLAG 8*	*PLAG 9*	*PLAG 11*	*PLAG 12*	*PLAG 16*	*PLAG 17*	*PLAG 18*	*PLAG 20*	*PLAG 26*	*PLAG 27*	*PLAG 21*	*PLAG 22*
SiO_2	62.52	61.91	58.27	58.94	56.06	58.60	59.55	56.52	56.24	58.46	57.79	53.93	58.13	53.95	58.90	58.73	59.27	60.07
Al_2O_3	24.10	23.98	26.78	26.10	28.44	26.45	25.79	28.06	27.85	25.99	26.95	29.58	26.50	28.86	26.01	26.19	25.64	26.01
FeO	–	–	–	–	–	–	–	–	–	–	–	–	–	0.27	–	–	–	–
CaO	5.00	4.98	7.99	7.57	10.00	7.52	7.05	9.94	9.75	7.47	8.52	11.43	8.09	10.85	7.55	7.75	7.06	6.99
Na_2O	9.09	9.09	7.06	7.46	5.81	7.03	7.68	6.44	6.46	7.54	7.25	5.29	7.38	5.56	7.37	7.46	7.69	7.94
K_2O	–	–	–	–	–	0.16	0.16		0.15	–	–	–	–	–	–	0.13	–	–
Total	**100.71**	**99.96**	**100.10**	**100.06**	**100.31**	**99.75**	**100.24**	**100.96**	**100.46**	**99.45**	**100.51**	**100.22**	**100.10**	**99.50**	**99.83**	**100.50**[a]	**99.67**	**101.01**
An	23.3	23.2	38.5	35.9	48.8	36.8	33.3	46.0	45.1	35.4	39.4	54.4	37.7	51.9	36.1	36.2	33.7	32.7
Ab	76.7	76.8	61.5	64.1	51.2	62.3	65.7	54.0	54.1	64.6	60.6	45.6	62.3	48.1	63.9	63.0	66.3	67.3
Or	–	–	–	–	–	0.9	0.9	–	0.8	–	–	–	–	–	–	0.7	–	–

NOTES: (a) Includes 0.23% NiO

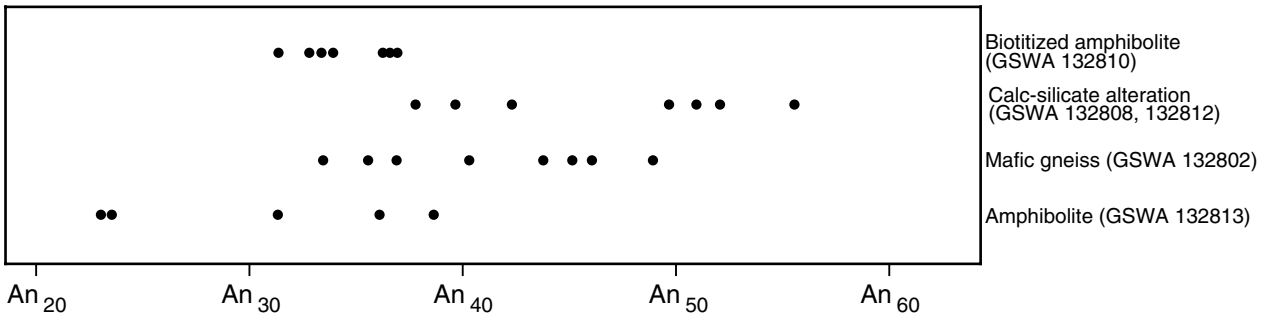

Figure 6.10. Composition of plagioclase in amphibolite and altered amphibolite, Karonie Main Zone deposit

Table 6.3. Selected SEM analyses of amphibole, Karonie Main Zone deposit

	GSWA 132813 amphibolite			*GSWA 132802 mafic gneiss*		*GSWA 132812 calc-silicate alteration*		*GSWA 132810 biotitized mafic gneiss*			
				amphibole–plagioclase band		*amphibole-rich selvage to diopside–plagioclase band*		*amphibole–plagioclase band*		*amphibole-rich margin to biotite-rich band*	
	HB 1	*HB 3*	*HB 4*	*HB 6*	*HB 9*	*HB 20*	*HB 22*	*HB 11*	*HB 12*	*HB 13*	*HB 14*
SiO_2	44.16	44.53	43.71	41.30	41.26	39.50	40.10	43.83	41.37	40.36	41.54
TiO_2	0.17	–	0.27	0.36	0.46	0.82	0.46	0.52	0.38	0.36	0.61
Al_2O_3	12.25	12.18	13.32	12.87	12.16	15.08	13.94	10.99	13.06	14.51	13.33
FeO	17.41	17.60	18.17	23.47	24.15	22.73	22.69	22.48	22.96	21.91	21.37
MnO	0.21	0.27	0.28	0.35	0.37	0.25	0.33	0.34	0.31	–	0.56
MgO	9.39	9.52	9.07	4.79	5.10	5.13	5.32	6.28	5.40	5.27	6.23
CaO	11.57	11.70	11.72	11.90	11.43	11.78	11.96	11.14	11.51	11.64	12.07
Na_2O	1.35	1.17	1.65	0.94	1.06	1.45	1.55	1.00	1.16	1.49	1.54
K_2O	0.20	0.12	0.18	1.09	0.92	1.33	1.32	0.60	0.68	0.86	0.86
Total	**96.70**	**97.08**	**98.37**	**97.07**	**96.91**	**98.14**	**97.67**	**97.18**	**96.83**	**96.40**	**98.10**
Fe/Fe+Mg	51.0	50.9	52.9	73.3	72.6	71.3	70.5	66.8	70.5	70.0	65.8
K_2O/Na_2O	0.15	0.10	0.11	1.16	0.87	0.92	0.85	0.60	0.59	0.58	0.56

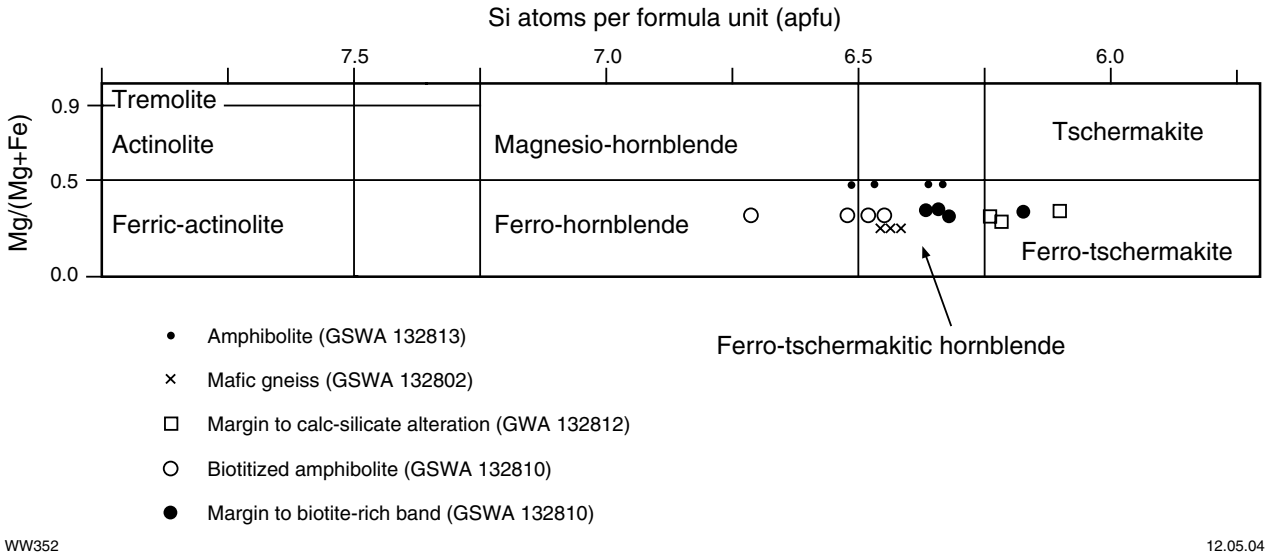

Figure 6.11. Composition of amphibole in amphibolite and altered amphibolite, Karonie Main Zone deposit (after Leake, 1978)

(Figs 6.14b,c, and 6.17), and coarse, crystalline pyroxene is in the necks of boudinaged calc-silicate layers (observed in the south face of the Main Zone pit; Fig. 6.20). Also, progressive, syndeformational development of pyroxene-bearing calc-silicate bands is indicated by overprinting relationships between more- and less-deformed bands of altered rock. Biotite and amphiboles in alteration zones tend to be randomly oriented and overgrow the ilmenite–titanite fabric, suggesting post-ductile-deformation, high-temperature recrystallization. Similarly, pyroxene in calc-silicate bands demonstrates evidence of post-deformation strain recovery.

Crosscutting relationships observed in the pit and in drillcore indicate that calc-silicate alteration post-dates biotite alteration (Fig. 6.13). Relicts of biotite-rich assemblages are separated from enclosing calc-silicate alteration by intermediate zones of randomly oriented amphibole at about 79.0 m in drillhole KD-91. Dalstra (1995) also noted such relationships. Biotite alteration is

Table 6.4. Selected SEM analyses of pyroxene, Karoni Main Zone deposit

	GSWA 132802 *mafic gneiss*		*GSWA 132808* *calc-silicate alteration*				*GSWA 132808* *calc-silicate alteration*				*GSWA 132812* *calc-silicate alteration*	
	porphyroblast diopside in diopside–plagioclase band		*calcite–diopside vein*		*diopside veinlet*		*porphyroblast diopside in diopside–plagioclase band*				*porphyroblast diopside in diopside–plagioclase band*	
	DI1	*DI4*	*DI 5*	*DI 6*	*DI 8*	*DI 10*	*DI13*	*DI14*	*DI 15*	*DI 17*	*DI 19*	*DI 21*
SiO_2	49.38	49.83	49.55	50.74	49.20	49.57	50.35	50.17	49.97	50.10	49.37	50.19
Al_2O_3	1.23	0.16	1.11	0.19	0.51	0.43	0.46	0.33	–	0.22	0.74	0.29
Cr_2O_3	–	–	–	–	–	–	0.22	–	–	–	–	–
FeO	17.92	17.56	19.22	19.54	19.50	18.66	19.52	19.10	17.94	19.39	20.30	19.86
MnO	0.52	0.61	0.74	0.73	0.46	0.42	0.41	0.59	0.43	0.47	0.65	0.65
MgO	6.36	6.44	6.11	6.08	5.53	5.83	5.82	6.00	6.61	5.70	5.06	5.63
CaO	23.23	23.47	23.40	23.77	23.28	23.50	23.36	23.27	23.26	23.43	23.52	23.81
Na_2O	0.38	0.26	0.51	0.23	0.25	–	0.30	0.43	0.21	0.41	0.39	0.38
Total	**99.01**	**98.33**	**100.63**	**101.29**	**98.72**	**98.41**	**100.44**	**99.90**	**98.41**	**99.72**	**100.04**	**100.81**
Fe/Fe+Mg	61.3	60.5	63.8	64.3	66.4	64.2	65.3	64.1	60.3	65.6	69.2	66.4
$CaSiO_3$	50.4	50.9	49.9	50.1	50.4	50.9	50.0	50.0	50.1	50.4	50.7	50.5
$MgSiO_3$	19.2	19.4	18.1	17.8	16.6	17.5	17.3	17.9	19.8	17.1	15.2	16.6
$FeSiO_3$	30.4	29.7	32.0	32.1	33.0	31.5	32.6	32.0	30.1	32.5	34.1	32.9

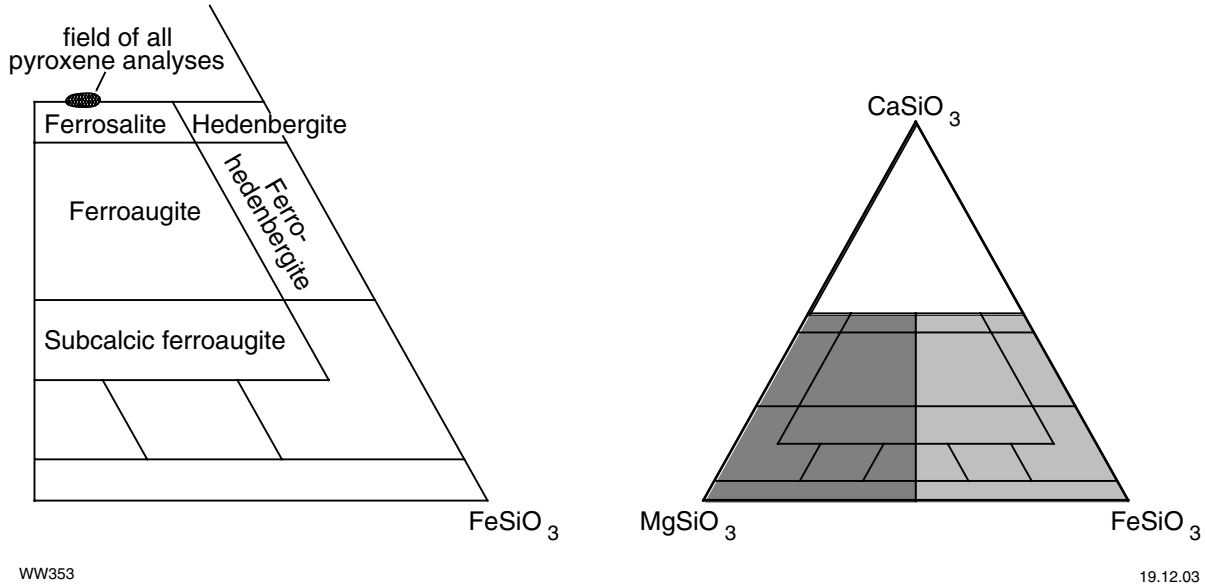

Figure 6.12. Composition of clinopyroxene in veins and altered amphibolite, Karonie Main Zone deposit

Table 6.5. Selected SEM analyses of biotite, Karonie Main Zone deposit

	GSWA 132810 biotitized mafic gneiss		
	biotite-rich band		
	BI 1	*BI 2*	*BI 5*
SiO_2	34.74	32.73	33.90
TiO_2	2.40	1.96	2.47
Al_2O_3	17.30	18.43	17.22
FeO	23.12	24.09	22.60
MnO	0.22	0.19	0.15
MgO	8.25	9.06	7.97
K_2O	9.78	7.95	9.61
Total	**95.79**	**94.39**	**93.93**
Fe/Fe+Mg	61.1	59.9	61.4

Table 6.6. Selected SEM analyses of carbonates, Karonie Main Zone deposit

	GSWA 132808 calc-silicate alteration		
	coarse carbonate in carbonate–diopside vein		
	CB 5	*CB 6*	*CB 7*
FeO	0.43	0.29	0.42
NiO	–	–	0.20
MnO	0.24	0.24	0.28
MgO	–	–	–
CaO	55.15	58.34	57.19
Total	**55.82**	**58.88**	**58.08**
$FeCO_3$	0.60	0.39	0.57
$NiCO_3$	–	–	0.25
$MnCO_3$	0.35	0.33	0.38
$MgCO_3$	–	–	–
$CaCO_3$	99.05	99.28	98.80
Nomenclature	Calcite	Calcite	Calcite

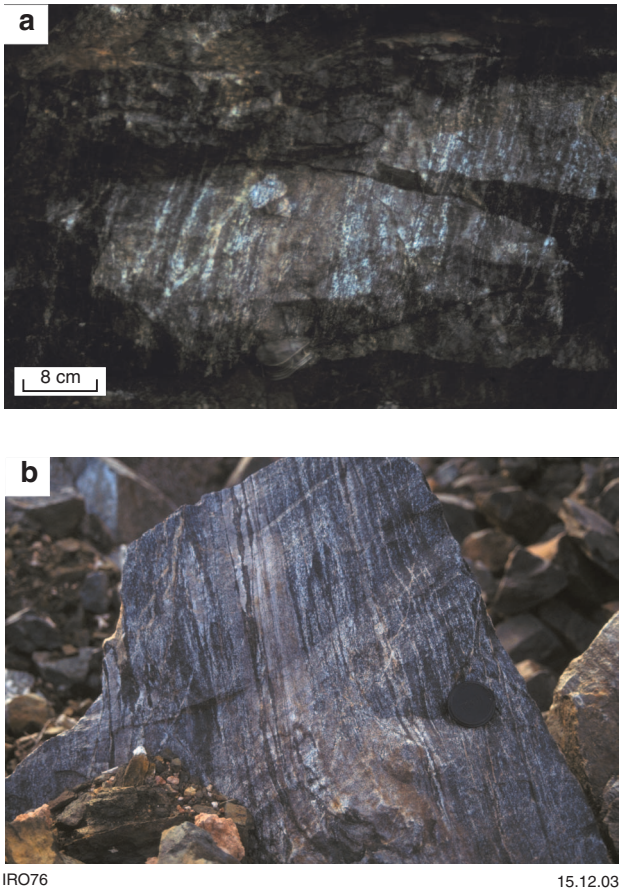

Figure 6.13. Relict bands and lenses of biotite alteration within mafic gneiss: a) cut by veins and bands of plagioclase–hornblende assemblages in the north face of Karonie Main Zone pit; and b) cut by pyroxene-rich assemblages in float from the north face of Karonie Main Zone pit

cut by veins and bands of plagioclase–hornblende assemblages (Fig. 6.13a) and, elsewhere, pyroxene-rich assemblages (Fig. 6.13b). Retrograde minerals variably developed in all assemblages are sericite (especially replacing feldspars), chlorite, and prehnite. A later phase of calc-silicate alteration is represented by small bands and veinlets of plagioclase–hornblende(–calcite), which locally overprint pyroxene-rich assemblages and alteration associated with 'marker units'.

Mineralized zones are in mafic gneiss, biotitized mafic gneiss, and pyroxene-bearing calc-silicate assemblages, but there is no consistent association with any of these rock types. However, in plan (Fig. 6.5) and in some drillcore intersections (Fig. 6.6), mineralized zones are flanked by pyroxene-bearing, calc-silicate alteration. 'Marker units' are commonly associated with ore-grade mineralization, but mineralization is more widespread. Up to 5% sulfides (mainly pyrrhotite, less pyrite) are present in all rock types within the ductile shear zone, but do not correlate well with mineralization (Figs 6.6 – 6.8). Gold exists as 'clouds' of fine inclusions in hornblende, epidote–clinozoisite, and prehnite (Piggot and Green, 1990; de Luca, 1995), together with minor Au–Ag–Ni–Pb–Bi tellurides and native tellurium. Coarser gold is interstitial to, and along fractures and cleavage planes in, these same silicate minerals, and these are commonly higher grade ore zones.

References: Pigott and Green (1990), Hopwood (1991), Poseiden Exploration Ltd (1992), de Luca (1995), Bogacz (1995), Dalstra (1995).

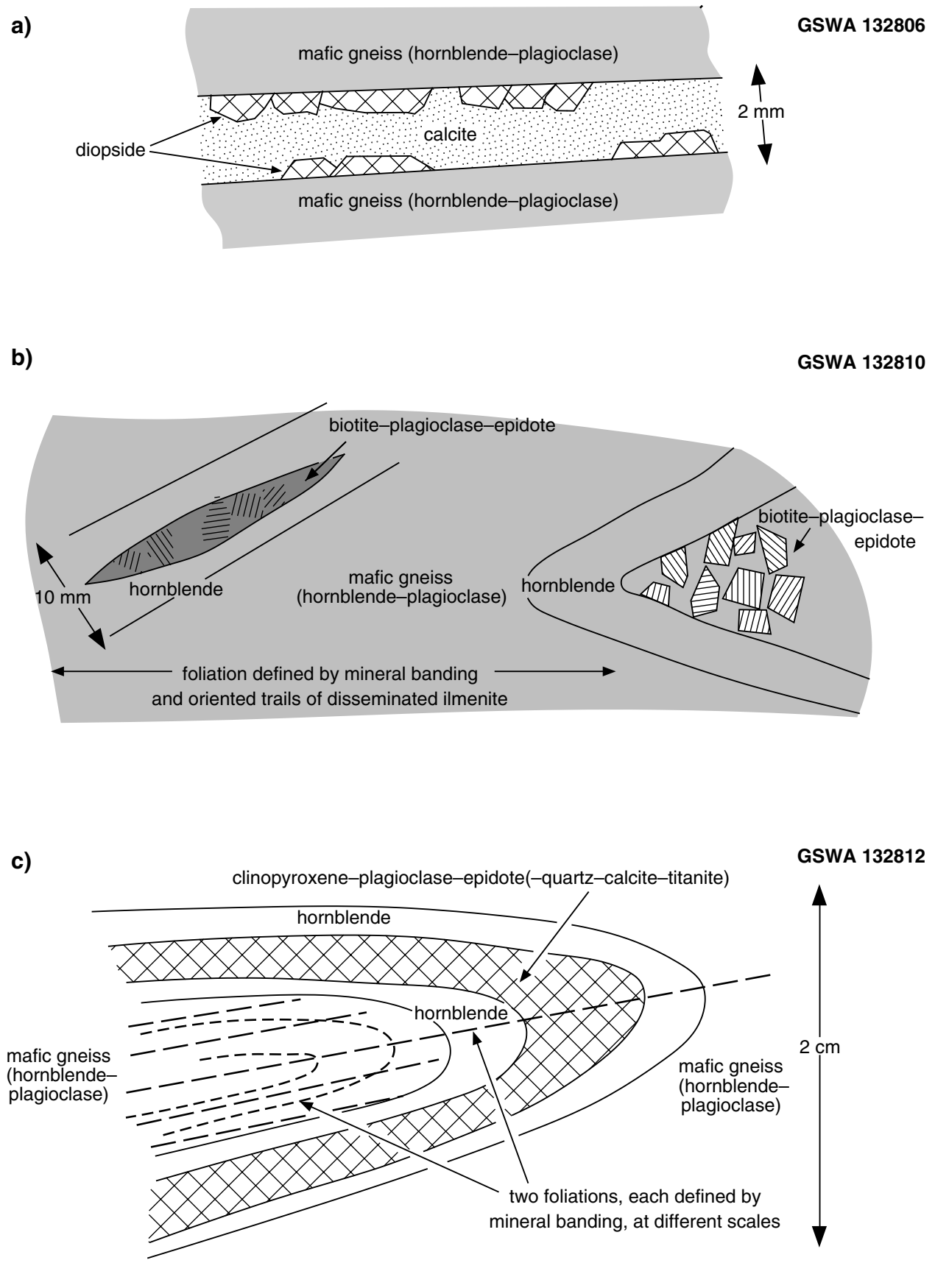

Figure 6.14. Sketches showing the relationship between deformation fabrics, veins, and various alteration assemblages, Karonie Main and West Zones and Harrys Hill deposits (continued over page)

d) **GSWA 132816**

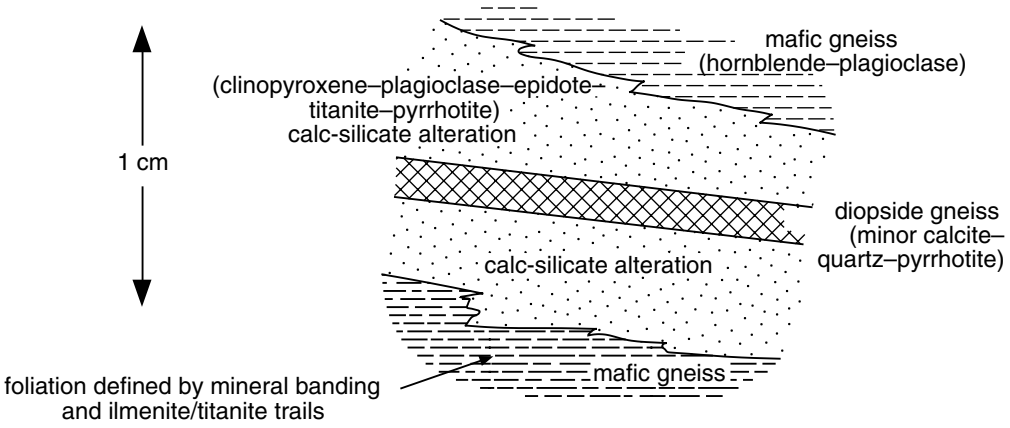

e) **GSWA 132821B**

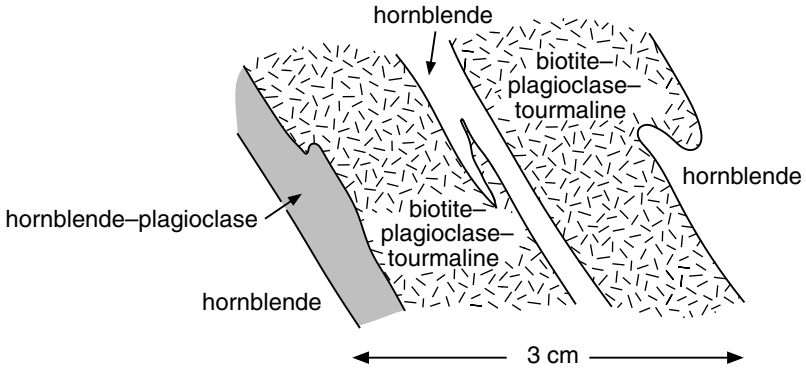

f) **GSWA 132923**

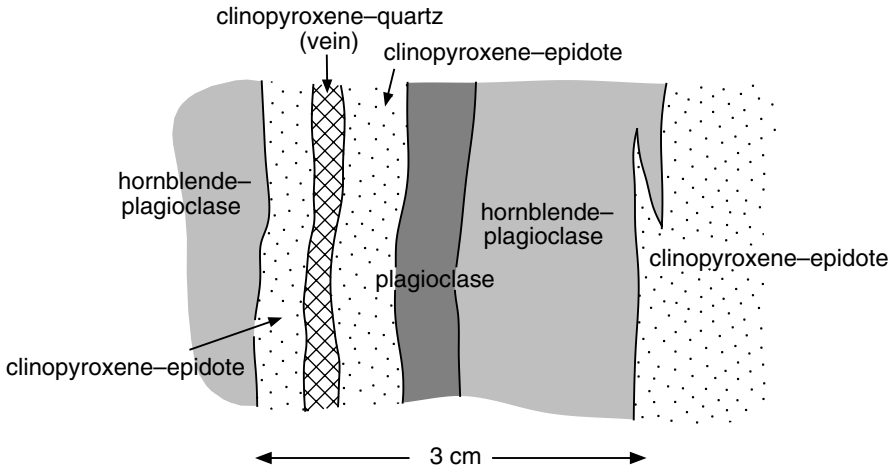

WW354A 26.11.03

Figure 6.14. (continued)

g) **GSWA 132823B**

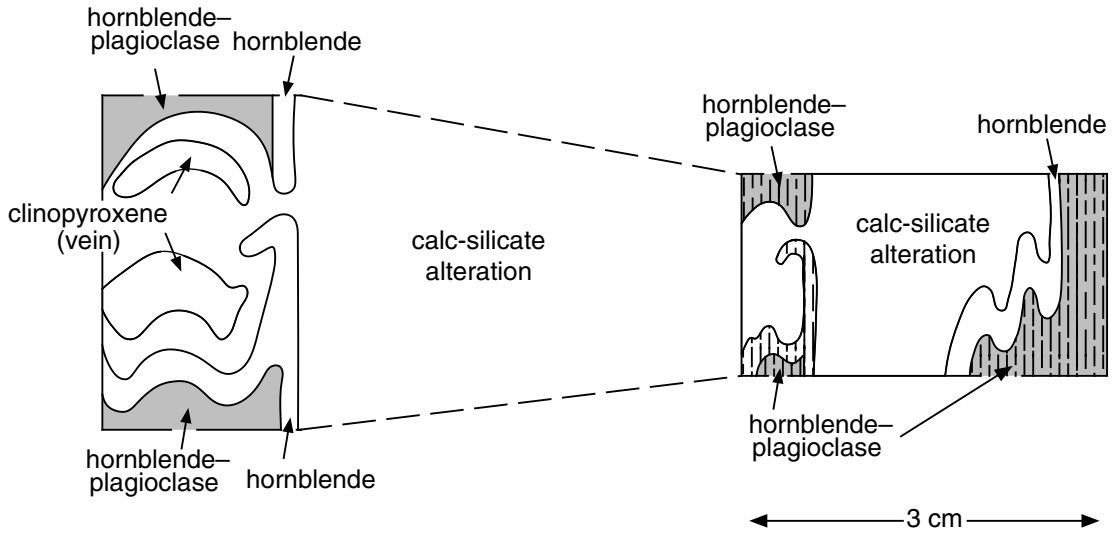

h) **GSWA 132828**

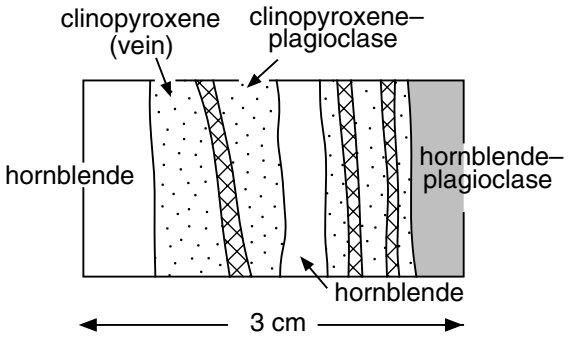

WW354b 13.02.03

Figure 6.14. (continued)

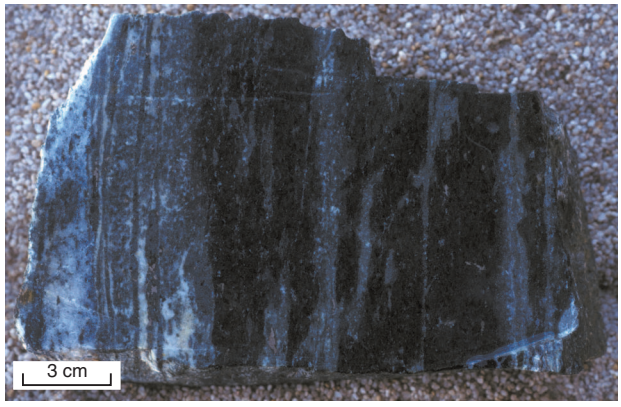

IRO78 15.12.03

Figure 6.15. Mafic gneiss, Karonie Main Zone pit

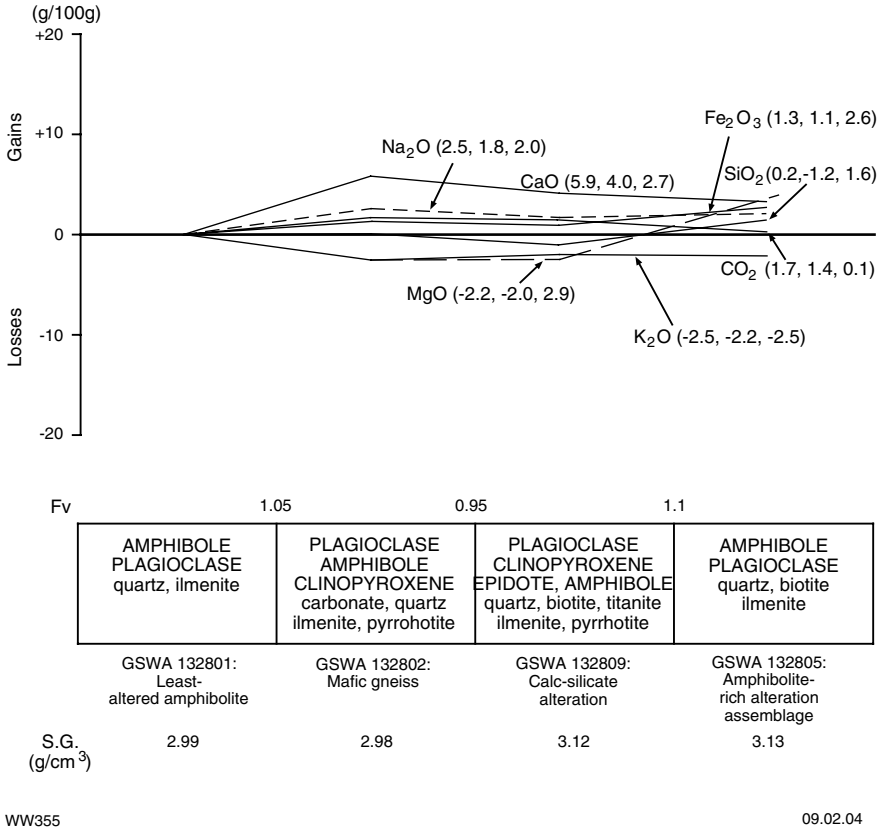

Figure 6.16. Mass-balance changes (calculated using the method of Gresens, 1967) associated with formation of mafic gneiss and calc-silicate alteration, Karonie Main Zone deposit. Mineral components of alteration assemblages are listed in approximate order of abundance, with main mineral components in upper case and minor mineral components in lower case

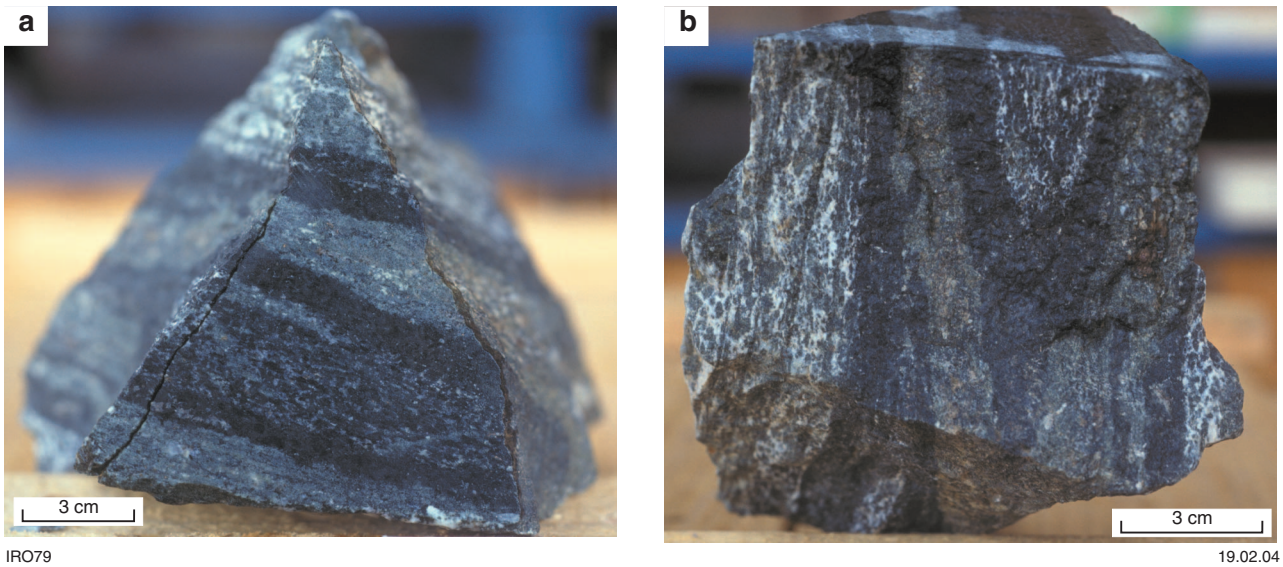

Figure 6.17. Calc-silicate alteration in mineralized amphibolite, Karonie Main Zone deposit: a) amphibole-rich bands (dark) alternate with clinopyroxene-rich bands. Note clinopyroxene veins parallel to banding in the clinopyroxene-rich assemblage at the right of the photo; and b) amphibole-rich bands (black) separate clinopyroxene-rich calc-silicate alteration (green) assemblages from mafic gneiss

Harrys Hill

Coordinates: 31°02'47"S, 122°33'22"E

Production: No historic production. The openpit mine accounts for a minor component of the total combined production from the Main and West Zones and Harrys Hill openpit mines, of 4960.349 kg Au during the period 1987–92. Separate figures for these deposits are not available. The remaining resource (measured) at the time of writing is 1.732 Mt of ore at 2.75 g/t Au (4763 kg Au; MINEDEX site code S00389).

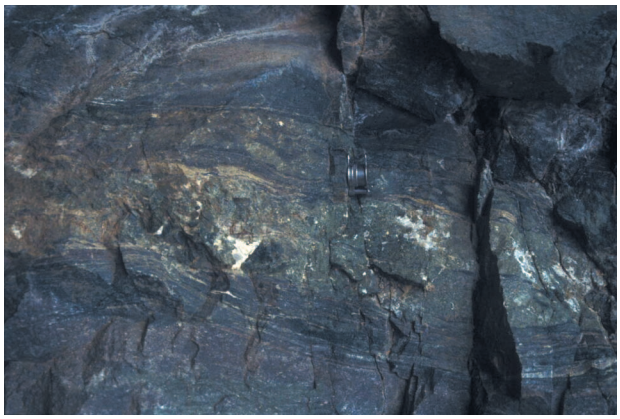

IRO100 10.02.04

Figure 6.18. Amphibole-rich alteration assemblage in the north face of Karonie Main Zone pit

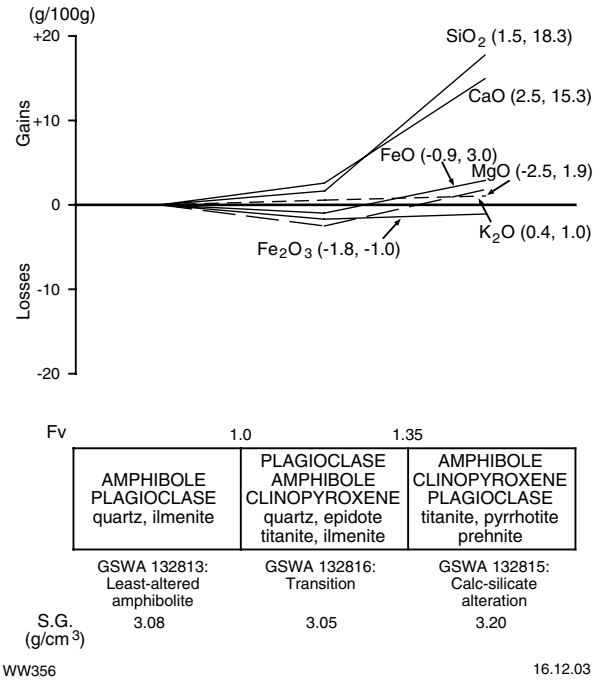

Figure 6.19. Mass-balance changes (calculated using the method of Gresens, 1967) associated with calc-silicate alteration, Karonie West Zone deposit. Mineral components of alteration assemblages are listed in approximate order of abundance, with main mineral components in upper case and minor mineral components in lower case

Host rock: The medium- to coarse-grained amphibolite is a more melanocratic rock (about 20% quartz and feldspar) than at Main and West Zones, but with paler coloured calcic amphibole and minor cummingtonite, suggesting a more magnesian precursor.

Structure: The orebody lies within a similar (possibly the same) north-trending ductile shear zone as the Main and West Zones deposits, but the strain intensity and width of the shear zone may not be as great. It is about 400 m long and up to 20 m wide. It consists of a series of steeply west dipping, right-stepping, ?en echelon lenses (Figs 6.20 and 6.21). Foliation-parallel quartz veins (1–15 cm wide) are relatively common and include some late, flat-lying veins.

Alteration: As for the Main and West Zones orebodies, mineralized zones tend to be flanked by pyroxene-bearing calc-silicate assemblages (Fig. 6.21). Ore lenses tend to be biotitized (up to 40% biotite) and there is a more consistent presence of biotite in ore zones compared to the Main and West Zones orebodies (de Luca, 1995; see also Fig. 6.22). As in Main and West Zones, biotite-rich alteration assemblages are separated from mafic rock (amphibolite) by amphibole-rich assemblages (Fig. 6.14e). Also, there is a clear relationship between ore zones, veining, and abundance of pyrite (Fig. 6.22). The pyrite to pyrrhotite ratio increases towards veins. Tourmaline is common in some veins, and alteration zones associated with quartz–tourmaline(–amphibole) veins are dominantly amphibole with variable biotite, tourmaline, chlorite, and sulfide minerals. These alteration amphiboles are a paler green than in the host amphibolite, which may indicate a relatively magnesian (Fe-poor) composition. The veins and their alteration halos are commonly mineralized (Fig. 6.22).

Mass-balance calculations, based on whole-rock geochemical data, indicate addition of CaO (±Na_2O, Fe_2O_3) to calc-silicate alteration zones, but depletion of SiO_2 (Figs 6.23a,b). Alteration associated with a late, brittle–ductile fault, equivalent to one of the 'marker units' in Main and West Zones, involves addition of SiO_2 and K_2O but depletion of most other elements, including CaO,

IRO82 15.12.03

Figure 6.20. Coarsely crystalline clinopyroxene and calcite in necks of calc-silicate boudins, south face of Karonie Main Zone pit

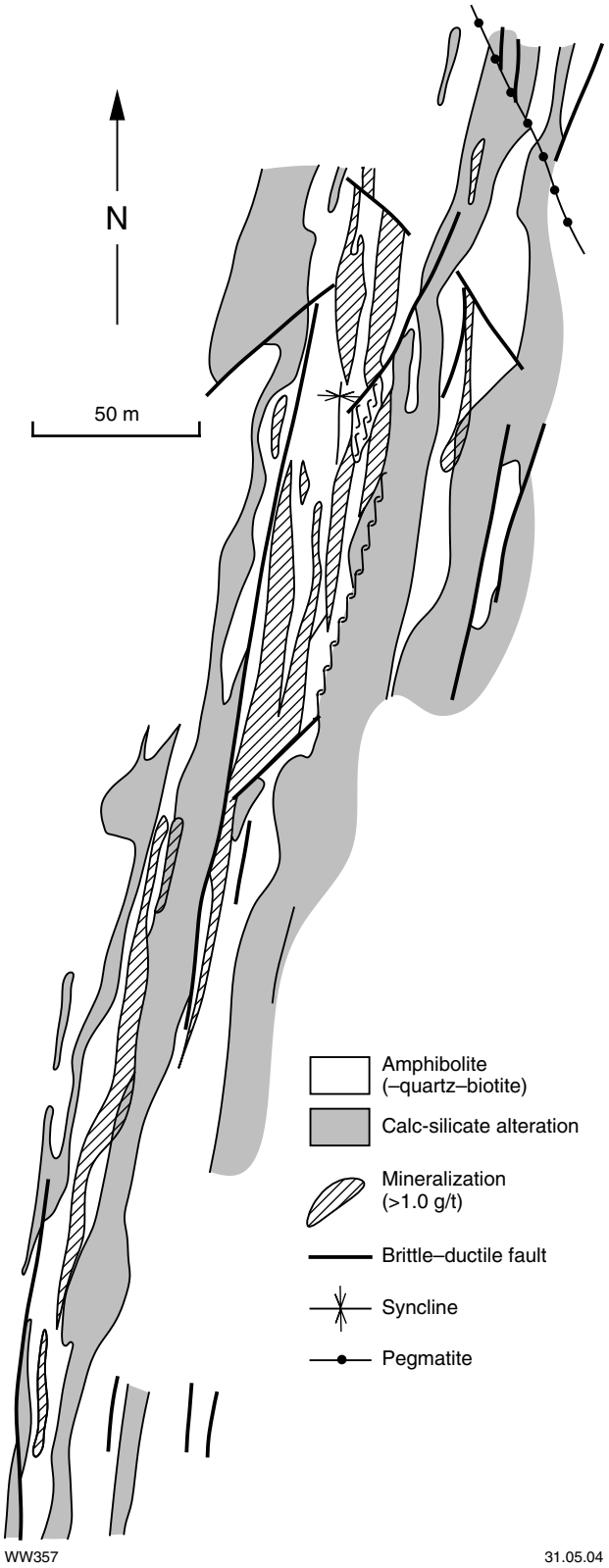

Figure 6.21. Geological plan of the Harrys Hill orebody at the 300-m level, Karonie

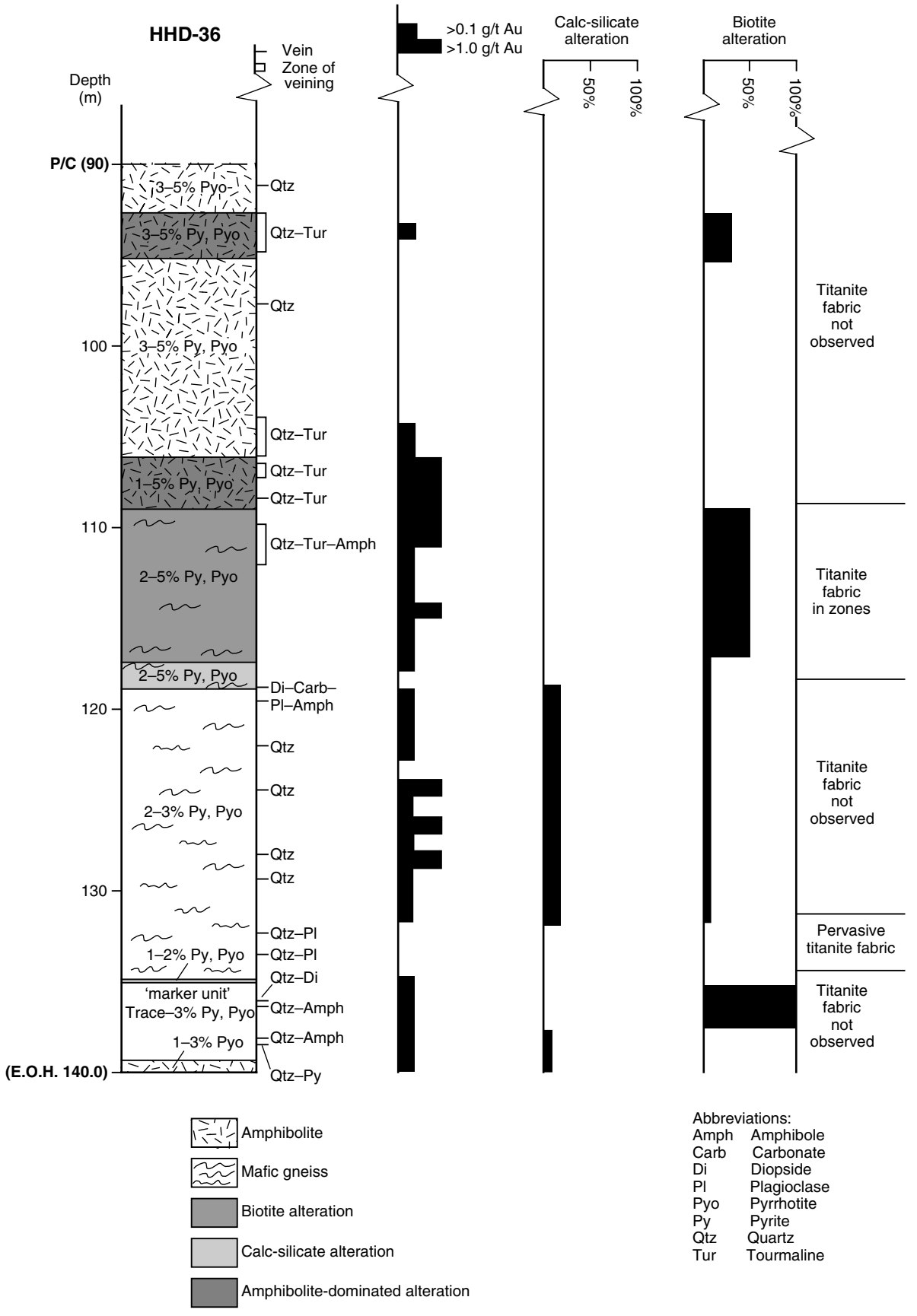

Figure 6.22. Summary log, HHD-36, Harrys Hill, Karonie

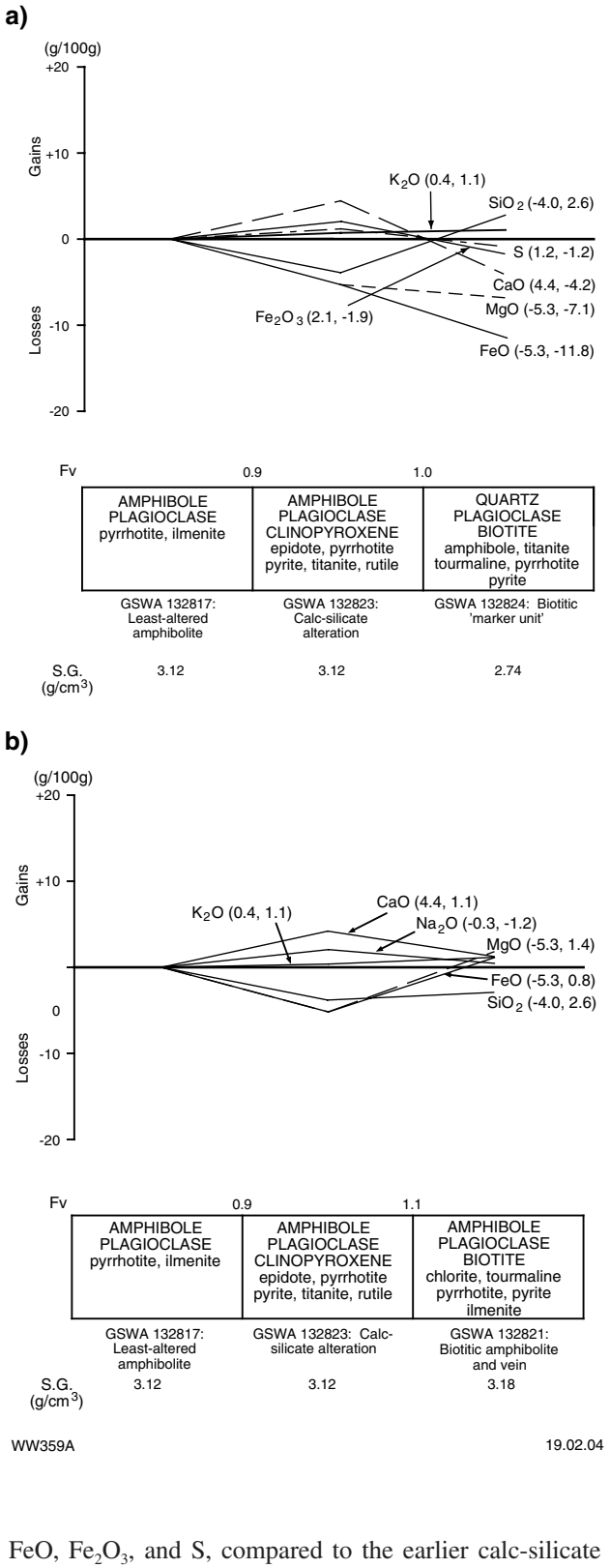

Figure 6.23. Mass-balance changes (calculated using the method of Gresens, 1967) associated with: a) calc-silicate alteration and retrograde alteration associated with late brittle–ductile shear zones; b) calc-silicate alteration and biotite alteration; and c) a quartz–tourmaline vein and alteration selvage, Harrys Hill deposit, Karonie. Mineral components of alteration assemblages are listed in approximate order of abundance, with main mineral components in upper case and minor mineral components in lower case

FeO, Fe_2O_3, and S, compared to the earlier calc-silicate alteration (Fig. 6.23a). Alteration related to a prominent quartz–tourmaline vein involves depletion of SiO_2, FeO, and MgO from the outer part of the alteration halo and redeposition of those same components in an inner, proximal alteration zone (Fig. 6.23c).

Although 'clouds' of fine-grained inclusions have been observed, gold is more commonly present as coarser grains, interstitial to, and along grain boundaries of, quartz and hornblende. The association with epidote observed in Main and West Zones is not well developed at Harrys Hill.

References: Poseiden Ltd (1990), Bogacz (1995), de Luca (1995), Dalstra (1995).

French Kiss

Other names: French Kiss South

Coordinates: 30°12'47"S, 122°34'35"E

Production: No historic production. The inferred resource is 28 000 t of ore at 3.47 g/t Au (1050 kg Au; MINEDEX site code S04351). The French Kiss South prospect has an indicated resource of 652 000 t at 4.34 g/t Au (2829 kg Au) and inferred resource of 207 000 t at 4.0 g/t Au (828 kg Au; MINEDEX site code S06415).

Host rock: The deposit is a supergene orebody hosted by the regolith overlying mafic and felsic greenstones.

Structure: There is little information regarding the structure in the underlying greenstones.

Alteration: There is little information regarding the nature of any alteration in the underlying greenstones.

References: de Luca (1995).

References

BOGACZ, V., 1995, Structural geometry and kinematics, tectogenetic explanation of exploration potential, Karonie prospect, Appendix *in* BORDER GOLD LTD, 1995, Annual report, Nov 1994 to Oct 1995, on E28/469–472, P28/841, P28/897–899 and M28/43: Western Australia Geological Survey, Statutory mineral exploration report, A46712 (confidential)*.

DALSTRA, H., 1995, The Kanonie gold deposits; gold mineralization and alteration characteristics, Appendix *in* BORDER GOLD LTD, 1995, Annual report, Nov 1994 to Oct 1995, on E28/469–472, P28/841, P28/897–899 and M28/43: Western Australia Geological Survey, Statutory mineral exploration report, A46712 (confidential)*.

de LUCA, K. E, 1995, Gold mineralisation in the Karonie greenstone belt, Eastern Goldfields, Western Australia: Western Australian School of Mines, MSc thesis (unpublished).

GRESENS, R. L., 1967, Composition–volume relationships of metasomatism: Chemical Geology, v. 2, p. 47–65.

HILL, R. I., CHAPPELL, B. W., and CAMPBELL, I. H., 1992, Late Archaean granites of the southeastern Yilgarn Block, Western Australia: age, geochemistry and origin: Transactions of the Royal Society of Edinburgh, v. 83, p. 211–226.

HOPWOOD, T., 1991, Structure and rock type controls at the Karonie mine, W.A.: a guide to exploration, Appendix *in* BORDER GOLD LTD, 1994, Annual report, Jan 1993 to Dec 1993, on M28/43: Western Australia Geological Survey, Statutory mineral exploration report, A46712 (confidential)*.

KNIGHT, J. T., GROVES, D. I., and RIDLEY, J. R., 1993, The Coolgardie Goldfield, Western Australia: district-scale controls on an Archaean gold camp in an amphibolite facies terrane: Mineralium Deposits, v. 28, p. 436–456.

LEAKE, B. E., 1978, Nomenclature of amphiboles: American Mineralogist, v. 63, p. 1023–1053.

McCUAIG, T. C., KERRICH, R., GROVES, D. I., and ARCHER, N., 1993, The nature and dimensions of regional and local gold-related hydrothermal alteration in tholeiitic metabasalts in the Norseman goldfields: the missing link in a crustal continuum of gold deposits?: Mineralium Deposita, v. 28, p. 420–435.

MIKUCKI, E. J., and RIDLEY, J. R., 1993, The hydrothermal fluid of Archaean lode-gold deposits at different metamorphic grades: compositional constraints from ore and wallrock alteration assemblages: Mineralium Deposits, v. 28, p. 469–481.

MYERS, J. S., 1995, Geology of the Esperance 1:1000 000 sheet, W.A.: Western Australia Geological Survey, 1:000 000 Geological Series Explanatory Notes, 10p.

PIGOTT, G. F., and GREEN, N. P., 1990, Karonie gold deposit, *in* Geology of the mineral deposits of Australia and Papua New Guinea *edited by* F. E. HUGHES: Australasian Institute of Mining and Metallurgy, Monograph 14, p. 531–535.

POSEIDEN LTD, 1990, Annual report, 1989, on P28/600, P28/477, M28/27–31, M28/53, M28/50 and M28/43: Western Australia Geological Survey, Statutory mineral exploration report, Item 11665 A30325 (unpublished).

POSEIDEN EXPLORATION LTD, 1992, Annual report, Jan 1991 to Jan 1992, on M28/53, M28/50–51, M28/43 and M28/27–31: Western Australia Geological Survey, Statutory mineral exploration report, Item 11665 A35404 (unpublished).

RIDLEY, J. R., 1990, Alteration assemblages, *in* Gold deposits of the Archaean Yilgarn Block, Western Australia: Nature, genesis and exploration guides *edited by* S. E. HO, D. I. GROVES, and J. M. BENNETT: University of Western Australia, Geology Department (Key Centre) and University Extension, Publication no. 20, p. 268–272.

SMITHIES, R. H., 1994, Geology of the Roe 1:100 000 sheet: Western Australia Geological Survey. 1:100 000 Geological Series Explanatory Notes, 15p.

SWAGER, C. P., and NELSON, D. R., 1997, Extensional emplacement of a high-grade granite gneiss complex into low-grade greenstones, Eastern Goldfields, Yilgarn Craton, Western Australia: Precambrian Research, v. 83, p. 203–219.

WITT, W. K., 1991, Regional metamorphic controls on alteration associated with gold mineralization in the Eastern Goldfields Province, Western Australia: implications for the timing and origin of Archaean lode-gold deposits: Geology, v. 19, p. 982–985.

WITT, W. K., 1993, Gold mineralization in the Menzies–Kambalda region, Eastern Goldfields, Western Australia: Western Australia Geological Survey, Report 39, 165p.

WITT, W. K., SWAGER, C. P., and NELSON, D. R., 1996, $^{40}Ar/^{39}Ar$ and U–Pb constraints on the timing of gold mineralization in the Kalgoorlie gold field, Western Australia: a discussion: Economic Geology, v. 91, p. 792–795.

*Confidential references are used with the permission of companies.

7. Eucalyptus – Pykes Hollow

The Eucalyptus and Pykes Hollow mining centres are located in a north-trending greenstone belt between Yundamindera and Lake Carey, southwest of Laverton. The geology of this area is dominated by a north-northwesterly trending F_2 fold (Fig. 7.1) that has been variously interpreted as an anticline (Williams et al., 1976; Hallberg and Wilson, 1983; Hallberg, 1985) or a syncline (Gower, 1976). The western limb of the fold has been complicated by the emplacement of large granite plutons to the west. In the north of the area, a large ultramafic body may have been thrust over the folded greenstones (Hallberg, J. A., 1996, written comm.). The fold axis terminates in the south against a north–south shear zone that separates the mineralized greenstones from meta-andesite-bearing greenstones to the east. Late (D_4) deformation produced northeast-trending dextral faults and northwest-trending sinistral faults.

In combination, the two mining centres have produced about 150 kg of gold, the bulk of which came from Pykes Hollow. Dollied and alluvial gold accounts for most of this production, with the largest production of alluvial and lode gold coming from the Yando Leases (about 45 kg Au from each). The largest historic deposit in the Eucalyptus mining centre is the Cardigan mine (about 10 kg Au). In both centres, supergene gold was produced from the oxidized zone and few workings penetrated fresh rock. There has been no modern reworking of the old underground mines, but there has been widespread, small-scale reworking of the alluvial deposits. Small-scale, openpit mining was conducted in the 1990s at the Zelica deposit, about 3.5 km south of the old Eucalyptus mining centre (pre-mining resource of 119 kg Au).

The Zelica deposit and the old Eucalyptus mining centre are both located near the nose of the F_2 fold. Mineralization at Zelica is associated with stockwork veining in metabasalt and is related to shear movement on a metamorphosed thin interflow sedimentary rock between metamorphosed komatiitic and tholeiitic basalt flows. The Cardigan workings are located in metabasalt and metadolerite on the western limb of the F_2 fold and appear to follow west-northwesterly to northwesterly trending D_4 faults. Other, smaller workings are located on small structures with a variety of orientations in mafic rocks within the core and eastern limb of the fold.

Most deposits in the Pykes Hollow centre are hosted by thin metasedimentary units within mafic sequences. Mineralization is associated with strike-parallel zones of brittle–ductile shear. These shears appear to have accommodated dextral movement, followed by later subvertical movement. Mineralized northeast-trending structures are less common, but may be related to D_4 faults with a similar orientation. The orientation of splay structures off one such lode, south of Harlech Castle, suggests sinistral movement.

The Triumph mine, about halfway between the two mining centres, is located on the hangingwall of a 3–4 m-wide, northeast-striking quartz blow. Mineralization appears to be associated with coarse, idioblastic pyrite in strongly sheared and silicified, metamorphosed feldspar-phyric dolerite.

Alteration at most deposits has been obscured by weathering. However, limited amounts of fresh material on mine dumps and from exploration drilling suggest mineralized metasedimentary rocks are silicified sericitic schist with idioblastic pyrite. Mafic-hosted mineralization at Zelica, Eucalyptus, and Pykes Hollow is associated with pyritic(–pyrrhotite) quartz–sericite schist enveloped in an outer halo of chlorite–carbonate alteration.

The orientation of sinistral and dextral brittle–ductile shears at Pykes Hollow implies formation during east–west compression. The similarity of alteration styles at these deposits and others associated with D_4 faults suggests all the mineralization in these two mining centres formed late in the deformation history of the greenstones. The north–south orientation of the greenstones at Eucalyptus and Pykes Hollow is favorable for the failure of competent units by brittle fracture (Ridley, 1993), particularly at Pykes Hollow, where the mafic sequence is bound by less-competent metasedimentary rocks to the west and east. Although historic mining focused on contact-parallel shears, further exploration should be directed towards quartz-vein arrays in brittle mafic units, particularly near contacts with less-competent rock units.

The proximity of the Pykes Hollow mining centre to a late thrust surface suggests that the thrust fault was a capping horizon that caused local build-up of high fluid pressures, leading to rock fracture and mineralization. The area north of Pykes Hollow has a high potential for undiscovered gold mineralization, particularly where north-trending contacts between rock units of contrasting rheology are overlain by the thrust sheet.

Deposits of Eucalyptus – Pykes Hollow area

Zelica

Coordinates: 29°13'06"S, 122°10'26"E

Production: No significant historic production was recorded. The measured resource is 70 000 t of ore at 1.7 g/t Au (119 kg Au). Small-scale, openpit mining has taken place in recent times; however, no production figures are available.

Host rock: Mainly metabasalt; some ore is in a metamorphosed narrow interflow sedimentary unit. Figure 7.1 shows that the deposit is located in metamorphosed tholeiitic basalt; however, M. Longman (1995, written comm.) indicated that the interflow sedimentary unit separates mainly metamorphosed komatiitic basalt to the west from metamorphosed tholeiitic basalt to the east, in which case the deposit is hosted by metamorphosed komatiitic basalt.

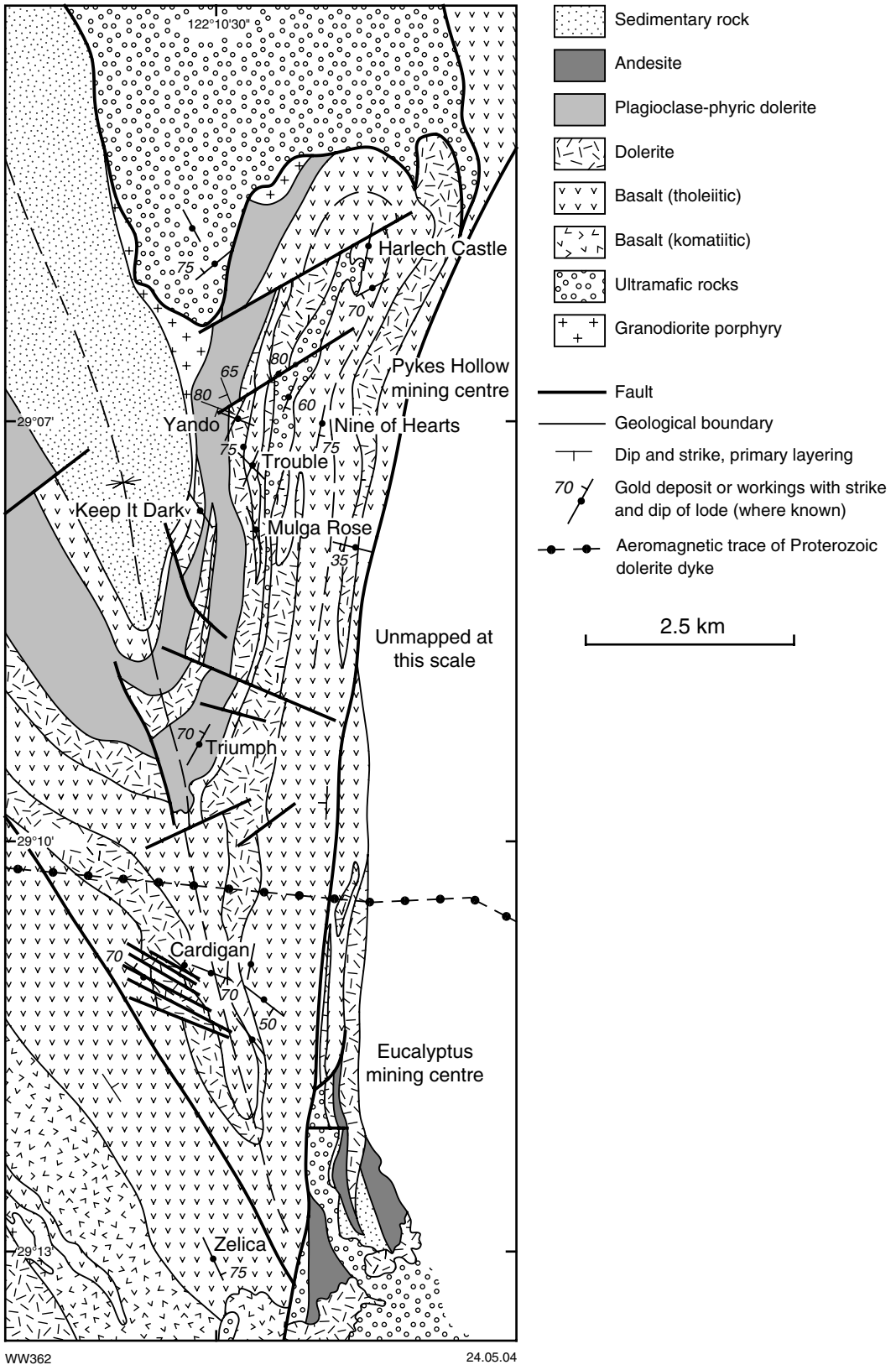

Figure 7.1. Interpreted geological map of the Eucalyptus and Pykes Hollow mining areas (based on regional maps and aeromagnetic data) showing the location and nature of gold deposits

Structure: Mineralization is associated with a sheared metamorphosed interflow sedimentary rock that strikes 335° and dips 60–80°E. The main orebody is a zone of stockwork veining in the footwall of the sheared metasedimentary rock and is separated from the metasedimentary rock by 5–7 m of barren mafic rock. There is also a relatively narrow ore zone within the sheared metasedimentary rock. Ore-zone widths are variable along strike and with depth, but at the present level of exposure, the main ore zone is about 5 m thick and the metasedimentary-rock-hosted ore zone is about 1 m wide. Quartz veins within the mineral-ized stockwork have a range of orientations, including prominent sets parallel to the sheared metasedimentary unit and subhorizontal veins.

A broad zone of foliated mafic rock in the footwall of the sheared metasedimentary rock dips more steeply to the east than the metasedimentary unit, suggesting reverse movement on the shear zone.

Alteration: Alteration is obscured by weathering, but drilling indicates that the ore zone (yellow in openpit exposures) is quartz–sericite–carbonate–pyrite schist with minor but variable amounts of chlorite and silicification. In the openpit, the main ore zone is separated from the sheared metasedimentary rock by chocolate-brown rock after chloritized and carbonated mafic rock.

References: Jarrahmond Holdings Pty Ltd (1988).

Cardigan

Other names: Round Hill, Shannon, Shannon Gold Mining Company, Lady Pascoe

Coordinates: 29°10'50"S, 122°10'15"E

Production: 284.5 t of ore for 10.38 kg Au (36.5 g/t Au) between 1899 and 1936.

Host rock: Mafic rocks (metabasalt and metadolerite). Fresh metadolerite is found on dumps surrounding the deepest shafts. Regional mapping (Fig. 7.1) indicates a metamorphosed tholeiitic basalt host rock, but exploration drilling indicates the presence of metamorphosed komatiitic basalt with pyroxene spinifex texture in the vicinity of the workings.

Structure: The main group of mine workings is distributed over about 250 m on a 305° trend, more or less parallel to a series of late faults that, in combination, sinistrally offset the metabasalt–metadolerite contact by about 500 m (Fig. 7.1). Mine dumps are dominated by weathered, but little-deformed, mafic rock and abundant quartz–carbonate vein fragments. There is also a small amount of more-strongly foliated rock containing thin quartz–carbonate veins. Evidence from dump samples suggests the mineralized structure is probably a brittle–ductile fault with a large component of brittle deformation.

There is a second group of shallower workings on a similar structure, about 15 m east of the main line of workings.

Alteration: Undeformed mine-dump samples display little evidence of alteration, which may have been obscured by weathering. Foliated samples with veins are sericitized, carbonated, and sulfidized (pyrite±pyrrhotite).

Reference: Maitland (1903).

Keep It Dark

Other names: Battlers Rest, Knights Errant

Coordinates: 29°07'31"S, 122°10'16"E

Production: 45.7 t of ore for 4.28 kg Au (93.6 g/t Au) between 1898 and 1904. Additionally, 5.83 kg of dollied gold was produced in the same period.

Host rock: Weathered mafic rock.

Structure: Shallow to moderately deep workings trend 325° over a strike length of about 70 m, but the mineral-ized structure is not well exposed.

Alteration: Alteration is obscured by weathering.

Mulga Rose

Coordinates: 29°07'25"S, 122°10'55"E

Production: 315.0 t of ore for 6.56 kg Au (20.8 g/t Au) between 1944 and 1947.

Host rock: Weathered mafic rock (?metabasalt).

Structure: Shallow workings lie on a 345° trend, but the host structure is poorly exposed. Vein quartz is moderately common on most mine dumps, indicating a possible veined brittle–ductile shear.

Alteration: Alteration is obscured by weathering, but sericitic schist with idioblastic pyrite has been observed on some mine dumps.

Trouble

Other names: Vera

Coordinates: 29°07'08"S, 122°10'45"E

Production: 260.6 t of ore for 7.45 kg Au (28.6 g/t Au) between 1939 and 1946.

Host rock: Thin (5–10 m wide) metasedimentary unit between metadolerite units.

Structure: Mine workings, distributed over about 150 m, are located on a north–south trend (000–010°), following the strike of the metasedimentary unit. The workings expose a 1–2 m-wide, brittle–ductile (veined) shear zone that dips 60–70°W, conformable with the metasedimentary host rock. Exposed sections of the mineralized shear suggest that veins (up to 10 cm wide) constitute 10–20% of the total shear zone width.

The mineralized shear is located near the hangingwall contact of the metasedimentary unit. There are two main vein sets within the mineralized shear: one is parallel to subparallel to the shear fabric (approximately north–south and dipping 60–70°W), and the other is markedly discordant (dipping about 20°N to NNE). There is also a less common set of subvertical veins that trend about 290°.

Rare, early veins are tightly folded about northerly to north-northwesterly trending axial planes. The subhorizontal vein set post-dates the steeper veins and offsets them by a few centimetres with a top-block-to-the-west movement direction.

At the northern end of the mineralized structure, workings follow a 1–2 m-thick quartz blow that trends 025° and dips about 80°E and is wholly contained within the metasedimentary unit.

The orientation of the quartz blow within the northern part of the mineralized shear, and the rotation of the regional foliation adjacent to the shear, indicate a predominantly dextral movement on the shear zone. The subhorizontal veins formed during a later stage of subvertical movement.

Alteration: Within the mineralized shear, the metasedimentary unit is altered to carbonated sericitic schist with idioblastic pyrite up to 5 mm across. A minor component of silicified metasedimentary rock may represent zones of more-intense alteration.

Nine of Hearts

Other names: Cornucopia

Coordinates: 29°06'55"S, 122°11'12"E

Production: 886.6 t of ore for 25.43 kg Au (28.7 g/t Au) between 1898 and 1901.

Host rock: Although the regional map shows this deposit to be within metabasalt (Fig. 7.1), inspection of mine workings indicates that the main host rock is a metasedimentary unit — probably a thin interflow unit.

Structure: Mine workings are quite scattered, but appear to follow two or more brittle–ductile (veined) shears that strike 010° and dip 70–80°E. The largest workings appear to be located on the sheared footwall of a large (about 1 m wide) quartz blow. Minor mineralization is also apparent within shears that are conformable with the regional foliation (340–350°, subvertical). Both the regional foliation and the conformable shears are deflected against the 010°-trending structures. The direction of this deflection suggests dextral movement on the 010°-trending structures. Another prominent 010°-trending quartz blow extends about 100 m south beyond the workings, but has not supported any production.

Alteration: The mineralized metasedimentary unit contains idioblastic pyrite (up to 5 mm across) but the details of alteration have been obscured by weathering.

References: Honman (1917).

Harlech Castle

Coordinates: 29°05'50"S, 122°11'37"E

Production: 7.11 t of ore for 2.90 kg Au (407.9 g/t Au) between 1903 and 1905. Also 31.93 kg of dollied gold.

Host rock: Regional mapping indicates the host unit is metabasalt (Fig. 7.1). However, exploration drill chips indicate the presence of metadolerite and pyritic black shale at depth. The host rock is probably metadolerite.

Structure: A deep shaft has been sunk at the northern end of a 1–2 m-thick quartz vein that strikes 010°. Exploration drilling suggests the vein dips to the east.

Alteration: Mine dumps are dominated by vein quartz and weathered mafic rock. Exploration drill chips indicate the presence of chlorite–carbonate schist at depth.

References: Honman (1917).

Yando Leases

Coordinates: 29°06'52"S, 122°10'35"E

Production: 78.8 t of ore for 45.08 kg Au (572.1 g/t Au) between 1900 and 1905. Also 45.0 kg dollied gold. Some of this production may have come from Trouble.

Host rock: The main host rock is a thin metasedimentary unit (quartz–sericite schist and metamorphosed black shale) that separates metadolerite units; there appears to have been some production from adjacent metadolerite units.

Structure: Mineralization is centred on a 1–3 m-wide, brittle–ductile (veined) shear zone that trends 025° and dips 70–80°E, following the metasedimentary unit. The mineralized shear is apparently located at or near the hangingwall of the metasedimentary unit. Quartz veins (up to 30 cm thick) within the mineralized shear have variable orientations, but are commonly subparallel to shear margins. There are also some subhorizontal veins and another set that strikes about 290° and dips 80°S. Deflection of fractures adjacent to the mineralized shear, exposed in an exploration trench, suggest a period of reverse movement.

A second mineralized shear, to the north and west of that described above, strikes 350° and dips 60–70°W in metadolerite. This structure is a 0.5 m-wide zone of strongly foliated rock with foliation-parallel quartz veins up to 10 cm wide.

A third mineralized shear, about 100 m northwest of the first, is located on another thin metasedimentary horizon between metadolerite units. This subvertical zone of deformation is about 1 m wide and trends 015°. Sheeted, subvertical veins ($\leq$2 cm) of quartz in the adjacent metadolerite to the west are oriented 275°. The orientation of these sheeted veins suggests dextral movement on the mineralized shear.

Alteration: Mineralized shears are characterized by sericitic schist with idioblastic pyrite up to 3 mm across. Silicified metasedimentary rock on mine dumps may represent zones of more-intense alteration. Alteration of doleritic host rocks is obscured by weathering, but appears to be defined by narrow bleached zones (?sericite–carbonate alteration) coincident with zones of strong deformation and veining, enveloped in broader zones (0.5 to 1 m) of chlorite–carbonate alteration.

References: Honman (1917).

References

GOWER., C. F., 1976, Laverton, W.A.: Western Australia Geological Survey, 1:250 000 Geological Series Explanatory Notes, 30p.

HALLBERG, J. A., 1985, Geology and mineral deposits of the Leonora–Laverton area, northeastern Yilgarn Block, Western Australia: Perth, Western Australia, Hesperian Press, 140p.

HALLBERG, J. A., and WILSON, P., 1983, Relative timing of igneous intrusion in the Eucalyptus area, northeastern Yilgarn Block, Western Australia: Journal of the Geological Society of Australia, v. 30, p. 383–392.

HONMAN, C. S., 1917, The Geology of the North Coolgardie Goldfield — Part I. The Yerilla District: Western Australia Geological Survey, Bulletin 73, 98p.

JARRAHMOND HOLDINGS PTY LTD, 1988, Annual report on GML39/00982, M39/00056, M39/00178–00182 and M39/00114–00115: Western Australia Geological Survey, Statutory mineral exploration report, Item 11658 A25363 (unpublished).

MAITLAND, A. G., 1903, Notes on the country between Edjudina and Yundamindera, North Coolgardie Goldfield: Western Australia Geological Survey, Bulletin 11, 58p.

RIDLEY, J. R., 1993, The relations between mean rock stress and fluid flow in the crust: with reference to vein- and lode-style gold deposits: Ore Geology Reviews, v. 8, p. 23–27.

WILLIAMS, I. R., GOWER, C. F., and THOM, R., 1976, Edjudina, W.A.: Western Australia Geological Survey, 1:250 000 Geological Series Explanatory Notes, 29p.

8. Jubilee–Kurnalpi

The Kurnalpi mining centre is located within the Steeple Hill domain of the Kurnalpi Terrane (Swager, 1997). In this area, the greenschist-facies greenstones strike north–south and young to the east. They lie in faulted contact with roughly east–west oriented greenstones of slightly higher metamorphic grade to the north. The greenstones are predominantly metabasalt and metadolerite with minor lenses and slices of ultramafic schist. A high proportion of the total gold production from the Kurnalpi mining centre (about 180 kg Au) is from detrital sources, including both deep leads and surficial (supergene) gold. Small-scale working of surficial deposits continues to be the main mining activity in the area. The most important of the deep leads were those at Minters Gully and Scottish Lass Well. Large amounts (>10 kg) of dollied and alluvial gold were produced from the Kurnalpi Pride – Kurnalpi King – Kurnalpi Gem area and the Kurnalpi Wonder area.

Although some gold mineralization is spatially associated with large-scale faults or shear zones (e.g. Success is adjacent to the Avoca Fault), the main lode-style mineralization at Kurnalpi is in a wedge-shaped, fault-bound, low-strain domain (Fig. 8.1). The main host rocks are metamorphosed basalt and komatiitic basalt, although there is also some mineralization in ultramafic rocks. Gold is in quartz veins, quartz-vein arrays, and brittle–ductile shear zones with a variety of orientations and attitudes (Fig. 8.1). Many of the mineralized structures, particularly those that dip to the east, have relatively flat attitudes (≤45°). The Six Mile deposit is an east–west, tabular zone of veining and brecciation that lies mostly within a differentiated metadolerite sill in the higher grade greenstones to the north (Fig. 8.1). A prominent focus of historic workings within this zone is a large, northwest-striking quartz vein that dips about 35°NE. The structures in the Kurnalpi mining area are, for the most part, poorly exposed, and it has not been possible to establish their primary controls. They may have formed in response to uplift related to the emplacement of granite plutons to the north, or may be related to late-tectonic fluid focusing in a domain of low mean stress. During late-tectonic east–west compression, the Kurnalpi mining area lay in the pressure shadow of the large granitoid body immediately to the north. The strike of the greenstones, normal to regional σ_1, is ideally oriented to exploit differences in mean stress at contacts between units of contrasting competency (Ridley, 1993). Under these circumstances, brittle fracture of competent units can be anticipated.

Mineralized mafic rocks are altered to pyritic assemblages dominated by plagioclase (albite), carbonate (ankerite), and quartz with minor but variable amounts of chlorite, muscovite, and biotite (Table 8.1). Fuchsite has been observed at some deposits hosted by metamorphosed komatiitic basalt and ultramafic rock. Less-altered samples are dominated by chlorite, biotite, and carbonate. The mineralized lodes are characterized by the addition of SiO_2, Na_2O, CO_2, and S, and depletion of FeO and MgO. CaO may be enriched (Kurnalpi Pride) or lost (Six Mile). Similar alteration assemblages are present at the Mulgabbie mining centre.

The Jubilee mining centre is located within the Jubilee domain of the Kurnalpi Terrane (Swager, 1997), in a northwest-striking sequence of greenschist-facies greenstones. It has produced only about 40 kg of gold, mainly from the Jubilee Gift South deposit. Mineralization at Jubilee Gift South is within a sinistral shear zone, in metamorphosed felsic volcaniclastic sedimentary rocks. The deposit is close to a contact with ultramafic rocks to the southwest. The interpreted sinistral movement on the mineralized shear zone is consistent with quartz-fibre orientations at Mountain Maid (not the same as Jubilee Gift South), which suggest a σ_1 oriented at about 250°. Weathering has obscured alteration at Jubilee Gift South, but ultramafic rocks at Mountain Maid have been carbonated, and mineralized mafic rocks at a small deposit about 1.5 km west of Mountain Maid are quartz–ankerite–muscovite(–chlorite) assemblages with numerous quartz–carbonate veins and veinlets. The intense carbonation at Mountain Maid and other localities in the Jubilee domain may have been an important factor in localizing mineralized vein systems and converting relatively ductile ultramafic rocks to more-brittle carbonate rocks. Shear strain was localized at the contacts between northwest-trending carbonated ultramafic rocks and felsic schists because of the competency contrast between these units. Local changes in the strike of this contact shear may have caused rock dilation and fluid focusing, potentially explaining localized accumulations of gold, for example, at Jubilee Gift South.

There are a few small workings in the Jubilee domain greenstones, south of Lake Yindarlgooda. Auriferous quartz veins, 1–2 m wide and oriented 325–350°, are in weathered metavolcaniclastic rocks near Pineapple Dam, east of Gundockerta Hill, to the south of the Kurnalpi mining centre. These deposits are located adjacent to the contact with metasedimentary rocks of the Mount Belches Formation and may be related to the northern termination of the Railway Fault (Swager, 1995). The greenstone sequence in this area is also cut by late, northerly to north-northeasterly trending dextral faults. These may have generated the contacts, oriented at a large angle to the regional east–west σ_1, between units of contrasting competency. Other, similar quartz veins in metamorphosed felsic volcaniclastic rocks have been mined for gold at Gessners Find and Kurnalpi South in the southern Kurnalpi Terrane.

Deposits of the Jubilee–Kurnalpi area

Jubilee Gift South

Other names: Mountain Maid, Iron Prince

Coordinates: 30°31'18"S, 122°03'15"E

Production: 1728.2 t of ore for 38.70 kg Au (22.4 g/t Au) between 1898 and 1903.

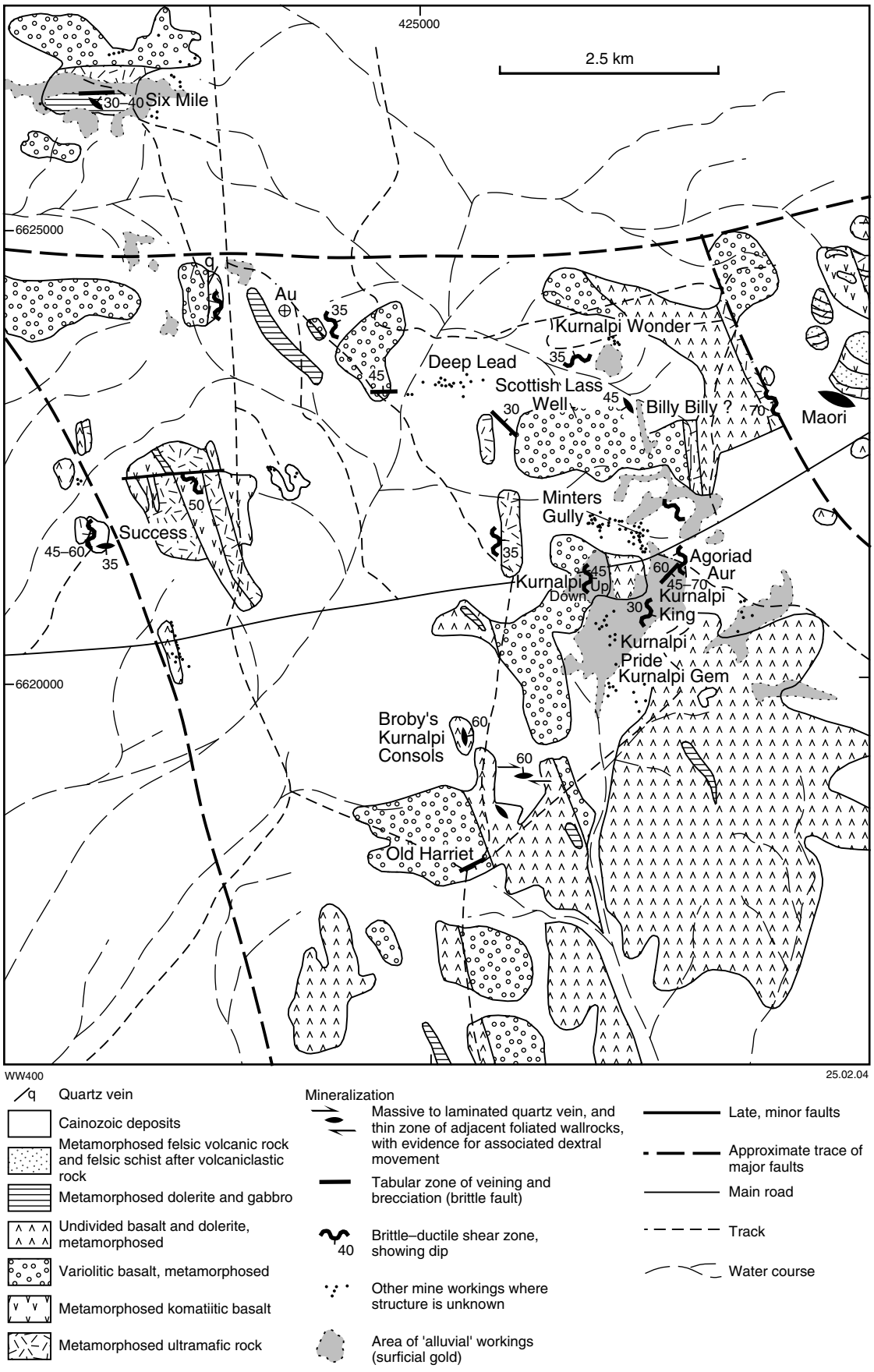

Figure 8.1. Geological map of the Kurnalpi mining area showing locations and styles of gold deposits (modified from Laverton Gold NL, 1987)

Table 8.1. Generalized summary of metamorphic and alteration assemblages in mafic rocks, Kurnalpi mining area

Metamorphic assemblage	*Outer alteration assemblage*	*Intermediate alteration assemblage*	*Inner alteration assemblage*
PLAGIOCLASE	PLAGIOCLASE	PLAGIOCLASE (ALBITE)	PLAGIOCLASE (ALBITE)
AMPHIBOLE	CHLORITE	CHLORITE	ANKERITE
Ilmenite	CARBONATE	ANKERITE	QUARTZ
	Quartz	QUARTZ	MUSCOVITE
	Epidote	Biotite	Leucoxene
	Leucoxene	Muscovite	Rutile
	Pyrrhotite	Leucoxene	Pyrite
	Pyrite	Rutile	
		Pyrite	

NOTES: Both the inner and intermediate zones of alteration are mineralized. Chlorite-absent assemblages (inner zones) are quite limited in occurrence and mostly restricted to narrow selvages adjacent to quartz–carbonate veins (Fig. 8.4)
Minerals shown in upper case are essential minerals and commonly form >10% of the rock
Minerals shown in lower case are minor to accessory phases

Host rock: Felsic schist after volcaniclastic rock.

Structure: One deep shaft and several shallower shafts, pits, and open stopes extend over about 250 m on a trend of 310°. The mineralization is in two to three subparallel, possibly en echelon, veined brittle–ductile shear zones (terminology of Witt, 1993). The shear zones are 1–2 m wide and dip steeply at greater than 70°NE. Massive to laminated, cherty looking veins (≤10 cm wide) within the shear zones are mostly subparallel to the shear-zone margins, but many are curved or branching, or both. Quartz-vein splays observed at the northwestern end of the workings are steep and oriented east–west, indicating a predominantly sinistral strike-slip movement on the shear zone. Locally, subhorizontal veins have also been observed, and probably formed during later, subvertical movements.

Alteration: Alteration is obscured by weathering. The mine dump at the main shaft, at the southeastern end of the workings, contains weathered felsic schist and vein quartz, commonly with a thin veneer of sericitic schist. There is also minor carbonated metadolerite, indicating the presence of mafic rocks at depth.

Agoriad Aur

Other names: Perseverance, Kurnalpi, Turn of the Tide

Coordinates: 30°32'24"S, 122°14'47"E

Production: 128.5 t of ore for 8.85 kg Au (68.8 g/t Au) between 1908 and 1922. An additional 26.15 kg Au has been produced from dollied and alluvial sources.

Host rock: Weathered metamorphosed tholeiitic basalt.

Structure: Shallow, scattered workings are on quartz veins that display a variety of orientations. The structures are very poorly exposed, except in a shallow costean where several small veins (3 cm) are oriented 220° and dip 45–70°SE. These veins are associated with shearing of the mafic host rock and are cut by a set of flatter en echelon veins.

Historic records describe the mineralization as being in a 10–12 m-wide 'lode' that strikes 005° and dips 60°W. The sigmoidal form of the steeper set of veins implies oblique dextral and reverse movement.

Alteration: Alteration is obscured by weathering.

References: Metana Minerals NL (1985a).

Billy Billy

Coordinates: 30°31'16"S, 122°15'34"E

Production: 823.0 t of ore for 22.44 kg Au (27.3 g/t Au) between 1903 and 1905.

Host rock: Metamorphosed tholeiitic basalt.

Structure: A moderately deep shaft and some shallower workings have been sunk on a quartz vein (0.25 m thick) that strikes north-northwest and dips 45°W.

Alteration: Larger mine dumps contain chlorite–carbonate rock and schist, and vein quartz.

References: Montgomery (1904).

Scottish Lass Well

Other names: Hampton Hill GMs Ltd, Scottish Lass

Coordinates: 31°31'16"S, 122°13'39"E

Production: 852.5 t of ore for 11.26 kg Au (13.2 g/t Au) between 1898 and 1901.

Host rock: Metamorphosed variolitic (?komatiitic) basalt.

Structure: Several workings, including a moderately deep decline, extend for about 100 m on a structure that is oriented 300° and dips 30°NE. Mine-dump samples and limited observations suggest that the structure is a 1–2 m-thick, veined brittle–ductile shear zone or a tabular zone of veining and brecciation (terminology of Witt, 1993). The decline plunges 20–30°N, which may also be

the plunge of the ore shoots. Altered mine-dump samples are mostly moderately to strongly foliated, with the foliation defined by fine-scale modal and grain-size banding of metasomatic minerals, trails of disseminated ilmenite/leucoxene, and a weak to moderate preferred orientation of chlorite. The foliation is axial planar, with some locally developed tight folding of veins.

Alteration: Mineralization is associated with quartz–ankerite–albite veins within a broad zone of quartz–ankerite–albite alteration with varying amounts of chlorite, muscovite, and pyrite. Representative mineral analyses of albite and ankerite are given in Tables 8.2 and 8.3. Disseminated anhedral to idioblastic pyrite (≤1 mm) is associated with trace chalcopyrite and, in some samples, minor arsenopyrite. Accessory minerals are rutile and ilmenite, the latter extensively altered to leucoxene. The quartz, albite, and carbonate form an interlocking, granular mosaic of anhedral, subequant grains. Chlorite, where present, defines a weak to moderate foliation. Subhedral lath-shaped books of muscovite (0.2 – 0.3 mm long) display a preferred orientation at a large angle to the fabric in foliated samples.

Within this zone, narrow selvages of intense albitization adjacent to quartz–ankerite–albite veins overprint a less-intense, chlorite-bearing (intermediate) alteration assemblage (Fig. 8.2; cf. Table 8.1). The overprinting relationships do not necessarily indicate a temporal gap between alteration assemblages. Instead, they probably reflect a dynamic environment in which fractures and veins are continually forming and allowing access of unmodified ore fluids to relatively distal parts of a zoned alteration assemblage.

Table 8.2. Selected SEM analyses of plagioclase, Scottish Lass Well deposit, Kurnalpi

	GSWA 132985B ankerite–albite veins in pyritic ankerite–albite alteration assemblage after mafic rock					
	ankerite–albite alteration assemblage			*ankerite–albite vein*		
	P1	*P3*	*P5*	*P6*	*P8*	*P9*
SiO_2	68.56	66.86	68.38	68.05	68.40	68.20
Al_2O_3	19.33	19.01	19.30	19.58	19.32	19.27
FeO	0.24	0.93	0.26	-	-	-
MgO	0.17	-	-		-	-
CaO	0.28	0.14	0.26	-	-	-
Na_2O	11.55	11.54	11.35	11.70	11.58	11.57
K_2O	0.11	0.11	-	0.15	0.07	0.07
Total	**100.24**	**100.28**	**99.29**	**99.03**	**99.37**	**99.04**
An	1.3	0.6	1.3	-	-	-
Ab	98.1	98.7	98.7	99.2	99.6	100
Or	0.6	0.6	-	0.8	0.4	-

NOTE: Minor amounts of FeO and MgO in P1, P3, and P5 probably reflect some contamination from fine-grained ankerite

Table 8.3. Selected SEM analyses of carbonate, Scottish Lass Well deposit, Kurnalpi

	GSWA 132985B ankerite–albite veins in pyritic ankerite–albite alteration assemblage after mafic rock						
	ankerite–albite alteration assemblage			*ankerite–albite vein*			
	CB1	*CB3*	*CB4*	*CB8*	*CB9*	*CB10*	*CB11*
FeO	8.43	10.19	8.84	17.17	10.17	18.61	8.20
MnO	0.58	0.53	0.67	0.18	0.34	0.28	0.44
MgO	14.94	13.39	14.33	10.09	13.62	8.66	14.53
CaO	29.36	29.09	29.90	28.09	29.53	27.92	29.48
Total	**53.31**	**53.21**	**53.73**	**55.53**	**53.6**	**55.47**	**52.65**
$FeCO_3$	11.5	14.2	12.0	24.1	14.0	26.5	11.3
$MnCO_3$	0.8	0.7	0.9	0.3	0.5	0.4	0.6
$MgCO_3$	36.3	33.2	34.8	25.2	33.4	22.0	35.8
$CaCO_3$	51.4	51.9	52.2	50.4	52.1	51.0	52.2

NOTE: CB8 and CB10 are high-Fe/Mn+Mg carbonates from grain-boundary margins against albite. Carbonates farther (greater than about 200 microns) from the grain boundaries are similar in composition to the carbonate in the altered wallrocks

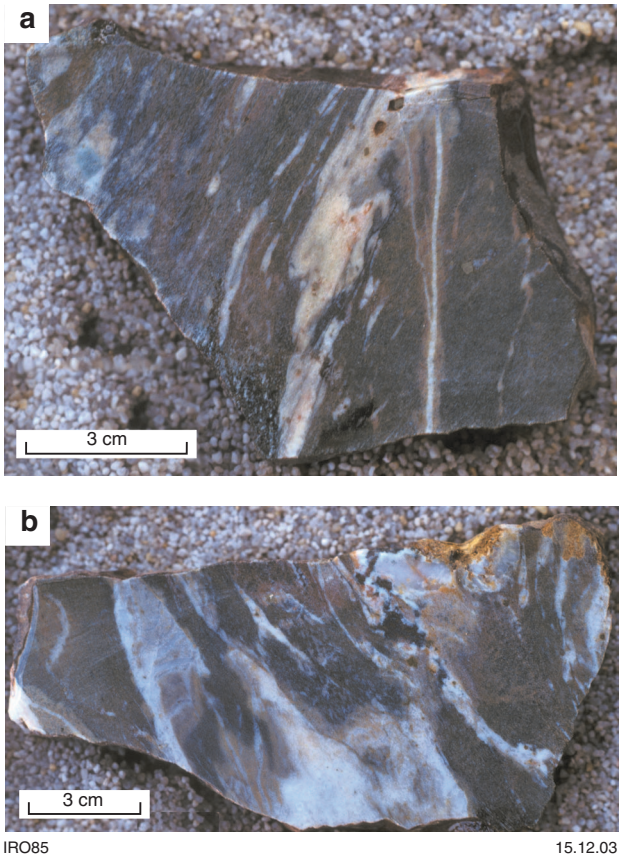

Figure 8.2. Deformed quartz–albite–carbonate veins with narrow, bleached alteration halos (intermediate zone, Table 8.1) within chlorite–carbonate alteration assemblage (outer zone, Table 8.1), mineralized mafic rock, Scottish Lass Well, Kurnalpi mining area

The proportion of chlorite increases at the expense of carbonate outwards from the central fluid conduits and is accompanied by minor amounts of biotite in some samples. The outer alteration zone is a chlorite–carbonate–plagioclase(–biotite) assemblage.

Whole-rock geochemical data are presented in Appendix 4, but mass-balance calculations have not been carried out because suitable samples of relatively unaltered metabasalt were not collected. Qualitatively, the samples of altered metabasalt from mine dumps display very high CO_2, CaO, and FeO concentrations, but lower amounts of SiO_2 than in altered samples from Kurnalpi King and Six Mile. These changes are consistent with intense carbonation (ankerite) of the host metabasalt.

References: Laverton Gold NL (1987), Montgomery (1904).

Kurnalpi King

Coordinates: 30°32'33"S, 122°14'42"E

Production: 15.8 t of ore for 9.53 kg Au (603.0 g/t Au) between 1912 and 1913. An additional 25.61 kg Au has been produced from dollied and alluvial sources.

Host rock: Metamorphosed tholeiitic basalt.

Structure: Shallow to moderately deep shafts lie on a structure that strikes 200°. Mine dumps are dominated by massive to moderately foliated, weathered metabasalt and vein quartz, suggesting that the mineralized structure is a veined brittle–ductile shear zone (Witt, 1993). Historic records refer to a 'hematitic indicator' up to about 0.25 m wide and dipping 30°SE. Gold is present where small (1–7 cm-wide) quartz veins intersect the 'indicator'.

Alteration: Alteration is obscured by weathering, but the weathered mafic rocks and schist are clearly strongly carbonated.

References: Metana Minerals NL (1985b), quoting Jutson (1914).

Kurnalpi Pride

Coordinates: 30°32'31"S, 122°14'42"E

Production: 34.2 t of ore for 11.45 kg Au (334.4 g/t Au) between 1915 and 1921. An additional 19.93 kg Au has been produced from dollied and alluvial sources.

Host rock: Metamorphosed amygdaloidal tholeiitic basalt.

Structure: The structure is not well exposed, but a deep shaft and some shallower excavations are associated with mullock that is mainly massive metabasalt in which essentially brittle fracture has produced widespread veining. These observations suggest that the orebody is a tabular zone of veining and hydraulic brecciation (brittle fault).

Alteration: Quartz–ankerite veining is associated with alteration of metabasalt to a quartz–ankerite–albite(–muscovite)–pyrite assemblage. Idioblastic pyrite up to 1 mm across is present in these assemblages. Less-intensely altered samples are chloritic with small biotite porphyroblasts. Mass-balance calculations, based on whole-rock geochemical data, indicate addition of large amounts of SiO_2, CO_2, Na_2O, and CaO, and small amounts of S to the mineralized albitic alteration assemblage (Fig. 8.3). MgO and FeO are lost when weakly to moderately carbonated metabasalt is altered to this assemblage.

Old Harriett

Coordinates: 30°34'00"S, 122°13'20"E

Production: 992.12 t of ore for 34.43 kg Au (34.7 g/t Au) between 1931 and 1937.

Host rock: Metamorphosed variolitic (komatiitic) basalt.

Structure: Shallow to moderately deep workings extend over about 100 m on a 245° trend. The mineralized structure is not exposed, but mine-dump samples include vein quartz, massive to weakly foliated, altered metabasalt with numerous branching veinlets, and small zones of

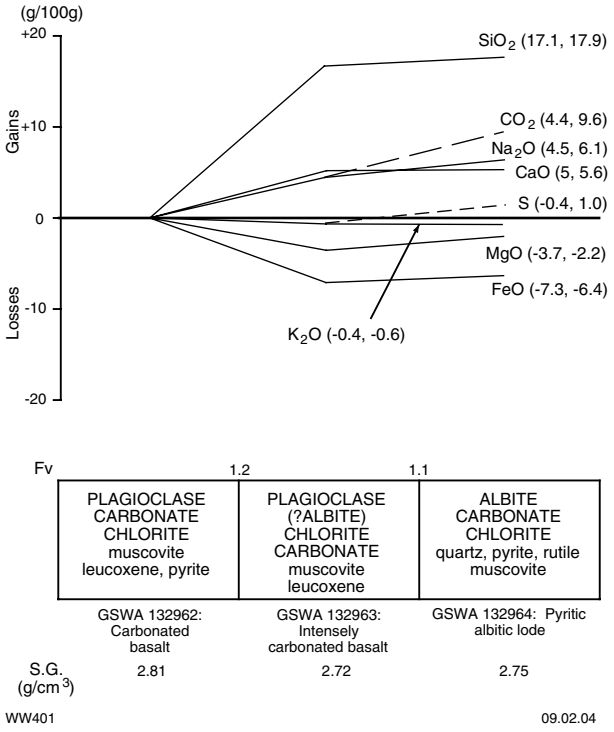

Figure 8.3. Mass-balance changes (calculated using the method of Gresens, 1967) associated with altered, mineralized mafic rock, Kurnalpi Pride, Kurnalpi mining area. GSWA 132962 is equivalent to the outer alteration assemblage, and GSWA 132963 and GSWA 132964 are equivalent to the intermediate alteration assemblage in Table 8.1. Mineral components of alteration assemblages are listed in approximate order of abundance, with main mineral components in upper case and minor mineral components in lower case

hydraulic breccia and minor chloritic schist. These observations suggest that the orebody is a tabular zone of veining and brecciation. The location of the deepest shaft suggests a dip to the south-southeast.

Alteration: Mineralized metabasalt is altered to a quartz–albite–ankerite assemblage containing accessory ilmenite and up to several percent disseminated, idioblastic pyrite (≤1 mm). Less-intensely altered samples are characterized by the assemblage plagioclase–carbonate–chlorite with minor quartz, epidote, and leucoxene.

Six Mile

Coordinates: 30°29'17"S, 122°10'59"E

Production: There is no recorded production against this group of leases, although the scale and number of workings suggest that there was significant production (?20–50 kg Au) from primary gold lodes.

Host rock: Metadolerite, meta-quartz-dolerite and, at the western end of the orebody only, olivine orthocumulate and pyroxenite. Metabasalt is mineralized at the eastern end of the workings. The main locus of development appears to have been in the meta-quartz-dolerite.

Structure: Several moderately deep shafts have been sunk to access a 200–300 m-wide, subvertical structure that strikes approximately east–west. Several of the deepest shafts appear to access a quartz vein within this zone that is several metres wide, strikes 310°, and dips 30–40°NE. The orebody is exposed at the surface, in the central part of the workings, as a massive, altered meta-quartz-dolerite with extensive veining and hydraulic breccia. However, mine-dump samples generally contain a moderate to strong, fine-scale (mm) ductile fabric defined by modal and grain-size banding of metasomatic minerals. In some samples, the banding is tightly folded and otherwise deformed and cut by later brittle features (veins). These observations suggest that the mineralized structure is a tabular zone of veining and brecciation or a veined brittle–ductile shear zone (terminology of Witt, 1993).

Alteration: Doleritic host rocks are altered to quartz–plagioclase(?albite)–carbonate-dominated assemblages. These minerals are accompanied by varying amounts of chlorite and, less commonly, biotite. Quartz–carbonate–albite assemblages are related to numerous quartz–carbonate and quartz–albite veins that cut a foliation in a less-intense, chlorite-bearing alteration assemblage, commonly at a large angle (Fig. 8.4). Most of the quartz and plagioclase form a fine-grained granular mosaic of anhedral grains, but there are some porphyroclasts of tabular, metamorphic plagioclase. Carbonate forms aggregates of coarser, anhedral grains (0.2 – 0.5 mm) that, in some samples, are elongate in the plane of the foliation. Chlorite is absent in more-intensely altered metadolerite, which may contain up to 10% sericite. Relict plagioclase porphyroclasts are absent in these more-intensely altered samples. Disseminated, idioblastic pyrite (2 mm), with minor chalcopyrite, is present in most samples and generally increases in abundance to several percent with proximity to veins. There is also an association of pyrite with carbonate aggregates in some samples.

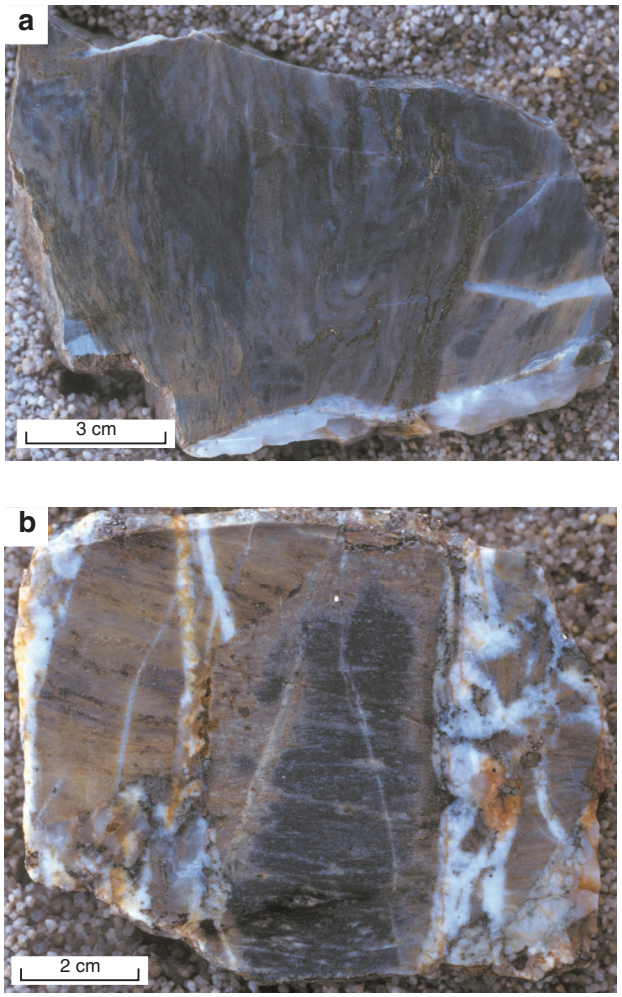

Figure 8.4. Examples of alteration in mineralized mafic rock from Six Mile, Kurnalpi mining area: a) deformed bands of chlorite–carbonate alteration (outer zone) and bleached, albitic alteration (intermediate zone); b) bleached, albitic alteration halos (intermediate zone) related to quartz–albite–carbonate veins (right) and hydraulic breccia (left) overprinting foliated chlorite–carbonate alteration assemblage (outer zone). Refer to Table 8.1 for a summary of the outer and intermediate alteration zones

Mass-balance calculations, based on whole-rock geochemical data, show that mineralized quartz–carbonate–albite assemblages are extremely enriched in SiO_2, and also enriched in CO_2, Na_2O, and S, compared to deformed but relatively unaltered mafic host rocks (Fig. 8.5). These chemical enrichments are accompanied by losses of FeO, CaO, and MgO.

Ultramafic rock at the western end of the workings is altered to a chlorite- and serpentine-bearing talc–carbonate assemblage that is cut by fibrous carbonate-rich veins and contains minor disseminated pyrite.

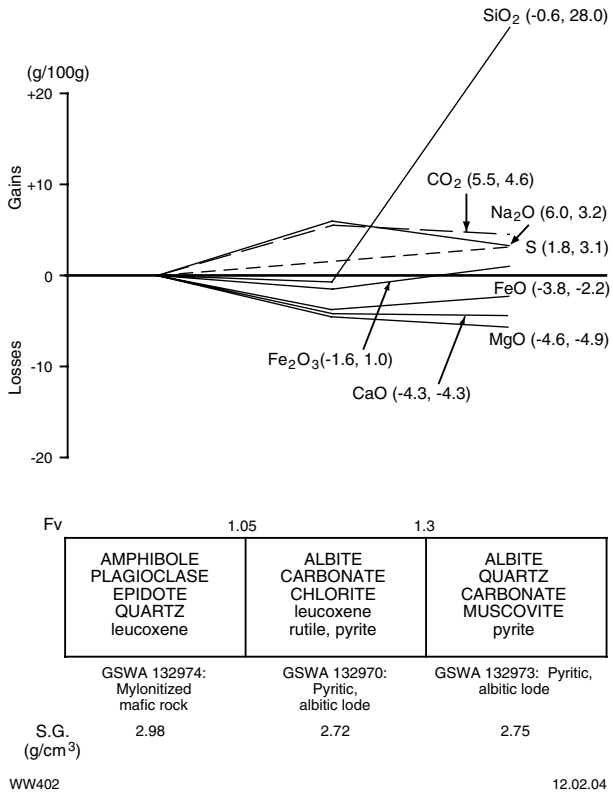

Figure 8.5. Mass-balance changes (calculated using the method of Gresens, 1967) associated with mineralized albitic alteration assemblages, Six Mile, Kurnalpi mining area. GSWA 132970 is equivalent to the intermediate zone, and GSWA 132973 is equivalent to the inner zone in Table 8.1. Mineral components of alteration assemblages are listed in approximate order of abundance, with main mineral components in upper case and minor mineral components in lower case

References

GRESENS, R. L., 1967, Composition–volume relationships of metasomatism: Chemical Geology, v. 2, p. 47–65.

JUTSON, J. T., 1914, Kurnalpi, North-east Coolgardie Goldfield: Western Australia Geological Survey, Bulletin 59, p. 13–30.

LAVERTON GOLD NL, 1987, Report on P28/00440, Scottish Lass Well: Western Australia Geological Survey, Statutory mineral exploration report, Item 3815 A21738 (unpublished).

METANA MINERALS NL, 1985a, Report on E28/00141 and E28/00135: Western Australia Geological Survey, Statutory mineral exploration report, Item 4188 A15630 (unpublished).

METANA MINERALS NL, 1985b, Report on E28/00141 and E28/00135: Western Australia Geological Survey, Statutory mineral exploration report, Item 4188 A17315 (unpublished).

MONTGOMERY, A., 1904, Annual Report for the year 1903: Western Australia, Department of Mines, p. 77–80.

RIDLEY, J. R., 1993, The relations between mean rock stress and fluid flow in the crust: with reference to vein- and lode-style gold deposits: Ore Geology Reviews, v. 8, p. 23–27.

SWAGER, C. P., 1995, Geology of the greenstone terranes in the Kurnalpi–Edjudina region, southeastern Yilgarn Craton: Western Australia Geological Survey, Report 47, Plate 1.

SWAGER, C. P., 1997, Tectono-stratigraphy of late Archaean greenstone terranes in the southern Eastern Goldfields, Western Australia: Precambrian Research, v. 83, p. 11–42.

WITT, W. K., 1993, Gold mineralization in the Menzies–Kambalda region, Eastern Goldfields, Western Australia: Western Australia Geological Survey, Report 39, 165p.

9. Mulgabbie – Old Plough Dam

The historic workings of the Mulgabbie mining centre lie within the Mulgabbie domain (Kurnalpi Terrane) of Swager (1997). At Mulgabbie, the greenstones of this domain form a homoclinal sequence that dips steeply to the southwest and youngs in the same direction. A depositional age of 2673 ± 7 Ma for a felsic volcanic unit from this sequence was determined from SHRIMP U–Pb dating of zircons (Nelson, 1995). The metamorphic grade is estimated at close to the greenschist–amphibolite transition (Morris, 1994). Relatively high strain in the Mulgabbie mining area apparently resulted from compression between the Galvalley Monzogranite to the east and another large granitic body to the west.

The Mulgabbie deposits produced about 250 kg of gold from very rich but small quartz veins. The main group of workings are in metamorphosed tholeiitic basalt, close to a contact with deformed and recrystallized komatiitic basalt to the west. This contact lies in the hanging-wall, about 1 km southwest of the Rebecca Shear, which is a splay off the Claypan Fault (Fig. 9.1). The main mineralization is along 1500 m of strike, in a zone that is conformable with lithological trends. The structure is not well exposed, but published descriptions and samples collected from mine dumps suggest that gold is within a veined brittle–ductile shear zone or, more probably, a brittle fault zone. The fault is several metres wide and characterized by cataclasis, hydraulic fracture, and relatively minor zones of ductile deformation. The fault may be a splay off the Rebecca Shear and may have been partly localized by the ductility contrast between metamorphosed, massive tholeiitic basalt and tremolite–chlorite schist (after komatiitic basalt). Mineralized rocks within the fault zone are characterized by a massive to strongly foliated, plagioclase (?albite)-dominant assemblage with a 'bleached' appearance. Plagioclase is accompanied by smaller amounts of pale-green chlorite, sericite, biotite, carbonate, epidote, and sulfide minerals (pyrite and pyrrhotite, minor chalcopyrite). Telluride minerals are locally common. Fabric relations indicate overlapping or alternating periods of ductile and brittle deformation within the 'bleached' zone. Gold was won mainly from quartz veins within the 'bleached' metabasalt, most of which do not exceed a few centimetres in thickness. 'Bleached' metabasalt is associated with zones of chloritic schist, locally with abundant small biotite porphyroblasts, in zones of strong ductile deformation within the fault zone. It is uncertain whether the chloritic schist represents a temporally separate (earlier) phase of hydrothermal activity or a less-intense (outer) zone of alteration related to the same fluid event that produced the 'bleached' rock. Early descriptions (Jackson, 1905) suggest the former. Mineralized, 'bleached' metabasalt is characterized by the addition of SiO_2, Na_2O, and S, and depletion of MgO, CaO, FeO, and Al_2O_3 (Fig. 9.2).

Relatively minor amounts of gold have been produced from quartz veins and narrow, strike-parallel shear zones in felsic schist at several localities (e.g. Cora, Ernbill) to the south and west of the main group of workings at Mulgabbie. There has been extensive, recent working of surficial units for alluvial gold in the vicinity of all historic workings.

The northwest orientation of the greenstone sequence at Mulgabbie is not favourable for brittle failure of competent units during late-tectonic east–west compression, but would maximize shear strain along contacts (Ridley, 1993). The presence of gold associated with dilational structures (veining and brecciation) in the contact-parallel shear zone probably reflects subtle changes in the strike of the shear zone, which may have been deflected around the small but relatively rigid monzogranite unit immediately to the west of the Mulgabbie Perseverance mine.

Recent exploration, 15 km northwest of the historic Mulgabbie mining area, has identified two orebodies with a combined resource of about 6 t of gold. The Twin Peaks and Monty Dam deposits lie within metamorphosed felsic volcaniclastic and related epiclastic sedimentary rocks in the eastern part of the Kurnalpi Terrane (Table 9.1; Swager, 1995). The deposits are within 2 km of the Yilgangi Fault — a major structure that forms the eastern boundary of the Kurnalpi Terrane (Fig. 9.1). The greenstone sequence in this area strikes north-northwest; it youngs and dips moderately to steeply to the east, but is locally overturned near the Twin Peaks deposit. Most of the lithological contacts in this area are deformed and both deposits are near north–south splays off these strike-parallel faults. Mineralization is within zones of intense brittle (hydraulic) fracture and associated silicification and pyritization. There is a broad association of gold with hematitization at Monty Dam and a closer association with arsenopyrite at Twin Peaks.

There are some features of the Twin Peaks and Monty Dam deposits that set them apart from the majority of gold deposits in the Eastern Goldfields Granite–Greenstone Terrane, and the origins of the deposits are equivocal. The deposits display some characteristics that are typical of many late-tectonic, epigenetic (mesothermal) gold deposits in the Eastern Goldfields Granite–Greenstone Terrane. They are spatially associated with late (D_4), northerly to north-northeasterly trending faults (cf. Kalgoorlie, Clout et al., 1990; Porphyry and Yarri, this Report). Veins in both mineralized stockworks overprint a foliation in the wallrocks, and reconnaissance fluid-inclusion studies indicate the presence of low-salinity H_2O–CO_2 fluids during mineralization (Pancontinental Mining Ltd, 1993, 1994). On the other hand, the host rocks to gold mineralization (metamorphosed volcaniclastic sedimentary rocks) are not typical of late-tectonic gold deposits. Under late-tectonic stress, brittle failure would be predicted in the more competent felsic volcanic unit that separates host rocks at Twin Peaks and Monty Dam (Fig. 9.1). Both deposits are associated with silicification of metamorphosed felsic volcaniclastic rocks that may have promoted brittle fracture of otherwise incompetent metavolcaniclastic rocks during regional deformation. However, the origin of silicification that pre-dated brittle fracture is unclear and not easily related to late-tectonic

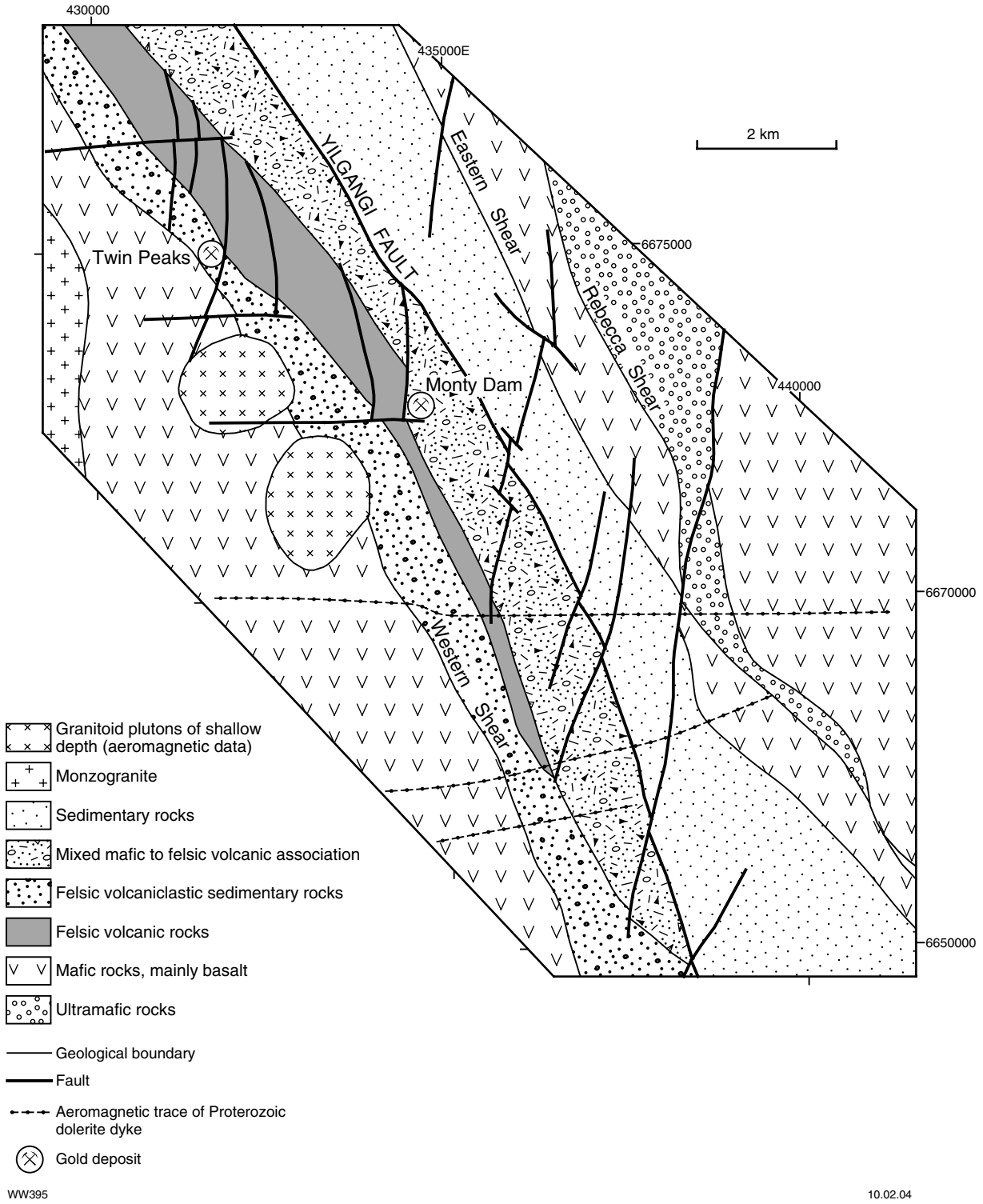

Figure 9.1. Interpreted geological map of the Old Plough Dam area showing the location of the Twin Peaks and Monty Dam deposits. Compiled from regional maps, maps from Pancontinental Mining Ltd (1993, 1994), and aeromagnetic data

events. The Twin Peaks deposit in particular, displays evidence for relatively early formation and two periods of subsequent deformation:

1. During regional deformation, strain was partitioned around the margins of the massive, silicified metasedimentary rock, producing an envelope of brittle–ductile deformation and chloritization. Although undeformed in the massive, silicified alteration zone, stockwork veins have been deformed with the host rocks in the enveloping zone of chloritization and brittle–ductile deformation. Narrow zones of chloritic alteration and ductile deformation also cut the main body of mineralized and silicified metasedimentary rock.
2. The Twin Peaks orebody is a stockwork of quartz veins that is transgressive with respect to stratigraphy. The shape of the orebody suggests that it has been deflected against a sheared contact with felsic volcanic rocks during late-tectonic, reverse fault movements (Fig. 9.3).

These observations are consistent with a pre-regional-deformation, possibly synvolcanic, origin for the Twin Peaks orebody. The mineralized stockwork may represent a feeder zone from a subvolcanic magma chamber, in a mesothermal to epithermal environment. If Monty Dam also formed in a similar environment, the tabular form and strike-parallel orientation of the orebody may reflect a shallow-level zone of hydrofracture, and boiling of hydrothermal fluids.

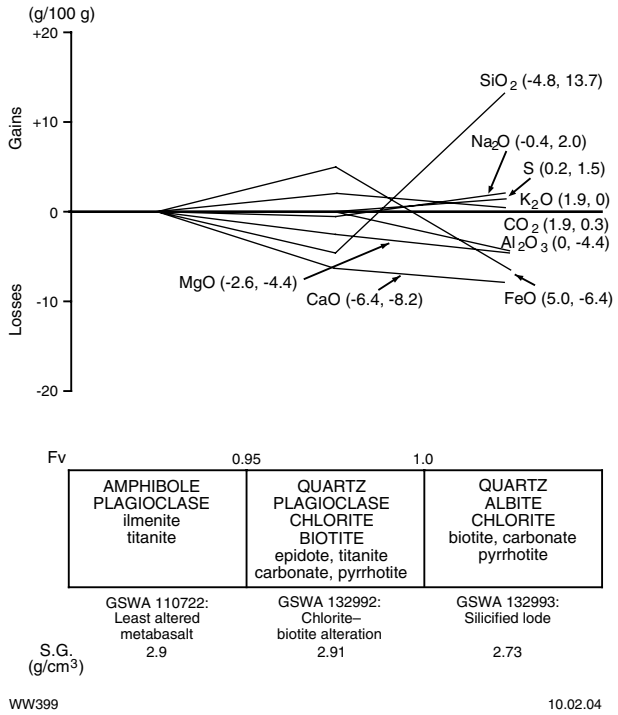

Figure 9.2. Mass-balance changes (calculated using the method of Gresens, 1967) associated with silicification of mineralized mafic rock, Mulgabbie Perseverance, Mulgabbie mining area. Mineral components of alteration assemblages are listed in approximate order of abundance, with main mineral components in upper case and minor mineral components in lower case

Deposits of the Mulgabbie – Old Plough Dam area

Twin Peaks

Coordinates: 30°03'20"S, 122°17'40"E

Production: No historic production. The inferred resource is 490 000 t of ore at 3.2 g/t Au (1568 kg Au) and the indicated resource is 1.27 Mt of ore at 3.88 g/t Au (4927.6 kg; MINEDEX site code S04205).

Host rock: Metamorphosed, massive to weakly foliated, fine-grained, felsic volcaniclastic sedimentary rock. The metasedimentary rocks are well sorted but unbedded and matrix supported, suggesting rapid deposition, possibly as the distal facies of mass-flow deposits. Clasts are predominantly quartz and plagioclase with minor lithic

Table 9.1. Descriptions of main rock types at Monty Dam and Twin Peaks

Rock type	*Description*
Metalatite	Metamorphosed, fine- to medium-grained, generally well sorted tuff and epiclastic sedimentary rock. Angular to subrounded, sand-sized particles of quartz, feldspar, and ferromagnesian minerals (mainly biotite), minor lithic clasts (≤1 cm), and rare megacrysts of plagioclase (about 8 mm), in a very fine grained quartzofeldspathic matrix. Quartz is generally a relatively minor component. Grain-size variation and variation in the abundance of biotite (up to 30–40%) and lithic clasts define a metre-scale bedding and, locally, millimetre-scale bedding. Cross-bedding and scour structures are present in some finely bedded sections. Probably includes metamorphosed air-fall tuff and related epiclastic sedimentary rocks
Meta-andesite	Massive to weakly bedded rock containing up to 10% plagioclase (≤3 mm) and hornblende (≤2 mm) crystal fragments, and subrounded to subangular, amphibole-rich lithic clasts (≤1 cm) in a fine-grained, mesocratic matrix. Probably includes metamorphosed ash-flow tuff and air-fall tuff and related epiclastic sedimentary rocks
Metamorphosed felsic volcaniclastic sedimentary rock	Massive (unbedded), well-sorted, fine-grained, volcaniclastic sedimentary rock. Angular to subangular grains (≤0.5 mm) of quartz (10%) and feldspar (90%) in a finer grained matrix of quartz, feldspar, sericite, biotite, and chlorite. Feldspar clasts are mainly plagioclase and there are rare lithic clasts with an andesitic to dacitic composition. Unbedded and matrix-supported structure of the metasedimentary rocks suggests rapid deposition from mass-flow deposits and an andesitic to dacitic provenance

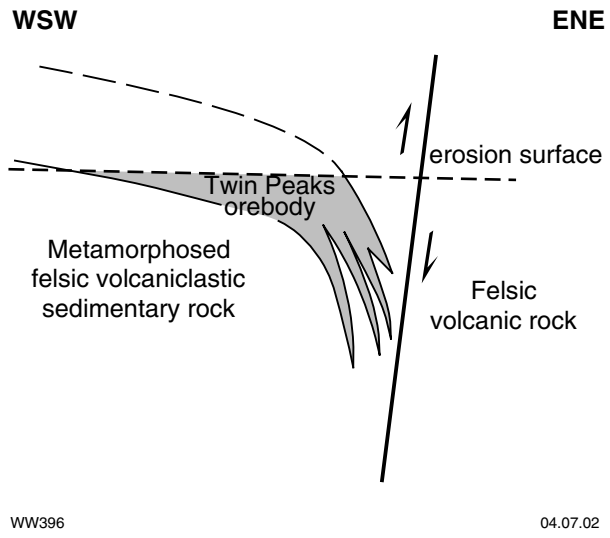

Figure 9.3. Schematic section through the Twin Peaks orebody, showing the relation to nearby reverse fault

fragments, and a dacitic provenance seems likely. The sequence is locally overturned near Twin Peaks and dips steeply to the west-southwest.

Structure: Several subparallel lodes strike parallel to the regional lithological trends, but dip steeply to the east-northeast. These lodes take on a shallower dip and merge upwards to form a 'bulge', up to 45 m thick, that extends over about 90 m of strike length at the surface (Fig. 9.3). This 'bulge', which forms the main part of the orebody (as presently known), plunges approximately 25°SE to a vertical depth of at least 280 m.

Mineralization is associated with extensive brittle fracture that produced a stockwork of brecciation and quartz veining in massive to weakly foliated metasedimentary rocks (Fig. 9.4). The irregular, branching nature of the veins, and their tapered terminations suggest an origin by hydraulic fracture. The veins and veinlets overprint a weak foliation defined by the preferred orientation of short, discontinuous seams of chlorite and biotite. This central mineralized zone is also cut by several thin zones of ductile deformation that post-date vein formation. Drillhole JDDH-122 (Fig. 9.5), which intersected one of the deeper, east-northeasterly dipping lodes, indicates that the stockwork-forming veins are variably deformed by folding, faulting, and narrow zones of ductile deformation in thin chloritic zones that envelope the main intersected ore zone.

Analysis of vein orientations in JDDH-1, which intersected the 'bulge', indicate three main groups of veins (Pancontinental Mining Ltd, 1993): 300–315°, 40–65°NE; 255–280°, dipping to the north; and 200–225°, dipping to the east-southeast. There are also some flatter lying veins that dip less than 25°WNW and ESE. These later, flatter vein sets are interpreted to have formed in en echelon series along zones of late-tectonic reverse faulting (Fig. 9.3).

Alteration: Mineralized zones are characterized by intense silicification, carbonation, and zones of sericitization. This alteration is associated with abundant quartz(–ankerite–pyrite) veins and quartz–biotite veinlets. Fine-grained, disseminated biotite exists locally, in association with quartz–biotite veinlets. Up to several percent pyrite forms as fine-grained, idioblastic disseminations and veinlets, and coarse idioblastic arsenopyrite is also common (Fig. 9.4b,d).

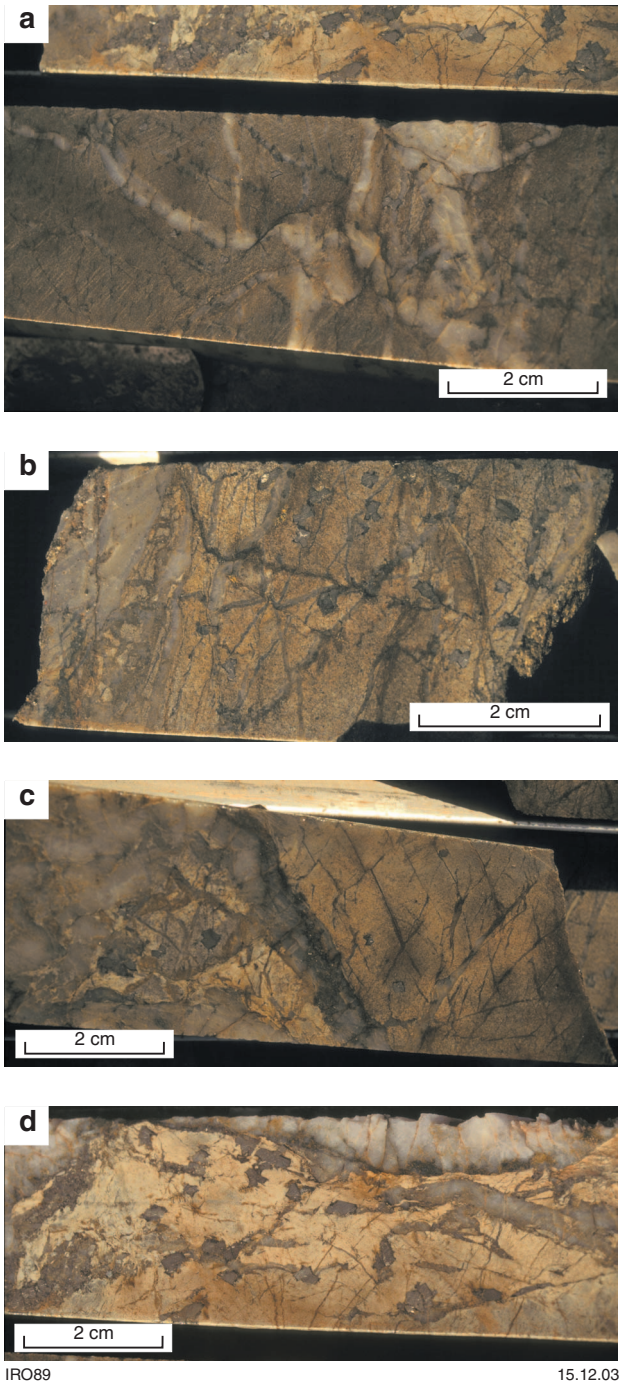

Figure 9.4. Series of photographs illustrating the nature of stockwork quartz veining and idioblastic arsenopyrite in mineralized metamorphosed volcaniclastic sedimentary rocks, Twin Peaks deposit

The main ore zone in JDDH-122 is enveloped by narrow zones of chloritization and carbonation (Fig. 9.5) in which quartz veins have been deformed during later stages of deformation. Chlorite–carbonate-dominated assemblages also characterize narrow zones of ductile deformation that cut the main ore zone and post-date vein formation.

References: Pancontinental Mining Ltd (1993, 1994), Longworth (1996).

Monty Dam

Other names: This deposit is very close to the historic Old Plough Dam workings, but is a distinctly separate orebody.

Coordinates: 30°04'32"S, 122°19'19"E

Production: No historic production. Indicated resource is 1.31 Mt of ore at 2.32 g/t Au (3039.2 kg Au; MINEDEX site code S04429).

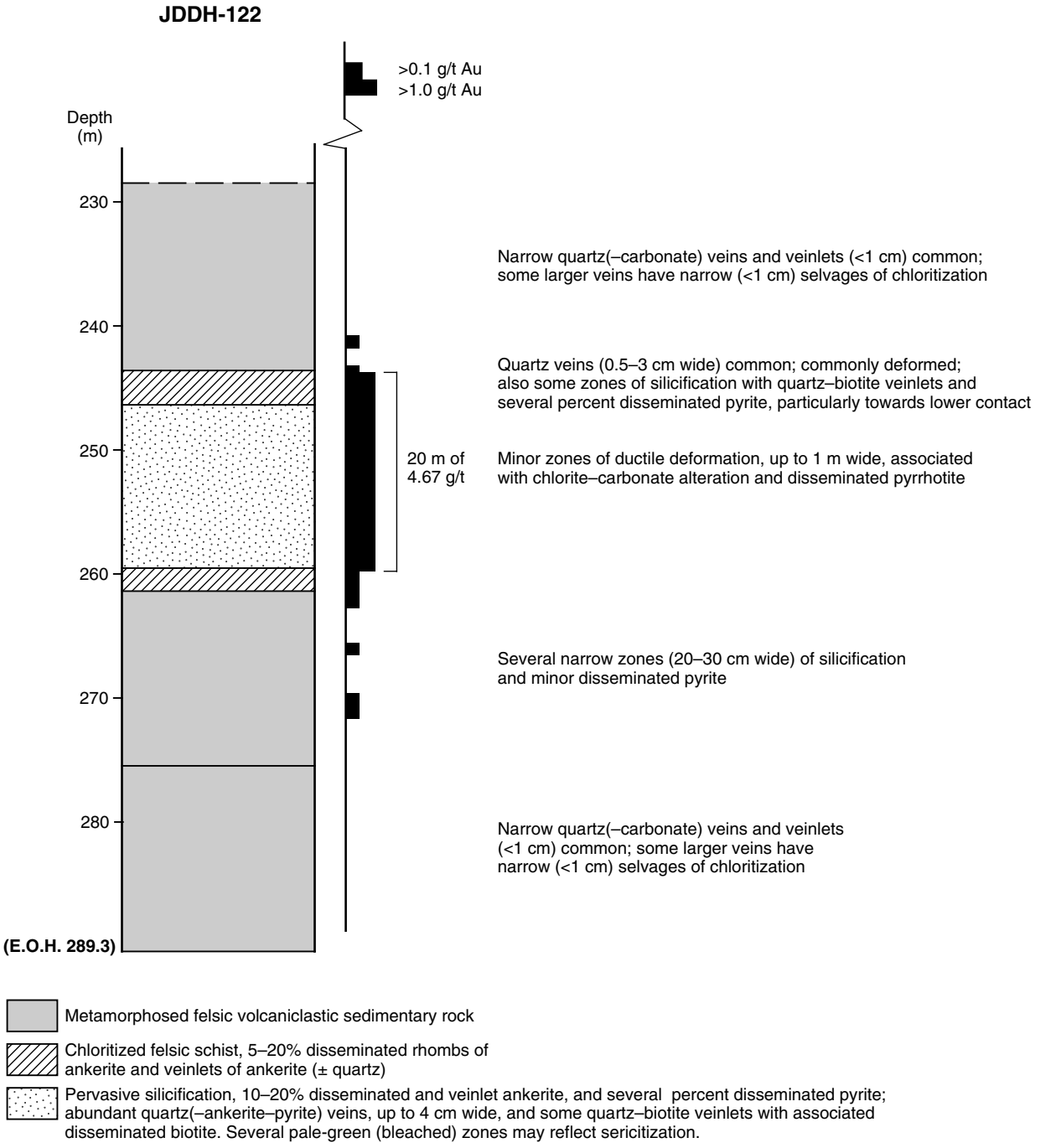

Figure 9.5. Summary log, diamond drillhole JDDH-122, Twin Peaks, Old Plough Dam mining area

Host rock: Massive to finely bedded metatuff and related metamorphosed epiclastic sedimentary rocks, with angular to subangular crystal fragments of quartz, plagioclase, and microcline in a fine-grained, quartzofeldspathic matrix. The overall composition of the metavolcaniclastic rocks ranges from andesitic to latitic. Some lamprophyre dykes are associated with the mineralization.

Structure: The Monty Dam orebody strikes north-northwest, parallel to regional lithological trends (325°), and dips 60°NE. The orebody has a strike length of over 240 m at the surface and extends to a depth of at least 250 m. It consists of a stockwork of veins and veinlets (Fig. 9.6) that overprints a weak foliation defined by the preferred orientation of short, discontinuous seams of chlorite and biotite.

Alteration: Quartz(–pyrite–rutile–hematite) veins and veinlets in the orebody (Fig. 9.6) are associated with intense silicification and hematitization, several percent of fine-grained, disseminated pyrite, and destruction of ferromagnesian mineral phases (Fig 9.7). Although hematitization is common within the ore zone, there is no consistent relationship with mineralization. Gold mineralization appears to be more closely associated with silicification and pyritization. Sericitization of silicified rocks is associated with crosscutting fractures and microshears.

References: Pancontinental Mining Ltd (1993, 1994).

Perseverance – Hope – General Rodiski

Other names: Cables, John Bull, White Elephant, Star, Lucknow, Try Again

Coordinates: 30°09'40"S, 122°25'48"E

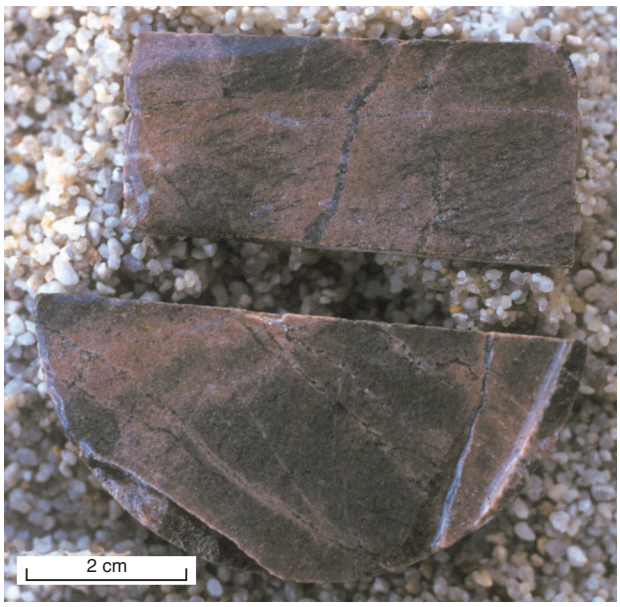

IRO94 15.12.03

Figure 9.6. Bleached and hematitized alteration halos around quartz veinlets in mineralized latite, Monty Dam, Old Plough Dam mining area

Production: 86.0 t of ore for 231.10 kg Au (2687.2 g/t Au) between 1903 and 1924. An additional 33.93 kg Au has been produced from dollied and alluvial sources.

Host rock: Metamorphosed tholeiitic basalt, locally with small (≤1 mm) plagioclase phenocrysts. Minor amounts of metamorphosed black shale have been observed on some mine dumps.

Structure: Gold mineralization extends over a strike length of about 1500 m, in a northwest-trending zone, several metres wide. Although historic records recognize several production centres along this structure, the mineralization is essentially contiguous, with the most productive section (represented by several deep shafts and numerous pits) encompassing the 350 m between Mulgabbie Perseverance and White Elephant (Lucknow).

Jackson (1905) showed a section through the mineralized structure at Mulgabbie Perseverance as a series of southwest-dipping quartz veins that cut a subvertical zone of chloritic schist. The zone of chloritic schist varies greatly in thickness, up to a maximum of about 1 m. The main quartz veins ('leaders') are oriented northwest within the northwest-trending zone of mineralization, but there are also some shorter northeast-trending veins. The veins are up to 1 m thick, but much of the historic production has come from thin 'leaders' only a few centimetres thick. Some of the quartz 'leaders' pass into 'crush zones' (?cataclastic faults) at depth. Mine-dump samples vary greatly in the amount of ductile strain they record, but relict igneous textures are still recognizable in many, including strongly altered and mineralized samples. In combination with published descriptions, these observations suggest that the mineralized structure is either a veined brittle–ductile shear zone or a fault zone dominated by brittle failure. Fabric/vein relationships (see below) suggest overlapping or alternating periods of brittle and ductile deformation.

Alteration: Altered metabasalt samples collected from mine dumps fall into two main groups:

1. Chloritic schist: moderately to strongly foliated quartz–plagioclase–chlorite schist with accessory titanite and epidote. The foliation in these rocks is defined by oriented chlorite in discontinuous seams and lenses, and trails of anhedral titanite. Irregularly distributed, randomly oriented porphyroblasts of subhedral, subequant biotite (0.2 – 0.5 mm) overprint the chloritic shear fabric (Fig. 9.8a). The chloritic schist also contains numerous small (mostly <1 mm), deformed carbonate veinlets, commonly associated with minor disseminated pyrrhotite.
2. Plagioclase-rich assemblages: massive to strongly foliated, bleached metabasalt (Fig. 9.8b), composed predominantly of plagioclase (?albite) and secondary quartz, and associated with branching veins and hydraulic breccia. These rocks contain minor amounts of carbonate, chlorite, biotite, sericite, epidote, and titanite. The bleached appearance of the rocks is due to both a decrease in the abundance of ferromagnesian minerals and a change in the composition of the chlorite (paler green). Oriented chlorite and sericite define a (mostly weak) fabric that is overprinted by

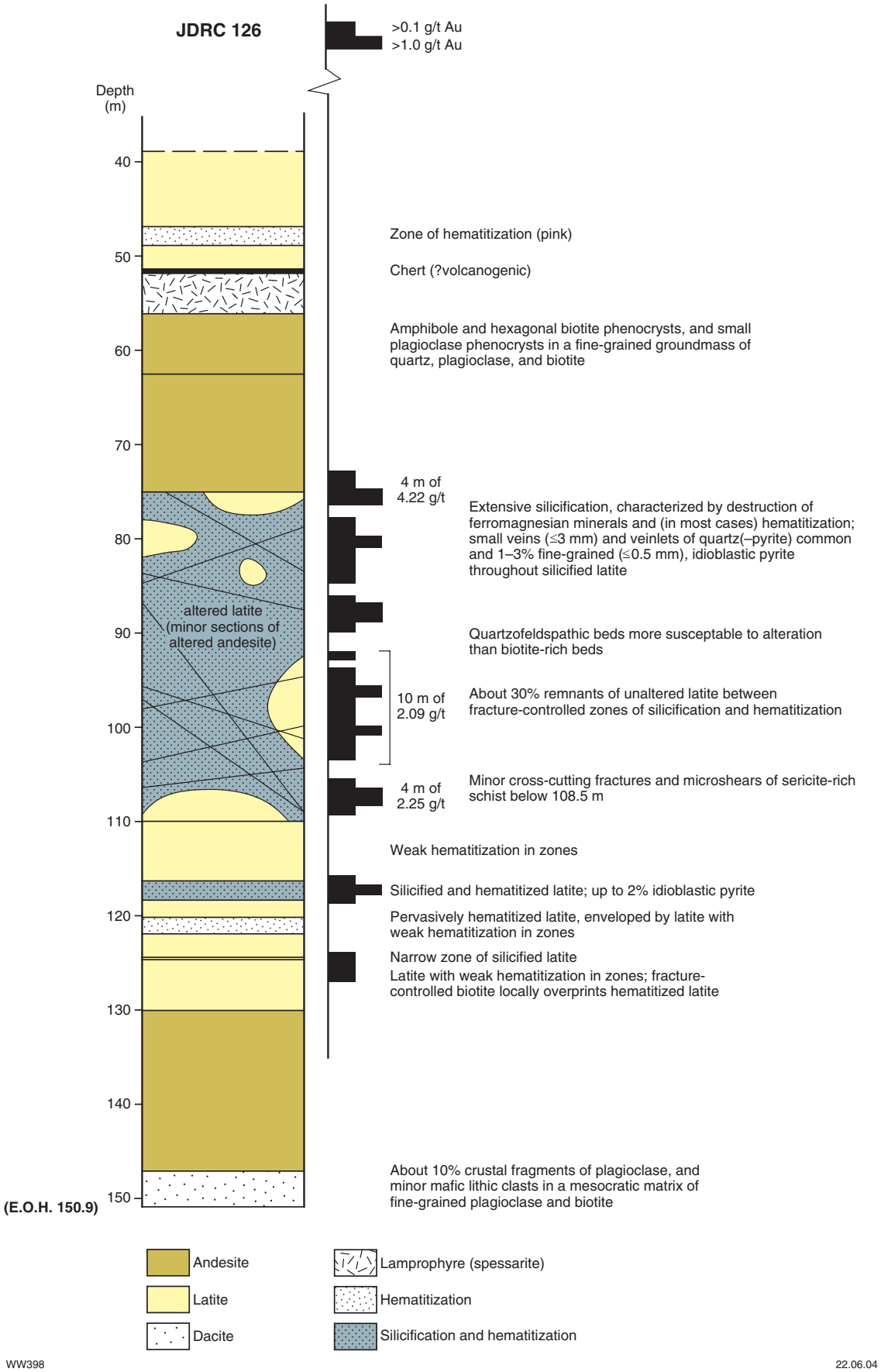

Figure 9.7. Summary log, diamond drillhole JDRC-126, Monty Dam, Old Plough Dam mining area

Figure 9.8. Altered metabasalt from Mulgabbie Perseverance, Mulgabbie mining area: a) randomly oriented biotite porphyroblasts in chloritic schist; and b) quartz–albite vein and bleached, plagioclase (?albite)-rich alteration assemblage (below) and darker chloritic alteration assemblage (above)

massive to laminated veins containing quartz–carbonate with minor albite, chlorite, biotite, and epidote, and carbonate–albite veinlets. There is a narrow (≤2 mm) zone of strong ductile deformation adjacent to some of the veins (Fig. 9.8b). Other veins, in zones of relatively strong ductile deformation, are variably deformed by the shear fabric. The plagioclase-rich assemblage is associated with up to several percent disseminated pyrrhotite and pyrite, commonly with minor chalcopyrite. Gold mineralization and sulfide minerals are most consistently associated with these plagioclase-rich assemblages. Local concentrations of rich telluride ore were recorded by Jackson (1905).

Inaccessibility of in situ exposures of the lode system preclude a confident assessment of spatial and temporal relations between these alteration assemblages, or even the relative volumes of each. Mine-dump samples indicate that contacts between the two are sharply transitional, with the amount of biotite porphyroblasts increasing towards the plagioclase-dominated assemblage. Comparison of alteration assemblages at Perseverance with those at Victory–Defiance, Kambalda, suggests that the chlorite schist and plagioclase-rich assemblages are the outer and inner zones, respectively, of a single hydrothermal event (Clark et al., 1989; Witt, 1993). Alternatively, the chloritic shears may post-date an earlier period of albitization and silicification.

Mass-balance calculations, based on whole-rock geochemical data, indicate depletion of MgO and CaO in both alteration assemblages (Fig. 9.2). SiO_2 is depleted in the chloritic schist, but large amounts of SiO_2 are added to the plagioclase-rich assemblage. Conversely, FeO and K_2O are added to the chloritic schist and depleted in the plagioclase-rich assemblage. The mineralized, plagioclase-rich assemblage is characterized by large amounts of SiO_2 addition together with smaller amounts of Na_2O and S, and depletion of CaO, FeO, MgO and Al_2O_3. Al_2O_3 is normally considered an immobile component under hydrothermal conditions. Apparent mobility at Mulgabbie may indicate an incorrect choice of volume factor (Gresens, 1967). Use of a volume factor greater than 1.0 (volume expansion during alteration) for mass-balance calculations would make Al_2O_3 immobile and simultaneously increase the calculated enrichments of SiO_2, Na_2O, and S, while minimizing the calculated depletions of MgO, CaO, and FeO.

References: Montgomery (1904), Jackson (1905).

Ernbill

Other names: Mulgabbie Queen, V.R.C.

Coordinates: 30°10'40"S, 122°25'43"E

Production: 125.0 t of ore for 6.71 kg Au (53.7 g/t Au) between 1938 and 1940. An additional 8.20 kg Au has been produced from dollied and alluvial sources.

Host rock: Felsic schist after volcaniclastic rock.

Structure: Shallow workings and a moderately deep shaft are centred on thin (≤10 cm) 255–260°-trending quartz veins that dip 45–70°SSE and are markedly oblique to the regional north-northwest foliation.

Alteration: Alteration has been obscured by weathering.

References: Jackson (1905).

Golden Gleam

Coordinates: 30°11'04"S, 122°26'10"E

Production: 10.26 t of ore for 6.08 kg Au (595.6 g/t Au) in 1938.

Host rock: Historic workings were sited in talc–carbonate schist and felsic schist after volcaniclastic rock, but they have been obscured somewhat by recent developments, including extensive alluvial workings.

Structure: Some historic workings are developed upon a subvertical shear zone with thin (≤5 cm) quartz veins that trend 160°.

Alteration: Alteration has been obscured by weathering.

Carosue Dam

Other names: The alternative name is Khartoum. The Carosue Dam mining operation includes the Karari, Luvironza, and Whirling Dervish opencut pits.

Coordinates: 30°09'10"S, 122°21'13"E

Production: Carosue Dam was discovered in 1997, 6 km west of the Mulgabbie mining centre. The pre-mining resource (indicated and inferred) was 40.1 Mt of ore for 68 170 kg Au (1.7 g/t Au; Langworthy and Joyce, 1999). Pre-mining probable reserves were 16.53 Mt for 32 398.8 kg Au (1.96 g/t Au; Langworthy and Joyce, 1999). Production figures for the individual opencut pits are not available. However, combined mineral production up to 30 September 2002 was 7019.625 kg Au (MINEDEX site code S18887). The deposit is still in production.

Host rock: Mineralization at the Carosue Dam mine (Fig. 9.9) is hosted by felsic volcanic-epiclastic rocks of the Gundockerta Formation (Langworthy and Joyce, 1999). The lithological mine sequence includes metamorphosed andesitic, trachytic, and rhyodacitic volcanic

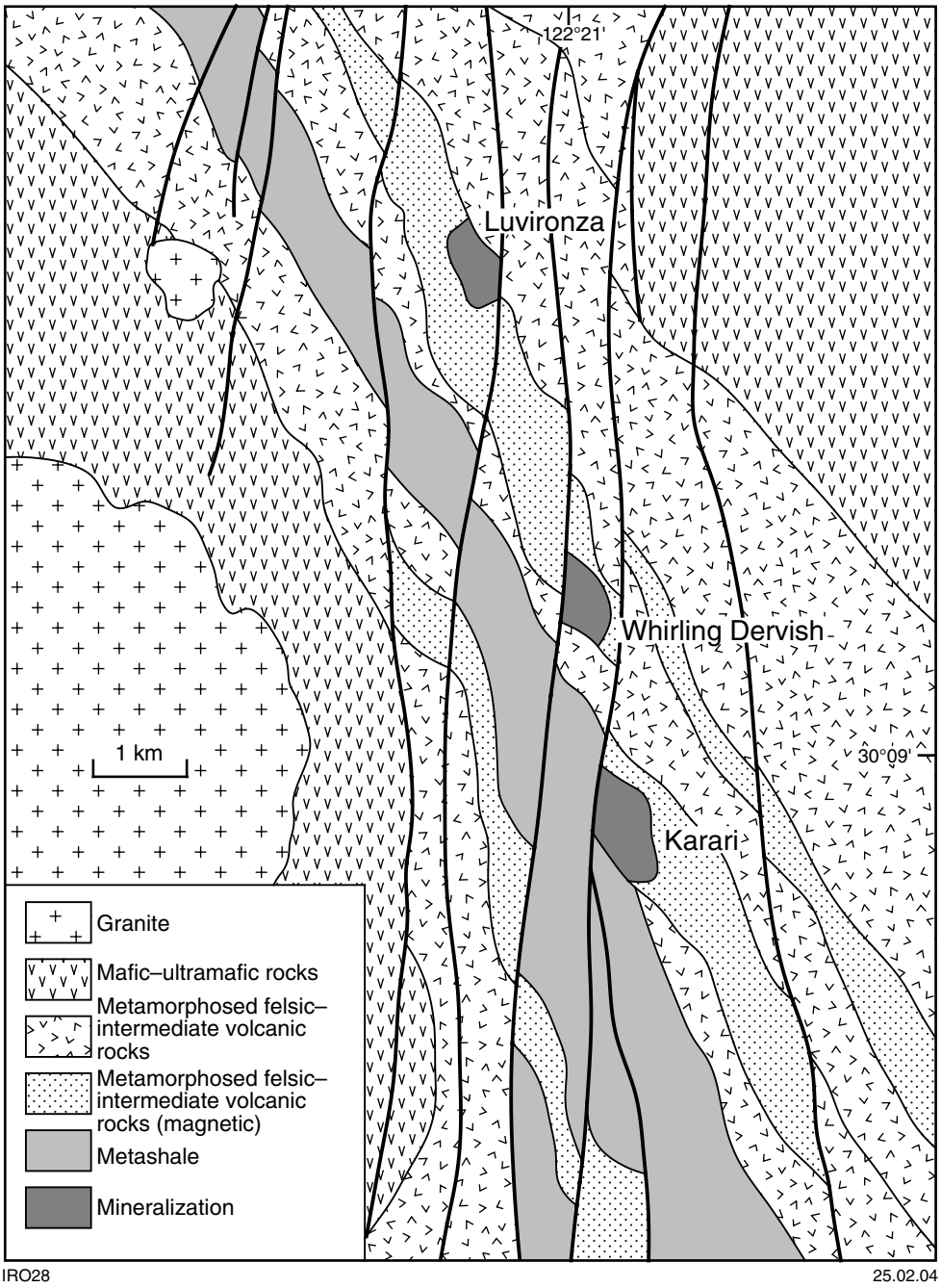

Figure 9.9. Geological sketch map of the Carosue Dam area (after Langworthy and Joyce, 1999)

rocks, metamorphosed intermediate–felsic volcaniclastic sandstones and crystal tuffs, and metashale–metasiltstone (Langworthy and Joyce, 1999; Fig. 9.9).

Structure: The Carosue Dam deposit lies in the Yabboo domain of the Edjudina Terrane (Swager, 1997). The mineralized sequence trends in a northwesterly direction and has a moderate northeasterly dip. Significant mineralized horizons are moderately to strongly magnetic, which Langworthy and Joyce (1999) considered had a control on the mineralization.

Mineralization has two orientations: parallel to stratigraphy, and flat to shallowly west dipping. Langworthy and Joyce (1999) considered that these orientations were consistent with mineralization in a steeply east dipping, reverse ductile shear zone, with shallower dipping, more-tensional links between them.

Alteration: The alteration assemblage comprises albite, K-feldspar, quartz, hematite, carbonate, and pyrite. Mineralization within lodes parallel to the stratigraphy is associated with quartz–albite–pyrite alteration, while the flat to shallow-dipping lodes have a strong hematite–carbonate–pyrite alteration (Langworthy and Joyce, 1999).

References: Langworthy and Joyce (1999).

References

CLARK, M. E., CARMICHAEL, D. M., HODGSON, C. J., and FU, M., 1989, Wall-rock alteration, Victory Gold Mine, Kambalda, Western Australia: Process and P–T–X_{CO_2} conditions of metasomatism, *in* The geology of gold deposits: the perspective in 1988 *edited by* R. R. KEAYES, W. R. H. RAMSAY, and D. I. GROVES: Economic Geology, Monograph 6, p. 445–459.

CLOUT, J. M. F., GLEGHORN, J. H., and EATON, P. C., 1990, Geology of the Kalgoorlie Gold Field, *in* Geology of the mineral deposits of Australia and Papua New Guinea *edited by* F. HUGHES: Australasian Institute of Mining and Metallurgy, Monograph 14, p. 411–431.GRESENS, R. L., 1967, Composition–volume relationships of metasomatism: Chemical Geology, v. 2, p. 47–65.

GRESENS, R. L., 1967, Composition–volume relationships of metasomatism: Chemical Geology, v. 2, p. 47–65.

JACKSON, C. F. V., 1905, Note on the geology and ore deposits of Mulgabbie: Western Australia Geological Survey, Bulletin 18, p. 25–33.

LANGWORTHY, P., and JOYCE, M., 1999, Carosue Dam gold project — evolution of a discovery, *in* New Generation Gold Mines '99 — case histories of discovery: Australian Mineral Foundation Conference Proceedings, p. 143–149.

LONGWORTH, N. M., 1996, The Twin Peaks Resource — a case study: Western Australia School of Mines Symposium, Kalgoorlie, 1996, Abstracts, p. 73–75.

MONTGOMERY, A., 1904, Annual Report for the year 1903: Western Australia, Department of Mines, p. 77–80.

MORRIS, P. A., 1994, Geology of the Mulgabbie 1:100 000 sheet: Western Australia Geological Survey, 1:100 000 Geological Series Explanatory Notes, 18p.

NELSON, D. R., 1995, Compilation of SHRIMP U–Pb zircon dates, 1994: Western Australia Geological Survey, Record 1995/03, 244p.

PANCONTINENTAL MINING LTD, 1993, Annual report, Jun 1992 to Jun 1993, on E31/107, E31/101, E28/444, E28/359, E28/256 and P31/1391: Western Australia Geological Survey, Statutory mineral exploration report, Item 11664 A39118 (unpublished).

PANCONTINENTAL MINING LTD, 1994, Annual report, Jun 1993 to Jun 1994, on Keith Kilkenny gold exploration: Western Australia Geological Survey, Statutory mineral exploration report, Item 11664 A42513 (unpublished).

RIDLEY, J. R., 1993, The relations between mean rock stress and fluid flow in the crust: with reference to vein- and lode-style gold deposits: Ore Geology Reviews, v. 8, p. 23–27.

SWAGER, C. P., 1995, Geology of the greenstone terranes in the Kurnalpi–Edjudina region, southeastern Yilgarn Craton: Western Australia Geological Survey, Report 47, 31p.

SWAGER, C. P., 1997, Tectono-stratigraphy of late Archaean greenstone terranes in the southern Eastern Goldfields, Western Australia: Precambrian Research, v. 83, p. 11–42.

WITT, W. K., 1993, Gold mineralization in the Menzies–Kambalda region, Eastern Goldfields, Western Australia: Western Australia Geological Survey, Report 39, 165p.

10. Porphyry

The central part of the Mulgabbie domain of the Kurnalpi Terrane is dominated by metamorphosed volcaniclastic andesite, andesitic basalt, and related epiclastic sedimentary rocks. In the southern part of the belt, relatively undeformed metamorphosed basalt and andesitic basalt are intensely and pervasively carbonated. Both units have been intruded by numerous small granitoid plutons. Although most of these intrusions are poorly exposed or very weathered, known compositions range from metamorphosed biotite syenogranite to quartz monzonite and tonalite. Most appear to be discordant with respect to lithological layering and major regional structures, suggesting emplacement late in the tectonic evolution of the greenstone belt. The Porphyry Quartz Monzonite was emplaced at 2667 ± 4 Ma (Hill et al., 1992). The Outcamp Bore Tonalite (2719 ± 5 Ma) may be a subvolcanic equivalent of the metamorphosed intermediate volcanic rocks. The belt also contains several D_1 thrust faults interpreted from low-angle stratigraphic 'cut-outs' on aeromagnetic images.

Gold mineralization is in a belt stretching from Porphyry North (Fig. 10.1) to the Wallbrook area, about 8 km to the south-southeast. Historic production has been patchy, but significant quantities of gold have been extracted from deposits hosted by the Porphyry Quartz Monzonite (e.g. Porphyry, Million Dollar; >4 t Au). Present inferred resources in the Porphyry Quartz Monzonite (Porphyry, Million Dollar, Pioneer Paddock) are estimated at to a further 3 t of gold or more. Inferred resources have also been estimated in several meta-andesite-hosted deposits to the east of Porphyry, including Margaret (about 1000 kg Au) and Enterprise (about 2000 kg Au). A small inferred resource (about 200 kg Au) has been estimated at Porphyry North.

Meta-andesite-hosted deposits east of Porphyry appear to be associated with north-northwesterly trending zones of left-lateral shear. These zones correspond to relatively magnetic bands on aeromagnetic images. However, the resolution of aeromagnetic images is not high enough to show whether the shear zones are localized at contacts between lithologically and magnetically distinct units, or if the magnetic signature is due to secondary magnetite in the actual shear zones. Subhorizontal mineral lineations in the shear zones attest to a mainly subhorizontal movement vector. Mineralized vein systems that are rotated anticlockwise with respect to the strike of the shear zones indicate sinistral movement, at least during the latest stages. The Enterprise deposit is a gently plunging array of brittle quartz veining that formed in a relatively low strain domain between the shear zones. The mineralized quartz veins at Enterprise have a similar orientation to those in the shear zones, suggesting formation during the same stress regime. The pipe-like nature of the Enterprise orebody may reflect partial stratigraphic control, involving brittle failure of a relatively competent andesitic unit.

Left-lateral, strike-slip movement was also important at Porphyry North, where gold is associated with right-stepping en echelon vein arrays in a small quartz-monzonite intrusion. The competency contrast between the granitoid intrusion and andesitic wallrocks was probably important in localizing the mineralized vein system. Competency contrast is also implicated at Wallbrook, where a mineralized quartz vein stockwork has developed within a small syenogranitic intrusion within metabasalt. Locally however, the wallrocks at Wallbrook comprise relatively incompetent felsic schists. Quartz veins formed a conjugate set while the local principal stress axis was oriented northeast–southwest.

Deposits hosted by the Porphyry Quartz Monzonite (Fig. 10.1) are in discontinuous brittle–ductile shears that dip about 20–45°E. Cross sections through Porphyry Audax that cut the granitoid–greenstone contact appear to indicate a reverse movement. More work is required to determine the kinematic history of these structures and their relationship to the regional deformation history.

In summary, the main sites of gold mineralization in the Porphyry area are the eastern margin of the Porphyry Quartz Monzonite and the Enterprise – Mad Dog area. North-northwesterly to northerly trending contacts between greenstones and relatively competent granitoid plutons appear to have been important sites of mineralization, particularly at Porphyry. The relatively shallow dips of mineralized shears in the Porphyry Quartz Monzonite may be related to proximity to the roof of the intrusion (Fig. 10.2). The shear-zone-hosted and related deposits in the Enterprise – Mad Dog area are a short distance west of a north-trending D_4 fault. The significance of this association, if any, is not clear, but the D_4 fault is oriented normal to the regional σ_1 — an orientation that should promote high shear strain on lithological contacts and brittle failure of competent units (Ridley, 1993). The orebodies in the Enterprise – Mad Dog area may be second- and third-order splay structures related to dextral movement on the D_4 fault. Gently inclined D_1 structures may have provided a semi-permeable capping surface (Fig. 10.2) that led to buildup of fluid pressures and vein formation after the main ductile phase of deformation. Other, mostly smaller meta-andesite-hosted deposits are well south of this fault. These appear to be related to different structures from those to the north. Although exposure is poor, mineralization in the south appears to be associated with discontinuous structures oriented about 300–320°, which could be interpreted as sinistral shear bands similar to those documented in the Yarri Monzogranite (Swager, 1995).

Ductile deformation in meta-andesite-hosted shear zones was accompanied by the introduction of reduced fluids that produced quartz–plagioclase–chlorite–carbonate and quartz–chlorite–carbonate–muscovite schists with accessory titanite and up to 5% porphyroblasts of secondary magnetite. Gold is associated with pyrite, ankerite, and brick-red albite in intensely hematitized assemblages adjacent to quartz–ankerite–albite–pyrite(–rutile–apatite) veins that overprint the magnetite-bearing shear-zone assemblage. Titanite is replaced by rutile in these oxidized assemblages. Mineralization in the

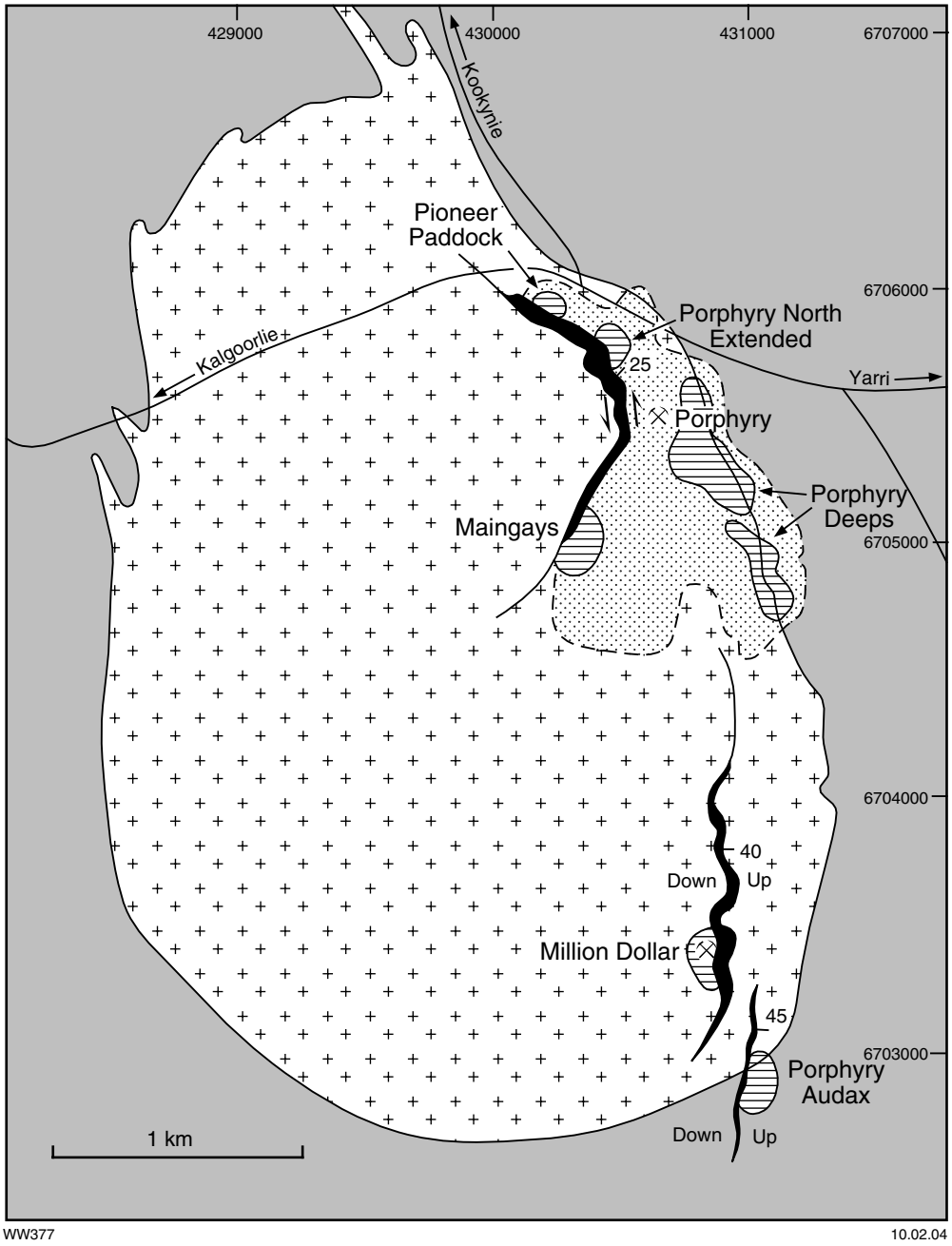

Figure 10.1. Geological map showing gold deposits in the Porphyry Quartz Monzonite, Porphyry mining area (modified from Allen, 1987; Cole, R., 1995, written comm.)

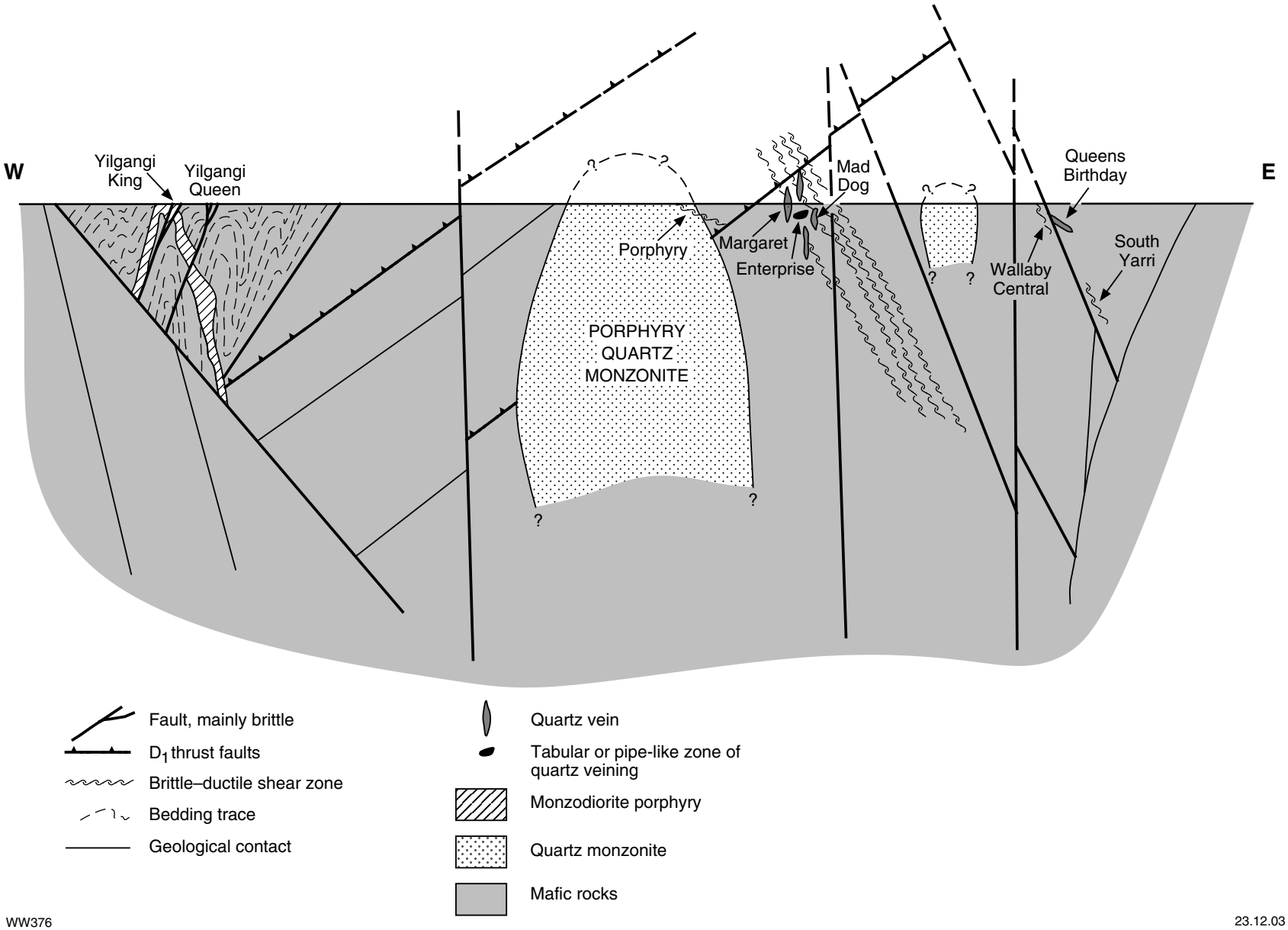

Figure 10.2. Schematic east–west cross section through the Yilgangi, Porphyry, and Yarri mining areas showing the various styles of mineralization

Porphyry Quartz Monzonite is accompanied by silicification, pyritization, and hematitization, suggesting an origin related to similar oxidizing fluids to those that precipitated gold in andesitic rocks. However, two feldspars remain stable in altered Porphyry Quartz Monzonite. Tourmaline is also present in mineralized alteration assemblages in both andesitic and granitoid host rocks, as a common or accessory phase.

Separate reserve figures for many of the deposits in the Porphyry area are not available and have been reported as a combined figure for the Edjudina group — the measured resource is 0.519 Mt of ore at 2.09 g/t Au for 1084.71 kg Au, indicated resource is 2.149 Mt at 3.63 g/t for 7800.87 kg Au, and inferred resource is 0.817 Mt at 3.16 g/t for 2581.72 kg Au (MINEDEX site code S05006).

Deposits of the Porphyry area

Wallbrook

Other names: Mount Wallbrook, Redbrook, Golden Brook, Black Rooster

Coordinates: 29°52'12"S, 122°19'01"E

Production: 3658.1 t of ore for 26.23 kg Au (7.2 g/t Au) between 1921 and 1937. Note that there is considerable uncertainty as to the relative production of Wallbrook and Selbourne, but production from Wallbrook was clearly the greater of the two. Redbrook has an inferred resource of 73 000 t of ore at 2.46 g/t Au (179.58 kg Au; MINEDEX site code S05530).

Host rock: Coarse-grained (1–3 mm), equigranular quartzofeldspathic intrusion (?syenogranite) with interleaved lenses or slices of quartz–sericite schist (?after felsic volcaniclastic sedimentary rocks).

Structure: A small group of historic workings and a more recent, small opencut mine about 70 m long by 10 m deep expose an orebody that has a total strike length of about 150 m oriented about 290°. The relatively competent granitoid is host to an extensive stockwork of quartz veining (Fig. 10.3). The veins are of variable width (most up to several centimetres), display a wide variety of orientations and attributes, and branch along strike. However, the veins can be resolved into two main groups (Fig. 10.4), which can be interpreted as a conjugate vein array formed in response to a principal axis of compression oriented 035–040°. No consistent cross-cutting relationships among veins of different orientations could be distinguished. Most quartz veins are sharply

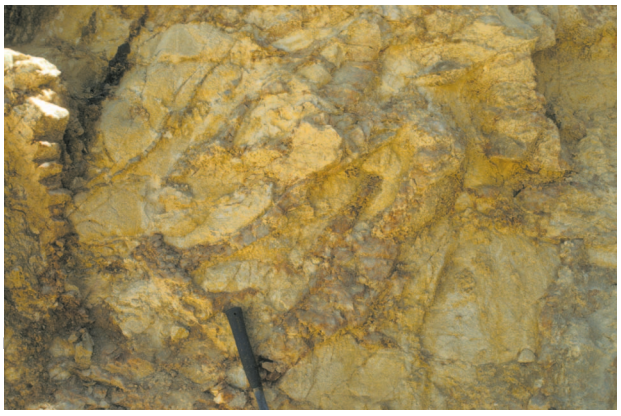

IRO44 15.12.03

Figure 10.3. Stockwork of quartz veins in a granitoid intrusion, Wallbrook mine, Porphyry mining area. The field of view shown in the photo is about 2 m wide

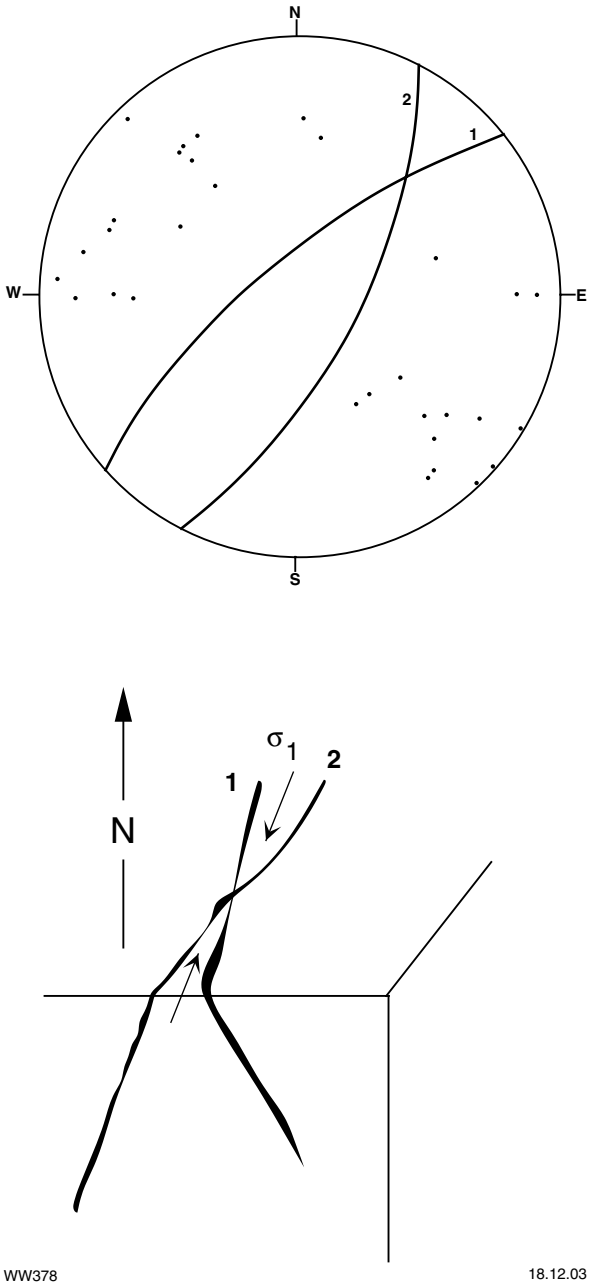

Figure 10.4. Stereoplot showing poles to quartz veins, Wallbrook mine, Porphyry mining area

terminated against sheared contacts between the granitoid and the interleaved lenses and slices of felsic schist.

The dominant schistosity (?shear fabric) in the felsic schist units is oriented approximately northwest and dips about 60°SW. Quartz veins are less common in the schist than in the granitoid, but there are some veins that are mostly subparallel to the schistosity, and are locally boudinaged. Drag on a folded, locally flat-lying quartz vein suggests that the felsic schist unit exposed in the northern corner of the opencut was a locus for normal (west side down) movement.

There is a second, smaller line of workings on a 245°-trending shear that dips 70–80°SE and intersects the main structure at the northwestern end of the opencut.

Alteration: Alteration in the granitoid and schist is obscured by deep weathering. There are no visible alteration assemblages adjacent to quartz veins. Coarse limonite (after idioblastic pyrite, up to 1 cm across) is present within some quartz veins and in the immediate wallrocks.

References: Swager (1995).

Selbourne

Other names: Towers

Coordinates: 29°52'00"S, 122°18'47"E

Production: 800.35 t of ore for 3.22 kg Au (4.0 g/t Au) between 1937 and 1942. See comments for Wallbrook (above).

Host rock: Coarse-grained (1–3 mm), equigranular quartzofeldspathic intrusion (?syenogranite) and quartz–sericite schist (after felsic volcaniclastic sedimentary rocks).

Structure: Collapsed stopes and moderately deep shafts outline two main trends:

1. Stockwork veining over a strike length of about 100 m in weathered granitoid, in a zone adjacent to its contact with felsic schist to the west. The contact and mineralized zone trend 320° and dip 70°SW.
2. A smaller group of workings extending over about 50 m on a 1–2 m-wide shear zone with quartz veins. Veins display minor boudinage structures. The shear zone trends 350° and dips 70°W within felsic schist. Deflection of the shear fabric at the margins of the shear zone suggests reverse movement.

Alteration: Alteration is obscured by weathering.

References: Swager (1995).

Eastward Gold Reefs

Other names: Silver

Coordinates: 29°39'32"S, 122°20'02"E

Production: 1348.6 t of ore for 9.22 kg Au (6.8 g/t Au) between 1936 and 1985.

Host rock: Metamorphosed andesitic volcanic and volcaniclastic rocks.

Structure: Shallow workings selectively expose subvertical to steeply north dipping, 060–085°-trending quartz veins, up to 10 cm thick. These veins are present over about 100 m, within and overprinting a 320–330°-trending zone of deformation. Asymmetric pressure shadows on magnetite porphyroblasts imply simple shear. Geometric relationships suggest that en echelon quartz veins formed during sinistral movement on the deformation zone in which they lie.

Alteration: Alteration is obscured by weathering. Exploration drilling indicates that the veins are within quartz–sericite(–carbonate–chlorite) schist with minor pyrite, tourmaline, and hematite. Tourmaline is locally abundant, forming up to 20% of the alteration assemblage.

References: Cyprus Minerals Australia Co. (1988), Consolidated Resources NL (1994), Swager (1995).

Penola

Coordinates: 29°48'40"S, 122°19'00"E

Production: 162.6 t of ore for 2.90 kg Au (17.8 g/t Au) between 1905 and 1906. Resources have been quoted as a combined figure for the Edjudina group.

Host rock: Metamorphosed andesitic volcanic and volcaniclastic rocks.

Structure: Shallow to moderately deep workings are developed over about 150 m on a 300°-trending structure. Exposure is poor, but exploration drilling indicates that the structure dips northeast. A small openpit (about 30 m long and 15 m wide) is located northeast of the first structure. This pit exposes a north-trending brittle–ductile shear zone that dips 60°W.

Alteration: Altered, deformed andesitic rocks are quartz–muscovite–carbonate(–chlorite) schist with abundant secondary magnetite as small ($\leq$2 mm), idioblastic porphyroblasts, minor pyrite, and irregularly distributed fine, dusty hematite.

References: Cyprus Minerals Australia Co. (1988), Swager (1995).

Porphyry Audax

Coordinates: 29°48'11"S, 122°17'11"E

Production: No historic production. Resources have been quoted as a combined figure for the Edjudina group.

Host rock: Mainly metamorphosed andesitic volcanic and volcaniclastic rocks; minor mineralization in massive, coarse-grained, porphyritic biotite–quartz monzonite.

Structure: Mineralization is hosted by a north-trending shear zone that dips about 45°E and cuts the southeastern contact of the Porphyry Quartz Monzonite. Exploration drilling has shown the shear zone to be a 20–30 m-thick zone of interleaved quartz monzonite, sheared quartz

monzonite, and schist after altered andesitic rocks. Displacement of a subvertical intrusive contact indicates reverse movement across the mineralized shear zone.

The ore zone is about 120 m long and consists of between two and four stacked lenses, up to 80 m in depth, within the shear zone (Fig. 10.5). Most mineralized lenses terminate at the meta-andesite – quartz monzonite contact, although some do penetrate the pluton. Ore lenses are associated with zones of quartz veining within andesitic schist, and to a lesser extent within interleaved, deformed quartz monzonite.

Alteration: Deformed andesitic rocks and interleaved quartz monzonite are silicified, hematitized, and pyritized. Andesitic schist locally contains secondary magnetite. Ore lenses tend to be associated with quartz veining and pyrite. Intense tourmalinization of the quartz monzonite has been recorded adjacent to the deformed margins of the intrusion.

References: AuDAX Resources (1989), Enterprise Gold Mines NL (1992a).

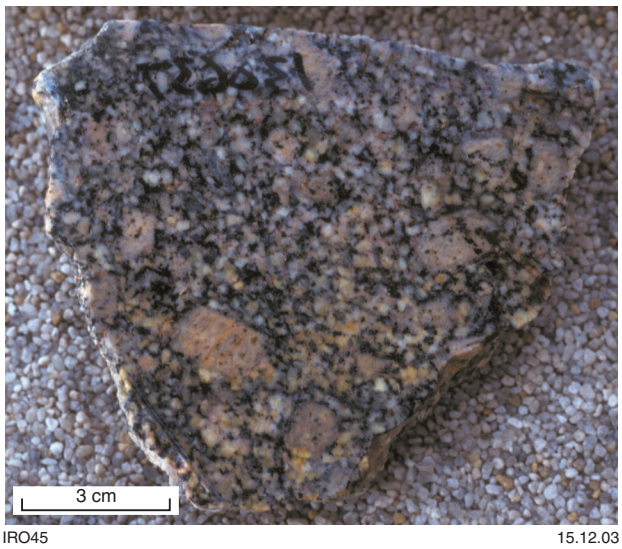

Figure 10.6. Porphyry Quartz Monzonite, Million Dollar deposit, Porphyry mining area

Million Dollar

Coordinates: 29°47'54"S, 122°17'13"E

Production: The Million Dollar openpit mine produced 133 151 t of ore for about 270 kg Au (2.02 g/t Au) between 1988 and 1989. A further inferred resource of 245 000 t at 2.90 g/t Au (710.5 kg Au) is located about 2 km north at Million Dollar North.

Host rock: The massive, coarse-grained, porphyritic quartz monzonite host rock contains about 15% phenocrysts of K-feldspar and 5–10% biotite (partly after hornblende) in the groundmass (Fig. 10.6). The quartz monzonite forms a plug-like pluton, about 12 km^2, which intruded andesitic volcanic rocks.

Structure: The Million Dollar opencut mine is located near the southern end of a north-trending brittle–ductile shear zone that can be traced for over a kilometre of strike length (Fig. 10.1). The western wall of the pit exposes stacked zones of fracturing, quartz veining, and hydraulic brecciation (Fig. 10.7). The larger quartz veins are up to 30 cm thick, dip 35–45°SE, and appear to splay off a basal, 1–2 m-thick zone of veining and hydraulic

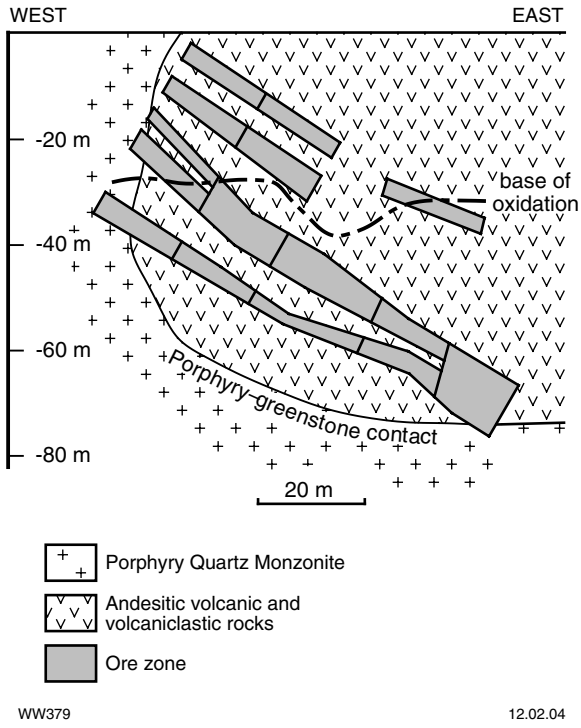

Figure 10.5. Cross section through the Porphyry Audax deposit, Porphyry mining area, showing stacked ore lenses on the margin of the Porphyry Quartz Monzonite (after AuDAX Resources NL, 1989)

Figure 10.7. Stacked zones of quartz veining and hydraulic brecciation in Porphyry Quartz Monzonite, Million Dollar openpit, Porphyry mining area

IRO48 15.12.03

Figure 10.8. Basal zone of quartz veining and brittle–ductile shear in Porphyry Quartz Monzonite, Million Dollar openpit, Porphyry mining area

IRO49 15.12.03

Figure 10.10. Hematitization of Porphyry Quartz Monzonite in the basal zone of quartz veining and brittle–ductile shear, Million Dollar openpit, Porphyry mining area

brecciation (Fig. 10.8). Altered wallrocks to the veins are characterized by anastomosing zones of feldspar cataclasis and quartz grain-size reduction. Quartz veins overprint quartz-monzonite cataclasite, but they have been locally recrystallized themselves during progressive ductile deformation. Thus the veins display zones of grain-size reduction, and elongate quartz subgrains are oriented parallel to the ductile fabric in the wallrocks. Small quartz veinlets in feldspar porphyroclasts, oriented normal to the ductile fabric, are terminated against zones of ductile deformation and grain-size reduction. These relationships indicate overlapping periods of ductile and brittle deformation. Mylonitized quartz monzonite similar to that described for the Porphyry deposit was not observed.

Alteration: The mineralized zones are characterized by a strong, red colouration that reflects pervasive hematitization (Figs 10.9 and 10.10). Hematite forms fine, dusty disseminations, mainly in feldspars, and along fractures and cleavage planes. Zones of brittle–ductile deformation contain minor carbonate and disseminated, idioblastic pyrite. Biotite is replaced by chlorite and muscovite. Titanite is replaced by rutile, and magnetite by hematite and pyrite. Two feldspars remain stable throughout the alteration zone and there is an increase in modal abundance of quartz, especially in the basal zone of deformation.

Mass-balance calculations, based on whole-rock geochemical data, indicate addition of K_2O, CO_2, and S, and depletion of Na_2O, to the altered, mineralized quartz monzonite. Enrichment of SiO_2 is apparently extreme (Fig. 10.11), but this is at least partly due to the presence of numerous quartz veins that could not be readily separated from the altered wallrocks.

References: Weatherstone (1990), Swager (1995).

IRO46 15.12.03

Figure 10.9. Hematitization, quartz veins, and cataclasis in Porphyry Quartz Monzonite, Million Dollar openpit, Porphyry mining area

Porphyry

Other names: Chateau Tanunda, Welshs Find, Edjudina G.M., Porphyry G.M.

Coordinates: 29°46'45"S, 122°17'00"E

Production: 103 648.8 t of ore for 495.34 kg Au (4.8 g/t Au) between 1933 and 1978. Production during openpit (1984–87) and underground (1987–88) mining produced 781 424 t of ore at 3.38 g/t Au (2641.2 kg Au) and 476 645 t at 2.88 g/t Au (1370.9 kg Au), respectively. Resources have been quoted as a combined figure for the Edjudina group of Sons of Gwalia Ltd.

Host rock: The massive, coarse-grained, porphyritic quartz monzonite contains about 15% phenocrysts of K-feldspar and 5–10% biotite (partly after hornblende) in the groundmass. The quartz monzonite forms a plug-like pluton, about 12 km^2, which intruded andesitic volcanic rocks.

Structure: Mineralization is within a north-trending brittle–ductile shear zone that dips 20–25°E, close to, and subparallel to, the eastern margin of the host intrusion (Fig. 10.2). Predominantly ductile deformation produced

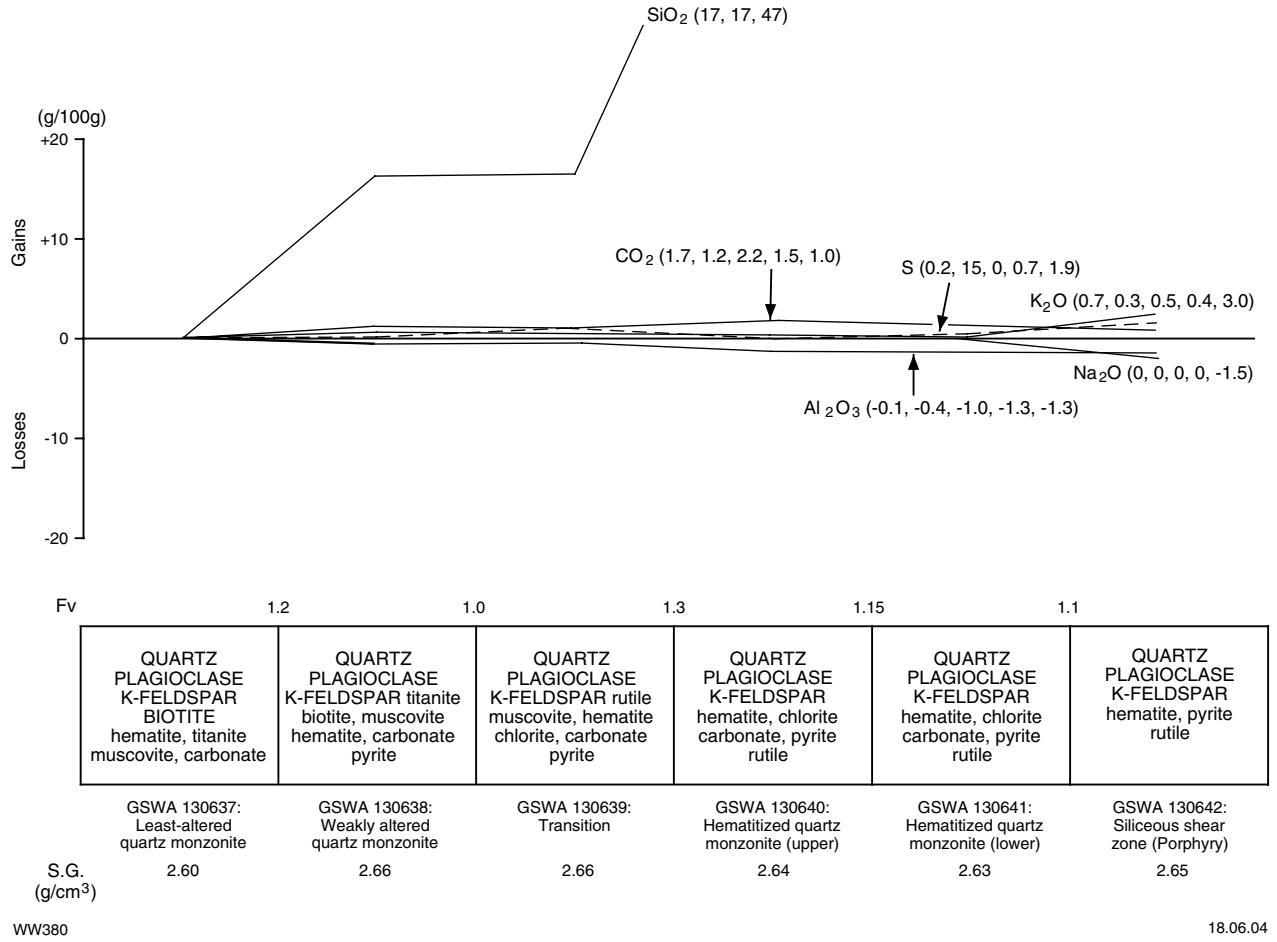

Figure 10.11. Mass-balance changes (calculated using the method of Gresens, 1967) associated with hematitization of pyritic lodes in Porphyry Quartz Monzonite, Million Dollar openpit, Porphyry mining area. The siliceous ductile shear in the Porphyry openpit, which is situated within a broader zone of hematitized quartz monzonite similar to that at Million Dollar, is included for comparison. Mineral components of alteration assemblages are listed in approximate order of abundance, with main mineral components in upper case and minor mineral components in lower case

banded quartz–phyllosilicate rock with rounded and fractured, relict microperthite porphyroclasts, and ultimately mylonitic quartz monzonite (Fig. 10.12). The shear zone varies in width up to 25 m and is about 1.5 km long. The surface trace of this structure is gently arched, but much of the curvature can be attributed to the shallow dip of the shear zone. The orebody plunges southeast within the shear zone. Ore forms a series of stacked lenses that step to the right in longitudinal section (Weatherstone, 1990), suggesting sinistral movement on the north–south portion of the mineralized structure. Allen (1987) suggested that microtextural evidence in some samples indicates a dominant sinistral displacement with a minor reverse component of movement.

Alteration: Weakly deformed quartz monzonite is mildly carbonated, but silicification, pyritization, and hematitization become more intense with increasing deformation toward the centre of the shear zone. Alteration involves addition of quartz and conversion of biotite to muscovite and pyrite. There is also minor addition of hematite and carbonate throughout the shear zone. Hematitization is characteristic of alteration associated with the shear zone but is broader than ore sections.

Alteration has introduced massive amounts of SiO_2 (possibly mainly as quartz veins), and also K_2O, CO_2, and S (Fig. 10.11; see also Allen, 1987). Intense silicification in the mylonitic shear zone reflects depletion of most other components, including Al_2O_3 (Fig. 10.11). Gold is associated with S in the form of pyrite. Mo is also moderately enriched in mineralized sections.

Other data: Allen (1987) reported the presence of three-phase fluid inclusions containing a low-salinity, H_2O–CO_2 fluid in undeformed vein quartz from the mineralized shear.

References: Blatchford (1935), Allen (1987), Weatherstone (1990), Swager (1995).

Pioneer Paddock

Coordinates: 29°46'35"S, 122°16'50"E

IRO42 15.12.03

Figure 10.12. Flat-lying ductile shear zone within altered (hematitized) Porphyry Quartz Monzonite, Porphyry openpit, Porphyry mining area. Remains of historic workings are shown on either side of the pillar that exposes the shear zone

Production: No historic production. Resources have been quoted as a combined figure for the Edjudina group of Sons of Gwalia Ltd.

Host rock: Massive, coarse-grained, porphyritic quartz monzonite, as for Porphyry.

Structure: Mineralization lies on the northern extension of the same structure that hosts the Porphyry deposit. At this location, the structure is flatter, dipping very gently to the north.

Alteration: Similar to that at Porphyry and Million Dollar.

Nil Desperandum

Other names: Valerie May

Coordinates: 29°47'35"S, 122°18'46"E

Production: 722.1 t of ore for 8.47 kg Au (11.7 g/t Au) between 1947 and 1986. The inferred resource is 124 000 t of ore at 2.2 g/t Au (273 kg Au).

Host rock: Metamorphosed andesitic volcanic and volcaniclastic rocks.

Structure: Mineralization lies within a 30–40 m-wide, brittle–ductile shear zone that trends 350° and dips about 70°E. The orebody within the shear zone is 170 m long and several metres wide. Mineral lineations and the orebody plunge south. Sheeted, subvertical quartz veins at the margins of the shear zone are oriented 310°, suggesting sinistral movement.

Alteration: Surface exposures are deeply weathered, but exploration drilling indicates that mineralized andesitic schist is altered to pyritic quartz–muscovite–carbonate(–tourmaline) assemblages. Ore zones are associated with As anomalies.

References: Gondwana Resources NL (1987), Swager (1995).

Enterprise

Coordinates: 29°46'42"S, 122°18'52"E

Production: No historic production. Resources have been quoted as a combined figure for the Edjudina group of Sons of Gwalia Ltd.

Host rock: Metamorphosed andesitic volcanic and volcaniclastic rocks.

Structure: Exploration drilling has identified a zone, about 300 m long, in which mineralization is related to a gently west dipping, southerly plunging (25°S) zone of brittle quartz veining. The mineralized zone of veining is 3–20 m wide and about 100 m below the surface at its southern end. It is located in moderately deformed andesitic rocks in which plagioclase, chlorite, and even biotite are still stable. Vein-related mineralization overprints more-intensely deformed schists, typical of assemblages within shear-zone hosted mineralization (e.g. Margaret, Dead Dog) in the deeper parts of diamond drillhole G-94-2 (Fig. 10.13). Asymmetric tails on carbonate porphyroblasts suggest a degree of simple shear even in the moderately deformed rocks.

Veins up to about 1 m wide are in a particularly wide zone of brittle deformation, at about 50 m depth in G-94-2. This zone can be correlated across several adjacent drillholes from which the southerly plunge of the orebody is deduced. Several thinner zones of brittle deformation containing quartz veins ($\leq$5 cm wide) lie above (mostly) and below this wide zone of mineralization. Mineralized veins cut the steeply east dipping regional foliation and shear-related fabrics in the shear zone intersected by the lower part of drillhole G-94-2. Vein orientation is variable, but subvertical, 325°-trending veins, similar to those in shear-related mineralization (e.g. Dead Dog), are common. Subhorizontal veins have also been noted.

Alteration: Alteration assemblages in moderately to strongly foliated meta-andesitic rocks are summarized in Tables 10.1 and 10.2 and illustrated in Figures 10.14 to 10.18. Analytical data for metamorphic and metasomatic minerals are summarized in Figure 10.19 and Tables 10.3 to 10.6. Persistent features in strongly foliated (sheared) meta-andesitic rocks are carbonation and hydration, and secondary magnetite porphyroblasts. More-strongly deformed and altered rocks record silicification and potassic alteration (muscovite). Massive albite-rich assemblages with smaller amounts of ankerite, rutile, and pyrite are adjacent to late quartz–ankerite–albite(–pyrite) veins (Figs 10.14a and c). These assemblages are brick red, reflecting addition of abundant fine, dusty hematite, and overprint the foliation in adjacent schists (Figs 17 and 18). Alteration selvages vary from several millimetres to several centimetres wide. Magnetite porphyroblasts are severely corroded or absent from intensely hematitized alteration halos. At the margins of these alteration halos, magnetite porphyroblasts are partly pseudomorphed by hematite, and idioblastic pyrite contains inclusions of carbonate, silicate minerals, and magnetite.

Weaker hematitization of andesitic schists (pink in colour; Fig. 10.16) extends beyond the veins and their

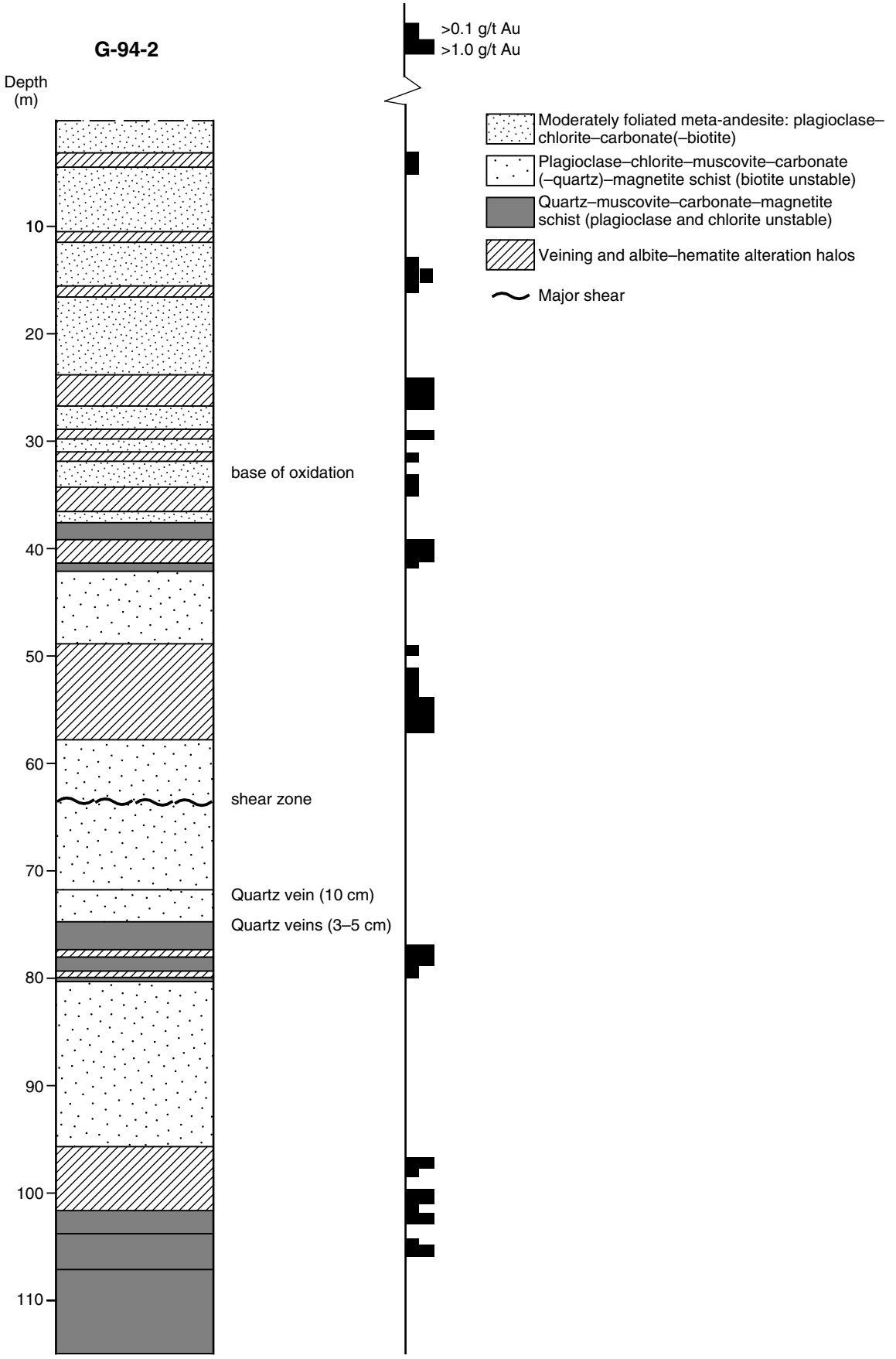

WW381 13.02.04

Figure 10.13. Summary log, diamond drillhole G-94-2, Enterprise deposit, Porphyry mining area

Table 10.1. Metamorphic and metasomatic assemblages in meta-andesitic rocks, Enterprise deposit, Porphyry area

Metamorphism	*Ductile deformation*		*Brittle deformation*
metamorphic assemblage	*moderate deformation/metasomatism*	*intense deformation/metasomatism*	*late vein-related alteration*
PLAGIOCLASE	PLAGIOCLASE	QUARTZ	ALBITE
AMPHIBOLE	CHLORITE	CARBONATE	HEMATITE
BIOTITE	CALCITE	MUSCOVITE	ANKERITE
Ilmenite	QUARTZ	Magnetite	MUSCOVITE
	MUSCOVITE	Titanite	Rutile
	Magnetite	Pyrite	Pyrite
	Titanite		Chalcopyrite

NOTES: Minerals shown in upper case are essential minerals and commonly form >10% of the rock
Minerals shown in lower case are minor to accessory phases

immediate brick-red halos (Figs 10.14a and b). Magnetite porphyroblasts in these more-weakly hematitized schists are unaltered, suggesting that kinetic effects have prevented equilibration with oxidizing fluids.

Although trace pyrite is found throughout drillhole G-94-2, idioblastic pyrite is more abundant in hematitized rocks (including pink schists distal from quartz veins). There is a strong correlation between gold and zones of quartz veining, idioblastic pyrite, and hematitization (Fig. 10.13).

Mass-balance calculations, based on whole-rock geochemical data, show that K_2O, CO_2, and CaO ($\pm SiO_2$, Fe_2O_3) have been added to the strongly foliated andesitic schists in the shear zone (Fig. 10.20). Chemical changes accompanying mineralization (hematitic quartz–carbonate–albite–pyrite lodes) include further enrichment of CO_2, Fe_2O_3, and CaO, as well as lesser Na_2O and S. SiO_2 is depleted from these zones.

References: Enterprise Gold Mines NL (1992a,b), Consolidated Resources NL (1994).

Margaret

Coordinates: 29°46'52"S, 122°18'39"E

Production: 7504.6 t of ore for 51.84 kg Au (6.9 g/t Au) between 1940 and 1980. Resources have been quoted as a combined figure for the Edjudina group of Sons of Gwalia Ltd.

Host rock: Metamorphosed andesitic volcanic and volcaniclastic rocks.

Structure: Moderately deep shafts and shallow workings are sited over a strike length of about 400 m, on a brittle–ductile shear zone that trends 345° and dips 60–80°E. Further workings on the same structure are located 500 m to the north. The mineralized lode is associated with veining within this shear zone and is 1–2 m wide. A subhorizontal linear fabric is present within the shear zone. Subvertical quartz veins in the margins of the shear are oriented 325°, suggesting sinistral movement.

Alteration: Meta-andesitic rocks within the mineralized lode are altered to quartz–muscovite–carbonate schist with disseminated, idioblastic pyrite. Widespread hematitization is indicated by pink to brick-red colouration. Quartz–albite–carbonate–pyrite(–tourmaline) veins are present within the altered schist. Secondary magnetite porphyroblasts in quartz–muscovite–chlorite–carbonate schists marginal to the mineralized lode have asymmetric pressure shadows indicative of simple shear.

References: Cyprus Minerals Australia Co. (1988), Enterprise Gold Mines NL (1992a,b), Consolidated Resources NL (1994), Swager (1995).

Tonbridge

Coordinates: 29°47'21"S, 122°18'54"E

Production: No historic production. Resources have been quoted as a combined figure for the Edjudina group of Sons of Gwalia Ltd.

Host rock: Metamorphosed andesitic volcanic and volcaniclastic rocks.

Structure: Mineralization is associated with quartz veining in a subvertical brittle–ductile shear zone that strikes about 350°.

Alteration: Deformed andesitic rocks are altered to quartz–muscovite(–chlorite) schist, locally with secondary magnetite. Widespread pink colouration reflects hematitization.

References: Cyprus Minerals Australia Co. (1988), Enterprise Gold Mines NL (1992a,b), Consolidated Resources NL (1994).

Mad Dog and Mad Dog South

Coordinates: 29°46'54"S, 122°18'56"E

Production: Historic production is less than 5 kg Au. Resources have been quoted as a combined figure for the Edjudina group of Sons of Gwalia Ltd.

Table 10.2. Petrographic descriptions of metamorphic and metasomatic assemblages related to ductile deformation and quartz veining in diamond drillhole G-94-2, Enterprise deposit, Porphyry area

Assemblage type	*Assemblage minerals/description*
Metamorphic assemblage	**Plagioclase–amphibole(–biotite)–leucoxene/titanite** Swager (1995) described intermediate volcanic rocks in the Porphyry area as consisting mainly of plagioclase and light-green amphibole with accessory leucoxene or titanite and minor secondary muscovite, chlorite, and epidote. Textural features including plagioclase phenocrysts (1–2 mm) and quartz-filled amygdales are preserved, as are the original lath shapes of plagioclase in the groundmass. Amphiboles in least-altered and least-deformed andesitic rocks from G-94-2 are entirely replaced by chlorite and biotite
Shear-zone assemblages	**Quartz(–plagioclase)–carbonate–muscovite(–chlorite)–magnetite–titanite(–hematite–pyrite–tourmaline)** Amphibole and biotite are unstable in moderately to strongly deformed meta-andesitic rocks in G-94-2. Plagioclase and chlorite are unstable in more-strongly altered zones Where preserved, **plagioclase** commonly retains its original lath-like form, but is variably recrystallized. In contrast to metasomatic albite, metamorphic plagioclase contains a small but detectable component of anorthite (Table 10.4). **Quartz** forms a fine-grained, granoblastic mosaic of anhedral grains. **Chlorite** and **muscovite** are strongly oriented parallel to the shear fabric. Anastomosing chloritic seams envelope carbonate-rich domains to produce a pseudo-fragmental structure (Fig. 10.15). Where less abundant, chlorite may form thin, elongate aggregates (‘flecks’) that define a subhorizontal lineation. **Carbonate** (calcite) is coarser grained (0.1 – 0.3 mm) than most other minerals and commonly forms elongate, sigmoidal porphyroblasts. Inclusion trails in early carbonate (cores) are commonly oriented at a high angle to the external shear fabric. These features indicate carbonate growth during simple shear. **Titanite** forms short, granular trails in the plane of the shear fabric. Secondary **magnetite** forms foliation-parallel trails and more-irregular disseminations of subhedral to euhedral porphyroblasts up to about 2 mm across, which overgrow, but locally deflect, the shear fabric. The main accessory minerals are **tourmaline** and **pyrite** Weak, foliation-controlled hematitization is evident as pink colouration in several zones (Fig. 10.16). Fine, dusty hematite appears selectively in quartz and muscovite but is less common in carbonate-rich bands. Magnetite is commonly unaltered in weakly hematitized schist, probably because of kinetic effects (Fig. 10.14b). In some cases, the weak hematitization is distal to more-intense, hematite-bearing alteration selvages adjacent to late veins (Figs 10.14a and 10.17), but in others there is no obvious relationship between hematitization and veins. Rutile forms in place of titanite where hematitization has occurred
Late veins and related alteration halos	**Quartz–carbonate–albite(–muscovite)–pyrite–rutile** Late quartz–ankerite–albite(–minor pyrite–rutile–apatite) veins cut the shear fabric and have alteration halos that overprint the foliation in adjacent schists after altered meta-andesite (Figs 10.14a and 10.17). Albite-rich alteration selvages are brick-red, reflecting intense hematitization (Fig. 10.18). They also contain smaller amounts of ankerite, rutile, and idioblastic pyrite (up to about 5 mm across). Ankerite compositions (mainly Fe/Mg) vary between samples (Fig. 10.19), perhaps reflecting the chemistry of the original metamorphic rocks. Albite in the veins and alteration selvages is essentially pure albite (Ab_{100}). Muscovite is present in some alteration halos. Trace chalcopyrite is locally associated with pyrite. Secondary magnetite porphyroblasts in intensely hematitized assemblages are absent or severely corroded. Replacement of magnetite by hematite is evident near intense hematitization fronts. Idioblastic pyrite contains inclusions of silicates, carbonate, and magnetite. In GSWA 130684, muscovite in altered schist adjacent to the replacement front is randomly oriented and post-dates oriented chlorite, suggesting recrystallization of the shear zone assemblage Where a late vein cuts less-altered schist containing plagioclase and chlorite (GSWA 130694), there is a narrow rim of magnetite–muscovite separating the vein from the albitized wallrock (Fig. 10.14c)

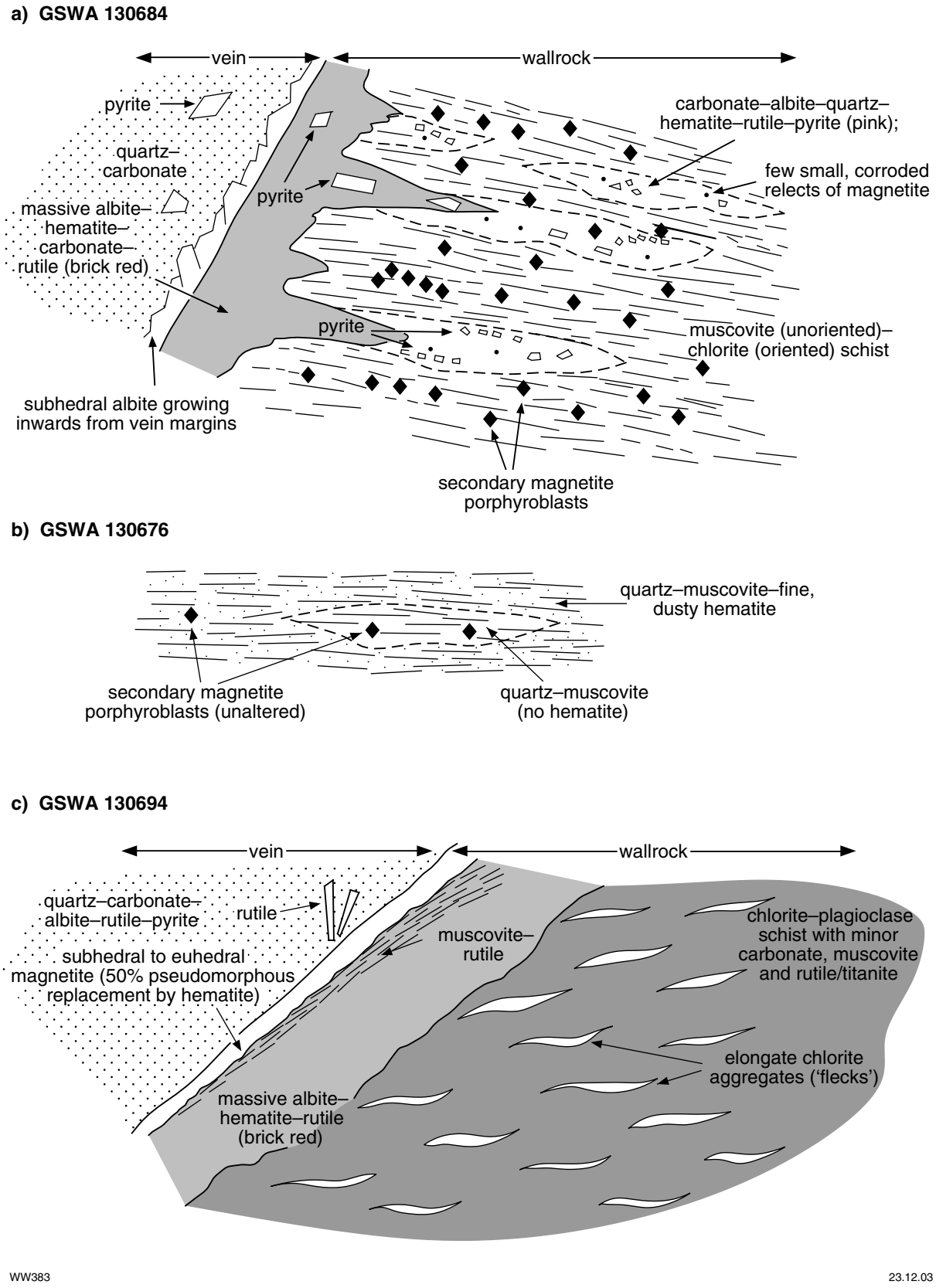

Figure 10.14. Sketches showing microtextural and fabric relations among various alteration assemblages, Enterprise deposit, Porphyry mining area

IRO97 21.07.03

Figure 10.15. Pseudo-fragmental structure formed by isolated relicts of carbonate-rich alteration assemblage in anastomosing, chlorite-rich seams, Enterprise deposit, Porphyry mining area

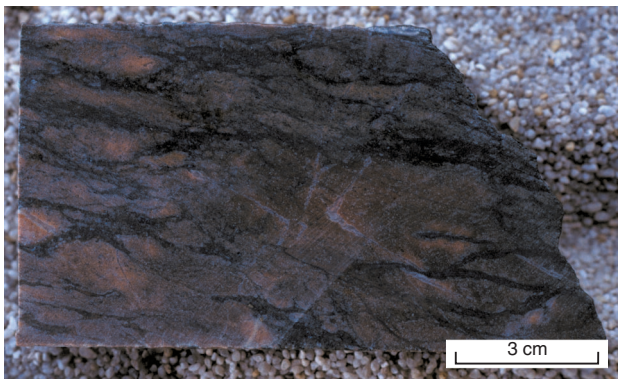

IRO43 15.12.03

Figure 10.16. Relict weak hematitized meta-andesite within anastomosing zones of chlorite-rich assemblage, Enterprise deposit, Porphyry mining area

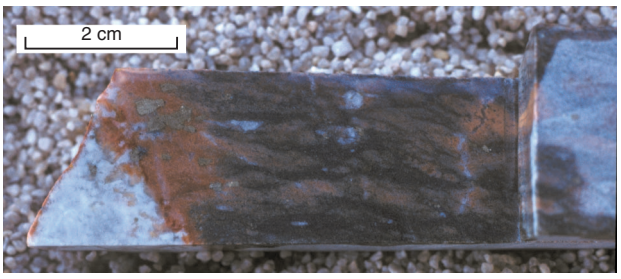

IRO98 15.12.03

Figure 10.17. Massive, hematitic, albite-rich alteration assemblage with disseminated pyrite adjacent to a late quartz vein, overprinting earlier shear-related alteration (relict weak hematitized meta-andesite within anastomosing zones of chlorite-rich assemblage), Enterprise deposit, Porphyry mining area

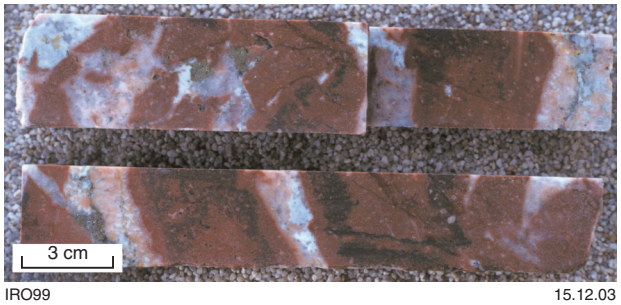

IRO99 15.12.03

Figure 10.18. Quartz–carbonate–albite–pyrite veins within brick-red albite-rich alteration assemblage, Enterprise deposit, Porphyry mining area

Host rock: Andesitic volcanic and volcaniclastic rocks.

Structure: At Mad Dog, moderately deep stopes and shafts extend over about 100 m on a 345°-trending brittle–ductile shear zone. The mineralized zone is 3–10 m wide and dips about 60°E. Subvertical quartz(–carbonate–albite) veins up to 20 cm wide, within the zone of brittle–ductile deformation, are oriented 325°, suggesting sinistral movement on the shear zone.

At Mad Dog South, the orebody is a 350°-trending lens, about 60–80 m long, 10–15 m wide, and extending 30–90 m below the surface. This orebody lies within a broader zone of hematitization, similar to that at Enterprise.

Alteration: Ore is in pyritic quartz–sericite–carbonate–hematite schist and associated quartz–carbonate–albite veins. This mineralized schist lies within a broader envelope of lower grade quartz–sericite–chlorite–carbonate–hematite–(secondary) magnetite(–tourmaline–pyrite) schist.

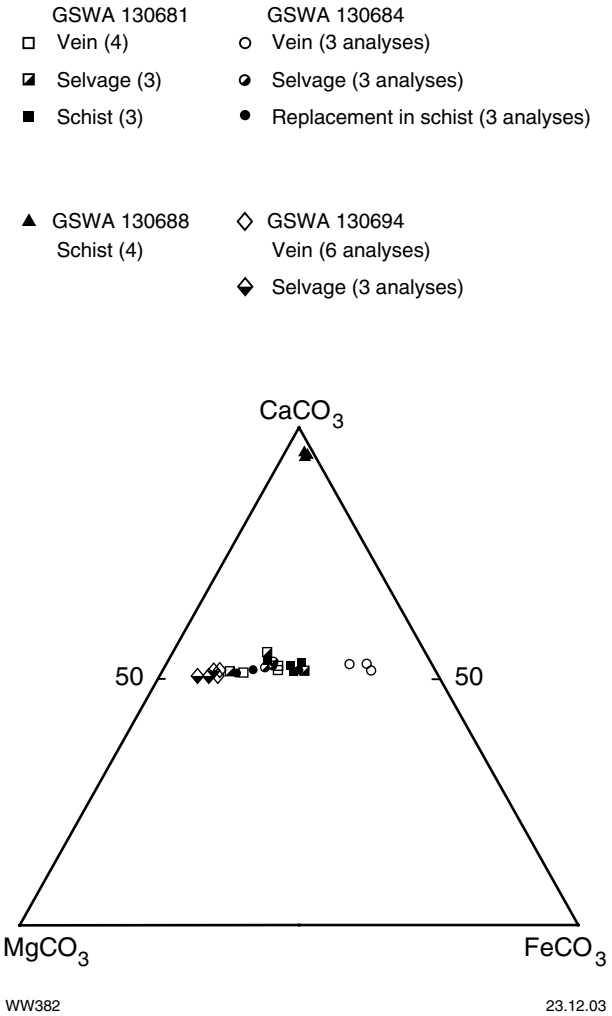

WW382 23.12.03

Figure 10.19. Carbonate mineral compositions, Enterprise deposit, Porphyry mining area, plotted on a $MgCO_3$–$CaCO_3$–$FeCO_3$ triangular diagram

Table 10.3. Representative analyses of carbonate minerals, Enterprise deposit, Porphyry area

	GSWA 130681									*GSWA 130684*						*GSWA 130688*		*GSWA 130694*				
	vein in quartz–chlorite–muscovite schist									*vein in altered schist*						*chl– pl– cb schist*		*vein in chl– pl– cb schist*				
	vein (quartz–carbonate–albite–pyrite)				*vein selvage (hem–ab–cb–ms–py)*		*wallrock schist (qtz–chl–ms–cb–mag)*			*vein (qtz–cb–ab–py–ap)*		*massive ab–hem alteration selvage*		*albitic replacement front in schist*				*quartz–carbonate–albite vein*			*albite–hematite alteration selvage*	
	CB1	*CB2*	*CB3*	*CB4*	*CB5*	*CB6*	*CB7*	*CB8*	*CB9*	*CB10*	*CB12*	*CB15*	*CB17*	*CB18*	*CB19*	*CB22*	*CB26*	*CB29*	*CB30*	*CB32*	*CB34*	*CB44*
FeO	14.25	14.88	11.47	10.46	12.51	17.08	13.18	16.28	15.89	20.54	22.27	13.52	14.03	16.48	11.12	2.83	2.72	9.83	9.86	9.73	9.23	9.34
MnO	0.48	0.42	0.50	0.60	0.83	-	0.51	0.35	0.35	0.31	0.44	0.65	0.68	0.48	0.89	0.76	0.91	0.46	0.52	0.37	0.44	0.30
MgO	10.75	10.76	12.95	13.88	11.00	9.87	11.36	9.70	10.29	7.16	6.12	11.59	10.97	9.81	13.49	0.48	0.38	14.76	14.16	14.55	14.64	15.23
CaO	28.23	28.11	28.27	28.78	30.03	27.79	29.05	28.80	28.14	28.34	27.58	28.80	28.63	28.15	28.49	54.32	54.28	29.04	28.83	28.91	29.16	29.38
Total	**53.71**	**54.17**	**53.20**	**53.72**	**54.37**	**54.74**	**54.10**	**55.13**	**54.67**	**56.35**	**56.41**	**54.55**	**54.31**	**54.93**	**53.98**	**58.39**	**58.29**	**54.09**	**53.37**	**53.57**	**53.47**	**54.25**
$FeCO_3$	20.34	21.11	16.09	14.40	17.52	24.30	18.52	23.00	22.50	29.38	32.29	18.84	19.77	23.38	15.32	3.82	3.68	13.31	13.59	13.32	12.61	12.55
$MnCO_3$	0.69	0.60	0.71	0.83	1.18	-	0.73	0.49	0.49	0.45	0.64	0.91	0.97	0.69	1.25	1.04	1.26	0.64	0.72	0.51	0.61	0.41
$MgCO_3$	27.34	27.20	32.38	34.03	27.44	25.02	28.44	24.41	25.97	18.25	15.83	28.80	27.56	24.80	33.12	1.17	0.91	35.64	34.79	35.49	35.69	36.48
$CaCO_3$	51.63	51.09	50.80	50.73	53.86	50.67	52.30	52.10	51.03	51.92	51.23	51.45	51.70	51.14	50.31	93.98	94.15	50.41	50.91	50.68	51.09	50.57
Nomen-clature	← ankerite →															← calcite →		← ferroan dolomite →				

NOTES: ab: albite; ap: apatite; cb: carbonate; chl: chlorite; hem: hematite; mag: magnetite; ms: muscovite; pl: plagioclaise; py: pyroxene; qtz: quartz

Table 10.4. Representative analyses of albite, Enterprise deposit, Porphyry area

	GSWA 130681						*GSWA 130684*						*GSWA 130688*				*GSWA 130694*					
	vein in quartz–chlorite–muscovite schist						*vein in altered schist*						*chlorite– plagioclase– carbonate schist*				*vein in chlorite–plagioclase–carbonate schist*					
	qtz–cb–ab–py vein margin		*vein selvage (hem–ab–cb–ms–py)*		*wallrock schist (qtz–chl–ms–cb–mag)*		*qtz–cb–ab–py vein*		*aassive ab–hem alteration selvage*		*albitic replacement front in schist*						*qtz–cb–ab vein*		*ab–hem alteration selvage*		*chl–pl–cb schist*	
	AB1	*AB4*	*AB6*	*AB7*	*AB8*	*AB10*	*AB12*	*AB13*	*AB15*	*AB16*	*AB18*	*AB19*	*AB20*	*AB25*	*AB26*	*AB28*	*AB30*	*AB31*	*AB33*	*AB34*	*AB35*	*AB39*
SiO_2	67.09	68.12	68.16	68.31	68.15	68.64	68.34	68.50	67.81	67.96	67.72	67.61	67.52	67.00	67.42	66.34	68.82	68.76	68.43	68.11	69.26	67.69
Al_2O_3	19.38	19.58	19.36	20.14	19.49	19.52	19.72	19.97	19.38	19.53	19.43	19.49	19.89	20.74	19.75	19.93	19.55	19.60	19.87	20.21	20.00	19.86
FeO	–	–	–	–	–	–	–	–	–	–	–	–	–	0.17	0.27	0.31	–	–	0.29	–	–	–
CaO	–	11.87	–	–	–	–	–	–	–	–	0.19	–	0.19	1.13	0.37	0.55	–	–	–	0.22	–	0.32
Na_2O	11.68	–	11.94	11.93	11.90	12.11	12.22	12.25	12.01	11.93	11.91	11.78	11.88	11.55	11.72	11.42	12.17	11.55	12.17	11.77	12.08	11.95
K_2O	–	–	–	–	–	–	–	–	–	–	–	–	–	0.23	–	–	–	–	–	–	0.10	–
Total	**98.15**	**99.57**	**99.46**	**100.37**	**99.54**	**100.27**	**100.28**	**100.72**	**99.20**	**99.41**	**99.25**	**98.88**	**99.48**	**100.83**	**99.54**	**98.56**	**100.54**	**99.91**	**100.77**	**100.31**	**101.44**	**99.82**
Ab	100.00	100.00	100.00	100.00	100.00	100.00	100	100	100	100	99.12	100	99.13	93.70	98.27	97.39	100	100	100	98.98	99.48	98.5
Or	–	–	–		–		–	–		–	–	–	–	1.22	–	–	–	–	–	–	0.52	–
An	–	–	–		–		–	–		–	0.88	–	0.87	5.08	1.73	2.61	–	–	–	1.02	–	1.5

NOTES: ab: albite; cb: carbonate; chl: chlorite; hem: hematite; mag: magnetite; ms: muscovite; pl: plagioclaise; py: pyroxene; qtz: quartz

Table 10.5. Representative analyses of chlorite, Enterprise deposit, Porphyry area

	GSWA 130681				*GSWA 130684*			*GSWA 130688*			*GSWA 130694*	
	vein in quartz–chlorite–muscovite schist				*vein in altered schist*			*chlorite–plagioclase–carbonate schist*			*vein in chl–pl–cb schist*	
	outer vein selvage (qtz–ms–chl–cb–py)		*wallrock schist (qtz–chl–ms–cb–mag)*		*recrystallized chlorite–muscovite schist*						*chlorite–plagioclase–carbonate schist*	
	chlorite in pressure shadow of pyrite				*coarse-grained chlorite*		*chl replacing magnetite*					
	CH2	*CH3*	*CH4*	*CH5*	*CH9*	*CH10*	*CH11*	*CH14*	*CH15*	*CH17*	*CH50*	*CH53*
SiO_2	24.08	24.59	24.41	24.94	24.63	24.76	22.64	23.30	22.56	22.43	25.44	24.93
Al_2O_3	21.66	21.87	21.55	21.57	21.22	21.65	19.93	21.62	22.80	22.69	21.14	21.48
Cr_2O_3	-	-	-	-	-	0.15	-	-	-	-	-	-
FeO	26.30	23.98	23.82	24.96	26.37	24.84	41.71	31.35	31.55	32.10	19.61	20.47
NiO	0.37	0.21	-	0.27	-	-	-	-	-	-	-	-
MgO	14.04	15.09	15.43	15.14	13.91	15.120	3.34	9.95	9.09	9.18	18.82	18.38
Na_2O	-	0.26		0.26	0.21	0.20	-	-	-	-	-	-
Total	**86.45**	**86.00**	**82.51**	**87.13**	**86.34**	**86.72**	**87.61**	**86.21**	**86.00**	**86.40**	**85.02**	**85.27**
Fe/Fe+Mg	51.2	56.2	46.4	48.0	51.5	48.0	87.5	63.9	66.1	66.2	36.7	38.5

NOTES: cb: carbonate; chl: chlorite; mag: magnetite; ms: muscovite; pl: plagioclaise; py: pyroxene; qtz: quartz

Table 10.6. Representative analyses of muscovite, Enterprise deposit, Porphyry area

	GSWA 130684 vein in altered schist recrystallized chlorite–muscovite schist	
	MU1	*MU3*
SiO_2	46.69	45.76
TiO_2	0.17	0.38
Al_2O_3	28.52	32.14
FeO	4.50	3.55
MgO	1.97	1.01
Na_2O	0.33	0.52
K_2O	10.89	10.75
Total	**93.08**	**94.11**

References: Cyprus Minerals Australia Co. (1988), Enterprise Gold Mines NL (1992a,b), Consolidated Resources NL (1994).

Porphyry North

Coordinates: 29°41'24"S, 122°16'23"E

Production: There are historic workings in the area, but production appears to have been insignificant (<5 kg Au). The inferred resource is 200 000 t of ore at 2.2 g/t Au (440 kg Au; MINEDEX site code S02379).

Host rock: Mineralization is in a medium-grained (≤1 mm), equigranular granitoid (quartz monzonite) intrusion, about 1000 m long and 300 m wide at the surface. This pluton intrudes metamorphosed mafic to intermediate (mainly andesitic) country rocks.

Structure: A 340°-trending zone in the northern part of the granitoid intrusion supports small historic workings and has been the focus of more-recent exploration. The mineralized zone consists of a series of right-stepping, en echelon zones of fracturing, veining, and foliation. These en echelon zones are 1–3 m wide, strike about 300°, and dip 60–75°SW. They project into the mafic to andesitic country rocks but are mostly unmineralized outside the intrusion. The right-stepping nature of the en echelon series suggests formation within a zone of sinistral shear.

Alteration: Alteration at the surface is obscured by weathering. However, drill chips from exploration drilling suggest the granitoid has been sericitized, and contain disseminated pyrite and minor tourmaline. There are also some zones of hematitization.

References: Audimco Ltd (1987), Swager (1995).

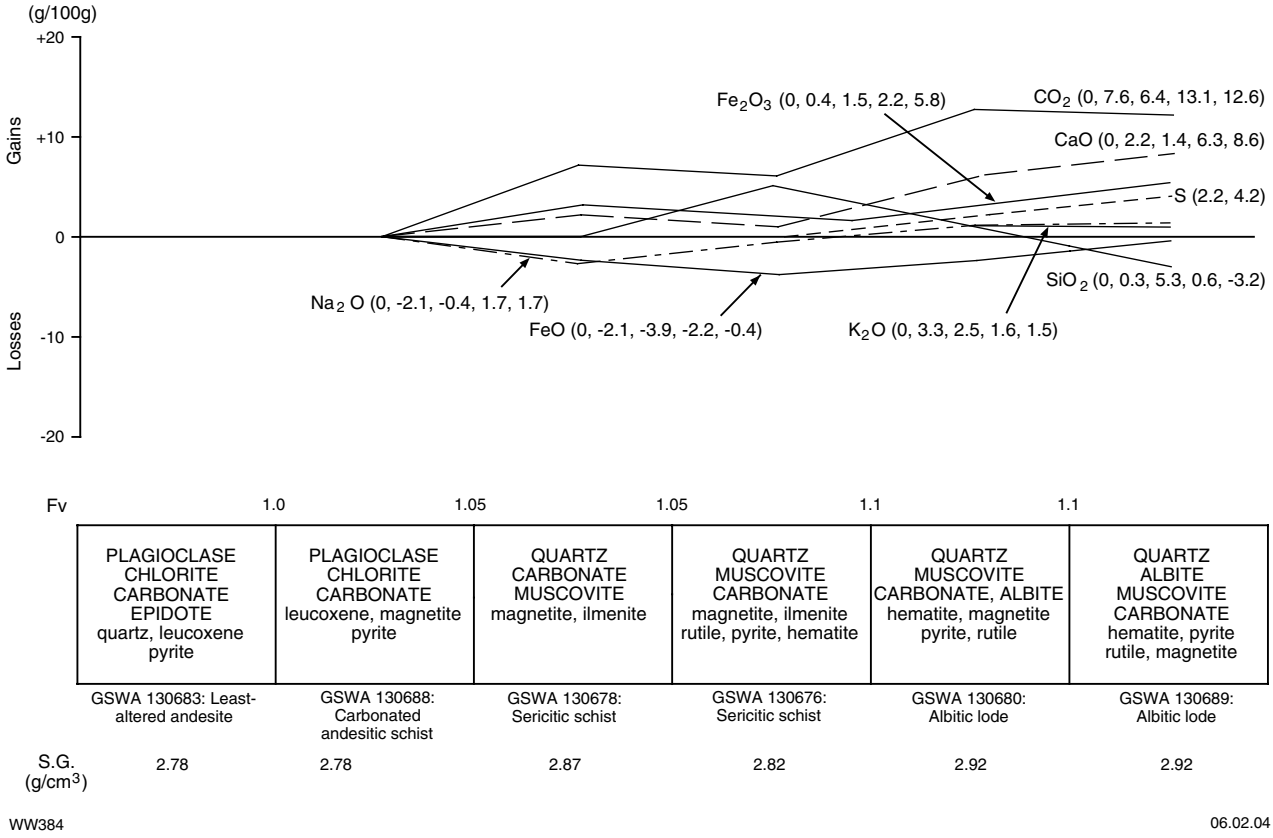

Figure 10.20. Mass-balance changes (calculated using the method of Gresens, 1967) associated with ductile-deformation-related alteration and later, brittle-deformation-related albitic lode formation, Enterprise deposit, Porphyry mining area. Mineral components of alteration assemblages are listed in approximate order of abundance, with main mineral components in upper case and minor mineral components in lower case

References

ALLEN, C. A., 1987, The nature and origin of the Porphyry gold deposit, Western Australia, *in* Recent advances in understanding Precambrian gold deposits *edited by* S. E. HO and D. I. GROVES: University of Western Australia, Department of Geology and University Extension, Publication no. 11, p. 137–146.

AUDAX RESOURCES NL, 1989, Report on P31/01114–01116, P31/01083–01087, P31/01010 and M31/00076: Western Australia Geological Survey, Statutory mineral exploration report, Item 11649 A28892 (unpublished).

AUDIMCO LTD, 1987, Annual report, 1986–1987, P31/00–00163: Western Australia Geological Survey, Statutory mineral exploration report, Item 5459 A22909 (unpublished).

BLATCHFORD, T., 1935, Report on Welch's Find near Yarri, North Coolgardie Goldfields: Western Australia Geological Survey, Annual progess report for the year 1934.

CONSOLIDATED RESOURCES NL, 1994, Annual report, Dec 1992 to Dec 1993, on Edjudina gold exploration: Western Australia Geological Survey, Statutory mineral exploration report, Item 11652 A40259 (unpublished).

CYPRUS MINERALS AUSTRALIA CO., 1988, Annual report 1986 to 1987 on P31/00561–00565, P31/00391–00393, P31/00313–00314, 31/00307 and M31/00028–00032: Western Australia Geological Survey, Statutory mineral exploration report, A21686 (confidential)*.

ENTERPRISE GOLD MINES NL, 1992a, Report on P31/113, P31/1417–1418, M31/99, M31/76 and M30/30: Western Australia Geological Survey, Statutory mineral exploration report, Item 11655 A37396 (unpublished).

ENTERPRISE GOLD MINES NL, 1992b, Report on P31/1417–1418, M31/99, M31/76 and M31/30: Western Australia Geological Survey, Statutory mineral exploration report, Item 11655 A37397 (unpublished).

GONDWANA RESOURCES NL, 1987, Report on GML31/1482: Western Australia Geological Survey, Statutory mineral exploration report, Item 11645 A40823 (unpublished).

GRESENS, R. L., 1967, Composition–volume relationships of metasomatism: Chemical Geology, v. 2, p. 47–65.

HILL, R. I., CHAPPELL, B. W., and CAMPBELL, I. H., 1992, Late Archaean granites of the southeastern Yilgarn Block, Western Australia: age, geochemistry and origin: Transactions of the Royal Society of Edinburgh, v. 83, p. 211–226.

RIDLEY, J. R., 1993, The relations between mean rock stress and fluid flow in the crust: with reference to vein- and lode-style gold deposits: Ore Geology Reviews, v. 8, p. 23–27.

SWAGER, C. P., 1995, Geology of the Edjudina and Yabboo 1:100 000 sheets: Western Australia Geological Survey, 1:100 000 Geological Series Explanatory Notes, 43p.

WEATHERSTONE, N., 1990, Porphyry gold deposit, *in* Geology of the mineral deposits of Australia and Papua New Guinea *edited by* F. E. HUGHES: Australasian Institute of Mining and Metallurgy, Monograph 14, p. 525–530.

* Confidential references are used with permission of companies

11. Randalls

The Randalls mining area (Fig. 11.1), with a modern production (1992–97) of 2.73 Mt of ore for 7409.969 kg Au (2.7 g/t), lies within the Mount Belches Formation of Painter and Groenewald (2001). This unit broadens to the south and is bound to the west by the curved Randall Fault. This fault is interpreted as a folded D_1 structure across which mafic and ultramafic rocks of the Kalgoorlie Terrane were thrust over felsic volcanic rocks of the Gindalbie Terrane. The Mount Belches Formation is a thick sequence of metamorphosed, mainly clastic sedimentary rocks. Metamorphosed polymictic conglomerate in the northern part of the sequence indicates a provenance to the north. At Randalls, the metasedimentary rocks are dominated by metasandstone and metasiltstone, with minor chloritic (metashale) interbeds. Psammitic units consist mainly of angular quartz, feldspar, and biotite, suggesting derivation from an immature sediment with a volcanic or volcano-plutonic provenance. Dunbar and McCall (1971) interpreted these metasedimentary rocks as being derived from turbiditic deposits. Two to three units containing detrital magnetite grains lie within metamorphosed turbiditic siltstone and sandstone in the Randalls area. These units have been referred to as banded iron-formation (BIF). The upper unit is the thickest and most prominent in outcrop. Diamond-drill logs (Fig. 11.2) indicate that, in detail, the BIF units are interbedded with metamorphosed quartzofeldspathic siltstone and sandstone, and chlorite-rich units interpreted as Fe-metashale (Table 11.1; Figs 11.3 and 11.4). The BIF units are layered on several scales and vary from quartz–magnetite(–grunerite) to sulfide rich and amphibole rich (Table 11.1). Intersections of sulfide-rich layers coincide with quartz veining (Fig. 11.5).

Despite regional folding and local zones of shearing, the metasedimentary rocks in the examined drillcore show little evidence of ductile deformation, and primary sedimentary structures (e.g. graded bedding and basal grit beds; Table 11.2; Figs 11.6 and 11.7) are widely preserved. Representative mineral analyses are presented in Tables 11.3 – 11.8, and arsenopyrite and calcic amphibole compositions are plotted in Figures 11.8 and 11.9. Mineral assemblages in BIF units, especially the widespread presence of grunerite and calcic amphibole, suggest medium-grade (amphibolite facies — about 500°C or more) regional metamorphism (Gole, 1981; Ahmat, 1986). Quartz–biotite – opaque oxide pseudomorphs after andalusite in metasiltstone are also consistent with medium-grade metamorphism. The presence of orthopyroxene (eulite; Table 11.3) in a magnetite-rich sample (GSWA 132923; Santa Claus) is normally regarded as indicative of upper amphibolite- to granulite-facies metamorphism (Robinson et al., 1982), but its restricted occurrence (on the contact between magnetite-rich and Fe-metashale) at Randalls makes the significance of this observation unclear.

The regional structure in the Randalls area is dominated by D_2 chevron folds that plunge 40–50°N and are overturned to the west (Fig. 11.1). The relatively steep plunge of these folds is attributed to rotation during D_3. The folds tighten progressively towards the west, and fold axes are rotated towards the north-trending Bare Hill Shear Zone, which is interpreted to be a D_3 splay off the Randall Fault. Mapping of openpits by Newton et al. (1998) has identified two main fault sets: steep, northwesterly to north-northwesterly trending, and bedding-parallel, brittle to brittle–ductile faults with reverse movement have been identified in the southern part of the Santa Claus pit; and similar north-northwesterly to north-northeasterly trending faults exist at Cock Eyed Bob. Regionally, these faults are equivalent to D_3 faults in the Kalgoorlie Terrane, which also display reverse movement during late D_3 (Witt, 1990; 1993). These faults are post-dated by north-northeasterly to east-northeasterly trending brittle and brittle–ductile dextral faults that formed during D_4.

Most gold deposits (Santa Claus, Craze, Rumbles, Santa North, Cock Eyed Bob, and Knob Hill) are hosted by the upper BIF unit, but there are also several deposits (Dunlevy, Maxwells, Flora Dora, and Browns) in the lower unit or units. Mineralization in all the main deposits is related to brittle quartz(–siderite–chlorite) veining in the relatively competent BIF units (Fig. 11.10), with most quartz veins dipping 25–40°SW. Many are terminated against contacts with metasiltstone units, but some persist for a short distance into the adjacent metasiltstones. The relatively flat lying nature of the mineralizing quartz veins implies subvertical extension consistent with formation during reverse movement on north-northwesterly trending and bedding-parallel faults. Vein formation may also, or alternatively, be related to strike-slip movement on north-northeasterly to east-northeasterly trending faults. Local stockwork veining may account for an increase in grade adjacent to these faults.

The quartz(–siderite–chlorite) veins generally have low gold contents, and most of the gold is located in sulfidized wallrocks. Sulfidation (pyrrhotite, arsenopyrite) of BIF units is accompanied by addition of biotite, carbonate (siderite), and possibly chlorite. However, the volume of metasomatic minerals other than sulfides is generally low. Arsenopyrite geothermometry at Santa Claus and Rumbles yields temperatures of crystallization between about 390 and 460°C, which is up to about 100°C below estimated peak metamorphic temperatures (Fig. 11.8). The arsenopyrite compositions are consistent with the presence of coexisting pyrite at Rumbles, but are not consistent with the presence of pyrrhotite at Santa Claus, where the two sulfides may not be in equilibrium (Fig. 11.8). At Santa Claus, idioblastic arsenopyrite overprints banded pyrrhotite, suggesting an evolution towards lower temperatures and higher sulfur fucacity (a_{S2}) during the hydrothermal event. At Rumbles, arsenopyrite contains relict inclusions of pyrrhotite, and 'birds-eye' structure in coexisting pyrite suggests a similar temporal evolution from pyrrhotite to pyrite. Pyrrhotite and carbonate in some samples from Santa Claus and Maxwells display textures that suggest equilibration with metamorphic amphiboles. Furthermore, veins with pyrrhotite contain minor

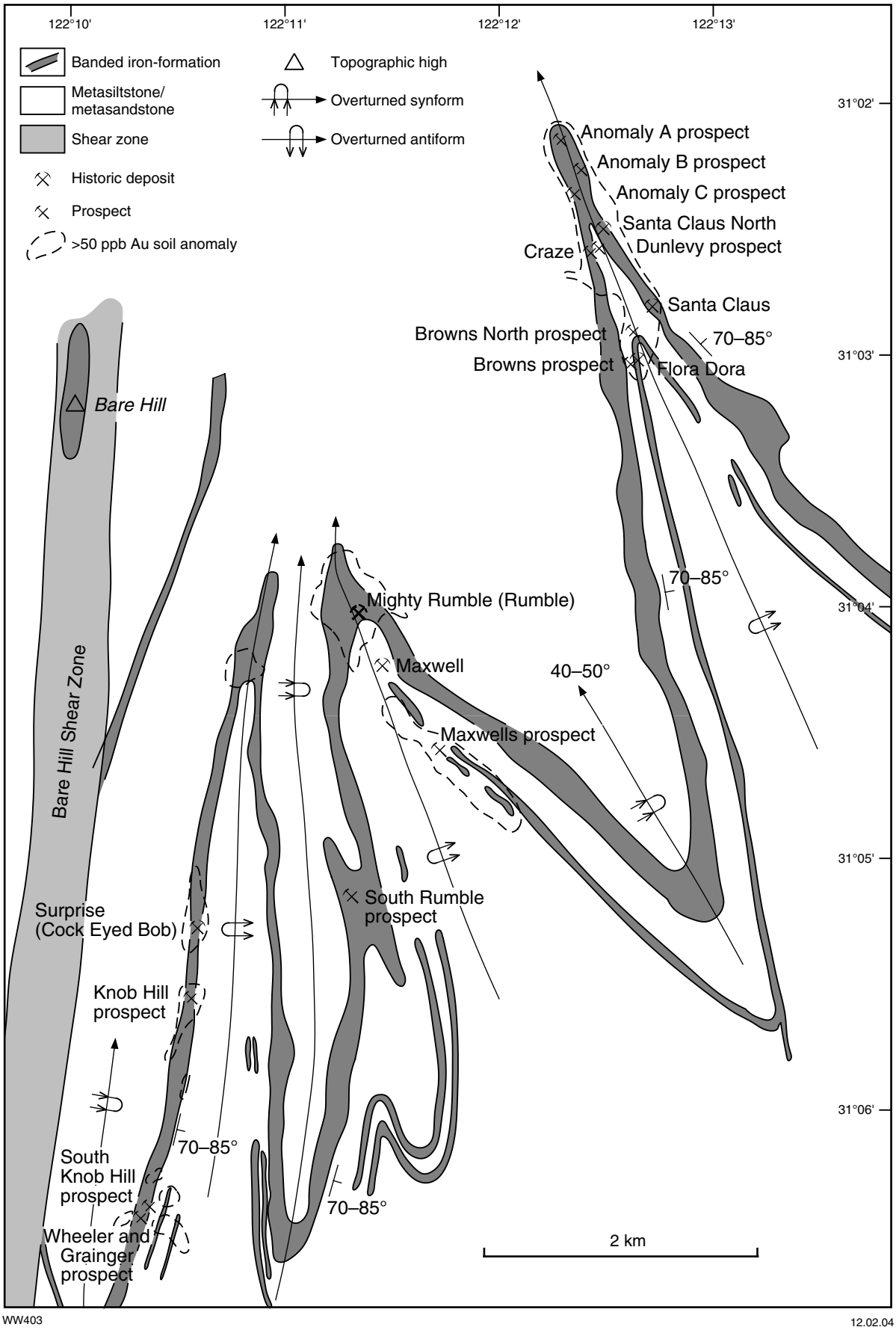

Figure 11.1. Geological map of the Randalls mining area (modified from Ramsgate Resources Ltd, 1994)

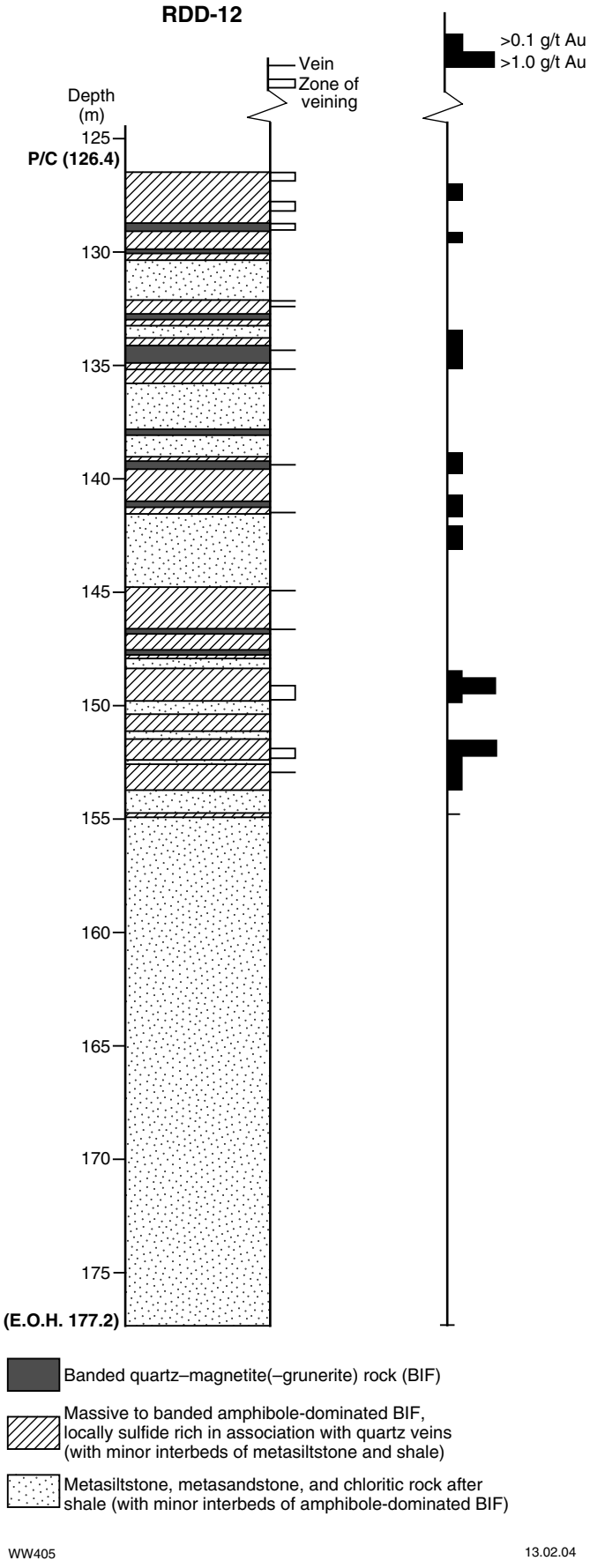

Figure 11.2. Summary log, diamond drillhole RDD-12, Santa Claus

Table 11.1. Petrographic descriptions of rock types encountered in drillholes RDD-12 (Santa Claus), RMD-1 (Rumbles), and MD-1 (Maxwells), Randalls mining centre

Rock type	*Description*
1. Metamorphosed magnetite-rich (quartz–magnetite±grunerite) metasedimentary unit	Millimetre- to centimetre-scale bands are defined by modal variation of the main rock-forming minerals. Bands of granoblastic quartz alternate with bands of coarse-grained magnetite and bands of fibrous to acicular, randomly oriented grunerite. Chlorite and carbonate are subordinate phases in some samples. Carbonate forms transgressive veinlets and anhedral grains that are concentrated into bands. Limited SEM analyses have identified the carbonate as calcite (Table 6). Accessory phases include biotite and apatite.
2. Sulfide-rich BIF	Millimetre- to centimetre-scale bands are defined by modal variation of quartz and iron sulfide, together with subordinate chlorite, grunerite, magnetite, and carbonate. Sulfide-rich, magnetite-rich units are present mainly in RMD-1, where the sulfide is pyrite. Thin intervals of pyrrhotite-rich, magnetite-rich units are also present within amphibole-dominated BIF units in RDD-12. Pyrite and pyrrhotite form fine-grained disseminations, rounded aggregates (about 1 mm in diameter), bedding-parallel bands and, less commonly, transgressive veinlets. Minor biotite and ?titanite or ?scheelite are present in some sections, and coarse-grained, idioblastic arsenopyrite is locally common. In RMD-1, banding is locally strongly contorted and quartz–pyrite banding defines a foliation oblique to the main mineral banding (bedding). Pyrite and magnetite display minor alteration to marcasite and hematite, respectively.
3. Massive to banded amphibole-dominated BIF	Banding at a scale of 1 to 10 cm is defined by variable grain size and modal concentrations of quartz, grunerite, calcic amphibole, chlorite, and magnetite. Grunerite is widespread in RDD-12, but calcic amphibole is dominant in Maxwells. Banding is generally not strongly contorted, but attitude varies between steep east and 50°W. Some examples of isoclinal folding were observed (e.g. RDD-12, 152.0 m). Quartz forms near-monomineralic bands with granoblastic fabric as a minor phase interstitial to amphiboles in quartz-poor bands. Grunerite forms near-monomineralic bands, blotchy aggregates, and radiating 'starbursts' of randomly oriented, columnar to acicular grains up to 3 mm long. Grunerite is commonly intergrown at the grain scale with calcic amphibole. Calcic amphibole (ferrotschermakite, Table 11.5, Fig. 11.9) forms randomly oriented, subhedral, bladed to stubby prisms up to 3 mm long. Grain-scale intergrowths with grunerite are widespread. Calcic amphibole tends to form the margins and terminations of grunerite grains; however, the opposite relationship was observed locally in MD-1. Fine-grained chlorite with a weak to moderate preferred orientation parallel to banding forms felted masses interstitial to amphiboles. Disseminations and aggregates of subhedral magnetite are also mainly interstitial to amphiboles, indicating contemporaneous metamorphic recrystallization. Accessory zircon is concentrated into thin, banding-parallel seams. Other accessory minerals are apatite, pyrrhotite, titanite, and garnet.
4. Interbedded sulfide-rich BIF and Fe-metashale	Alternating sections (1 to 10 cm thick) of pyrite-rich, magnetite-rich units (see above) and Fe-metashale (see below).
5. Fe-metashale	Massive to coarsely bedded, chlorite-rich rock with minor to sparse, randomly oriented porphyroblasts of biotite (about 2 mm across) also contains minor quartz and carbonate. Accessory minerals are ilmenite, zircon and ?minnesotaite. Fine-grained chlorite forms a felted mass with a weak to moderate preferred orientation parallel to bedding. Basal grit beds overlie some contacts with magnetite-rich units (e.g. sample GSWA 132924; Table 11.2). Zircon is concentrated into thin, bedding-parallel seams that are draped over exotic clasts of magnetite-rich units (Fig. 11.3a). Local quartz–biotite–magnetite pseudomorphs after ?andalusite are common in some sections. Magnetite porphyroblasts (about 2 mm across) are also common, particularly adjacent to contacts with BIF units. Starbursts of grunerite(–calcic amphibole) are also adjacent to some contacts with BIF units (Fig. 11.3b). Some starbursts appear to be centred on irregular quartz(–magnetite) domains. These amphibole starbursts formed by metamorphic reaction of quartz in clasts of magnetite-rich units with Fe-chlorite in chloritic metasedimentary rock. Magnetite porphyroblasts and relict magnetite in amphibole starbursts are replaced by pyrite or pyrrhotite adjacent to sulfide-rich sections of BIF units (Fig. 11.3c). Similarly, some contacts between quartz–magnetite–grunerite magnetite-rich units and Fe-metashale are marked by a thin band containing calcic amphibole (Fig. 11.4). This may be due to exchange of chemical components between adjacent rock units during regional metamorphism (bimetasomatic or reaction skarns; Einaudi and Burt, 1982).
6. Metamorphosed siltstone and metasandstone	Massive to coarsely bedded quartz–feldspar–biotite(–chlorite) rock contains minor carbonate and trace to 2% fine-grained, disseminated pyrrhotite. Some sections have rhomb-shaped pseudomorphs of quartz(–feldspar)–biotite–opaques after ?andalusite (about 2 mm across). These are commonly zoned from leucocratic cores to biotite-rich margins. The original detrital fabric is still preserved despite metamorphic recrystallization. Quartz forms angular to subangular clasts. Anhedral feldspar (?dominantly plagioclase) has undergone extensive grain-size reduction and widespread sericitization. Tabular to lath-shaped shreds of chlorite and biotite are randomly oriented. Accessory phases are magnetite, pyrite, pyrrhotite, and tourmaline. Many contacts between siltstone and chlorite-rich rocks after metashale are transitional over several centimetres via a gradual increase in the proportion of chlorite. This is interpreted as reflecting original graded bedding (see also Table 11.2)

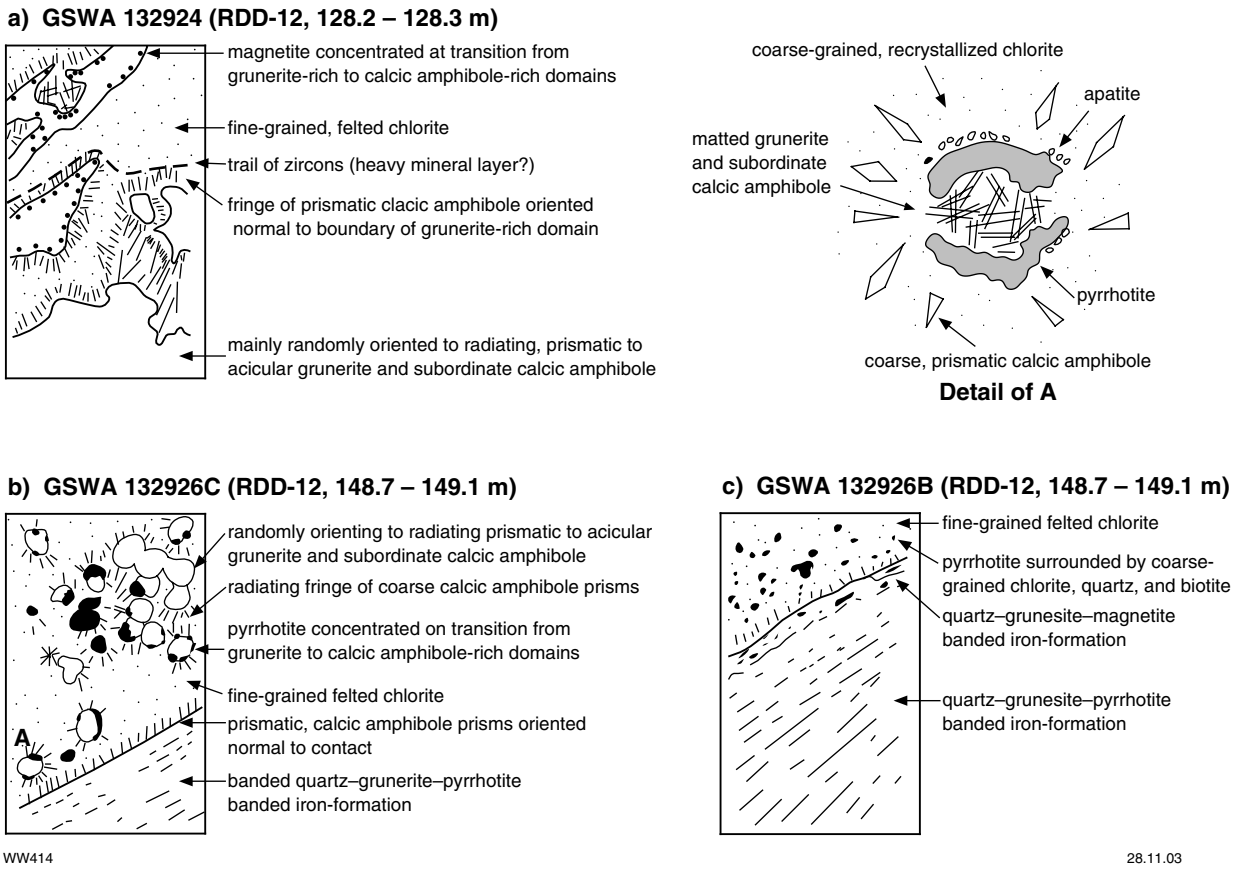

Figure 11.3. Sketches showing some structures and relationships in mineralized BIF, Santa Claus, Randalls mining area. Length of illustrated sections is about 4 cm

amphibole and biotite, suggesting that pyrrhotite grew in approximate thermal equilibrium with peak metamorphic assemblages in the wallrocks. Thus, mineralization in the Randalls area appears to have been initiated with the introduction of pyrrhotite at or close to peak metamorphic temperatures and evolved to pyrite–arsenopyrite assemblages during retrograde cooling to around 400°C.

The competency contrast between thin, relatively brittle BIF units within a thick sequence of metamorphosed clastic sedimentary rocks was essential to the formation of gold deposits at Randalls. Brittle fracture and fluid focusing in BIF units is predicted at sites of low mean stress in and adjacent to BIF units, especially where such units are oriented north–south, close to normal to the regional east–west axis of compression (Oliver et al., 1990; Ridley, 1993), as they are, for example, at Cock Eyed Bob.

Tight hinge zones of isoclinal folds are also favourable sites for mineralization at Randalls (e.g. Santa Claus and Rumble). This is not due to bedding-plane extension, as is the case in many turbidite-hosted deposits, but may reflect similar structural controls to those described above, as the hinge zones are also oriented at a large angle to the regional σ_1. Suitable sites of brittle failure may also exist where the BIF units are cut by north-northeasterly trending faults, particularly if displacement on such faults was

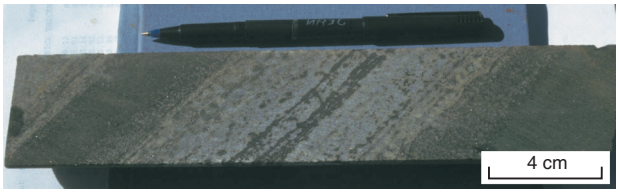

IRO51 15.12.03

Figure 11.4. Calcic amphibole-rich, bimetasomatic band separating quartz–grunerite–magnetite BIF (centre) from chlorite-rich Fe-metashale (dark green, at ends of core) Santa Claus, Randalls mining area

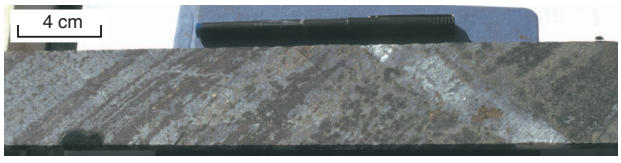

IRO53 15.12.03

Figure 11.5. Quartz–grunerite–pyrrhotite vein cutting across bedding in quartz–grunerite–magnetite BIF, Santa Claus, Randalls mining area. Note sulfide-rich bands (brassy) adjacent to the vein

Table 11.2. Primary sedimentary structures in drillcore from Randalls mining centre

Sedimentary structure	*Description*
Graded bedding in siltstone and Fe-metashale	There are numerous units with graded bedding in the drillcores examined. Bedded units range from metamorphosed quartz–feldspar–biotite sandstone or siltstone through increasing amounts of chlorite to chlorite-dominated Fe-metashale, which is overlain by BIF. In one example, at 152.5 m in RDD-12 (Fig. 11.6), there is a thin, K-rich metashale unit represented by a biotite-rich assemblage on the contact between the chlorite-rich Fe-metashale and BIF. Biotite porphyroblasts increase in abundance within Fe-metashale as the contact with BIF is approached. In the example cited, the younging direction deduced from graded bedding is downhole, opposite to the regional younging direction (northeast limb of anticline). However, isoclinal fold closures noted at 152 m imply rapid reversals of younging directions in this area. In some other Fe-metashales, including graded units, an increasing development of magnetite porphyroblasts in the vicinity of contacts with BIF units was noted. The porphyroblasts are probably concentrated towards the upper contact of the Fe-metashale.
Basal grit beds in Fe-metashale	There are several examples of enigmatic, mineralogically zoned domains observed in the drillcores. These are generally in Fe-metashale and are adjacent to contacts with BIF. Domains vary from equant and slightly rounded (1–3 mm across) to quite irregular in shape and up to about 2 cm across. Examples from RDD-12 are shown in Figures 11.3 and 11.7. These domains are compositionally distinct from the enclosing chloritic metashale and are mineralogically zoned as shown in Figure 11.16. Although all zones are not present in every example, essential components include a grunerite-rich core and a radiating fringe of calcic amphibole prisms. Magnetite(–apatite) tends to be concentrated at the transition between these two zones, and the calcic amphibole prisms may grow within a coarse, recrystallized chloritic matrix, which contrasts with the fine-grained, felted chlorite of the Fe-metashale. Rarely, there is some quartz in the grunerite-rich core. These domains are interpreted as fragments of quartz or quartz–magnetite BIF that have been incorporated into the basal part of the overlying Fe-metashale unit. Interpretation of these domains in GSWA 132924 as clasts in basal grit beds is consistent with the presence of zircon concentrated into thin layers that are draped over the domains, and can be interpreted as heavy-mineral beds (Fig. 11.3a). Interpretation of the domains in GSWA 132924 as clasts in basal grit beds implies uphole younging, consistent with the sample's location on the northeast limb of a regional anticline. Regional metamorphism of the basal grit beds may explain the mineralogically zoned nature of the domains interpreted as miniature reaction skarns (Einaudi and Burt, 1982). Coexisting quartz and Fe-chlorite became thermally unstable during regional metamorphism, initiating a complex set of metamorphic reactions that stabilized the a_{SiO_2} gradient between quartz in the BIF and chlorite in the Fe-metashale (note that SiO_2 decreases regularly through the sequence quartz–grunerite– calcic amphibole –chlorite). Magnetite remained stable but was mobile on a local scale and may have been selectively replaced by pyrrhotite during the auriferous hydrothermal event. The thin contact zone of calcic amphibole prisms in Fe-metashale, oriented more or less normal to the contact with quartz–grunerite–pyrrhotite BIF in GSWA 132926 (Figs 11.3b,c), is attributed to a similar high-temperature reaction during regional metamorphism.

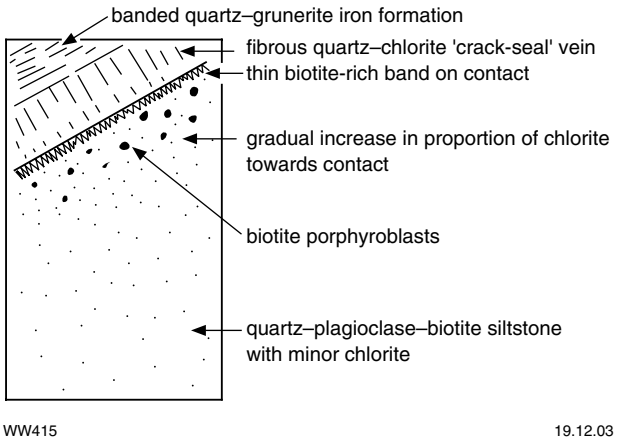

Figure 11.6. Sketch showing a contact between quartz–grunerite–magnetite BIF and graded meta-siltstone to chlorite-rich Fe-metashale unit, Santa Claus, Randalls mining area

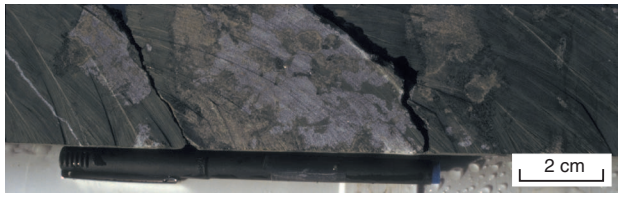

Figure 11.7. Irregularly-shaped domains (clasts) of BIF in basal section of Fe-metashale, Santa Claus, Randalls mining area. Note radiating selvage of calcic amphibole and grunerite that surrounds the iron-formation clasts and separates them from the chlorite-rich Fe-metashale

sufficient to isolate blocks of BIF units within less-competent metashale. North-northeasterly trending faults appear to have been important at Santa Claus and may also have played a role at Maxwells, where the northwest orientation of the fold limb would not be expected to promote brittle fracture (Ridley, 1993).

There is potential for further discoveries in the Randalls area. Other Archaean epigenetic gold deposits in amphibolite-facies, magnetite-rich units (BIF) include the Lupin deposit, in Canada, which is attributed a pre-mining resource of more than 100 t Au (Bullis et al., 1994).

Deposits in the Randalls area

Santa Claus

Other names: Santa Claus G.M. Co. Ltd, New Santa Claus G.M. Co. Ltd, Transcontinental leases, North Santa Claus. The recent openpit mine incorporates the Santa Claus, Craze, and Dunlevy deposits.

Coordinates: 31°02'44"S, 122°12'48"E

Production: Historic production amounts to 27 584.3 t of ore for 269.68 kg Au (9.8 g/t) between 1903 and 1934. Openpit mining commenced in 1993 and, to the end of December 1995 has produced the following amounts:

- Santa Claus – Dunlevy – Craze pit — 439 624 t for 1604.63 kg Au (3.65 g/t).
- Santa Claus North pit — 92 601 t for 226.87 kg Au (2.45 g/t).
- Anomaly C — 48 081 t for 103.37 kg Au (2.15 g/t).

Demonstrated reserves at the end of June 1996 were 197 000 t at 4.3 g/t Au (841 kg Au), contained within Santa Deeps and Santa Claus North – Anomaly C. A further demonstrated resource of 81 000 t at 3.0 g/t Au (245 kg Au) is present at Browns and Browns North (see Figs 11.1 and 11.11 for locations of orebodies).

Host rock: Magnetite-rich unit (mainly amphibole dominated) interbedded with Fe-metashale and fine- to medium-grained clastic units (metasiltstone; Figs 11.2 and 11.4).

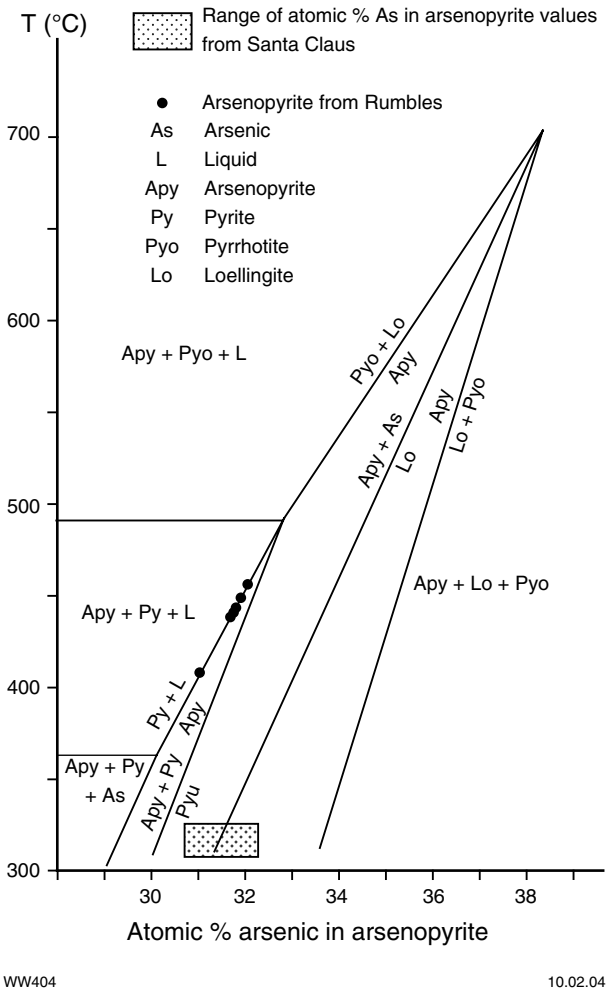

Figure 11.8. Arsenopyrite compositions, Santa Claus and Rumbles, plotted on a temperature versus atomic% As in arsenopyrite diagram (after Kretschmar and Scott, 1976)

Table 11.3. Representative SEM analyses of arsenopyrite and pyrite, Randalls mining centre

	Santa Claus									*Rumbles*										
	GSWA 132926A									*GSWA 132931C*								*GSWA 132933B*		
	banded quartz–pyrrhotite BIF									*quartz–carbonate–chlorite–pyrite lode*								*quartz–chlorite–sulfide lode*		
	disseminated, idioblastic arsenopyrite									*disseminated, idioblastic arsenopyrite*				*banded pyrite*		*pitted pyrite with pale-green tint*		*disseminated, idioblastic arsenopyrite*		
	grain 1			*grain 2*			*grain 3*													
	core	*internal*	*margin*	*core*	*internal*	*margin*	*core*	*internal*	*margin*											
	AY1	*AY4*	*AY3*	*AY10*	*AY9*	*AY8*	*AY5*	*AY6*	*AY7*	*AY15*	*AY16*	*AY17*	*AY19*	*PY1*	*PY2*	*PY3*	*PY4*	*AY21*	*AY23*	*AY24*
Fe	34.03	34.21	34.58	34.69	34.89	34.55	34.65	35.14	35.50	35.64	35.61	35.61	35.81	47.35	47.35	46.76	46.68	35.10	35.08	35.69
Co	–	–	–	–	–	–	–	–	–	–	0.23	–	–	–	–	–	0.16	0.17	0.14	–
Sb	–	–	–	–	–	–	–	–	–	0.21	–	–	0.25	–	–	–	–	0.19	–	–
As	42.87	43.53	41.56	42.94	43.31	43.05	43.23	41.98	44.53	44.47	44.28	44.11	43.68	–	–	–	–	44.26	44.49	44.64
S	18.79	19.22	20.06	19.26	19.52	19.52	19.05	20.14	19.59	20.01	20.00	19.70	20.71	52.65	52.46	52.53	52.41	19.88	20.01	19.77
Total	**95.69**	**97.10**	**96.35**	**96.88**	**97.72**	**97.12**	**96.94**	**97.26**	**99.62**	**100.32**	**100.12**	**99.42**	**100.44**	**100.00**	**99.82**	**99.29**	**99.25**	**99.61**	**99.72**	**100.10**
At.% Fe	34.5	34.1	34.4	34.6	34.5	34.3	34.6	34.6	34.4	34.36	34.35	34.64	34.25	34.05	34.13	33.82	33.80	34.09	33.99	34.52
At.% As	32.4	32.4	30.8	31.9	31.9	31.9	32.2	30.8	32.1	31.95	31.84	31.98	31.14	–	–	–	–	32.04	32.12	32.18
At.% S	33.2	33.4	34.74	33.5	33.6	33.8	19.0	34.6	33.5	33.60	33.60	33.37	34.51	65.95	65.87	66.18	66.09	33.63	33.76	33.30
Fe/S	–	–	–	–	–	–	–	–	–	–	–	–	–	–0.516	0.518	0.511	0.511	–	–	–

NOTE: although totals for arsenopyrite from Santa Claus are low, some repeat analyses which totalled 100 (±1%) give atomic% As which deviated <0.3 atomic% from the values shown

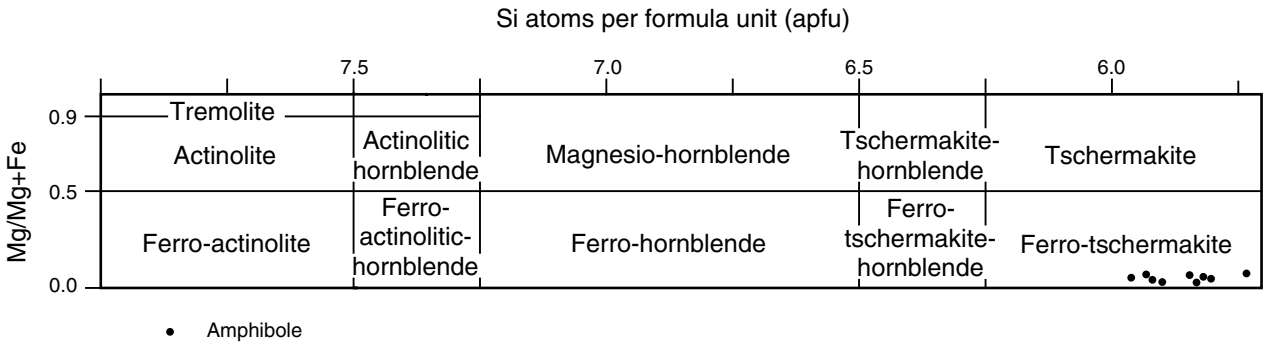

Figure 11.9. Calcic amphibole compositions, Santa Claus, Randalls mining area (see Table 11.5)

Structure: The deposits are located on opposing fold limbs near the hinge zone of a north-plunging, overturned isoclinal anticline (Fig. 11.1). Both limbs of the fold dip steeply to the northeast. Mineralization is associated with sheeted quartz veins (Figs 11.10 and 11.11) that dip 25–40°SW (Figs 11.12 and 11.13). Although veining is concentrated in BIF units, individual veins extend into the adjacent metasiltstone (Newton, 2000). There is also a second, less-abundant set of bedding-parallel veins. The deformation style is essentially brittle. There is little foliation development associated with the mineralized veins, and although some bedding-parallel brittle–ductile faults are shown in Figure 11.12, lithological contacts are mostly unstrained and primary sedimentary structures are widely preserved (Table 11.2). Ore shoots plunge shallowly to the south, consistent with the intersection between veins and bedding (Figs 11.12 and 11.13).

Table 11.4. Representative SEM analyses of pyroxene, Randalls mining centre

	Santa Claus, GSWA 132923 amphibole-rich BIF in contact with chlorite-rich rock after shale	
	relict pyroxene in calcic amphibole prisms chlorite-rich rock and oriented normal to contact	
	PX2	*PX4*
SiO_2	48.52	48.51
Al_2O_3	0.50	0.36
Cr_2O_3		
FeO	41.90	42.18
MnO	0.21	0.40
MgO	4.24	4.43
CaO	0.27	0.18
Na_2O		0.47
Total	**95.98**	**96.54**
Fs	84.1	83.8
En	15.2	15.7
Wo	0.7	0.5

NOTE: low totals probably reflect incipient alteration of pyroxene

Steep, north-northwesterly trending and bedding-parallel brittle–ductile reverse faults have been identified in the southern part of the Santa Claus pit. Locally, subhorizontal veins splay off these reverse faults, and the veins and faults were probably at least partly contemporaneous. Geometric relationships among these faults and their mineralized veins are shown in Figure 11.14. Steep, north-northeasterly to northeasterly trending oblique-normal faults with subhorizontal slickensides are present throughout the orebody and offset lithological layering, commonly with dextral movement. For example, dextral displacement on a prominent set of these faults near the northern end of the Santa Claus deposit offsets a magnetite-rich unit by about 80 m. The offset unit hosts mineralization at Santa Claus North. These faults may have played a role in the development of the vein system by isolating rigid bodies of BIF units within more-ductile, metamorphosed clastic sedimentary rocks. There is a local increase in gold grades in vein stockwork systems developed adjacent to these faults (Newton, P. G. N., 1995, written comm.).

Alteration: Mineralized intervals in drillhole RDD-12 (Fig. 11.2) are associated with coarse, disseminated to banded pyrrhotite and idioblastic arsenopyrite

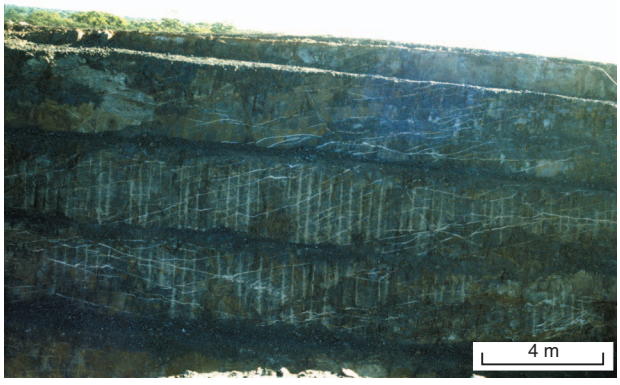

Figure 11.10. Brittle quartz-vein array, western wall, Santa Claus openpit, Randall mining area

Table 11.5. Representative SEM analyses of calcic amphiboles, Randalls mining centre

	Santa Claus					
	GSWA 132923 amphibole-rich BIF in contact with chlorite-rich rock after shale				*GSWA 132926A banded quartz–pyrrhotite BIF*	
	amphibole-rich BIF		*amphiboles on contact with Fe-metashale*			
	AM9	*AM10*	*AM5*	*AM6*	*AM1*	*AM2*
SiO_2	39.08	39.29	39.23	38.96	38.06	39.36
TiO_2	–	0.14	–	0.19	–	–
Al_2O_3	17.18	16.67	16.51	16.98	18.05	18.63
FeO	26.47	27.38	27.47	27.27	26.31	26.55
MnO	–	–	–	–	0.15	–
MgO	1.53	1.66	1.50	1.53	1.31	1.22
CaO	11.46	11.46	11.25	10.92	11.33	11.28
Na_2O	1.05	1.02	1.03	1.39	0.87	0.89
K_2O	0.51	0.57	0.49	0.52	0.51	0.43
Total	**97.29**	**98.18**	**97.50**	**97.76**	**96.59**	**98.38**
Fe/Fe+Mg	90.6	90.3	91.1	90.9	91.8	92.4

Table 11.6. Representative SEM analyses of carbonates, Randalls mining centre

	Santa Claus		*Rumbles*					
	GSWA 132926A banded quartz–pyrrhotite BIF		*GSWA 132931C quartz–carbonate–chlorite–pyrite lode*		*GSWA 132933B quartz–chlorite–sulfide lode*		*GSWA 132936 quartz–magnetite BIF*	
	disseminated, fine-grained carbonate		*coarse carbonate with pyrite*		*carbonate intergrown with biotite and pyrite*		*coarse, disseminated carbonate*	
	CB2	*CB3*	*CB6*	*CB8*	*CB10*	*CB12*	*CB13*	*CB16*
FeO	2.09	2.37	59.56	60.41	59.65	58.21	3.07	3.12
MnO	–	–	0.56	0.45	0.25	0.47	0.22	0.19
MgO	–	–	–	–	–	–	–	–
CaO	55.11	53.90	–	–	–	0.62	51.25	52.96
Total	**57.46**	**56.58**	**60.12**	**60.87**	**59.90**	**59.30**	**55.16**	**56.75**
$FeCO_3$	2.9	3.3	99.1	99.2	99.6	97.9	4.4	4.4
$MnCO_3$	–	–	0.9	0.8	0.4	0.8	0.3	0.3
$MgCO_3$	–	–	–	–	–	–	–	–
$CaCO_3$	97.1	96.7	–	–	–	1.3	95.2	95.3
Nomenclature	Calcite	Calcite	Siderite	Siderite	Siderite	Siderite	Calcite	Calcite

Table 11.7. Representative SEM analyses of biotite, Randalls mining centre

	Santa Claus							*Rumbles*						
	GSWA 132923					*GSWA 132926A*		*GSWA 132931C*			*GSWA 132933B*			
	amphibole-rich BIF in contact with Fe-shale					*banded quartz–pyrrhotite BIF*		*quartz–carbonate–chlorite–pyrite lode*			*quartz–chlorite–sulfide lode*			
	amphibole-rich BIF		*biotite porphyroblasts in Fe-metashale*			*?metasomatic biotite near arsenopyrite*		*with recrystallized felted chlorite*	*coarse biotite with arsenopyrite*		*medium-grained biotite with carbonate and pyrite*		*coarse biotite with arsenopyrite*	
	BI11	*BI12*	*BI6*	*BI7*	*BI8*	*BI2*	*BI3*	*BI14*	*BI16*	*BI19*	*BI20*	*BI21*	*BI22*	*BI24*
SiO_2	31.86	32.23	30.35	32.37	32.82	31.88	31.92	33.22	32.75	32.29	32.33	32.57	32.04	32.16
TiO_2	2.11	2.36	1.53	2.29	1.93	2.15	2.48	2.04	1.81	1.74	1.67	1.56	2.13	2.20
Al_2O_3	14.79	14.98	16.12	15.63	15.64	16.48	16.04	15.09	15.39	15.64	15.31	15.53	15.59	15.87
FeO	33.70	32.72	35.11	32.88	32.06	34.59	34.56	29.08	29.72	31.43	31.50	30.87	31.22	31.86
MgO	3.03	3.10	3.53	3.02	2.89	1.21	1.43	6.49	4.82	4.63	5.34	4.68	4.59	4.81
Na_2O	–	–	0.25	–	–	–	–	–	0.27	0.24	0.35	–	–	–
K_2O	8.70	9.20	5.97	9.30	9.41	8.81	8.73	8.41	8.95	8.34	7.81	9.26	8.80	8.58
Total	**94.19**	**94.59**	**92.87**	**95.49**	**94.76**	**95.12**	**95.16**	**94.33**	**93.71**	**94.31**	**94.32**	**94.47**	**94.38**	**95.47**
Fe/Fe+Mg	86.2	85.5	84.8	85.9	86.2	94.1	93.1	71.5	77.6	79.2	76.8	78.7	79.2	78.8

Table 11.8. Representative SEM analyses of chlorite, Randalls mining centre

	Santa Claus					*Rumbles*					
	GSWA 132923					*GSWA 132931C*				*GSWA 132936*	
	amphibole-rich BIF in contact with Fe-metashale					*quartz–carbonate–chlorite–pyrite lode*				*quartz–magnetite BIF*	
	felted chlorite in Fe-metashale		*interstitial to amphiboles on contact*		*chlorite in ampibole-rich BIF*	*felted chlorite*		*recrystallized chlorite with metasomatic biotite*		*disseminated chlorite*	
	CH5	*CH7*	*CH10*	*CH11*	*CH13*	*CH16*	*CH17*	*CH20*	*CH21*	*CH22*	*CH24*
SiO_2	22.24	22.51	21.90	22.18	22.45	23.18	23.34	23.44	24.04	21.95	22.47
Al_2O_3	20.96	20.34	20.11	20.23	19.82	20.09	19.78	19.73	18.99	19.38	20.11
FeO	40.98	40.93	41.12	40.97	41.67	36.47	35.89	35.67	36.17	39.31	39.68
MgO	4.22	4.41	4.05	4.27	4.18	7.49	8.23	8.18	8.22	4.58	4.27
Na_2O	0.35	–	–	–	–	–	0.32	0.29	–	–	–
Total	**88.75**	**88.20**	**87.19**	**87.65**	**88.13**	**87.23**	**87.74**	**87.30**	**87.42**	**85.21**	**86.87**
Fe/Fe+Mg	84.5	83.9	85.1	84.3	84.8	73.2	71.0	71.0	71.2	82.8	83.9

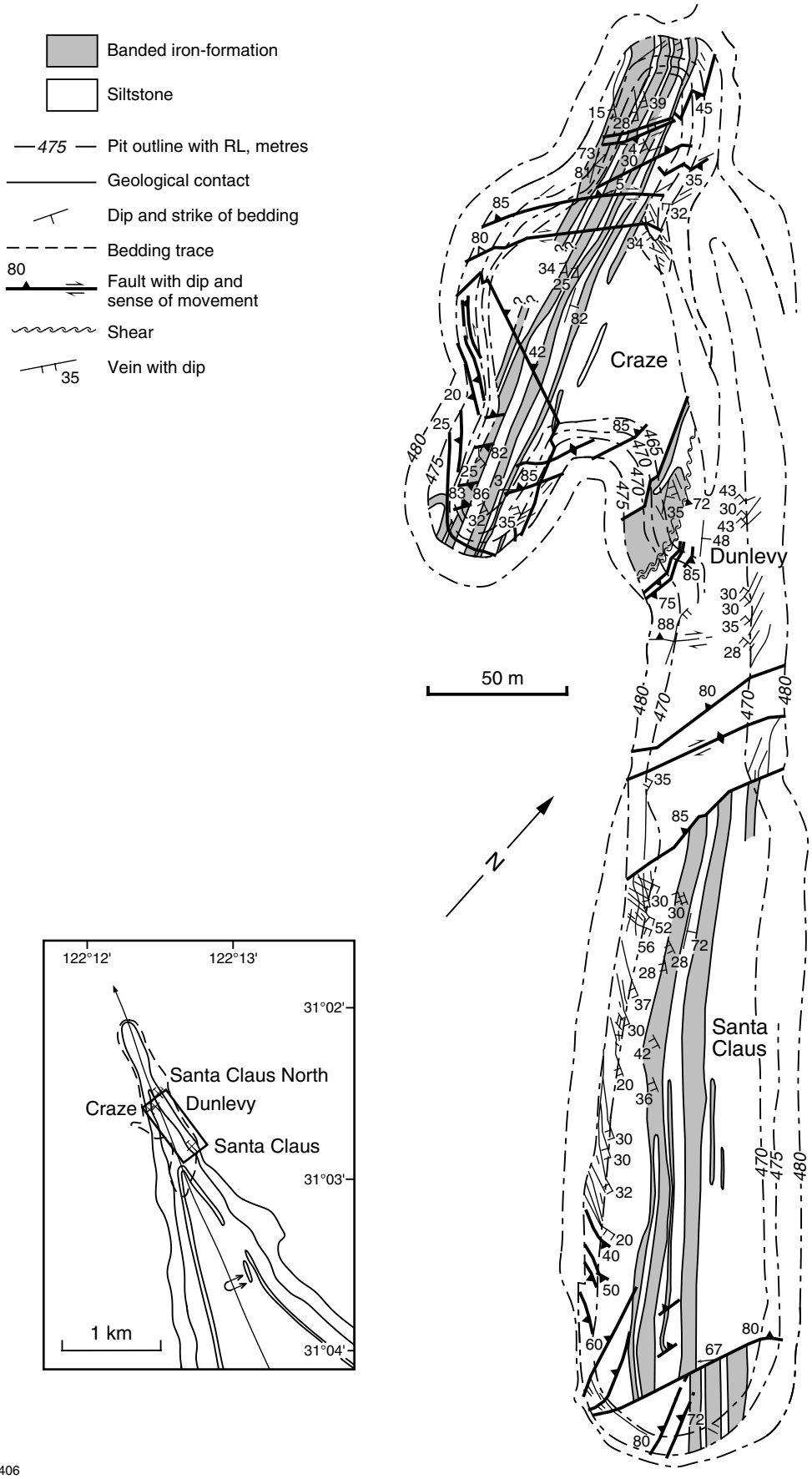

WW406 12.02.04

Figure 11.11. Geological plan, Santa Claus openpit (after Newton et al., 1998)

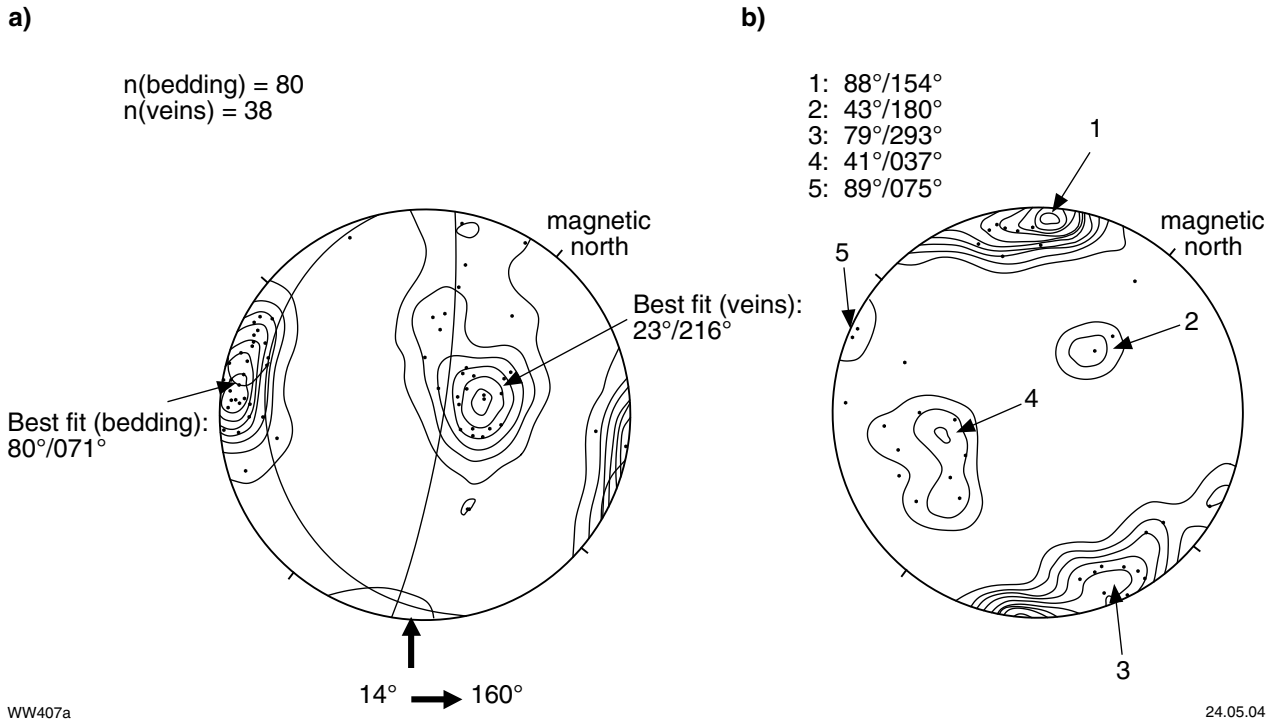

Figure 11.12 Structure of the Craze orebody: a) contoured equal-area stereoplot of Craze bedding planes and flat-dipping extensional veins; and b) contoured equal-area stereoplot of Craze faults and fractures. Data from Newton (2000)

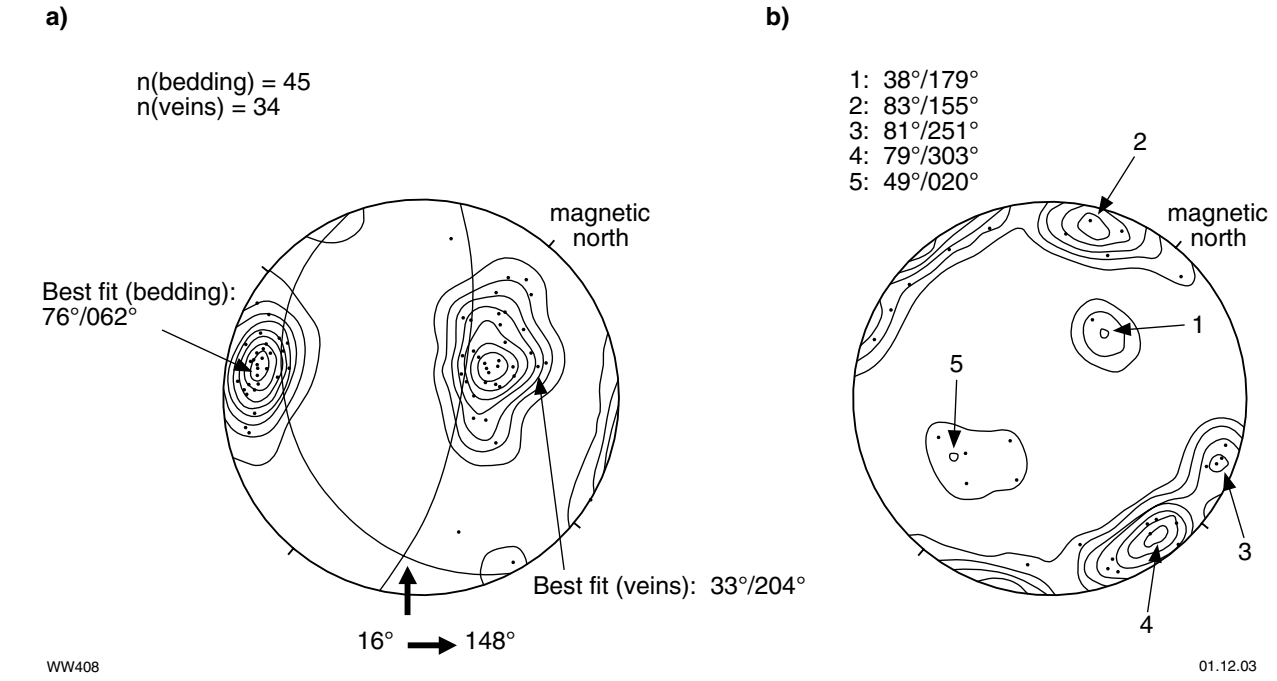

Figure 11.13. Structure of the Santa Claus orebody: a) contoured equal-area stereoplot of bedding planes and flat-dipping extensional veins (note shallow southerly plunge of the intersection point between veins and bedding); and b) contoured equal-area stereoplot of faults and fractures. Data from Newton (2000)

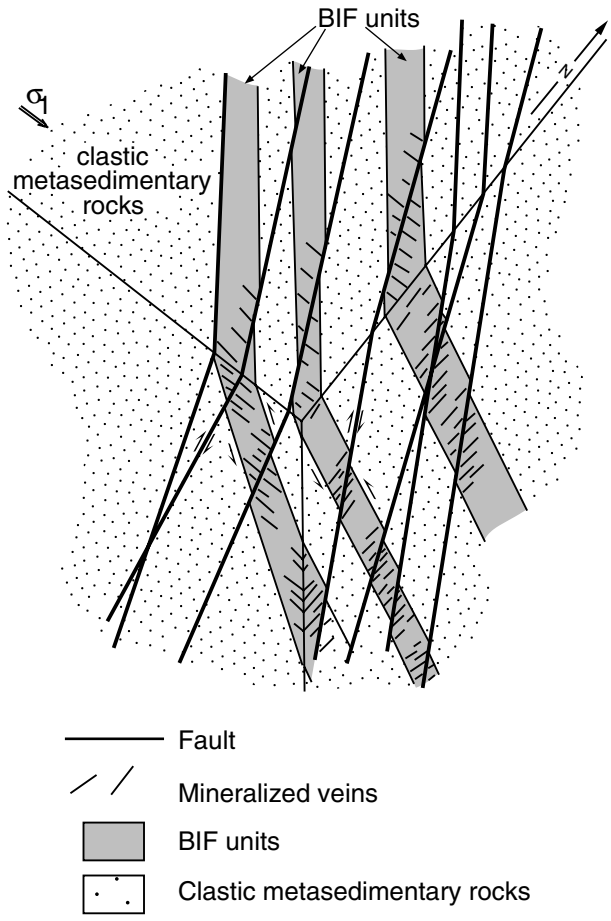

Figure 11.14. Block diagram showing relationships between bedding, D_3 reverse faults, and mineralized veins, Santa Claus orebody (schematic only)

(Fig. 11.15), which is in turn related to quartz(–siderite–chlorite) veins. Magnetite layers in the BIF units grade to pyrrhotite along strike, and relicts of magnetite in pyrrhotite clearly indicate a replacement relationship. These sulfides are commonly associated with variable amounts of metasomatic carbonate (calcite — see Table 11.4), biotite, and minor chalcopyrite. Biotite forms randomly oriented, subhedral grains, consistent with the essentially brittle nature of the quartz veining. Arsenopyrite analyses show that As varies between 30.8 and 32.4 atomic wt% (Table 11.8), indicative of temperatures of 390–460°C (Kretschmar and Scott, 1976) and suggesting disequilibrium between arsenopyrite and pyrrhotite (Fig. 11.8).

Whole-rock geochemical data are presented in Appendix 4. The assumption that mineralized samples were originally the same composition, as unaltered samples could not be made with confidence because of the small-scale chemical heterogeneity related to layering in unaltered BIF units. Nevertheless, qualitative assessment of the data clearly indicates addition of S and As to the quartz–magnetite–grunerite units.

References: Newton et al. (1996), Newton et al. (1998), Newton (2000).

Flora Dora

Other names: New Chum, Father Christmas

Coordinates: 31°03'03"S, 122°12'46"E

Production: 1471.7 t of ore for 19.73 kg Au (13.4 g/t Au) between 1905 and 1942.

Host rock: Banded iron-formation.

Structure: Observations of historic workings are obscured by recent mine development.

Alteration: Observations of historic workings are obscured by recent mine development.

Rumble

Other names: Mighty Rumble, Mighty Rumble Extended, Rumbles

Coordinates: 31°04'01"S, 122°11'17"E

Production: Historic production amounts to 460.6 t of ore for 3.96 kg Au (8.58 g/t Au) between 1902 and 1909.

Openpit mining has commenced and to the end of December 1995 had produced 68 119 t of ore for 155.31 kg Au (2.28 g/t Au).

The current demonstrated resource for this deposit (reported at the end of March 1996) is 149 000 t at 4.0 g/t Au (590 kg Au).

Host rock: Banded iron-formation (mainly sulfide rich) interbedded with Fe-rich metashale and metasiltstone (Fig. 11.16).

Structure: Rumble is located in the hinge zone of a north-plunging, overturned anticline (Fig. 11.1). As with Santa Claus, mineralization is associated with brittle deformation of BIF units, producing sheeted quartz veins that dip shallowly to moderately to the southwest.

Alteration: The drill log shown in Figure 11.16 shows that zones of gold mineralization correlate with quartz veining and sulfide-rich, magnetite-rich units.

Sulfide-rich, magnetite-rich units consist chiefly of alternating bands of quartz and pyrite (Table 11.1). Pyrite contains relict inclusions of magnetite and is variably

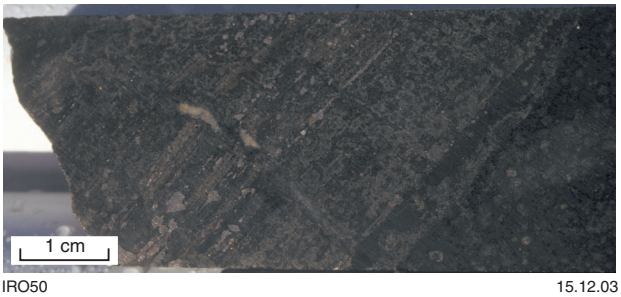

Figure 11.15. Coarse, idioblastic arsenopyrite and banded pyrrhotite in amphibole-rich BIF, Santa Claus, Randalls mining area

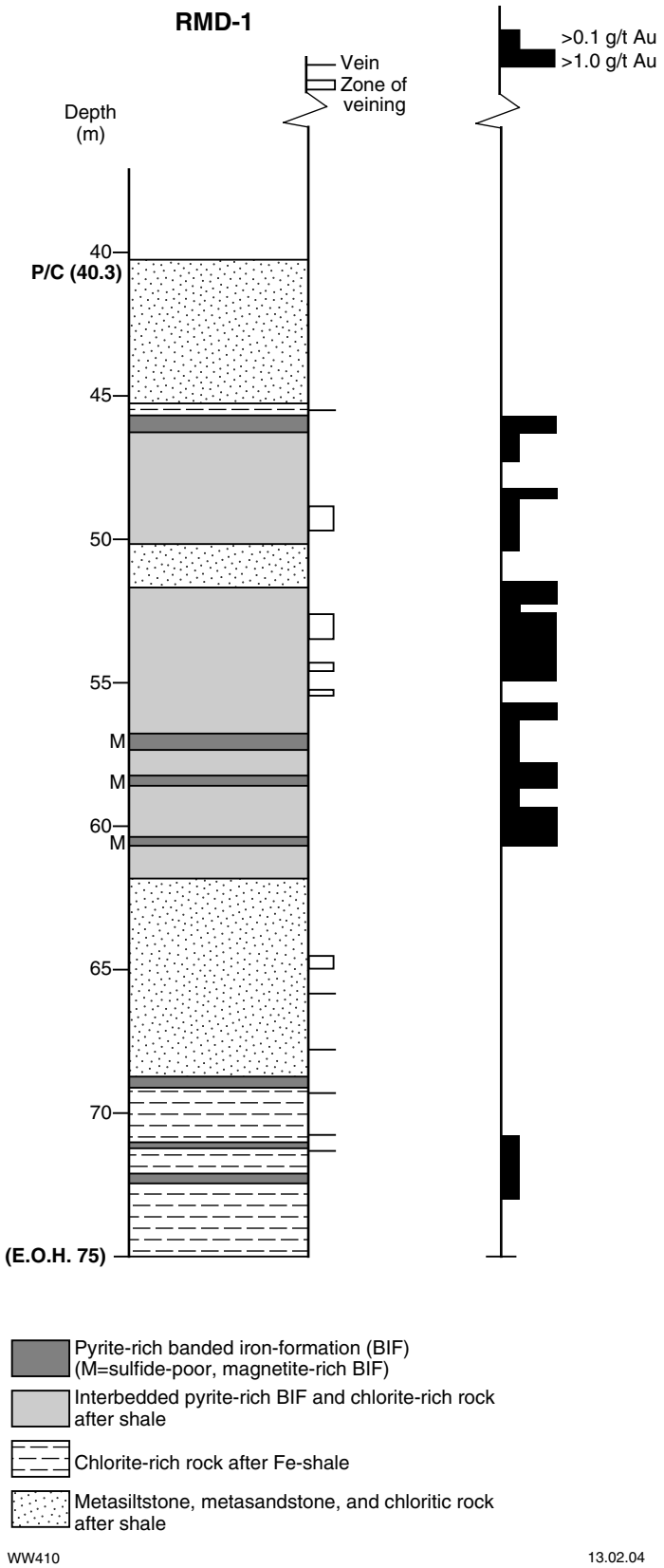

Figure 11.16. Summary log, diamond drillhole RMD-1, Rumbles, Randalls mining area

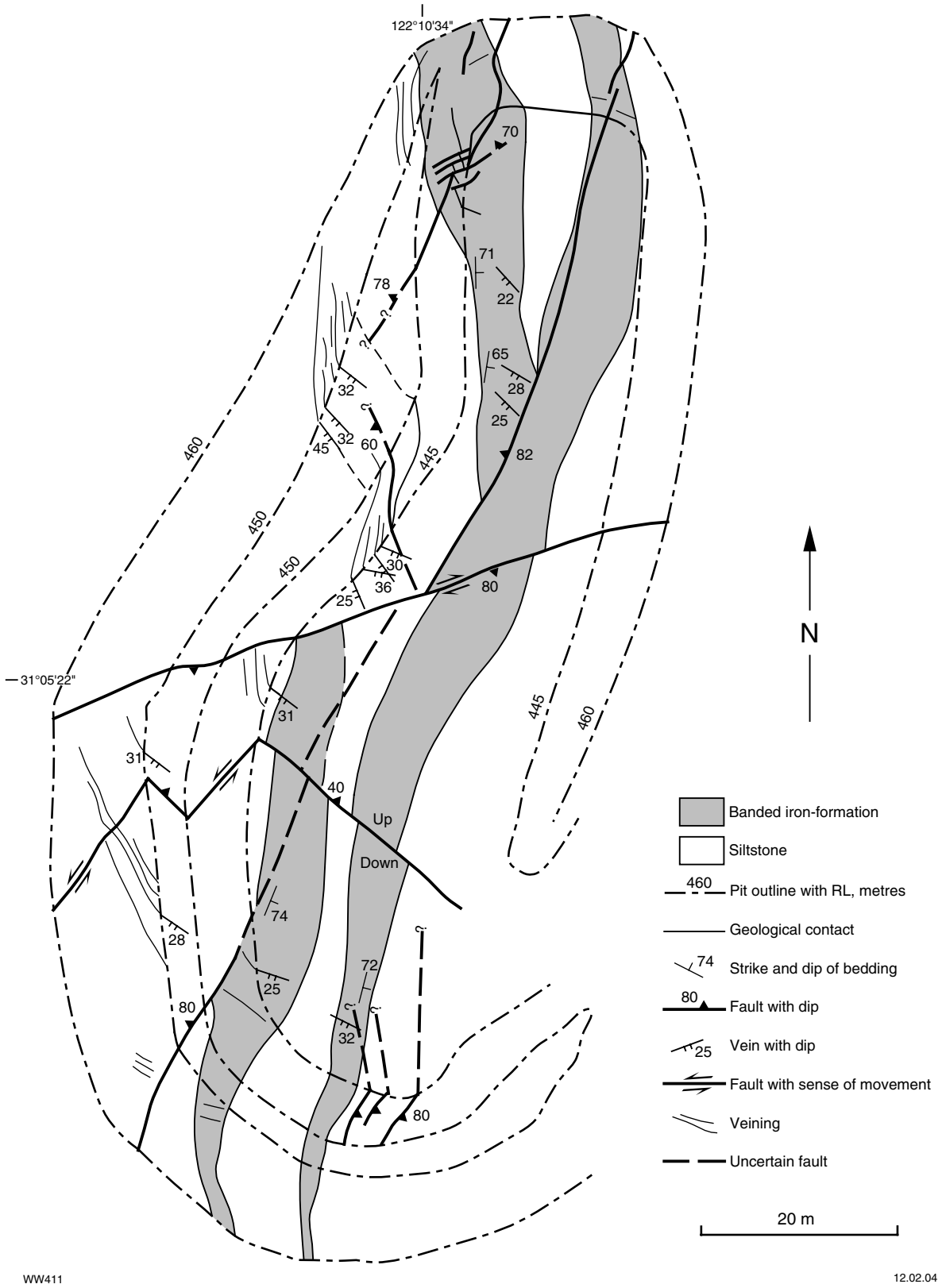

Figure 11.17. Geological plan of the Cock Eyed Bob openpit, Randalls mining area (after Newton et al., 1998)

altered to marcasite. It is commonly associated with idioblastic arsenopyrite and minor amounts of chalcopyrite. Associated metasomatic minerals are biotite, siderite, and possibly chlorite.

Representative mineral analyses are presented in Tables 11.3 – 11.8 and calcic amphibole compositions are plotted in Figure 11.9. Whole-rock geochemical data are presented in Appendix 4.

References: Newton et al. (1996), Newton et al. (1998), Newton (2000).

Cock Eyed Bob

Other names: Comstock W.A., Surprise

Coordinates: 31°05'22"S, 122°10'34"E

Production: Historic production from Comstock W.A. and Surprise amounts to 806.3 t of ore for 23.95 kg Au (29.7 g/t Au) between 1904 and 1916. These mines are both in the Cock Eyed Bob – Knob Hill area (Fig. 11.1), but there was no historic production from the site of the current Cock Eyed Bob resource.

Recent openpit mining at Cock Eyed Bob produced 251 341 t of ore for 785.29 kg Au (3.1 g/t Au). Demonstrated reserves at end of June 1996 were 96 000 t at 6.75 g/t Au (648 kg Au), mainly in the Cock Eyed Bob Deeps orebody.

Host rock: Banded iron-formation.

Structure: The Cock Eyed Bob openpit mine (Fig. 11.17) lies on the eastern limb of an overturned, north-plunging, isoclinal anticline, about 1 km east of the Bare Hill Shear Zone (Fig. 11.1). Mineralization is associated with sheeted quartz veins that are mainly located in BIF units but extend into the adjacent metasiltstone. The veins, which are essentially brittle features, dip 25–40°SW (Fig. 11.18). Steep, north-northwesterly to north-northeasterly trending faults apparently produce small normal displacements of lithological layering. They are probably post-dated by steep, northeast-trending dextral faults that in turn may be post-dated by a flatter lying, northwest-trending reverse fault (Fig. 11.17). Timing relations between vein formation and the northeast-trending dextral faults are difficult to establish, but the vertical extension implied by gently dipping quartz veins is consistent with formation mainly during subvertical movements on north-trending contacts between magnetite-rich units and metasiltstone (Fig. 11.1). Later reverse faults appear to offset veins.

Alteration: There has been no investigation of alteration in this deposit, but it is probably similar to that in other deposits in the Randalls area.

References: Newton et al. (1996), Newton et al. (1998), Newton (2000).

Maxwells

Other names: Maxwell

Coordinates: 31°04'51"S, 122°11'56"E

Production: Historic production at Maxwell mine amounts to 99.2 t of ore for 0.52 kg Au (5.3 g/t Au) between 1904 and 1905.

Mining has not yet commenced on a demonstrated resource (May 1995) of 2.066 Mt of ore at 3.5 g/t Au (7231 kg Au) at the Maxwells prospect (Fig. 11.1).

Host rock: Banded iron-formation (mainly amphibole dominated) within a sequence of interbedded metasiltstone and Fe-metashale (Fig. 11.19).

Structure: The Maxwells deposit lies on the northwest-trending limb of a north-plunging, overturned anticline (Fig. 11.1). Mineralization is associated with brittle-style sheeted quartz veins that dip 25–40°SW, similar to those described above.

Alteration: Mineralized intervals in drillhole MD-1 (Fig. 11.19) are associated with disseminated and banded pyrrhotite and idioblastic arsenopyrite with variable amounts of biotite and carbonate. Pyrrhotite commonly forms interstitial grains between randomly oriented calcic amphibole prisms. Pyrrhotite is also associated with minor pyrite (minor alteration to marcasite) and trace chalcopyrite. Whole-rock geochemical data are presented in Appendix 4. Qualitative assessment of the data clearly indicates addition of sulfur and arsenic to the sulfide-poor BIF units.

References: Newton et al. (1996), Newton et al. (1998), Newton (2000).

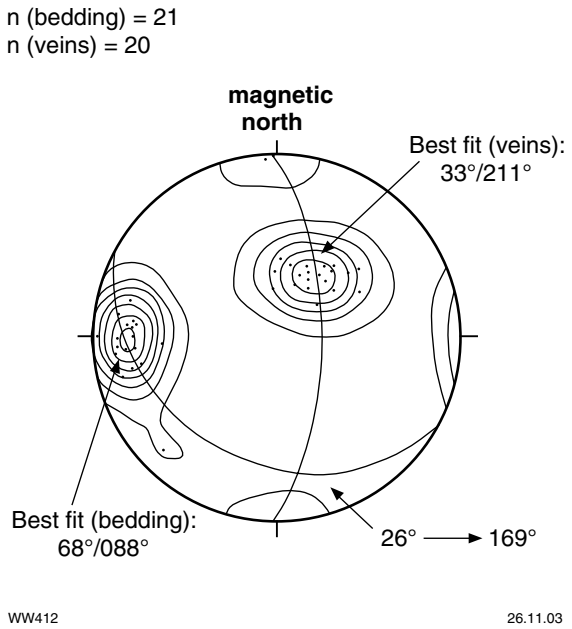

Figure 11.18. Contoured equal-area stereoplot of bedding planes and flat-dipping extensional veins, Cock Eyed Bob, Randalls mining area. Note shallow southerly plunge of the intersection between veins and bedding planes. Data from Newton (2000)

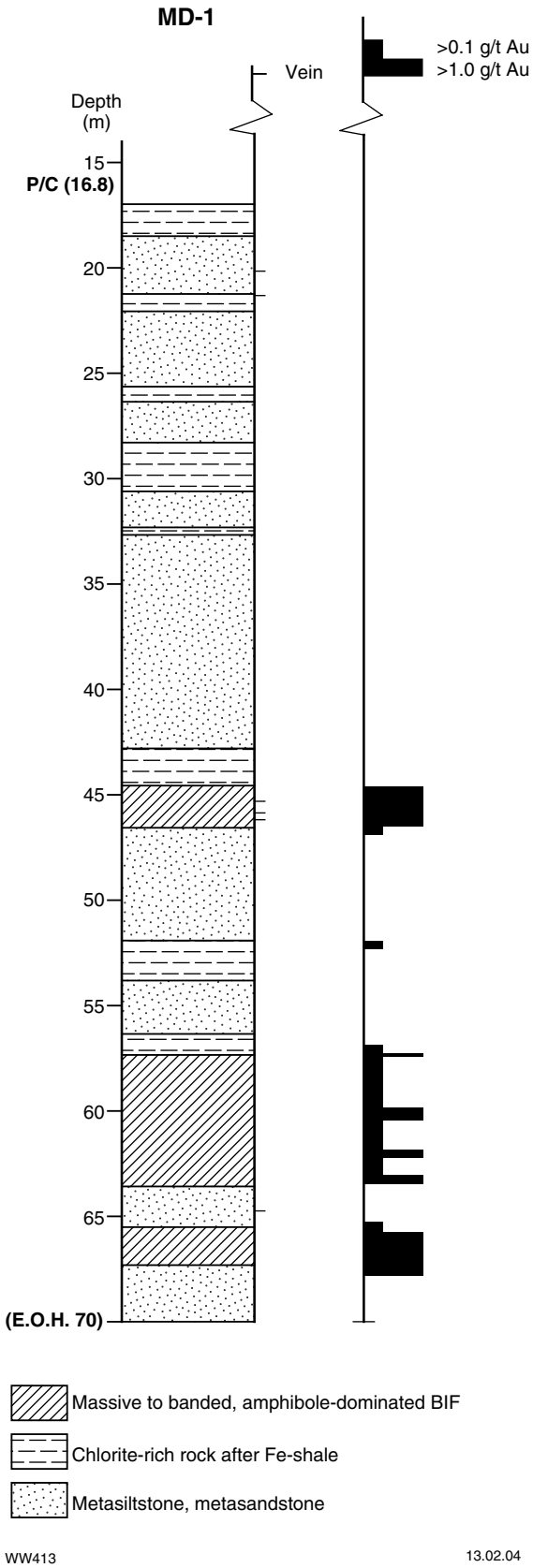

Figure 11.19. Summary log, diamond drillhole MD-1, Maxwells, Randalls mining area

References

AHMAT, A. L., 1986, Metamorphic patterns in the greenstone belts of the Southern Cross Province, WA: Western Australia Geological Survey, Report 19, Professional Papers for 1984, p. 1–21.

BULLIS, H. R., HUREAU, R. A., and PENNER, B. D., 1994, Distribution of gold and sulfides at Lupin, Northwest Territories: Economic Geology, v. 89, p. 1217–1227.

DUNBAR, G. J., and McCALL, G. J. H., 1971, Archaean turbidites and banded ironstones of Mt Belches area (Western Australia): Sedimentary Geology, v. 5, p. 93–133.

EINAUDI, M. T., and BURT, D. M., 1982, Introduction — terminology, classification, and composition of skarn deposits: Economic Geology, v. 77, p. 745–754.

GOLE, M. J., 1981, Archean banded iron-formations, Yilgarn Block, Western Australia: Economic Geology, v. 76, p. 1954–1974.

KRETSCHMAR, U., and SCOTT, S. D., 1976, Phase relations involving arsenopyrite in the system Fe–As–S and their application: Canadian Mineralogist, v. 14, p. 364–386.

NEWTON, P. G. N., 2000, The integration of structural geology and directional variography at three orogenic gold deposits: implications of orebody geometry and mine practice: University of Western Australia, PhD thesis (unpublished).

NEWTON, P., KHOSROWSHAHI, S., and SMITH, B., 1996, The integrated use of directional variography and structural geology at the Randalls BIF-hosted Au deposit, Kalgoorlie, Western Australia: Western Australia School of Mines Symposium, Kalgoorlie, W.A., 1996, Abstracts Volume, p. 64–72.

NEWTON, P. G. N., SMITH, B., BOLGER, C., and HOLMES, R., 1998, Randalls gold deposits, *in* Geology of Australian and Papua New Guinean mineral deposits *edited by* D. A. BERKMAN and D. H. MACKENZIE: Australasian Institute of Mining and Metallurgy, Monograph 22, p. 225–231.

OLIVER, N. H. S., VALENTA, R. K., and WALL, V. J., 1990, The effect of heterogeneous stress and strain on metamorphic fluid flow, Mary Kathleen, Australia, and a model for large-scale fluid circulation: Journal of Metamorphic Geology, v. 8, p. 311–331.

PAINTER, M. G. M., and GROENEWALD, P. B., 2001, Geology of the Mount Belches 1:100 000 sheet: Western Australia Geological Survey, 1:100 000 Geological Series Explanatory Notes, 38p.

RAMSGATE RESOURCES LTD, 1994, Annual report, Jul 1993 to Jun 1994, on Randalls/Karnilbinia copper-zinc/gold exploration: Western Australia Geological Survey, Statutory mineral exploration report, Item 11663 A41751 (unpublished).

RIDLEY, J. R., 1993, The relations between mean rock stress and fluid flow in the crust: with reference to vein- and lode-style gold deposits: Ore Geology Reviews, v. 8, p. 23–27.

ROBINSON, P., SPEAR, F. S., SCHUMACHER, J. C., LAIRD, J., KLEIN, C., EVANS, B. W., and DOOLAN, B. L., 1982, Phase relations of metamorphic amphiboles: natural occurrence and theory, *in* Amphiboles: petrology and experimental phase relations *edited by* D. R. VEBLEN and P. H. RIBBE: Reviews in Mineralogy, v. 9B, p. 1–227.

WITT, W. K., 1990, The geology of the Bardoc 1:100 000 sheet, Western Australia: Western Australia Geological Survey, Record 1990/14, 111p.

WITT, W. K., 1993, Gold mineralization in the Menzies–Kambalda region, Eastern Goldfields, Western Australia: Western Australia Geological Survey, Report 39, 165p.

12. Balagundi–Bulong–Taurus

The Bulong and Balagundi mining areas both lie in a belt of north-trending greenstones in the western part of the Gindalbie Terrane. The greenstones dip moderately to steeply to the west, and young in the same direction. They are located on the western limb of the D_2 Bulong Anticline and are within 11 and 3 km, respectively, of the north-northwesterly striking Kanowna Shear. Ultramafic rocks of the Bulong Complex are interleaved with mafic rocks and metamorphosed felsic volcaniclastic rocks (Ahmat, 1995). A felsic volcanic rock from this association has been dated at 2705 ± 4 Ma (Nelson, 1995). This package of interleaved units was thrust over the younger felsic volcanic complex (2672 ± 12 Ma) in the core of the Bulong Anticline during D_1 (Swager, 1995). The presence of andalusite in weathered, metamorphosed volcaniclastic sedimentary rocks suggests that the metamorphic grade in this area is mid- to upper greenschist facies. The greenstones are dissected by numerous north-trending faults, some of which originated as D_1 structures, although they were almost certainly active during the later (D_3 and D_4) stages of regional deformation, probably as splays off the Kanowna Fault.

The Bulong mining area has produced around 2500 kg of gold, mainly from the Queen Margaret mine, whereas the Balagundi mining area has produced only about 50 kg. A relatively small amount of gold has been produced from a deep lead that drained south from the Queen Margaret deposit at Bulong. Primary deposits in the two mining areas have much in common, and these features are consistent with formation during late-tectonic east–west compression. Mineralization at both localities is in quartz veins and veined brittle–ductile shears that seem to be largely controlled by the contrasting competency of metamorphosed felsic volcaniclastic units and adjacent, more-brittle units. At Bulong, the sheared contacts are between metamorphosed felsic volcaniclastic rocks and intensely carbonated ultramafic rocks, whereas at Balagundi, the contacts are with metabasalt and metadolerite (including metamorphosed granophyric quartz-dolerite). Contact-parallel shears were probably active during D_3 as second- and third-order splays off the Kanowna Shear – Mount Monger Fault system. For example, sinistral movement on a north-northwesterly trending contact, where the strike of the contact changes to northwesterly, may be responsible for the large mineralized quartz vein at Balagundi.

Gold is also produced from quartz-vein systems in less-deformed rocks adjacent to the sheared contacts. At Balagundi, there is an association of mineralization with northeast-striking cross-faults that displace lithological contacts (Fig. 12.1). Mineralization is most intense where closely spaced cross-faults have isolated relatively brittle metabasalt units within more-ductile metasedimentary rocks. There is also a small intrusive (porphyry) body about 1 km west of the Balagundi workings, which may have contributed to local stress inhomogeneity and localized dilation and vein formation.

At Bulong, there are two main subparallel lines of workings. Most gold production was from the western of these two lines, which contains the Queen Margaret mine (2200 kg Au). Mine development is almost continuous for about 1500 m on a north-trending shear zone, but there are further scattered workings, including Storm King, on the same structure for about 4 km to the north. The eastern line of workings appears to be controlled by several shorter, en echelon shear zones, which produced more than 250 kg Au, principally from the Great Oversight and Green Harp groups of mines. The Great Oversight group, to the south, lies on the eastern and western contacts of a thin metamorphosed felsic volcaniclastic unit within carbonated ultramafic rock. The Green Harp workings are also on the contact between carbonated ultramafic rock and felsic schist. Workings are scattered for several kilometres to the north of the Green Harp group.

Alteration of metamorphosed felsic volcaniclastic rocks at Balagundi and Bulong is generally restricted to narrow zones of bleaching adjacent to quartz veins, and a broader, more diffuse halo of disseminated carbonate and pyrite. Biotite is unstable within the bleached zones, which consist predominantly of quartz, plagioclase (albite), and carbonate, with minor chlorite and pyrite. Ultramafic rocks are intensely carbonated, and although the timing of this carbonation is uncertain, it appears to pre-date gold mineralization. The brittle, carbonate-rich rocks are commonly traversed by a network of quartz(–carbonate) veins that have introduced a second generation of carbonate and disseminated pyrite. Mafic rocks at Balagundi are altered to pyritic quartz–albite–carbonate–chlorite assemblages.

There has been no significant recent mining in the area, although there is evidence of a small heap-leaching operation at Balagundi (locality B, Fig. 12.1). A resource (the Jarvis lode) of 179 000 t of ore averaging 3.1 g/t Au (555 kg Au) has been identified near Great Oversight.

The Taurus mining centre has produced about 20 kg of gold, mainly from the Great Ophir deposit. There are numerous other small, historic workings scattered over an area of about 4 km^2, but these appear to have produced very little gold. The mining centre is located about 8 km northeast of Bulong, within the younger felsic volcanic complex, and just below a gently north dipping D_1 fault surface. The Great Ophir mine has extracted gold from a large, massive quartz vein that dips at a moderate angle to the southeast. Some mineralization potential exists in the area because it is likely that high fluid pressures developed where hydrothermal fluids in steep structures ponded against the gently dipping D_1 fault surface. In fact, a resource of 217 kg of gold has been announced at the Central Zone — a quartz-vein complex bounded by northwest-trending faults, about 2 km southwest of Great Ophir.

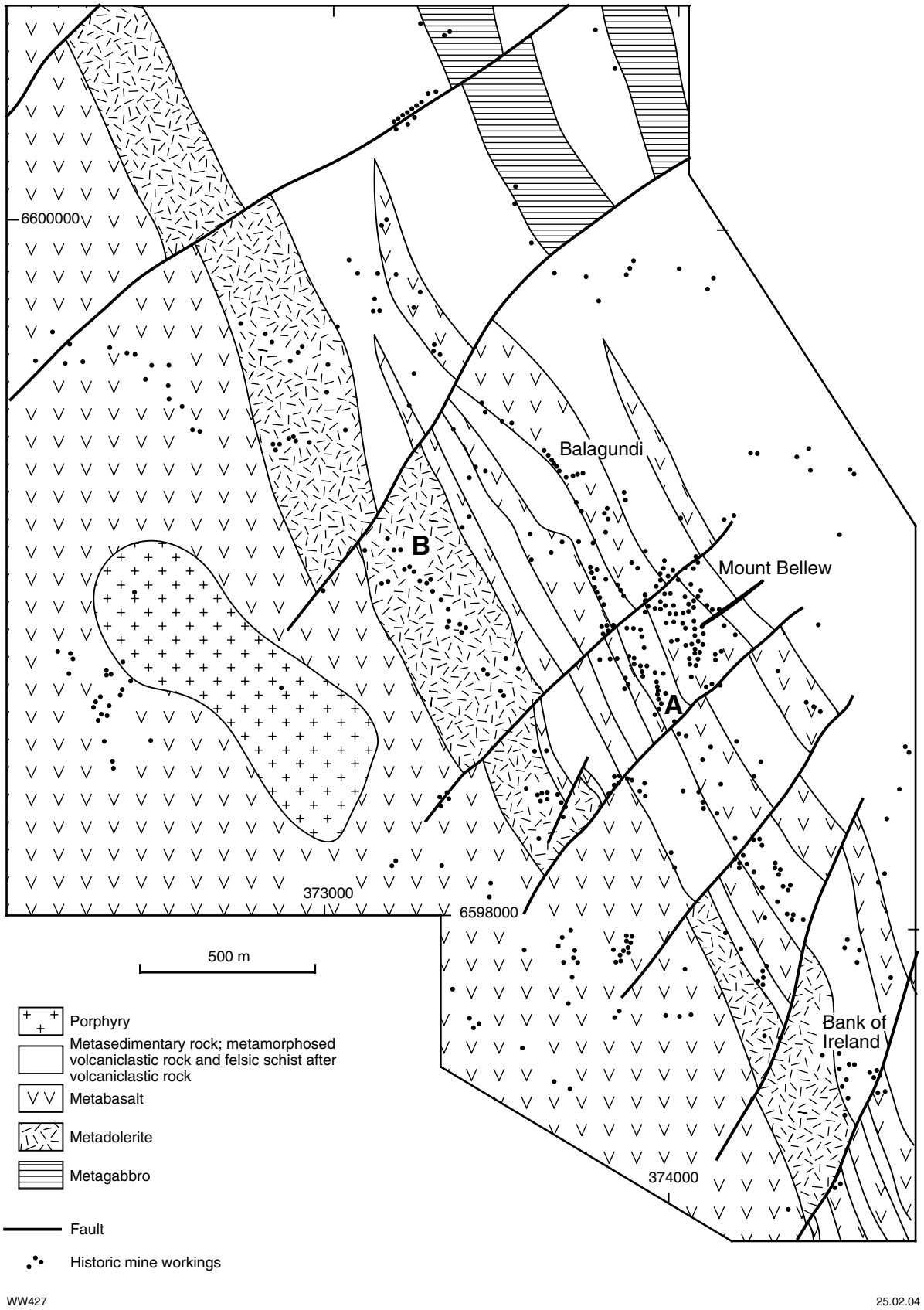

Figure 12.1. Geological map of Balagundi mining area (adapted from Delta Gold Ltd, 1993)

Deposits of the Balagundi–Bulong–Taurus area

Mount Bellew

Other names: Balagundi, Croagh Patrick, Lady Molly

Coordinates: 30°44'03"S, 121°51'54"E

Production: 388.4 t of ore for 42.07 kg Au (108.3 g/t Au) between 1900 and 1973.

Host rock: The main host rock is metabasalt, but there is also some mineralization in felsic volcaniclastic sedimentary rock and schist. Other workings (locality B, Fig. 12.1), about 500 m west of the Mount Bellew workings, are on a unit of metamorphosed dolerite and granophyric quartz-dolerite.

Structure: Shallow to moderately deep pits and shafts extend over about 500 m along strike (Fig. 12.1). Within this zone of mineralization, groups of workings suggest that individual mineralized structures trend north-northwest, north, and east. There are several linear groups of workings on contacts between metabasalt and felsic rocks, but others are within these units. One of the main group of workings is focused on the footwall of a 1–3 m-wide, gossanous quartz vein that strikes north–south and dips 60–70°W (locality A, Fig. 12.1). Massive to vuggy, white, crystalline vein quartz is common on most mine dumps, and the orebodies have been described as containing quartz veins and stockworks (Stroud, 1987). Primary igneous textures and structures are widely preserved in altered, metamorphosed basalt and volcaniclastic sedimentary rocks. The deformation appears to have been mainly brittle, although lithological contacts have probably been zones of brittle–ductile shear. Most of the mineralization is between two northeast-striking cross-faults, and the cross-faults also seem to carry some gold.

Alteration: Surface samples are generally weathered, but widespread carbonation of the metadolerite is evident. Limonite after pyrite is present in much of the vein quartz. Petrographic descriptions (Stroud, 1987) indicate that the mafic rocks have been altered to a quartz–albite–carbonate–chlorite rock with disseminated pyrite. Felsic rocks have been silicified, sericitized, and pyritized.

References: Stroud (1987), Delta Gold Ltd (1993).

Balagundi Consolidated

Other names: Day Dawn, Queen of Balagundi, Sunday Gift, May Queen

Coordinates: 30°43'41"S, 121°40'47"E

Production: 646.2 t of ore for 7.26 kg Au (11.2 g/t Au) between 1901 and 1910.

Host rock: The main host rock is metabasalt, but there is also some mineralization in felsic volcaniclastic sedimentary rock and schist, metadolerite, and metamorphosed granophyric quartz-dolerite.

Structure: Shallow to moderately deep workings lie over about 300 m strike length on a 0.5 – 1.5 m-wide quartz vein that strikes 320° and dips 70–80° NE. The massive to vuggy to laminated vein is on or near the contact between metabasalt and metasedimentary rocks.

Alteration: Alteration has been obscured by weathering, but carbonation of the metadolerite can be recognized and coarse, idioblastic pyrite is common. Gold appears to have been associated with pyritic, laminated quartz in the footwall part of the vein.

Queen Margaret

Other names: Princess Margaret, Furness Abbey, Queen Margaret South, New Queen Margaret South, Queen Margaret South Extended, Melbourne United, Melbourne United North, White Horse

Coordinates: 30°45'02"S, 121°46'32"E

Production: 69 789.1 t of ore for 2168.4 kg Au (31.1 g/t Au) between 1897 and 1935.

Host rock: Mine-dump samples suggest that gold mineralization is mainly within metamorphosed fine-grained felsic volcaniclastic sedimentary rocks. However, metamorphosed black shale and ultramafic and mafic rocks, including metadolerite, are also present on mine dumps and may also be mineralized. Some samples of probable lamprophyre were observed on mine dumps.

Structure: Moderately deep shafts and shallower pits exist over about 1500 m, on a veined, brittle–ductile shear zone that strikes 010° and dips 50–80°W, more or less parallel to the major lithological trends in this area. The historic workings lie on or close to a contact between ultramafic rock (to the west) and felsic schist after volcaniclastic rock (to the east). This contact is locally associated with a thin unit of metamorphosed black shale. This contact zone probably includes thin, interleaved units of ultramafic and felsic rock. For example, local observations (towards the southern end of the workings) indicate a mineralized shear zone that lies on the contact between intensely carbonated ultramafic rocks (on the footwall) and metamorphosed felsic volcaniclastic sedimentary rocks (on the hanging-wall). The orientation of sheeted quartz veins (070°) in the footwall unit at this location suggests a component of dextral movement on the shear zone. Quartz veins within the shear zone are mostly subparallel to vein margins but are variably deformed, and there are also some late, branching veins that cut across the shear fabric. Minor folds defined by relatively early veins, observed at the northern end of the workings, plunge about 45°N.

Quartz-vein samples on mine dumps commonly have fine-grained, blue-grey margins and vuggy interiors.

Alteration: Altered ultramafic rocks record carbonation, producing talc–chlorite–carbonate(–biotite) schist with minor pyrite. Intensely carbonated ultramafic rocks consist mainly of carbonate, but are commonly cut by a complex array of quartz–carbonate(–chlorite) veins and hydraulic breccia associated with narrow (several millimetres) zones of intense bleaching (albitization) and the more widespread introduction of disseminated pyrite.

Brittle fracture of metamorphosed felsic volcaniclastic sedimentary rocks produced quartz–carbonate(–chlorite–albite–pyrite) veins and veinlets associated with narrow zones of bleaching (biotite unstable), up to about 1 cm wide (Fig. 12.2). Broader zones of bleaching are present where fractures are closely spaced. Bleached alteration assemblages are quartz–plagioclase(albite)–carbonate assemblages with minor chlorite and disseminated pyrite. Plagioclase in this zone is extensively sericitized. Broader zones of disseminated carbonate and pyrite extend beyond the zone of bleaching.

Mass-balance calculations, based on whole-rock geochemical data (Appendix 4), indicate addition of Na_2O and S, and depletion of K_2O and SiO_2, to altered metamorphosed felsic volcaniclastic rocks (Fig. 12.3). These chemical changes are consistent with petrographic observations that suggest albitization and pyritization of bleached wallrocks. Note that the starting composition ('least-altered' sample) already contains several percent CO_2, but there is no significant further addition of CO_2 in samples of alteration more directly related to auriferous quartz veins.

Slug Hill Proprietary

Other names: Slug Hill

Coordinates: 30°44'56"S, 121°46'45"E

Production: 764.0 t of ore for 21.20 kg Au (27.7 g/t Au) between 1899 and 1902.

Host rock: The mine workings are in the headwaters of a south-draining deep lead. A deep shaft on the edge of the deep lead probably worked a primary lode deposit in what appears to be deeply weathered felsic schist after volcaniclastic rock.

Structure: The structure is not exposed and no information could be ascertained.

Alteration: The mine dump consists of weathered quartz–muscovite(–chlorite) schist.

IRO55 21.07.03

Figure 12.2. Quartz–carbonate veins with thin, bleached (quartz–albite–carbonate) alteration selvages in metavolcaniclastic rock

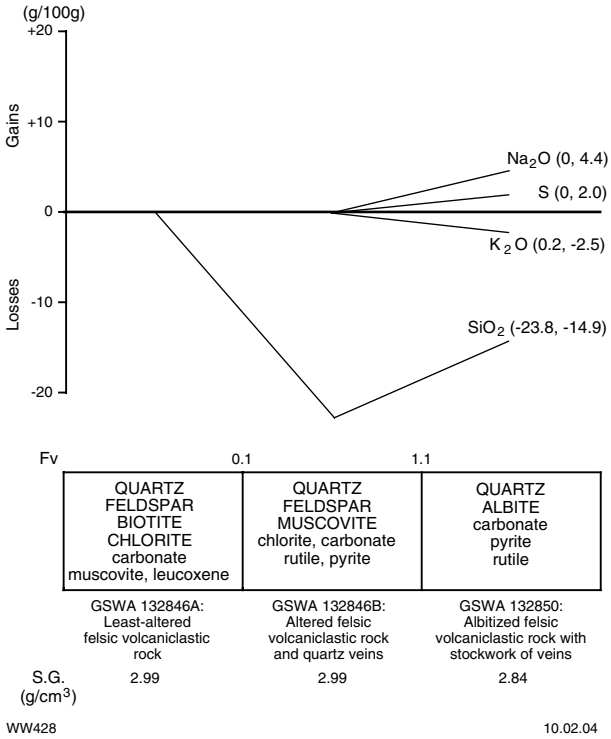

Figure 12.3. Mass-balance changes (calculated using the method of Gresens, 1967) associated with bleached alteration assemblages in metamorphosed felsic volcaniclastic rock, Queen Margaret mine, Bulong. Mineral components of alteration assemblages are listed in approximate order of abundance, with main mineral components in upper case and minor mineral components in lower case

Storm King

Other names: Castle Corner, Castle Corner Extended

Coordinates: 30°44'04"S, 121°46'43"E

Production: 286.65 t of ore for 12.37 kg Au (43.2 g/t Au) between 1902 and 1909.

Host rock: Weathered metamorphosed felsic volcaniclastic sedimentary rocks.

Structure: Two subparallel lines of shallow to moderately deep workings extend over about 300 m on north–south trends. Limited exposures suggest mineralization is within brittle–ductile shear zones that dip 70°W.

Alteration: Alteration has been obscured by deep weathering.

Trump

Other names: Fuairoe

Coordinates: 30°43'46"S, 121°46'28"E

Production: 470.9 t of ore for 30.21 kg Au (64.1 g/t Au) between 1902 and 1911.

Host rock: Most mine dumps consist of white, kaolinitic clay, quartz, and weathered rock of uncertain origin.

Structure: There are numerous shallow pits and a deeper shaft on a roughly north–south trend. Mine-dump material suggests the workings exploited a deep-lead deposit.

Alteration: Not applicable.

Peacehaven

Other names: Stratford

Coordinates: 30°43'41"S, 121°46'55"E

Production: 122.1 t of ore for 6.54 kg Au (53.6 g/t Au) between 1899 and 1930.

There is no further information for this deposit.

Golden West

Other names: New Golden West

Coordinates: 30°43'59"S, 121°47'36"E

Production: 960.7 t of ore for 36.18 kg Au (37.7 g/t Au) between 1902 and 1910.

Host rock: Weathered felsic volcaniclastic sedimentary rock.

Structure: Shallow pits extend over about 100 m on a poorly exposed, north-trending structure that dips to the west. Vein quartz is common on most mine dumps.

Alteration: Alteration has been obscured by deep weathering.

Sinn Fein

Other names: Blue Quartz North, Ninety Eight, Toby Barton

Coordinates: 30°44'03"S, 121°47'20"E

Production: 2898.7 t of ore for 29.33 kg Au (10.1 g/t Au) between 1898 and 1941.

Host rock: Weathered felsic volcaniclastic sedimentary rock.

Structure: Shallow to moderately deep pits and shafts extend over about 200 m on a poorly exposed, north–south structure that dips 70° to the west. Fine-grained, blue-grey vein quartz is common on most mine dumps.

Alteration: Alteration has been obscured by deep weathering.

Green Harp Leases

Other names: Green Harp, Green Harp South, Green Lode, Lady Gwen, Bulong Proprietary, Bulong Surprise

Coordinates: 30°44'45"S, 121°47'33"E

Production: 9530.9 t of ore for 104.06 kg Au (10.9 g/t Au) between 1898 and 1948.

Host rock: Felsic volcanic and volcaniclastic rock, schist, and ultramafic rock.

Structure: Shallow to moderately deep pits and shafts extend over about 700 m on a trend that is oriented about 010°. The structure is poorly exposed, but is probably a shear zone similar to those at Great Oversight (see below). The mineralized shear overlaps, in an en echelon fashion, with the western line of workings at Great Oversight. Mine dumps contain ultramafic schist, but most quartz veining is in relatively undeformed, fine-grained felsic porphyry (?acid volcanic rock).

Alteration: Ultramafic rock is altered to (commonly fuchsitic) talc–carbonate schist. Alteration of felsic rocks is obscured by weathering.

Great Oversight

Other names: Oversight, Gascoyne, Don, Christmas Box, Great Oversight G.M. Co., Good Hope Leases, Southern Cross Leases, Brilliant, Eastern Extended, Annabelle

Coordinates: 30°44'45"S, 121°47'33"E

Production: 23 105.4 t of ore for 149.71 kg Au (6.5 g/t Au) between 1897 and 1971.

Host rock: Metamorphosed felsic volcaniclastic sedimentary rocks appear to be the main host rock, but several mine dumps, particularly the deeper ones, contain deformed and altered ultramafic rock that may also be a significant host rock.

Structure: Shallow to moderately deep pit shafts and open stopes extend for about 400 m on two subparallel north–south to 010° trends. The two lines of workings appear to be concentrated on or near contacts between the metamorphosed felsic volcaniclastic unit and ultramafic rocks to the west and a doleritic unit to the east. Limited exposures suggest that mineralization is associated with veined brittle–ductile shear zones that are localized by these contacts and dip 40–50°W. Quartz veins up to 1 m thick are common, both within the shear zones and in adjacent, less-deformed rocks. They are commonly subparallel to shear-zone margins, but display a wide variety of orientations, particularly in relatively low strain domains outside the main zones of shearing.

Alteration: Quartz–carbonate(–pyrite) veining in metamorphosed felsic volcaniclastic rock and schist is accompanied by widespread, disseminated carbonate and pyrite. Ultramafic rocks are altered to chlorite–carbonate schist and talc–carbonate schist, the latter commonly containing minor amounts of fuchsite.

Central Zone

Coordinates: 30°42'54"S, 121°50'38"E

Production: No past production. The indicated resource is 93 000 t of ore at 2.33 g/t Au (0.217 t Au).

Host rock: The orebody is hosted by a 100 m-thick metamorphosed crystal-lithic tuff within a thicker, north-striking sequence of metamorphosed felsic volcaniclastic sedimentary rocks (metaconglomerate).

Structure: The overall form of the orebody is still uncertain, but appears to be an east-northeasterly striking zone of quartz veining and alteration that lies between two northwest-trending faults. Mineralized quartz veins within this zone are 'crustiform' (vuggy?) and dip 30° towards 270–280°.

Alteration: Mineralized quartz veins are associated with bleaching of the felsic host rocks. Bleached rocks are ankerite–sericite–pyrite–leucoxene(–tourmaline–fuchsite) assemblages. The bleaching overprints a broader zone of alteration characterized by disseminated chlorite and carbonate. The metamorphosed felsic volcaniclastic rocks adjacent to the mineralized metatuff display hematitic alteration that is associated with or overprints chlorite–carbonate alteration.

References: Manor Resources NL (1995).

Great Ophir

Other names: Fremantle Leases, Golden Jumble, Great Reefs Ltd, La Mascotte, Macquarie, Macquarie Extended, Marmont, Rangatiri, Raub

Coordinates: 30°41'42"S, 121°51'30"E

Production: 1360.6 t of ore for 17.74 kg Au (13.0 g/t Au) between 1897 and 1940. Records of cancelled gold mining leases (Department of Mines, 1954) attribute this production to 'same ground', but the mines listed above are at several sites up to several kilometres apart. Nevertheless, it is clear from the scale of the workings that the greater part of the listed production came from the Great Ophir mine (described below).

Host rock: Metamorphosed coarsely bedded, fine-grained, felsic volcaniclastic rock.

Structure: An open stope has exploited a massive quartz vein that strikes 060° and dips 40–50°SE. The vein orientation is rotated to about 080° at its northeastern and southwestern ends. The vein overprints a weak to moderate, pervasive regional foliation and is associated with only a narrow zone (≤20 cm) of weak to moderate shearing adjacent to the vein. Thinner quartz veins (≤20 cm) are common in both the footwall and hanging-wall of the main vein and display a variety of orientations, commonly 110–140° and dipping 30–60°S.

Alteration: Wallrocks to the main vein are cut by smaller quartz–carbonate and carbonate–quartz veins and veinlets and sericitic microshears. The altered metamorphosed volcaniclastic sedimentary rocks contain up to about 20% secondary carbonate with minor chlorite and disseminated pyrite.

References

AHMAT, A. L., 1995, Geology of the Kanowna 1:100 000 sheet: Western Australia Geological Survey, 1:100 000 Geological Series Explanatory Notes, 28p.

DEPARTMENT OF MINES WESTERN AUSTRALIA, 1954, List of cancelled gold mining leases which have produced gold: Western Australia Department of Mines, 271p.

DELTA GOLD LTD, 1993, Annual report, Mar 1992 to Mar 1993, on P25/1186–1188: Western Australia Geological Survey, Statutory mineral exploration report, Item 11653 A38918 (unpublished).

GRESENS, R. L., 1967, Composition–volume relationships of metasomatism: Chemical Geology, v. 2, p. 47–65.

MANOR RESOURCES NL, 1995, Annual Report, Jan 1994 to Mar 1995 on Bulong/Manor Ni/Co/gold exploration project: Western Australia Geological Survey, Statutory mineral exploration report, Group M5163 A45341 (confidential)*.

NELSON, D. R., 1995, Compilation of SHRIMP U–Pb zircon dates, 1994: Western Australia Geological Survey, Record 1995/03, 244p.

STROUD, R. A., 1987, Report on P26/00339–00340 and P26/00311–00312: Western Australia Geological Survey, Statutory mineral exploration report, Item 8043 A21541 (unpublished).

SWAGER, C. P., 1995, Geology of the greenstone terranes in the Kurnalpi–Edjudina region, southeastern Yilgarn Craton: Western Australia Geological Survey, Report 47, 31p.

---

* Confidential references are used with permission of companies.

13. Trans Find – Juglah and Majestic

The Trans Find – Juglah area is located in the southern part of the Gindalbie Terrane (Swager, 1995), on the eastern limb of the Bulong Anticline, and north of the mining centres at Randalls and Mount Monger. The mines in this area structurally underlie a D_1 thrust fault that has emplaced older mafic volcanic rocks above the mineralized felsic volcanic sequence (Swager, 1995). Metamorphic grade is difficult to estimate but is probably mid- to upper greenschist facies. The main mining area is at Trans Find, where gold is in felsic volcanic and metavolcaniclastic rocks and a subvolcanic granodiorite pluton. A felsic volcanic rock from this sequence has yielded a SHRIMP date of 2672 ± 12 Ma (Nelson, 1995). The Trans Find openpit has produced about 150 kg of gold, and a resource of 4.58 t Au at Curtin remains unmined. Both deposits are in north-northeasterly striking (010–020°) brittle–ductile shear zones, but northwest-trending faults or fracture zones are widespread in the area (Fig. 13.1) and appear to be an important control, at least at Trans Find. Gold is associated with quartz veining and pyrite. Quartz veins within the mineralized shears strike northeast to east-northeast. At Curtin, the veins dip 30–50° south and north, consistent with a synmineralization deformation regime in which σ_1 was oriented east-northeast and σ_3 was subvertical. A further association with secondary silica and biotite has been recognized at Curtin. The Juglah deposit, about 7 km north-northwest of Curtin, lies near the eastern margin of the Juglah Monzogranite and is another mineralized 010°-trending brittle–ductile shear or fracture zone in metamorphosed felsic volcaniclastic rocks. At Jones Find, 10 km west of Curtin, gold has been mined from steep, brittle–ductile shears that strike 310–350°, in felsic volcaniclastic and metasedimentary rocks.

The origin of deposits in the Trans Find – Juglah area is somewhat enigmatic. The association with late, linear fracture zones (Fig. 13.1) suggests a late tectonic origin. However, the pyrite-rich nature of veins and the association with subvolcanic intrusions and biotite alteration invite comparisons to porphyry copper styles of mineralization.

The Majestic mining centre is located about 8 km south-southeast of Morelands Find, within felsic volcanic rock and volcaniclastic schist, on the western limb of the Bulong Anticline. Like Curtin, Majestic is located between overlapping sections of the same east–west Proterozoic dolerite dyke. The Majestic deposit displays some features that are similar to those that characterize younger porphyry gold systems (Beane and Titley, 1981). Gold is in a subvolcanic intrusive complex containing at least three distinct igneous phases, all of which are mineralized. Mine-dump samples indicate the presence of a stockwork vein and fracture system in massive to weakly deformed porphyry host rocks. Alteration related to veins and fractures (summarized in Table 13.1) are superimposed upon a pervasive alteration that involves replacement of primary igneous ferromagnesian minerals by secondary chlorite and epidote. Wallrock alteration adjacent to mineralized (pyritic) veins includes chloritization and sericitization. Relict biotite is present locally within the chloritic alteration assemblages, suggesting that the chlorite may have formed by retrograde metamorphism of biotite-rich (potassic alteration) assemblages.

A locally developed foliation appears to overprint veins and suggests early formation of the vein system. Shear strain during regional deformation may have been partitioned into early zones of phyllosilicate alteration. This would explain the presence of ductile shear zones associated with some of the mineralization intersected by diamond drilling north of the old Majestic workings.

In contrast to most mesothermal gold deposits, relict high-temperature alteration minerals at the Majestic mine (including biotite and garnet) are apparently out of equilibrium with conditions indicated by regional metamorphic assemblages in the surrounding districts. Alteration zoning is also different from that in most mesothermal (late-orogenic) gold deposits. Mesothermal gold deposits that contain biotite in the alteration assemblage are commonly associated with zoned alteration halos that comprise an outer, biotitic assemblage and an inner zone that contains albite and muscovite (e.g. Kambalda; Phillips and Groves, 1984). The latter reflects increasing fluid X_{CO_2} towards the vein (Clark et al., 1989). At Majestic, alteration zoning is from an outer, albite- and muscovite-bearing assemblage to an inner, biotite-rich (or chlorite-rich) assemblage. This zoning can be attributed to increasing fluid Mg^{2+}/H^+ or Fe^{2+}/H^+, or both, and decreasing fluid K^+/H^+ towards the veins (Beane and Titley, 1981). More-detailed investigations, including fluid-inclusion and isotope studies, are required to determine the timing and nature of the hydrothermal system that deposited gold at Majestic.

Two further resources in this area are listed in MINEDEX, but there is little available information about the geology of these two deposits. Nicknames Find (34 000 t of ore at 1.8 g/t Au for 61.2 kg Au) and Duchess of York (132 000 t at 2.3 g/t Au for 303.6 kg Au) are located about 20 km south of Curtin, above the D_1 thrust fault. Both deposits are in north-striking zones, on or near the contact between quartz–feldspar (?metadacite) metaporphyry and carbonated mafic or ultramafic units. Gold at Duchess of York is associated with quartz–carbonate–pyrite stockwork veining on the deformed contact between the porphyry and mafic rocks (Hampton Hill Mining NL, 1994). Mineralization is associated with silicification of the porphyry and carbonation of mafic rocks. At Nicknames Find, mineralization is in a thin metachert unit, possibly an exhalite, that contains 5–15% pyrite and trace chalcopyrite. Anomalous Cu and Bi are associated with 0.1 – 2.0 g/t Au (Hampton Hill Mining NL, 1994). A sea-floor origin has been suggested for this deposit (Hampton Hill Mining NL, 1994).

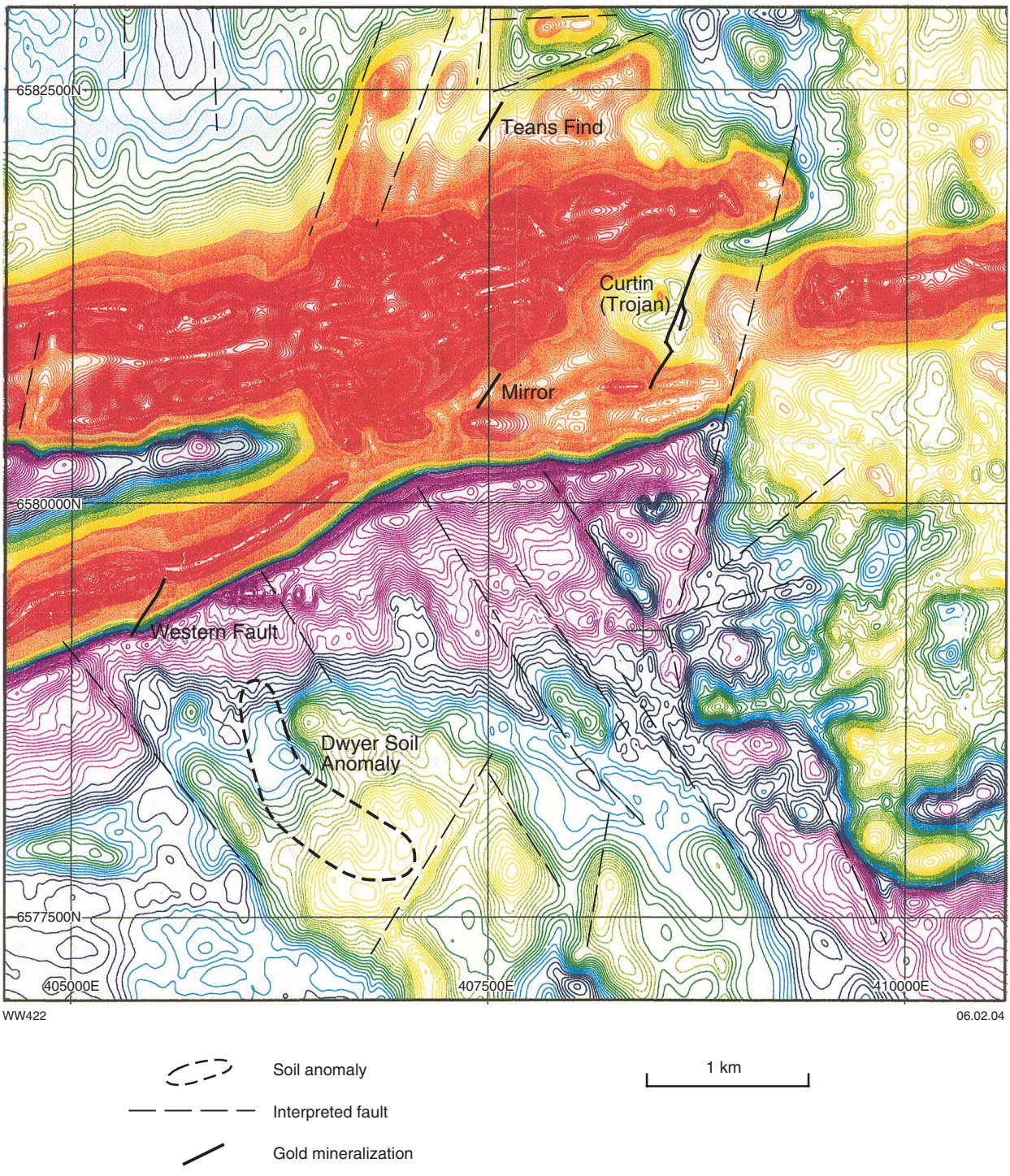

Figure 13.1. Contoured aeromagnetic data, showing location of mines and prospects, and interpreted late faults and fractures (aeromagnetic data from Taipan Resources NL, 1995)

Table 13.1. Generalized summary of vein and alteration assemblages in mineralized metaporphyries at the Majestic mine

Alteration/vein type	*Assemblage*		
Pervasive alteration (propylitic or metamorphic) in metaporphyry host rocks	Plagioclase Quartz Biotite Chlorite Epidote Ilmenite Titanite		
Larger quartz-dominant veins	**veins**	**inner zone*(darkened)**	**outer zone (bleached)**
	Quartz	Plagioclase (albite)	Plagioclase (albite)
	Chlorite (Biotite?)#	Chlorite (Biotite)#	Muscovite
	Epidote	Quartz	Quartz
	Carbonate	Pyrite	Chlorite (Biotite)#
	Pyrite	Titanite	Pyrite
	Titanite	Rutile	Titanite
Smaller calc-silicate veins and fractures	**vein/fracture**	**inner zone (lime green)**	**outer zone (pink to brick red)**
	Epidote	Epidote	Plagioclase (albite)
	Carbonate	Chlorite	Chlorite (Biotite)
	Chlorite	Muscovite	Quartz
	Quartz	Plagioclase (albite)	Hematite
	Garnet	Pyrite	Pyrite
		Titanite	Titanite
		Rutile	
Retrograde alteration (?synmetamorphic)	Prehnite after plagioclase, epidote, and garnet Chlorite after biotite, garnet Sericite after plagioclase		

NOTES: All assemblages are listed in the approximate order of mineral abundance.
* The inner zone can be subdivided into two subzones in which primary textures are destroyed in the inner subzone and plagioclase phenocryst forms are still evident in the outer subzone.
# Chlorite is ubiquitous, whereas biotite is generally a minor phase. Much or all of the chlorite may be secondary after earlier biotite.

Deposits of the Trans Find – Juglah and Majestic areas

Curtin

Other names: Trojan

Coordinates: 30°53'49"S, 122°02'43"E

Production: No historic production is recorded for this deposit. The measured resource is 1.223 Mt of ore at 2.3 g/t Au (2812.9 kg Au) and indicated resource is 798 000 t at 2.0 g/t Au (1596 kg Au; MINEDEX site code S00143).

Host rock: The main host rock is massive biotite granodiorite. Minor gold is present in metabasaltic country rock. The fine-grained, porphyritic texture suggests a subvolcanic origin for the granitic host rock.

Structure: Historic workings are located on northeasterly to north-northeasterly trending brittle–ductile shears (Figs 13.1 and 13.2). A series of northwest-striking structures in this area have also been identified from aeromagnetic data. The modern resource lies on a north-northeasterly striking shear, between overlapping portions of an easterly trending Proterozoic dyke. A small, exploratory pit has been excavated at the southern end of this lode (Fig. 13.2). The mineralized shear dips 50–80°W. There are two main ore zones, which have a tabular form and are more or less conformable within the brittle–ductile shear. The 'upper zone' is 5–20 m thick and about 300 m long. The 'footwall zone' extends for a similar strike length, but is only 1–3 m wide and slightly offset to the south with respect to the main ore zone (Fig. 13.2). The 'upper zone' contains higher grade ore (3–5 g/t Au) compared to the 'footwall zone' (0.7–1 g/t Au).

Diamond-drill intersections reveal the mineralized lodes to be zones of shearing, veining, fracture and, locally, brecciation. The exploratory pit exposes a stockwork of veins, mostly less than 5 mm wide, with a variety of orientations. Random observations on veins with three-dimensional exposure showed that most strike east-northeast and dip 30–50° north and south; another set of veins dip steeply with a north-northwesterly strike.

Alteration: The biotite granodiorite host rock contains up to about 3% secondary pyrite and 2% magnetite throughout most diamond-drill intersections (Titan Resources NL, 1995). Fractures filled with secondary biotite are also present locally. Mineralized sections contain more-abundant pyrite (5–15%) as disseminations in veins (±quartz) and on fracture surfaces. Mineralization is commonly associated with: moderate to intense silicification of the granodiorite, secondary biotite in fractures and as disseminations, and minor secondary carbonate. Secondary carbonate is more abundant in altered, mineralized metabasalt. The granodiorite also contains zones of hematitization, but these do not appear

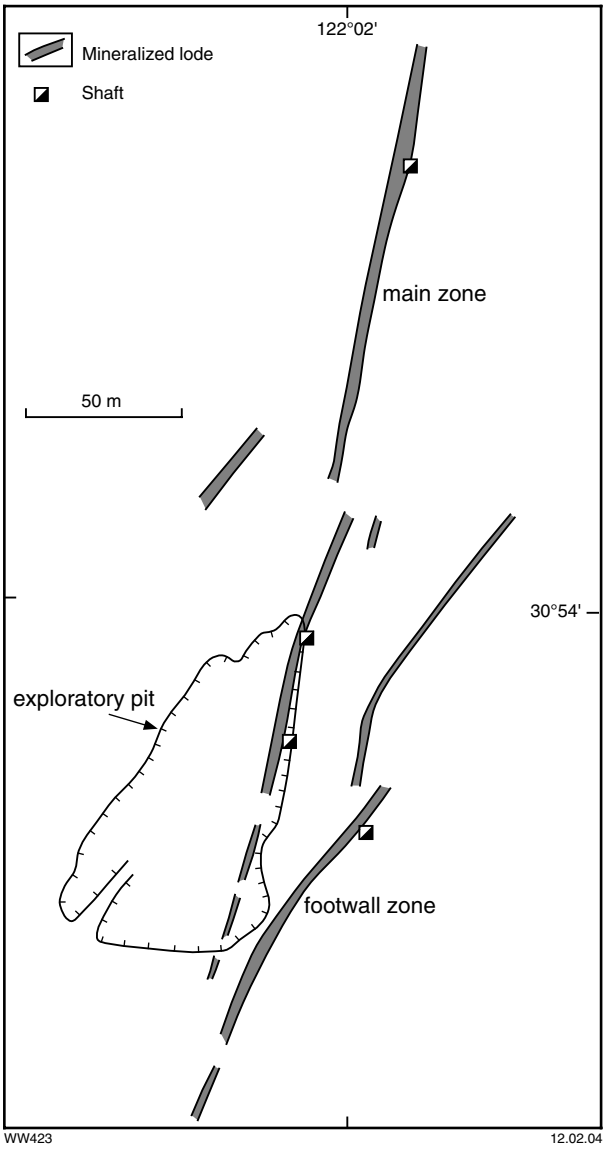

Figure 13.2. Geometry of the lode system, historic shafts, and recent exploratory pit at Curtin (after Titan Resources NL, 1995)

to correlate directly with gold mineralization. They may represent barren, distal alteration zones similar to those described from the granitoid-hosted Lady Bountiful deposit (Cassidy and Bennett, 1993; Witt, 1993).

Whole-rock analyses (Titan Resources NL, 1995) report low levels of As, Sb, Co, Ag, Mo, and W, but samples have not been analyzed for base metals.

References: Titan Resources NL (1995).

Trans Find

Other names: Dawn of Hope South

Coordinates: 30°53'49"S, 122°02'42"E

Production: Records of cancelled gold mining leases (Department of Mines, 1954) document no historic production for this locality. Openpit operation produced 152.7 kg Au from 31 050 t of ore (4.9 g/t Au) between July 1991 and February 1992. Initial mining was based on a resource of 69 000 t of ore at 5.7 g/t Au (393 kg Au; Imperial Resources NL, 1992).

Host rock: The main locus of mining appears to have been a relatively massive metarhyolitic or metadacitic unit within a sequence of metabasalt and metamorphosed bedded volcaniclastic sedimentary rocks. The latter includes coarse, clastic units (clasts up to 12 cm across) and minor thin beds of banded chert or jasperoidal quartz. The relatively massive host rock is a metamorphosed crystal-lithic tuff breccia.

Structure: The openpit operation was based on a north-northeasterly trending zone of brittle–ductile shearing that is concordant with the lithological layering (strike 010–015°, dip 30–40°E). Broadest zones of mineralization are where the main host unit is cut by 320°-trending faults. Quartz veins (mostly less than 5 cm wide) are widespread, and most strike 030–070° and dip shallowly (30–50°) southeast, north, and northwest. Those that are subparallel to the bedding surfaces are boudinaged.

Alteration: Gold is associated with quartz veins and pyrite, but exposures in the openpit are weathered. No alteration selvages adjacent to quartz veins could be identified.

References: Imperial Resources NL (1992), Taipan Resources NL (1994, 1995).

Juglah

Other names: Transville, Mount Juglah

Coordinates: 30°50'38"S, 122°00'22"E

Production: 995.1 t of ore for 25.94 kg Au (26.1 g/t Au) between 1923 and 1937.

Host rock: Weathered felsic volcanic or metavolcaniclastic rock.

Structure: Moderately deep shafts and some shallower workings extend over about 200 m strike length, on a trend of 010°. Open stopes expose metre-wide, north–south zones of fracturing and veining with subordinate ductile deformation. Right-stepping, en echelon zones dip 70°W and suggest sinistral movement on the mineralized fault. Vein quartz is common on mine dumps and in exposed stopes.

Alteration: Although weathered, the felsic host rocks appear to be carbonated and sericitized adjacent to veins. Disseminated pyrite is widespread and some quartz veins contain up to 20% pyrite as veinlets and stringers.

Long Looked For

Coordinates: 30°54'55"S, 121°55'43"E

Production: 239.1 t of ore for 6.80 kg Au (28.4 g/t Au) between 1921 and 1924.

Host rock: Weathered metamorphosed felsic volcaniclastic sedimentary rocks.

Structure: Shallow workings are located on four or five en echelon, massive, white to blue-grey quartz veins. The veins, which are up to about 20 cm wide, strike between 340° and north, and dip 70°W. The veins are associated with zones of fracturing and minor ductile deformation that extend beyond the quartz veins, along strike.

Alteration: Quartz veins contain minor limonitic pseudomorphs after pyrite. Alteration has been obscured by weathering.

Majestic

Other names: Majestic G.M.s Ltd

Coordinates: 30°55'00"S, 121°55'48"E

Production: 1312.7 t of ore for 20.44 kg Au (15.6 g/t Au) between 1902 and 1909.

Host rock: The main host rocks are a leucocratic feldspar(–quartz–amphibole) porphyry and a later, mesocratic plagioclase porphyry. Primary mineralogy in both intrusive phases has been extensively modified by metamorphism or propylitic alteration, or both. Both phases contain phenocrysts up to about 2 mm across in an aphanitic, quartzofeldspathic groundmass. The groundmass in the mesocratic porphyry contains 10–20% chlorite and biotite. A third magmatic phase, consisting of finer grained microporphyritic dykes intrudes both the earlier porphyries.

Structure: Shallow workings and a deeper shaft lie on a 080° trend. The structure is poorly exposed, but mine-dump samples and all three intrusive phases display evidence of an extensive stockwork of quartz veining and fracturing. Quartz veins are up to about 30 cm thick.

IRO57 10.02.04

Figure 13.3. Regional foliation overprinting an alteration zone in mineralized porphyry, Majestic mine. To the right of the photo (missing from the sample) is a fluid conduit (probably a vein); alteration ranges from proximal (dark) to distal (bleached), with relatively unaltered porphyry to the left of the photograph. See Table 13.1 for details of alteration assemblages. Foliation runs from left to right, across the photograph

Although the mineralized porphyries are mostly massive, a foliation, where present, appears to overprint the veins and attendant alteration assemblages (Fig. 13.3).

Alteration: The alteration history and assemblages at Majestic are summarized in Table 13.1. Tables 13.2 to 13.5 present analyses of minerals in altered porphyries from the Majestic deposit.

Larger veins are mainly quartz with minor carbonate, chlorite (or biotite), epidote, and pyrite (Fig. 13.4). Wallrock alteration is zoned from an inner, chlorite-rich zone (with relict biotite) to an outer, bleached zone (Figs 13.3 – 13.5). The inner zones are 1–5 cm wide and

Table 13.2. Selected SEM analyses of chlorite, altered metaporphyry from the Majestic mine

	GSWA 132864								
	altered, mineralized feldspar–quartz–amphibole metaporphyry								
	wallrocks						*wallrocks*		
	secondary after ferromagnesian mineral phenocryst			*chlorite in calc-silicate veinlet*			*secondary chlorite in chloritic veinlets*		
	CH1	*CH2*	*CH3*	*CH5*	*CH6*	*CH7*	*CH9*	*CH13*	*CH14*
SiO_2	26.12	25.88	26.32	25.99	25.56	24.99	25.92	26.13	26.14
Al_2O_3	18.55	18.06	18.69	18.43	19.03	18.10	18.48	18.36	18.56
FeO	28.45	29.46	28.79	28.21	28.44	31.00	28.32	29.52	28.64
MnO	0.54	0.42	0.44	0.68	0.65	0.76	0.81	0.53	0.77
MgO	13.45	12.77	13.50	13.38	12.54	11.43	13.35	12.95	13.37
CaO	–	–	–	0.13	–	–	–	–	–
Na_2O	–	–	0.20	0.19	–	–	–	0.25	–
Total	**87.11**	**86.59**	**87.95**	**87.00**	**86.31**	**86.28**	**86.87**	**87.74**	**87.48**
Fe/(Fe+Mg)	54.3	56.4	54.5	54.2	56.0	60.3	54.3	56.1	54.6

Table 13.3. Selected SEM analyses of plagioclase, altered metaporphyry from the Majestic mine

	GSWA 132864 *altered, mineralized feldspar–quartz–amphibole metaporphyry*							
	calc-silicate veinlet			*wallrocks*				
				plagioclase phenocryst		*groundmass plagioclase*		
	P12	*P14*	*P15*	*P16*	*P17*	*P22*	*P23*	*P24*
SiO_2	68.53	68.14	68.66	67.70	68.24	68.97	67.97	68.19
Al_2O_3	18.94	19.02	19.37	18.93	19.05	19.25	18.87	19.24
FeO	–	–	–	0.14	–	–	–	–
CaO	–	0.10	0.18	0.08	0.14	0.20	–	0.15
Na_2O	11.32	11.20	11.71	11.28	11.36	11.30	11.14	11.34
K_2O	–	0.16	0.10	0.07	–	0.08	0.07	0.22
Total	**98.79**	**98.62**	**100.02**	**98.21**	**98.80**	**99.80**	**98.04**	**99.13**
An	–	0.5	0.8	0.4	0.7	1.0	–	0.7
Ab	100	98.6	98.6	99.2	99.3	98.6	99.6	98.0
Or	–	0.9	0.5	0.4	–	0.4	0.4	1.2

Table 13.4. SEM analyses of garnet, altered metaporphyry from the Majestic mine

	GSWA 132864 *altered, mineralized feldspar–quartz–amphibole metaporphyry*					
	garnet in calc-silicate veinlet					
	GT1	*GT2*	*GT3*	*GT4*	*GT5*	*GT6*
SiO_2	34.81	35.36	35.53	35.06	34.97	35.12
Al_2O_3	–	0.86	1.94	–	–	0.16
FeO	27.53	26.60	25.64	27.84	28.18	27.93
MnO	–	–	0.37	–	–	0.24
MgO	–	–	–	–	–	–
CaO	33.30	33.93	33.68	33.62	33.58	33.95
Total	**95.64**	**96.75**	**97.16**	**96.52**	**96.73**	**97.39**
Andradite	100	95.6	90.5	100	100	99.7
Grossular	–	4.4	8.6	–	–	–
Spessartine	–	–	0.9	–	–	0.3

Table13.5. Selected SEM analyses of epidote and prehnite, altered metaporphyry from the Majestic mine

	GSWA 132864 *altered, mineralized feldspar–quartz–amphibole metaporphyry*										
	calc-silicate veinlet										
	prehnite after garnet			*coarse-grained epidote*		*epidote after plagioclase*		*fine-grained epidote, prehnite, and calcite*			
	PR2	*PR3*	*PR5*	*EP1*	*EP3*	*EP6*	*EP7*	*PR8*	*PR9*	*EP8*	*EP11*
SiO_2	43.06	42.83	43.03	37.65	38.08	37.85	37.80	43.06	42.92	37.28	37.43
Al_2O_3	22.99	23.02	23.29	23.72	23.52	24.91	23.77	23.66	23.64	22.48	23.20
FeO	0.72	0.96	0.79	11.78	10.98	10.32	10.67	0.65	0.57	12.21	10.98
MnO	–	–	–	0.21	–	0.45	0.19	–	–	–	0.31
CaO	27.10	27.01	27.31	23.77	23.43	23.57	24.19	27.23	27.62	23.59	23.76
Total	**93.87**	**93.82**	**94.52**	**97.13**	**96.01**	**97.10**	**96.62**	**94.60**	**94.75**	**95.56**	**95.67**

can be subdivided into two subzones of more or less equal width. Phenocryst forms are poorly preserved in the outer part, whereas nearer the vein the primary igneous texture is completely destroyed. The outer, bleached (albitic) zone varies from a few millimetres in width up to several centimetres. Modal chlorite and biotite contents in these outer zones are low, and although sericitized and sausuritized, the forms of the plagioclase phenocrysts are still clearly visible. Each zone contains disseminated pyrite (± minor chalcopyrite and galena).

Smaller veinlets and fractures (less than about 5 mm wide) are epidote or adularia rich and also contain variable amounts of carbonate, chlorite, and garnet (Figs 13.6 and 13.7). Garnet is variably retrogressed to chlorite and prehnite. These small veinlets are associated with narrow zones (up to a few millimetres wide) of bleaching and hematitization. They generally post-date the larger quartz-rich veins and attendant alteration halos (Figs 13.4 – 13.6).

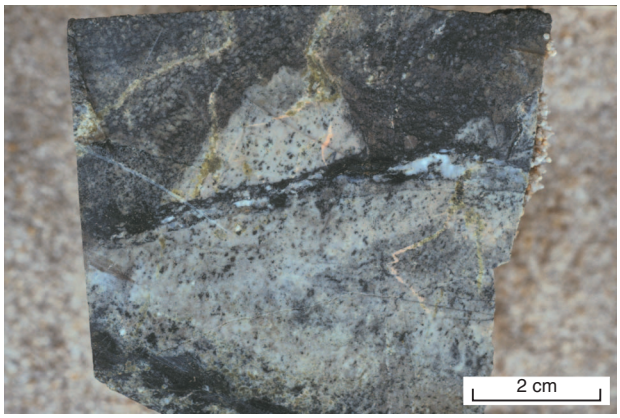

IRO61 15.12.03

Figure 13.6. Late veinlets of pink adularia cutting altered, mineralized porphyry, Majestic mine

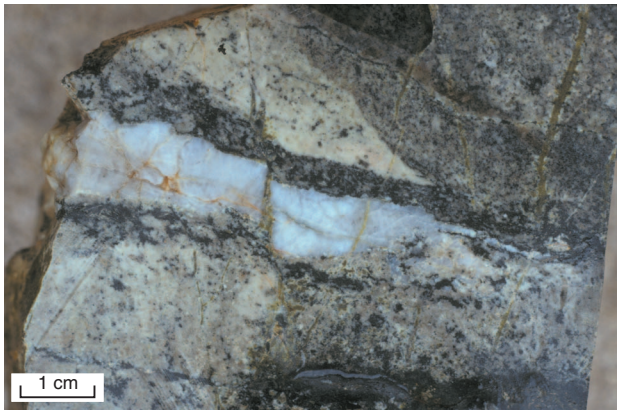

IRO58 15.12.03

Figure 13.4. Mineralized quartz vein in altered porphyry, Majestic mine. Note the proximal (dark) and distal (bleached) alteration halos on either side of the vein

IRO59 18.12.03

Figure 13.5. Altered porphyry, Majestic mine, showing an alteration halo between a quartz vein (left) and relatively unaltered porphyry (centre). The alteration halo consists of a broad inner zone (dark) and a thin distal zone (bleached). Note late, pink adularia veinlets cutting the vein and alteration halo at a large angle. A second alteration halo at the right end of sample shows the closely spaced nature of the veins in the mineralized stockwork system. See Table 13.1 for details of alteration assemblages

Diamond drilling 750 m and 1.9 km north of the old workings indicates that zones (up to 5 m wide) of quartz veining, weak to strong shearing, and alteration (quartz–sericite–albite–carbonate–chlorite–pyrite) are enveloped in slightly broader zones of fracturing, brecciation, chloritization, and hematitization. These zones are in similar host rocks (termed granodiorite and diorite by Western Mining Corporation, 1993) to those at Majestic and are probably equivalent to the two alteration and veining styles described above. Gold is present in both alteration zones and is commonly associated with secondary biotite and pyrite.

Whole-rock samples of altered, mineralized porphyry from the Majestic mine dumps are presented in Appendix 4. Altered samples were unbrecciated. Deformation fabrics

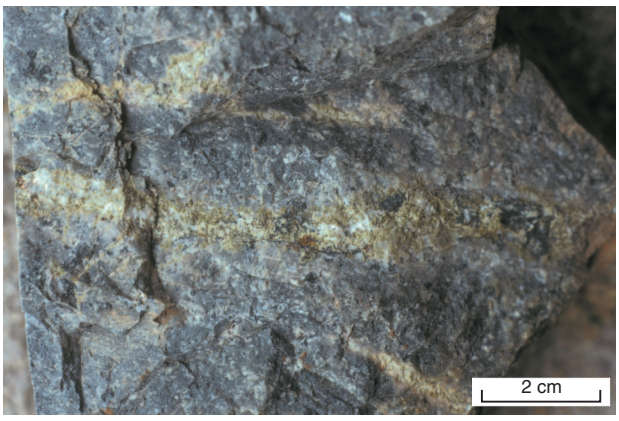

IRO62 15.12.03

Figure 13.7. Late epidote–calcite–biotite vein (left to right across centre of photograph) cutting across biotite/chlorite alteration (dark, at right) and relatively unaltered porphyry, Majestic mine

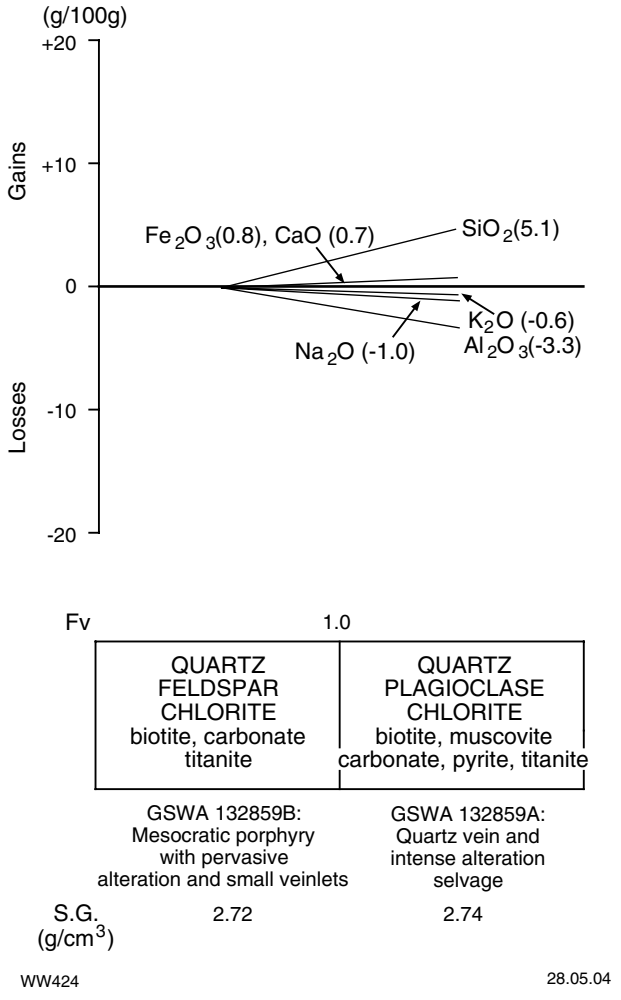

Figure 13.8. Mass-balance changes (calculated using the method of Gresens, 1967) associated with alteration adjacent to mineralized quartz veins in felsic porphyry, Majestic mine. Mineral components of alteration assemblages are listed in approximate order of abundance, with main mineral components in upper case and minor mineral components in lower case

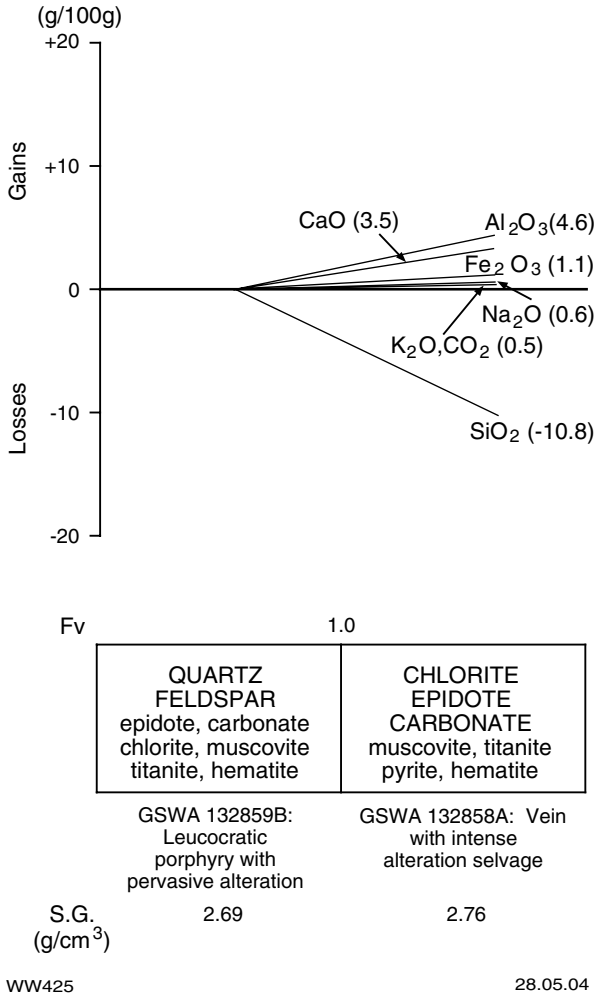

Figure 13.9. Mass-balance changes (calculated using the method of Gresens, 1967) associated with epidote–carbonate alteration adjacent to a late, chlorite-rich vein. Mineral components of alteration assemblages are listed in approximate order of abundance, with main mineral components in upper case and minor mineral components in lower case

were absent from the innermost zones of alteration, and primary textures preserved in the remainder of the alteration halos. Based on these observations, mass-balance calculations were carried out assuming no volume change (i.e. Fv=1). These calculations indicate that SiO_2 has been added, and alkalis and Al_2O_3 depleted from alteration halos adjacent to early quartz veins (Figs 13.8 and 13.9). Calculations based on the alternative assumption that Al_2O_3 is immobile indicate more-extreme enrichment of SiO_2 and addition of Fe_2O_3, CaO, and minor K_2O. Alteration around a late, chlorite-rich vein with an epidote-rich alteration selvage involves depletion of SiO_2 and addition of Al_2O_3, CaO, and Fe_2O_3. The assumption of Al_2O_3 immobility infers more extreme SiO_2 depletion, and enrichment of CaO and minor amounts of Fe_2O_3 and CO_2. Whichever assumption is favoured, the two styles of alteration give rise to opposing mass movements of SiO_2.

References: Western Mining Corporation Ltd (1993).

References

BEANE, R. E., and TITLEY, S. R., 1981, Porphyry copper deposits, Part II. Hydrothermal alteration and mineralization: Economic Geology, 75th Anniversary Volume, p. 225–269.

CASSIDY, K. F., and BENNETT, J. M., 1993, Gold mineralization at the Lady Bountiful Mine, Western Australia: an example of a granitoid-hosted Archaean lode-gold deposit: Mineralium Deposits, v. 28, p. 388–408.

CLARK, M. E., CARMICHAEL, D. M., HODGSON, C. J., and FU, M., 1989, Wall-rock alteration, Victory Gold Mine, Kambalda, Western Australia: Process and P–T–X_{CO_2} conditions of metasomatism, *in* The geology of gold deposits: the perspective in 1988 *edited by* R. R. KEAYES, W. R. H. RAMSAY, and D. I. GROVES: Economic Geology, Monograph 6, p. 445–459.

DEPARTMENT OF MINES WESTERN AUSTRALIA, 1954, List of cancelled gold mining leases which have produced gold: Western Australia Department of Mines, 271p.

GRESENS, R. L., 1967, Composition–volume relationships of metasomatism: Chemical Geology, v. 2, p. 47–65.

HAMPTON HILL MINING NL, 1994, Annual report, Feb 1993 to Feb 1994, on P25/1228–1230: Western Australia Geological Survey, Statutory mineral exploration report, Item 11657 A40611 (unpublished).

IMPERIAL RESOURCES NL, 1992, Transfind project East Coolgardie Mineral Field, Mining Lease M25/60 Kurnalpi SH51-10, Surrender report to Mines Department 28/3/91 to 28/2/92: Western Australia Geological Survey, Statutory mineral exploration report, Item 9573 A35285 (unpublished).

NELSON, D. R., 1995, Compilation of SHRIMP U–Pb zircon dates, 1994: Western Australia Geological Survey, Record 1995/03, 244p.

PHILLIPS, G. N., and GROVES, D. I., 1984, Fluid access and fluid–wallrock interaction in the genesis of the Archaean gold–quartz vein deposit at Hunt mine, Kamblada, Western Australia, *in* Gold '82: The geology, geochemistry and genesis of gold deposits *edited by* R. P. FOSTER: Geological Society of Zimabwe, Special Publication No. 1, p. 389–416.

SWAGER, C. P., 1995, Geology of the greenstone terranes in the Kurnalpi–Edjudina region, southeastern Yilgarn Craton: Western Australia Geological Survey, Report 47, 31p.

TAIPAN RESOURCES NL, 1994, Annual report, Sept 1993 to Sept 1994, on Transfind gold exploration: Western Australia Geological Survey, Statutory mineral exploration report, Item 9984 A43372 (unpublished).

TAIPAN RESOURCES NL, 1995, Annual report on exploration activities within E25/86, E25/87, M25/105 and P25.1233, Sep 1994–95 Jones Find project, Kalgoorlie, Western Australia: Western Australia Geological Survey, Statutory mineral exploration report, Item 9984 A46714 (unpublished).

TITAN RESOURCES NL, 1995, Annual report, Nov 1994 to Nov 1995, on M25/104: Western Australia Geological Survey, Statutory mineral exploration report, Item 11669 A46618 (unpublished).

WESTERN MINING CORPORATION LTD, 1993, Annual report, Jan 1990 to Dec 1992, Majestic North gold exploration: Western Australia Geological Survey, Statutory mineral exploration report, A38266 (confidential)*.

WITT, W. K., 1993, Gold mineralization in the Menzies–Kamblada region, Eastern Goldfields, Western Australia: Western Australia Geological Survey, Report 39, 165p.

---

* Confidential references are used with permission of companies.

14. Morelands Find – Black Hills – Wombola

This group of mining centres has produced only about 300 kg of gold in total, including production of about 50 kg from the Wombola openpit.

The Morelands Find mining centre is located at the southern end of Lake Yindarlgooda in a north-trending belt of greenstones dominated by metadolerite, metagabbro, and metabasalt. The greenstones are interpreted as a thrust slice that was tectonically emplaced over younger felsic volcanic rocks (Swager, 1995). The mineralization is located near the axis of an F_1 anticline. The main group of workings, at Sweet Nell, lies at the southern end of a small, felsic intrusion, in a domain that would have registered low mean stress in an east–west compressive regime (cf. Oliver et al., 1990). Mineralization is centred on a subvertical quartz vein that is more or less concordant with the greenstones. Other, shallower workings in the surrounding area were excavated on similar quartz veins.

On the eastern limb of the F_1 fold and adjacent to the basal thrust fault, copper- and bismuth-rich gold deposits are in a thick doleritic unit. East-southeast of Sweet Nell, copper-rich quartz–pyrite(–plagioclase) veins with malachite and calcite lie within a shear that dips steeply to the west and is more or less conformable with the enclosing greenstones (Fig. 14.1). Wallrocks are epidotized and chloritized (Fig. 14.2). Farther to the north, gold and bismuth are present in a subvertical quartz vein that strikes 140°. The vein, up to 0.5 m wide, is within metadolerite near the eastern contact of a metamorphosed quartz–feldspar porphyry. Mine-dump samples include quartz–carbonate–epidote–pyrite(–coarse, secondary apatite) veins with halos of altered wallrock that contain epidote–amphibole–quartz–titanite.

Farther north along strike, at Yindarlgooda, there are several small workings in metadolerite and metabasalt, with little recorded production. Gold was produced from quartz veins and shears, most of which are steep and subconformable with the north-northwesterly striking mafic unit. Alteration of the iron-rich, metamorphosed quartz dolerite host rock includes addition of biotite, quartz, pyrrhotite, and pyrite. Plagioclase remains stable in the presence of up to about 10% sulfides.

The Black Hills mining centre is within a north-trending, steeply west dipping sequence of metabasalt and metadolerite. Most gold deposits in this centre lie to the west of an isoclinal anticline interpreted as a D_1 structure by Swager (1995), and are located beneath a moderately west dipping D_1 fault (the Goddard Fault). The largest historic producers (Black Hill and Warnambool) and recent alluvial activity were concentrated around small historic mines are on the western flank of the D_1 fold axis. Mineralized quartz veins are associated with the eastern contacts of doleritic units or metamorphosed thick, differentiated basalt flow units, and also with late, transgressive, dextral faults that strike east-northeast to north-northeast. The north–south orientation of the greenstones, and the competency contrast between mafic rocks and broad packages of ultramafic rock to the west and felsic schist to the east, may have promoted brittle failure of the more brittle mafic rocks (Oliver et al., 1990; Ridley, 1993). The relatively flat lying Goddard Fault may also have promoted brittle failure by acting as a hydraulic seal and causing localized build-up of fluid pressure.

The Wombola mining centre is located above the D_1 Goddard Fault. The mineralized greenstone sequence is interpreted as a thrust slice of Kalgoorlie Terrane greenstones (Swager, 1995). The mining centre is spatially associated with the Simplex Fault — an irregular, east-southeasterly trending structure that links the Goddard Fault with the Mount Monger Fault to the west. The Simplex Fault separates north-striking greenstones (predominantly ultramafic rocks) to the north from an east-southeasterly striking sequence of metamorphosed felsic volcaniclastic rocks and mafic rocks to the south. The Wombola mining centre is located close to where an east-trending section of the fault changes to a southeast trajectory (Fig. 14.1). Gold is associated with quartz veins in an east-trending section of the Simplex Fault (Lady Agnes) and in an east-trending metadolerite unit to the south of the fault (Wombola openpit mines, equivalent to the historic Just In Time mine).

The structural origin of the Wombola deposits is uncertain. The Hoffman deposits are located on north-northeasterly to northeasterly oriented quartz veins within a north-trending zone of talc–carbonate rock and schist. The latter represents a shear zone within massive, strongly carbonated ultramafic rocks (Fig. 14.1). Mineralized quartz veins are associated with an asymmetric, Z-shaped section of the shear zone that may have formed a dilational jog during late-tectonic compression. Other, less-productive, gold-bearing quartz veins with similar orientations are associated with a fault that is subparallel to the Goddard Fault. These veins exist over a distance of about 5 km, from a point about 3 km north of Hoffman to a second point about 3 km east of Lady Agnes (Fig. 14.1). The east–west orientation of the Simplex Fault may have led to dilation and vein formation within the fault zone during late-tectonic compression. Thin ductile units (the shear zone) oriented parallel to the regional σ_1 direction are likely sites of brittle failure and rock dilation (Ridley, 1993). However, where the orientation of the layered sequence is east–west, failure of the more brittle metadolerite host rock is not predicted by the modelling of Ridley (1993). It may be that unrecognized northerly to north-northeasterly trending faults, in combination with splays off the Simplex Fault, have isolated relatively small sections of the metadolerite within less-competent schist after felsic volcaniclastic rocks. This geometry would be more favourable for brittle fracture of the metadolerite unit.

Deposits of the Morelands Find – Black Hills – Wombola area

Sweet Nell

Coordinates: 30°50'55"S, 122°53'09"E

Production: 407.3 t of ore for 30.48 kg Au (74.8 g/t Au) between 1922 and 1927.

Host rock: Massive to weakly deformed metabasalt.

Structure: Shallow workings are developed over about 150 m, on a north–south trend. The workings appear to exploit a 20–50 cm-wide quartz vein that is more or less parallel to the strike of the enclosing greenstones. There is little or no evidence of ductile deformation in the metabasalt adjacent to the vein, but the structure is poorly exposed. Most dumps contain samples of quartz–feldspar porphyry, suggesting that the vein may be localized near a contact between porphyry and metabasalt.

Alteration: No visible alteration of metabasalt or porphyry is evident in mine-dump samples.

Black Hill

Coordinates: 30°58'06"S, 121°50'18"E

Production: 3.4 t of ore for 8.61 kg Au (2460.0 g/t Au) in 1917.

Host rock: Weathered mafic rock.

Structure: Shallow workings on an apparent northerly to northwesterly trend.

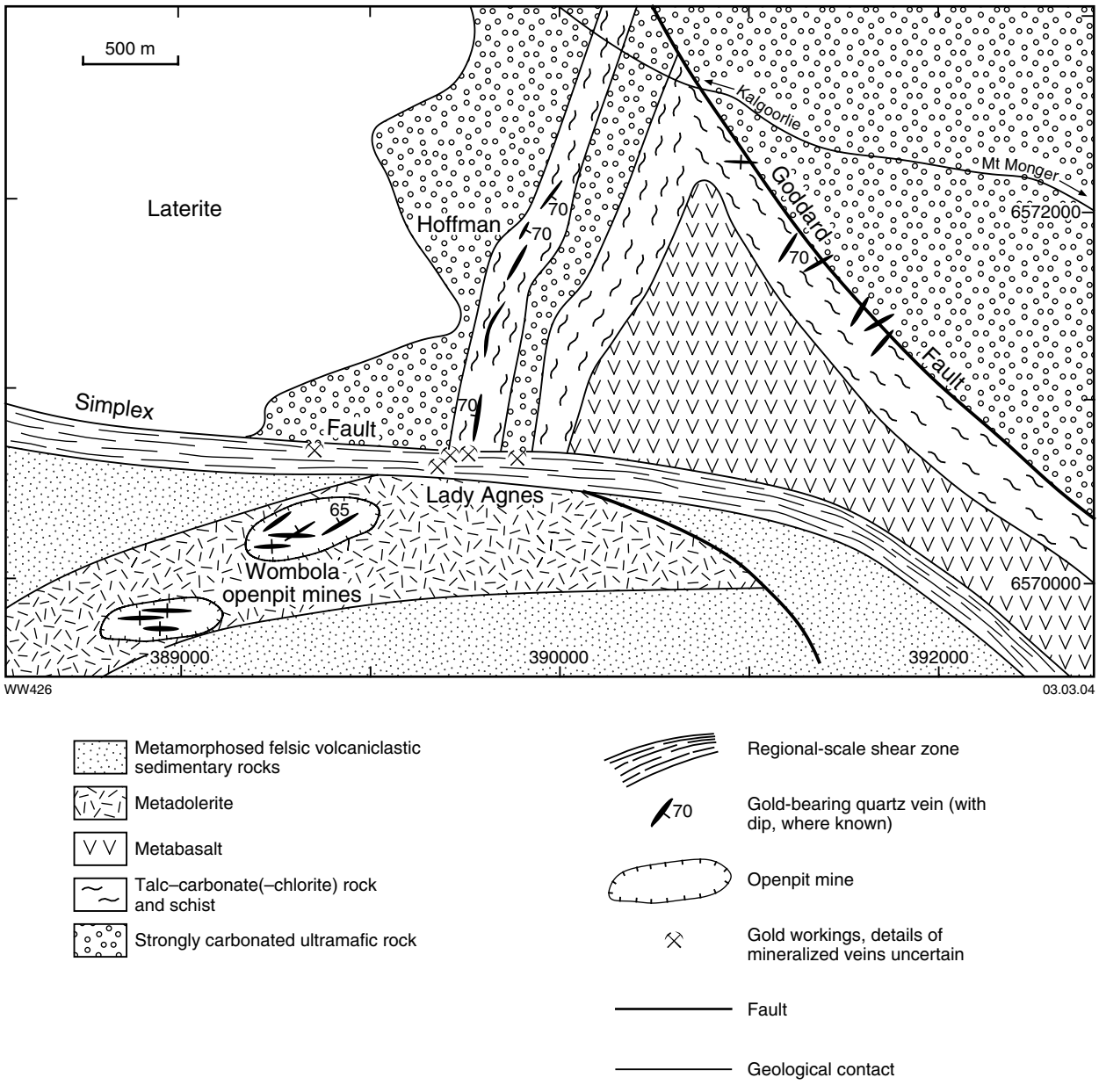

Figure 14.1. Geological map of the Wombola mining area (constructed from regional maps and 1:25 000 air photography)

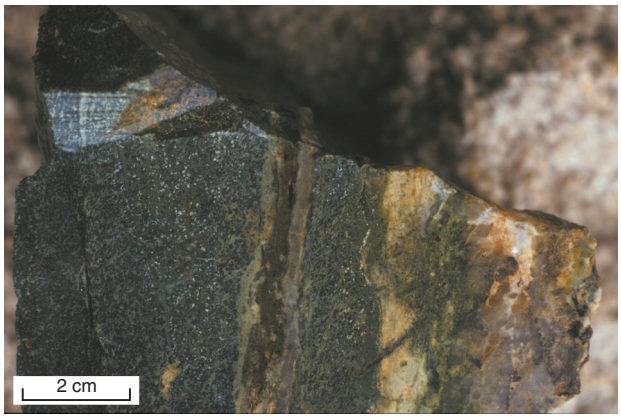

IRO56 15.12.03

Figure 14.2. Quartz–pyrite–plagioclase–epidote veins in epidotized and chloritized metadolerite from a copper-rich gold mine east-southeast of Sweet Nell, Morelands Find mining area

Alteration: Alteration has been obscured by weathering.

References: West Coast Holdings Ltd (1988).

Warnambool

Other names: Black Hills, Scotch Star

Coordinates: 30°56'08"S, 121°52'30"E

Production: 10.1 t of ore for 7.33 kg Au (725.7 g/t Au) between 1900 and 1902. Also 36.5 kg of dollied gold were produced in the same period.

Host rock: Shallow workings and a moderately deep shaft have been sunk into deeply weathered mafic rock (?metadolerite).

Structure: The mine workings trend north-northwest and apparently follow the contact between metadolerite and a thin interflow sedimentary rock horizon that has been intruded by a felsic porphyry. The deposit is located where a 060°-trending fault intersects the sheared contact of the metadolerite. The mineralized structure is not exposed, but minor amounts of vein quartz are present on mine dumps.

Alteration: Alteration has been obscured by weathering.

References: Ramsgate Resources Ltd (1992).

Hoffman

Other names: Rainbow, Kalgoorlie–Boulder Firewood Co. Ltd, Wombola

Coordinates: 30°59'06"S, 121°50'42"E

Production: 2516.8 t of ore for 29.98 kg Au (11.5 g/t Au) between 1906 and 1941.

Host rock: Talc–carbonate rock and schist after komatiite.

Structure: Shallow to moderately deep workings define a north-trending shear zone that is developed over a strike length of 350 m within ultramafic rock (metakomatiite). The deposits are located near the north-trending contact of metakomatiite with metamorphosed komatiitic basalt. In more detail, gold mineralization is associated with four shorter, 030–040°-trending structures that dip about 70°SE. These structures are poorly exposed, but the available evidence, including mine-dump samples, suggests that they lie in a zone of strong ductile deformation with quartz veins of many sizes, up to a maximum of about 1 m. The en echelon arrangement of the mineralized veins suggests dextral movement on the shear zone. At the southern end of the Hoffman 'line', coinciding with the intersection of the shear zone and the Simplex Fault (Fig. 14.1), there are numerous quartz veins that strike 040° (dip 70°NW) and 080° (dip 60°N). Farther north, workings coincide with a change in the strike direction of the ductile deformation zone. Dextral movement on the shear zone would have generated a dilational jog at this locality. Most veins appear to dip steeply to the southeast, but northwest-dipping veins may become more important towards the southern part of the mine group.

Alteration: Quartz veins are within talc–carbonate(–chlorite) schist after ultramafic rock. A strong shear fabric is defined by the preferred orientation of phyllosilicate minerals. Locally, the schist contains coarse carbonate porphyroblasts, up to 5 mm across. Thin selvages (up to a few millimetres wide) of coarser grained muscovite have been observed adjacent to some quartz veins. Randomly oriented prisms and needles of tremolite overprint the shear fabric.

Lady Agnes

Other names: Inverness, Inverness Extended, Logans, December

Coordinates: 30°04'50"S, 122°11'54"E

Production: 18 671.9 t of ore for 112.61 kg Au (6.0 g/t Au) between 1906 and 1986.

Host rock: Deeply weathered rock of uncertain origin. Talc–carbonate rock and schist after komatiite have been identified, but weathered mafic and sedimentary rocks are also likely to be present.

Structure: Shallow to moderately deep workings, confined to the oxidized zone, trend east–west over about 1 km. The structure is poorly exposed, but appears to coincide with an east-trending section of the Simplex Fault. Vein quartz is common on most mine dumps. Montgomery (1907) described the area as containing 'a great number of lodes' that strike about 075° and dip 60°NW.

Alteration: Alteration has been obscured by weathering.

References: Montgomery (1907).

Just In Time (Wombola openpit)

Other names: Knight St George, Tamerlane, Lady Dorothea, May Flower, Sindan

Coordinates: 30°59'56"S, 121°49'48"E

Production: 3653.4 t of ore for 27.72 kg Au (7.6 g/t Au) between 1906 and 1987. In addition, the Wombola openpit mine produced 25 640 t of ore for 56.08 kg Au (2.2 g/t Au) in 1988.

Host rock: Coarse-grained metadolerite unit within a thicker sequence of metamorphosed volcaniclastic sedimentary rocks.

Structure: Mineralization is associated with an east-trending sheeted quartz vein system confined within the metadolerite unit. Veins within the sheeted vein system are steep and strike east–west, although there is another, less common set that strikes east-northeast to northeast and dips 60–70°N. Individual veins are 10–100 cm thick and spaced about 5–10 m apart.

Alteration: Alteration has been obscured by weathering, but there appears to have been widespread chlorite–carbonate alteration of the metadolerite unit within the openpit mines. Quartz–carbonate(–pyrite) veins are associated with bleaching of wallrocks. Chlorite is unstable in the bleached zone and the assemblage is probably dominated by carbonate, sericite, and plagioclase with minor disseminated pyrite. Secondary biotite has been noted by Croesus Mining NL (1987).

References: CRA Exploration Pty Ltd (1986), Croesus Mining NL (1987).

References

CRA EXPLORATION PTY LTD, 1986, Annual report on P26/00314 and P26/00310–00312:Western Australia Geological Survey, Statutory mineral exploration report, Item 7785 A19826 (unpublished).

CROESUS MINING NL, 1987, Report on P26/00339–00340 and P26/00311–00312: Western Australia Geological Survey, Statutory mineral exploration report, Item 7785 A21393 (unpublished).

MONTGOMERY, A., 1907, Report on the mines of the Mount Monger District: Western Australia Department of Mines, Annual Report for 1906, p. 82–97.

OLIVER, N. H. S., VALENTA, R. K., and WALL, V. J., 1990, The effect of heterogeneous stress and strain on metamorphic fluid flow, Mary Kathleen, Australia, and a model for large-scale fluid circulation: Journal of Metamorphic Geology, v. 8, p. 311–331.

RIDLEY, J. R., 1993, The relations between mean rock stress and fluid flow in the crust: with reference to vein- and lode-style gold deposits: Ore Geology Reviews, v. 8, p. 23–27.

RAMSGATE RESOURCES LTD, 1992, Annual report, Jul 1991 to Jul 1992, on P26/1941–1943 and P25/1101–1102: Western Australia Geological Survey, Statutory mineral exploration report, Item 11663 A36566 (unpublished).

SWAGER, C. P., 1995, Geology of the greenstone terranes in the Kurnalpi–Edjudina region, southeastern Yilgarn Craton: Western Australia Geological Survey, Report 47, 31p.

WEST COAST HOLDINGS LTD, 1988, Annual report 1987 on P26/01048–01050, P25/00570, P25/00517, P25/00503–00508, M25/00030and M25/00025: Western Australia Geological Survey, Statutory mineral exploration report, Item 11670 A22258 (unpublished).

15. Sudden Jerk – Mount Monger

The Sudden Jerk and Mount Monger mining centres lie within the southern part of the Gindalbie Terrane (Swager, 1997). This area exposes an imbricate thrust package of greenstones derived from the Kalgoorlie Terrane that structurally overlies younger felsic volcanic rocks on the western limb of the Bulong Anticline. The thrust package was emplaced over the felsic volcanic rocks during D_1 and subsequently folded about the D_2 Bulong Anticline (Swager, 1995). The main D_1 thrust surface was named the Goddard Fault (Ahmat, 1995) but, in the Sudden Jerk and Mount Monger mining areas, the floor thrust lies below the Goddard Fault. The intervening horse contains a D_1 anticline that may be a hangingwall fold (Fig. 15.1). Felsic volcanic rocks within the thrust package have been dated at 2705 ± 4 Ma, whereas the felsic volcanic rocks below the thrust package were deposited at 2672 ± 12 Ma (Nelson, 1995).

The Mount Monger and Sudden Jerk mining centres have produced about 8 t of gold, and there have been recent openpit developments in both areas. The main historic producers were Haoma (2.1 t Au), Daisy–Milano (1.2 t Au), and Great Hope (0.6 t Au). Recent openpit mines include Sibu, Baguss, Futi Baguss, Fingals Fortune, and Lorna Doone (about 2.5 t Au) and Mirror Magic (799.328 kg Au). The remaining resource at Mirror Magic, and Costello about 1.5 km to the north, amounts to 1.8 t Au.

Gold deposits are in a north-northwesterly trending zone about 9 km long, mainly within the mafic horse beneath the Goddard Fault as well as in overlying metamorphosed felsic volcaniclastic rocks (Fig. 15.2). The greatest concentration of mining activity is located directly below the Goddard Fault. Relatively little gold has been produced from above the Goddard Fault and there has been insignificant gold production from rocks above the structurally higher Carowlyme Fault (another D_1 thrust).

Gold mineralization at Mount Monger is associated with north-northwesterly trending brittle–ductile shear zones that dip steeply to moderately steeply to the southwest (Fig. 15.2). Felsic porphyry dykes have the same orientation (Mt Monger Gold Project Pty Ltd, 1995). It is difficult to determine the sense of movement on most of these poorly exposed structures, but underground exposures in the Daisy mine show evidence for reverse and sinistral components of movement, consistent with late-tectonic east–west compression. These structures are parallel to the axial plane of the Bulong Anticline and may have initially formed during D_2. However, the orebodies appear to have formed late and probably developed during later reactivation as reverse-sinistral shear zones in a stress regime dominated by east–west compression. Orebodies plunge 40–60°S, which, as noted by Hickman (1986), is colinear with the intersection between the brittle–ductile shears and the Goddard Fault.

Deposits in the Sudden Jerk mining area lie within the mafic horse confined between the floor thrust to the east and the Goddard Fault to the west. Gold is found in brittle–ductile shear zones that have a similar orientation to those at Mount Monger but which dip only moderately (45°) to the east and west (Fig. 15.2). Evidence from the Baguss and Futi Baguss pits suggests reverse movement on the east-dipping structures, and the two sets of faults may be complimentary structures that formed in response to late-tectonic east–west compression. The deposits contain one or more zones of quartz veining, which form stacked ore lenses within the shear zones. These ore lenses are conformable with the enclosing shear zones and plunge gently to the south. The Fingals Fortune pits lie at the intersection between one of these west-dipping shear zones and a steeper, northwest-trending fault (Fingals Fault) that appears to have accommodated sinistral movement. Small porphyry intrusions exposed in the Sibu and Baguss openpits may have played a role in creating domains of stress heterogeneity within the shear zones.

The apparent control of D_1 thrust faults on gold mineralization in both mining centres, particularly at Mount Monger, suggests that the early structures may have capped further ascent of fluids and thereby promoted the high fluid pressures necessary for rock dilation and vein formation.

Hydrothermal alteration associated with gold mineralization in the recent pits in the Sudden Jerk mining area has been obscured by weathering. However, colour changes in the weathering products suggest that mineralization is associated with destruction of ferromagnesian minerals ('bleaching') and is enveloped by chlorite–carbonate alteration. Fresh samples from historic workings at None Such and Lurgan indicate that mineralized mafic rocks are altered to assemblages that contain chlorite, biotite, carbonate, and quartz in addition to disseminated pyrite or pyrrhotite, or both. The mineralized felsic rocks at Mount Monger are quartz–plagioclase(?albite)–sericite–chlorite–carbonate assemblages with abundant fine-grained, disseminated and veinlet pyrite. Biotite is present in some deposits (e.g. Caledonian and Mirror Magic) where the original host rock was relatively mafic. Tourmaline is present and locally abundant in many mines in both mining areas.

Geochemical data are presented but are difficult to interpret (see Appendix 5). The most likely mass changes involve addition of SiO_2, CO_2, Fe_2O_3, and S, reflecting the addition of secondary quartz, ankerite, and pyrite.

Deposits of the Sudden Jerk – Mount Monger area

Lurgan

Other names: Sonda Ditch

Coordinates: 30°58'58"S, 121°55'08"E

Production: 2708.4 t of ore for 29.25 kg Au (10.8 g/t Au) between 1936 and 1987.

Host rock: Mafic rocks (metadolerite and metabasalt). There is evidence in altered rocks of quartz–plagioclase

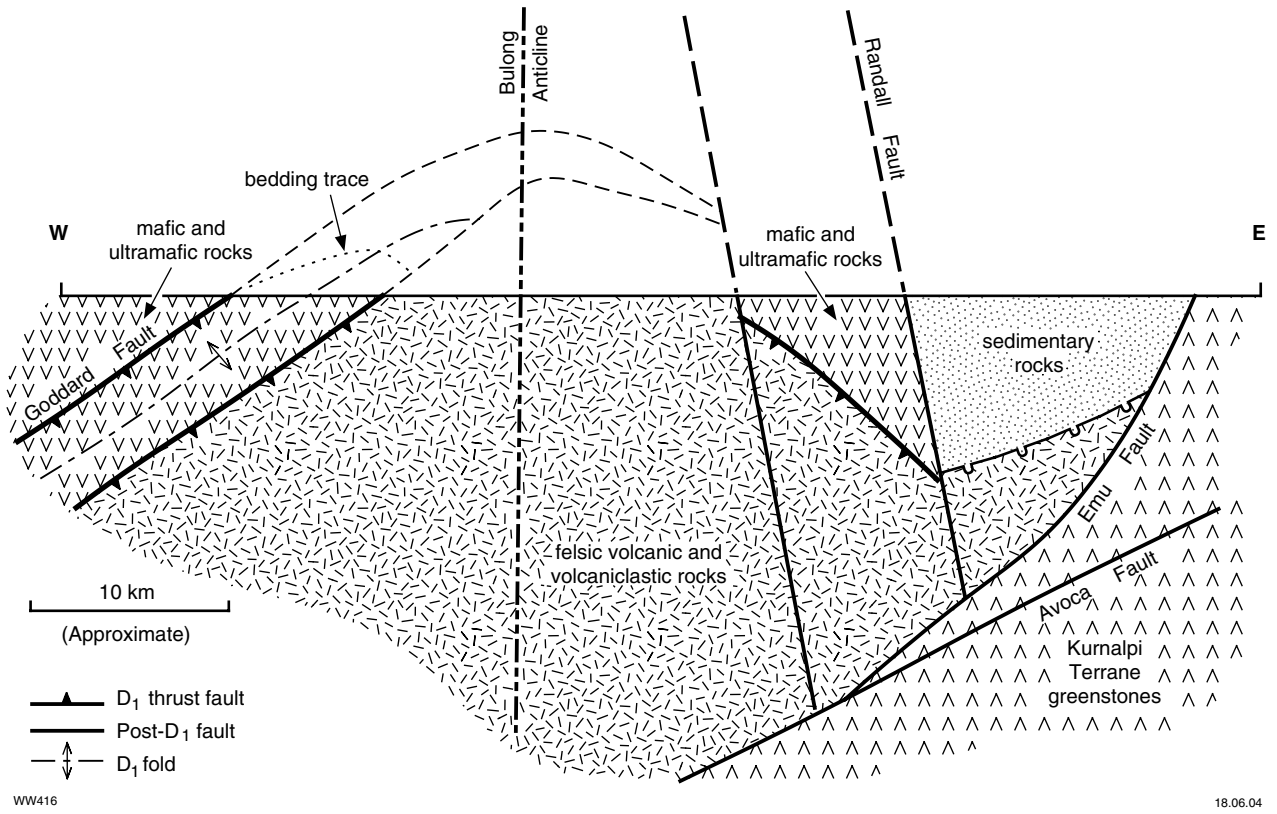

Figure 15.1. Interpreted cross section through the Bulong Anticline (based on regional geological maps and Swager, 1995)

granophyre, suggesting that gold mineralization is hosted at least partly by meta-quartz-dolerite. Minor meta-komatiite is also present on mine dumps, but does not appear to have been a significant host rock.

Structure: Moderately deep workings extend over about 1 km on a 2–3 m-wide zone of altered mafic schist and brittle fracture that strikes 350°. Good exposures of the mineralized structure can be seen in the stope that is cut into the side of the doleritic hill north of the main shaft. There are only minor exposures of quartz veins, and vein quartz is uncommon on the main mine dumps. These characteristics suggest that gold is hosted by a brittle–ductile fault in which the main process of brittle deformation was cataclasis rather than hydraulic fracture. Another stope has been sunk on a second, shorter structure that strikes 290°, at the northern end of the 350°-trending mineralized fault.

Alteration: Mafic rock within the mineralized fault is altered to quartz–plagioclase–chlorite–carbonate schist. This assemblage is augmented with minor disseminated leucoxene, tourmaline, and pyrite, and trace chalcopyrite. Fine-scale mineral banding and the preferred orientation of phyllosilicate minerals define a strong, pervasive foliation. More-intensely altered mafic rock collected from mine dumps contains up to 25% biotite, up to 10% muscovite, and several percent sulfides (mainly pyrrhotite). Biotite forms randomly oriented porphyroblasts (0.1 – 0.2 mm across) or, where more abundant, anastomosing seams with strong preferred orientation. Muscovite forms small (0.01 – 0.05 mm), randomly oriented, tabular grains that are irregularly distributed. Albite porphyroblasts (0.5 – 2 mm) with numerous inclusions of carbonate, chlorite, and biotite are present in some biotite-rich samples. The pervasive foliation is cut by carbonate veinlets with minor biotite or muscovite. Muscovite–carbonate veinlets cut biotite–carbonate veinlets. The amount of carbonate and pyrrhotite increases, and biotite decreases, towards late, discordant quartz veinlets.

Sibu

Coordinates: 30°57'28"S, 121°54'41"E

Production: 26 243 t of ore for 78.99 kg Au (3.0 g/t Au) from the Sibu openpit mine. Mining operations have ceased and there is no resource for this site listed in MINEDEX.

Host rock: Metamorphosed pillowed basalt. A massive, felsic porphyry unit exposed at the southern end of the openpit is probably not a major host rock.

Structure: The deposit lies on a brittle–ductile shear zone that strikes about 330° and dips 35°E, more or less parallel to interpreted primary layering (S_0). The 20–30 m-thick felsic porphyry unit has intruded the shear zone and dips about 45°E. The interior of the porphyry is extensively fractured and veined. The marginal zones, up to about 0.5 m wide, display intense ductile deformation, and a

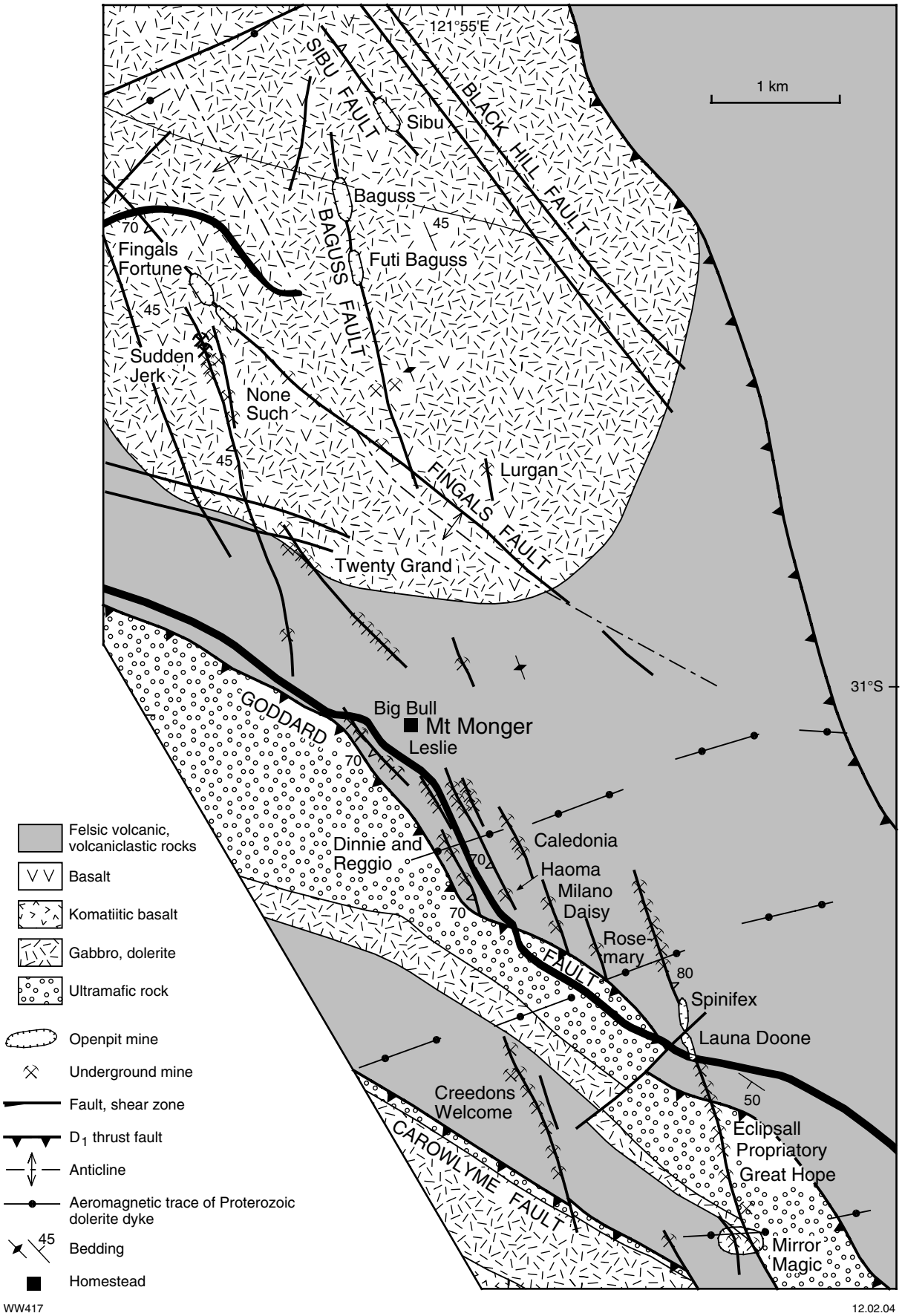

Figure 15.2. Geological map of the Sudden Jerk – Mount Monger area (based on regional maps and Ramsgate Resources Ltd, 1992)

much broader zone (several metres wide) of foliated metabasalt and quartz veining is present on the footwall of the porphyry. Veins observed in the pit fall into three groups: west to west-northwest striking with a dip of 40–70°S; west-southwest striking with a dip of 50°N; and southwest striking with a dip of 20°SE. The first two vein sets include examples with subhorizontal quartz fibres. The latter set is represented by fine-scale fractures and minor shears.

Alteration: Alteration has been obscured by weathering, but 'bleached' clays suggest that mineralized quartz veins are associated with sericitization and carbonation.

References: Ramsgate Resources Ltd (1993).

Baguss

Coordinates: 30°57'45"S, 121°54'26"E

Production: The Baguss openpit mine produced 75 397 t of ore for 225.44 kg Au (3.0 g/t Au) post-1988. Mining operations have ceased and there is no resource for this site listed in MINEDEX.

Host rock: The main host rock is metamorphosed pillowed basalt. A felsic porphyry is present at the northern end of the pit, but is probably not a significant host rock.

Structure: The Baguss openpit mine lies on a brittle–ductile shear zone that strikes 340–350° and dips 30–50°E. The orebody consists of quartz veins and altered metabasalt in a single, tabular lens, 3 to 6 m thick, that dips 40–60°E. Quartz veins are most abundant in the zone of high shear strain, which is about 5 m wide. Veins up to about 20 cm wide strike 310–300° and dip 60–70°SW and 60–90°NE. The orientation of these veins within the 345°-trending shear zone suggests a component of sinistral movement on the mineralized shear. Thick quartz veins that formed by dilation in the pressure shadow of a sigmoidal porphyry body also suggest a component of reverse movement on the mineralized shear zone. The mineralized shear zone is offset about 40 m by a late, sinistral fault.

Alteration: Deformed metabasalt is altered to chlorite–carbonate schist within the brittle–ductile shear zone.

References: Ramsgate Resources Ltd (1992, 1993), Mt Monger Gold Project Pty Ltd (1995).

Futi Baguss

Coordinates: 30°58'04"S, 121°54'29"E

Production: The Futi Baguss openpit mine produced 109 204 t of ore for 325.43 kg Au (3.0 g/t Au) post-1988. Mining operations have ceased and there is no resource for this site listed in MINEDEX.

Host rock: Metamorphosed pillowed basalt and metadolerite.

Structure: The Futi Baguss openpit mine lies about 500 m south of Baguss, on the same brittle–ductile shear zone (Fig. 15.2). Within the pit, metamorphosed basalt pillows are slightly flattened between anastomosing zones of high shear strain. The orebody consists of one to three tabular lenses, each 3–6 m thick, that dip 30–50°E and plunge 20–30°S. The ore lenses consist of quartz veins and veinlets with associated hydrothermal alteration. Veins exposed in the openpit strike west-northwest to north-northwest and dip either 40–60°NE or 70–90°SW, consistent with a sinistral component of movement. Mutual crosscutting relationships between veins and zones of high shear strain suggest that the veins formed during shear movements. Local drag and offset of veins against zones of high shear strain imply a reverse component of movement across the shear zone.

Alteration: Alteration has been obscured by oxidation, but descriptions based on drill logs indicate that mineralized quartz veins are associated with pyritic quartz–carbonate–albite alteration assemblages. Tourmaline is locally abundant and minor galena and chalcopyrite have also been recorded.

References: Ramsgate Resources Ltd (1992, 1993), Mt Monger Gold Project Pty Ltd (1995).

Fingals Fortune

Other names: Fingalls Fortune

Coordinates: 30°58'09"S, 121°53'43"E

Production: The Fingals Fortune group of orebodies (Fingals, Fingals South, Fingals East North, and Fingals East South) produced 424 469 t of ore for 1138.23 kg Au (2.7 g/t Au). Mining operations have ceased and there is no resource for this site listed in MINEDEX.

Host rock: The host rock is a thin unit of felsic schist (deformed quartz–feldspar–phyric rock) within a broader sequence of metabasalt. Some mineralization is also present in the adjacent metamorphosed pillowed basalt.

Structure: The Fingals Fortune deposit was mined from two openpits, which lie on a northwest-trending brittle–ductile shear zone (the Fingals Fault, Fig. 15.2) that dips 70°SW. In the southern pit, this structure forms a faulted contact between the felsic schist and metabasalt to the east. A pervasive foliation subparallel to S_0 (340°, 45°W) is well developed in the felsic schist unit and may be the northern continuation of the None Such Shear Zone. The pervasive foliation is deflected by (and therefore pre-dates) brittle–ductile deformation on the steeper Fingals Fault. The nature of this deflection suggests sinistral movement on the Fingals Fault.

Mineralized vein systems form two to three stacked lenses, 3–6 m thick, in the felsic schist unit and its hangingwall. The ore lenses dip 40–50°W but with some flatter sections. Metamorphosed basalt pillows west of the felsic schist unit become progressively more flattened towards the contact with felsic schist. Quartz veins (mostly ≤20 cm thick) in the western mafic unit strike about 115° and dip 45°S, consistent with sinistral movement on the deformed contact. There are also some steeper veins with a similar strike that seem to post-date the flatter vein set.

The Fingals ore system is cut by a Proterozoic dolerite dyke, which is exposed in the southern wall of the northern pit.

Alteration: Alteration of metabasalt adjacent to quartz veins has produced a pyritic quartz–carbonate–albite assemblage with minor galena and chalcopyrite.

References: Ramsgate Resources Ltd (1992), Mt Monger Gold Project Pty Ltd (1995).

Sudden Jerk

Other names: Struck Oil, None Such

Coordinates: 30°58'37"S, 121°53'56"E

Production: 73.3 t of ore for 13.83 kg Au (188.7 g/t Au) between 1900 and 1914. This locality has also produced 13.31 kg of dollied gold.

Host rock: Metabasalt.

Structure: A deep shaft and several moderately deep shafts extend for 300 m on a 350° trend. The mineralized structure is poorly exposed but appears to be a veined, brittle–ductile shear zone.

Alteration: Mine-dump samples are altered to chloritic schist, with unoriented biotite porphyroblasts (0.5 – 2 mm across). Biotite becomes more abundant and strongly oriented in zones adjacent to massive to laminated quartz (–carbonate–pyrite) veins. Coarse, idioblastic pyrite is present in the altered wallrocks. Laminae in quartz veins are composed of biotite(–chlorite).

Twenty Grand

Coordinates: 30°59'32"S, 121°54'26"E

Production: 647.5 t of ore for 12.3 kg Au (19.00 g/t Au) between 1936 and 1941.

Host rock: Weathered mafic rock (?metabasalt) and schist after felsic volcaniclastic rock.

Structure: Shallow to moderately deep workings are concentrated in two sections, on north-northwest to north-west trends.

The northern group of workings extends over 400 m on a thin (<0.5 m), subvertical, veined brittle–ductile shear zone that strikes 350° in mafic rock. At the southern end of this shear, shallow pits are developed over about 100 m on a splay structure that strikes 320°. The second group of workings is located about 500 m to the southeast on an extension of this 320°-trending structure. Shallow workings extend over about 350 m in schist after felsic volcaniclastic rock.

Alteration: Alteration is obscured by weathering but chloritic schist is present on some of the mine dumps in the northern group of workings. The altered schist consists of mainly quartz, plagioclase, chlorite, and carbonate with accessory titanite and minor epidote and biotite, and contains minor disseminated sulfides. Sericite increases in abundance at the expense of chlorite in more-intensely altered samples. The ratio of pyrite to pyrrhotite increases towards zones of higher strain (at the hand-specimen scale). Biotite forms randomly oriented porphyroblasts (0.5 – 1 mm) that overprint a shear fabric defined by oriented chlorite and sericite.

Big Bull

Other names: Leslie, Venezia, Taurus, Bull and Leslie Shafts

Coordinates: 30°59'56"S, 121°54'26"E

Production: 4775.2 t of ore for 112.38 kg Au (23.5 g/t Au) between 1934 and 1988.

Host rock: Metamorphosed felsic volcaniclastic rock (tuff, agglomerate, and related epiclastic rocks).

Structure: Moderately deep shafts extend over about 500 m on a trend of 330°. The workings lie in two groups (Big Bull and Leslie) on the same structure or two en echelon structures that dip 70°SW. Ore shoots plunge 60°SSE (Hickman, 1986). The mineralized structure is unexposed, but mine-dump samples record variable ductile strain. The foliation intensity is locally greater than the pervasive S_2 fabric, and implies an element of shear strain. However, strongly foliated rocks are not necessarily mineralized and many of the mineralized samples are intensely veined, with little evidence for flattening of clasts or preferred orientation of metasomatic minerals. The host structure is most probably a veined brittle–ductile shear zone, but mineralization appears more directly related to late brittle fracture and veining.

Alteration: Mineralized samples from mine dumps are quartz–plagioclase(?albite)–sericite–chlorite–carbonate assemblages with accessory leucoxene and several percent of fine- to medium-grained, disseminated and veinlet pyrite. Trace chalcopyrite has also been observed. Some larger quartz veins (>1 cm) are laminated with lamellae composed of chlorite, epidote, biotite, epidote, and pyrite. Abundant tourmaline is present in some of the lamellae. Less-intensely altered samples are chloritic but contain less carbonate and only minor sericite and pyrite.

Whole-rock geochemical analyses of altered rocks from Big Bull are presented in Appendix 5. The least-altered sample contains several percent CO_2. Chemical mass-balance additions and depletions are not apparent, apart from addition of S to more-intensely altered samples, and a mass-balance plot is not presented.

References: Hickman (1986).

Dinnie–Reggio

Other names: Dinnie North, I.V.M., Jerry

Coordinates: 31°00'40"S, 121°54'58"E

Production: 2468.9 t of ore for 69.87 kg Au (28.3 g/t Au) between 1916 and 1988.

Host rock: Metamorphosed felsic volcaniclastic rock (tuff, agglomerate, and related epiclastic rocks).

Structure: Deep and moderately deep shafts extend for several hundred metres on a 330° trend with the deepest shafts at the southeast end of the group. Mineralization is associated with one or more 1–2 m-wide, brittle–ductile shear zones that dip subvertically to 70°W. The distribution of workings suggests that they are located on a number of en echelon shear zones. The shear zones are not exposed, but are interpreted from mine-dump samples that include strongly foliated samples and widespread vein quartz.

Alteration: Hydrothermal alteration is similar to that described for Big Bull.

Haoma

Other names: Maranoa, Capitol, Business Risk, Jimberella, Pauline, J.J.

Coordinates: 31°00'40"S, 121°55'07"E

Production: 82 061.7 t of ore for 2160.2 kg Au (26.3 g/t Au) between 1916 and 1985.

Host rock: Metamorphosed felsic volcaniclastic rock (tuff, agglomerate, and related epiclastic rocks).

Structure: Several deep shafts extend over about 100 m on an unexposed structure that strikes 320–330° and dips 70°SW. Gold was extracted from several vertical, north-striking quartz veins, in a shoot that plunges 40–60°S.

Alteration: Hydrothermal alteration is obscured by weathering, but appears similar to that described for Big Bull.

References: Hickman (1986).

Caledonian

Other names: North Caledonia, Venture

Coordinates: 31°00'30"S, 121°55'13"E

Production: 4581 t of ore for 36.0 kg Au (7.9 g/t Au) between 1917 and 1983.

Host rock: Metamorphosed felsic volcaniclastic rock (tuff, agglomerate, and related epiclastic rocks).

Structure: The mineralized structure strikes 330° and is the locus for some deep and moderately deep workings that extend over about 100 m. There is little evidence for strong ductile deformation in exposures or samples on mine dumps, but quartz(–carbonate–chlorite–tourmaline) veins and veinlets are common. By comparison with other, similarly oriented lodes in this district, the ore structure is most probably a veined brittle–ductile shear zone.

Alteration: Mineralized samples are quartz–plagioclase(?albite)–chlorite–sericite–carbonate assemblages with several percent of fine-grained, disseminated pyrite and up to about 10% porphyroblasts of biotite (≤1 mm).

References: Hickman (1986).

Daisy–Milano

Other names: Happy Go Lucky

Coordinates: 31°00'44"S, 121°55'22"E

Production: 41 799.4 t of ore for 1166.4 kg Au (4.0 g/t Au) between 1917 and 1985.

Host rock: Metamorphosed felsic volcaniclastic rock (tuff, agglomerate, and related epiclastic rocks).

Structure: The Daisy and Milano lodes lie on the same 330°-striking structure. The Milano lode is a vein that dips 70°NE and contains an ore shoot that plunges 45°SE (Hickman, 1986).

The Daisy mine provides access to two lodes. The Eastern lode strikes 340° and dips 70°E (this may be a continuation of the Milano lode), whereas the Western lode strikes 345° and is subvertical. Both lodes are 3–5 m thick and ore shoots plunge 40–45°SE. Underground exposures (7 level) indicate that the lodes are zones of brittle–ductile shearing in which quartz veins (3–5 cm) are common. Veins are commonly conformable with the shear zone (340° and steep) or slightly oblique (325°, 50–60°SW), and are variably deformed, indicating formation during and after shear movement. The 325°-trending vein set suggests sinistral movement on the shear zone; however, there is little evidence of boudinage, suggesting that ductile strain was not intense. The asymmetry of folds defined by disrupted veins suggests reverse movement, as does the geometry of en echelon vein sets. The quartz vein in the Eastern lode is more or less continuous along strike, whereas veins in the Western lode are more irregular and discontinuous.

Alteration: Altered felsic rocks in the mineralized brittle–ductile shear zones are altered to a quartz–plagioclase–sericite–chlorite–carbonate assemblage with accessory ilmenite. A foliation is defined by anastomosing, chlorite-rich seams. More-intensely altered ('bleached') rock adjacent to quartz- and carbonate-rich veins has less and paler coloured chlorite, in addition to larger amounts of sericite and several percent fine-grained, disseminated and veinlet pyrite. Ilmenite is replaced by leucoxene or rutile, or both. The pyrite (≤1 mm) tends towards an idioblastic form and is commonly associated with small aggregates of quartz, chlorite, carbonate, and tourmaline. Very small inclusions of pyrrhotite and gold are present in the pyrite. Carbonate and fibrous quartz have been recognized in some veins.

Quartz–carbonate breccia zones are locally developed within the lodes. They contain minor amounts of muscovite, chlorite, and acicular (?secondary) ilmenite (altered to leucoxene). Fine-grained pyrite and tourmaline are common, and locally abundant. The breccias appear to have evolved from an early, barren, carbonate-rich phase to a later phase in which quartz, pyrite, and tourmaline are the main constituents.

Mass-balance calculations, based on whole-rock geochemical data (Appendix 5), indicate addition of SiO_2, CO_2, CaO, Fe_2O_3, and S to altered rocks associated with pyritic veins (Figs 15.3 and 15.4). These changes reflect

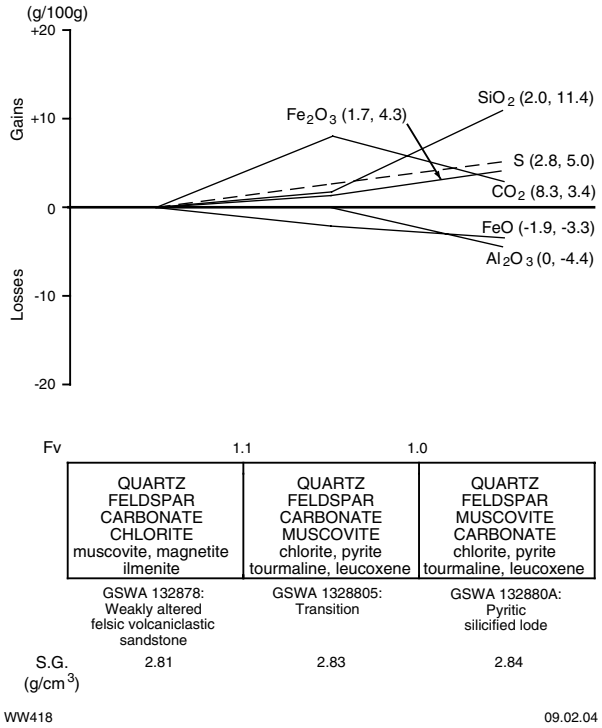

Figure 15.3. Mass-balance changes (calculated using the method of Gresens, 1967) associated with silicification and pyritization of felsic volcanic rock at the Daisy mine, Mount Monger. Mineral components of alteration assemblages are listed in approximate order of abundance, with main mineral components in upper case and minor mineral components in lower case

formation of secondary quartz, ankerite, and pyrite. Minor K_2O has been added as muscovite, and Na_2O depleted, in one sample (Fig. 15.4). The loss of FeO shown in Figure 15.3 could reflect the larger amount of pyrite in these samples because pyrite deposition may be accompanied by wallrock oxidation (Mikucki and Heinrich, 1993). The loss of Al_2O_3 assumes approximately constant volume during alteration. This assumption seems reasonable in view of the lack of brecciation or ductile deformation fabrics in the altered rock samples. The alternative assumption, that Al_2O_3 is immobile, requires a volume expansion of 50% (Fv=1.5). This assumption appears unreasonable but yields qualitatively similar mass-balance results. Apart from Al_2O_3, the main difference is the more extreme enrichment of SiO_2 in the most altered sample. Note that the loss of SiO_2 and Al_2O_3 from GSWA 132883 (quartz–carbonate breccia, see Appendix 5) reflects the formation of very large amounts of ankerite.

References: Hickman (1986).

Rosemary

Coordinates: 31°00'56"S, 121°55'33"E

Production: 1668.4 t of ore for 27.1 kg Au (16.2 g/t Au) between 1942 and 1982.

Host rock: Metamorphosed felsic volcaniclastic rock (tuff, agglomerate, and related epiclastic rocks).

Structure: Three deep shafts have been sunk on one (?or more, en echelon) structures that strike 320°. The structure is not exposed at the surface, but Hickman (1986) describes mineralization as being associated with a quartz vein that dips 70°NE.

Alteration: Hydrothermal alteration is similar to that described for Daisy–Milano.

References: Hickman (1986).

Creedons Welcome

Other names: Dry Mount, Hodad, Little Jean, Southern Cross

Coordinates: 31°01'34"S, 121°55'19"E

Production: 6233 t of ore for 127.0 kg Au (20.4 g/t Au) between 1916 and 1984.

Host rock: Metamorphosed felsic volcaniclastic rock (tuff, agglomerate, and related epiclastic rocks).

Structure: Moderately deep shafts have been excavated over a strike length of about 1 km, on a steep structure

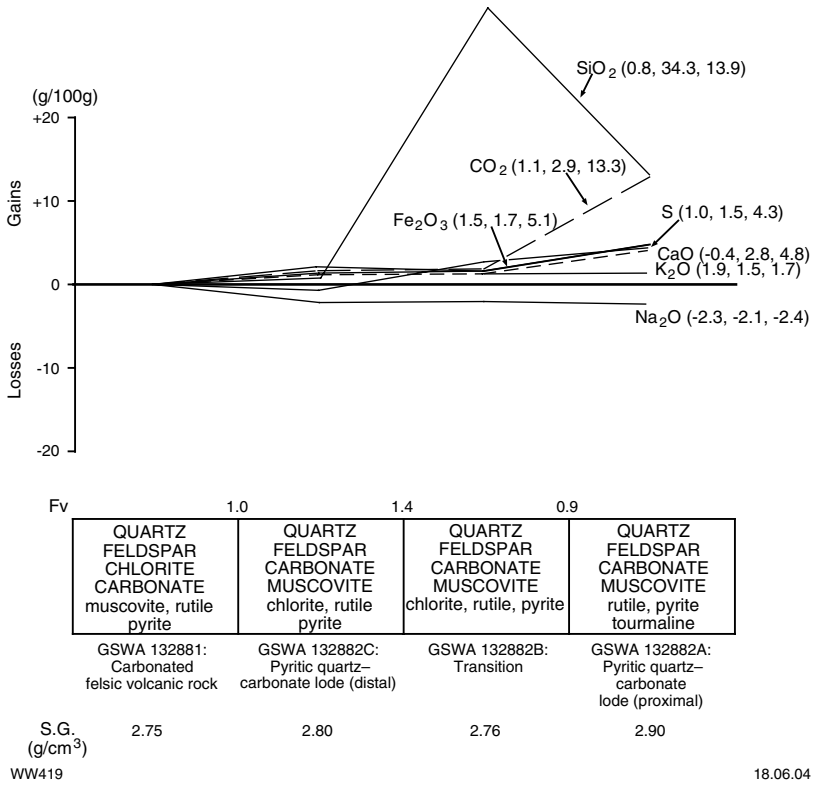

Figure 15.4. Mass-balance changes (calculated using the method of Gresens, 1967) associated with pyritic quartz–carbonate lode in felsic volcanic rock, Daisy mine, Mount Monger. Mineral components of alteration assemblages are listed in approximate order of abundance, with main mineral components in upper case and minor mineral components in lower case

that strikes 340°. The mineralized structure is poorly exposed, but is probably a veined brittle–ductile shear zone similar to those described for the Daisy deposit.

Alteration: Hydrothermal alteration has been obscured by weathering, but quartz–sericite schist is exposed on mine dumps associated with deeper workings.

References: Clarke (1925), Hickman (1986).

Lorna Doone

Other names: M.L.S., Everley, Spinifex

Coordinates: 31°01'17"S, 121°55'59"E

Production: 5349.0 t of ore for 73.2 kg Au (13.7 g/t Au) between 1935 and 1980. The Lorna Doone openpit mine produced 184 802 t of ore for 437.98 kg Au (2.4 g/t Au). The Spinifex openpit mine produced 121 157 t of ore for 333.18 kg Au (2.75 g/t Au).

Host rock: The Lorna Doone and Spinifex deposits are both hosted by felsic volcanic and metavolcaniclastic rocks.

Structure: The Lorna Doone and Spinifex deposits lie about 200 m apart, on steep, veined, brittle–ductile shear zones (10–15 m wide) that strike 340–350°. Four separate ore shoots plunge 45–50°S. The mineralization coincides with the intersection of a northeast-striking dextral fault and the mineralized shear zone.

The mineralized shear in the Spinifex pit dips 80°E and is controlled by the contact of metamorphosed felsic volcaniclastic rocks with a 340°-striking felsic porphyry dyke.

The Lorna Doone deposit contains two elements: broad, bedding-parallel zones of mineralization that strike 320° and dip 40°SW are cut by narrow, high-grade zones that dip 70–80°W.

Alteration: Ore shoots are characterized by zones of 'bleaching'. Altered zones are quartz–plagioclase–chlorite–sericite–carbonate assemblages with associated pyrite and tourmaline.

References: Mt Monger Gold Project Pty Ltd (1995).

Eclipsall

Other names: Great Hope North, Proprietary, Mount Monger Proprietary East

Coordinates: 31°01'40"S, 121°56'08"E

Production: 4066.9 t of ore for 150.8 kg Au (37.1 g/t Au) between 1926 and 1953.

Host rock: Ultramafic rock (metaperidotite).

Structure: Shallow stopes have been sunk on a 1–2 m-wide, subvertical zone of shearing that strikes 345°.

Alteration: Sheared ultramafic rock has been altered to talc–carbonate schist.

References: Clarke (1925).

Great Hope

Other names: P.G.M. Ltd, Marise

Coordinates: 31°01'52"S, 121°56'10"E

Production: 5899.7 t of ore for 609.89 kg Au (103.4 g/t Au) between 1920 and 1984.

Host rock: Ultramafic rock (metaperidotite).

Structure: A deep shaft and stopes have been developed over a strike length of about 200 m, on a subvertical shear zone that strikes 345°, with an ore shoot that plunges 45°S. A second, shorter structure, about 50 m east of the first, dips 70°E. The main mineralized structure is exposed in the stope as a 1 m-wide, purely ductile shear zone with some low-strain fragments of ultramafic rock but no quartz veins.

Alteration: Within the shear zone, the ultramafic rock is altered to talc–carbonate rock and schist, locally with abundant metasomatic biotite and minor disseminated pyrite. Chlorite-rich schist with abundant euhedral magnetite octahedra (≤2 mm) is common on mine dumps. The precursor to this rock is unknown. Gold was reported to have come from thin seams in the deformed and altered ultramafic rock.

References: Clarke (1925), Hickman (1986).

Lass O'Gowrie

Other names: Loganberry

Coordinates: 31°03'03"S, 121°57'39"E

Production: 555.0 t of ore for 6.89 kg Au (12.4 g/t Au) between 1920 and 1943.

Host rock: Ultramafic rock (metaperidotite).

Structure: Shallow to moderately deep workings are developed over about 200 m on a trend of about 310°, which is more or less parallel to lithological layering in this area. Mining has focused on a 1 m-wide shear zone that dips 60–70°SW, but some 340°-trending shears that dip 60–70°W also seem to have been mined. Quartz veins are uncommon, but a few thin stringers of quartz are present on mine dumps.

Alteration: Mine dumps are dominated by talc–chlorite–carbonate schist and talc–carbonate rock and schist. Chlorite–magnetite rock, similar to that at Great Hope North, is also present. Gold exists as thin stringers and disseminations. Small concentrations of high-grade scheelite have also been reported (Ellis, 1944). The deposits have previously been mined for talc (Ellis, 1944).

References: Clarke (1925), Ellis (1944), Hickman (1986).

Mirror Magic

Other names: Mirror, Costello, Magic

Coordinates: 31°02'08"S, 121°56'11"E

Production: Openpit mining in 1993 produced 266 443 t of ore for 799.32 kg Au (3.0 g/t Au). An inferred resource of 166 000 t at 4.00 g/t Au (663 kg Au) remains unmined. Additional underground resource is 75 000 t at 8.88 g/t Au (666 kg Au; MINEDEX site code S03350). For Costello the indicated resource is 137 000 t at 3.5 g/t Au (479.5 kg Au; MINEDEX site code S04450). For the Magic openpit the indicated resource is 223 000 t at 4.14 g/t Au (923.22 kg Au).

Host rock: Mineralization in drillhole MMD-5 is in a metamorphosed dacitic ash-flow tuff (about 10 m thick) within a thicker sequence of metamorphosed andesitic volcaniclastic sedimentary rocks (Fig. 15.5).

Structure: Flooding of the openpit prevented close examination of the orebody, which appears to be associated with a homoclinal structure defined by S_0. The dominant foliation (and S_0) in the pit is north-northwest to north trending and dips 45° to 70°W, and is probably related to D_3 fault movement on the structure that hosts the nearby Great Hope and Lorna Doone deposits. Mineralization appears to be associated with vein formation in a zone of mainly brittle deformation that dips 20–30° towards 195°, in the relatively competent dacitic unit.

Alteration: The metamorphosed andesitic volcaniclastic sequence is strongly carbonated, with a secondary mineral assemblage dominated by carbonate, chlorite, and biotite (Table 15.1). Disseminated pyrrhotite and secondary sericite form a halo, several metres wide, around the mineralized dacitic unit. Mineralization in the dacitic unit is associated with carbonation, sericitization, biotitization, and pyritization (Table 15.1). Fine-grained disseminated sulfides form up to 5% of the rock. These are mainly pyrite with minor pyrrhotite, but in some sections arsenopyrite is the major or sole sulfide mineral.

Whole-rock geochemical data for one sample each of meta-andesite and metadacite are presented in Appendix 5. With less-altered equivalents of each rock type unavailable for analysis, it is difficult to quantify mass changes associated with alteration. However, compared to average andesite compositions (Cox et al., 1979), it seems likely that the meta-andesite sample has lost Na_2O and gained K_2O and CO_2. Similarly, the mineralized metadacite has probably gained SiO_2, CO_2, S, and As and lost Na_2O and possibly Al_2O_3.

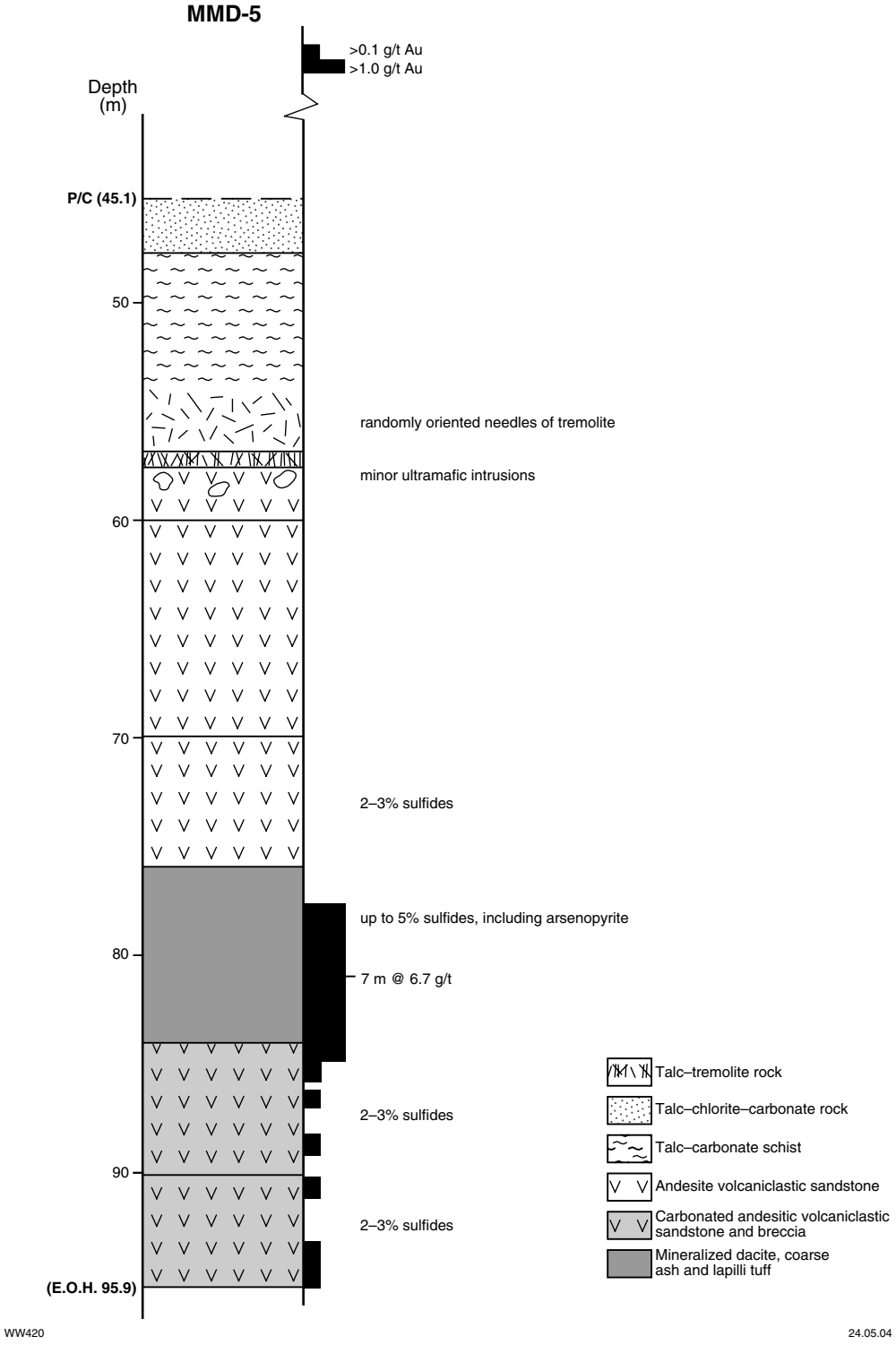

Figure 15.5. Summary log of diamond drillhole MMD-5, Mirror Magic deposit, Mount Monger

Table 15.1. Petrographic descriptions of rock units in diamond drillhole MMD-5, Mirror Magic gold deposit

Rock unit	*Lithology and petrography*	*Interpretation*	*Alteration*
Metamorphosed andesitic volcaniclastic unit	Well-sorted, matrix-supported, intermediate volcaniclastic sandstone. The unit is unbedded except for variation in the size of clasts on a scale of several metres or more. Lithic clasts and crystal fragments (1–2 mm) are contained within a fine- to medium-grained matrix of quartz, feldspar, and chlorite. Subangular to subrounded lithic clasts comprise very fine grained, leucocratic volcanic rock (dacite or rhyolite) and mesocratic clasts that contain 10–30% chlorite and biotite. Crystal fragments of quartz and plagioclase are less common than lithic clasts. Accessory minerals are titanite and rutile Coarser metavolcaniclastic units, containing lithic clasts up to several centimetres across, are interbedded with the metamorphosed volcaniclastic sandstone	This unit probably represents an immature volcaniclastic sandstone with a mixed, felsic to intermediate volcanic provenance	The meta-andesitic unit contains about 10% carbonate as disseminations and irregular aggregates. Several percent disseminated sulfides (mainly pyrrhotite, minor pyrite) are present below 70 m. Up to 20% of oriented sericite in the matrix defines a weak, anastomosing foliation
Metadacite	Unbedded, massive, leucocratic volcaniclastic rock with well-preserved, angular shard shapes up to 3 mm across	This unit is interpreted as a metamorphosed vitric lapilli and ash-flow tuff	Intense fracturing has produced quartz–carbonate veins up to 1 cm wide and hydraulic breccia. Extensive sulfidation has produced 2–5% fine-grained, disseminated pyrite and pyrrhotite, although arsenopyrite accounts for the full sulfide content in some sections. Disseminated carbonate (10%) and sericite (10–20%) are extensively distributed. Biotite and sulfides increase in abundance towards quartz–carbonate veins and veinlets

References

AHMAT, A. L., 1995, Geology of the Kanowna 1:100 000 sheet: Western Australia Geological Survey, 1:100 000 Geological Series Explanatory Notes, 28p.

CLARKE, E, De C., 1925, The geology of a portion of the East Coolgardie and Northeast Coolgardie Goldfields, including the mining centres of Monger and St Ives: Western Australia Geological Survey, Bulletin 90, 41p.

COX, K. G., BELL, J. D., and PANKHURST, R. J., 1979, The interpretation of igneous rocks: London, George Allen and Unwin, 450p.

ELLIS, H. A., 1944, Talc and soapstone deposits, Mount Monger, 37.5 miles southeast of Kalgoorlie, Western Australia: Western Australia Geological Survey, Annual Progress Report 1943, p. 10–11.

GRESENS, R. L., 1967, Composition–volume relationships of metasomatism: Chemical Geology, v. 2, p. 47–65.

HICKMAN, A. H., 1986, Stratigraphy, structure, and economic geology of the Mount Monger area, Eastern Goldfields Province: Western Australia Geological Survey, Report 16, 21p.

MIKUCKI, E. J., and HEINRICH, C. A., 1993, Vein- and mine-scale wall-rock alteration and gold mineralization in the Archaean Mount Charlotte deposit, Kalgoorlie, Western Australia: Australian Geological Survey Organisation, Record 1993/54, p. 135–140.

MT MONGER GOLD PROJECT PTY LTD, 1995, Annual report, May 1994 to Apr 1995, on Mount Monger gold exploration: Western Australia Geological Survey, Statutory mineral exploration report, Item 11663 A45072 (unpublished).

NELSON, D. R., 1995, Compilation of SHRIMP U–Pb zircon dates, 1994: Western Australia Geological Survey, Record 1995/03, 244p.

RAMSGATE RESOURCES LTD, 1992, Annual report, Apr 1991 to Apr 1992, on Mount Monger gold exploration: Western Australia Geological Survey, Statutory mineral exploration report, Item 11663 A36347 (unpublished).

RAMSGATE RESOURCES LTD, 1993, Annual report, May 1992 to Apr 1993, on Mount Monger gold exploration: Western Australia Geological Survey, Statutory mineral exploration report, Item 11663 A38628 (unpublished).

SWAGER, C. P., 1995, Geology of the greenstone terranes in the Kurnalpi–Edjudina region, southeastern Yilgarn Craton: Western Australia Geological Survey, Report 47, 31p.

SWAGER, C. P., 1997, Tectono-stratigraphy of late Archaean greenstone terranes in the southern Eastern Goldfields, Western Australia: Precambrian Research, v. 83, p. 11–42.

16. Linden

The Linden mining centre is located immediately south of Lake Carey, near the abandoned townsite of Linden. It lies within the high-strain Laverton Tectonic Zone of Hallberg (1985) and the Linden Terrane of Swager (1997). The Linden Fault, which forms the western boundary of the Linden Terrane, lies 2–3 km west of the main group of mines. A large area of granitoid gneiss and intrusive granite lies several kilometres to the east of the Linden mining centre. The greenstones in the Linden area consist of mainly ultramafic to mafic rocks (metabasalt and metamorphosed komatiitic basalt) with minor interbeds of ferruginous metachert. Several metadoleritic units intrude the mafic volcanic rocks, and one of these, in the northeastern part of the mining centre, is a layered sill consisting of metamorphosed peridotite, gabbro–norite, gabbro, dolerite, anorthosite, and granophyre. To the south, these rocks are interbedded with meta-andesite and metamorphosed felsic volcaniclastic rocks. The greenstones form the upper part of Association 2 of Hallberg (1985) and exhibit greenschist-facies metamorphic assemblages. In the Linden area, the greenstones define open to moderately tight, northwest-plunging folds. These are probably equivalent to the regional D_2 folds of Swager (1995). A distinctive feature of the district is the large number of granitoid plutons and irregular bodies of feldspar–quartz porphyry. The largest granitoid pluton (about 10 km in diameter) is centred on Kurrajong Well. The Kurrajong Monzogranite intrudes northwest-plunging folds and was therefore emplaced after folding.

The Linden mining centre has produced about 2 t of gold, mainly from the Democrat (641 kg Au), Bindah (349 kg Au), and Local Lady (280 kg Au) deposits. Although small openpit developments in the 1980s produced further gold from Bindah and Second Fortune, the ore was crushed elsewhere and production has been incorporated with other, larger production centres in MINEDEX. The more significant production took place in the late 19th and early 20th Centuries. There is no single preferred host rock to gold mineralization in the Linden area. The larger deposits are in ultramafic and mafic rocks and metamorphosed felsic volcaniclastic rocks.

Gold mineralization in the Linden mining centre appears to have formed in response to the partitioning of regional stress around the Kurrajong Monzogranite and therefore must have formed after regional folding. There are two main structural regimes where gold is found: in the pressure shadow at the northern end of the Kurrajong Monzogranite, and in high-strain zones on the western and eastern margins of the intrusion.

Most of the deposits are located in what would have been a strain shadow to the north of the Kurrajong Monzogranite during post-folding, regional east–west to east-northeast–west-southwest compression. Low mean stress in the pressure shadow of the Kurrajong Monzogranite promoted fracture dilation of the greenstones and focused flow of hydrothermal fluids into these dilational sites. Dilational sites (vein arrays and hydraulic breccias) formed in brittle–ductile shear zones that were localized at the contacts between felsic porphyry dykes and stocks and mafic to ultramafic country rocks, as a result of the competency contrast between the intrusions and the greenstones. Of far greater economic significance are the relatively brittle veins and vein arrays (Democrat and Local Lady) that formed in ultramafic rocks, at a large angle to the north-northwesterly oriented regional fabric.

Gold is also present in brittle–ductile shear zones in high-strain zones on the western (Great Carbine, Second Fortune, and Linden Star) and eastern (Bindah) margins of the Kurrajong Monzogranite. The mineralized shears are parallel or subparallel to the contacts between the monzogranite and the greenstones. These high-strain zones are comparable to those along the eastern margin of the Granny Smith Granodiorite, which is also in the Laverton Tectonic Zone, 54 km north of Linden. The Granny Smith deposit (35 700 kg Au) is a mineralized stockwork of quartz veins in the eastern margin of the granodiorite intrusion. It formed in a domain of low mean stress adjacent to a contact-parallel high-strain zone that developed in response to the competency contrast between the pluton and the greenstones (Ojala et al., 1993).

Hydrothermal alteration related to gold mineralization at Linden varies with the nature of the host rock, but is generally compatible with a relatively low temperature (300–400°C) environment (Mueller and Groves, 1991; Witt, 1991). Ultramafic rocks have been altered to talc–chlorite–carbonate(–biotite) assemblages, and mafic rocks have been altered to chlorite–carbonate–sericite assemblages. Biotite is present with sericite and chlorite in mineralized metabasalt at Lake View and Boulder East. Mineralized felsic rocks (porphyry intrusions and metamorphosed volcaniclastic sedimentary rocks) have been silicified and sericitized but contain relatively minor amounts of carbonate. All mineralized assemblages contain pyrite as the main sulfide phase. Many of the deposits contain minor chalcopyrite, but the Bindah and Second Fortune deposits contain a significant copper component as chalcopyrite, malachite, and digenite. Minor garnet and tourmaline are present in the alteration assemblages at Second Fortune.

Comparison with the Granny Smith area suggests that there is further exploration potential for gold mineralization in high-strain zones along the western and eastern sides of the Kurrajong Monzogranite. The contact zones of the monzogranite intrusion, especially along the eastern margin, warrant further investigation for Granny Smith-style mineralization.

The interpreted geology of the Linden area is shown in Figure 16.1. Ferruginous metachert horizons outline a northwest-plunging anticline around Mount Linden, with poorly exposed intermediate and sedimentary rocks in its core. Just north of the fold closure are talc–chlorite schists that host the Golden Ridge, Wimmera, Local Lady, Democrat, and Compensation deposits. North of this unit

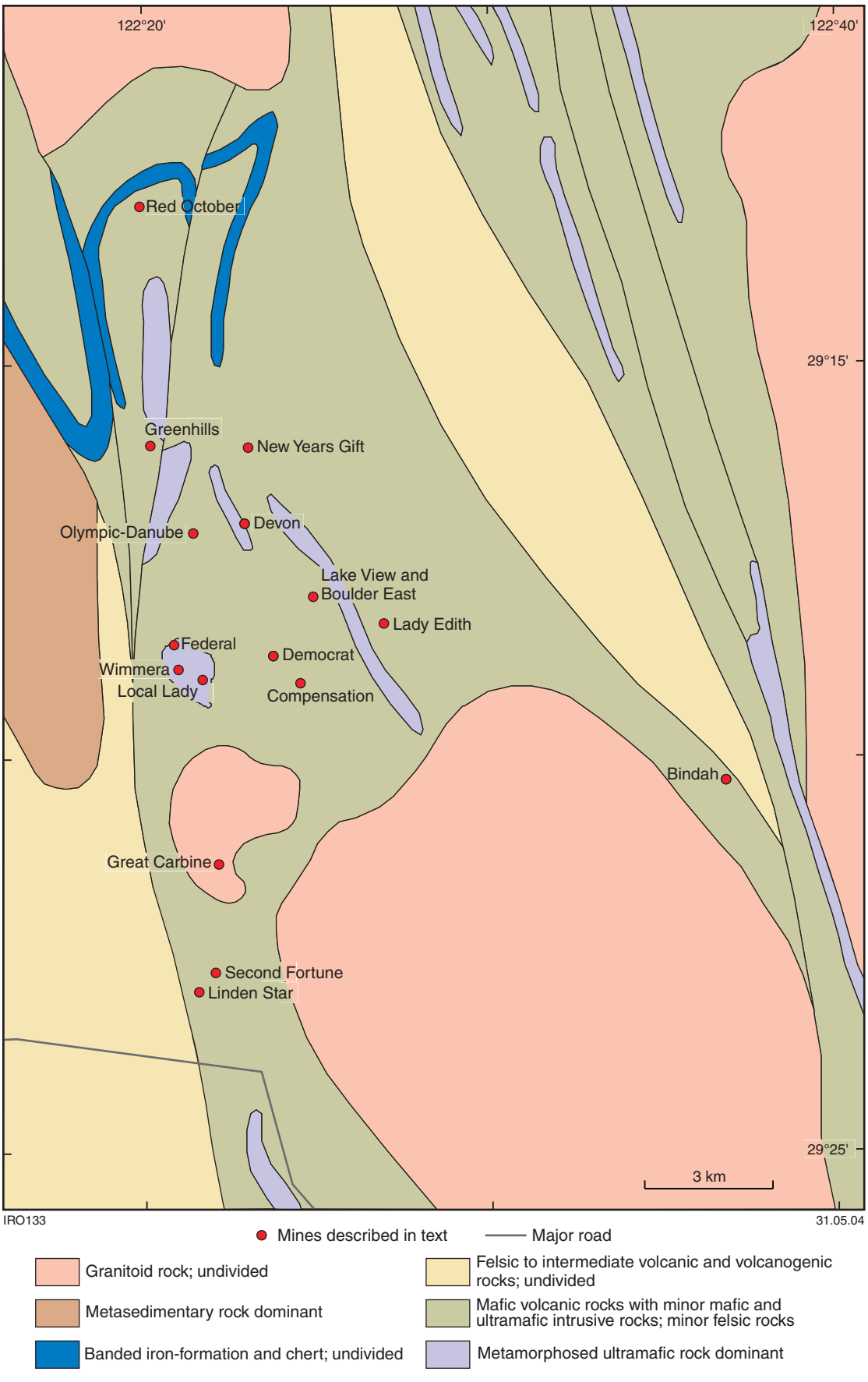

Figure 16.1. Interpreted geology of the Linden area

is a 'wedge' of metamorphosed komatiitic basalt interbedded with several ferruginous metachert horizons. This sequence is generally well exposed. The metamorphosed komatiitic basalt commonly exhibits a variolitic texture in some areas, and in others is metamorphosed to a tremolite–chlorite schist. Pillow structures and small amounts of hyaloclastite have been recognized in this metabasalt on the dumps at the Danube mine.

A large body of metaperidotite cuts the metachert and metamorphosed komatiitic basalt to the west and is host to the Greenhills gold mine, where it has been converted to talc–chlorite schist. Along the northeastern margin of the metamorphosed komatiitic basalt is a differentiated sill consisting of metamorphosed peridotite, gabbronorite, anorthosite, granophyre, gabbro, and dolerite. This sill is host to the Torquay and possibly the Lake View Boulder East gold mines. Metamorphosed tholeiitic basalt lies to the east of the sill and is host to the Lady Edith mine.

To the south of the main mining centre, lie the Great Carbine and Second Fortune gold mines. Unlike the other deposits in the area, these are hosted in metamorphosed felsic and sedimentary rocks. Great Carbine is hosted by a fine-grained deformed dacitic porphyry, which is probably a volcanic rock. Second Fortune is within a sequence of metamorphosed felsic volcaniclastic rocks, metashales, metatuffs, and a coarse-grained metamorphosed felsic volcanic conglomerate.

A distinctive feature of the Linden area is that it has been intruded by small granite pods, and numerous irregular bodies and dykes of feldspar–quartz porphyry (Fig 16.1). All of the mines studied either lie on contacts between the host rocks and these intrusions, or are in very close proximity to them.

The Linden mining area lies within the interpreted position of the Laverton Tectonic Zone of Hallberg (1985). There are two major north-trending sinistral faults in the Linden area; these have been named the Olympic and Quartz Ridge Faults and are thought to converge to the north under Lake Carey (Shaw and Associates, 1993). The Olympic Fault is host to the Olympic and Danube mines. The Quartz Ridge Fault runs from east of the Democrat mine through to New Years Gift. Its surface expression is marked by a series of vein-quartz outcrops. Some of the deposits such as Devon, and Lake View and Boulder East G.M., may be related to splays of these faults.

Gold is hosted in narrow lodes generally less than 0.5 m wide. It is in quartz–carbonate–sulfide stringer zones and veins, although with the exception of Second Fortune, quartz-vein material is not significant. There is a strong correlation between sulfide content and gold grade. With the exception of the Devon mine, which is arsenopyrite dominated, all of the mines in the Linden area have pyrite as the main sulfide with chalcopyrite as a common accessory. The Bindah mine is relatively copper rich, containing native copper and traces of bornite in addition to chalcopyrite. Carbonate and chlorite are the main alteration assemblages at Linden, with smaller amounts of sericite, biotite, and tourmaline found in some of the mines.

Deposits of the Linden area

Greenhills

Coordinates: 29°16'11"S, 122°25'06"E

Production: 3813.1 t of ore for 184.11 kg Au (48.3 g/t Au) between 1898 and 1909, and in 1973.

Host rock: Mineralization is hosted by metamorphosed felsic porphyry intrusions and talc–chlorite–carbonate schist after peridotite, and is mostly along the contact between these two rock types.

Structure: Mineralization was accessed by several shafts, most of which have been incorporated into a north-trending openpit (flooded at time of visit). The deepest shaft was worked down to 40 m and the lode was documented as being 1–2 m wide (Honman, 1917). Quartz-vein material found on the dumps is up to 20 cm across, but usually forms thin quartz–carbonate stringers about 1 cm wide that are parallel to, and crosscut, the foliation. The ore zone is thought to be steeply west dipping (Burrows, 1985). There is a minor outcrop with an anastomosing foliation that strikes between 330° and 010° and wraps around relatively low strain, centimetre-scale domains of ultramafic rock.

Alteration: Serpentinized metaperidotite has been altered to talc–carbonate–chlorite rock. The felsic porphyry is silicified and carbonated and is intersected by numerous thin carbonate and quartz veinlets. Both rock types contain minor disseminated pyrite. There is significant enrichment of gold in the oxidized zone and visible gold has been documented (Burrows, 1985).

References: Honman (1917), Burrows (1985).

Olympic

Other names: Jack and Doris, True Blue Leases

Coordinates: 29°17'05"S, 122°25'55"E

Production: 631.5 t of ore for 26.06 kg Au (41.3 g/t Au) between 1897 and 1920, and in 1971.

Host rock: Mine workings are hosted in weathered metamorphosed komatiitic basalt, in between two ferruginous metachert horizons (Fig. 16.1).

Structure: Several shafts and two open stopes lie on a mineralized shear zone that strikes 330° and dips steeply to the east. This structure, named the Olympic Fault, also hosts the adjacent Danube mine to the south. The shear zone is about 1 m wide and contains a quartz reef that varies from a few centimetres to 0.6 m wide.

Historical investigations found that there is a shoot about 11 m long that pitches about 30°S. There is also a footwall reef; the intersection between this and the lode pitches about 45° to the north. Honman (1917) suggested that there is a series of parallel shoots that begins where the lode intersects with the footwall reef, as shown in Figure 16.2.

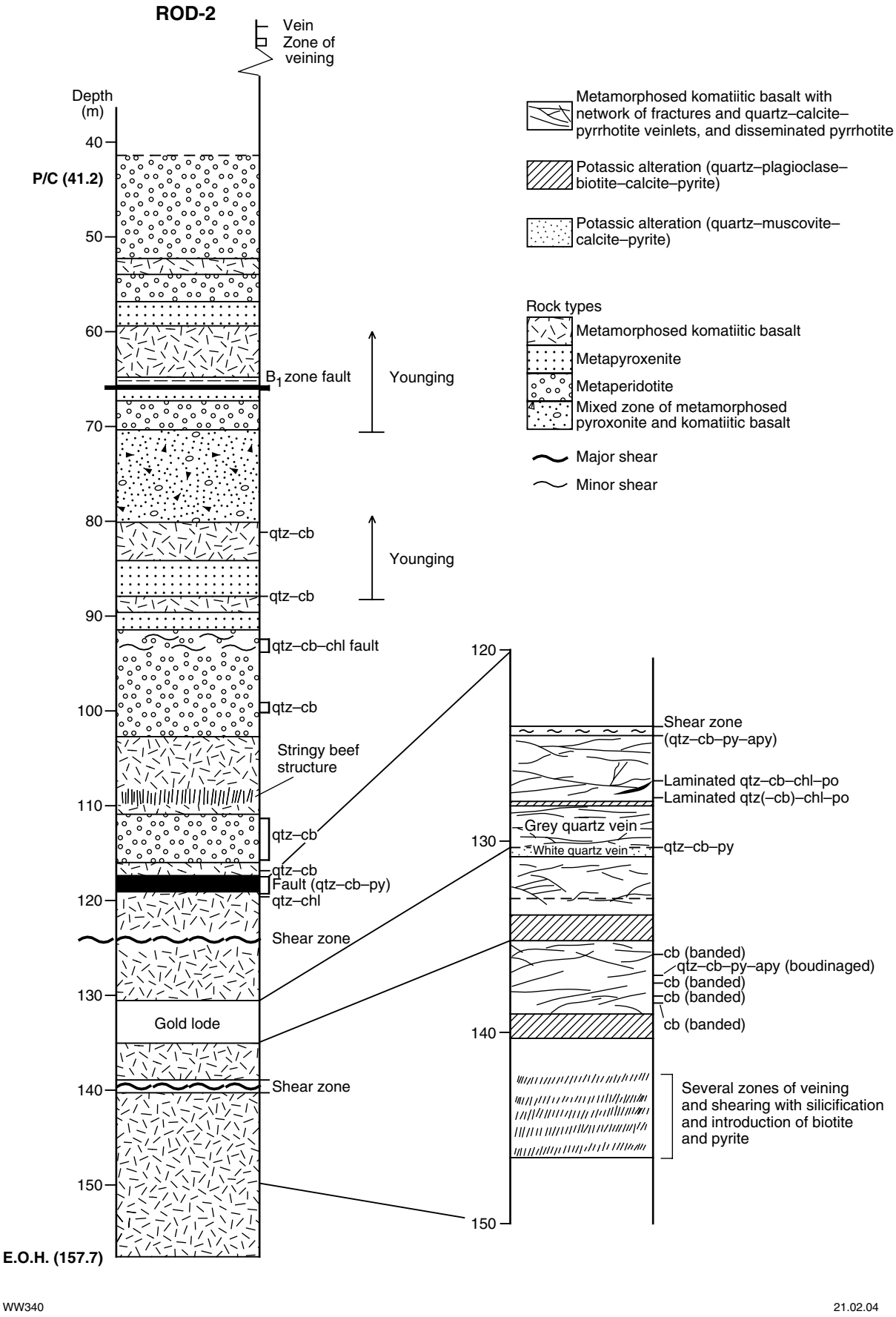

Figure 16.2. Summary log, diamond drillhole ROD-2, Red October deposit, Linden mining area

Alteration: Alteration is obscured by weathering.

References: Honman (1917), Shaw and Associates (1993).

Danube

Coordinates: 29°17'13"S, 122°26'01"E

Production: 895.4 t of ore for 29.74 kg Au (33.2 g/t Au) between 1911 and 1919.

Host rock: Metamorphosed variolitic komatiitic basalt hosts the deposit. Some primary features have been preserved, including pillow structures and hyaloclastite. A steeply west dipping felsic porphyry dyke outcrops just to the east of the workings and probably cuts the lode at depth.

Structure: The Danube lode is continuous with that of the Olympic gold mine, along the Olympic Fault. Several shafts and open stopes were placed into four ore shoots in the lode, over a surface distance of about 115 m. Historical studies (Honman, 1917) report that the longest shoot is about 30 m on the surface. North of this are two vertical shoots about 23 m and 8 m long. The lode dips steeply to the east and is no greater than 0.5 m wide. A quartz seam is reported to be on either side of the shear zone.

Alteration: Within the Olympic Fault the host rock has been altered to an assemblage containing chlorite–carbonate–sericite–quartz–albite(–pyrite–chalcopyrite).

References: Honman (1917).

New Years Gift

Other name: New Years Gift G.M. Co. Ltd

Coordinates: 29°16'06"S, 122°26'30"E

Production: 538.0 t of ore for 12.25 kg Au (22.8 g/t Au) between 1899 and 1912.

Host rock: Dump material around the deepest shaft comprises metamorphosed komatiitic basalt and medium-grained meta-quartz-dolerite. Felsic porphyry intrusive rocks have also been documented (Thompson, 1991), and recent drilling confirms that these are common (Peters, J., 1996, written comm.).

Structure: Several shafts and shallow pits form a line that trends 345° over a distance of about 250 m. The main shaft lies about 15 m to the east of this line. One dump contains abundant milky vein quartz, with a maximum block size of 0.5 m across. The metabasalt is strongly jointed and the metadolerite has a weak foliation. Exploration drilling has delineated a steeply east dipping mineralized zone.

Alteration: Meta-quartz-dolerite has the assemblage chlorite–carbonate–quartz–plagioclase–leucoxene. In addition to these minerals, the metamorphosed komatiitic basalt contains epidote, titanite, amphibole, and pyroxene.

References: Thompson (1991).

Devon

Other names: Torquay Leases, Devon Leases, Devon deep levels, Westralia United Goldfields Ltd, Dreadnought, Dreadnought South

Coordinates: 29°17'05"S, 122°26'29"E

Production: 11 043.1 t of ore for 210.95 kg Au (19.1 g/t Au) between 1913 and 1947.

Host rock: Mineralization is hosted by a layered sill comprising metamorphosed gabbro, dolerite, leucodolerite, quartz dolerite, and granophyre. Metadacite and metamorphosed porphyritic basalt are also found on some of the dumps.

Structure: The Devon leases extend over 500 m into Lake Carey to the south. The mineralized structure strikes about 330°, dips moderately to the southwest, and is interpreted as having a reverse sense of movement (Shaw and Associates, 1993).

Historical observations of the workings (Honman, 1917) describe two lodes. The main lode is within a shear zone, up to about 30 cm wide, striking 330° and dipping 50°W. This lode is cut by a footwall lode that comes in from the north, striking 340° and dipping 55°W. The highest grades were found in the main lode between the Main shaft and Dreadnought shaft, where a 107 m-long block was stoped out between depths of about 6 and 15 m.

The lode in the northern workings is small. Underground workings that extend into the lake have not been documented due to inaccessibility.

There is little evidence of thick quartz-vein material on the mine dumps, with the largest quartz vein observed being 7 cm across. Dump samples are generally weakly deformed and contain irregular quartz–carbonate–sulfide veinlets less than 1 cm wide (average width 1–2 mm). Some samples have slickensided surfaces, indicating movement along fault surfaces.

Alteration: Mafic rocks from this deposit have the alteration assemblage chlorite–carbonate–plagioclase–sericite–leucoxene–sulfides. Quartz veinlets contain carbonate as well as subhedral arsenopyrite, minor pyrite, and a trace of chalcopyrite and covellite. Historic observations document that the best grades coincide with where sulfides are prominent.

References: Honman (1917), Blatchford (1927), Shaw and Associates (1993).

Lake View and Boulder East G.M. Co. Ltd

Other names: Lake View and Boulder East G.M. Co. Ltd, Hoffnung, Blair Athol Leases, Hill East

Coordinates: 29°18'02"S, 122°27'25"E

Production: 893.1 t of ore for 43.12 kg Au (48.3 g/t Au) between 1897 and 1909.

Host rock: The deposit is hosted by a fine-grained mafic rock (probably metabasalt).

Structure: One deep shaft and three smaller shafts lie in a line that trends about 100° over 50 m. Vein quartz on the dumps is up to 20 cm wide. The host rock is also intersected by numerous quartz–carbonate veinlets, averaging 5 mm wide, that are both parallel to, and transgressive across, the moderate to strong foliation, and many are folded.

Alteration: The host rock has been altered to a chlorite–biotite–sericite–carbonate assemblage. Selvages around the veins have a higher proportion of chlorite and biotite. Veinlets of quartz and carbonate contain pyrite (some of which have been pseudomorphed by goethite), minor pyrrhotite, and chalcopyrite. Sulfides are also disseminated throughout the rock and are present on fracture surfaces.

References: Peters, J. (1996, written comm.).

Lady Edith

Other name: Reward, Audy Fisher

Coordinates: 29°18'20"S, 122°28'28"E

Production: 192.8 t of ore for 14.44 kg Au (74.9 g/t Au) between 1899 and 1916.

Host rock: The deposit is hosted by metabasalt that has been intruded by a metamorphosed feldspar–quartz–(?hornblende) porphyry.

Structure: Two shafts and a shallow digging form a line that trends 300° over about 100 m. The pit exposes a faulted contact, dipping steeply to the southwest, between metabasalt and metaporphyry. A 5 cm-wide, discontinuous quartz vein lies on this contact, and the adjacent metabasalt and metaporphyry are locally brecciated.

A second shallow pit lies at 340° to the westernmost shaft and is located wholly within metamorphosed felsic porphyry. The pit appears to have been centred on a joint plane that is gently folded and dips moderately to the southwest.

Alteration: Some of the quartz veins cutting metabasalt contain carbonate or coarse epidote. There is minor pyrite and ?chalcopyrite lining fracture surfaces, and goethite pseudomorphs after pyrite are weakly disseminated throughout the metaporphyry.

Federal

Other names: Golden Ridge, Lease 978R

Coordinates: 29°43'49"S, 122°28'24"E

Production: 463.99 t of ore for 18.82 kg Au (40.6 g/t Au) between 1898 and 1911.

Host rock: Medium-grained equigranular granodiorite with aplitic veins, talc–chlorite schist, and minor talc–chlorite–carbonate schist.

Structure: Two shafts about 20 m apart, as well as two small stopes immediately north, form a line that trends 350°. A quartz vein in one of the stopes follows the granodiorite–ultramafic contact, which dips moderately to the south-southeast. Quartz-vein material on the dumps is up to 40 cm wide. The granodiorite is cut by numerous thin comb-quartz veins with open spaces, possibly due to the weathering out of carbonate. Joints in the granodiorite dip steeply to the northwest, and those in the ultramafic rocks dip steeply south-southeast. Slickensides on the joint surfaces plunge shallowly towards the west-southwest.

Alteration: The granodiorite is sericitized and in some parts all minerals except quartz have been completely replaced by chlorite. Pyrite alteration is present in both rock types and is typically replaced by goethite in the more weathered rocks.

References: Maitland (1903).

Democrat

Other names: North Democrat, Moree

Coordinates: 29°18'45"S, 122°26'51"E

Production: 11 189.7 t of ore for 640.70 kg Au (57.3 g/t Au) between 1908 and 1951.

Host rock: Tremolite–chlorite–carbonate(–talc) rock after metamorphosed komatiitic basalt or sedimentary rock, talc–chlorite schist, and minor metamorphosed quartz–feldspar porphyry are on the mine dumps.

Structure: One very deep shaft and three smaller shafts make up the main workings. In 1917 the main shaft of this mine was the deepest in the Linden mining centre at about 120 m depth. An irregular quartz reef strikes about 110° and dips 75° to the north.

The North Democrat workings form a line trending about 110°. Simple and laminated quartz vein material found on the mine dumps averages 5 cm in width. There are minor quartz veins up to 20 cm wide. Some of the thinner veins are boudinaged.

Alteration: Metamorphosed quartz–feldspar porphyry is strongly silicified, with hematite and carbonate alteration, and minor sericite, chlorite, and pyrite alteration. The mafic–ultramafic rocks are carbonated and contain varying amounts of chlorite, tremolite, and talc. Sulfides or magnetite, or both, constitute up to 5% of the mafic–ultramafic rocks and include varying proportions of pyrite, pyrrhotite, pentlandite, and chalcopyrite. One inclusion of unidentified ?Bi telluride was found in pyrite. The gold is mostly quartz-vein hosted, but a minor amount has also been found within the schist.

References: Honman (1917).

Wimmera

Coordinates: 29°18'53"S, 122°25'33"E

Production: 562.9 t of ore for 19.16 kg Au (34.0 g/t Au) between 1897 and 1909.

Host rock: Ultramafic–mafic schist.

Structure: Four shafts and several shallow diggings are in a cluster. Dump samples are strongly deformed, with narrow quartz–carbonate veins (typically 2–3 cm, but up to 15 cm wide), some of which are folded or boudinaged.

Alteration: Talc–carbonate–chlorite schists from the mine contain minor biotite and limonite pseudomorphs after pyrite. Quartz veins are rich in coarse carbonate (probably ankerite and siderite) and contain fine-grained tourmaline. Fine rosettes of gypsum less than 4 mm wide fill open spaces and are interpreted as a later groundwater feature.

Local Lady

Other names: Great Junction, Old Kelley, Lady Ethel, Ailsa

Coordinates: 29°18'58"S, 122°25'47"E

Production: 9558.8 t of ore for 280.50 kg Au (29.3 g/t Au) between 1898 and 1953.

Host rock: Talc–chlorite schist and fine-grained, buff-coloured metasedimentary rock are found on the mine dumps.

Structure: The structure at Local Lady is rather complex, with a cluster of several shafts and shallow diggings intersecting two broadly parallel reefs that strike northeast across northwesterly striking schists. Both the host rocks and the lodes are strongly deformed. The reefs follow an irregular path, both parallel to, and cutting across, the foliation in the host rocks and commonly forming quartz 'kidneys'. As of 1917, the main reef had been worked down to about 30 m. The northeastern end of this reef is said to be northwest dipping and the southeastern end dips to the southeast. Gold was apparently found in the quartz 'kidneys' and where the reef was contorted.

References: Honman (1917).

Compensation

Coordinates: 29°19'05"S, 122°27'15"E

Production: 528.3 t of ore for 8.72 kg Au (16.5 g/t Au) between 1935 and 1936.

Host rock: Small mine dumps of talc–carbonate schist are found on laterite outcrop.

Structure: One deep shaft and a few shallow shafts and diggings lie over about 200 m with no obvious strike. Only minor quartz was found on the dumps.

Alteration: Carbonate.

Bindah

Other names: New Bindah, Bindah G.M.s Ltd, Bindah Leases

Coordinates: 29°20'05"S, 122°33'13"E

Production: 26 984.7 t of ore for 349.14 kg Au (12.9 g/t Au) between 1913 and 1937. Opencut mining was conducted in the mid- to late 1980s, but no figures for modern production are available.

The openpit was flooded at the time of inspection, so the following description has been taken from various company reports.

Host rock: Mineralization at the Bindah gold mine lies along the contact between tholeiitic metabasalt and a package of komatiitic metabasalt and ultramafic units. These rocks have been intruded by several generations of felsic metaporphyry dykes, one of which also hosts mineralization.

Structure: Gold mineralization is present along three main lodes: the main, central, and west lodes. These are on or along a north-northwesterly trending fault that separates metabasalt to the west from komatiitic metabasalt and ultramafic units to the east. The main and central lodes trend between 310° and 320° and the west lode between 330° and 320°. The southern end of these shoots plunge steeply to the north.

Mineralization forms breccia infills of dilation zones along two subparallel shear zones. These infills consist of ferruginous quartz, carbonate, cherty material (some jasperoidal), and country rock.

The felsic dykes generally lie subparallel to the fault system and mineralization, and they intrude and are truncated by the shear zones.

Alteration: The main alteration phases documented are silica, carbonate, chlorite, and sulfides. There is ferruginous alteration and narrow quartz stringers around the lodes. Gold is free milling to a depth of about 40 m and is readily visible. At 17 m depth there is a 5 m-thick supergene enriched zone. Malachite is present at the top of the sulfide zone, which is between 27 and 38 m depth, and native copper forms a halo around the sulfide mineralization.

The sulfide assemblage is dominated by pyrite and smaller amounts of chalcopyrite. Traces of bornite, sphalerite, pyrrhotite, and arsenopyrite have been found, and nickel sulfide has been inferred from assay data. Sulfides form bands and blebs associated with Mg-chlorite between chert–quartz–carbonate layers.

References: Stewart (1986), Bonwick (1987).

Great Carbine

Other names: Greenhill G.M. Co. Ltd

Coordinates: 29°21'23"S, 122°26'03"E

Production: 2254.4 t of ore for 41.66 kg Au (18.5 g/t Au) between 1898 and 1923.

Host rock: Fine-grained, metamorphosed felsic to intermediate feldspar porphyry (probably felsic volcanic rock) is found on the mine dumps.

Structure: Several shafts and open stopes follow a reef that strikes 085° and dips steeply to the north. This joins

another line of shafts and stopes that trends northeast. The deepest reported workings go down to 37 m and follow quartz reefs up to 1 m wide.

Alteration: Free gold and pyrite have been found in the quartz. The host rocks are sericite, chlorite, and carbonate altered.

References: Maitland (1903), Honman (1917), Vigar (1985).

Second Fortune

Other names: Mess Fury, Star of the Sea

Coordinates: 29°22'38"S, 122°26'07"E

Production: Between 1937 and 1953 production was 686.8 t of ore for 11.72 kg Au (17.06 g/t Au). Recent production figures for Second Fortune are not available. The indicated resource is 77 000 t of ore at 12.6 g/t Au (970.2 kg; MINEDEX site code S00709).

Host rock: The Second Fortune gold deposit is hosted within a west-facing sequence of intercalated metamorphosed felsic volcaniclastic rocks, metashale, metatuff, meta-lapilli-tuff, and coarse-grained metamorphosed volcanic conglomerate (?meta-agglomerate), and is intruded by irregular metamorphosed albite porphyry bodies. The metaconglomerate is poorly sorted and made up of fine-grained felsic volcanic clasts with rare porphyry.

The succession has been divided into three broad units:

- The hangingwall sequence is composed of fine-grained metamorphosed felsic tuffs and local metashales, and tuffaceous metashales. This sequence includes a gold-bearing quartz zone associated with metashales.
- The reef sequence includes the main vein and numerous quartz veins and stringers in a zone of rapid facies changes. The host rocks are metaconglomerate, meta-lapilli-tuff, metashale, metamorphosed tuffaceous shale, fine-grained metatuff, and metamorphosed felsic porphyry intrusions.
- The footwall sequence consists of a metamorphosed coarse-grained, matrix-supported conglomerate with minor metatuff.

Structure: Gold mineralization at Second Fortune is hosted within a north-striking quartz vein that dips steeply to the west and has an arcuate trend, convex to the east. This vein is between 0.3 and 1.5 m thick, is discontinuous over a strike length of over 400 m, and is still present at 300 m depth. In addition to the main vein, there are a number of other quartz veins (possibly splays) and stringer zones in the hangingwall and footwall, some of which are gold bearing. The vein system is cut off at both the northern and southern ends by oblique faults.

The host rocks strike 350–360° and are subvertical to steeply west dipping and rarely steeply east dipping. They are moderately to strongly deformed, with a subvertical foliation striking 330°. There are two sets of cross-faults: one striking east–west and vertically dipping, and the other subparallel to the foliation direction. Clasts in the metaconglomerate have been stretched and plunge north, parallel to the foliation.

Alteration: The dominant alteration phases at Second Fortune are sericite, carbonate, chlorite, and pyrite. Other alteration minerals observed include chalcopyrite, garnet, tourmaline, rutile, biotite, digenite, covellite, and pyrrhotite. The alteration halo around the ore zone is intense but generally less than 0.5 m wide.

Most of the gold is in quartz veins, and is more abundant in the main vein than it is in the smaller splays or stringer zones; it is also more common near areas rich in sulfides and carbonate. Only a minor amount is found in the wall rocks. There is a strong correlation between the gold and sulfides, with the best grades where pyrite is most abundant. Gold is also found as inclusions in pyrite and within microfractures associated with quartz, calcite, garnet, pyrite, and digenite. These microfractures cut across the foliation and therefore indicate that some of the mineralization is post-deformation.

Mineralized zones contain between 2 and 10% pyrite, disseminated throughout and less commonly filling late fractures. Pyrite is euhedral to anhedral and forms cubes up to 1 cm across. Chalcopyrite forms anhedral patches associated with pyrite, calcite, and quartz, and as inclusions in pyrite. Digenite partly replaces pyrite and heals fractured pyrite grains.

References: Mason (1987), Rutter (1987).

Linden Star

Other names: Oldfield Proprietary, Star

Coordinates: 29°22'55"S, 122°25'52"E

Production: 413.8 t of ore for 22.14 kg Au (53.5 g/t Au) between 1908 and 1916.

Host rock: Mafic to ultramafic schist.

Structure: Several shafts and open stopes follow a mineralized structure that trends 015° and then bends around to 130°. The lode is about 0.5 m wide and is made up of a stockwork of numerous quartz–carbonate stringers up to 5 cm wide.

Alteration: The host rock has strong carbonate alteration and contains minor pyrite.

References: Honman (1917).

Red October

Coordinates: 29°13'02"S, 122°24'57"E

Production: Production figures for Red October are not available. The inferred resource is 3.7 Mt of ore for 17 760 kg Au (4.8 g/t Au; MINEDEX site code S05338).

Host rock: The host rock is metamorphosed variolitic komatiitic basalt. In drillhole ROD-2, the host unit is separated by a fault (at around 119 m) from a series of metamorphosed layered komatiitic basalt – peridotite flows

(Fig. 16.2; Table 16.1). Contacts between many of the units in this sequence are gradational; macro-layering within metamorphosed fractionated komatiitic basalt flows indicates that the younging direction is uphole (i.e. towards the northwest).

Structure: The deposit is located at depths of up to 75 m beneath Lake Carey, in the Laverton Tectonic Zone of Hallberg (1985). Aeromagnetic data suggest that the host metamorphosed komatiitic basalt unit strikes roughly northeast and lies on the northwest limb of a tight fold, which has a northeast-trending fold axis. These trends are at a large angle to the dominant (northwest to north) regional structural grain. The folded sequence forms a narrow (about 2 km) slice of greenstones between north-striking faults.

The Red October deposit is located near the contact between metamorphosed komatiitic basalt and a less competent ultramafic flow sequence. Four subparallel, tabular zones of mineralization dip subvertically to steeply northwest. A fifth subparallel zone of mineralization, about 1.5 km northwest of Red October, has been named the Nautilus prospect. Individual zones at Red October are about 5–10 m wide and up to 50 m apart. Mineralization exists over a strike length of 900 m.

The main ore zone in ROD-2 (4.1 m of 8.87 g/t Au between 130.3 and 134.4 m) coincides with an interval of complex quartz veining and brecciation and the attendant potassic alteration zones (Fig. 16.2). This zone strikes northeast, roughly parallel to primary layering in the metabasaltic host rocks. Early, coarse-grained vein quartz is brecciated and cut by an irregular network consisting of numerous fractures, crush zones (cataclasis), and veinlets.

Table 16.1. Main rock types encountered in ROD-2, Red October deposit

Rock type	*Description*
Metaperidotite	Massive, medium-grained talc(–tremolite) serpentinite after olivine orthocumulate
Metapyroxenite	Massive, medium-grained tremolitic amphibole–chlorite(–plagioclase) rock with pseudomorphs after subsequant pyroxene (1–2 mm); probable cumulate layer at base of metamorphosed komatiitic basalt flow
Metamorphosed komatiitic basalt	Massive, medium- to coarse-grained tremolite–chlorite(–plagioclase) rock with pyroxene-spinifex texture; elongate prisms and needles (up to 2 cm long) after supercooled pyroxene are abundant and widespread; 'stringy-beef' texture at 109.8 – 110.0 m. Possible flow-top breccias observed in unit between 102.6 and 110.4 m. Variolitic texture is widespread in all metamorphosed komatiitic basalt units below 102.6 m

Adjacent zones of potassic alteration are relatively narrow (≤1 m) but contain one or more foliations. The footwall alteration zone contains millimetre-scale mineral banding and is overprinted by a pervasive fabric, defined by oriented micas, at 30–40° to the banding. Thin veins within this interval are locally boudinaged. The orientation of these fabrics with respect to the mineralized quartz vein is uncertain, but in ROD-2 the vein margin is transgressive across the mineral banding. The banding may represent a shear fabric that has been overprinted by a later regional shortening fabric. The main ore zone is enveloped in a broad zone (about 10 m wide) of intense fracturing and veinlets. These enveloping zones are generally uneconomic but contain a number of thin, discrete shear zones that are mineralized.

The mineralized lode is a brittle–ductile structure, but gold and sulfide minerals are closely related to brittle features such as quartz veins, fractures, and zones of cataclasis. The thickness of the mineralized quartz vein and enveloping zone of fracturing, compared to the thickness of the foliated wallrocks, suggest that gold deposition was related to a large-scale brittle deformation event. Brittle-deformation features overprint less-extensive ductile fabrics (e.g. mineral banding) that may have formed during an earlier period of contact-parallel shearing. These earlier structures may have acted as conduits for focused fluid flow and were therefore the locus for later, but more widespread, brittle deformation as a result of hydraulic fracture.

Alteration: The entire mafic–ultramafic volcanic sequence intersected by ROD-2 displays minor to moderate carbonation, characterized by the presence of carbonate porphyroblasts, fine-scale quartz–carbonate veining, and trace to minor pyrrhotite. Quartz–carbonate veinlets and fractures and disseminated pyrrhotite become more abundant in the broad zone (about 10 m wide) that envelops the ore zone. The ore zone consists of a complex quartz vein and relatively narrow (≤1 m) halos of potassic alteration (Fig. 16.2). Irregular zones of cataclasis, brecciation, and veining in the quartz vein are characterized by heterogeneous grain-size reduction of quartz and introduction of carbonate (calcite), muscovite, chlorite, and pyrite. Minor arsenopyrite and chalcopyrite accompany the pyrite. In addition, fine disseminations of several unidentified phases containing various combinations of Cu, Fe, As, Sb, and S phases were encountered in the course of SEM mineral analysis. Although the carbonate component of the vein is predominantly calcite, minor fine-grained euhedral rhombs of ankerite have also been identified. Potassic alteration in the footwall of the mineralized quartz vein consists of quartz–calcite–biotite schist with disseminated pyrite, minor arsenopyrite, and chalcopyrite. A similar assemblage is present in discrete shears in the hangingwall and footwall of the main ore zone, some of which are mineralized. The hangingwall to the mineralized quartz vein is characterized by a similar assemblage, but with muscovite instead of biotite. Some representative analyses of metamorphic and metasomatic minerals at Red October are given in Tables 16.2 – 16.6 and presented graphically in Figures 16.3 – 16.5.

Table 16.2. Selected SEM mineral analyses of metamorphic and metasomatic plagioclase

	GSWA 132946 metabasalt			*GSWA 132952 potassic alteration zone*		
				quartz–plagioclase–carbonate–biotite–pyrite		
	PLAG 9	*PLAG 10*	*PLAG 11*	*PLAG 2*	*PLAG 3*	*PLAG 6*
SiO_2	66.84	64.27	67.63	61.06	52.69	58.39
Al_2O_3	20.78	22.00	19.93	24.15	30.42	25.62
FeO	1.06	0.77	0.23	–	–	0.58
CaO	1.57	3.26	0.87	9.37	14.04	9.26
Na_2O	10.50	9.87	10.86	4.98	3.87	5.60
K_2O	0.08	–	0.10	0.07	–	0.41
Total	**100.83**	**100.17**	**99.62**	**99.64**	**101.02**	**100.36**
An	7.61	15.45	4.22	50.7	66.7	46.5
Ab	91.93	84.55	95.20	48.8	33.3	51.1
Or	0.46	–	0.58	0.5	–	2.4

Table 16.3. Selected SEM analyses of metamorphic amphibole and relict igneous pyroxene

	GSWA 132946 metabasalt					
	PX1	*PX3*	*PX4*	*AM1*	*AM2*	*AM5*
SiO_2	53.44	53.22	52.85	47.21	51.32	49.59
TiO_2	0.17	0.19	0.28	0.17	0.15	–
Al_2O_3	1.77	1.91	1.95	8.94	5.48	5.44
Cr_2O_3	0.36	–	0.41	–	–	–
FeO	7.14	8.80	7.52	17.16	13.01	19.45
MnO	–	0.19	–	0.23	0.28	0.22
MgO	18.14	19.28	18.25	11.38	14.43	10.21
CaO	19.76	16.74	18.39	12.03	12.51	12.28
Na_2O	0.21	–	0.22	0.92	0.52	0.70
K_2O	–	–	–	0.17	–	–
Total	**100.99**	**100.32**	**99.87**	**98.2**	**97.71**	**97.90**
Fe/Fe+Mg	18.10	20.4	18.77	45.8	33.6	51.7
Enstatite	49.9	46.8	51.1	–	–	–
Ferrosalite	11.0	12.0	11.8	–	–	–
Wollastonite	39.1	29.2	37.0	–	–	–

Table 16.4. Selected SEM analyses of carbonates

	GSWA 132952 potassic alteration zone		*GSWA 132950 ore vein*							
	quartz–plagioclase–carbonate–biotite–pyrite		*quartz–carbonate–pyrite*							
			late carbonate veinlet		*irregular disseminations*		*anhedral porphyroblasts*		*small, euhedral rhombs*	
	CB4	*CB5*	*CB6*	*CB8*	*CB10*	*CB13*	*CB15*	*CB16*	*CB17*	*CB19*
FeO	0.83	0.90	–	0.19	0.81	1.13	0.21	1.26	41.20	57.42
MnO	0.72	0.68	–	0.58	0.33	0.21	0.61	0.36	9.25	0.19
MgO	0.55	0.93	–	–	0.43	–	0.19	0.76	2.72	0.34
CaO	55.75	56.28	57.92	57.29	54.97	54.82	56.76	53.39	6.00	3.05
Na_2O	–	–	–	–	–	–	–	–	0.91	–
Total	**57.86**	**58.79**	**57.92**	**58.06**	**56.53**	**56.16**	**57.78**	**55.77**	**60.08**	**60.99**
$FeCO_3$	1.13	1.19	–	0.26	1.11	1.57	0.28	1.76	64.23	92.43
$MnCO_3$	1.00	0.91	–	0.78	0.46	0.29	0.84	0.51	14.60	0.31
$MgCO_3$	1.33	2.20	–	–	1.06	–	0.46	1.91	7.54	0.96
$CaCO_3$	96.55	95.69	100.0	98.95	97.36	98.13	98.41	95.82	11.07	6.29
Na_2CO_3	–	–	–	–	–	–	–	–	1.64	–
Nomenclature	Calcite	Calcite	Calcite	Calcite	Calcite	Calcite	Calcite	Calcite	Ankerite	Ankerite

Table 16.5. Selected SEM analyses of metasomatic biotite and chlorite

	GSWA 132952 potassic alteration zone			*GSWA 132950 ore vein*	
	quartz–plagioclase–carbonate–biotite–pyrite			*quartz–carbonate–pyrite*	
	BI1	*BI2*	*BI5*	*CH1*	*CH3*
SiO_2	36.99	38.14	39.12	31.93	30.64
TiO_2	1.58	1.66	1.50	–	–
Al_2O_3	18.26	17.66	21.40	15.98	15.63
Cr_2O_3	0.13	–	–	–	–
FeO	15.18	15.29	12.97	16.24	18.20
MnO	0.17	–	0.20	–	–
MgO	13.50	13.88	11.14	20.73	21.73
CaO	0.25	–	0.23	–	0.13
Na_2O	–	–	–	–	0.21
K_2O	9.80	10.08	8.00	1.76	0.17
Total	**95.84**	**96.70**	**94.56**	**86.64**	**86.71**
Fe/Fe+Mg	38.7	38.2	39.5	30.5	32.0

Table 16.6. SEM analyses of sulfide minerals

	GSWA 132951 ore vein (quartz–carbonate–pyrite)					
	S4	*S5*	*AY6*	*AY7*	*AY8*	*AY9*
Cu	77.47	77.06	–	–	–	–
Fe	1.32	1.26	35.36	34.23	34.81	34.48
As	–	–	44.28	44.54	42.60	43.05
S	20.01	20.14	22.77	21.06	22.35	22.31
Sb	0.30	0.20	–	0.23	0.27	0.30
Total	**99.08**	**98.66**	**102.42**	**100.06**	**100.03**	**100.14**
At.% Fe	–	–	32.7	32.9	33.0	32.7
At.% As	–	–	30.5	31.9	30.1	30.4
At.% S	–	–	36.7	35.2	36.9	36.8
Nomenclature	?Antimonial cuprite; ?Tetrahedrite		–	–	–	–
			–	–	–	–

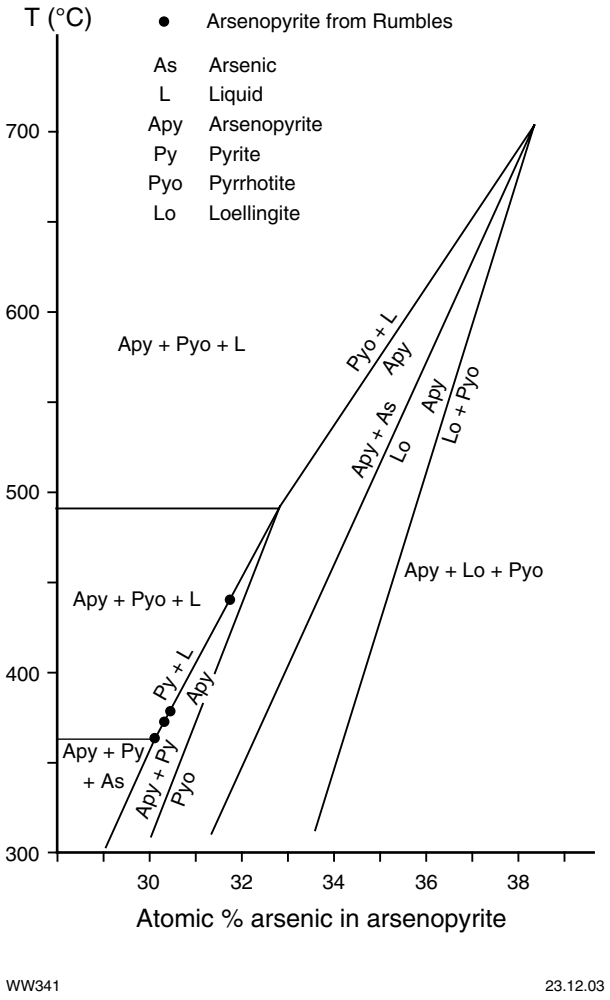

Figure 16.3. Arsenopyrite compositions, Red October, plotted on a diagram of temperature versus atomic% As in arsenopyrite (after Kretschmar and Scott, 1976)

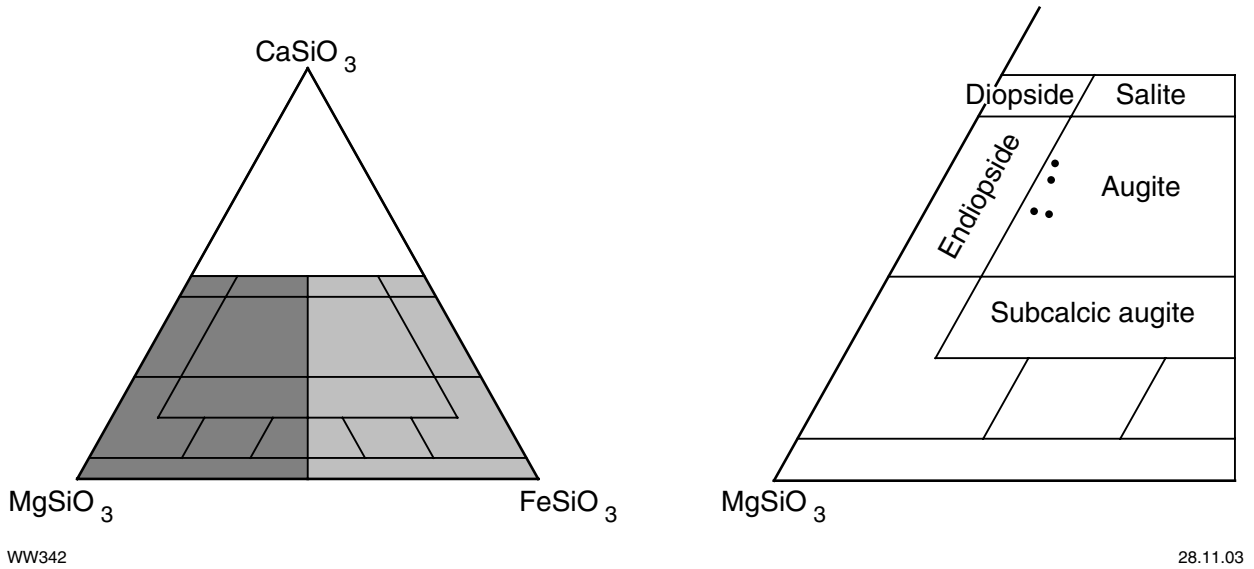

Figure 16.4. Compositions of relict igneous clinopyroxene from mineralized metamorphosed komatiitic basalt, Red October, Linden mining

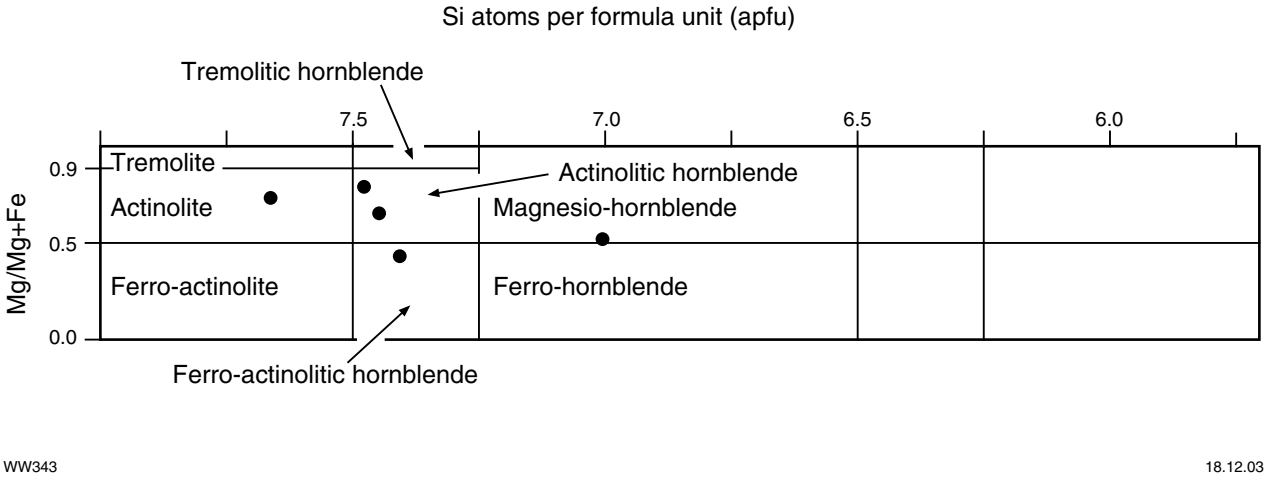

Figure 16.5. Compositions of metamorphic amphibole, Red October, Linden mining area

The main potassic alteration assemblages that accompany mineralization at Red October (biotite plus calcite dominant) suggest depositional temperatures of around 400–450°C (Mueller and Groves, 1991; Witt, 1991). These relatively high temperatures are supported by the presence of calcic plagioclase (andesine–labradorite) instead of albite in the alteration assemblages. Mineral banding defined by these minerals suggests that this higher temperature alteration may have been associated with the early, relatively ductile deformation proposed in the preceding discussion on the structure of the Red October deposit. Fine-grained, disseminated ankerite, and Cu–F–As–Sb–S phases in the ore zone probably indicate a lower temperature stage of mineralization that may be correlated with the muscovite-dominant alteration assemblage in the hangingwall of the main mineralized vein. Arsenopyrite compositions (Fig. 16.3) support a range of ore depositional temperatures, from almost 450°C to around 360°C.

Gold is typically fine grained (mostly <50 μm), sometimes has a vein-like character, and is occasionally argentian (Jones et al., 1997).

Mass-balance calculations using the method of Gresens (1967) indicate enrichment of the hangingwall alteration zone in CO_2, K_2O, CaO, and S (Fig. 16.6). Although the addition of CaO is somewhat unusual,

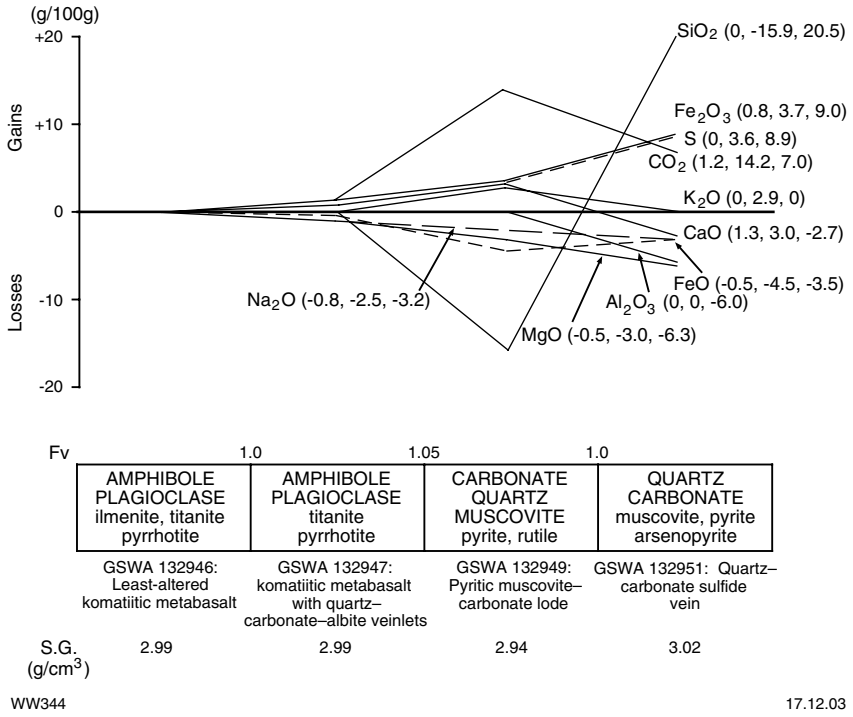

Figure 16.6. Mass-balance changes (calculated using the method of Gresens, 1967) associated with mineralized quartz–carbonate lodes, Red October, Linden mining area. Mineral components of alteration assemblages are listed in approximate order of abundance, with main mineral components in upper case and minor mineral components in lower case

enrichment of K, CO_2, and S is typical for hydrothermally altered rocks in lode-gold deposits (Kerrich, 1986; Barley et al., 1990; Witt, 1993). SiO_2 is depleted in the alteration zone, which may have been a source for SiO_2 deposited in the mineralized quartz vein. Although not analysed, the biotite-bearing alteration zones can be expected to display qualitatively similar chemical gains and losses.

References: Mt Burgess Gold Mining Co. NL (1994, 1995), Jones et al. (1997).

References

BARLEY, M. E., CASSIDY, K. F., GOLDING, S. D., GROVES, D. I., and McNAUGHTON, N. J., 1990, Alteration haloes, *in* Gold deposits of the Archaean Yilgarn Block, Western Australia: nature, genesis and exploration guides *edited by* S. E. HO, D. I. GROVES, and J. M. BENNETT: University of Western Australia, Geology Department (Key Centre) and University Extension, Publication no. 20, p. 317–327.

BLATCHFORD, T., 1927, Devon mine, Linden: Western Australia Geological Survey, Annual Report, 1926, p. 66–67.

BONWICK, C. M., 1987, Annual Report, Bindah Project: 1 July 1986 to 30 June 1987 by Western Mining Corporation Limited Exploration Division: Western Australia Geological Survey, Statutory mineral exploration report, Item 11651 A21501 (unpublished).

BURROWS, G. F., 1985, Summary Exploration Report, Greenhills Project P39/489, 633, 679–681, 769, Mt Morgans District, Mt Margaret Mineral Field, Western Australia. Edjudina Gold Mines Pty, Ltd.: Western Australia Geological Survey, Statutory mineral exploration report, Item 3803 A18243 (unpublished).

HONMAN, C. S., 1917, The Geology of the North Coolgardie Goldfield — Part I. The Yerilla District: Western Australia Geological Survey, Bulletin 73, 98p.

JONES, C., MOORE, J., and FLEMING, S., 1997, The discovery of the Red October gold deposit, Lake Carey, Western Australia, *in* New Generation Gold Mines, 1997: Australian Mineral Foundation, p. 12.1–12.9.

KERRICH, R., 1986, Archaean lode gold deposits of Canada: Part I — A synthesis of geochemical data from selected mining camps, with emphasis on pattern of alteration: University of Witswatersrand, Johannesburg, Economic Geology Research Unit Information Circular 182, 30p.

KRETSCHMAR, U., and SCOTT, S. D., 1976, Phase relations involving arsenopyrite in the system Fe–As–S and their application: Canadian Mineralogist, v. 14, p. 364–386.

MAITLAND, A. G., 1903, Notes on the country between Edjudina and Yundamindera, North Coolgardie Goldfield: Western Australia Geological Survey, Bulletin 11, 58p.

MASON, D. R., 1987, Native gold in drill core SFH21 from the Second Fortune gold mine, *in* Annual Report for Gold Mining Leases 39/706, 767, Appendix 4: Western Australia Geological Survey, Statutory mineral exploration report, Item 3014/1 A24487 (confidential)*.

* Confidential references are used with permission of companies

MUELLER, A. G., and GROVES, D. I., 1991, The classification of Western Australian greenstone-hosted deposits according to alteration mineral assemblages: Ore Geology Reviews, v. 6, p. 293–331.

MT BURGESS GOLD MINING CO. NL, 1994, Annual report, Jan 1993 to Dec 1993, on Butcher Well gold exploration: Western Australia Geological Survey, Statutory mineral exploration report, Item 11662 A40601 (unpublished).

MT BURGESS GOLD MINING CO. NL, 1995, Annual report, Jan 1994 to Dec 1995, on Camelback gold exploration: Western Australia Geological Survey, Statutory mineral exploration report, Item 11662 A43925 (unpublished).

OJALA, V. J., RIDLEY, J. R., GROVES, D. I., and HALL, G. C., 1993, The Granny Smith gold deposit: the role of hetergeneous stress distribution at an irregular granitoid contact in a greenschist facies terrane: Mineralium Deposita, v. 28, p. 409–419.

RUTTER, J. H., 1987, Annual Report for Gold Mining Leases 39/706 and 39/767, Second Fortune Mine, Linden area, Mount Margaret Goldfield, Period: 1/1/87–31/12/87: Western Australia Geological Survey, Statutory mineral exploration report, Item 11667 A24487 (unpublished).

SHAW, J., and ASSOCIATES, 1993, Haoma Northwest NL, Annual report year ending 18 September 1993, Linden Project E39/293, Mount Margaret Mineral Field W.A.: Western Australia Geological Survey, Statutory mineral exploration report, Item 11668 A39523 (unpublished).

STEWART, K. P., 1986, Annual Report on the Bindah Project for the Period 4 April 1984 to 30 June 1986, by Western Mining Corporation Limited Exploration Division: Western Australia Geological Survey, Statutory mineral exploration report, Item 11651 A18673 (unpublished).

SWAGER, C. P., 1995, Geology of the greenstone terranes in the Kurnalpi–Edjudina region, southeastern Yilgarn Craton: Western Australia Geological Survey, Report 47, 31p.

SWAGER, C. P., 1997, Tectono-stratigraphy of late Archaean greenstone terranes in the southern Eastern Goldfields, Western Australia: Precambrian Research, v. 83, p. 11–42.

THOMPSON, R. L., 1991, Initial exploration programme for 1991, Linden gold project, Western Australia, Annual Report for Sept 1990–Sept 1991, Haoma Northwest NL/ Consolidated Gold Mining Areas NL joint venture: Western Australia Geological Survey, Statutory mineral exploration report, Item 11668 A34576 (unpublished).

VIGAR, A. J., 1985, Map *in* STEWART, K. P., 1986, Annual Report on Great Carbine Project for the Period 1 January, 1985 to 31 December, 1985, Western Mining Limited, Exploration Division: Western Australia Geological Survey, Statutory mineral exploration report, Item 3210 A18359 (unpublished).

WITT, W. K., 1991, Regional metamorphic controls on alteration associated with gold mineralization in the Eastern Goldfields Province, Western Australia: implications for the timing and origin of Archaean lode-gold deposits: Geology, v. 19, p. 982–985.

WITT, W. K., 1993, Gold mineralization in the Menzies–Kambalda region, Eastern Goldfields, Western Australia: Western Australia Geological Survey, Report 39, 165p.

17. Butcher Well and Tin Dog Flats

The Butcher Well and Tin Dog Flats mining areas are in the northern extension of the Edjudina Terrane of Swager (1997), which is made up of felsic to mafic volcanic and metavolcaniclastic rocks with intercalated BIF. Prominent jaspilite ridges of the Edjudina Range outcrop just west of both mining areas. These mining areas lie within the Murrin Margaret Sector of Hallberg (1985), and the rocks in these areas are part of Association 2 immediately west of the Laverton Tectonic Zone. The metamorphic grade of this area is lower greenschist facies.

Both groups of deposits lie within the north-northwesterly trending Mount Hornet Shear Zone (which is interpreted to be 1 km wide) or associated splay faults. The Mount Hornet Shear Zone is a complex zone of ductile deformation marked by mylonitization, sheared lithological contacts, and syenite intrusions (Mt Burgess Gold Mining Co. NL, 1994). Recent exploration along this structure has identified several gold deposits.

The Butcher Well mining area to the north consists of eight known gold deposits and prospects over a strike length of about 2.5 km. The deposits are (from north to south) Marchelayo, Butcher Well North, Sizzler, Enigmatic North, Hronsky, Mambo, Enigmatic South, and Old Camp (Fig. 17.1).

There is no significant historic production recorded for the Butcher Well area. Three opencut mines exploited gold from the above deposits between April 1993 and 1994, firstly Butcher Well North and Enigmatic South, and then Hronsky. In total, these deposits, as well as Yundamindera, produced 1832.472 kg of gold. The pits were full of water at the time of field examination, so the following descriptions are based on drillcore logs from each pit and various company reports.

The Butcher Well deposits are located in a package of metamorphosed basalt, intermediate to mafic volcaniclastic rocks, black shale, and komatiitic basalt, within a broader sequence of schistose felsic volcaniclastic rocks. Some of these rocks have been deformed into chlorite schists. Metabasalt is the dominant host rock for the southern deposits, whereas at Butcher Well North, metamorphosed intermediate to mafic volcanic rocks and black shale interbeds host the mineralization. The mining area has been intruded by several generations of syenite, monzonite, and lamprophyre stocks, dykes, and veins. Lamprophyres identified include kersantite and camptonite (Bush, 1994).

A broad zone of chlorite schist envelops the relatively competent mafic host-rock package, in which primary volcanic structures and textures are widely preserved. This mafic rock package contains zones of moderately foliated sericite–carbonate–plagioclase rock and schist after mafic rocks.

Gold is typically associated with zones of intense, fine-scale fracturing (Fig. 17.2), and to a lesser extent brecciation (some of which may be primary; Fig. 17.3). Larger quartz veins (>1 cm) are uncommon and apparently unrelated to gold mineralization.

Ore zones are oriented north to north-northwest, dip steeply east and west, and tend to be associated with the contacts of the relatively competent mafic rock package. They are also commonly focused along the margins of syenitic stocks and dykes.

Fractures in the mineralized zones typically have bleached alteration halos in the order of 1–10 mm wide, some of which are red, reflecting the presence of fine-grained hematite. Where fracturing has been relatively intense, alteration halos merge into a broad zone of pervasive alteration containing the alteration assemblage carbonate–silica–sericite–albite–pyrite(–arsenopyrite). Gold is directly related to zones of intense silicification and sulfidation. This massive alteration assemblage overprints sericite–carbonate alteration associated with zones of ductile deformation. Strongly mineralized zones contain up to 10% sulfides, with euhedral to anhedral pyrite and slightly less abundant euhedral arsenopyrite. Other sulfides include anhedral chalcopyrite, which forms as disseminations or in fractures within pyrite, and very minor traces of sphalerite and galena.

No visible gold was observed in any of the three diamond drillholes logged. One strongly mineralized sample from the Butcher Well North deposit was examined for solid-solution gold using wavelength dispersive spectrometry, and analysed pyrite and arsenopyrite grains contained up to 150 and 460 ppm (by wt%) gold respectively (Mt Burgess Gold Mining Co. NL, 1994).

All of the deposits in the Butcher Well mining area have significant zones of supergene gold mineralization.

The Tin Dog Flats deposit, about 16 km south of the Butcher Well mining area, is also associated with the Mount Hornet Shear Zone. It is similar to the Butcher Well deposits, in that the mineralization is in intermediate to mafic volcanic and metavolcaniclastic rocks that have been intruded by syenite and lamprophyre dykes, veins, and stocks. Both mining areas show excellent preservation of primary rock textures and are characterized by brittle (fracture-related) rather than ductile deformation. Mineralization in both deposits is locally focused around contacts between the volcanic rocks and the intrusive bodies.

The deposits at Butchers Well and Tin Dog Flats are brittle structures spatially associated with the Mount Hornet Shear Zone, but post-date ductile movements on that structure. The competency contrast between the relatively thin package of mafic rocks and the broader expanse of felsic schists was probably important in creating local heterogeneity in the distribution of stress. On a smaller scale, the competency contrast between syenitic intrusions and volcanic country rocks would have played a similar role in localizing brittle failure and focusing of hydrothermal fluids in domains of low mean stress (cf. Oliver et al., 1990; Ridley, 1993). The mineralized brittle fault system comprises northerly trending, dextral, dip-slip (?reverse) faults and north-northwesterly trending P structures (Tchalenko, 1970). Offset on the

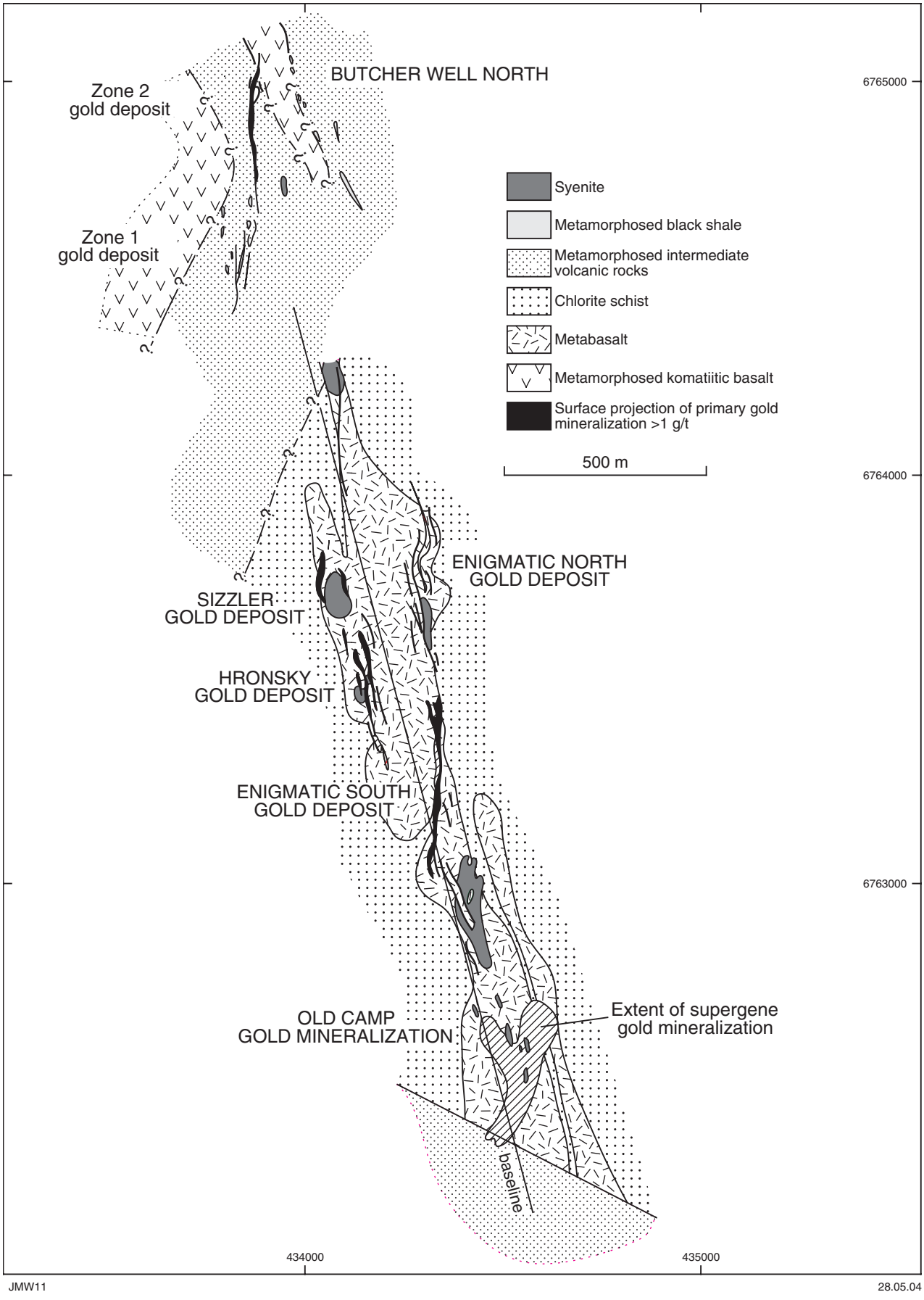

Figure 17.1. Sketch map of the Butcher Well mining area

northerly trending faults may have assisted the brittle deformation process by breaking the competent unit into smaller bodies in a situation similar to that at Mount Charlotte (Clout et al., 1990).

Deposits at the Butcher Well and Tin Dog Flats mining areas

Mount Florence

Other names: Camelback, Camel Back, Edna

Coordinates: 29°15'12"S, 122°16'52"E

Production: 496.6 t of ore for 10.33 kg Au (20.8 g/t Au) between 1911 and 1942.

Host rock: Host rocks are not exposed at the surface but mine dumps are composed of weathered schist after metamorphosed volcaniclastic sedimentary rocks.

Structure: Moderately deep shafts and pits extend over about 300 m on a bearing of 145°. The mineralized structure is subvertical to steeply northeast dipping, although the northernmost shaft has been sunk on a 170°-trending structure that dips 70°E. The nature of the orebody is not well exposed in the mine workings, but

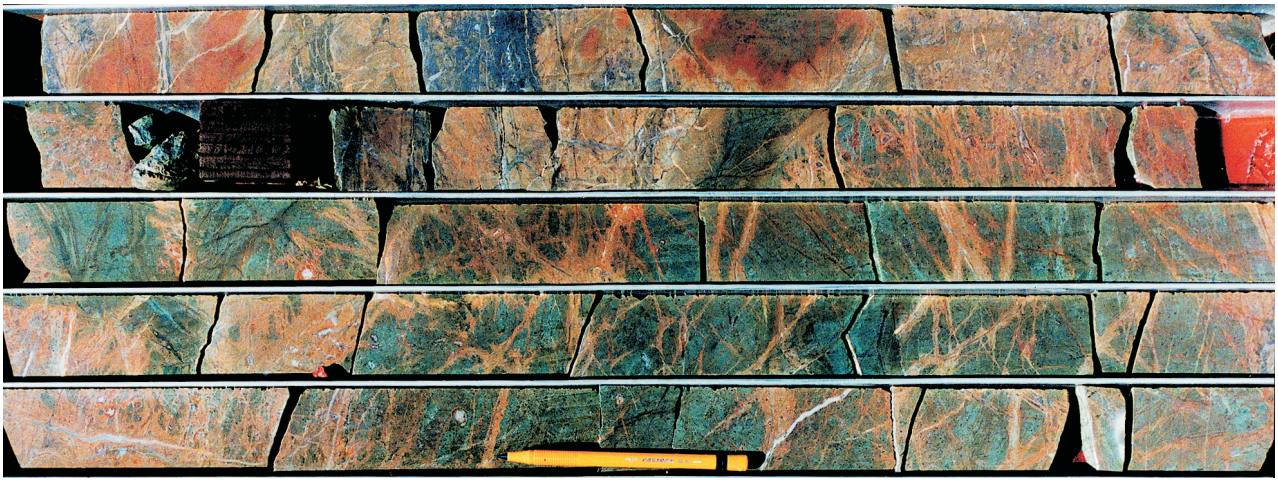

IRO138 03.05.04

Figure 17.2. Intense, fine-scale fracturing in drillcore from ESDH-7, Enigmatic South

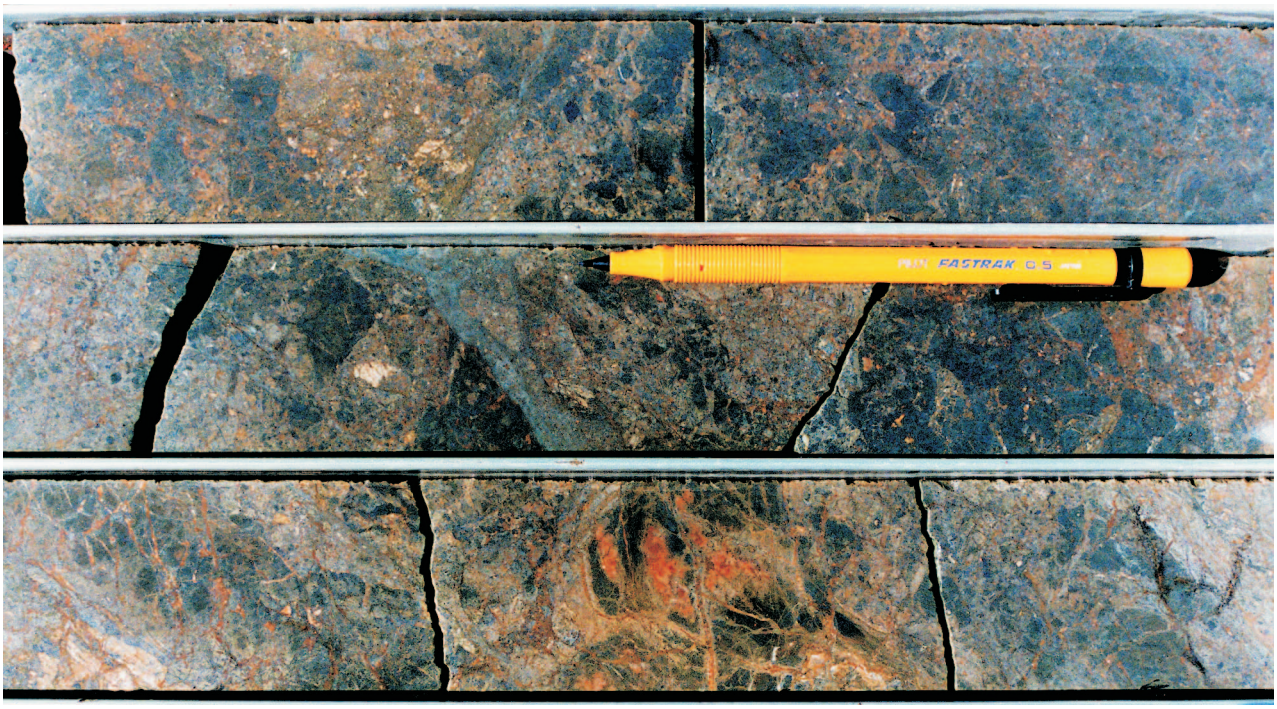

IRO139 03.05.04

Figure 17.3. Brecciation in drillcore from ESDH-7, Enigmatic South

mine dumps contain minor quartz–limonite (after ?pyrite) veins that probably came from a veined brittle–ductile shear zone.

Alteration: Alteration characteristics have been obscured by weathering.

Butcher Well North

Other names: Marchelayo

Coordinates: 29°14'42"S, 122°19'11"E

Production: A total of 198 006 t of ore at 2.99 g/t Au (592.0 kg Au) have been mined. A further resource (inferred) of 380 000 t at 2.80 g/t Au (1064 kg Au) remains at Butcher Well North.

Host rock: Gold is hosted mostly within very strongly altered intermediate to mafic metavolcaniclastic and volcanic rocks. Associated pyritic black metashale and metamorphosed komatiitic basalt are not major host rocks. A graphic log of diamond drillhole CMBD-15 is shown in Figure 17.4.

Structure: Butcher Well North lies in a sequence of rocks that strike 340°, subparallel to the regional foliation. Mineralization is in two moderately to steeply dipping planar zones of brittle deformation that strike 020° and cut the stratigraphy and regional foliation. The southern zone has a strike length of about 170 m and dips about 60°E. The northern zone has higher gold grades, and extends over a strike length of about 320 m, with a dip of about 75°W (Mt Burgess Gold Mining Co. NL, 1993). In CMBD-15, the mafic rocks become more foliated and altered as the ore zone is approached.

The Marchelayo prospect (MGA51 433890E, 6764850N) is the northernmost gold deposit in the Butcher Well area. It comprises a 200 m-long north-northwesterly trending zone of mineralization, subvertical to steeply east dipping and up to 9 m wide. It is probably structurally continuous with the Butcher Well North deposit (Mt Burgess Gold Mining Co. NL, 1994).

Alteration: Moderately foliated mafic to intermediate rocks that overlie the ore zone in CMBD-15 are altered to a non-pyritic carbonate–sericite(–quartz–plagioclase (?albite)–chlorite) assemblage. This style of alteration forms as relicts between anastomosing zones of chloritic alteration between 180–200 m. The resulting rock resembles a metaconglomerate, but is here interpreted as a pseudo-fragmental rock (Fig. 17.5).

The mineralized alteration assemblage comprises massive carbonate–sericite–chlorite–quartz–albite–pyrite(–arsenopyrite–chalcopyrite). Sulfides may constitute up to 10% of the strongly mineralized rocks. This alteration has resulted in the intense bleaching of the host rocks. The bleached mineralized alteration assemblage contains numerous fine-scale quartz–carbonate(–albite) veinlets.

Four samples of variously altered metabasalts from diamond drillhole CMBD-15 were subjected to whole-rock analyses (Appendix 5). On a TiO_2/Zr diagram (Hallberg, 1985) they plot in the metabasalt field (Fig. 17.6). Gresens (1967) mass-balance calculations indicate that CO_2, FeO, CaO, MgO, K_2O, and Fe_2O_3 were added to the least-altered metabasalt (already carbonated) to form the moderately foliated, altered, but unmineralized metabasalt (GSWA 130556; Fig. 17.7). These components were probably stabilized as ankerite and sericite. A mineralized pyritic metabasalt sample (GSWA 130558) formed by further addition of these same components and minor amounts of S. Formation of the most intensely altered sample (GSWA 130560) involved slight depletion of FeO, CaO, and CO_2, and addition of S, Na_2O, and SiO_2, as pyrite, arsenopyrite, albite, and quartz.

References: Mt Burgess Gold Mining Co. NL (1993, 1995).

Sizzler

Coordinates: 29°15'14"S, 122°19'12"E

Production: The Sizzler deposit has yet to be mined and, combined with the adjacent Enigmatic North area, has an estimated resource of 750 000 t of ore at 1.90 g/t Au (1425 kg Au; Jones, C., 1997, written comm.).

Host rock: The host rock is metabasalt intruded by syenite.

Structure: Mineralization at the Sizzler prospect is present over a strike length of about 200 m, flanking the western margin of a syenite intrusion. A parallel zone of primary mineralization is located about 50 m to the east, on the other contact of the syenite. Mineralization is largely supergene and has formed over a narrow, northerly trending shear zone, which is the northern extension of the main Hronsky shear structure (see **Hronsky/Mambo** below).

Alteration: No details are available.

References: Mt Burgess Gold Mining Co. NL (1994, 1995).

Enigmatic North

Coordinates: 29°15'16"S, 122°19'26"E

Production: This deposit has yet to be mined and, combined with the Sizzler deposit, has an estimated resource of 750 000 t of ore at 1.90 g/t Au (Jones, C., 1997, written comm.).

Host rock: The main host rock is metabasalt with smaller amounts of felsic rock.

Structure: Ore zones up to 5 m thick strike north–south and dip moderately to steeply to the west. The eastern margin of the mineralized zone is a shear zone within barren chlorite schist. The deposit itself is a zone of brittle fracture. The Z-shaped, sigmoidal ore zones suggest formation during dextral movement on the brittle fault.

A zone of supergene mineralization, which is subhorizontal and averages 4 m in thickness, overlies the deposit.

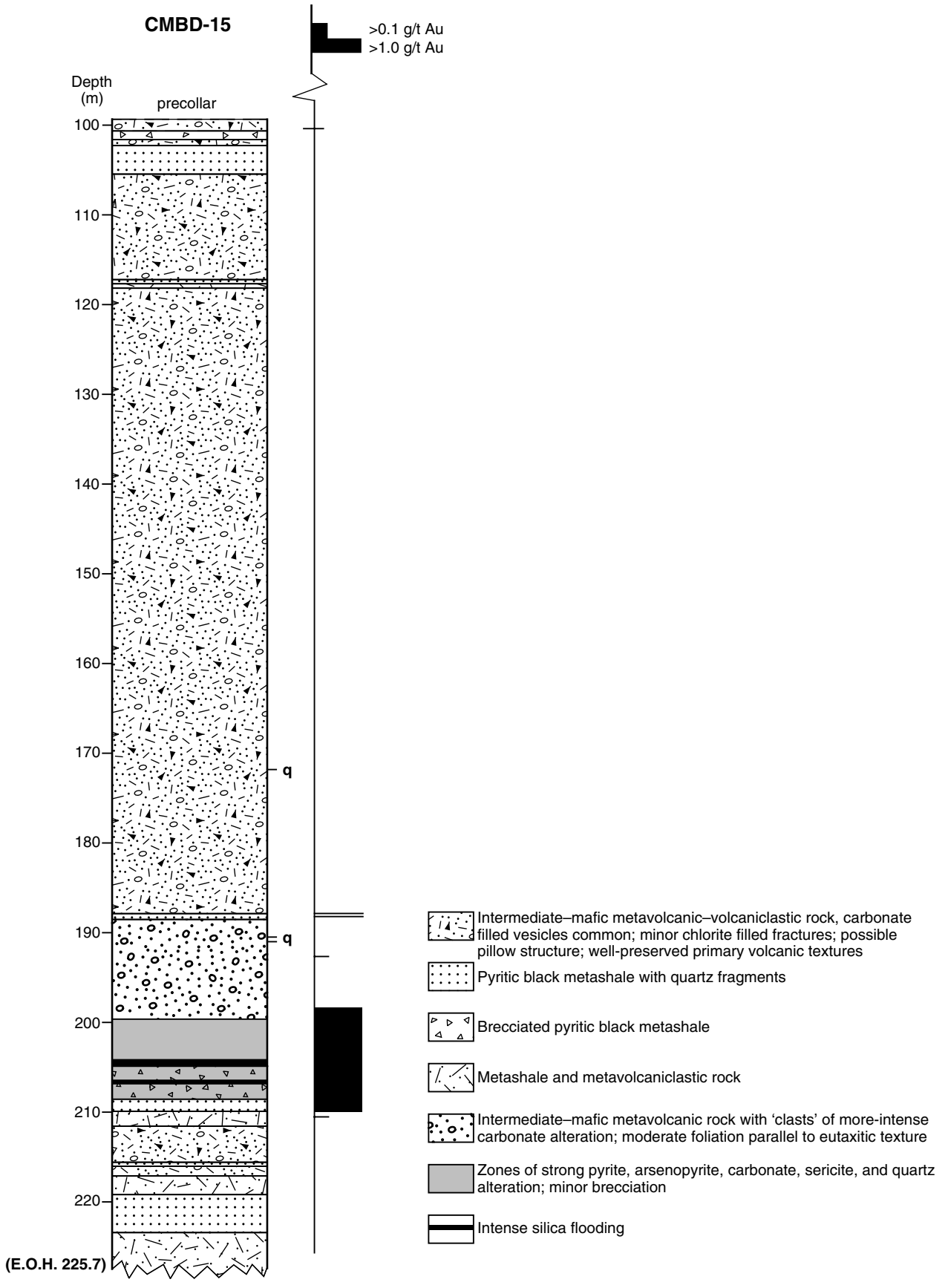

Figure 17.4. Summary log of drillcore from diamond drillhole CMBD-15, Butcher Well North

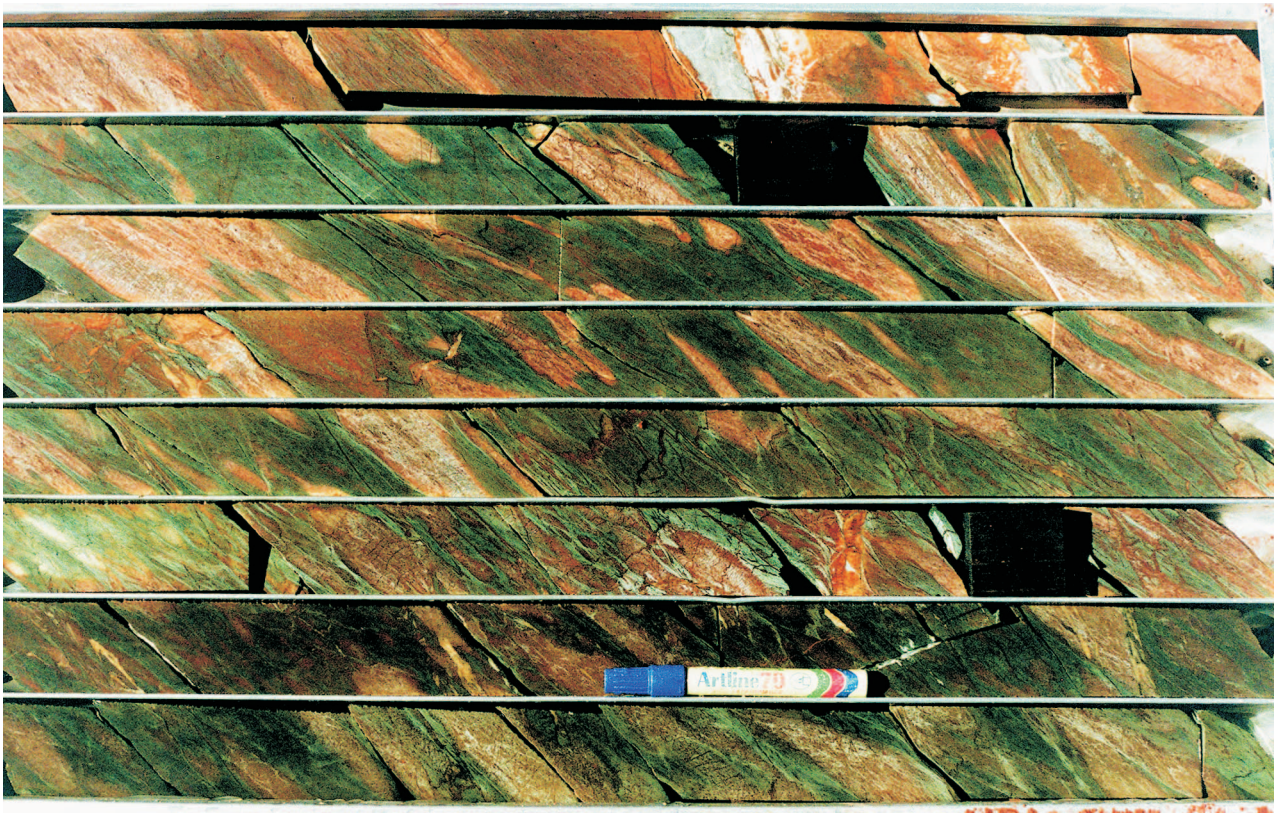

IRO140 03.05.04

Figure 17.5. Pseudo-fragmental rock from drillhole CMBD-15, Butcher Well North

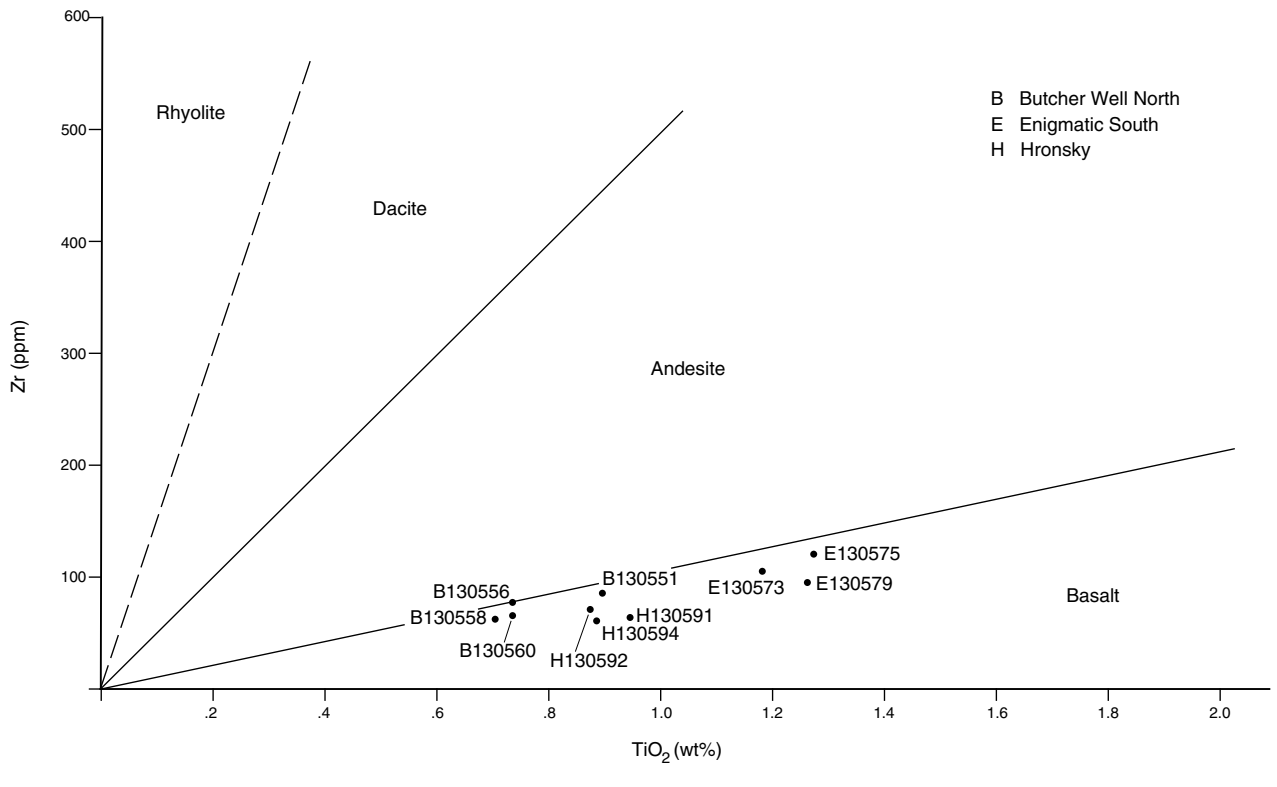

JMW4 26.11.03

Figure 17.6. TiO_2/Zr diagram for rock samples from Butcher Well, Enigmatic South, and Hronsky

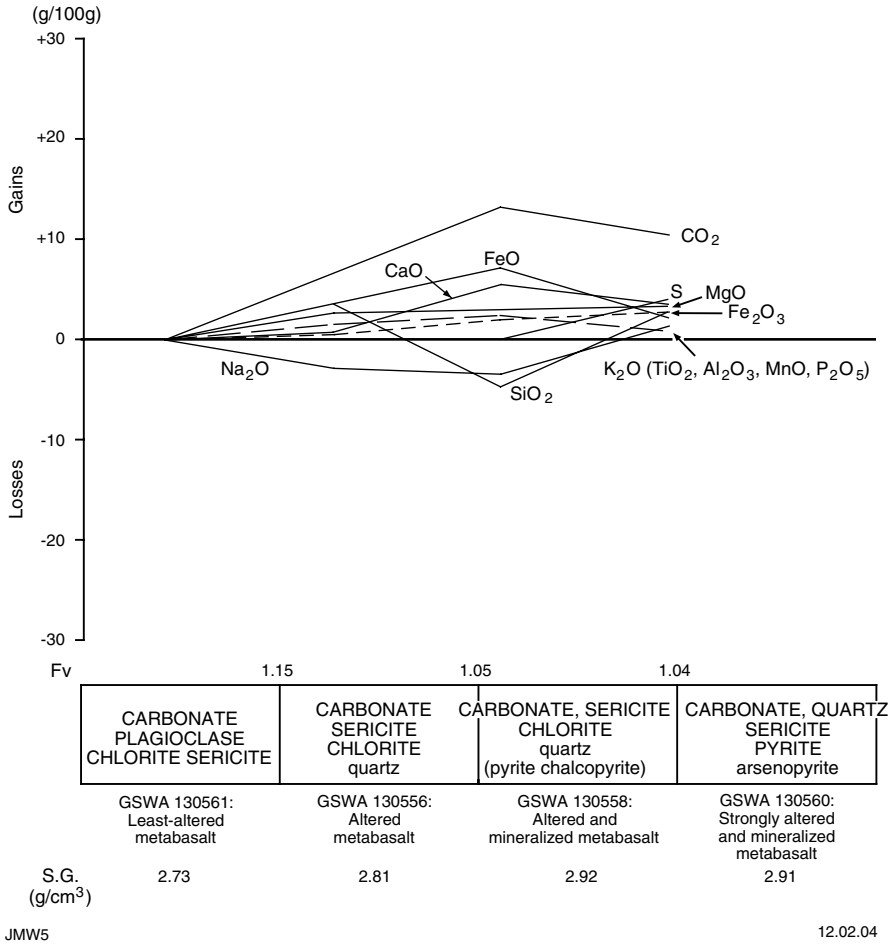

Figure 17.7. Mass-balance changes (calculated using the method of Gresens, 1967) for samples from Butcher Well North. Mineral components of alteration assemblages are listed in approximate order of abundance, with main mineral components in upper case and minor mineral components in lower case

Alteration: Mineralization is associated with silica- and pyrite-rich alteration zones.

References: Bush (1994), Mt Burgess Gold Mining Co. NL (1995).

Enigmatic South

Coordinates: 29°15'33"S, 122°19'26"E

Production: The Enigmatic South deposit was mined as an opencut on the southeastern edge of the Hronsky deposit during 1993 and 1994. A total of 316 071 t of ore at 2.85 g/t Au (900.8 kg Au) have been mined. A further inferred resource of 640 000 t at 1.90 g/t Au (1216 kg Au) remains (Jones, C., 1997, written comm.).

Host rock: The dominant host rock is metabasalt cut by numerous dykes and veins of syenite, monzonite, and lamprophyre. A summary log of diamond drillcore from the Enigmatic South deposit is shown in Figure 17.8.

Structure: Enigmatic South is continuously mineralized over a north–south strike length of 500 m. The ore zone, which may be a continuation of the Enigmatic North lode system, dips steeply to the west and is 2–8 m thick. Gold mineralization is directly related to zones of intense fracturing (Fig. 17.2). Both the hangingwall and the footwall of the ore zone are zones of ductile shear. Offset of a contact between metabasalt and chlorite schist, and the shape of a syenite body in the footwall, suggest a dextral component of movement on the mineralized brittle fault. The primary ore is overlain by an asymmetric supergene zone up to 8 m thick (Mt Burgess Gold Mining Co. NL, 1990).

Examination of core from drillhole ESDH-7 indicates a weak foliation throughout, but mineralization appears to be associated with zones of later, predominantly brittle styles of deformation. The metabasalt is cut by numerous carbonate- and quartz-lined fractures less than 1 cm wide. Higher gold grades are present where this fracturing is more intense. Larger quartz veins are rare to absent. Localized zones of brecciation, which also carry mineral-

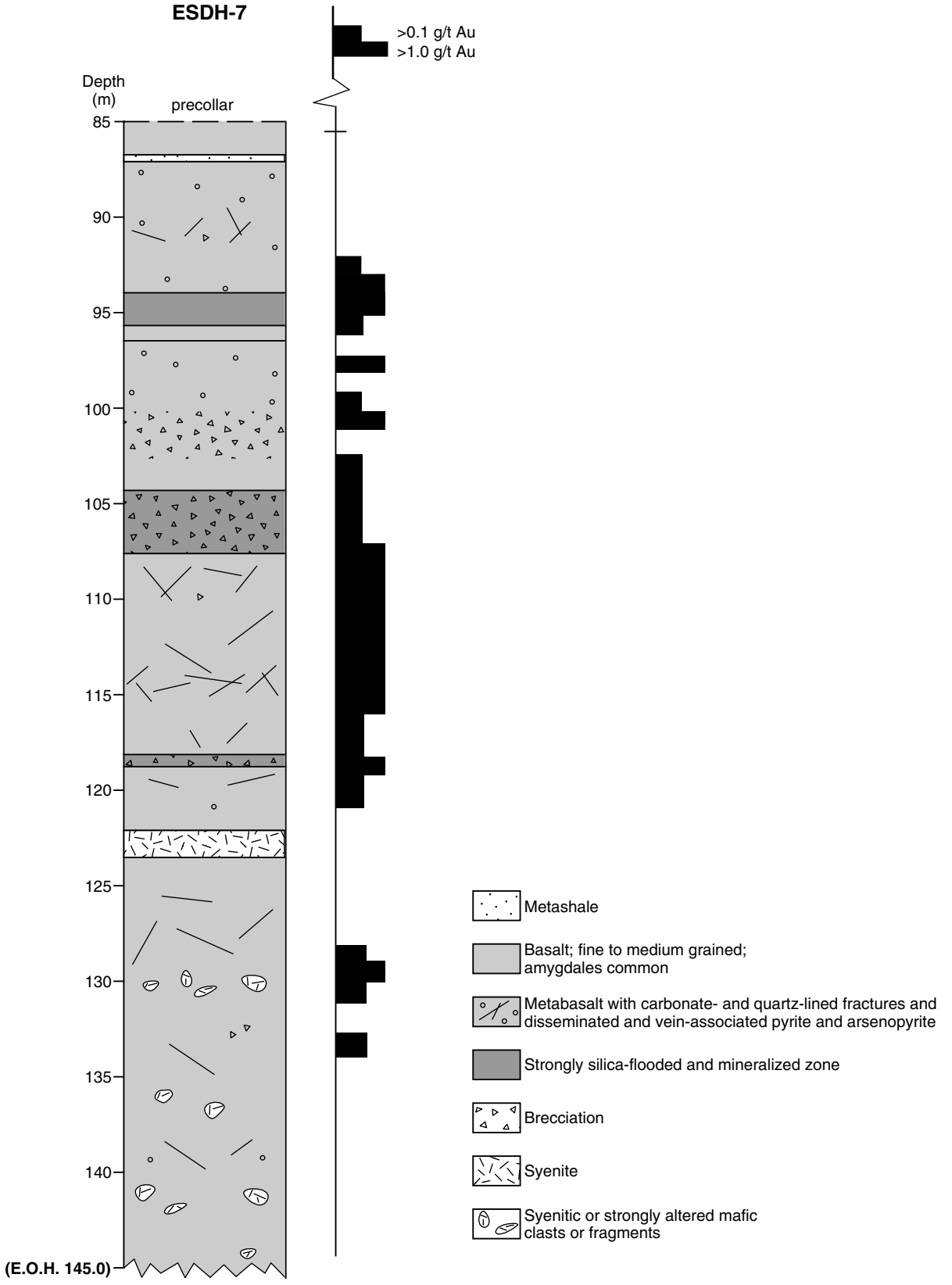

JMW2 13.02.04

Figure 17.8. Summary log of drillcore from diamond drillhole ESDH-7, Enigmatic South

ization, appear to be primary volcanic (?flow-top) features, rather than a product of deformation.

Alteration: The alteration assemblage comprises chlorite–carbonate–sericite–biotite–plagioclase(?albite)–quartz–pyrite(–leucoxene–ilmenite–magnetite–tourmaline). High gold values are directly related to high pyrite and silica contents.

Three altered metabasalt samples from diamond drillhole ESDH-7 were subjected to whole-rock analyses (Appendix 5) and plot in the metabasalt field on a diagram of TiO_2 versus Zr (Fig. 17.6). Gresens (1967) mass-balance calculations (Fig. 17.9) show a steady increase in CO_2, with minor increases in CaO, MgO, S, FeO, Fe_2O_3, and K_2O, from least- to most-altered metabasalt samples. SiO_2 decreased and then increased significantly, whereas Na_2O showed a steady decrease from the least to most altered samples. These chemical changes are consistent with observed secondary mineral assemblages. Qualitatively, they are mostly similar to those established for Butcher Well North, except that albite is absent.

References: Mt Burgess Gold Mining Co. NL (1990).

Hronsky/Mambo

Coordinates: 29°15'25"S, 122°19'21"E

Production: A total of 174 102 t of ore at 2.63 g/t Au (457.9 kg Au) have been mined at Hronsky/Mambo. A further inferred resource of 270 000 t at 3.0 g/t Au (810 kg Au) remains (Jones, C., 1997, written comm.).

Host rock: The main host rock at Hronsky is metabasalt with minor black metashale and siltstone. These have been cut by ubiquitous syenite, monzonite, and lamprophyre intrusive bodies, mostly in the form of narrow dykes and veins. Primary volcanic textures are commonly well preserved. A summary log of diamond drillcore from the Hronsky deposit is shown in Figure 17.10.

Structure: Mineralization is present along zones of shearing as well as zones of brittle fracturing and syenite contacts. Gold deposition occurred along a ductile dip-slip shear zone that trends 350°. Deformation became more brittle late in the shearing event, and gold was remobilized into tensional fractures. Clockwise rotation of the syenite intrusions may also have occurred, causing remobilization of gold into associated pressure shadows and marginal shear zones (Mt Burgess Gold Mining Co. NL, 1995).

Gold lodes at Hronsky strike 340–350° and dip to the west. Gold is in ore zones up to 5 m thick, which display intense fine-scale fracturing. Larger quartz veins are rare to absent. Several of these ore zones are localized at contacts between syenite and metabasalt. A predominantly dip-slip movement on this fault has been interpreted by Mt Burgess Gold Mining Co. NL (1995).

Mineralization in the Mambo deposit may be associated with a pressure shadow or sheared contacts along the margins of syenitic intrusions (Mt Burgess Gold Mining Co. NL , 1995).

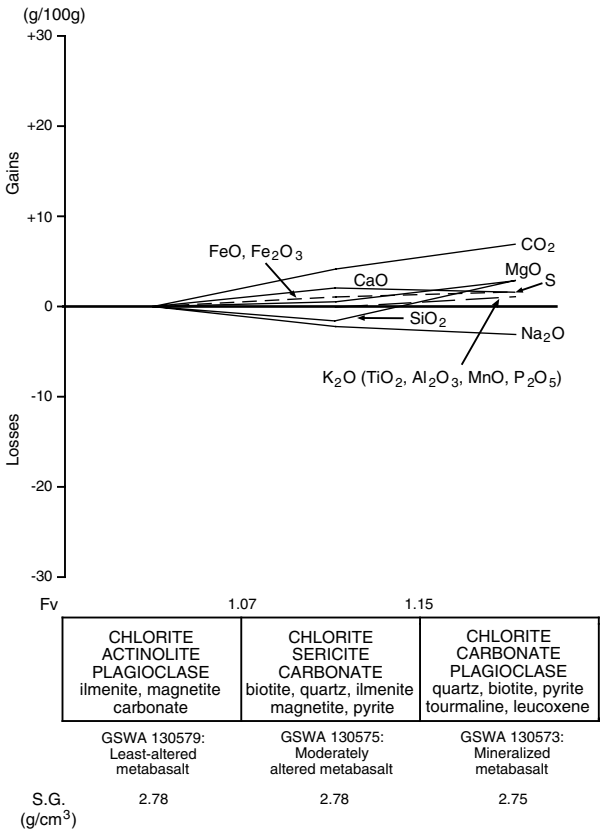

Figure 17.9. Mass-balance changes (calculated using the method of Gresens, 1967) for samples from Enigmatic South. Mineral components of alteration assemblages are listed in approximate order of abundance, with main mineral components in upper case and minor mineral components in lower case

The primary mineralization is overlain by a supergene zone averaging 6 m in thickness.

Alteration: The main alteration assemblage is carbonate–silica–sericite–chlorite–leucoxene–pyrite(–chalcopyrite–arsenopyrite).

Hronsky is the most deeply weathered deposit in the Butcher Well area, with the average depth of weathering being about 44 m.

Three whole-rock analyses from diamond drillhole HDH-8 are shown in Appendix 5. These samples fall into the metabasaltic field when plotted on a diagram of TiO_2 versus Zr (Fig. 17.6). Gresens (1967) mass-balance calculations were performed on variously altered metabasalts (Fig. 17.11) and indicate an increase of CO_2 and S during alteration, as reflected in the increasing carbonate and sulfide contents respectively. SiO_2 was lost from GSWA 130594, but added to the more intensely altered, mineralized sample GSWA 130592.

References: Bush (1994), Mt Burgess Gold Mining Co. NL (1995).

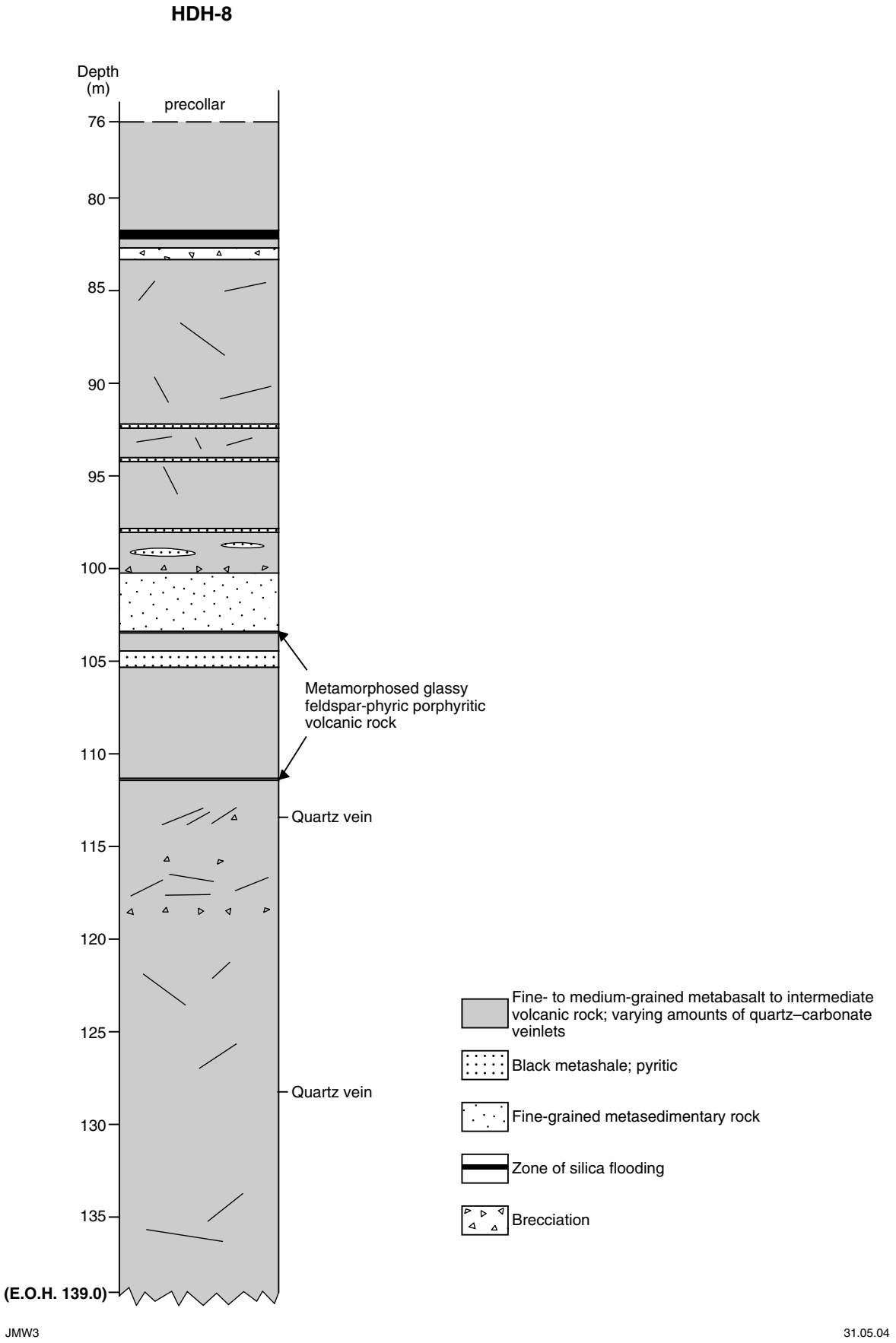

Figure 17.10. Summary log of drillcore from diamond drillhole HDH-8, Hronsky

Old Camp

Coordinates: 29°15'40"S, 122°19'12"E

Production: The inferred resource for the Old Camp prospect is 1.704 Mt of ore at 1.43 g/t Au (2436.72 kg Au) and the indicated resource is 1.681 Mt at 1.65 g/t Au (2773.65 Kg Au).

Host rock: Gold is hosted within an outcropping syenite that intrudes metabasalt.

Structure: The Old Camp prospect is a flat-lying supergene zone, overlying primary gold mineralization, that extends over 500 m. Mineralization is controlled by a shear zone and second-order shears (Mt Burgess Gold Mining Co. NL, 1994).

Alteration: No details are available.

References: Mt Burgess Gold Mining Co. NL (1995).

Tin Dog Flats

Coordinates: 29°23'23"S, 122°21'51"E

Production: Although a few small shafts are developed on the prospect, no official production or resource figures exist for this site.

Host rock: A map of the Tin Dogs prospect is shown in Figure 17.12, and a summary log of drillcore from Tin Dog Flats is shown in Figure 17.13.The deposit is hosted by andesitic volcanic rocks and metavolcaniclastic rocks, including amygdaloidal, variolitic, and fragmental varieties (Fig. 17.14). This sequence has been intruded by multiple phases of syenite that also host mineralization. Syenites (Fig. 17.15) vary from biotite rich to hornblende rich, and some contain riebekite or pyroxene. Grain sizes are variable, and both porphyritic and non-porphyritic varieties exist. Several phases of lamprophyre have also been noted in the deposit, some of which are weakly anomalous in gold.

Structure: The Tin Dog Flats prospect lies along the interpreted position of the Mount Hornet Shear Zone, lying on the fault itself or on an associated splay. Gold is in zones of intense fracturing and quartz–carbonate veining. It is found in brecciated zones within the meta-andesites and also appears to be more prevalent adjacent to contacts between the meta-andesites, syenites, and lamprophyres. Mineralized veins are predominantly flat lying and are generally less than 1 cm thick.

Alteration: The mineralized syenite has the assemblage K-feldspar–plagioclase–carbonate–chlorite–pyrite with accessory quartz, apatite, and hematite. Minor amounts of biotite, amphibole, rutile, ilmenite, fluorite, pyroxene, magnetite, chalcopyrite, galena, and molybdenite are present in some samples. Zones of high-grade mineralization are brick red due to intense hematite alteration and are silicified with complete destruction of the original biotite, amphibole, and pyroxene. Sulfides are generally disseminated throughout the syenite. Some molybdenite has been observed in quartz–carbonate veins.

The andesitic rocks have an alteration assemblage that includes chlorite, biotite, amphibole, carbonate, plagioclase, epidote, sericite, ?hematite, leucoxene(–quartz), magnetite, pyrite, chalcopyrite, garnet, and tourmaline. The most strongly mineralized zones are intensely silicified and contain limonite after carbonate. Distinct, bleached alteration fronts containing varying proportions of carbonate, hematite, pyrite, or biotite are present around veins and fractures in the meta-andesite. Epidote veining is common, and some of the more strongly deformed zones contain abundant coarse epidote. Some of the epidote veins also contain andradite, sulfide, and carbonate. Late quartz–carbonate–riebekite veins have been observed near contacts.

Whole-rock analyses of the Tin Dog Flats syenite and meta-andesite are shown in Appendix 5.

References: Newmont Australia Ltd (1991), Newcrest Mining Ltd (1992).

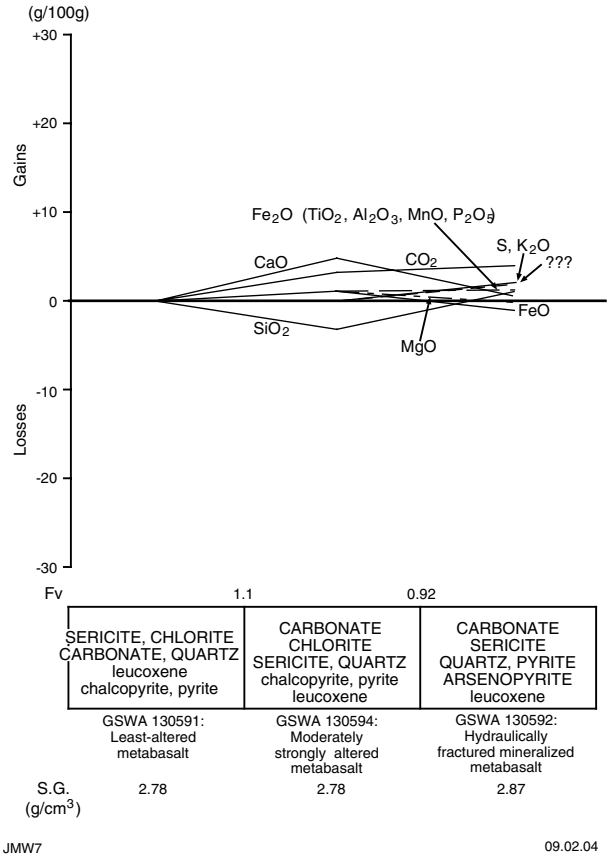

Figure 17.11. Mass-balance changes (calculated using the method of Gresens, 1967) for samples from the Hronsky/Mambo deposit. Mineral components of alteration assemblages are listed in approximate order of abundance, with main mineral components in upper case and minor mineral components in lower case

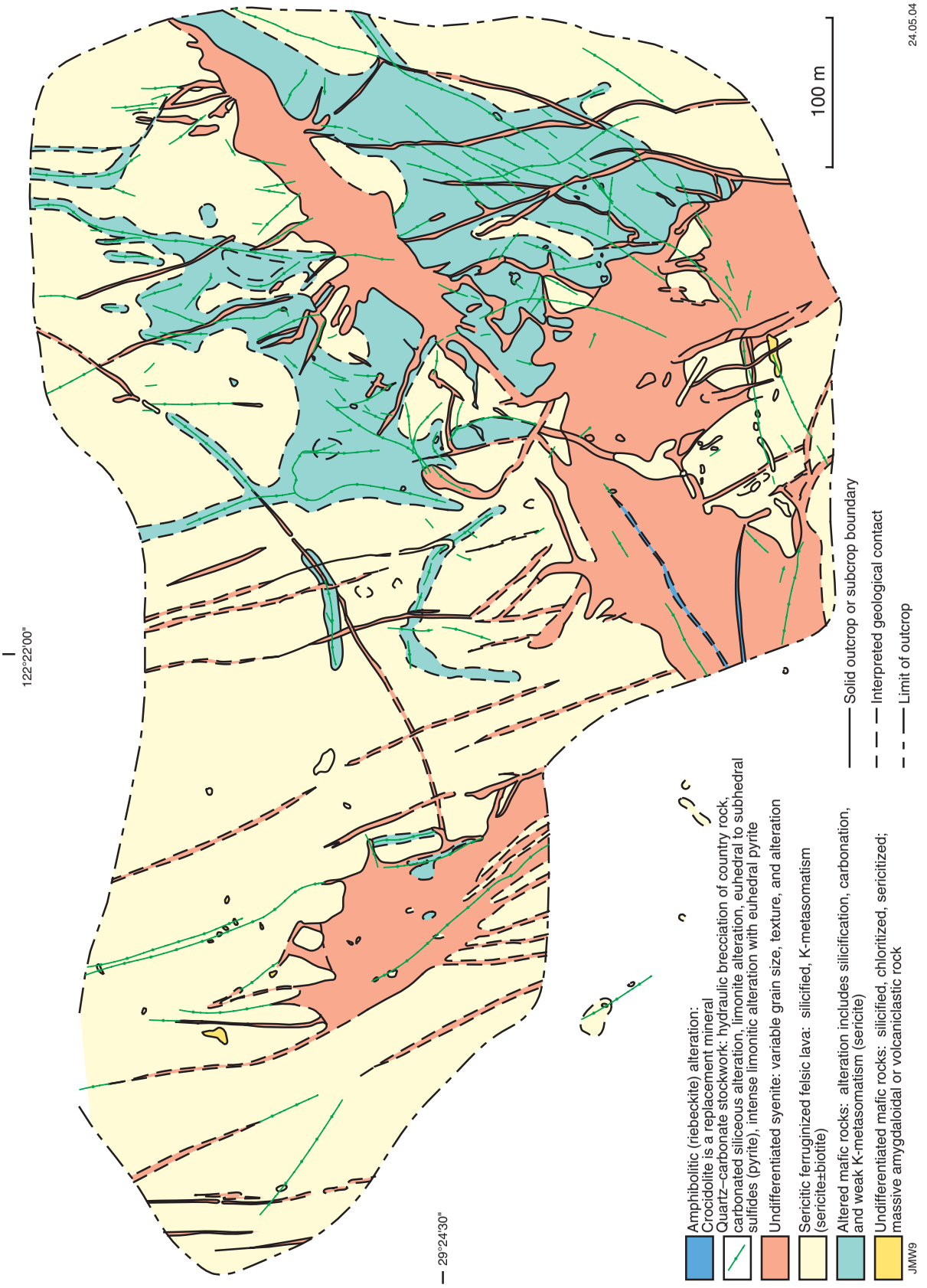

Figure 17.12. Geological map of the Tin Dog Flats deposit

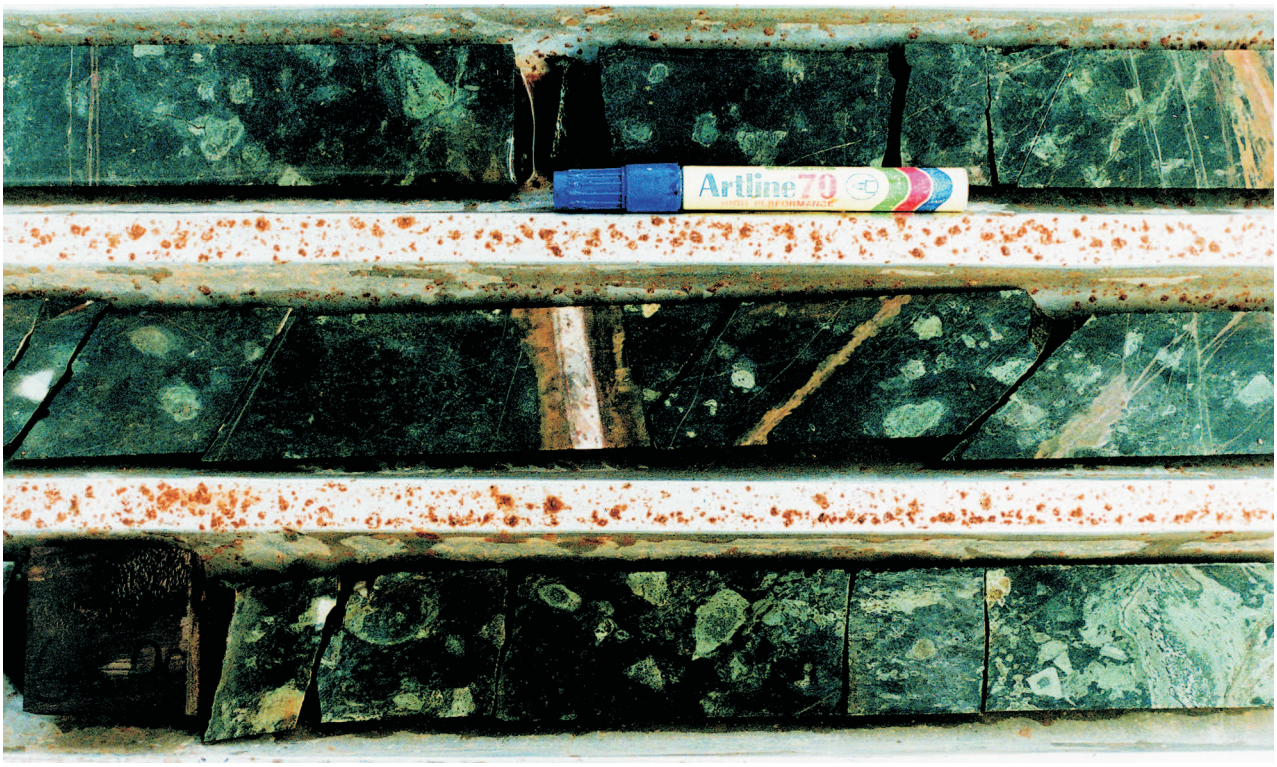

IRO141 03.05.04

Figure 17.13. Fragmental meta-andesite from diamond drillhole TDDH-5, Tin Dog Flats

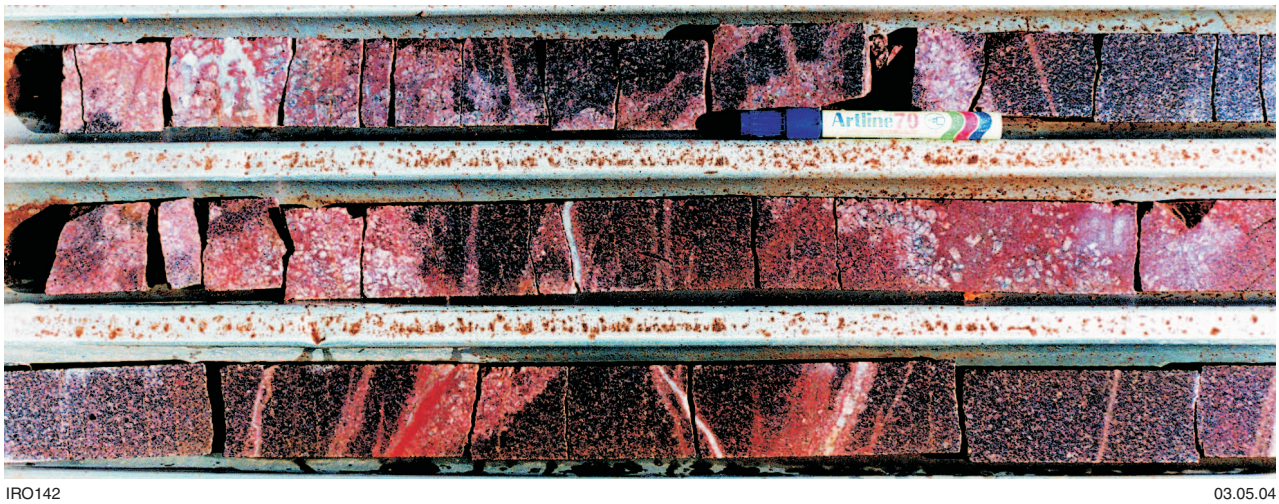

IRO142 03.05.04

Figure 17.14. Moderately fractured syenite from diamond drillhole TDDH-5, Tin Dog Flats. Note more-intense hematitization adjacent to fractures, and the destruction of biotite

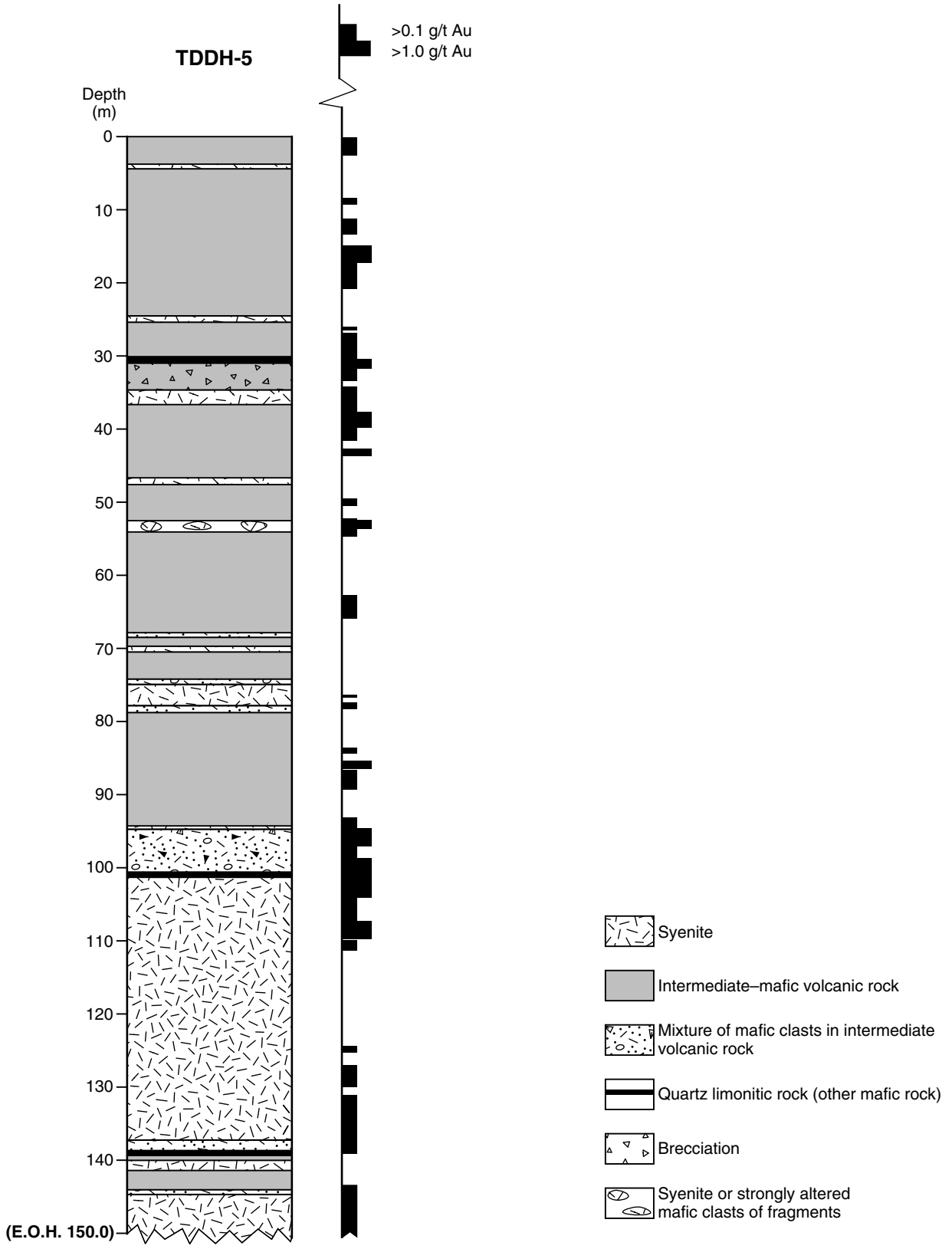

JMW8 18.02.04

Figure 17.15. Summary log of drillcore from diamond drillhole TDDH-5, Tin Dog Flats

References

BUSH, M. E., 1994, The spatial and temporal relationships between metamorphism, emplacement of intrusive dykes, gold mineralization, and hydrothermal alteration at Butcher Well Gold Mine, Linden, Western Australia: Curtin University of Technology, BSc (Hons) thesis (unpublished).

CLOUT, J. M. F., GLEGHORN, J. H., and EATON, P. C., 1990, Geology of the Kalgoorlie Gold Field, *in* Geology of the mineral deposits of Australia and Papua New Guinea *edited by* F. HUGHES: Australasian Institute of Mining and Metallurgy, Monograph 14, p. 411–431.

GRESENS, R. L., 1967, Composition–volume relationships of metasomatism: Chemical Geology, v. 2, p. 47–65.

HALLBERG, J. A., 1985, Geology and mineral deposits of the Leonora–Laverton area, northeastern Yilgarn Block, Western Australia: Perth, Western Australia, Hesperian Press, 140p.

MT BURGESS GOLD MINING CO. NL, 1990, Annual report, 1988 to 1989, on M39/00165–00166: Western Australia Geological Survey, Statutory mineral exploration report, Item 11661 A29849 (unpublished).

MT BURGESS GOLD MINING CO. NL, 1993, Annual report, Sep 1992 to Sep 1993, on M39/232, M39/230, M39/118–120: Western Australia Geological Survey, Statutory mineral exploration report, Item 11662 A39628 (unpublished).

MT BURGESS GOLD MINING CO. NL, 1994, Annual report, Jan 1993 to Dec 1993, on Camelback gold exploration: Western Australia Geological Survey, Statutory mineral exploration report, Item 11662 A40601 (unpublished).

MT BURGESS GOLD MINING CO. NL, 1995, Annual report, Jan 1994 to Dec 1995, on Camelback gold exploration: Western Australia Geological Survey, Statutory mineral exploration report, Item 11662 A43925 (unpublished).

NEWCREST MINING LTD, 1992, Annual report, Feb 1991 to Feb 1992, on M39/172–173, 39/147–148, 39/55 and M39/38: Western Australia Geological Survey, Statutory mineral exploration report, Item 11661 A35370 (unpublished).

NEWMONT AUSTRALIA LTD, 1991, Annual report, 1990–1991, on M39/172–173, 39/147–148, 39/55 and M39/38: Western Australia Geological Survey, Statutory mineral exploration report, Item 11601 A33208 (unpublished).

OLIVER, N. H. S., VALENTA, R. K., and WALL, V. J., 1990, The effect of heterogeneous stress and strain on metamorphic fluid flow, Mary Kathleen, Australia, and a model for large-scale fluid circulation: Journal of Metamorphic Geology, v. 8, p. 311–331.

RIDLEY, J. R., 1993, The relations between mean rock stress and fluid flow in the crust: with reference to vein- and lode-style gold deposits: Ore Geology Reviews, v. 8, p. 23–27.

SWAGER, C. P., 1997, Tectono-stratigraphy of late Archaean greenstone terranes in the southern Eastern Goldfields, Western Australia: Precambrian Research, v. 83, p. 11–42.

TCHALENKO, J. S., 1970, Similarities between shear zones of different magnitudes: Geological Society of America, Bulletin, v. 81, p. 1625–1640.

18. Mount Celia

The Mount Celia mining area lies within the Linden Terrane of Swager (1997). It is located in a narrow (about 5 km) belt of greenstones, bound by the Linden Fault to the west and a sheared contact with granitoids to the east (Fig. 18.1). The gold deposits are in the same greenstone sequence as those at Linden, and lie south of the Kurrajong Monzogranite. This area is also intruded by several small granitoid plutons. The metamorphic grade adjacent to the granitoid–greenstone contact, including rocks in the Mount Celia mine area, is estimated to be amphibolite facies. Quartz–andalusite-rich assemblages in a felsic volcaniclastic sedimentary unit at Mount Celia trigonometric station were noted by Hallberg (1985). Quartz–pyrophyllite assemblages at Kangaroo Bore suggest a maximum temperature of about 370°C in this area (Barnes, 1979), equivalent to lower greenschist-facies meta-morphism.

The Mount Celia mining area has produced about 100 kg of gold, mainly from historic mining. Recent exploration has identified resources of about 1 t Au at Deep Well and 2 t at Kangaroo Bore. Historic production has come from amphibolite host rocks, but the recently identified resources are located in BIF (Deep Well) and quartz–pyrophyllite schist (Kangaroo Bore).

Historic gold production was from zones of quartz veining subparallel to the north-northwesterly trending greenstone sequence. At Kangaroo Bore, the mineralized veins are associated with a high-strain zone that has been interpreted as a sinistral shear zone (Ransom, 1988). This shear zone is on the contact between a quartz-rich quartz–pyrophyllite rock and less-siliceous, more-ductile units. Coronation and Dunns Reward appear to be located near a contact between metabasalt and metagabbro. Mineralization at Deep Well is associated with quartz veins in metamorphosed ferruginous chert (?BIF) within a broader sequence of relatively ductile metamorphosed felsic volcaniclastic rocks. There is no clear relationship between quartz veins and gold at Deep Well, but this may be an effect of gold dispersion associated with weathering. These observations suggest that competency contrasts between adjacent units may have played a role in localizing gold-bearing structures. However, the lodes are not well exposed and further work is required to establish such a relationship in this area.

Alteration adjacent to mineralized quartz veins in the amphibolite-hosted Mount Celia deposit is dominated by muscovite with minor carbonate and biotite. The muscovite-dominant assemblage passes outwards into biotite amphibolite, but it is not clear whether this biotite-bearing assemblage represents an outer alteration halo or a metamorphic assemblage. The presence of muscovite-dominant alteration in amphibolite-facies host rocks at Mount Celia is indicative of hydrothermal alteration that was distinctly retrograde with respect to peak metamorphic temperatures. This contrasts with gold mineralization in other amphibolite-facies greenstones of the Yilgarn Craton, where alteration assemblages are compatible with metamorphic temperatures (Mueller and Groves, 1991; Witt, 1991).

Quartz–pyrophyllite host rocks at Kangaroo Bore record the activity of a very low pH fluid, more commonly associated with epithermal styles of mineralization (Barnes, 1979; Hedenquist et al., 1994) than with the late-tectonic, structurally controlled gold deposits that are widespread in the Yilgarn Craton. More-detailed studies are required to determine whether the gold mineralization is related to early epithermal activity or if the quartz–pyrophyllite rock, being more competent than associated rock types, preferentially reacted to regional deformation by brittle fracture and quartz-vein formation.

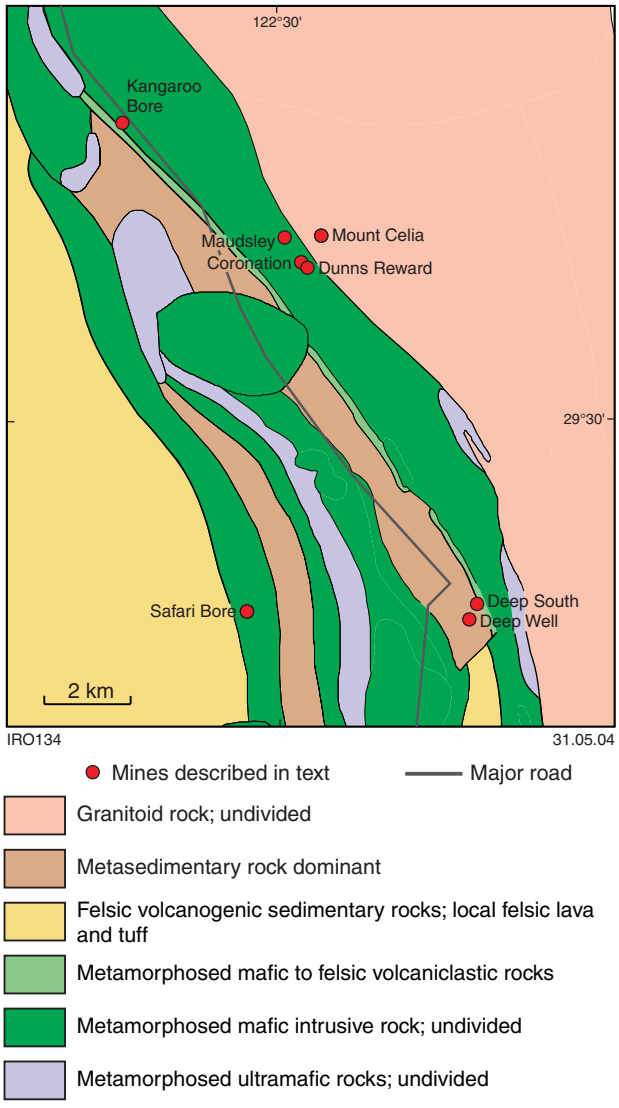

Figure 18.1. Map of the Mount Celia mining area

Deposits of the Mount Celia mining area

Mount Celia

Other names: Caledonian, Blue Peter, Red Star

Coordinates: 29°32'23"S, 122°29'32"E

Production: 1489.0 t of ore for 20.05 kg Au (13.5 g/t Au) between 1898 and 1945.

Host rock: The Mount Celia gold mine is hosted by a fine- to medium-grained amphibolite.

Structure: The main area of workings, consisting of a series of open stopes and shafts, appears to follow two structures about 10 m apart and trending approximately 310° over a distance of about 100–200 m. The workings access a series of simple quartz veins, less than 20 cm wide, that dip steeply to the northeast within the main foliation of the host rock. Smaller-scale quartz and carbonate veinlets are both parallel to, and cut across, the foliation.

About 250 m south of the main workings, another line of shafts, stopes, and shallow diggings trend 300° over a distance of about 300 m. The mineralized structure dips steeply to the northeast, and at the eastern end, strikes 320°. The structure is poorly exposed, but there is minor vein quartz on the dumps, with the largest block being 20 cm across.

Alteration: The least-altered rock from the Mount Celia mine is amphibolite containing a significant amount of 'fox-red' biotite. Minor chlorite cuts across the biotite. The amphibolite also has zones containing tabular grains of clinozoisite that cut across the foliation, which is defined by the preferred orientation of amphiboles and micas. In more-strongly foliated samples of amphibolite, most of the amphibole has been destroyed and the dominant minerals are chlorite, carbonate, clinozoisite, and biotite, with minor amounts of sericite. This assemblage is probably from an outer zone of hydrothermal alteration around the lodes.

The lodes consist mostly of quartz veins with local high concentrations of pyrite. Thin selvages of host rock between quartz veins have been altered to an assemblage dominated by muscovite, with smaller amounts of biotite and carbonate, and accessory chlorite and epidote. Pyrite tends to form within the altered host rock slivers rather than in the quartz. It forms as subhedral to anhedral grains up to 15 mm in diameter. Limited petrographic observations suggest that gold is present as inclusions up to 0.5 mm across within pyrite, along with smaller inclusions of chalcopyrite and pyrrhotite. It is relatively pale, indicating a high silver content.

Coronation

Coordinates: 29°28'02"S, 122°30'20"E

Production: 311.7 t of ore for 72.17 kg Au (231.6 g/t Au) between 1938 and 1943.

The relative scale of workings at this locality and at Mount Celia does not seem consistent with the corresponding production figures. It is possible that some of the production attributed to Coronation resulted from ore that was transported from Mount Celia.

Host rock: The deposit is hosted by fine-grained amphibolite.

Structure: A few shafts and shallow diggings follow a zone of small, subparallel, steeply dipping quartz veins that trend about 300°. The veins are less than 20 cm wide.

Alteration: Alteration is obscured by weathering.

Dunns Reward

Other names: Dunn's Reward

Coordinates: 29°28'06"S, 122°30'25"E

Production: 103.1 t of ore for 5.32 kg Au (51.6 g/t Au) between 1939 and 1944.

Host rock: The deposit is hosted by fine- to medium-grained amphibolite.

Structure: Several relatively deep shafts trend about 310° over a distance of about 200 m. The foliation dips steeply to the northeast. Quartz-vein material on dumps is up to 20 cm thick.

Deep Well

Coordinates: 29°32'17"S, 122°32'42"E

Production: Though old workings of a significant size exist in the area, no official historical production has been recorded for this site. The indicated resource is 34 700 t of ore at 2.9 g/t Au (101.5 kg Au; MINEDEX site code S02378).

Recent drilling 0.5 km south of Deep Well intersected gold mineralization, with the best values being 17 m at 6.94 g/t Au and 11 m at 16.4 g/t (Red Back Mining NL, 2001).

Host rock: The deposit is hosted by the central unit of three oxidized metamorphosed ferruginous chert horizons. These units lie within a sequence of quartz–sericite schist and altered metasedimentary and metavolcaniclastic rocks that have been intruded by metamorphosed felsic porphyry. Some of the mineralization, which is mainly within the oxidized zone, extends into these other rock units.

Structure: A series of shafts and shallow workings trend about 340°, parallel to bedding and the main foliation, over a distance of about 1.2 km. The BIF is 1.5 to 13 m thick and dips steeply to the west. Vein quartz on the mine dumps is up to 30 cm wide, but a clear relationship between the quartz veins and mineralization has not been established, with the best grades found in areas that lack quartz.

Alteration: The ore zone at depth contains quartz, pyrite, chlorite, amphibole, and magnetite.

References: Redback Mining NL (Burrow, G., 1997, written comm.)

Maudsley

Coordinates: 29°27'43"S, 122°30'06"E

Production: 263.2 t of ore for 6.65 kg Au (25.3 g/t Au) between 1909 and 1911.

The mine could not be located in the field.

Kangaroo Bore

Coordinates: 29°26'19"S, 122°27'53"E

Production: 61.0 t of ore for 0.74 kg Au (12.13 g/t Au) between 1898 and 1908. The measured resource is 1.31 Mt at 1.45 g/t Au (1899.5 kg Au; MINEDEX site code S02362).

Host rock: Mineralization at Kangaroo Bore is hosted by quartz–pyrophyllite schist within a sequence that also contains chlorite–carbonate schist (probably after metamorphosed basalt or komatiitic basalt), quartz-eye schist (interpreted to be after porphyritic dykes), and metasedimentary rocks including metamorphosed black shale. Ransom (1988) identified quartz-rich and quartz-poor varieties of quartz–pyrophyllite rock.

Structure: Several shafts and open stopes trend between 310° and 340° over a strike length of nearly 1 km. Mineralization is interpreted to be in a high-strain zone within a larger sinistral shear zone. Gold is associated with quartz veining within the high-strain zone on the contact between quartz-rich quartz–pyrophyllite schist and less-siliceous units to the west.

In the more siliceous rocks a crenulation cleavage has been observed and has been interpreted to be a result of later shearing within the high-strain zone. Later gold mineralization is present within quartz-filled fractures and net-vein arrays associated with brittle failure of the quartz–pyrophyllite schist.

Alteration: The host quartz–pyrophyllite schist is strongly silicified and locally contains carbonate. Sulfides are disseminated throughout the host rock and are associated with quartz–carbonate veins. Pyrite is the dominant sulfide and forms up to 5% of the host rock. Up to 1% arsenopyrite has also been observed, along with traces of sphalerite and galena. Most of the gold is within quartz–carbonate–sulfide veins.

Significant amounts of pyrite are in metamorphosed black shales within the sequence and in the footwall 'quartz-poor' quartz–pyrophyllite schist. Some pyrite is also in the metabasalt, which is also chloritized and carbonated.

References: Ransom (1988).

Safari

Other names: Safari Bore

Coordinates: 29°32'23"S, 122°29'32"E

Production: No historical production. The inferred resource is 3.0 Mt of ore at 2.9 g/t Au (8700 kg Au).

Deep South

Other names: Deep South Project

Coordinates: 29°32'10"S, 122°32'47"E

Production: No historical production. The inferred resource is 700 000 t of ore at 4.0 g/t Au (6000 kg Au).

References

BARNES, H. L., 1979, Solubilities of ore minerals, *in* Geochemistry of hydrothermal ore deposits (2nd edition) *edited by* H. L. BARNES: New York, John Wiley and Sons, p. 404–460.

HALLBERG, J. A., 1985, Geology and mineral deposits of the Leonora–Laverton area, northeastern Yilgarn Block, Western Australia: Perth, Western Australia, Hesperian Press, 140p.

HEDENQUIST, J. W., MATSUHISA, Y., IZAWA, E., WHITE, N. C., GIGGENBACH, W. F., and OAKI, M., 1994, Geology, geochemistry, and origin of high sulfidation Cu-Au mineralization in the Nansatsu district, Japan: Economic Geology, v. 89, p. 1–30.

MUELLER, A. G., and GROVES, D. I., 1991, The classification of Western Australian greenstone-hosted deposits according to alteration mineral assemblages: Ore Geology Reviews, v. 6, p. 293–331.

RANSOM, D. M., 1988, Structure of the Kangaroo Bore Gold Prospect, Mt Celia area, Western Australia, *referenced in* J. M. GRAINDORGE and P. PENNA, 1989, Mt Celia Project, Annual Technical Report for the period ended 23 May 1989, Union Oil Development Corporation: Western Australia Geological Survey, Statutory mineral exploration report, Item 11666 A27843 (unpublished).

RED BACK MINING NL, 2001, Quarterly report for the period ending 30 June 2001, viewed 9 December 2002, <http://www.redbackmining.com.au/quart_reports/2001/2001jun/2001jun.pdf>.

SWAGER, C. P., 1997, Tectono-stratigraphy of late Archaean greenstone terranes in the southern Eastern Goldfields, Western Australia: Precambrian Research, v. 83, p. 11–42.

WITT, W. K., 1991, Regional metamorphic controls on alteration associated with gold mineralization in the Eastern Goldfields Province, Western Australia: implications for the timing and origin of Archaean lode-gold deposits: Geology, v. 19, p. 982–985.

19. Edjudina

Covering the southeastern part of the EDJUDINA and northwestern part of the YABBOO 1:100 000 sheets, the Edjudina mining centre comprises an almost continuous line of workings trending 320° over 13 km (Fig. 19.1). The southern 3 km of this line have been combined under the one ownership and have been worked in modern times as the Paget leases. Modern production figures (post-1988) are not available for individual deposits; however, combined gold production between 1984 and 1991 was 4679.031 kg. Resources for the Edjudina mining centre are: measured, 519 000 t of ore at 2.09 g/t Au (1084.7 kg Au); indicated, 2.149 Mt at 3.63 g/t Au (7800.87 kg Au); and inferred, 817 000 t at 3.16 g/t Au (2581.72 kg Au).

Deposits of the Edjudina mining centre

Paget

Other names: Edjudina Goldfields Ltd, Neta, Neta Extended, Neta Junction, Geneve, Senate, Gawler, Gawler G.M. Co. Ltd, Fingall, Louie Mary, Vulcan, Bulger, Lord Nelson, Paget Gold Mines of Edjudina Ltd

Coordinates: 29°51'11"S, 122°33'15"E

Production: Paget is a conglomeration of gold mining leases covering the southern 3 km of the 'Edjudina Line', the more significant leases being Neta, Senate, and Gawler. These leases were mined separately and intermittently from the late 1890s until 1921. In 1936, they all came under the single ownership of Paget Gold Mines of Edjudina Ltd, who carried out rehabilitation and further exploration over the leases. Further production by this company was halted due to lack of funds and the onset of World War II.

There is no documentation of further work on Paget until the early 1970s, when various companies began exploration programs carrying out mapping, drilling, and costeaning. In 1983, the Paget Gold Mining Company Ltd was floated, and from 1984 to 1986 this company carried out further mining and development, although, due to poor grade control and mining technique, the mine was not profitable. Further exploration and feasibility studies have been carried out under various joint venture agreements and the mine is now under care and maintenance.

Production between 1898 and 1921 totalled 22 409.9 t of ore for 1069.44 kg Au (47.7 g/t Au). Recent production figures (post-1988) are not available.

Host rocks: The mine sequence is bounded by BIF and metachert horizons and is hosted mostly by chlorite schists interpreted to be derived from intermediate to mafic volcanic rocks. There are also some chlorite–carbonate schists, chlorite–tremolite–magnetite schists, quartz–sericite schists, and metadolerite. Metamorphosed felsic porphyry dykes can be traced for up to 750 m throughout the mine sequence and are 30 cm to 1.5 m wide.

Structure: The mine sequence is located in a regional, isoclinally folded zone within a series of parallel and subparallel, narrow, quartz-filled shear zones that strike 320–340° and dip steeply to the northeast. Mineralization is associated with quartz veining that varies from 2 cm to 2 m in width. The quartz veins are boudinaged in both the horizontal and vertical directions, producing pod-shaped orebodies historically known as 'kidney ore'.

Three major categories of veins have been recognized: normal veins, en echelon veins, and multiple vein systems (Davis, 1981; Howell, 1983). Normal veins are relatively simple and continuous. These boudinaged veins parallel the foliation, trending about 320°, and are generally less than 0.5 m thick. The best examples are the Nos 1 and 2 reefs, which were mined in the deep shafts (e.g. Maitland, 1903).

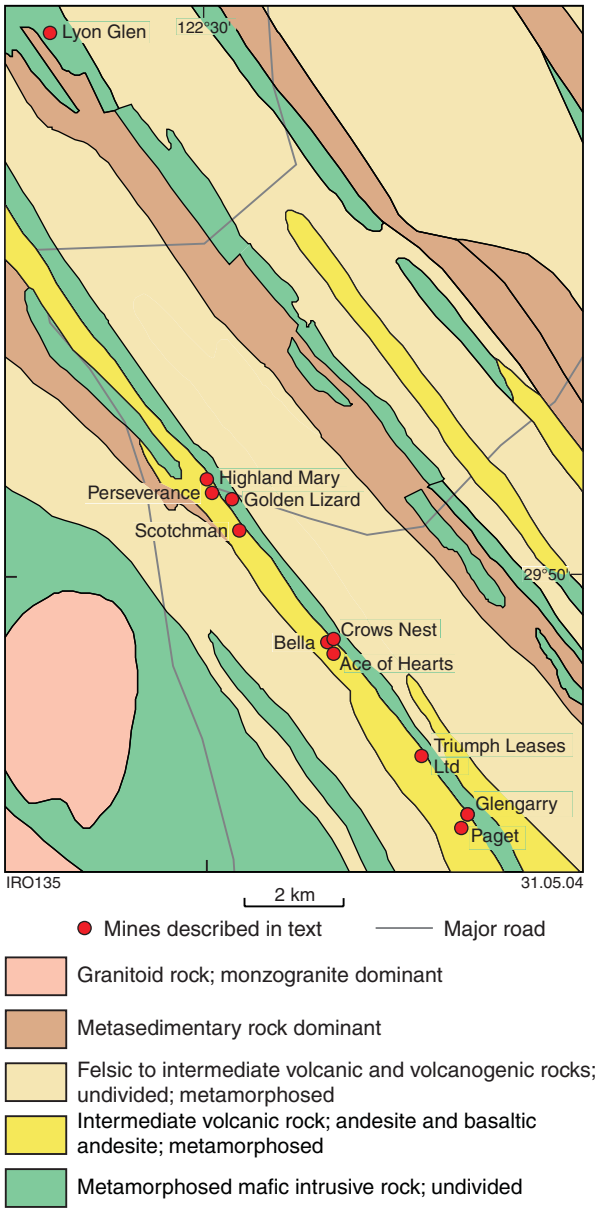

Figure 19.1. Map of the Edjudina mining area

Two en echelon vein systems have been recognized. The first are the Jep I, II, and III veins, about 200 m southeast of the Gawler Shaft. The Southeast vein system lies farther to the southeast (between the Vulcan and Highland Mary deposits). The en echelon veins are very strongly boudinaged, up to 3 m thick, and 3–5 m long.

The multiple vein systems are made up of numerous narrow (2–10 cm), foliation-parallel, commonly boudinaged veins in zones up to 5 m wide. The 'Gold Lode' intersected in the Neta workings (e.g. Maitland, 1903) is described as a multiple vein system. Part of the Jep II vein is also a multiple vein system.

The felsic dykes intruded late- to post-deformation, and are both foliated and non-foliated. They have a similar trend to the shear zones, with a slightly shallower dip. Where the dykes crosscut the lodes or shear zones, they may have a deleterious effect on the ore grades, as barren silicifications are present at dyke margins; where the dykes are parallel, grades are unaffected.

Rugless (1975), Clayton (1988), and Lidbury (1988) described the gold-bearing veins as being within a shallow, northwest-plunging isoclinal anticline. Findlay (1986) described several different lodes hosted on the limbs of a steep, northwest-plunging syncline.

Alteration: The chloritic schists contain up to 50% carbonate, which is disseminated throughout the rock and also forms as abundant parallel and crosscutting veinlets and blebs. There is minor quartz intergrown with this carbonate. The alteration halos around the thicker veins are up to 15 m wide. The sulfide assemblage consists of pyrite with subordinate chalcopyrite, pyrrhotite, arsenopyrite, sphalerite, and galena. Minor amounts of wolframite have been found in the Jep veins, and there is abundant siderite and common arsenopyrite and pyrite in the southeast vein system; scheelite and tourmaline have also been documented.

Gold is about 75% free milling, with the rest associated with sulfides. It is mostly associated with the quartz veining, and the best gold grades are on the margins of the quartz veins. Only minor gold is present in the host rock and rarely within the metamorphosed felsic porphyry dykes.

References: Maitland (1903), Montgomery (1904, 1906), Honman (1917), Rugless (1975), Wilding (1975), Davis (1981), Loftus Hills (1981), Greg Kater and Associates Pty Ltd (1983), Howell (1983), Gifford (1985), Sanders (1985), Findlay (1986), Stroud (1986), Burrows (1987), Mulholland (1987), Clayton (1988), Lidbury (1988), Swager (1995).

Highland Mary

Other names: Digger, Heathcote

Coordinates: 29°47'17"S, 122°29'53"E

Production: 493.8 t of ore for 12.71 kg Au (25.7 g/t Au) between 1900 and 1915.

Host rocks: Chlorite schist, minor chlorite–carbonate schist, and some metamorphosed ferruginous chert.

Structure: One moderately deep shaft and a few shallow diggings trend 320° over less than 100 m. Blocks of vein quartz on the dumps are up to 30 cm thick.

Alteration: Pyrite cubes are scattered throughout the host rock. Many of the quartz blocks have ankerite and quartz–sericite schist on their margins.

Reference: Maitland (1903).

Perseverance

Coordinates: 29°47'32"S, 122°30'06"E

Production: 169.7 t of ore for 5.43 kg Au (32.0 g/t Au) between 1902 and 1905.

Host rocks: Quartz–sericite schist (quartz-eye schist), and minor chlorite schist.

Structure: A few deep shafts and several shallower workings follow a structure trending 320° over a distance of about 100–200 m.

Reference: Maitland (1903), Montgomery (1904).

Golden Lizard

Other names: Fingall, Trio

Coordinates: 29°47'36"S, 122°30'20"E.

Production: 733.92 t of ore for 15.57 kg Au (21.2 g/t Au) between 1911 and 1939.

Host rocks: Chlorite schist and sericite schist.

Structure: Several moderately deep vertical shafts, developed over about 200 m, follow a quartz-veined structure that trends 320°.

Alteration: Quartz on the mine dumps is gossanous and many fragments are ankerite bearing.

Scotchman

Other name: Success

Coordinates: 29°48'08"S, 122°30'32"E

Production: 400.3 t of ore for 7.66 kg Au (19.1 g/t Au) between 1902 and 1905.

Host rocks: Quartz–sericite schist and chlorite schist.

Structure: Several vertical shafts follow a structure that trends 320° over 200–300 m.

Reference: Maitland (1903), Montgomery (1904).

Bella

Other names: Jack Wren, Turn of the Tide

Coordinates: 29°49'11"S, 122°31'32"E

Production: 1018.1 t of ore for 28.69 kg Au (28.2 g/t Au) between 1900 and 1908.

Host rock: Intermediate schist.

Structure: A few small shafts and costeans, developed over a strike length of 100–200 m, follow a structure that trends 310° and dips steeply 80°E. A subhorizontal lineation can be seen in the foliation plane. Blocks of quartz-vein material found on the dumps are up to 30 cm wide.

Reference: Maitland (1903), Montgomery (1904).

Crows Nest

Coordinates: 29°49'09"S, 122°31'36"E

Production: 1054.4 t of ore for 32.29 kg Au (30.6 g/t Au) between 1902 and 1913.

Host rocks: Quartz–sericite schist with local quartz-eyes, and minor chlorite schist.

Structure: Several shafts and open stopes are developed over a strike length of about 300 m. Quartz veins up to 40 cm wide follow a structure that trends 320° and dips steeply 80°NE. Boudinage in some quartz veins is in two directions within the foliation plane. The main set of boudin necks is subhorizontal, and a second, less-strongly developed set has a subvertical plunge.

Alteration: Alteration is obscured by weathering.

References: Maitland (1903), Montgomery (1904, 1906).

Ace of Hearts

Coordinates: 29°49'23"S, 122°31'40"E.

Production: 621.3 t of ore for 10.31 kg Au (16.6 g/t Au) between 1936 and 1937.

Host rock: Chlorite schist.

Structure: Several shafts follow a structure trending 320° over a strike length of about 300 m. A parallel set of workings lies about 30 m east of the main lode. Dump samples have a strong pervasive lineation.

Alteration: Quartz veins have ankerite on their margins.

Triumph Leases Ltd

Other names: Glory Qualve, Marawa, Yale Lock; includes Three Crosses to the north, and Martin, Old Edjudina, Triumph South, Old Guard, and Eva to the south.

Coordinates: 29°50'26"S, 122°32'43"E

Production: 3102 t of ore for 82.95 kg Au (26.7 g/t Au) between 1897 and 1925.

Host rocks: Quartz-eye-bearing quartz–sericite schist, chlorite schist, and chlorite–carbonate schist.

Structure: A series of relatively deep shafts are distributed along a considerable strike length of at least 300 m, more or less continuous with ?Martin to the south and ?Three Crosses to the north. The dominant foliation (?shear fabric) strikes 325° and is vertical to steeply dipping to the northeast. A strong, pervasive intersection lineation plunges shallowly towards 325°. Thin quartz stringers, some of which are boudinaged, lie parallel to the foliation. Large blocks of quartz on the dumps indicate that there is much thicker veining that is not exposed.

Alteration: Idioblastic limonite after pyrite is present in all rock types. The chlorite schist contains numerous rounded carbonate porphyroblasts, 1 mm across, and minor carbonate veins less than 3 mm thick.

References: Maitland (1903), Montgomery (1904, 1906), Burrows (1987), Swager (1995).

Glengarry

Other names: London and Coolgardie Explorers Ltd, Golden Girl

Coordinates: 29°51'05"S, 122°33'17"E

Production: 747.8 t for 16.09 kg Au (21.5 g/t Au) between 1901 and 1905.

Host rocks: Felsic to intermediate quartz–sericite schist with quartz and feldspar ‘eyes’, and minor chloritic schist and some metachert in the northern workings.

Structure: A few open stopes and shallow pits and several moderately deep (up to about 46 m) shafts have been sunk over a strike length of about 200 m. These follow a shear zone that trends 320°. Quartz veins up to 20 cm wide lie parallel to the shear fabric, which dips steeply to the northeast. Some quartz veins are boudinaged and plunge shallowly to the north, suggesting subvertical displacement. The southern workings are in a parallel structure that dips steeply to the southwest.

Alteration: Mine-dump samples are generally deeply weathered. The quartz–feldspar–sericite schist has minor limonite after idioblastic pyrite.

References: Maitland (1903), Montgomery (1904), Swager (1995).

Lyon Glen

Other names: Broken Hill North, Broken Hill

Coordinates: 29°42'25"S, 122°28'09"E

Production: 345.4 t of ore for 9.07 kg Au (26.3 g/t Au) between 1902 and 1904.

Host rock: Deeply weathered felsic to intermediate schist amongst outcropping metamorphosed banded chert.

Structure: Several small shafts, open stopes, and shallow diggings, trending 320°, follow narrow (maximum width of 30 cm) brittle–ductile quartz veins.

Alteration: Idioblastic limonite pseudomorphs after pyrite are present, as well as 1 mm limonite spots ?after carbonate.

Reference: Swager (1995).

References

BURROWS, G. F., 1987, W. A. Mines Department 1987 Annual/ Surrender Report, Prospecting Licences P31/176–181, "Triumph" Project, Yerilla District, North Coolgardie Mineral Field, Picon Exploration Pty Ltd: Western Australia Geological Survey, Statutory mineral exploration report, Item 5980 A 1632 (unpublished).

CLAYTON, W., 1988, Paget Gold Mine, Edjudina, Annual Report for Period 11/10/87 to 10/10/88, ML 31/18, PL's 31/747, 748, 749 and PL's 31/770, 771. Associated Gold Fields NL: Western Australia Geological Survey, Statutory mineral exploration report, Item 4304 A24802 (unpublished).

DAVIS, G., 1981, Paget Gold Mines, Edjudina WA, Preliminary Geological Report: Western Australia Geological Survey, Statutory mineral exploration report, Item 4304 A29522 (unpublished).

FINDLAY, D., 1986, The structural controls on the mineralization at the Paget mine Edjudina, Western Australia: Western Australia Geological Survey, Statutory mineral exploration report, Item 4304 A29522 (unpublished).

GIFFORD, A. C., 1985, Commentary on the orientation surface mining and sampling programme at the Paget Gold Mine, Edjudina in June 1985: Western Australia Geological Survey, Statutory mineral exploration report, Item 4304 A29522 (unpublished).

GREG KATER AND ASSOCIATES PTY LTD., 1983, Report of Consulting Geologist, *in* Prospectus dated 13th October, 1983, Paget Gold Mining Company Limited.

HONMAN, C. S., 1917, The Geology of the North Coolgardie Goldfield — Part I. The Yerilla District: Western Australia Geological Survey, Bulletin 73, 98p.

HOWELL, W. J. S., 1983, Paget Gold Mines, Edjudina WA, Preliminary report on percussion drilling program: Western Australia Geological Survey, Statutory mineral exploration report, Item 4304 A29522 (unpublished).

LIDBURY, R. O., 1988, Report on the Paget gold mining area: Western Australia Geological Survey, Statutory mineral exploration report, Item 4304 A24802 (unpublished).

LOFTUS HILLS, 1981, The geological significance and practical importance of work done by Paget Gold Mines of Edjudina Limited: Western Australia Geological Survey, Statutory mineral exploration report, Item 4304 A12568 (unpublished).

MAITLAND, A. G., 1903, Notes on the country between Edjudina and Yundamindera, North Coolgardie Goldfield: Western Australia Geological Survey, Bulletin 11, 58p.

MONTGOMERY, A., 1904, Annual Report for the year 1903: Western Australia, Department of Mines, p. 77–80.

MONTGOMERY, A., 1906, Report on the state of mining progress in the Kurnalpi, Mulgabbie, Pinjin, Edjudina, Yarri, and Yerilla Districts: Western Australia Department of Mines, Annual Report for 1905, p. 82–97.

MULHOLLAND, I. R., 1987, Paget Gold Mine, Edjudina, Annual Report for Period 11/10/86 to 10/10/87, ML 31/18, PL 31/747, 748,749, PL 31/770, 771, Associated Gold Fields NL: Western Australia Geological Survey, Statutory mineral exploration report, Item 4304 A29521 (unpublished).

RUGLESS, C. S., 1975, Report to Department of Mines, W.A. — Results of Exploration on Mineral Tenements During 1974, Edjudina Gold Line: Western Australia Geological Survey, Statutory mineral exploration report, Item 4304 A5744 (unpublished).

SANDERS, T. S., 1985, Report on the hydraulic excavator programme conducted on the Paget Group Leases, Edjudina: Western Australia Geological Survey, Statutory mineral exploration report, Item 4304 A29522 (unpublished).

STROUD, R. A., 1986, Mines Department Report — October 1985–October 1986, Edjudina, M31/18, Paget Gold Mining Company Limited: Western Australia Geological Survey, Statutory mineral exploration report, Item 4304 A19030 (unpublished).

SWAGER, C. P., 1995, Geology of the Edjudina and Yabboo 1:100 000 sheets: Western Australia Geological Survey, 1:100 000 Geological Series Explanatory Notes, 43p.

WILDING, I. G. P., 1975, Final report on Edjudina Gold Project — Results of Exploration of Mining Tenements during 1975: Western Australia Geological Survey, Statutory mineral exploration report, Item 4304 A6189 (unpublished).

20. Pinjin

The Pinjin mining centre lies within the Yabboo domain of the Edjudina Terrane (Swager, 1997), on and to the west of the Pinjin Fault, which forms the margin between the Yabboo and Pinjin domains (Fig. 20.1). The Edjudina Terrane is characterized by BIF marker units and is dominated by intermediate schist, several metamorphosed basalt–andesite–dacite–rhyolite volcanic complexes, and some thin ultramafic units. This terrane is bound to the west by the Claypan Fault and to the east by a zone of strongly foliated granitoids.

The Pinjin domain consists of felsic, intermediate, and mafic schists, minor ultramafic rock, and BIF, all of which are metamorphosed to amphibolite facies. It is thought that the Pinjin domain may represent a higher grade, uplifted portion of the Edjudina Terrane, with uplift occurring along the Pinjin Fault (Swager and Nelson, 1997). SHRIMP dating of zircons from a felsic volcanic rock about 4.5 km north of Pinjin Homestead, just east of the Pinjin Fault, has given an age of 2713 ± 4 Ma (Nelson, 1995).

The gold deposits within the Pinjin mining centre lie within a sequence of metamorphosed intermediate volcanic rocks and derived feldspathic sedimentary rocks and mafic and ultramafic rocks with minor chemical sedimentary rocks, on the interpreted position of the Pinjin Fault and associated splays.

There are three mineralized trends that strike north-northwest over a length of 11 km: the King Pin – Harbour Lights, Pinjin King, and Anglo Saxon trends. The King Pin – Harbour Lights trend comprises (from north to south) King Pin, Pinjin North, Coles, Pinjin Queen, Exile, Lillian, Harbour Lights North, and Harbour Lights, and is hosted by ultramafic schists, minor mafic rocks, and sedimentary rocks. The Pinjin King trend is made up of the Lily of Australia, Pinjin King, and Shamrock gold mines, and is hosted by metamorphosed quartzo-feldspathic sedimentary rocks and felsic to mafic schists. The Anglo Saxon trend, which in terms of gold production is the most significant, lies along the interpreted position of the Pinjin Fault and is hosted by intermediate to felsic schists plus minor BIF. Metagabbro and metadolerite units are associated with many of the deposits and intrude throughout the sequence.

Mineralized structures within these trends are discontinuous brittle–ductile shears. Boudinage structures are common, but not as abundant as in the Edjudina mining area 20 km north. Gold is generally quartz-vein hosted, with only minor mineralization within the host rocks.

Alluvial workings are present between the Exile and Lillian mines.

Deposits of the Pinjin mining area

Anglo Saxon

Other names: Ajax, Mona May Gold Mine, Sirdar, Saxon Extended (Anglo Saxon North is included in this group)

Coordinates: 30°04'36"S, 122°43'55"E

Production: 10 530 t of ore for 199.87 kg Au (18.98 g/t Au) between 1899 and 1940. Saxon Extended has an indicated resource of 270 000 t at 4.1 g/t (1107 kg Au) and an inferred resource of 440 000 t at 6.5 g/t (2860 kg Au; MINEDEX site code S19028).

Modern openpit mining took place between January and July 1987. Mining ceased when fresh rock was

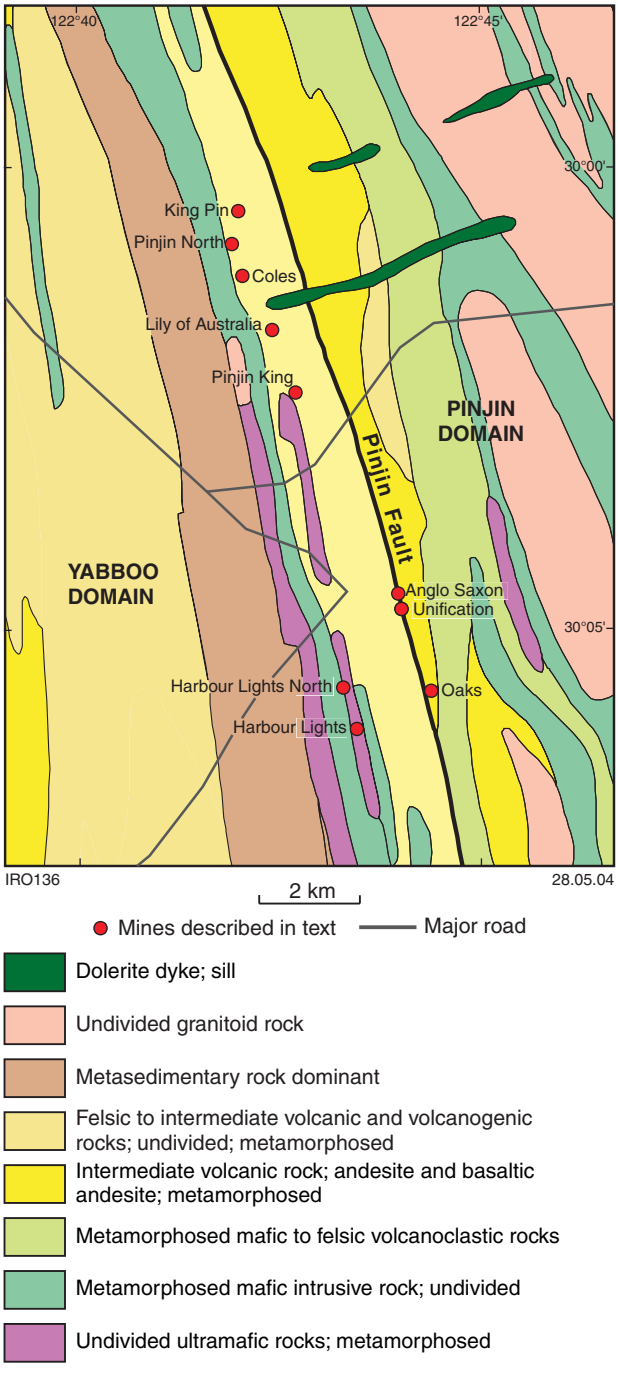

Figure 20.1. Map of the Pinjin mining area

encountered and pit instability problems were anticipated. Production at Anglo Saxon North between 1905 and 1910 was 780.6 t for 16.85 kg Au (21.6 g/t Au) .

Host rocks: Deeply weathered felsic to intermediate volcanic and metavolcaniclastic rocks, chlorite–sericite(–biotite) schists, and minor metadolerite.

Structure: The Anglo Saxon mine lies on the interpreted position of the Pinjin Fault. The foliation in the pit strikes north-northwest and is subvertical to steeply east dipping. There is a stretching lineation that plunges moderately to the south-southeast. In addition to these structural elements there is a regularly spaced jointing normal to the foliation. Coarse-grained muscovite is commonly found on these joint surfaces.

Mineralization is in three broad vein types: an early set of quartz stringers lying subparallel to the main foliation and commonly folded; a series of steep, east-dipping, en echelon quartz-vein sets that trend north-northwest (also subparallel to the main foliation), which are boudinaged and typically 10–20 cm wide (but up to 50 cm wide in places); and shallow, northeast-dipping veins that are boudinaged and folded, with the axial planes of the folds parallel to the dominant regional foliation. The flat veins and the steep, east-dipping veins appear to be contemporaneous.

Historical workings at Anglo Saxon North were on eight lines of narrow quartz veins.

Alteration: As the rocks in the Anglo Saxon pit are deeply weathered, the following description of alteration is based on examination of drillcore. Mineralization is in zones of silicification characterized by irregular quartz stringers and silica replacement. However, not all silicified zones are mineralized. Disseminated chlorite, and to a lesser extent, biotite, is present throughout the deposit and could possibly be of purely metamorphic origin. Carbonate is abundant, constituting 10–20% of most of the rock types, and is dominantly ankeritic in composition (Appendix 5). Ankerite forms as disseminations and irregular elongate aggregates oriented parallel to the foliation. The only rock type examined without significant carbonate alteration is metadolerite; in this unit sericite and silica alteration is predominant.

There are broad zones containing up to 5% sulfides, dominantly pyrrhotite with smaller amounts of pyrite, minor chalcopyrite, and traces of native bismuth, bismuthinite, and pentlandite. These form as disseminations and irregular elongate aggregates oriented parallel to the foliation. The amount and grain size of sulfides increases slightly towards areas of more-intense quartz veining.

Disseminated magnetite porphyroblasts are present in intervals up to 3 m wide and constitute up to 5% of the rock. The foliation wraps around some of these porphyroblasts, producing pressure shadows, whereas others crosscut the fabric, indicating that the growth of magnetite is syntectonic. These zones of magnetite disseminations do not appear to be related to the mineralization.

In addition to quartz veins, there are numerous narrow (generally less than 1 cm wide) veins, rich in coarse-grained calcite and subordinate ankerite. These irregular veins cut across the fabric and appear to fill fractures and voids. Coarse-grained muscovite, chlorite, biotite, and acicular ilmenite are present towards the margins of these veins. The carbonate veins and, to a lesser extent, quartz veins, have narrow alteration selvages (generally less than 1 cm wide) of bleaching, which reflects the destruction of chlorite and biotite. In places they have biotite(–sulfide) rich alteration halos, with some red alteration selvages due to the presence of fine-grained hematite. However, hematite alteration is generally patchy throughout.

Gold forms in quartz veins or in areas of intense silicification as coarse blebs generally associated with sulfides or tourmaline, or both, or as a fine ‘paint’ on fracture surfaces.

Geochemistry: Analyses from sections of drillcore from holes PDD004 and 005 can be found in Appendix 5.

References: Montgomery (1906), Amoco Minerals Aust Co. (1987), Swager (1994).

Coles

Coordinates: 30°01'11"S, 122°42'02"E

Production: 1348.8 t of ore for 12.97 kg Au (9.6 g/t Au) between 1909 and 1910.

Host rocks: Fine-grained, silicified, intermediate to mafic schist.

Structure: One small openpit (<10 m in diameter) with a few open stopes and shafts are developed over a strike length of about 200 m. The ore-bearing structure strikes 350° and is subvertical to steeply west dipping.

Alteration: Mine-dump samples are moderately to deeply weathered. Fresh drill chips were found to be silicified and carbonate altered.

References: Swager (1994).

Harbour Lights

Other name: Harbour Lights South

Coordinates: 30°06'06"S, 122°43'27"E

Production: 351.3 t of ore for 8.72 kg Au (24.8 g/t Au) between 1905 and 1908.

Host rocks: Deeply weathered talc–carbonate schist and subordinate fine-grained metasedimentary rock.

Structure: Several shafts and a few shallow workings lie on at least two parallel structures that strike 340° and dip steeply to the east. The main workings are developed over a strike length of about 100 m and follow a quartz vein up to 1.2 m wide. Gold was obtained from both this and the surrounding wallrock.

Alteration: Alteration is obscured by weathering, although some of the dump material contains small pits due to the weathering out of ankerite and possibly pyrite.

References: Montgomery (1906), Swager (1994).

Harbour Lights North

Other name: Harbour Lights Extended

Coordinates: 30°05'38"S, 122°43'17"E

Production: 148.3 t of ore for 7.11 kg Au (47.9 g/t Au) in 1906.

Host rocks: Talc–chlorite–carbonate schist and deeply weathered fine-grained ?metasedimentary rock.

Structure: A line of shafts, shallow diggings, and stopes follows a 340°-striking, subvertical quartz-veined structure over a distance of 500 m.

Alteration: Alteration is obscured by weathering, although some of the dump material contains holes after carbonate or pyrite, or both.

References: Montgomery (1906), Swager (1994).

King Pin

Coordinates: 30°00'29"S, 122°41'59"E

Production: 682.3 t of ore for 21.42 kg Au (31.4 g/t Au) between 1908 and 1910.

Host rocks: Silicified felsic to intermediate schist, minor fuchsitic schist, and deeply weathered medium- to coarse-grained mafic rock.

Structure: A line of shafts over a strike length of about 400 m follows a subvertical 1 to 1.5 m-wide quartz vein that trends 335°. There is an open stope at the northern end of the workings.

Alteration: Sericite alteration dominates, with minor fuchsite. Vugs caused by the weathering out of carbonate are common, and there are also holes after pyrite in both the quartz and wallrock.

References: Swager (1994).

Lily of Australia

Coordinates: 30°01'46"S, 122°42'25"E

Production: 305.3 t of ore for 7.60 kg Au (24.9 g/t Au) between 1906 and 1907.

Host rock: Felsic to intermediate schist (?metasedimentary rock), generally deeply weathered. There is a small ridge of ultramafic caprock outcropping a few hundred metres south of the workings.

Structure: A few shafts and several open stopes follow a steep, west-dipping structure that strikes 340° over about 100 m.

Alteration: Silica and sericite alteration dominates, with minor ?fuchsite. Numerous small holes are caused by the weathering out of pyrite and carbonate.

References: Swager (1994).

Oaks

Coordinates: 30°05'41"S, 122°44'22"E

Production: 366.8 t of ore for 7.55 kg Au (20.6 g/t Au) between 1905 and 1907.

Host rock: Fine- to medium-grained intermediate rock.

Structure: Numerous shafts and shallow diggings intersect at least nine parallel reefs that trend about 335° over a strike length of 200–300 m. Jointing (some containing coarse-grained muscovite), similar to that observed in the Anglo Saxon openpit, is perpendicular to the main subvertical to steep, east-dipping foliation. Quartz reefs are variable in size from a few centimetres up to 1 m wide.

Alteration: There is some iron-rich carbonate alteration. Relatively coarse muscovite forms on some joint planes in a similar fashion to that at Anglo Saxon, as well as on the margins of some quartz veins. Some of the wider quartz veins are tourmaline bearing, with minor pyrite and scheelite also present.

References: Montgomery (1906), Swager (1994).

Pinjin King

Coordinates: 30°02'27"S, 122°42'41"E

Production: 1713.6 t of ore for 27.48 kg Au (16.0 g/t Au) between 1905 and 1908.

Host rock: Fine-grained chlorite–sericite schist.

Structure: Several shafts and open stopes and one small pit, 5 m-deep, with three shafts on its western margin, follow several parallel, steep, west-dipping structures that strike about 345° over a distance of several hundred metres. Vein quartz on the dumps is up to 30 cm in diameter.

Alteration: Silica and carbonate.

References: Montgomery (1906).

Pinjin North

Other name: Sulphide

Coordinates: 30°00'51"S, 122°41'54"E

Production: 164.1 t of ore for 4.84 kg Au (29.5 g/t Au) between 1907 and 1908.

Host rock: Fine-grained chloritic schist; generally deeply weathered.

Structure: Several shafts follow a subvertical structure that strikes 340° over a distance of a few hundred metres. There is only minor quartz on the dumps, some of which contain cavities after carbonate.

Alteration: Alteration is obscured by weathering.

Unification

Other name: Anglo Saxon South

Coordinates: 30°04'46"S, 122°43'59"E.

Production: 634.0 t of ore for 10.36 kg Au (16.3 g/t Au) between 1911 and 1912.

Host rock: Deeply weathered, fine- to medium-grained feldspar–quartz–biotite rock.

Structure: Vertical shafts follow several subparallel structures that trend 330–340° over a distance of a few hundred metres. Vein quartz up to 30 cm in thickness is common on the mine dumps.

Alteration: Many of the quartz veins are very rich in tourmaline. Fresh drill chips from the mine are strongly silicified, with disseminated pyrite and minor chalcopyrite.

References: Montgomery (1906).

References

AMOCO MINERALS AUST CO., 1987, Annual report, 1987, on GML31/01458: Western Australia Geological Survey, Statutory mineral exploration report, Item 11648 A24068 (unpublished).

MONTGOMERY, A., 1906, Report on the state of mining progress in the Kurnalpi, Mulgabbie, Pinjin, Edjudina, Yarri, and Yerilla Districts: Western Australia Department of Mines, Annual Report for 1905, p. 82–97.

NELSON, D. R., 1995, Compilation of SHRIMP U–Pb zircon dates, 1994: Western Australia Geological Survey, Record 1995/03, 244p.

SWAGER, C. P., 1994, Geology of the Pinjin 1:100 000 sheet: Western Australia Geological Survey, 1:100 000 Geological Series Explanatory Notes, 22p.

SWAGER, C. P., 1997, Tectono-stratigraphy of late Archaean greenstone terranes in the southern Eastern Goldfields, Western Australia: Precambrian Research, v. 83, p. 11–42.

SWAGER, C. P., and NELSON, D. R., 1997, Extensional emplacement of a high-grade granite gneiss complex into low-grade greenstones, Eastern Goldfields, Yilgarn Craton, Western Australia: Precambrian Research, v. 83, p. 203–219.

21. Kalpini and Mayday

The Kalpini mining area is in an area of low regional strain within the Jubilee domain of the Kurnalpi Terrane (Swager, 1997). The Mayday mining area is located within the Gindalbie Terrane, which is separated from the Jubilee domain by the Emu Fault. These mining areas lie 2–4 km from the Emu Fault. Metamorphic grade has not been precisely determined, but appears to be lower to mid-greenschist facies.

A little over 300 kg of gold has been produced from the Kalpini mining area. Only very minor amounts of gold have been produced from the Mayday mining area, but a resource of 475 kg Au has been identified at the Mayday North deposit.

The interpreted geology of the Kalpini mining area is shown in Figure 21.1. Historic mining extracted gold from mafic host rocks — mainly metagabbro. Gold is associated with brittle to brittle–ductile shear zones, sheeted vein systems, and complex vein arrays. The relatively competent metagabbro host unit at Kalpini lies within a broader sequence of schistose felsic volcaniclastic rocks and metashale that is oriented at a large angle to the east–west axis of regional compression. This geometric arrangement favours brittle failure of the more competent unit (Ridley, 1993).

Metagabbroic host rocks in the Kalpini mining area are strongly altered, with an assemblage dominated by chlorite and carbonate. An inner zone of alteration, characterized by sericite–carbonate–pyrite, is present at Camelia and Primrose. Pyrite is the dominant sulfide mineral and is accompanied by minor amounts of chalcopyrite and trace sphalerite.

The Mayday North resource is an oxide-zone deposit located above mafic to intermediate volcanic rocks. Exploration drilling has indicated that hydrothermal alteration of the volcanic rocks beneath the oxide zone has produced sodic rather than potassic assemblages. These are predominantly carbonate–albite–apatite–sulfide assemblages that may be similar to the albite-rich alteration assemblages in mineralized metabasalt at Kurnalpi and Mulgabbie.

Deposits of the Kalpini and Mayday areas

Bank of Kalpini

Coordinates: 30°24'04"S, 121°56'41"E

Production: 16 179.5 t of ore for 46.89 kg Au (2.9 g/t Au) between 1968 and 1971.

Camelia

Other names: Atlas G.M.'s Ltd, Camelia Extended

Coordinates: 30°23'51"S, 121°56'54"E

Production: 12 154.5 t of ore for 183.10 kg Au (15.1 g/t Au) between 1898 and 1910. Some of the production attributed to Atlas G.M.'s Ltd may have come from the Primrose Leases.

Host rock: The principal host rock at Camelia is metagabbro, with mineralization extending into schistose felsic volcaniclastic rocks at depth. The Camelia Extended workings, west of the main shaft area, are in finer grained mafic volcanic rocks. Minor thinly banded and brecciated carbonate–quartz–tourmaline rock of uncertain origin found on mine dumps probably also carries some of the mineralization.

Structure: Several shafts and connecting stopes access a 105°-trending structure over a strike length of about 300 m. The main workings follow a brittle–ductile shear zone that strikes 060° and dips about 70°N, with the main Camelia shaft inclined 60–70°N. The mineralized structure is parallel to the strike of the greenstones, but dips in the opposite direction to the host rocks. Mineralization cuts across the contact between metagabbro and schistose felsic volcaniclastic rocks at depth. The mineralized shear consists of a central zone of strong ductile deformation enveloped by brittle fractures and veining. It has been offset by one or more later, north-striking, steeply east dipping reverse faults.

Two more mineralized structures, parallel to the main line of workings, are about 100 m (Middle Reef) and 170 m (Black Reef) north of the main line of workings (Montgomery, 1907).

Alteration: The mafic wallrocks are intensely altered, resulting in a quartz–plagioclase–chlorite–sericite–carbonate assemblage. This alteration assemblage extends for about 80 m from the centre of the shear zone (Enigma Gold Pty Ltd, 1994). Fuchsitic quartz–sericite–carbonate schist present on mine dumps probably comes from the central zone of strong ductile deformation. Carbonate alteration and fuchsitic assemblages both contain minor amounts of leucoxene, sulfide minerals, and tourmaline. Sulfide minerals are mainly pyrite with minor chalcopyrite and arsenopyrite. Gold forms, together with traces of pyrrhotite and sphalerite, as inclusions in pyrite.

Samples of moderately to strongly foliated tourmaline–quartz–carbonate rock have been found on mine dumps, and presumably form part of the lode system. This rock has the appearance of a breccia, with a tourmaline-rich matrix that has subsequently been deformed.

References: Montgomery (1907), Enigma Gold Pty Ltd (1994).

New Venture

Other names: Gambia, Gambier, Gambier West

Coordinates: 30°24'08"S, 121°56'39"E

Production: 975.9 t of ore for 5.84 kg Au (6.0 g/t Au) between 1902 and 1934.

A trial opencut operation produced 2000 t of ore for 10 kg Au (5 g/t Au) during the late 1970s.

Host rock: Metagabbro.

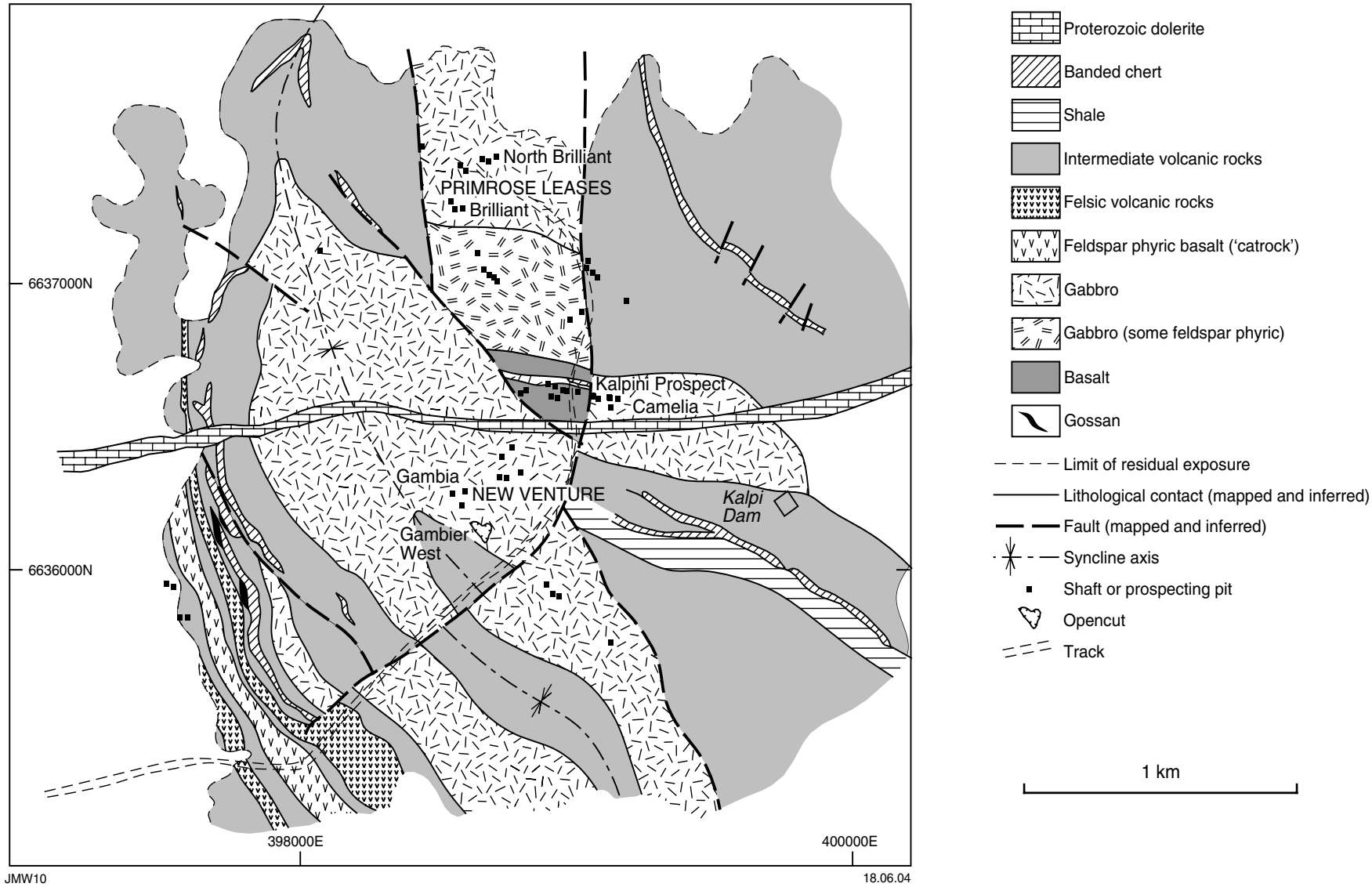

Figure 21.1. Interpreted geology of the Kalpini mining area (modified from Enigma Gold Pty Ltd, 1994)

Structure: The long axis of the trial openpit is oriented northwesterly and is at the southeastern end of what appears to be a larger, northwest-trending vein system. Historic shafts and shallow pits expose the northwestern end of this system. Gold is associated with sheeted quartz veins that dip shallowly to the east and northeast. Individual veins are commonly 1–2 cm wide, but range up to 30 cm and form vein systems that are 2–4 m wide.

Several shallow shafts and open stopes lie on a 250°-trending structure, 200 m northeast of the trail pit. Mine dumps contain abundant laminated vein quartz.

Alteration: Quartz–sulfide vein systems are enveloped by strongly carbonated metagabbro.

References: Kennecott Exploration Australia Pty Ltd (1981), Enigma Gold Pty Ltd (1994).

Gem

Coordinates: 30°23'05"S, 121°30'35"E

Production: 198.6 t of ore for 12.38 kg Au (62.3 g/t Au) between 1900 and 1908.

Host rock: The Gem lode is in mafic rocks (metabasalt, metagabbro, and meta-quartz-gabbro). Metamorphosed feldspar porphyry is also present in the mine environment and may be a significant host rock.

Structure: Shallow shafts and pits trend 325° over 100–200 m. The mineralized structure is not exposed, but mine-dump samples of vein quartz in massive mafic rock suggest gold is associated with a brittle vein array. Historic records indicate that the lode is about 40 cm wide and dips northeast. The main shaft is about 25 m deep and much of the lode was mined to a depth of about 15 m. Several shallow shafts have been sunk on a second structure, subparallel to the main lode and a few metres from it.

Alteration: The mafic wallrocks are intensely altered. The alteration assemblage is dominated by carbonate, with smaller amounts of chlorite, plagioclase, leucoxene, and sulfide minerals. Relict quartz is also present in altered meta-quartz-gabbro. Pyrite is the dominant sulfide mineral. The altered metaporphyry contains feldspar, quartz, chlorite, carbonate, and biotite. Plagioclase in both the altered mafic rock and metaporphyry is extensively sericitized. Quartz–chlorite–carbonate veinlets in the altered metaporphyry contain a chalcopyrite-rich sulfide assemblage.

References: Montgomery (1907).

Primrose Leases

Other names: Brilliant, Brilliant North

Coordinates: 30°23'32"S, 121°56'42"E

Production: 334.2 t of ore for 8.19 kg Au (24.5 g/t Au) between 1898 and 1907.

Host rock: Metagabbro.

Structure: At Brilliant North, shallow shafts and open stopes over a distance of about 100 m identify a west-northwesterly striking lode system that dips at a moderate angle to the north-northeast. Quartz veins exposed within the lode system are 20–30 cm thick, but historic records indicate that vein thicknesses range up to a little over 1 m.

The Brilliant workings, 200 m southwest of Brilliant North, lie on a parallel structure.

Mine dumps at Brilliant and Brilliant North contain samples of vein quartz in undeformed mafic rock. Strongly foliated samples are uncommon, suggesting that the lode system is essentially a quartz-vein array.

Alteration: Mafic wallrocks are intensely carbonated (60–70% carbonate). The alteration assemblage consists of carbonate, chlorite, sericite, leucoxene, and disseminated sulfides. The sulfide assemblage is dominated by pyrite and includes widespread, fine-grained chalcopyrite and a trace of sphalerite.

References: Montgomery (1907).

Mayday North

Coordinates: 30°26'48"S, 121°51'52"E

Production: Historic production amounts to less than 5 kg Au. Geopeko (1991) listed a resource of 127 100 t of ore at 3.74 g/t Au (475.4 kg Au).

Host rocks: The resource is located in a silica-enriched cap that lies between the oxide zone and a primary sulfide zone in metabasalt and meta-andesite.

Structure: The orebody in the silica-enriched cap is essentially flat lying, but little is known about the structure of the underlying primary mineralization at Mayday North. It lies within a north-northwesterly trending greenstone sequence. The mafic–intermediate host unit dips 40°E and lies within metamorphosed sedimentary and felsic volcaniclastic rocks, but is only a few hundred metres east of a major contact between felsic rocks to the east and mafic rocks to the west. Petrological observations suggest that hydraulic fracture and brecciation were important processes in the origin of the primary mineralization.

A north-northwesterly trending Proterozoic dolerite dyke lies directly west of the Mayday North orebody.

Alteration: Drilling beneath the resource in the silica-enriched cap has provided information about the hydrothermal alteration associated with the primary mineralization. Geopeko (1991) interpreted a zoned alteration sequence. Unlike many mafic-hosted lode-gold deposits in the Eastern Goldfields Granite–Greenstone Terrane, gold is not associated with sericite-bearing rocks, but with a carbonate–albite–pyrite–arsenopyrite–apatite assemblage cut by veins containing quartz, carbonate, albite, and apatite in various proportions. The sulfide minerals include minor pyrrhotite and chalcopyrite. Gold forms as inclusions in pyrite, but has not been observed in arsenopyrite.

The mineralized zone passes outwards into a less well mineralized chlorite–sericite(–epidote–albite)–leucoxene–pyrite assemblage.

References: Geopeko (1991).

References

ENIGMA GOLD PTY LTD, 1994, Annual report, Mar 1993 to Mar 1994, on P27/1260–1263: Western Australia Geological Survey, Statutory mineral exploration report, Item 11654 A43100 (unpublished).

GEOPEKO, 1991, Annual report, 1990, on Kalpini gold exploration: Western Australia Geological Survey, Statutory mineral exploration report, Item 11656 A33041 (unpublished).

KENNECOTT EXPLORATION AUSTRALIA PTY LTD, 1981, Annual report 1981, MC27/01880–01881 and GML27/01828–01834: Western Australia Geological Survey, Statutory mineral exploration report, Item 2785 A10473 (unpublished).

MONTGOMERY, A., 1907, Notes on Mines at Kalpini (1906) — Division II: Appendix 'F'.- Report of the Department of Mines for the year 1906, p. 70–71: Perth by Authority, P.P. No 2 of 1907.

RIDLEY, J. R., 1993, The relations between mean rock stress and fluid flow in the crust: with reference to vein- and lode-style gold deposits: Ore Geology Reviews, v. 8, p. 23–27.

SWAGER, C. P., 1997, Tectono-stratigraphy of late Archaean greenstone terranes in the southern Eastern Goldfields, Western Australia: Precambrian Research, v. 83, p. 11–42.

22. Gindalbie

The Gindalbie mining area (Fig. 22.1) lies within the northern part of the Gindalbie Terrane of Swager (1997). This region consists of a metamorphosed bimodal basalt – felsic volcanic (dacite–rhyolite) sequence. Felsic rocks near Old Wild Dog and Maggies dams have been dated at 2709 ± 4 and 2681 ± 5 Ma respectively (Nelson, 1995). The metamorphic grade in the area is lower greenschist facies.

Gold was mined from four main centres, the largest of which is near the old Gindalbie town site (South Gippsland Leases, Homeward Bound, United Leases, and Eclipse). The other centres are Whiteheads Find, Hayes New Find (Diamond Jubilee), and Lindsays Find. The total production from the area is about 1263 kg of gold, with most of this mined from the South Gippsland Leases.

Mineralization is hosted by metamorphosed felsic to intermediate volcaniclastic and clastic rocks, metabasalt, minor metagabbro, and metamorphosed intrusive porphyry.

Gold is hosted within northwesterly to north-northwesterly trending brittle–ductile shear zones. Lodes consisting of subparallel, closely spaced quartz veins are up to 3 m wide. Laminated quartz veins are common.

Exploration reports (e.g. Auralia Resources NL, 1993) interpreted mineralization to be in splays or conjugate faults of a major, north-northwesterly trending fault or shear zone that dominates the area and is clearly visible on aeromagnetic images. The same feature has been interpreted by Ahmat (1995) and Swager (1995) as a Proterozoic mafic to ultramafic dyke. The feature does not appear to offset any units, is at a different angle to the main structural trend of the greenstones, and is discontinuous at its southern end.

The main alteration phases are quartz, sericite, chlorite, carbonate, pyrite(–albite), biotite, tourmaline, epidote, rutile, chalcopyrite, and pyrrhotite. Quartz veins may contain carbonate, albite, tourmaline, sulfides, or muscovite.

Deposits of the Gindalbie area

Homeward Bound Leases

Other names: Cosmopolite, Red and White

Coordinates: 30°20'12"S, 121°46'05"E

Production: 394.5 t of ore for 10.55 kg Au (26.7 g/t Au) between 1897 and 1906.

Host rock: Mine dumps consist of a deeply weathered, fine-grained, metamorphosed felsic to intermediate volcaniclastic or volcanic rock.

Structure: These leases are immediately south of the South Gippsland mining leases and are therefore probably on the same structure. Several shafts and shallow trenches are sparsely scattered over a strike length of about 700 m. Foliations in and around the workings strike 330–340° and are subvertical to steeply west dipping.

Parts of lodes are exposed in the workings as zones of narrow quartz veins that lie subparallel to the foliation. A subvertical quartz vein up to 70 cm wide is exposed in some of the workings.

Alteration: Dump material has the alteration assemblage sericite–chlorite – iron oxide (after carbonate) – biotite–quartz(–tourmaline).

Diamond Jubilee

Other names: Diamond Jubilee Extended, Jubilee, Little Nell

Coordinates: 30°17'17"S, 121°43'42"E

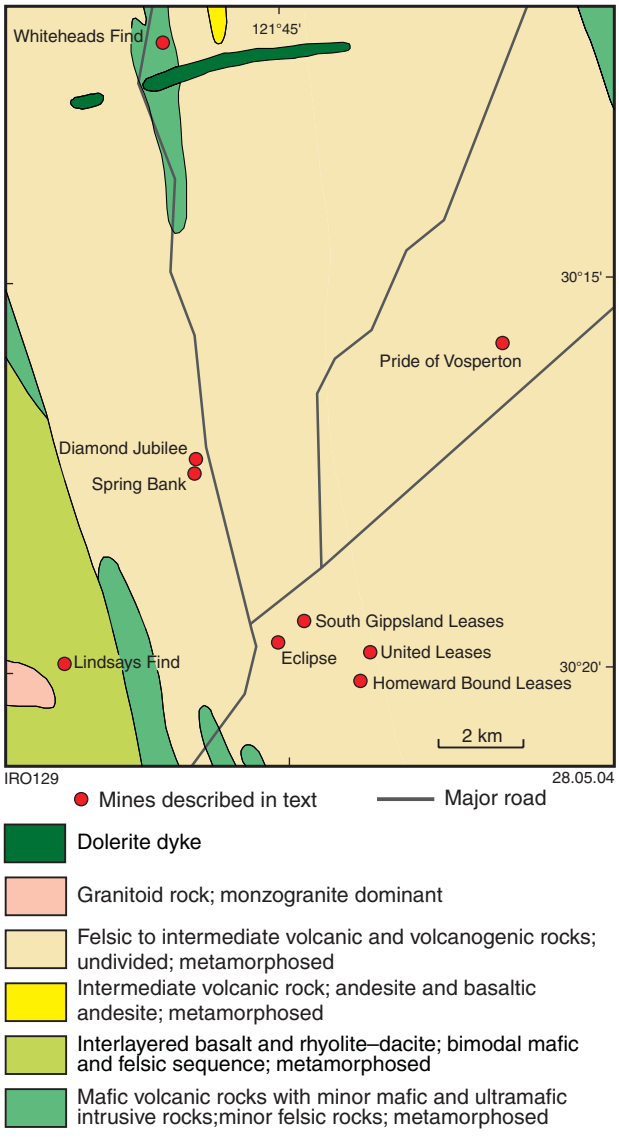

Figure 22.1. Map of the Gindalbie mining area

Production: 517.2 t of ore for 15.76 kg Au (30.5 g/t Au) between 1897 and 1907.

Host rock: The mine dumps consist of altered and deeply weathered intermediate to mafic rock. The precursor was possibly a metamorphosed intermediate to mafic volcaniclastic or sedimentary rock. Metagabbro intrusions are also present in the area.

Structure: A few shafts and open stopes follow a structure that trends 300° to 310°. Quartz-vein material on the dumps indicates that veins were up to 30 cm wide but predominantly narrow. Company reports state that mineralization is associated with zones of subparallel, closely spaced, narrow quartz veins.

Immediately south is the Spring Bank gold mine (<5 kg production), which lies on a north-trending structure that dips steeply to the west.

Alteration: Material found on the dumps has the mineral assemblage sericite–chlorite–quartz–biotite – iron oxide. Iron oxide pseudomorphs after pyrite are present in quartz veins and some of the wallrocks.

Rocks from the Spring Bank mine to the south are less-deeply weathered and, in addition to the above minerals, contain carbonate, feldspar, epidote, pyrite, chalcopyrite, and pyrrhotite.

References: Auralia Resources NL (1993).

Eclipse

Coordinates: 30°19'45"S, 121°44'60"E

Production: 954.1 t of ore for 23.46 kg Au (24.6 g/t Au) between 1903 and 1911.

Host rock: Gold mineralization is hosted by a fine-grained, metamorphosed felsic to intermediate volcaniclastic or sedimentary rock.

Structure: The main shaft is along strike from a subvertical stope (exposed in a costean) that trends 315°. This follows a 1–2 m-wide lode with quartz veins averaging 7 cm across (maximum 20 cm). Northwest of the shaft is a costean that exposes a 2 m-wide quartz–tourmaline vein.

About 100 m west of the main workings is another group of shafts and trenches that trend about 010°. The dominant foliation in the area strikes 320–345° and is subvertical to steeply southwest dipping. A shallow, southeast-plunging mineral lineation can be seen in some of the costeans.

On a thin-section scale, sulfides are associated with thin quartz–carbonate lenses that are probably disrupted veins. This suggests that mineralization occurred either before or, more likely, during ductile deformation.

Alteration: The alteration assemblage comprises sericite–chlorite–carbonate–pyrite–chalcopyrite – secondary Fe–Ti-oxides (–tourmaline).

Whiteheads Find

Other names: Gindalbie, Patches, Vosperton G.M.'s Ltd, Lady Betty

Coordinates: 30°11'56"S, 121°43'16"E

Production: 613.69 t of ore for 21.45 kg Au (35.0 g/t Au) between 1898 and 1908. Lady Betty produced 1031.49 t for 42.77 kg Au (41.5 g/t Au) between 1941 and 1954, but its location is uncertain.

Host rock: The main workings are hosted by metabasalt (some of which is coarsely feldspar phyric) as well as a fine-grained felsic to intermediate rock. Quartz–sericite schist is found on the mine dumps at Gindalbie.

Structure: At the main set of workings, several shafts form a line that trends 300° over a distance of about 300 m. A subvertical foliation in the mine area strikes 340° and a mineral lineation plunges shallowly to the south. Quartz-vein material on the dumps is up to 20 cm across. Veins and stringers of quartz are both parallel and transgressive to the foliation. Some dump samples show intense ductile deformation with coarse feldspar phenocrysts being flattened.

The Patches mine (Gindalbie) lies about 500 m southeast of the main Whiteheads Find workings. Here the workings trend 340° and consist of a small pit at the northern end and several shafts to the south. A costean south of the shafts exposes two narrow lode horizons and a 20 cm-wide quartz vein, all of which lie subparallel to the foliation, which dips steeply to the west. The Patches gold mine lies in a zone of strong ductile deformation with a sinistral sense of movement.

Alteration: The metamorphosed feldspar-phyric basalt has the assemblage chlorite–plagioclase–carbonate–sericite–ilmenite(–epidote–biotite–tourmaline–magnetite). Pyrite is the most common sulfide in the deposit, with minor chalcopyrite or pyrrhotite inclusions (or both), and chalcopyrite is also common. Traces of bornite, covellite, and sphalerite have also been observed.

In addition to quartz, veins are also rich in carbonate, tourmaline, or epidote; muscovite and sulfides are common accessories.

Quartz–sericite schist from the Patches gold mine has the assemblage quartz–sericite–feldspar–biotite–chlorite–pyrite–chalcopyrite. Tabular chlorite grains cut across the foliation defined by sericite.

References: Resource Service Group Pty Ltd (1990).

Pride of Vosperton

Other names: Moudland, Monkland

Coordinates: 30°15'50"S, 121°48'15"E

Production: 817.9 t of ore for 28.33 kg Au (34.6 g/t Au) between 1900 and 1906.

Host rock: The deposit is hosted by metamorphosed felsic volcaniclastic rocks.

Structure: Two shafts have been dug into a subvertical structure that trends about 350°. A moderate to strong foliation that strikes 330–350° is exposed in costeans along strike from the workings. Minor vein quartz is found on the dumps and is up to 20 cm across.

Alteration: Dump samples have the assemblage quartz–plagioclase–carbonate–sericite–chlorite(–biotite–pyrite–chalcopyrite).

South Gippsland Leases

Other names: South Gippsland Nos 1–5, Kalgoorlie Foundry Ltd, Melton, Melton G.M. Co. Ltd, Queen Margaret G.M. Co. Ltd

Coordinates: 30°19'23"S, 121°45'16"E

Production: 36 516.2 t of ore for 1013.85 kg Au (27.8 g/t Au) between 1897 and 1940.

Host rock: The South Gippsland group of workings is hosted by fine- to medium-grained, deeply weathered, metamorphosed felsic to intermediate clastic and volcaniclastic rock.

Structure: Several groups of workings host gold mineralization at South Gippsland, with the main leases being continuous with the Homeward Bound mine to the south. The group of leases has a northerly trend and the South Gippsland No 3 lease lies about 1 km northwest of the main leases.

Gold mineralization at the main workings is hosted within a steep, southerly plunging ore shoot that was worked to a depth of 230 m over an average strike length of 60 m. A network of laminated quartz veins makes up the shoot, and ranges from 0.5 to 2.75 m in width. To the east of this lies a ?west-dipping reef, which was reported to be partially stoped between the 74-m and 59-m levels (Auralia Resources NL, 1987b). Parallel veins are reported to be about 18 m east and 64 m west of the main reef, but have not been extensively mined (Auralia Resources NL, 1993).

Individual quartz veins, up to 1 m wide, are laminated and usually lie subparallel to the main foliation.

Alteration: The alteration assemblage comprises carbonate–chlorite–sericite–quartz(–pyrite–chalcopyrite–rutile–tourmaline–biotite–ilmenite–galena–sphalerite). Vein quartz is also rich in carbonate and may contain tourmaline as well as up to 5% sulfides. The alteration halo has been documented to extend for at least 40 m into country rocks (Auralia Resources NL, 1987b). The depth of weathering extends to about 50 m (Auralia Resources NL, 1993).

References: Auralia Resources NL (1987a,b, 1993)

United Leases

Other names: Occidental, Rising Star

Coordinates: 30°19'47"S, 121°46'14"E.

Production: 2921.1 t of ore for 81.35 kg Au (27.8 g/t Au) between 1897 and 1912.

Host rock: Mineralization at the United Leases is hosted by metamorphosed, fine- to medium-grained felsic to intermediate clastic and volcaniclastic rocks.

Structure: Lying immediately east of the South Gippsland Leases, the main workings at the United Leases consist of several shafts, open stopes, and small pits that follow a 350°-striking, steeply east dipping structure over a strike length of about 300 m. Several other groups of workings, north-northwest to northwest of the main workings, dip moderately to the west. The total lease area extends over a strike length of about 750 m. Gold is found in laminated quartz veins.

Alteration: The alteration assemblage comprises quartz–carbonate–sericite–plagioclase–chlorite(–tourmaline–biotite–pyrite–chalcopyrite–rutile–covellite).

Lindsays Find

Other name: ?Aberfoyle

Coordinates: 30°19'53"S, 121°41'43"E

Production: There is no official recorded historic or modern production for the Lindsays Find area. A trial openpit was mined by AUR NL during the twelve months proceeding May 1989. At the Mount Martin mill, 1700 t of ore was treated for about 6.8 kg Au (4 g/t Au).

Host rock: Gold mineralization is hosted by metabasalt intruded by a medium-grained, metamorphosed feldspar–quartz–biotite porphyry. Minor fine-grained, metamorphosed felsic to intermediate volcanic to volcaniclastic rock is also present in the pit.

Structure: The main structure seen in the pit is a well-developed, closely spaced jointing. The foliation varies from 290 to 310° and is subvertical to steeply northeast dipping. Metamorphosed feldspar–quartz porphyry dykes intrude the metabasalt sequence and are up to several metres wide. Gold mineralization is associated with the contacts between these dykes and the metabasalt.

Quartz veins are not common in the pit and are typically less than 4 cm wide. Mineralization is associated with stringers of quartz, carbonate, albite, and sulfides.

Alteration: The metamorphosed feldspar–quartz porphyry has the alteration assemblage plagioclase–quartz–sericite–carbonate–pyrite(–biotite–chlorite–?rutile). The original rock is strongly fractured, with fractures infilled by albite, quartz, and minor carbonate. Alteration is evident in the bleaching of the metaporphyry due to the strong silicification and destruction of ferromagnesian minerals such as biotite and ilmenite.

Metabasalt has the alteration assemblage plagioclase–carbonate–quartz–chlorite–biotite–pyrite. The rock is cut by carbonate and carbonate–albite veinlets up to 3 mm wide.

Sulfides constitute up to 10% of the rock and consist of pyrite, some samples of which contain inclusions of pyrrhotite and rare chalcopyrite. A sample of mineralized metabasalt examined in thin section contained at least 27 grains of gold, up to 0.05 mm in diameter, as inclusions and lining fractures within pyrite. Gold was also supposedly found in telluride minerals during historic mining from the original shaft (Smart, S., 1996, pers. comm.).

Geochemical analyses of three metaporphyry and metabasalt samples are shown in Appendix 5.

References: AUR NL (1989).

References

AHMAT, A. L., 1995, Geology of the Kanowna 1:100 000 sheet: Western Australia Geological Survey, 1:100 000 Geological Series Explanatory Notes, 28p.

AUR NL, 1989, Annual report on GML27/01721, GML27/01758, P27/00715, P27/00750, P27/00746–00747, P27/00758–00759, 27/00752–00754: Western Australia Geological Survey, Statutory mineral exploration report, Item 11650 A28065 (unpublished).

AURALIA RESOURCES NL, 1987a, Annual report, November 1986 to November 1987, for P27/00205–00210: Western Australia Geological Survey, Statutory mineral exploration report, Item 6402 A21025 (unpublished).

AURALIA RESOURCES NL, 1987b, Annual report, 1986 to 1987, on P27/00608, P27/00045, P27/00043, P27/00034–00077: Western Australia Geological Survey, Statutory mineral exploration report, Item 3545/1 A21655 (unpublished).

AURALIA RESOURCES NL, 1993, Report on E27/74, P27/1119 and M27/152: Western Australia Geological Survey, Statutory mineral exploration report, Item 11644 A39362 (unpublished).

NELSON, D. R., 1995, Compilation of SHRIMP U–Pb zircon dates, 1994: Western Australia Geological Survey, Record 1995/03, 244p.

RESOURCE SERVICE GROUP PTY LTD, 1990, Annual report, 1989, on Whiteheads Find gold exploration: Western Australia Geological Survey, Statutory mineral exploration report, A30569 (confidential)*.

SWAGER, C. P., 1995, Geology of the Edjudina and Yabboo 1:100 000 sheets: Western Australia Geological Survey, 1:100 000 Geological Series Explanatory Notes, 43p.

SWAGER, C. P., 1997, Tectono-stratigraphy of late Archaean greenstone terranes in the southern Eastern Goldfields, Western Australia: Precambrian Research, v. 83, p. 11–42.

* Confidential references are used with permission of companies.

23. Kanowna

The Kanowna mining area lies within the Boorara domain of the Kalgoorlie Terrane of Swager (1997). The geology and location of the main gold deposits are shown in Figure 23.1. The stratigraphy of the area consists of a basal metabasalt unit, metachert and ultramafic rocks, and upper metavolcanic and metasedimentary rocks. The metamorphic grade of the area is lower greenschist facies.

Gold was discovered at Kanowna in 1893. Production was initially from quartz reefs along the White Feather structure, and later from deep leads and cemented alluvium (Beckett et al., 1998). Historical production (>15 500 kg Au) in the Kanowna area peaked in about 1900 before rapidly declining after 1914 (Beckett et al., 1998). About half of the historical production was from alluvial and deep leads and half was from quartz reefs (Truelove et al., 1997).

The most significant gold deposit in the area, Kanowna Belle, was discovered in 1989 concealed beneath soil and leached saprolite. The deposit is not exposed at the surface, and as a consequence, remained undiscovered for more than 90 years (Gellatly et al., 1995). Mineralization is hosted by metamorphosed feldspar–quartz porphyry and volcaniclastic and clastic rocks, with the majority of the Kanowna Belle resource within metamorphosed feldspar-phyric porphyry. Mineralization at Kanowna Belle is juxtaposed with a major northeast-trending structural feature — the Fitzroy Shear Zone (Beckett et al., 1998).

There are three styles of gold mineralization in the Kanowna mining area:

- Alluvial and deep-lead mineralization in palaeochannels result from supergene alteration of ancient (?Tertiary) auriferous river channels. Gold within the palaeochannels was probably sourced from nearby gold lodes and structures within the saprolitic bedrock immediately beneath the channels.
- Stockwork mineralization consists of brittle, flat-lying, quartz-rich veins. Red Hill is the best example; Ho (1984) and Ross (1993) considered the Red Hill gold deposit to have formed as a consequence of the interaction of the ore fluids with oxidized metaporphyry. Gold precipitated with the change in oxidation state of the ore fluid, as indicated by a change in oxidation state of iron in the alteration zones (Ho, 1984; Ross, 1993).
- Brittle-shear-hosted mineralization are either vein stockworks and vein arrays with local brecciation (e.g. Kanowna Belle) or massive to laminated quartz veins (e.g. Kanowna Main Reef). Orogenic gold is a result of this style of mineralization. The Kanowna Belle deposit, and possibly the Kanowna Main Reef deposits, are related to D_2 deformation (Davis et al., 2000).

Based on gold composition and SHRIMP U–Pb dating of zircons, two generations of gold mineralization are proposed for the Kanowna Belle deposit: gold mineralization within clasts of the Grave Dam grit, related to a c. 2670 Ma epithermal system; and orogenic gold deposited during the later part of east-northeast to west-southwest regional D_2 deformation, following the intrusion of the Kanowna Belle metaporphyry at 2655 ± 6 Ma (Ross et al., 2001).

Deposits of the Kanowna mining area

Kanowna Six Mile

Other names: Chance, Signal Junction, Signal No. 3, Signal Success, Signals Consols Leases, William Tell

Coordinates: 30°34'48"S, 121°32'04"E

Production: 289 t of ore for 13.272 kg Au (21.8 g/t Au), plus 19.65 kg dollied gold, between 1900 and 1909. In 1987, the Kanowna Six Mile and Fletcher pits produced about 44 000 t of ore at 4.31 g/t Au and about 45 000 t of low-grade ore at 1.33 g/t Au (MINEDEX site code S02133).

Host rock: Soil and recent cover obscure the bedrock; however, the host rocks exposed in pits and shafts include metamorphosed mafic volcanic rocks, lenticular metacherts, and metamorphosed felsic volcanic and sedimentary rocks. The rock sequence is intruded by metamorphosed quartz–feldspar porphyry (Western Mining Corporation, 1989).

Structure: Mineralization is associated with quartz–carbonate–tourmaline veins, which commonly follow northeast-striking fractures (moderate to shallow northerly dip), and alteration zones adjacent to intrusive contacts or in faults and shears (Western Mining Corporation, 1989).

Most of the pits and shafts target quartz veining at metaporphyry–metabasalt contacts. Mineralization is also in metamorphosed banded and pyritic chert beds, which are mostly about 0.75 to 2 cm thick (Western Mining Corporation, 1989).

Some shafts target the laterite profile, and gold nuggets were recovered in the topsoil and eluvial material.

Alteration: The rocks at Kanowna Six Mile have been subjected to carbonate alteration, and are locally micaceous, siliceous, and pyritic. Alteration is intense in faults and shears, and to a lesser extent at metaporphyry contacts.

References: Western Mining Corporation (1989).

Golden Valley

Other names: Golden Valley (WA) G.M. Co. NL, Golden Valley East, Golden Valley Leases, Golden Valley Main Reef, Golden Valley West

Coordinates: 30°34'05"S, 121°35'56"E

Production: The estimated production from the Golden Valley mine, including deep leads is 28 585.6 t of ore for 526.983 kg Au (18.4 g/t Au; MINEDEX site code S00384).

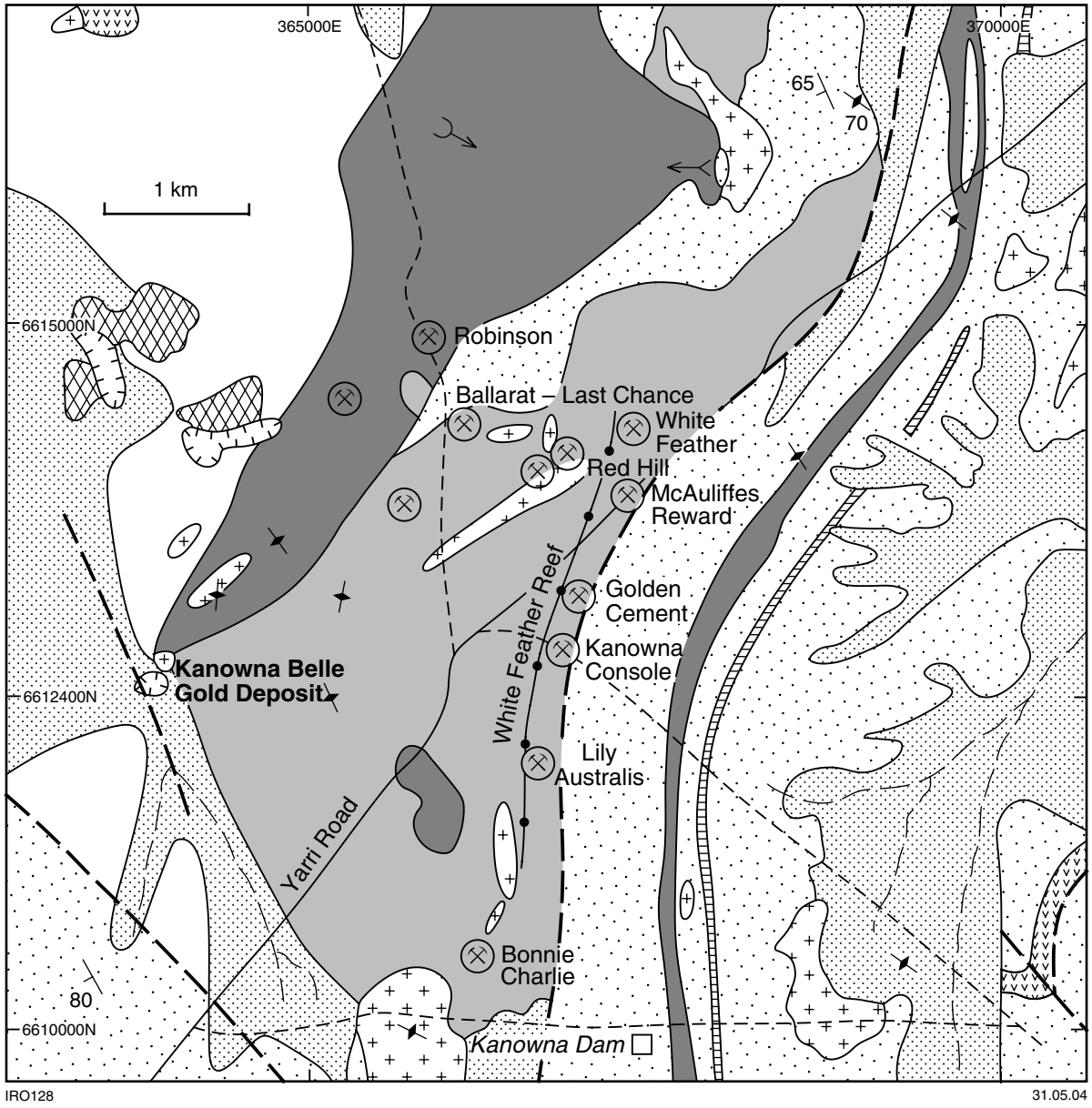

Figure 23.1. Simplified geology map of the Kanowna mining area

Host rock: Mafic and ultramafic units.

Structure: Two mineralized shoots, over 30 m in length, were mined from a 60°-striking, north-dipping quartz vein within the shear zone at the contact between mafic and ultramafic units (Peachey, 1993). Minor metaporphyry is present in the shear zone.

References: Peachey (1993).

Robinson

Other names: Robinson–O'Hallahans, Robinson Extended

Coordinates: 30°35'11"S, 121°36'16"E

Production: 3454 t of ore for 79.54 kg Au (23.0 g/t Au) between 1901 and 1936. However, historical production estimated by Truelove et al. (1997) was 48 440 t for 968.8 kg Au (20 g/t Au). Current resources are: measured — 1.79 Mt at 1.7 g/t Au (3043 kg Au); indicated — 1.6 Mt at 2.0 g/t (3360 kg Au); and inferred — 0.21 Mt at 2.2 g/t (462 kg Au; MINEDEX site code S00382).

Host rock: The host rock is a metamorphosed ultramafic volcanic rock. A brecciated metamorphosed felsic volcaniclastic sedimentary rock forms the hangingwall contact (Truelove et al., 1997).

Structure: Mineralization at Robinson is associated with subvertical, east-northeasterly trending laminated quartz veins and associated alteration (Truelove et al., 1997). There is also subhorizontal supergene gold mineralization below a 20-m depleted zone (Fig. 23.2) in the south-western part of the deposit (Truelove et al., 1997).

Alteration: Alteration zones of carbonate–fuchsite (Cr-sericite)–quartz–sulfide are associated with the quartz veining.

References: Truelove et al. (1997).

Ballarat – Last Chance

Other names: Ballarat and Prince Oscar Syndicate Ltd, Ballarat and Prince Oscar Co. Ltd

Coordinates: 30°35'39"S, 121°35'58"E

Production: Historical production took place mainly during 1903–12, with small productions in 1934 and 1946. The production reported to the Mines Department totalled 30 410 t of ore for 458.02 kg (15.06 g/t Au), as well as 22.414 kg of dollied gold and 0.122 kg of alluvial gold. Truelove et al. (1997), however, reported a historical production of 57 456 t for 913.55 kg Au (15.9 g/t Au). Between 1986 and 1987, opencut mining produced 187 000 t for 374 kg Au (2.0 g/t Au; Truelove et al., 1997). Current resources are: measured — 0.38 Mt at 2.8 g/t Au (1064 kg Au); indicated — 0.78 Mt at 2.2 g/t Au (1716 kg Au); and inferred — 0.73 Mt at 2.1 g/t Au (1533 kg Au; MINEDEX site code S00377).

Host rock: Gold mineralization is hosted by meta-komatiite, with lower grade gold within metamorphosed porphyry and felsic volcaniclastic sedimentary rocks.

Structure: Mineralization at Ballarat – Last Chance is within fault-bound wedges of ultramafic rocks within a broad, arcuate, northeast-trending, structurally complex zone known as the Kanowna Belle Mine Corridor (Truelove et al., 1997). The main gold-bearing structure is an east–west lens of alteration and subvertical and subhorizontal quartz veins, with smaller amounts of gold in narrow, subvertical, north-trending quartz veins orthogonal to the main mineralization (Truelove et al., 1997). Higher grade, pipe-like shoots are present at the intersection between north-trending quartz veins and alteration zones associated with east-trending veins (Truelove et al., 1997).

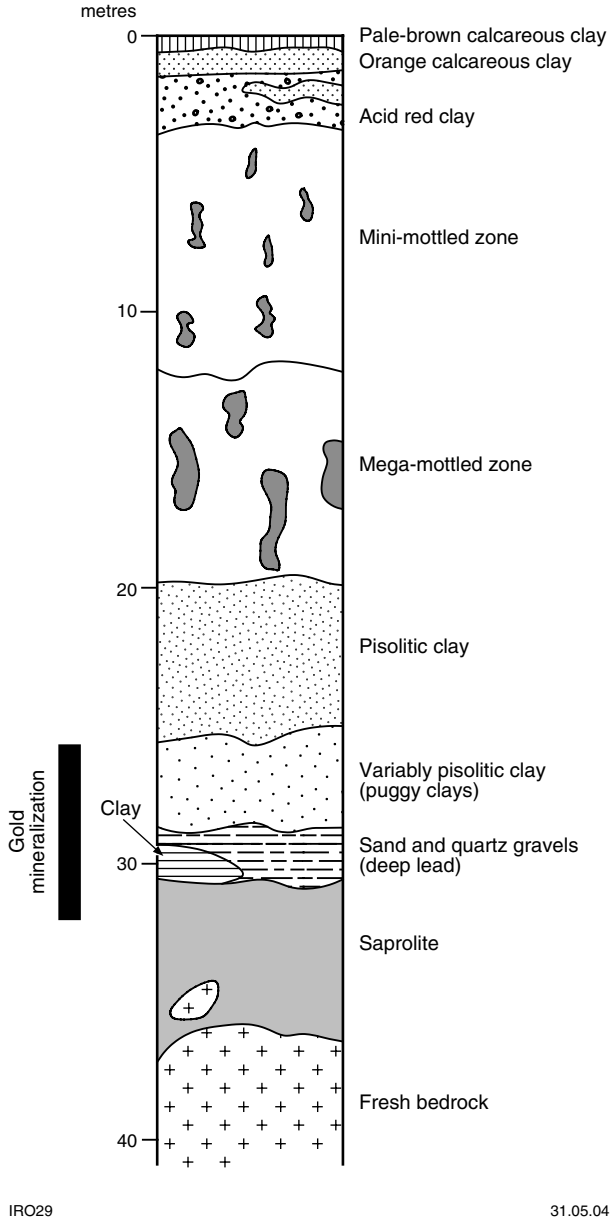

Figure 23.2. Schematic diagram of the profile of a palaeo-channel in the Kanowna mining area (after Dell and Anand, 2001)

The main mineralization (east–west quartz veins) continues east of a shear (locally known as the Isabella shear) that marks the contact between the metakomatiite and metamorphosed felsic volcaniclastic sedimentary rocks. East of this shear, as well as in east-trending porphyries, the gold mineralization is of a lower grade (Truelove et al., 1997).

Alteration: The alteration assemblage comprises fuchsite–carbonate–quartz–sulfide.

References: Truelove et al. (1997).

Red Hill

Other names: Gently Polly, Kintore, Madame Melba, Monte Christo

Coordinates: 30°35'48"S, 121°36'40"E

Production: 43 379.1 t of ore for 1507.42 kg Au (34.75 g/t Au) between 1902 and 1918. Current resources are: measured — 1.507 Mt at 1.9 g/t Au (2863.3 kg Au); indicated — 7.596 Mt at 1.7 g/t Au (12 913.2 kg Au); and inferred — 1.83 Mt at 1.6 g/t Au (2928 kg Au; MINEDEX site code S03419).

Host rock: The host rock to the gold mineralization is a metamorphosed massive dacitic porphyry that has intruded metamorphosed polymictic conglomerate. The metaporphyry comprises quartz, plagioclase, biotite, and rare carbonate–mica aggregates in a fine-grained, mosaic-textured groundmass of quartz and feldspar (Ho, 1984).

Structure: Gold mineralization at Red Hill is in vertically stacked, subhorizontal auriferous quartz veins within a metaporphyry boss (Ho, 1984). The quartz veins are convex upwards with a shallow northeast to southwest dip (10–20°), and range in thickness from 1 to 50 cm (typically between 5 and 30 cm; Ho, 1984). The mineralogy of the veins is mainly quartz, with smaller amounts of carbonate, albite, pyrite, galena, and native gold. Quartz within the veins is usually massive, but vughs containing randomly oriented quartz crystals are locally present (Ho, 1984). Carbonate and albite are typically present adjacent to the vein margins. Maitland (1919) noted that gold mineralization is higher grade in veins that have an arch- or dome-like form and are joined by smaller offshoots, and when galena is present.

Alteration: Alteration assemblages comprise fuchsite–chlorite–carbonate–albite–pyrite. The alteration halos adjacent to veins are up to 1 m wide, and due to the spacing of veins they typically overlap (Ho, 1984). These alteration zones show a marked increase in S, CO_2, and K_2O and smaller increases in CaO, MgO, and SiO_2 (Grigson, 1981).

Fluid-inclusion composition is H_2O–CO_2, with low salinity (<2 wt% equivalent NaCl). Trapping temperatures range from 280 to 320°C, with a pressure of about 100 MPa (Ho, 1984).

References: Maitland (1919), Grigson (1981), Ho (1984).

White Feather Main Reef

Other names: North White Feather, Black Feather Area, White Feather Reward, McAuliffes Reward, Lily Australis

Coordinates: 30°35'56"S, 121°36'56"E

Production: 446 254 t of ore for 7064.035 kg Au (15.8 g/t Au) between 1902 and 1924, in 1935, and between 1967 and 1974 (production figures include all mines located on the Kanowna Main Reef). Current resources (inferred) are 2.7 Mt for 3780 kg Au (1.4 g/t Au; MINEDEX site code S06548).

Host rock: The Kanowna Main Reef is hosted by a metamorphosed polymictic conglomerate. Pebbles and boulders are typically well rounded and vary in size from 1.3 to 76.2 cm, but are mostly 5.1 to 15.2 cm in diameter (Blatchford and Jutson, 1912). Clasts vary in composition and mainly include komatiite with cumulate and spinifex textures, metamorphosed mafic volcanic rocks, and metamorphosed felsic porphyry.

Structure: The Kanowna Main Reef is a large, massive to laminated quartz vein, with local branches and bifurcations, that extends for more than 3 km in a northerly to north-northeasterly direction (Ho, 1984). It dips at 40–70°E and is restricted to a shear zone (Ho, 1984). The quartz vein is typically 0.5 to 2 m thick, but can vary from a small stringer to about 3 m thick (Jutson, 1914). Most of the historical production of the Kanowna mining centre was from the Kanowna Main Reef, the main mines being (from north to south) North White Feather, White Feather Reward, White Feather Main Reef, and Lily Australis (Fig. 23.1).

The vein is composed of quartz and smaller amounts of carbonate, pyrite, and galena, with mineralization in the form of free gold (Blatchford and Jutson, 1912). Laminations in the vein are due to interlayered talc–chlorite, probably derived from adjacent rocks (Ho, 1984). Higher grades were obtained from laminated parts of the vein (Ho, 1984), and as was the case at Red Hill, galena was an indicator of higher grade gold mineralization (Maitland, 1919). Higher gold grades were also obtained where the strike of the vein changed and there was development of a spur or branch (Blatchford and Jutson, 1912).

The contact between the hangingwall and the host metaconglomerate is commonly sharp and contains slickensides, whereas the footwall is typically broken and irregular (Jutson, 1914). In places, the vein is in contact with intrusive porphyries (Ho, 1984). At the White Feather Main mine, the quartz vein bifurcates or wraps around a lenticular metaporphyry body. The metaporphyry contains flat-lying auriferous quartz veins similar to that at Red Hill (Blatchford and Jutson, 1912).

Alteration: Wallrock alteration is lithology specific: felsic clasts alter to carbonate (mainly ankerite)-dominated assemblages; mafic clasts and matrix fragments alter to pyrite–carbonate; and ultramafic fragments to carbonate–fuchsite (Ho, 1984). On the mine dumps at Lily Australis, felsic porphyry clasts within altered metaconglomerate

commonly show a distinct altered rim (typically about 0.5 cm wide).

Ho (1984) recognized two types of primary fluid inclusions within the vein quartz from the Kanowna Main Reef: CO_2-rich inclusions, typically with three phases at room temperature (H_2O liquid, and CO_2 liquid and vapour); and H_2O-rich inclusions, with two phases at room temperature (H_2O liquid and vapour). The main fluid phases are H_2O and CO_2, with low salinity (<2 wt% equivalent NaCl; Ho, 1984). Based on these fluid inclusions, a temperature of 250–325°C and pressure of about 100 MPa were estimated for the time of trapping (Ho, 1984).

References: Blatchford and Jutson (1912), Jutson (1914), Maitland (1919), Ho (1984).

Nemesis

Coordinates: 30°35'54"S, 121°36'34"E

Production: The amount of historical production is uncertain; however, Truelove et al. (1997) reported 270 t of ore for 1.524 kg Au (5.6 g/t Au). Present resources are: measured — 0.15 Mt at 2.4 g/t Au (360 kg Au); indicated — 0.69 Mt at 2.3 g/t Au (1587 kg Au); and inferred — 0.07 Mt at 2.2 g/t Au (154 kg Au; MINEDEX site code S05632).

Host rock: The host rock is a metamorphosed quartz–feldspar porphyry, trending north-northwesterly, that has intruded metamorphosed felsic volcaniclastic sedimentary rocks (Truelove et al., 1997).

Structure: The mineralized zone is located at the intersection of major north-northwesterly trending and subsidiary northwesterly, east-northeasterly, and subhorizontal structures, and is structurally complex (Truelove et al., 1997).

Alteration: The extent of alteration is dependent on the amount of micro-fracturing and quartz veining. The alteration assemblage comprises carbonate–sericite–silica–sulfide–albite (Truelove et al., 1997).

References: Truelove et al. (1997).

Kanowna Belle

Coordinates: 30°36'32"S, 121°34'46"E

Production: There was no historical gold production at Kanowna Belle. Total gold production from 1993 to September 2002 is 63 557 kg Au (2 043 413 oz Au). Current resources are: measured — 7.063 Mt at 4.0 g/t Au (28 252 kg Au); indicated — 10.219 Mt at 5.6 g/t Au (57 226 kg Au); and inferred — 1.544 Mt at 5.0 g/t Au (7720 kg Au; MINEDEX site code S03101).

Kanowna Belle was initially mined as an opencut operation (1993–98) to a depth of 220 m, and then an underground operation was developed using a decline to a depth of 1000 m. Drilling has intersected significant mineralization to a depth of 1400 m [*].

Host rock: Most of the gold mineralization is within metamorphosed intrusive feldspar porphyry, with smaller amounts in a metamorphosed sequence of volcaniclastic rocks, conglomerates, komatiitic basalt, and volcanic rocks (Ross et al., 2001). The metamorphosed volcaniclastic and sedimentary rock sequence dips 55° southwest to south, whereas the metaporphyry has a dip of 60°SSE (Ross et al., 1998).

Interbedded, mafic-dominated metaconglomerate (locally known as Golden Valley metaconglomerate) and felsic-dominated metaconglomerate (locally known as Cemetery metaconglomerate) constitute the footwall sequence (Beckett et al., 1998). The hangingwall contains cyclic sequences of felsic angular rudites and sporadic pebble-to-boulder beds, with minor mafic rocks (Beckett et al., 1998). These hangingwall units include the locally termed QED rudite, Lowes metasandstone, and Grave Dam grit (Beckett et al., 1998). The feldspar-phyric to aphyric Kanowna Belle metaporphyry (<10 to 80 m thick) has intruded along the pre-existing Fitzroy Shear Zone (Thomson and Peachey, 1993).

Structure: The dominant controlling structures for gold mineralization are the Fitzroy Shear Zone and associated oblique hangingwall structures (Beckett et al., 1998). The Fitzroy Shear Zone trends in an east to northeast direction, typically dips at 60°SSE, and is up to 10 m wide (Beckett et al., 1998). It is characterized by a mylonitic shear and fracture zone, and contains ductile C–S shear fabrics (Beckett et al., 1998).

The major structural style of the gold mineralization is brittle-shear-zone hosted with local brecciation (Ross et al., 1998). Ross et al. (2001) considered the Fitzroy Shear Zone to be a reactivated D_1 thrust ramp and suggested that the four main mineralized lodes were developed by sinistral shearing during a change in far-field compressive stress axes, from south–north during D_1, to east-northeast–west-southwest during D_2. The Kanowna Belle metaporphyry intruded after the D_2 deformation event (Ross et al., 1998). In the opencut pit there is a foliation, and a dextral fault offsets the shear zone. There are also breccia zones within the hangingwall and footwall units that are related to D_3 deformation (Beckett et al., 1998). Ross et al. (1998) stated that higher grade gold mineralization appears to be situated at sites of D_3 reactivation of the Fitzroy Shear Zone.

Alteration: The alteration envelope is asymmetrical and consists of an inner (ore) zone of pyrite–albite–quartz, an intermediate zone of sericite–carbonate–pyrite, and an outer zone of sericite–carbonate to chlorite–carbonate (Ross, 1993; Ross et al., 1998).

Most gold mineralization is associated with pyrite in the alteration envelopes adjacent to the Fitzroy Shear Zone and hangingwall shears, but is also in hydrothermal quartz breccias, sericite–pyrite veinlets, and pyritic quartz

[*] Taken from the Auriongold website (viewed September 2002) — now Placer Dome <http://www.placerdome.com/operations/kanowna/index.html>

stockworks (Ross, 1993). Flat-lying quartz veins locally contain free gold (Ross, 1993). Pyrite, in association with quartz and carbonate, is typically present within veinlets and breccia veins (Ross et al., 1998). Quartz veins with open-space-filling textures and recrystallized chalcedony suggest formation at a relatively high crustal level (Ross et al., 1998). Accessory opaque minerals reported to be present at Kanowna Belle include tennantite/tetrahedrite, galena, sphalerite, arsenopyrite, chalcopyrite, and altaite (Ross et al., 1998).

The principal ore lodes at Kanowna Belle are Lowes, Troy, Hilder, and Hangingwall, with most of the known resources within the Lowes lode, which generally strikes parallel to the Fitzroy Shear Zone (Ross et al., 1998). The Troy, Hangingwall, and Hilder lodes strike obliquely to the Lowes lode (Ross et al., 1998).

Average fluid-inclusion composition is H_2O–CO_2 ± CH_4, and the temperature of formation is about 250°C (Hagemann and Cassidy, 2001).

References: Ross (1993), Thomson and Peachey (1993), Beckett et al. (1998), Ross et al. (1998), Hagemann and Cassidy (2001), Ross et al. (2001).

Alluvial and deep leads

Historical production from the palaeochannels (alluvial and deep leads) in the Kanowna mining centre is estimated at about 3110 kg Au (Peachey, 1993). Most of the historical production from deep leads was from the North lead and its branches, Wilsons lead, Cemetery lead, Fitzroy lead, and Moonlight lead (Maitland, 1919). In addition, between 1989 and 1993, the QED heap-leach operation produced about 870 000 t of ore for 2332 kg Au (2.7 g/t Au) from the palaeochannels and underlying saprolitic bedrock (Beckett et al., 1998). Known production from alluvial and deep leads is shown in Table 23.1. A schematic representation of the palaeochannel profile in the Kanowna mining area is shown in Figure 23.3.

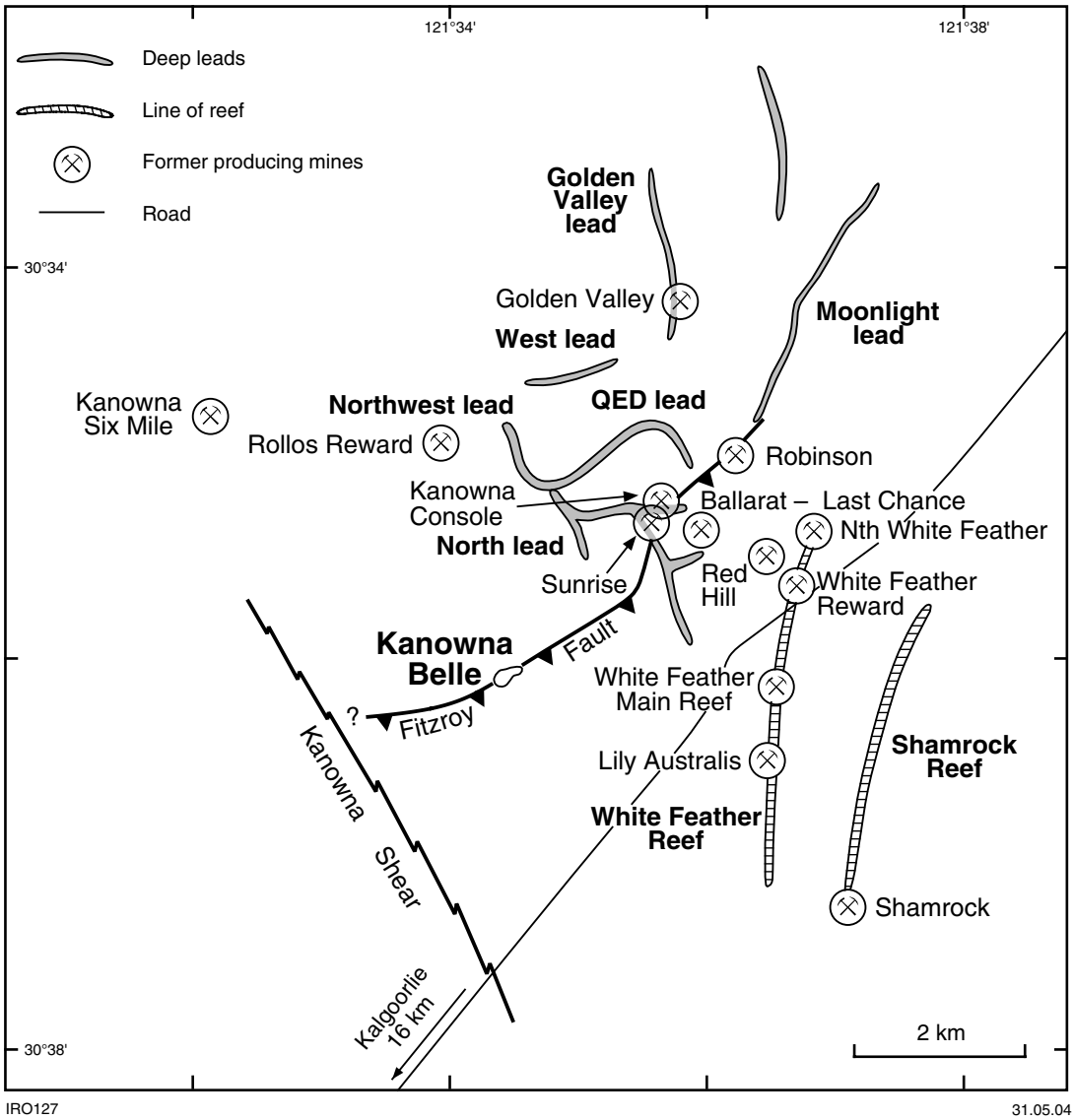

Figure 23.3. Location of deep leads in the Kanowna mining area

Table 23.1 Summary of known production from alluvial and deep leads in the Kanowna mining centre

Name	*Orientation*	*Production*	*Resources*	*Comments*
Moonlight lead	Northeast-trending palaeochannel overlying ultramafic units	Minimum historic production of 7101 t for 41.654 kg Au (5.9 g/t Au)	88 800 t for 320.568 kg Au (3.61 g/t Au)	–
Fenceline lead	North- to northwest-trending palaeo-channel overlying ultramafic and metaconglomerate units	–	–	Patchy gold within channel and overlying clays
Golden Valley lead	North-trending palaeochannel underlain by metabasalt and felsic metasedimentary units (partly sheared)	52 228 t for 124.3 kg Au (2.4 g/t Au)	–	Part of 1989–1993 QED operation
West lead	East–west palaeochannel overlying mafic and metasedimentary rocks	91 472t for 287.2 kg Au (3.14 g/t Au) (historical production unknown)	28 809 t for 105.153 kg Au (3.65 g/t Au)	Part of 1989–1993 QED operation (<10 % of resource is bedrock supergene mineralization)
Northwest lead	Northwest-trending palaeochannel overlying felsic metasedimentary units and minor metabasalt	218 493 t for 716.657 kg Au	49 510 t for 140.113 kg Au (2.83 g/t Au)	Extension of main North lead. Part of the 1989–1993 QED operation. Supergene gold in clays with about 10% of gold in saprolitic bedrock. Possible bedrock mineralization in northeast-trending shears or carbonaceous metashale, with some related to shallow-dipping quartz veins
North lead pit NLP9 — Rollos shaft	North-trending portion of North lead palaeo-channel and underlying saprolitic bedrock	Historical production (Rollos shaft) was 63 t for 0.526 kg Au (8.3 g/t Au). Recent production (1989–1993 QED operation) was 57 739 t for 180.146 kg Au (3.12 g/t Au)	11 411 t for 44.959 kg Au (3.94 g/t Au) (in fresh bedrock)	Part of the QED operation. Primary mineralization is at northeast-trending contact between ultramafic and metasedimentary units and shallow-dipping quartz vein mineralization
North lead	North-trending changing to west-trending palaeochannel overlying ultramafic and metaconglomeratic units	Historical production was 12 083.5 t for 89.014 kg Au (7.4 g/t Au) (total from Consuls area). Modern production (QED operation) 429 302 t for 1319.8 kg Au (3.07 g/t Au; 80% from puggy alluvial clay)	68 400 t for 191.52 kg Au (2.8 g/t Au) (mostly from alluvial puggy clay) and 6732 t for 21.278 kg Au (3.2 g/t Au) (fresh bedrock).	Part of QED operation. Supergene gold is present in puggy alluvial clays, channel sands, and saprolitic bedrock
Wilsons Gully lead	North- to northwest-trending palaeochannel overlying metamorphosed felsic lithic grit to metasandstone units	Known historical production is 1389 t for 10.241 kg Au (7.4 g/t Au). Modern production (1989–1993 QED operation) is included in North lead figures	–	Supergene gold in puggy alluvial clays, channel sands, and saprolitic bedrock
Cemetery lead	Extension of North lead, south of Fitzroy lead junction. Metasedimentary lithologies underlying palaeochannel	–	–	Supergene gold in channel and possibly minor amount in saprolitic bedrock
Fitzroy lead	Westerly to west-southwesterly trending palaeo-channel overlying metasedimentary units	Historical production was 1278.1 t for 54.089 kg Au (42.3 g/t Au)	–	Supergene gold in channel and upper saprolitic bedrock
QED lead	Curved palaeochannel (strike changes from northwest to southwest) overlying metaconglomeratic units	–	–	Gold in channel sands, overlying clays, and possibly saprolitic bedrock

SOURCE: Peachey (1993)

References

BECKETT, T. S., FAHEY, G. J., SAGE, P. W., and WILSON, G. M., 1998, Kanowna Belle gold deposit, *in* Geology of Australian and Papua New Guinean mineral deposits *edited by* D. A. BERKAMN and D. H. MACKENZIE: Australasian Institute of Mining and Metallurgy, Monograph 22, p. 201–206.

BLATCHFORD, T., and JUTSON, J. T., 1912, The mining geology of the Kanowna Main Reef line: Western Australia Geological Survey, Bulletin 47, 106p.

DAVIS, B., ARCHIBALD, N., and AALTONEN, A., 2000, Kanowna Belle gold mine — anatomy and history of a plumbing system: Geological Society of Australia, Abstracts, v. 59, p. 123.

DELL, M., and ANAND, R. R., 2001, Kanowna District, *in* Eastern Goldfields excursion field guide *edited by* C. R. M. BUTT, R. E. SMITH, M. DELL, R. R. ANAND, M. J. LINTERN, D. J. GRAY, J. VINAR, A. P. J. BRISTOW, H. M. CHURCHWARD, Z. S. VARGA, and J. E. WILINA: The Cooperative Research Centre for Landscape Environments and Mineral Exploration, Open-file Report 109, June, 2001, p. 1–13.

GELLATLY, D. C., PEACHEY, T. R., RYALL, A. W., and BECKETT, S., 1995, Discovery of Kanowna Belle gold deposit — one the old-timers missed, *in* New generation gold mines: case histories of discovery: Australian Mineral Foundation, p. 14.1–14.10.

GRIGSON, S. E., 1981, Nature and genesis of gold-quartz vein-type deposits, Kanowna, Western Australia: University of Western Australia, BSc (Hons) thesis (unpublished).

HAGEMANN, S. G., and CASSIDY, K. F., 2001, World-class gold camps and deposits in the eastern Goldfields Province, Yilgarn Craton: diversity in host rocks, structural controls, and mineralization styles, *in* World-class gold camps and deposits in the eastern Yilgarn Craton, Western Australia, with special emphasis on the Eastern Goldfields Province *edited by* S. G. HAGEMANN, P. NEUMAYR, and W. K. WITT: Western Australia Geological Survey, Record 2001/17, p. 7–44.

HO, S. E., 1984, Alternative host rocks for Archaean gold deposits: nature and genesis of hydrothermal gold deposits, Kanowna, Western Australia: Australasian Institute of Mining and Metallurgy, Regional Conference on Gold — Mining, Metallurgy and Geology, Kalgoorlie, October, 1984, Proceedings, p. 1–11.

JUTSON, J. T., 1914, Further notes on the mining geology of Kanowna: Western Australia Geological Survey, Bulletin 59, p. 215–227.

MAITLAND, A. G., 1919, The gold deposits of Western Australia, *in* The Mining Handbook of Western Australia: Western Australia Geological Survey, Memoir 1, Chapter II, 92p.

PEACHEY, T. R., 1993, Kanowna mining centre historic gold production and mine geology: Delta Gold N.L., Internal Report, March 1993 (unpublished).

ROSS, A., 1993, Archaean lode gold deposits of the Kanowna region, *in* Kalgoorlie '93: an international conference on crustal evolution, metallogeny and exploration of the Eastern Goldfields, Excursion 4 Guidebook — Gold mineralisation at various regional metamorphic grades *edited by* J. R. RIDLEY and D. I. GROVES: Australian Geological Survey Organisation, p. 122–126.

ROSS, A. A., BARLEY, M. E., RIDLEY, J. R. and McNAUGHTON, N. J., 2001, Two generations of gold mineralisation at the Kanowna Belle gold mine, Yilgarn Craton, *in* 4th International Archaean Symposium, 2001, Extended abstracts *edited by* K. F. CASSIDY, J. M. DUNPHY, and M. J. VAN KRANENDONK: AGSO — Geoscience Australia, Record 2001/37, p. 398–399.

ROSS, A. A., FAHEY, G., BECKETT, S., and VANDERHOF, F., 1998, Kanowna Belle gold mine, *in* MERIWA Project 195: Systematic documentation of Archaean gold deposits of the Yilgarn block *edited by* F. VANDERHOR and D. I. GROVES: Minerals and Energy Research Institute of Western Australia, p. II-58–II-63.

SWAGER, C. P., 1997, Tectono-stratigraphy of late Archaean greenstone terranes in the southern Eastern Goldfields, Western Australia: Precambrian Research, v. 83, p. 11–42.

THOMSON, R. M., and PEACHEY, T. R., 1993, The Kanowna Belle case study — the discovery of a concealed orebody, *in* An international conference on crustal evolution, metallogeny and exploration of the Eastern Goldfields, Extended Abstracts *edited by* P. R. WILLIAMS and J. A. HALDANE: Australian Geological Survey Organisation, Record 1993/53, p. 229–231.

TRUELOVE, A. J., WILSON, G. M., and SEYMOUR, K. M., 1997, New Resources in an old district — a case study of the discovery of Golden Feather, Kanowna, *in* New generation gold mines: case histories of discovery: Australian Mineral Foundation, p. 15.1–15.12.

WESTERN MINING CORPORATION LTD, 1989, Annual report, 1988 to 1989, on P27/00668: Western Australia Geological Survey, Statutory mineral exploration report, Item 5309 A27291 (unpublished).

Appendix 1

List of mineral deposits

Area	*Deposit*
Gordon–Mulgarrie	Sirdar
	Mount Eba
	North Kanowna Star
	Koh-I-Nor Leases
	Palm
	Gem
	Lady Clara
Pennyweight Point – Yundamindera	Dewey
	Problem
	Just In Time
	AWA
	Landed at Last
	Great Bonaparte
	Treasure North
	Maori Queen
	Golden Treasure
	Potosi
	Queen of the May
	Little Wonder
	Boer
Yarri	Great Banjo
	Wallaby North
	Wallaby Central
	Yarri Proprietary
	Star of Yarri
	Queens Birthday
	Yarri South
	Dostmund
Yerrilla – Mount Remarkable	Bull Terrier
	Dingo
	Westward Ho
	Yerilla Central
	Viola
	Yerilla King
	Melba Consols
	Queen of the Earth
	Lady Gertrude
	McGregor North
	La Tosca
Yilgangi	Yilgangi Queen
	Yilgangi
	Yilgangi King
Karonie–Roe	Karonie Main and West Zones
	Harrys Hill
	French Kiss
Eucalyptus – Pykes Hollow	Zelica
	Cardigan
	Keep It Dark
	Mulga Rose
	Trouble
	Nine of Hearts
	Harlech Castle
	Yando Leases
Jubilee–Kurnalpi	Jubilee Gift South
	Agoriad Aur
	Billy Billy
	Scottish Lass Well
	Kurnalpi King
	Kurnalpi Pride
	Old Harriett
	Six Mile

Area	*Deposit*
Mulgabbie – Old Plough Dam	Twin Peaks
	Monty Dam
	Perseverance – Hope – General Rodiski
	Ernbill
	Golden Gleam
	Carosue Dam
Porphyry	Wallbrook
	Selbourne
	Eastward Gold Reefs
	Penola
	Porphyry Audax
	Million Dollar
	Porphyry
	Pioneer Paddock
	Nil Desperandum
	Enterprise
	Margaret
	Tonbridge
	Mad Dog and Mad Dog South
	Porphyry North
Randalls	Santa Claus
	Flora Dora
	Rumble
	Cock Eyed Bob
	Maxwells
Balgundi–Bulong–Taurus	Mount Bellew
	Balagundi Consolidated
	Queen Margaret
	Slug Hill Proprietary
	Storm King
	Trump
	Peacehaven
	Golden West
	Sinn Fein
	Green Harp Leases
	Great Oversight
	Central Zone
	Great Ophir
Trans Find – Juglah and Majestic	Curtin
	Trans Find
	Juglah
	Long Looked For
	Majestic
Morelands Find – Black Hills – Wombola	Sweet Nell
	Black Hill
	Warnambool
	Hoffman
	Lady Agnes
	Just In Time (Wombola openpit)
Sudden Jerk – Mount Monger	Lurgan
	Sibu
	Baguss
	Futi Baguss
	Fingals Fortune
	Sudden Jerk
	Twenty Grand
	Big Bull
	Dinnie–Reggio
	Haoma
	Caledonian

Appendix 1 (continued)

Area	*Deposit*
Sudden Jerk – Mount Monger (continued)	Daisy–Milano
	Rosemary
	Creedons Welcome
	Lorna Doone
	Eclipsall
	Great Hope
	Lass O'Gowrie
	Mirror Magic
Linden	Greenhills
	Olympic
	Danube
	New Years Gift
	Devon
	Lake View and Boulder East
	Lady Edith
	Federal
	Democrat
	Wimmera
	Local Lady
	Compensation
	Bindah
	Great Carbine
	Second Fortune
	Linden Star
	Red October
Butcher Well and Tin Dog Flats	Mount Florence
	Butcher Well North
	Sizzler
	Enigmatic North
	Enigmatic South
	Hronsky/Mambo
	Old Camp
	Tin Dog Flats
Mount Celia	Mount Celia
	Coronation
	Dunns Reward
	Deep Well
	Maudsley
	Kangaroo Bore
	Safari
	Deep South
Edjudina	Paget
	Highland Mary
	Perseverance
	Golden Lizard
	Scotchman
	Bella
	Crows Nest
	Ace of Hearts
	Triumph Leases Ltd
	Glengarry
	Lyon Glen
Pinjin	Anglo Saxon
	Coles
	Harbour Lights
	Harbour Lights North
	King Pin
	Lily of Australia
	Oaks
	Pinjin King
	Pinjin North
	Unification
Kalpini and Mayday	Bank of Kalpini
	Camelia
	New Venture
	Gem
	Primrose Leases
	Mayday North
Gindalbie	Homeward Bound Leases
	Diamond Jubilee
	Eclipse
	Whiteheads Find
	Pride of Vosperton
	South Gippsland Leases
	United Leases
	Lindsays Find
Kanowna	Kanowna Six Mile
	Golden Valley
	Robinson
	Ballarat – Last Chance
	Red Hill
	White Feather Main Reef
	Nemesis
	Kanowna Belle

Appendix 2

Mineral occurrence definitions and explanation of terms

The methodology and terms used in this Report are based on Witt (1993a,b,c).

Other names: These may include names of nearby mines that have been grouped together, as well as alternative names for the same group of leases (or parts thereof) that have been held under different names at different times.

Production: Production has been divided into 'historic' and 'recent'. Following a scheme proposed by Witt (1993a,b,c), 'historic' production was generally the result of selective mining of narrow, high-grade ore bodies, and 'recent' mining was based mainly on large-tonnage, low-grade ore bodies, commonly as openpit mining operations. In many cases (as noted by Witt, 1993a,b,c), 'historic' and 'recent' mines have exploited the same orebody, with the 'recent' mine incorporating lower grade material previously considered uneconomic. The lower grade ores are generally over a relatively broad area, commonly enveloping the high-grade shoots and veins that were selectively mined in the past. 'Historic' production figures are based on production up to 1988. Also reported are the published resources obtained from MINEDEX*. The combined 'historic' and 'recent' production, plus published resource figures, approximate the total in-ground resource of gold prior to mining.

Host rocks: The host rock to mineralization is determined from the geological setting, published documentation, or from an assessment of mineralized dump samples. The proportion of gold yielded by host rocks in these mines has only been estimated, and accuracy should be considered no better than 10%.

Mineralized structures: Descriptions of the structural setting are based on regional mapping, whereas descriptions of ore-bearing structures are based on published documentation or direct observations.

Alteration: As for Witt (1993a,b,c), published documentation is available for some deposits, but for many the descriptions are based only on field observations and a limited number of petrographic samples. Many of the descriptions of alteration should therefore be regarded as of a reconnaissance nature only, but are nevertheless adequate for a regional study such as this.

References: This section lists the data on which the descriptions are based.

References

WITT, W. K., 1993a, Gold deposits of the Mt Pleasant–Ora Banda areas, Western Australia — Part 1 of a systematic study of the gold mines of the Menzies–Kamblada region: Western Australia Geological Survey, Record 1992/13, 158p.

WITT, W. K., 1993b, Gold deposits of the Mt Pleasant–Ora Banda areas, Western Australia — Part 2 of a systematic study of the gold mines of the Menzies–Kamblada region: Western Australia Geological Survey, Record 1992/14, 104p.

WITT, W. K., 1993c, Gold mineralization in the Menzies–Kambalda–St Ives area, Western Australia — Part 3 of a systematic study of the gold deposits of the Menzies–Kambalda region: Western Australia Geological Survey, Record 1992/15, 108p.

* MINEDEX is the Department of Industry and Resources' (DoIR's) mines and mineral deposits information database for Western Australia, and can be accessed through the Online Databases link on the DoIR homepage at <http//:www.doir.wa.gov.au>. Resource estimates detailed in MINEDEX are figures submitted by mining companies, and have not been verified by the Department.

Appendix 3

Description of digital datasets

The CD-ROM that accompanies this Report contains the following datasets.

Geology and regolith

Information on the geology and regolith has been extracted from the State 1:500 000 geology and regolith databases, with the major tectono-stratigraphic terranes and domains after Swager (1997). The separate layers or polygon themes supplied are:

- interpreted bedrock geology;
- regolith geology;
- major tectono-stratigraphic terranes and domains;
- major faults and shear zones.

Mineral deposits

This database is based on the investigation of more than 200 mineral deposits that produced more than 5 kg of gold within the Edjudina–Kanowna region. Field visits and geological observations were carried out for most of these deposits by W. Witt and J. Westaway between late 1995 and early 1997. Additional information is from publicly available company exploration reports.

For the purpose of description, the mineral deposits have been grouped together into 'mining centres'. These centres do not correspond to mining fields or subdivisions under the Mining Act, but are areas that encompass groups of deposits that lie within the same tectono-stratigraphic entities, are in close proximity to one another, and often have common geological settings.

The text and numeric information contained on the CD-ROM include:

- location of the deposits (GDA coordinates, latitude and longitude, mining centre);
- mineralization classification (mineralization-style group and mine structure style);
- orientation of mineralized and related structures;
- mineralized host rocks (type and grouping);
- alteration mineralogy, metamorphic zone based on alteration assemblage, and vein composition.

Mineralization-style group

The majority of the gold mineralization is classified as 'vein and hydrothermal — undivided' style, with the remainder as 'regolith — residual and supergene' and 'regolith — residual to eluvial'.

Mine structure style

This Report adopts the scheme of Witt (1993), in which mineralized structures are classified based on brittle–ductile relationships. This scheme includes the following types of structural style:

- simple quartz vein;
- flat-lying to subhorizontal quartz vein(s);
- quartz vein with relatively restricted adjacent zone of moderately to strongly foliated wallrock;
- pipe-like veins and breccia systems;
- quartz-vein sets between oblique bounding faults;
- quartz-vein sets between conformable bounding veined brittle–ductile shears;
- tabular vein–breccia systems (mainly brittle faults);
- veined brittle–ductile shear;
- banded brittle–ductile shear;
- ductile shear zone.

In addition, the following styles have been added for this Report:

- tabular to pipe-like vein stockworks in metamorphosed volcaniclastic sedimentary rocks;
- vein stockworks in metaporphyry;
- synvolcanic submarine vein systems;
- quartz veining, unclassified.

Mineralized host rocks

Following the scheme used by Witt (1993), the mineralized host rocks have been grouped into the following:

- surficial deposits (Tertiary to Quaternary host rocks; laterite and alluvial deposits);
- granitoid rocks;
- metaporphyry (post-volcanic intrusions);
- metamorphosed felsic volcanic rocks (including subvolcanic granitoids) and metasedimentary rocks (including metamorphosed interflow sedimentary beds);
- metagabbro, metadolerite;
- metamorphosed tholeiitic basalt;
- metamorphosed komatiitic basalt;
- amphibolite, undifferentiated mafic rocks;
- ultramafic rocks.

In addition, the following host-rock groups have been added for this Report:

- metamorphosed intermediate volcaniclastic and volcanic rocks;
- metamorphosed banded iron-formation (BIF).

Alteration mineralogy and metamorphic zone

Alteration mineralogy for the host rocks is tabulated in the database. Where possible, the mineralogy for the inner, intermediate, and outer zones are listed. Where no zonation is apparent, a general alteration-mineralogy assemblage is given.

The alteration mineralogy is consistent with Witt's (1993) findings that hydrothermal-alteration assemblages in the Eastern Goldfields vary systematically with metamorphic grade. The nomenclature for the metamorphic zones is based on assemblages of Witt (1993) and Mikucki and Roberts (2004). If information on mineral assemblage is insufficient, then no metamorphic zone is given.

The majority of the deposits contain veining and the vein composition is noted.

Production and resources

Production and resources for deposits were obtained from the MINEDEX* database. This information has been divided into:

- historical production (pre-1985) — ore tonnage, contained gold, gold grade, and period of production;
- modern production (post-1985) — ore tonnage, contained gold, and gold grade;
- current resource and reserve estimates — conforming to the code of the Joint Ore Reserves Committee of the Australasian Institute of Mining and Metallurgy, Australian Institute of Geoscientists, and Minerals Council of Australia (1999).

Other themes

A number of other themes are included on the CD-ROM. These themes are based Groenewald et al. (2000) and Groenewald et al. (2001) and include:

- TENGRAPH (DoIR's electronic tenement-graphics system);
- geophysics (total magnetic intensity, K–Th–U radiation ratios, and Bouguer gravity anomaly);
- Landsat TM imagery;
- cultural features.

* MINEDEX is the Department of Industry and Resources' (DoIR's) mines and mineral deposits information database for Western Australia, and can be accessed through the Online Databases link on the DoIR homepage at <http//:www.doir.wa.gov.au>. Resource estimates detailed in MINEDEX are figures submitted by mining companies, and have not been verified by the Department.

References

GROENEWALD, P. B., PAINTER, M. G. M., ROBERTS, F. I., McCABE, M., and FOX, A., 2000, East Yilgarn Geoscience Database, 1:100 000 geology Menzies to Norseman — an explanatory note: Western Australian Geological Survey, Report 78, 53p.

GROENEWALD, P. B., PAINTER, M. G. M., and, McCABE, M., 2001, East Yilgarn Geoscience Database, 1:100 000 geology of the north Eastern Goldfields Province — an explanatory note: Western Australian Geological Survey, Report 83, 39p.

JOINT ORE RESERVES COMMITTEE OF THE AUSTRALASIAN INSTITUTE OF MINING AND METALLURGY, AUSTRALIAN INSTITUTE OF GEOSCIENTISTS, and MINERALS COUNCIL OF AUSTRALIA, 1999, Australasian code for reporting of mineral resources and ore reserves: Australasian Institute of Mining and Metallurgy, Australian Institute of Geoscientists, and Minerals Council of Australia, 16p.

MIKUCKI, E. J., and ROBERTS, F. I., 2004, Metamorphic petrography of the Kalgoorlie region, Eastern Goldfields Granite Greenstone Terrane: METPET database: Western Australian Geological Survey, Record 2003/12, 40p.

SWAGER, C. P., 1997, Tectono-stratigraphy of late Archaean greenstone terranes in the southern Eastern Goldfields, Western Australia: Precambrian Research, v. 83, p. 11–42.

WITT, W. K., 1993, Gold mineralization in the Menzies–Kambalda region, Eastern Goldfields, Western Australia: Western Australia Geological Survey, Report 39, 165p.

Appendix 4

Key to geochemical samples and other samples used in mass-balance plots

GSWA sample no.	*Sample description*	*Drillhole*	*Depth interval (m)*
Gordon Sidar, Gordon mining area			
140102	Unmineralized metamorphosed polymicitic conglomerate	GSD-1	85.5 – 85.6
140108	Mineralized metamorphosed polymicitic conglomerate	GSD-1	228.0 – 228.1
140109	Mineralized metamorphosed polymicitic conglomerate	GSD-1	229.0 – 229.2
140110	Mineralized metamorphosed polymicitic conglomerate	GSD-1	234.1 – 234.2
AWA, Pennyweight Point mining area			
119966	Metabasalt	–	–
119967	Transition into quartz–sulfide lode	–	–
119970	Quartz–sulfide lode	–	–
Maori Queen, Yundamindera mining area			
119978	Least-altered metatonalite	–	–
119979	Metatonalite with low-temperature (adularia) veinlets and thin hematitization halos	–	–
119980	Metatonalite with thin amphibole veinlets and disseminated pyrite	–	–
119982	Pyritic, silicified lode	–	–
Potosi, Yundamindera mining area			
119991	Deformed (sheared) but little-altered metatonalite	–	–
119987	Mylonitized metatonalite with calc-silicate veins	–	–
119989	Pyritic, strongly deformed metatonalite with calc-silicate veins	–	–
Queen of the May, Yundamindera mining area			
119996	Strongly foliated metatonalite	–	–
119997	Transition from strongly foliated metatonalite to mylonitized tonlite (pyritic)	–	–
119998	Mylonitized metatonalite (pyritic)	–	–
120000	Silicified, sheared metatonalite (pyritic)	–	–
Boer, Yundamindera mining area			
132906	Calc-silicate veins in altered (bleached), weakly deformed metatonalite (pyritic)	–	–
132907	Bleached metatonalite with calc-silicate veins (pyritic) relict biotite in less-altered domains	–	–
132908	Calc-silicate vein (pyritic)	–	–
Wallaby Central, Yarri mining area			
115539	Unaltered monzogranite (Smithies and Witt, 1997)	–	–
130610	Least-altered monzogranite	–	–
130611	Moderately sericitized monzogranite	–	–
130613	Pyritic quartz–sericite lode	–	–
Yarri South, Yarri mining area			
110722	Unaltered metabasalt (Swager, 1995)	–	–
130614	Biotite amphibolite with minor calc-silicate alteration	–	–
130617	Biotite amphibolite with minor calc-silicate alteration	–	–
130615	Calc-silicate lode with K-feldspar	–	–
130619	Calc-silicate lode with K-feldspar	–	–
Bull Terrier, Yerilla mining area			
132919	Least-altered syenite	YBD-9	277.0 – 277.4
132921	Hematitized, carbonated syenite	YBD-9	181.1 – 181.2
132920	Intensely hematitized, pyritic syenite	YBD-9	175.4 – 175.6
Yilgangi Queen, Yilgangi mining area			
130657	Quartz–muscovite–carbonate–chlorite schist	–	–
130658	Quartz–muscovite–carbonate–chlorite schist (pyritic)	–	–
130659	Quartz–muscovite schist with quartz veins and disseminated arsenopyrite	–	–
Yilgangi, Yilgangi mining area			
130648	Least-altered metasedimentary rock	–	–
130649	Quartz–sericite lode	–	–
Yilgangi King, Yilgangi mining area			
130652	Least-altered monzodiorite with quartz veins	–	–
130653	Sericitized monzodiorite with quartz veins	–	–

Appendix 4 (continued)

GSWA sample no.	Sample description	Drillhole	Depth interval (m)
Main Zone, Karonie mining area			
132829	Quartz(–plagioclase)–biotite metasedimentary rock	KD-54	51.3 – 51.4
132804	Quartz–biotite metasedimentary rock	–	–
132801	Least-altered amphibolite	–	–
132802	Mafic gneiss	–	–
132828	Mafic gneiss	KD-55	55.1 – 55.3
132805	Amphibole-rich alteration assemblage	–	–
132803	Quartz–biotite–feldspar gneiss (?biotitized amphibolite)	–	–
132806	Carbonated mafic gneiss	–	–
132809	Calc-silicate alteration with minor biotite	–	–
West Zone, Karonie mining area			
132813	Least-altered amphibolite	–	–
132814	Quartz–biotite–amphibole–plagioclase gneiss	–	–
132816	Amphibolite with calc-silicate bands	–	–
132815	Calc-silicate alteration	–	–
Harrys Hill, Karonie mining area			
132817	Least-altered amphibolite (3% pyrrhotite)	HHD-36	90.6 – 90.7
132820	Distal alteration (transition between 132817 and 132819)	HHD-36	107.8 – 108.0
132819	Quartz vein and proximal (bleached, minor pyrhhotite) alteration halo	HHD-36	10.6.6 – 107.0
132821	Quartz vein with amphibole-rich halo in biotite amphibolite (2–3% pyrrhotite+pyrite)	HHD-36	11.7 – 11.95
132823	Calc-silicate lode	HHD-36	125.5 – 125.75
132824	Biotite–plagioclase rock (with pyrite and pyrrhotite) after amphibolite	HHD-36	136.6 – 136.9
Scottish Lass Well, Kurnalpi mining area			
132984	Pyritic, quartz–carbonate–albite lode	–	–
132985	Pyritic, quartz–carbonate–albite lode	–	–
132986	Pyritic, quartz–carbonate–albite lode	–	–
Kurnalpi Pride, Kurnalpi mining area			
132962	Carbonated metabasalt with minor pyrite	–	–
132963	Intensely carbonated metabasalt	–	–
132964	Pyritic lode with abundant albite and carbonate	–	–
Six Mile, Kurnalpi mining area			
132974	Strongly deformed (mylonitized) mafic rock	–	–
132970	Carbonated, albitic mafic rocks with quartz–carbonate–albite veins and disseminated pyrite	–	–
132973	Sericitie–carbonate altered, albitic mafic rock with disseminated pyrite	–	–
Perseverance and White Elephant, Mulgabbie mining area			
110722	Unaltered metabasalt from Mulgabbie Terrane (Morris, 1994)	–	–
132992	Chlorite–biotite altered mafic rock	–	–
132999	Transitional zone into silicified lode (no biotite)	–	–
132993	Silicified lode	–	–
Million Dollar, Porphyry mining area			
130637	Least-altered quartz monzonite	–	–
130638	Deformed, weakly altered quartz monzonite (minor pyrite)	–	–
130639	Transition into hematitized quartz-monzonite zone (pyritic)	–	–
130640	Upper hematitized quartz-monzonite zone (pyritic)	–	–
130641	Lower hematitized quartz-monzonite zone (pyritic)	–	–
130642	Siliceous shear zone (pyritic), Porphyry openpit mine	–	–
Enterprise, Porphyry mining area			
130683	Least-altered meta-andesite (trace pyrite)	–	–
130688	Chlorite–carbonate–plagioclase schist (minor pyrite)	–	–
130696	Carbonated plagioclase–chlorite–biotite schist (minor pyrite)	–	–
130674	Carbonated quartz–sericite–chlorite schist (trace pyrite, arsenopyrite)	–	–
130678	Quartz–carbonate–sericite schist	–	–
130676	Quartz–carbonate–sericite schist (minor pyrite)	–	–
130682	Quartz–carbonate–sericite schist (minor pyrite)	–	–
130680	Quartz veins in hematitic quartz–sericite lode (minor pyrite)	–	–
130689	Quartz veins in hematitic albite–sericite–carbonate lode (minor pyrite)	–	–
Santa Claus, Randalls mining area			
132923	Least-altered silicate-facies BIF unit (thin unit within larger magnetite facies BIF)	RDD-12	134.5 – 134.7
132925	Silicate-facies meta-BIF with disseminated pyrrhotite and quartz–carbonate vein	RDD-12	140.9 – 141.3
132926	Banded quartz–magnetite–pyrrhotite unit (lode)	RDD-12	148.7 – 149.1

Appendix 4 (continued)

GSWA sample no.	Sample description	Drillhole	Depth interval (m)
Rumble, Randalls mining area			
132932	?Least-altered BIF (pyritic)	RMD-1	46.8
132933	Massive to banded pyrrhotite-rich BIF (minor arsenopyrite)	RMD-1	49.2 – 49.5
132931	Sulfide-rich (pyrite, arsenopyrite) BIF	RMD-1	45.7 – 45.9
Maxwells, Randalls mining area			
132943	Transition from BIF to pyrrhotite-rich BIF	MD-1	59.8 – 60.0
132942	Pyrrhotite-rich BIF	MD-1	46.3 – 46.6
132941	Pyrrhotite-rich BIF (with arsenopyrite)	MD-1	45.5 – 46.0
Queen Margaret, Bulong mining area			
132846	Metamorphosed felsic volcaniclastic rock	–	–
132846A	Least-altered, metamorphosed felsic volcaniclastic rock	–	–
132846B	Altered (carbonate, sericite, pyrite), metamorphosed felsic volcaniclastic rock adjacent to quartz vein	–	–
132850	Stockwork of quartz–carbonate–pyrite veins in altered (?albitized), metamorphosed felsic metavolcaniclastic rock	–	–
Majestic, Majestic mining area			
132858	Chlorite–sericite–titanite–pyrite vein and epidote–carbonate alteration selvage in metamorphosed leucocratic porphyry	–	–
132858A	Vein and intensely altered halo	–	–
132858B	Less-strongly altered metaporphyry	–	–
132859	Quartz vein and alteration selvage in metamorphosed mesocratic porphyry	–	–
132859A	Vein and selvage of chlorite (after secondary biotite)	–	–
132859B	Small veinlets in least-altered, metamorphosed mesocratic porphyry	–	–
Big Bull, Mount Monger mining area			
132872	Weakly altered (chlorite, sericite), metamorphosed felsic volcaniclastic rock	–	–
132873	Moderately altered (chlorite, sercite, carbonate, pyrite), metamorphosed felsic volcaniclastic rock	–	–
132874	Strongly altered (quartz, sericite, carbonate, pyrite), metamorphosed felsic volcaniclastic rock	–	–
Daisy, Mount Monger mining area			
132878	Weakly altered (carbonate. chlorite, muscovite), metamorphosed felsic volcaniclastic sandstone	–	–
132880	Strongly altered (quartz, muscovite, pyrite), metamorphosed felsic volcaniclastic rock; samples A and B are proximal and distal, respectively, with respect to the same quartz–pyrite vein	–	–
132880A	Quartz vein and immediate selvage of silicified wallrock	–	–
132880B	Distal from vein	–	–
132881	Least-altered, metamorphosed felsic volcanic rock (metamorphosed dacitic or rhyolitic ash flow tuff)	–	–
132882	Strongly altered, pyritic felsic volcanic rock with quartz–carbonate veining; samples A–C are progressively farther from the same quartz–carbonate vein	–	–
132882A	Quartz–carbonate vein and immediate selvage	–	–
132882B	Intermediate distance from vein	–	–
132882C	Distal from vein	–	–
132883	Quartz–carbonate–pyrite breccia	–	–
Mirror Magic, Mount Monger mining area			
132987	Carbonated, metamorphosed andesitic volcaniclastic rock	MMD-5	69.0 – 69.2
132900	Mineralized dacitic rock	MMD-5	83.0 – 83.3
North Democrat, Linden mining area			
121667	Metamorphosed granodiorite porphyry (trace sulfides)	–	–
121668	Metamorphosed porphyritic dacitic dyke (pyritic)	–	–
Butcher Well North, Butcher Well mining area			
130551	Carbonated metabasalt	CMBD-15	126.24 – 126.49
130556	Strongly deformed, carbonated mafic rock (trace sulfides)	CMBD-15	193.27 – 193.44
130558	Strongly deformed, carbonated mafic rock (trace sulfides)	CMBD-15	200.46 – 204.96
130560	Carbonate–pyrite–arsenopyrite lode	CMBD-15	204.70 – 204.96
130561	Least-altered metabasalt	–	–
130556	Altered metabasalt	–	–
130558	Altered, mineralized metabasalt	–	–
130560	Strongly altered and mineralized metabasalt	–	–

Appendix 4 (continued)

GSWA sample no.	Sample description	Drillhole	Depth interval (m)
Enigmatic South, Butcher Well mining area			
130579	Least-altered metabasalt	–	–
130575	Moderately altered metabasalt	–	–
130573	Mineralized metabasalt	–	–
130579	Least-altered metabasalt (trace pyrite)	ESDH-7	138.30 – 138.50
130575	Carbonate–chlorite–pyrite-altered metabasalt	ESDH-7	123.58 – 123.75
130573	Carbonate–chlorite–biotite–pyrite-altered metabasalt	ESDH-7	116.70 – 116.86
Hronsky, Butcher Well mining area			
130591	Least-altered metabasalt	–	–
130594	Moderately to strongly altered metabasalt	–	–
130592	Hydraulically fractured and mineralized metabasalt	–	–
130591	Carbonated intermediate sedimentary rock (trace sulfides)	HDH-8	109.00 – 109.29
130594	Carbonated intermediate–mafic sedimentary rock (trace sulfides)	HDH-8	118.25 – 118.45
130592	Carbonate–silica–pyrite–arsenopyrite lode	HDH-8	113.6 – 114.0
Red October, Linden mining area			
132946	Least-altered, metamorphosed komatiitic basalt	–	–
132947	Metamorphosed komatiitic basalt with irregular quartz veinlets and minor disseminated sulfides	–	–
132948	Metamorphosed komatiitic basalt with irregular quartz veinlets and minor disseminated sulfides	–	–
132949	Pyritic muscovite–carbonate lode (with pyrite, arsenopyrite) after metamorphosed komatiitic basalt	–	–
132950	Grey, pyritic quartz–carbonate lode (vein)	–	–
132951	White, pyritic (and arsenopyrite) quartz–carbonate lode (vein)	–	–
132952	Quartz–carbonate–biotite lode (with arsenopyrite, pyrite) after metamorphosed komatiitic basalt	–	–
132953	Weakly altered (chlorite + biotite), metamorphosed komatiitic basalt	–	–
Tin Dog Flats, Tin Dog Flats mining area			
130543	Least-altered biotite syenite	TDDH-5	112.61 – 112.88
130542	Hematized, weakly carbonated pyritic syenite	TDDH-5	106.58 – 106.84
130530	Biotite–chlorite–sericite-altered mafic rock	TDDH-5	31.10 – 31.25
130529	Limonite–quartz lode	TDDH-5	30.64 – 30.83
Anglo Saxon, Pinjin mining area			
130716	Amphibole–biotite-bearing intermediate rock	PDD-002	228.60 – 228.90
130718	Amphibole–biotite-bearing intermediate rock	PDD-002	201.75 – 202.05
130717	Biotite–amphibole–(carbonate)-bearing intermediate rock	PDD-002	207.12 – 207.35
130731	Carbonate–sericite–chlorite–biotite–(trace sulfide) intermediate rock	PDD-005	106.23 – 106.47
130734	Quartz-veined, chlorite–biotite–carbonate–sericite(–trace sulfide) intermediate rock	PDD-005	118.10 – 118.42
130730	Quartz-veined, carbonate–sericite–biotite–chlorite(–trace sulfide) intermediate rock	PDD-005	81.39 – 89.61
130735	Chlorite–carbonate–magnetite–quartz–sericite intermediate rock	PDD-005	125.06 – 125.38
130733	Silica–carbonate–muscovite–chlorite(–minor sulfide) intermediate rock	PDD-005	112.38 – 112.54
130732	Strongly silicified and sericitized metadolerite	PDD-005	111.39 – 111.79
130740	Carbonate–biotite–sericite–chlorite–magnetite-bearing intermediate rock	PDD-004	79.80 – 79.95
130738	Carbonate–biotite–chlorite–magnetite-bearing banded intermediate rock	PDD-004	67.18 – 67.56
130736	Carbonate–biotite–chlorite–sericite–(sulfide)-bearing banded intermediate rock	PDD-004	66.65 – 66.90
130737	Carbonate–quartz–sericite–chlorite–biotite–pyrite-bearing intermediate rock	PDD-004	66.23 – 66.65
130741	Strongly deformed, quartz–carbonate–biotite–sericite–chlorite-bearing intermediate rock	PDD-004	90.00 – 90.32
130739	Strongly deformed, quartz–carbonate–sericite–biotite–hematite-bearing intermediate rock	PDD-004	75.30 – 75.56
Lindsays Find, Gindalbie mining area			
137325	Least-altered, metamorphosed biotite–feldspar porphyry (trace pyrite)	–	–
137326	Quartz–albite-veined, moderately altered, metaporphyry (minor pyrite)	–	–
137327	Quartz–albite-veined, silicified metaporphyry (minor pyrite)	–	–
137328	Least-altered metabasalt	–	–
137330	Moderately altered metabasalt (weathered)	–	–
137329	Gold-bearing, pyrite-rich altered metabasalt	–	–
Ballarat – Last Chance, Kanowna mining area			
137357	Carbonate-altered ultramafic rock	LCD-107	139.23 – 139.55
137356	Quartz–carbonate-veined, carbonate–fuchsite–arsenopyrite–pyrite-altered ultramafic rock	LCD-107	129.00 – 129.20
137359	Moderately altered ultramafic rock	LCD-122	275.54 – 275.72
137358	Carbonate-altered ultramafic rock	LCD-122	268.29 – 268.47
137362	Quartz–carbonate-veined, carbonate–fuchsite–arsenopyrite–pyrite-altered ultramafic rock	LCD-122	309.41 – 309.62

References

MORRIS, P. A., 1994b, Geology of the Mulgabbie 1:100 000 sheet: Western Australia Geological Survey, 1:100 000 Geological Series Explanatory Notes, 18p.

SMITHIES, R. H., and WITT, W. K., 1997, Distinct basement terranes identified from granite geochemistry in late Archaean granite–greenstones, Yilgarn Craton, Western Australia: Precambrian Research, v. 83, p. 185–201.

SWAGER, C. P., 1995, Geology of the Edjudina and Yabboo 1:100 000 sheets: Western Australia Geological Survey, 1:100 000 Geological Series Explanatory Notes, 43p.

Appendix 5

Whole-rock geochemical analyses of rocks from the Edjudina–Kanowna region

	Gordon Sirdar				*Lindsays Find*						*Ballarat – Last Chance*					*Queen Margaret, Bulong*			*Majestic*			
	140102	*140108*	*140109*	*140110*	*137325*	*137326*	*137327*	*137328*	*137330*	*137329*	*137357*	*137356*	*137359*	*137358*	*137362*	*132846A*	*132846B*	*132850*	*132858A*	*132858B*	*132859A*	*132859B*
Percentage																						
SiO_2	57.9	57.7	67.8	69.4	61	58.3	61.9	63.3	68.5	51.6	45	36.9	36.5	32.9	30.6	66	52.8	59.1	54.1	66.3	68.6	64
TiO_2	0.5	0.54	0.49	0.41	0.51	0.5	0.37	1.1	0.93	1.03	0.68	0.36	0.41	0.38	0.41	0.56	0.71	0.55	0.74	0.46	0.55	0.69
Al_2O_3	14.7	13.9	13.3	13.7	14	13.9	13	15.4	16.3	13.5	11.2	8.35	11.7	12.2	11.5	11.3	14.7	14.2	21.6	17.6	12.1	15.5
Fe_2O_3	1.64	0.606	0.634	0.353	0.9	0.86	1.3	2.09	1.89	9.38	0.4	7.29	1.27	2.84	1.62	1.36	1.43	2.41	1.86	0.746	1.78	0.966
FeO	2.9	5.6	3.3	3	3.2	3	2	4.6	0.2	5.8	6.5	5.2	7.4	8.8	5.2	2.2	3	1.4	2.3	1.8	3.6	3.6
MnO	0.18	0.34	0.14	0.18	0.08	0.08	0.1	0.09	-0.01	0.12	0.13	0.4	0.42	0.21	0.34	0.06	0.09	0.05	0.06	0.04	0.09	0.09
MgO	3.11	5.53	3.25	2.65	2.47	2.28	1.79	0.9	0.13	1.03	8.07	5.13	3.79	10	3.27	2.66	3.9	2.35	1.71	1.28	2.29	2.64
CaO	4.87	3.41	1.66	1.68	3.95	4.89	5.33	3.75	0.22	4.54	10.2	14.6	15.3	13.9	19.3	3.84	5.74	4.14	5.26	1.92	3.67	2.96
Na_2O	0.44	0.31	0.33	0.39	5.21	6.22	8.35	3.62	10.3	6.3	2.63	1.09	0.6	0.44	0.21	3.45	4.37	8.4	5.65	5.16	2.5	3.54
K_2O	3.5	2.3	2.76	2.82	2.21	1.25	0.52	1.22	0.1	1.29	0.9	2.53	2.8	0.64	4.08	2.11	2.95	0.2	3.23	2.83	2.48	3.1
P_2O_5	0.12	0.09	0.12	0.12	0.32	0.25	0.26	0.3	0.11	0.36	0.27	0.24	0.03	0.04	0.03	0.16	0.18	0.03	0.18	0.14	0.12	0.14
LOI	8.53	8.18	5.13	4.93	4.39	6.6	5.54	1.9	1.69	4.46	13.8	14.5	17.6	17	20.4	6.56	9.64	4.36	2.76	1.79	1.65	2.36
S	0.9	0.1	0	0	0.15	0.2	0.7	0.05	-0.05	3.6	-0.05	5.65	0.2	I.S.	0.55	0	0.15	1.95	0	0	0.2	0
TOTAL	99.29	98.606	98.914	99.633	98.39	98.33	101.16	98.32	100.31	103.01	99.73	102.24	98.02	99.35	97.51	100.26	99.66	99.14	99.45	100.066	99.63	99.586
CO_2	7.05	5.2	2.5	2.4	2.9	6.3	5.85	0.2	-0.05	2.5	11.3	12.9	16.4	12.2	20.2	5.4	7.4	6.4	0.75	0.3	0.65	0.35
H_20^+	–	–	–	–	–	–	–	–	–	–	–	–	–	–	–	–	–	–	–	–	–	–
H_2O^-	–	–	–	–	–	–	–	–	–	–	–	–	–	–	–	–	–	–	–	–	–	–
Parts per million unless otherwise indicated																						
Au (ppb)	141	55	12	149	10	90	130	10	100	15000	76	17500	22	I.S.	680	733	9400	267	4500	180	62	1
Ag	1.3	0.6	0.3	0.7	0.5	0.5	0.5	0.4	0.4	1	0.5	1.8	0.5	0.6	0.6	0.4	0	0.3	0.8	0.2	1	0.2
Pd (ppb)	0	0	0	0	-1	-1	-1	-1	-1	2	2	14	9	I.S.	11	0	0	0	0	0	6	0
Pt (ppb)	0	0	0	0	-5	-5	-5	-5	-5	-5	-5	10	5	I.S.	5	0	0	0	0	0	10	0
Cu	26	46	19	32	660	17	33	20	13	94	37	21	54	105	47	74	54	18	10	18	40	70
Pb	12	12	13	17	29	11	9	6	12	7	3	18	5	5	6	8	8	12	13	3	61	15
Zn	69	110	77	86	86	67	46	76	19	73	78	80	64	270	52	45	48	24	34	23	75	56
Cr	150	520	280	310	85	85	45	55	-5	5	600	1150	1450	1450	1300	175	200	40	30	20	50	55
Ni	53	250	140	175	42	37	23	16	-2	37	165	520	500	410	250	105	79	38	9	5	30	33
W	0	0	0	0	4	9	16	1	26	18	3	4	4	1	6	12	7	8	4	4	3	5
Mo	0.5	0	0	0.2	0.5	1.8	0.6	0.9	0.7	1.9	0.2	0.8	0.3	4.1	0.6	0.6	0	11	10.5	2	1.9	1.4
Sn	3	3	4	4	1	1	-1	2	-1	1	-1	2	-1	2	-1	4	4	3	4	3	5	5
As	2700	46	13	15	6	-2	3	14	12	3	48	14900	900	125	6250	9	10	13	17	9	17	10
Sb	17	3.2	2.5	1.7	0.4	0.5	0.5	1	0.5	0.7	2.9	11.5	2.3	2.3	4.9	0.5	0.5	0.4	0.3	0	0.2	0.3
Bi	0.2	0	0	0	0.2	0.1	0.5	0.2	0.7	2.5	-0.1	1.3	-0.1	-0.1	0.5	0	0	0.5	22.5	1.1	35	1.7
Cd	0.1	0	0	0	0.2	0.2	0.2	0.2	0.2	0.2	0.2	0.5	0.2	0.4	0.4	0	0	0.1	0	0	0.1	0
Be	0.5	0	0.5	0	2	1.5	1	0.5	0.5	1	-0.5	1.5	-0.5	-0.5	1.5	1	1	0	1	0.5	0	0.5
Co	19	30	17	19	12	11	10	24	-1	37	37	62	79	61	51	14	27	14	4	3	15	9
Sc	11	12	13	11	7	7	4	13	4	15	14	20	24	19	23	12	16	5	9	6	9	10
V	80	115	100	90	65	75	-5	180	15	270	100	100	170	140	165	90	120	35	75	55	90	100
Ga	20	17	16.5	18	18	17	13	18	12	25	14	18	12	15	16	16	17.5	22.5	25.5	19.5	17	22.5
Nb	1.5	1	1.5	1	4	3.5	2.5	5.5	5	5	2.5	0.5	0.5	1	-0.5	1	1	1	5	6	4	6.5
Zr	110	125	120	120	160	165	35	140	15	75	-5	-5	35	-5	25	120	160	120	250	185	115	165
Ba	380	580	720	520	1450	820	320	480	35	240	210	600	370	120	760	620	860	115	760	840	680	900
Rb	70	59	80	74	68	28.5	9	40	2.5	28	17.5	54	60	15.5	88	36	43.5	2	77	65	55	82
Sr	155	240	220	210	1300	980	580	640	330	470	110	300	120	120	195	390	620	580	210	185	145	230
Li	13	30	29	20	16	7	1.5	8	-0.5	6	54	4	19.5	70	5	11	16	2	18	19	25	28
U	1	0.5	1	1	2.9	2.8	1.65	0.59	0.63	0.7	0.79	0.16	0.28	0.45	0.17	1	1.5	1.5	3	2	1	1.5
Th	2.5	2	2.5	3	10	8.5	6.5	3.5	2.7	3.2	3.5	0.47	0.85	1.45	0.68	4	6	6	11	7.5	4.5	5.5
La	14	12	9	12	37	39	31	19	9	16	17	3	3	3	2	23	31	28	32	22	16	24
Ce	28	20	20	23	69	70	56	37	14	32	31	7	5	6	5	48	56	53	54	42	30	41
Y	6	16	7	10	12	11	9	16	8	13	12	5	9	7	9	8	11	13	19	14	8	16
Se	–	–	–	–	–	–	–	–	–	–	–	–	–	–	–	–	–	–	–	–	–	–

Appendix 5 (continued)

	Big Bull, Mt Monger			Daisy								Mirror Magic		Santa Claus, Randalls			Rumbles, Randalls			Maxwells, Randalls		
	132872	132873	132874	132878	132880A	132880B	132881	132882A	132882B	132882C	132883	132897	132900	132923	132925	132926	132932	132933	132931	132943	132942	132941
Percentage																						
SiO_2	62.1	64	61.7	58.9	64.2	55	62	51.4	69	61.7	36	53.8	72.9	43.6	51.3	40.6	43.3	48.1	29.4	53.8	52.5	41.6
TiO_2	0.5	0.43	0.44	0.72	0.45	0.69	0.41	0.65	0.3	0.42	0.17	0.53	0.3	0.34	0.38	0.34	0.29	0.13	0.26	0.41	0.22	0.13
Al_2O_3	14.5	13.2	14.2	14.3	8.15	12.6	14.6	11	9.93	14.5	4.12	13.8	8.76	7.98	8.36	7.14	6.3	1.89	4.43	9.38	6.32	7.52
Fe_2O_3	0.618	1.32	1.14	1.91	5.91	3.28	0.724	5.48	1.76	2.22	1.73	1.42	2.62	11.1	5.21	7.68	12.4	21.6	20.1	1.87	2.02	10.6
FeO	2.8	2	2.2	5.7	2	3.4	2.7	3	1.5	1.6	7.8	4.7	1.3	26.6	23	33	22.8	10.9	22	22.5	27.4	20.8
MnO	0.06	0.07	0.06	0.18	0.17	0.28	0.09	0.22	0.09	0.08	0.28	0.4	0.11	0.12	0.11	0.1	0.13	0.06	0.13	0.1	0.15	0.08
MgO	2.52	2.71	2.33	2.66	1.57	2.73	2.47	3.66	1.49	2.22	6.87	3.57	1.54	2.51	2.48	2.12	2.74	0.87	2.04	2.98	3.29	2.21
CaO	5.03	5.49	5.45	4.11	5.01	7.37	4.95	8.28	5.56	4.48	16.6	7.07	2.61	3.37	4.6	1.4	0.82	0.66	1.09	3.55	3.99	4.13
Na_2O	2.33	0.17	2.07	0.91	0.33	0.59	2.92	0.39	0.59	0.62	0.18	0.08	0.07	0.27	0.29	0.09	0.08	0.06	0.05	0.61	0.44	0.43
K_2O	2.52	3.39	2.57	2.54	2.05	3.07	2.48	3.2	2.8	4.27	0.89	4.52	3.07	0.35	0.27	0.39	0.68	0.23	0.2	0.44	0.21	0.19
P_2O_5	0.19	0.16	0.18	0.17	0.07	0.15	0.24	0.1	0.19	0.25	0.05	0.15	0.04	0.11	0.14	0.15	0.05	0.24	0.14	0.15	0.17	0.03
LOI	6.64	6.7	5.99	6.12	4.97	8.39	6.6	7.53	5.67	7.04	22.5	9.07	4.13	2.3	3.8	3.6	7.3	6.1	10.9	2.6	2.1	2.2
S	0	0.6	0.55	0.05	4.75	2.55	0.15	4.25	1.15	1.1	1.2	0.1	1.75	0.36	0.29	4.76	6.44	14.7	14.1	2.67	2.34	7.44
TOTAL	99.808	100.24	98.88	98.27	99.63	100.1	100.334	99.16	100.03	100.5	98.39	99.21	99.2	99.01	100.23	101.37	103.33	105.54	104.84	101.06	101.15	97.36
CO_2	4	4.6	4.25	3.4	5.65	10.6	5	17	5.7	6	25.4	5.75	3.35	0.3	1.1	0.8	4	4.9	7.6	0.4	0.5	0.8
H_20^+	–	–	–	–	–	–	–	–	–	–	–	–	–	2	2.7	2.8	3.3	1.2	3.2	2.2	1.6	1.4
H_2O^-	–	–	–	–	–	–	–	–	–	–	–	–	–	0	0	0	0	0	0.1	0	0	0
Parts per million unless otherwise indicated																						
Au (ppb)	6	0	353500	4400	58	1200	485	80	2300	427	29	145	151	210	130	9900	120	150	2	410	5600	31000
Ag	0	0.3	0.2	0.4	100	1	0.2	0.8	0.4	0.3	0.8	0	0.4	0	0	0.7	0.3	0.4	0.7	0.3	0.6	5
Pd (ppb)	0	0	0	0	0	0	0	0	0	0	0	0	0	0	0	0	0	0	0	0	0	5
Pt (ppb)	0	0	0	0	0	0	0	0	0	0	0	0	0	0	0	0	0	0	0	0	0	0
Cu	16	11	14	12	77	48	20	57	27	25	23	12	7	29	33	100	240	220	640	105	54	105
Pb	8	8	9	7	110	23	13	27	15	17	15	9	52	3	4	3	6	8	8	5	4	5
Zn	51	33	41	100	145	47	57	46	26	105	120	540	145	83	72	80	100	37	77	83	93	65
Cr	95	80	85	65	80	120	120	115	80	120	55	35	15	125	90	75	70	35	60	105	70	40
Ni	35	29	37	38	54	41	37	49	30	40	38	14	10	59	58	50	17	28	42	73	35	17
W	0	0	0	0	4	6	0	2	1	1	540	1	2	0	0	0	0	0	0	0	0	0
Mo	0	0.6	0	0	0.3	2.6	2.4	4.1	7.5	5.5	12	1	0.6	1.1	1	0.9	1.2	1.8	2.4	1.2	1.3	2.9
Sn	3	3	3	3	3	3	3	3	2	3	4	4	4	7	2	2	11	2	6	16	57	6
As	7	92	14	5	420	220	5	520	135	130	100	21	15200	3	7	7600	180	3500	5200	360	140	64000
Sb	0.4	0.6	0.6	0.9	1.4	1.3	0.6	1.2	1	0.9	0.8	0.5	58	0	0	1.9	0	0.9	2	0.2	0.2	15
Bi	0.4	0.1	0.1	0	0.6	0.1	0	0.3	0.1	0.1	0.1	0.5	0.2	0.3	0.2	0.6	0.5	0.9	1.2	0.2	0.3	1.7
Cd	0.2	0	0.1	0	1.5	0.3	0.1	0.3	0.2	0.1	0.4	0.5	0.2	0.4	0.2	0.1	0.4	0.2	0.3	0.7	1.9	0.5
Be	0.5	0.5	0.5	0.5	0.5	1	0.5	0.5	0.5	1	0	0.5	0	0.6	0.3	0.6	0.6	0.3	0.3	0.5	0.2	0.5
Co	10	9	15	17	18	15	14	22	9	11	11	11	10	10	13	14	0	15	10	15	6	30
Sc	7	7	6	11	9	14	7	14	7	8	6	10	6	9	10	9	7	3	7	11	6	5
V	75	65	60	130	80	120	65	110	70	75	75	90	45	65	80	60	60	30	55	75	50	65
Ga	15.5	14.5	16	19	12	15	17	14	13.5	18	5.5	16	11	14.5	13.5	14.5	12.5	5.5	10.5	14.5	12.5	15
Nb	1	0.5	1	3	0	1	1	1	0.5	1	0	5	2	6	5	6	5.5	0	0	5.5	0	0
Zr	180	135	130	150	85	130	150	105	105	230	55	125	80	90	90	85	80	55	75	80	55	40
Ba	620	540	580	720	480	720	700	720	600	840	200	1100	410	70	45	150	580	110	110	130	15	25
Rb	50	70	60	59	49.5	65	61	72	69	82	20	62	36.5	12.5	8.5	19	30.5	11.5	8.5	18	7.5	3.5
Sr	210	210	230	210	200	320	310	330	250	270	170	145	80	35	65	45	25	55	35	380	45	35
Li	12	12	13	25	4	7	15	5	4	4	4	15	8	3	3	3	2.5	1.5	2.5	7.5	2.5	3
U	1.5	1	1	1.5	0.5	1	1.5	1	1	1.5	1.5	1	1	1	1	0.5	0.5	0.5	1	1	0.5	0
Th	6	4.5	4.5	4.5	2.5	4	6.5	2.5	4.5	7	3.5	4	3.5	8	4	4.5	2.5	1	2.5	3.5	2.5	1.5
La	26	21	20	17	8	15	36	12	22	36	11	20	12	16	14	12	19	8	10	19	13	7
Ce	46	44	40	32	17	27	58	22	44	63	20	41	25	29	25	22	30	15	18	34	22	11
Y	12	10	30	17	16	16	10	19	8	0	11	11	5	9	14	10	9	9	11	13	11	6
Se	–	–	–	–	–	–	–	–	–	–	–	–	–	0	0	3	4	11	12	2	2	8

Appendix 5 (continued)

	Kurnalpi Pride			Scottish Lass, Kurnalpi			Six Mile, Kurnalpi			Mulgabbie			Bull Terrier, Yerilla			Yilgangi		Yilgangi King		Yilgangi Queen		
	132962	132963	132964	132984	132985	132986	132974	132970	132973	132992	132999	132993	132919	132921	132920	130648	130649	130652	130653	130657	130658	130659
Percentage																						
SiO_2	40.8	49.9	45.6	33.2	29.8	32.4	53.8	55.5	64	47.1	61.8	70	65.5	62.9	61.4	57.2	55.4	62.5	71.4	59.9	64.5	60
TiO_2	2	1.16	0.82	0.87	1.2	1.04	0.6	0.3	0.46	0.87	0.47	0.39	0.24	0.26	0.25	0.45	0.3	0.49	0.41	0.63	0.46	0.47
Al_2O_3	15.5	13.3	12.4	8.04	9.28	8.96	14.5	14.7	11.1	15.4	8.36	11.7	16.5	16.5	15.9	16.3	13.4	15.3	12.3	14.2	14.5	14.3
Fe_2O_3	5.41	5.35	3.45	2.59	9.95	4.51	3.69	2.18	3.66	2.76	1.22	2.71	1.59	1.77	2.32	2.52	1.99	2.05	2.15	1.44	1.58	1.92
FeO	12.7	4.6	4.8	8.9	4.1	8.3	5.9	2.2	2.9	14.5	7.6	3.4	1.3	1.5	1.1	2.1	2	1.5	1	5.4	2.6	1.9
MnO	0.16	0.17	0.19	0.21	0.2	0.19	0.17	0.1	0.1	0.35	0.28	0.06	0.06	0.05	0.06	0.07	0.11	0.06	0.04	0.06	0.03	0.07
MgO	5.66	1.71	2.94	7.63	8.62	8.09	5.82	1.31	0.79	5.33	2.97	1.83	1.08	0.9	0.98	3.51	3.42	1.36	0.44	3.78	1.94	1.8
CaO	4.9	8.54	8.21	12.7	12.1	11.3	10	5.95	4.57	3.62	6.75	1.92	1.97	2.52	2.32	3.75	5.82	3.21	2.35	2.51	1.98	4.17
Na_2O	2.13	5.71	6.57	3.09	3.06	2.76	2.26	8.72	4.46	1.87	1.44	4.51	6.42	6.05	5.75	4.47	2.9	5.78	3.7	1.02	3.36	4.47
K_2O	0.98	0.46	0.17	0.91	1	1.17	0.44	0.02	0.96	2.11	0.85	0.04	3.93	4.68	5.63	0.85	2.92	3.27	2.98	3.54	2.85	2.27
P_2O_5	0.26	0.15	0.17	0.05	0.07	0.05	0.06	0.13	0.09	0.06	0.03	0.11	0.13	0.14	0.14	0.18	0.14	0.18	0.17	0.12	0.15	0.16
LOI	8.85	10.8	13.3	23.4	19.8	21.6	1.8	7.9	5	5.1	7.4	2.4	0.2	3.2	3.1	5.9	10.6	5.1	2.8	5.8	4.7	6.1
S	0.45	0	1.25	0.7	0.34	0.06	0	1.86	2.52	0.25	0	1.65	0	0.06	2	0.4	0	0	0	0	0.06	0.37
TOTAL	99.80	101.85	99.87	102.29	99.52	100.43	99.04	100.87	100.61	99.32	99.17	100.72	98.92	100.53	100.95	97.70	99.00	100.80	99.74	98.40	98.71	98.00
CO_2	3.65	6.9	10.9	22.6	18.1	20.3	0.4	6.2	4	2	5.3	0.4	0	2.2	2.9	5.3	9.8	4.5	2	4.3	2.9	6
H_2O^+	5.2	3.9	2.4	0.8	1.7	1.3	1.4	1.7	1	3.1	1.9	2	0.1	1	0.1	0.6	0.8	0.6	0.8	1.4	1.8	0.1
H_2O^-	0	0	0	0	0	0	0	0	0	0	0.2	0	0.1	0	0.1	0	0	0	0	0.1	0	0
Parts per million unless otherwise indicated																						
Au (ppb)	41	7	89	185	435	81	6	185	1600	10	20	18	3	16	580	22	0	140	1300	4	85	180
Ag	0.8	0.3	0.5	1.2	4.6	1.2	0.9	1.3	2.6	0.3	0	1.1	0	0	0.3	0	0	0	0.3	0.3	0	0
Pd (ppb)	1	0	0	3	4	3	4	0	0	1	1	0	0	0	0	0	0	0	0	0	0	0
Pt (ppb)	0	0	0	0	0	0	0	0	0	0	0	0	0	0	0	0	0	0	0	0	0	0
Cu	220	170	93	94	48	200	96	28	155	77	73	300	5	21	43	36	6	20	31	25	42	23
Pb	11	6	26	5	6	4	3	15	15	1	0	3	7	7	7	18	7	12	21	16	13	19
Zn	260	110	66	110	150	135	90	17	44	320	65	56	46	33	28	74	61	98	67	120	83	93
Cr	140	15	15	360	680	580	50	20	65	280	150	50	35	40	45	40	75	30	25	125	105	120
Ni	95	34	26	125	220	195	77	21	39	170	77	43	14	16	15	37	72	11	8	145	76	72
W	3	2	3	4	4	3	0	6	3	0	0	0	0	6	14	2	0	8	7	2	3	9
Mo	0.9	5.5	14.5	0.5	5.5	1.2	1	110	3.6	0.3	0.2	2.4	0.8	0.7	0.8	5.5	7.5	0.8	1.7	3.4	0.7	1.6
Sn	13	4	4	3	4	5	5	4	6	4	5	5	4	3	3	3	6	3	3	3	5	2
As	21	5	2	0	0	0	3	3	7	3	0	0	4	6	32	1900	115	320	1800	140	74	7400
Sb	0.7	0.3	1.8	0	0.2	0	0	0	0.3	0.2	0	0.4	0.6	1	1.9	1.3	0.4	0.5	1.6	0.8	0.8	1.9
Bi	0.1	0	0.1	0.1	0.2	0	0	1.3	1	0	0	0.1	0	0	0.2	0.2	0	0.1	0.6	0.2	0	0.1
Cd	0.6	0.6	0.7	0.2	0.5	0.3	0.2	0.4	0.3	0.2	0.2	0.3	0.2	0.2	0.2	0.2	0.4	0.3	0.2	0.2	0.3	0.6
Be	1.7	0.9	0.6	1.2	1.5	1.3	1	0.9	1.5	1.2	0.8	1.3	5	3.7	2.7	3.1	1.8	2.4	2.6	1.9	1.7	2.2
Co	57	31	27	51	63	66	39	13	24	59	31	34	4	3	5	14	14	9	3	28	17	18
Sc	28	16	12	23	35	30	28	7	9	40	21	9	3	3	3	6	3	4	4	9	8	10
V	280	195	95	170	280	220	185	30	75	240	145	75	45	55	40	60	30	55	50	80	65	75
Ga	18.5	18	11.5	12.5	18	15	17	18.5	13.5	17.5	10.5	13	15.5	17.5	18.5	20.5	18	19	18	22	18.5	19.5
Nb	9	5	0	0	0	0	0	0	0	0	0	5	7	5.5	6	5	0	7.5	6.5	6	5.5	0
Zr	195	110	85	45	65	60	60	80	115	50	40	115	190	200	190	175	130	200	175	105	115	120
Ba	380	50	50	220	320	175	95	0	240	980	400	0	1300	1400	900	320	840	1700	1700	960	880	600
Rb	22	5.5	1.5	24.5	33	32	23.5	3	22.5	88	34	5.5	38.5	33	38	26.5	95	38	62	105	91	65
Sr	90	75	125	160	80	135	175	140	75	30	10	70	1600	900	680	660	660	1500	520	420	500	700
Li	24	6	2.5	3	5.5	6	6.5	1	6	17	10	5	1.5	12	3	6.5	9.5	9.5	13	24	12.5	4.5
U	0.5	0.5	0	0	0	0	0	0	1	0	0	1	2.5	4	2.5	3.5	2.5	3	2.5	3	2	2
Th	6	2	1	0.5	0.5	0	1	1.5	3	0.5	1	2.5	25	8.5	7	7.5	6.5	9	9	7.5	5.5	5.5
La	25	14	7	6	6	5	5	10	17	3	2	14	41	44	46	48	27	72	68	28	31	33
Ce	57	32	16	13	17	13	11	19	32	9	4	33	68	67	69	87	49	130	130	48	55	60
Y	38	21	18	13	20	15	15	13	13	16	14	16	13	10	13	9	6	11	10	10	10	12
Se	0	0	0	2	2	2	2	1	0	2	1	2	0	0	1	0	0	0	0	0	0	0

Appendix 5 (continued)

	Million Dollar, Porphyry						Enterprise, Porphyry									Wallaby Central, Yarri			Yarri South			
	130637	130638	130639	130640	130641	130642	130683	130688	130696	130674	130678	130676	130682	130680	130689	130610	130611	130613	130614	130617	130615	130619
Percentage																						
SiO_2	67.8	69.1	69.1	76.9	80.8	82.1	53.7	53.7	48.7	49.9	49.8	53.1	50	42.5	35.2	70	68	78.3	48.4	49.4	47.9	60.6
TiO_2	0.4	0.32	0.33	0.25	0.22	0.18	1.06	1.06	0.72	1.01	1.05	1.04	1.08	0.99	0.83	0.35	0.45	0.21	0.98	1	0.97	0.61
Al_2O_3	15.7	12.7	12.4	9.18	7.75	6.97	14.9	14.9	12	13.2	13.8	13.5	13.7	12.1	11	14.9	15.4	12.8	14.5	14.7	15.3	13.2
Fe_2O_3	1.84	1.15	2.12	1.83	1.58	1.4	2.13	2.06	1.82	0.35	2.3	3.32	1.65	3.49	6.47	1.69	1.83	0.95	3.18	1.97	4.23	1.99
FeO	1.1	1.1	0.9	0	0.4	0.9	8.2	8.3	4.8	6.6	5.8	3.8	4.9	4.8	6	1.3	2.1	0.9	9.5	10	6.5	6.6
MnO	0.03	0.04	0.03	0.03	0.02	0	0.15	0.15	0.12	0.15	0.13	0.12	0.12	0.2	0.24	0.06	0.06	0.02	0.2	0.19	0.18	0.11
MgO	0.99	0.76	0.45	0.3	0.16	0.08	2.68	2.7	6.9	2.82	2.79	2.31	3.11	3.74	4.49	0.8	1.18	0.44	7.73	6.42	5.77	3.42
CaO	1.02	2.29	1.65	1.61	0.92	0.16	5.67	5.67	6.84	7.8	7.27	6.23	7.06	9.78	11	3	3.62	0.01	10	11.6	14.8	8.39
Na_2O	5.23	4.26	4.68	3.49	2.98	1.21	3.03	3.03	2.87	0.93	0.84	2.51	1.11	4.05	3.69	3.64	1.93	0.16	2.08	2.29	1.81	2.11
K_2O	4.05	3.86	3.43	2.82	2.37	4.52	0.92	0.91	1.98	2.59	3.91	3.01	3.42	1.78	1.51	2.77	3.92	4.18	2.28	1.76	0.77	2.1
P_2O_5	0.19	0.15	0.14	0.11	0.09	0.04	0.21	0.21	0.28	0.18	0.22	0.18	0.21	0.56	0.18	0.1	0.09	0.01	0.06	0.05	0.05	0.08
LOI	2.1	2.2	1.8	2.2	1.3	0.7	6.5	6.6	11.3	12.6	11.5	10.1	12.1	14.8	13	1.5	1.4	1.4	0.5	1.2	1.7	0.7
S	0.1	0.23	1.53	0.02	0.61	1.59	0.1	0.1	0.02	0.78	0.02	0.03	0.08	1.97	3.56	0	0.17	0	0.18	0.86	0.36	1.58
TOTAL	100.55	98.16	98.56	98.74	99.20	99.85	99.25	99.39	98.35	98.91	99.43	99.25	98.54	100.76	97.17	100.11	100.15	99.38	99.59	101.44	100.34	101.49
CO_2	0.4	1.7	1.2	1.7	0.8	0.3	4.2	4.4	10.4	11.6	11.1	9.5	11.1	14.2	12.4	0.6	0	0	0	0.2	0.5	0.2
H_20^+	1.6	0.4	0.6	0.5	0.5	0.4	2.3	2.2	0.9	1	0.4	0.6	1	0.6	0.6	0.9	1.4	1.4	0.5	1	1.1	0.5
H_2O^-	0.1	0.1	0	0	0	0	0	0	0	0	0	0	0	0	0	0	0	0	0	0	0.1	0
Parts per million unless otherwise indicated																						
Au (ppb)	14	630	9600	3900	12500	8400	3	2	64	2	13	13	48	5500	13500	58	21	42	12	2	19	10
Ag	0	0	1.4	0	0.8	3.2	0	0	0	0	0	0	0	0.6	3.5	0	0	0	0	0.3	0.4	0.6
Pd (ppb)	0	0	0	0	1	0	0	0	0	0	0	0	0	0	0	0	0	0	0	0	0	0
Pt (ppb)	0	0	0	0	0	0	0	0	0	0	0	0	0	0	0	0	0	0	0	0	0	0
Cu	9	11	18	10	9	6	81	79	35	15	37	54	38	15	24	8	25	16	57	280	220	540
Pb	9	11	53	9	11	105	6	6	7	6	5	5	8	7	7	6	21	18	8	8	10	15
Zn	58	67	47	50	50	85	130	130	110	87	105	110	110	93	100	65	64	33	130	200	160	135
Cr	25	30	25	15	20	20	195	195	400	175	220	185	190	190	160	20	15	20	260	260	260	135
Ni	10	10	10	5	6	8	110	110	140	67	125	77	91	125	115	8	9	3	155	140	115	94
W	0	6	10	10	11	10	0	0	2	0	4	3	4	18	14	1	1	3	0	1	1	3
Mo	1	1.5	900	42.5	67	740	0.5	0.6	0.9	0.8	0.9	1	1.4	14	24.5	3.4	1.2	1.5	2	0.4	0.6	1.3
Sn	2	3	3	0	2	4	4	4	6	4	4	5	6	5	7	2	2	3	4	5	11	9
As	2	0	0	2	0	0	0	0	3	0	0	0	0	0	4	0	0	75	0	5	0	9
Sb	0.2	0.3	0.4	0.3	0.4	0.3	0.4	0.4	0.6	0.3	0.3	0.6	0.5	1	1.1	0	0	0.2	0	0	0.4	0
Bi	0.1	0.2	8	0.4	1.5	16.5	0	0	0	0	0	0	0	0.5	0.9	0.2	0.4	0.3	0.2	0.4	0.4	0.4
Cd	0.2	0.1	9	0.5	0.8	8.5	0.2	0.3	0.2	0.3	0.3	0.2	0.3	0.8	0.7	0.3	0.2	0.2	0.3	0.4	0.5	0.4
Be	3.5	2.3	1.9	0.8	1.1	0.9	1.8	1.9	2.4	1.9	2.6	2.2	1.9	2.6	2.4	1.8	1.8	2	0.8	1.9	2.2	1.4
Co	5	4	0	2	2	0	35	33	30	21	31	22	27	35	39	6	6	0	57	47	39	43
Sc	3	3	3	1	0	0	24	23	17	18	21	21	20	27	27	5	7	4	40	40	36	20
V	40	25	30	15	15	10	180	180	130	150	170	165	175	180	200	30	55	45	280	260	240	150
Ga	16.5	17	13	10.5	10	10.5	17.5	17.5	16	16	17	17	16	18.5	18.5	18.5	18	16.5	15.5	16	17	13.5
Nb	0	0	0	0	0	0	7	5	0	6	6	0	6	5	0	7.5	6.5	7.5	0	0	5	0
Zr	195	155	160	110	105	80	130	130	115	110	120	120	125	115	100	180	150	130	60	65	60	95
Ba	1600	1300	580	580	360	700	320	320	380	360	380	460	480	440	480	620	560	560	130	320	280	280
Rb	46	81	41	43	36	48.5	32.5	31	65	60	63	67	74	59	53	79	95	95	105	61	26	83
Sr	1300	620	320	220	135	115	145	145	280	90	105	140	130	340	380	130	130	20	55	80	100	100
Li	12.5	10.5	5.5	1.5	1	0	22	21	20	8	1.5	1	3.5	2	1.5	21	23.5	15	38.5	24.5	22	17.5
U	2	2.5	1.5	1	1	1	0.5	0.5	1	0.5	0.5	0	1	1	0.5	1	1.5	2	0	0	0	0
Th	10.5	7.5	7.5	4.5	4.5	3.5	1.5	1.5	2.5	1.5	1	1	1	1	1	4	4.5	7	2.5	0.5	1	1
La	74	55	52	34	35	28	13	14	26	14	15	12	12	9	13	25	13	16	3	3	4	7
Ce	110	96	94	63	61	50	30	30	55	32	35	27	27	20	29	44	24	23	8	8	10	15
Y	13	9	9	6	7	3	24	24	16	20	22	21	20	22	31	13	13	14	21	21	16	16
Se	0	0	2	0	1	2	2	2	1	2	2	2	2	2	4	0	1	0	0	1	1	2

Appendix 5 (continued)

	AWA, Pennyweight Point			Maori Queen, Yundamindera				Potosi, Yundamindera			Queen of the May, Yundamindera				Boer, Yundamindera			Butcher Well			
	119966	119967	119970	119978	119979	119980	119982	119991	119987	119989	119996	119997	119998	120000	132906	132907	132908	130551	130556	130558	130560
Percentage																					
SiO_2	51.7	48.4	65.4	63.6	63.5	58.5	66.9	52.8	66.3	69.3	63.4	74.3	57.8	78.8	75.3	65	74.9	55	49.6	38.1	44.1
TiO_2	0.77	0.75	0.72	0.65	0.65	0.71	0.56	0.88	0.54	0.49	0.6	0.36	0.78	0.21	0.3	0.48	0.43	0.9	0.74	0.71	0.74
Al_2O_3	15	14.9	14.2	15.5	15.7	16.1	14.2	15.4	14.4	11.9	15.4	11.8	18.8	8.69	11.9	12.3	11	15	12.7	11.7	11.2
Fe_2O_3	2.88	2.75	3.12	1.23	5.62	3.06	2.9	4.07	1.25	2.38	2.48	2.77	4.71	3.6	0	2.86	1.91	2.71	3.03	4.13	4.82
FeO	8.1	9.3	2.8	4	0.1	3.8	1.9	5.3	3	2.2	2.7	0.4	1.1	0.2	3.2	3.3	1.1	3.5	5.9	9	4.1
MnO	0.17	0.18	0.07	0.08	0.08	0.09	0.06	0.15	0.08	0.07	0.07	0.05	0.1	0.06	0.04	0.16	0.07	0.14	0.25	0.5	0.19
MgO	8.22	7.65	2.62	2.3	2.67	2.79	1.6	6.24	2.1	1.97	1.91	1.16	2.25	0.8	0.93	2.79	1.14	2.52	4.65	4.53	4.85
CaO	11.9	11.4	5.53	4.6	3.55	5.77	3.19	6.56	4.62	4.59	4.36	2.45	5.94	1.7	1.86	7.37	3.51	7.65	7.34	11	8.8
Na_2O	1.56	0.91	0.15	4.03	4.4	4.78	4.58	3.53	2.07	4.2	4.82	5.28	5.27	4.12	5.55	3.16	4.34	3.86	1.11	0.2	4.22
K_2O	0.18	1.83	2.48	1.19	2.15	2.19	1.68	1.92	2.9	1.24	2.1	0.4	2.01	0.21	0.25	1.22	0.5	0.8	2.33	2.86	1.42
P_2O_5	0.04	0.04	0.02	0.14	0.15	0.52	0.1	0.41	0.11	0.08	0.12	0.09	0.14	0.06	0.09	0.08	0.07	0.14	0.17	0.09	0
LOI	0.9	1.3	1.4	1.2	0.6	1.7	1.7	1.6	2.1	1.6	1	0.5	1	0.7	0.7	0.7	0.6	8.2	12	18.5	14
S	0	0.51	1	0	0	1.4	1.96	0.33	0.36	1.3	0.35	1.24	0.92	0.75	0.3	0.78	0	0.02	0.02	0.12	4.08
TOTAL	101.42	99.92	99.51	98.52	99.17	101.41	101.33	99.19	99.83	101.32	99.31	100.80	100.82	99.90	100.42	100.20	99.57	100.44	99.84	101.44	102.52
CO_2	0	0.7	0.2	0.2	0	0.3	0.5	0	0.6	0.7	0	0.1	0.5	0.3	0.3	0.5	0.5	6	10.5	15.9	13
H_2O^+	0.9	0.6	1.2	1	0.5	1.4	1.2	1.6	1.5	0.9	1	0.4	0.5	0.4	0.4	0.2	0.1	2.2	1.5	2.6	1
H_2O^-	0	0	0	0	0.1	0	0	0	0	0	0	0	0	0	0	0	0	0	0	0	0
Parts per million unless otherwise indicated																					
Au (ppb)	6	44	36	2	94	150	3700	44	240	3000	4500	5400	5300	2900	120	1700	80	2	0	4	2900
Ag	0.2	0	0.3	0	0	0	1.8	0	1.1	1.1	0.3	2.5	0.4	1	0.4	0.9	0	0	0.2	0.2	0.5
Pd (ppb)	8	11	11	0	0	0	0	1	0	1	1	0	0	1	0	0	0	0	0	0	0
Pt (ppb)	10	10	10	0	0	0	0	0	0	0	0	0	0	0	0	0	0	0	0	0	0
Cu	85	135	280	18	37	26	10	78	52	120	23	7	115	16	34	73	19	41	32	37	48
Pb	1	2	2	4	11	22	18	36	26	7	17	5	14	4	6	5	3	2	3	2	11
Zn	60	92	52	93	78	99	120	120	110	77	115	43	27	79	110	100	54	78	70	80	71
Cr	360	360	320	55	50	20	45	105	45	65	30	15	40	20	15	30	25	130	110	115	105
Ni	130	150	91	47	37	13	30	53	28	35	21	11	10	14	23	13	5	96	66	70	64
W	0	1	24	0	2	4	9	2	6	16	40	5	5	8	1	2	0	0	0	2	14
Mo	0.3	0.1	1.8	0.6	1.1	9.5	3	0.6	1.7	0.8	0.6	0.7	0.8	3.9	0.9	0.9	0.5	0.5	0.6	0.5	0.6
Sn	6	3	6	4	1	0	7	4	6	24	7	16	13	2	0	1	1	4	5	7	11
As	0	0	15	3	3	7	7	14	11	6	6	5	0	3	6	6	0	0	55	89	1800
Sb	0	0.3	0.3	0	0	0.2	0.3	0.3	0.2	0.2	0	0	0	0.4	0	0	0	0.5	6.5	5.5	33
Bi	0	0.2	1	0	0	0.5	0.1	0.2	0	0.1	0	0.2	0.2	0.1	0.1	0	0	0	0	0	0
Cd	0.2	0.2	0.4	0.2	0.2	0.2	0.6	0.3	0.8	0.8	0.3	0.4	0.3	0.3	0.7	0.2	0	0.3	0.2	0.3	0.4
Be	0.7	1.1	1	1.2	1.5	3.2	2	2.5	1.7	0.9	2.6	0.8	1.3	0.8	1	1.1	0.6	0.4	0.6	0.9	2.3
Co	44	36	31	22	21	26	17	44	12	18	16	7	8	25	17	12	6	36	32	27	27
Sc	43	42	38	10	10	10	8	25	9	11	9	5	12	2	3	10	4	18	18	20	20
V	260	260	240	80	85	110	105	195	75	90	80	50	105	10	15	70	25	160	140	145	360
Ga	13	14	14	18.5	19	19.5	21.5	20	19	16.5	19.5	14	12	8.5	22	15.5	9	14.5	12.5	12	13.5
Nb	0	0	0	6.5	5.5	LNR	0	5	5.5	0	5	0	0	0	7	0	0	0	0	0	0
Zr	45	40	35	120	110	200	105	125	125	90	105	100	195	35	65	80	70	85	80	65	65
Ba	30	185	520	260	620	1600	300	840	660	200	300	115	460	25	15	260	85	170	420	260	340
Rb	7	63	40.5	33.5	77	26.5	34	46	72	27.5	60	9.5	11.5	3	58	30.5	6	21.5	72	92	48.5
Sr	60	50	60	320	320	1100	195	520	240	220	320	150	300	80	120	195	100	170	180	190	980
Li	4	8.5	18	20	28	23.5	22.5	49	33.5	8.5	15	7	9	4.5	18	11.5	5.5	17.5	24	12.5	5
U	0	0	0	0.5	0.5	2.5	0.5	2	0.5	1	0.5	1	1	0	1	0.5	0.5	0.5	0.5	0.5	0.5
Th	0.5	0	0	3	2.5	10.5	2.5	4	2.5	1.5	2	1.5	4.5	1	1.5	2	1	2	2	2	2
La	3	3	3	17	17	77	18	23	16	12	15	13	19	7	10	7	11	9	12	7	9
Ce	7	8	6	33	29	150	32	48	31	22	28	20	34	10	17	11	20	21	23	14	17
Y	18	16	12	9	10	21	8	23	9	7	8	5	11	0	4	13	5	16	21	12	15
Se	0	1	1	0	0	0	0	1	0	0	0	0	0	0	0	0	0	0	0	0	0

Appendix 5 (continued)

	Enigmatic South			Hronsky			Tin Dog				Main Zone, Karonie									West Zone, Karonie			
	130579	130575	130573	130591	130594	130592	130543	130542	130530	130529	132829	132804	132801	132802	132828	132805	132803	132806	132809	132813	132814	132816	132815
Percentage																							
SiO_2	54.2	49.1	47.1	50.9	43.5	47.8	58.4	65.1	58	64.2	57.5	69.2	53.8	51.2	52.2	48.3	67.9	46.5	50.5	49.2	53.5	51.2	48.7
TiO_2	1.27	1.28	1.19	0.95	0.89	0.88	0.62	0.11	0.78	0.78	0.46	0.56	1.87	1.85	1.76	1.32	0.36	1.64	1.76	1.49	2.1	1.72	1.33
Al_2O_3	16.3	15.3	13.6	13.8	12.4	13	17.1	17.2	13.8	13.5	13.1	15.7	13.8	13.6	13.2	12.5	16.2	13.2	13.6	13.2	16.3	13.7	9.55
Fe_2O_3	4.98	4.61	5.65	2.13	3.11	3.35	3.41	1.41	5.41	8.19	1.03	0.91	0.95	2.15	1.54	3.18	0.74	1.66	1.96	3.96	0.91	2.16	2.08
FeO	4.3	3.2	5.1	5.7	6.3	4	1.2	0.2	7	0.7	4	1.7	11.1	9.5	9.6	13.5	1.8	9.4	10.8	10.4	10.6	9.6	9.5
MnO	0.2	0.17	0.14	0.21	0.31	0.2	0.06	0.02	0.18	0.27	0.37	0.1	0.37	0.29	0.27	0.39	0.04	0.22	0.35	0.27	0.18	0.3	0.4
MgO	3.71	4.01	5.41	3.97	4.54	3.64	2.28	0.12	3.58	0.28	1.31	0.77	5.12	2.81	2.62	7.35	1.65	3.29	2.99	7.25	4.03	4.84	6.53
CaO	5.36	6.88	5.6	9.3	12.7	7.76	2.41	0.84	3.48	0.39	12	3.97	8.81	14.1	14.6	9.98	3.84	15.4	12.3	9.94	4.65	12.6	18
Na_2O	6.73	4.36	3.07	2.12	2.28	2.27	5.9	3.45	0.77	3.46	0.5	2.92	2.9	2.78	2.87	2.07	4.78	3.65	2.06	2.04	2.27	2.03	1.07
K_2O	0.29	1.37	1	1.11	0.79	2.96	4.97	10	2.2	6.37	2.57	3.07	0.43	0.35	0.46	0.27	2.32	0.45	0.66	0.31	2.26	0.67	0.89
P_2O_5	0.22	0.24	0.21	0.16	0.16	0.08	0.45	0.01	0.11	0.31	0.11	0.12	0.16	0.16	0.15	0.12	0.11	0.13	0.15	0.14	0.17	0.14	0.11
LOI	2.4	7.3	9	9.9	12.1	12.4	1.8	1.3	5.9	0.2	7.8	0.7	0.5	2.3	0.9	0.3	0.3	4.4	2.06	0.85	0.8	0.7	2
S	0.19	0.41	1.14	0	0	2.28	0	0.56	0.05	0	0.27	0	0	0.14	0.51	0.13	0	0.22	0.21	0.02	0.18	0.06	0
TOTAL	100.15	98.23	98.21	100.25	99.08	100.62	98.60	100.32	101.26	98.65	101.02	99.72	99.81	101.23	100.68	99.41	100.04	100.16	99.40	99.07	97.95	99.72	100.16
CO_2	1.5	5.2	6.9	8	10.2	11.4	1.5	0.9	0.1	0.2	6.2	0.7	0	1.6	0.5	0	0.2	4.4	1.3	0.15	0	0.1	0.6
H_2O^+	0.9	2	2	1.9	1.9	1	0	0.2	5.6	0	1.6	0	0.5	0.7	0.4	0.3	0.1	0	0.76	0.7	0.8	0.6	1.4
H_2O^-	0	0.1	0.1	0	0	0	0.3	0.2	0.2	0	0	0	0	0	0	0	0	0	0	0	0	0	0
Parts per million unless otherwise indicated																							
Au (ppb)	9	44	220	0	28	7000	1	310	10	1400	33	18	3	82	945	8500	36	11	92	730	67	77	27
Ag	0.2	0.3	0.2	0	0.2	0	0.3	0.4	0.2	0	0.4	0	0	0.4	0.3	0.3	0	0	0	0	0	0.2	0.2
Pd (ppb)	0	0	0	0	0	0	0	0	0	0	0	0	0	0	0	5	0	0	0	0	0	0	0
Pt (ppb)	0	0	0	0	0	0	0	0	0	0	0	0	0	0	0	5	0	0	0	0	0	0	0
Cu	42	41	26	52	105	63	8	27	40	66	66	18	9	74	125	12	7	74	36	10	99	30	21
Pb	4	7	8	5	3	4	18	170	5	43	24	22	4	11	5	3	5	4	4	3	4	3	2
Zn	105	105	120	92	105	92	81	150	155	140	160	100	160	135	130	240	61	135	180	195	155	145	180
Cr	105	105	105	125	120	125	45	10	170	155	30	25	115	115	110	90	60	115	105	110	130	105	85
Ni	62	64	63	38	45	41	22	3	93	65	13	8	61	71	70	260	23	64	57	190	115	155	65
W	0	2	6	0	0	15	2	3	1	46	2	1	2	8	6	3	3	5	19	0	89	3	23
Mo	1.2	1.5	0.8	0.5	0.5	0.5	0.8	23.5	1	16.5	0.3	0.4	0.5	0.5	0.5	6	1.2	0.3	0.6	0.6	0.5	1.1	2.1
Sn	11	12	15	14	7	7	4	3	3	6	9	4	4	4	6	6	4	4	5	5	5	6	4
As	12	15	320	35	130	12400	4	3	3	5	0	0	0	0	0	0	0	0	0	0	0	0	0
Sb	1.5	5.5	17.5	4.2	7.5	47	0.7	1.5	0.4	4.8	0	0.2	0.4	0.2	0.2	0.3	0	0	0.2	0.5	0	0.4	0.3
Bi	0	0	0.1	0	0	0	0.2	1.1	0.1	2.9	0	0.2	0	0.2	1.6	0.9	0	0	0.2	0.8	0	0.2	0
Cd	0.5	0.4	0.6	0.5	0.4	0.4	0.2	0.9	0.1	0.5	0.5	0.3	0.3	0.4	0.4	0.5	0.3	0.3	0.4	0.4	0.3	0.3	0.3
Be	0.8	0.8	0.7	0.6	0.9	2.2	5.5	5	1.8	3.7	1.8	1.8	1.6	1.2	1.2	1.4	1.9	1.4	1.5	1.1	2.2	1.9	1.4
Co	37	34	38	25	28	24	11	1	42	42	7	6	41	42	43	69	9	42	44	69	56	64	35
Sc	23	23	21	22	27	22	6	0	24	16	10	5	45	46	42	32	4	39	43	36	50	42	31
V	195	190	180	165	170	175	70	10	145	145	60	60	400	400	400	280	45	340	400	340	460	380	280
Ga	18	16.5	17.5	13.5	13	13	16	20.5	17.5	19.5	17	18.5	21.5	20.5	20	20	19.5	19.5	21.5	20.5	25	20.5	14
Nb	5.5	0	0	0	0	0	10	9.5	7	7	5	6	7	6.5	6.5	5	0	5.5	5.5	5.5	7.5	6.5	5.5
Zr	95	120	105	65	60	70	400	195	120	160	150	160	145	135	125	100	130	105	115	115	150	115	95
Ba	115	420	240	150	75	280	1400	190	220	660	420	420	110	105	85	50	540	175	140	65	800	190	240
Rb	7.5	46.5	34.5	40.5	29	100	47.5	77	81	64	80	51	28.5	12.5	43	13	60	26.5	56	17.5	105	38.5	64
Sr	320	360	300	120	220	185	820	110	140	165	185	220	180	150	340	90	260	240	175	155	200	280	160
Li	10	25	55	32.5	25.5	2	48	0	28	20.5	38.5	29.5	30.5	26	48	49	56	26	38.5	42.5	160	22.5	32.5
U	0.5	1.5	0.5	0.5	0.5	0	2	9	0.5	3	4	0.5	0	0	1.5	0	1.5	1	0	0	0	0	0
Th	1.5	2.5	1.5	2	1.5	1.5	22	32.5	3.5	4.5	1	1.5	0.5	0.5	1	1	4	0.5	1	0.5	0.5	0.5	0.5
La	12	20	11	11	12	10	160	32	12	140	15	14	8	7	7	7	23	7	8	6	7	6	6
Ce	27	38	23	24	24	20	240	51	22	220	28	32	19	18	18	17	50	17	20	15	20	16	15
Y	19	22	20	13	13	14	17	7	15	22	19	11	39	46	44	32	6	35	38	33	41	36	29
Se	0	1	0	0	0	0	1	0	2	2	2	1	3	4	5	3	0	4	3	3	4	4	7

Appendix 5 (continued)

	Harrys Hill, Karonie						*Anglo Saxon, Pinjin*													
	132817	*132820*	*132819*	*132821*	*132823*	*132824*	*130716*	*130718*	*130717*	*130731*	*130734*	*130730*	*130735*	*130733*	*130732*	*130740*	*130738*	*130736*	*130737*	*130741*	*130739*
Percentage																					
SiO_2	46.7	45.5	40	43.4	47.5	61.6	62.3	61.6	60.9	58	52.2	64.4	43.2	90.9	64.3	60	46.7	48.1	47.2	57.6	57.6
TiO_2	1.14	1.03	1.35	1.26	0.85	0.75	0.7	0.76	0.69	0.57	0.71	0.57	0.67	0.03	0.92	0.66	1.61	1.62	1.69	0.69	0.63
Al_2O_3	12.6	10.9	13.5	13.1	14.1	16.4	14.9	15.6	14.5	14.4	15.1	15.3	13.4	1.09	19.6	14.2	13.4	14.2	14.1	16	13.7
Fe_2O_3	2.12	2.12	3.03	2.91	4.76	0.82	3.57	2.24	2.79	1.16	1.87	1.75	5.12	0.95	0.73	1.03	3.06	3.56	2.85	2.16	1.97
FeO	14	14.8	15.7	14.1	9.7	3.7	3.1	4.8	3.6	5.1	5.9	4.1	8.8	2.1	3	5.5	6.2	6.9	6.6	4.8	5.1
MnO	0.23	0.27	0.23	0.29	0.4	0.11	0.1	0.11	0.11	0.12	0.28	0.07	0.56	0.04	0.06	0.09	0.15	0.14	0.14	0.09	0.11
MgO	9.37	13.2	13	10	4.5	3.06	3.37	3.7	2.89	2.15	2.47	2.63	2.43	0.27	0.84	1.91	4.51	4.34	4.73	1.91	1.86
CaO	7.58	6.93	5.13	8.9	13.3	5.3	5.98	5	7.69	6.47	8.97	3.69	11.4	2.07	3.11	5.67	8.97	8.03	7.93	4.76	6.25
Na_2O	2.24	0.79	0.71	1.11	2.15	4.1	3.84	4.33	3.09	3.2	2.65	3.17	1.89	0.09	2.74	2.6	3.62	3.61	3.37	2.95	2.58
K_2O	0.31	0.82	0.74	1.27	0.75	1.85	0.78	0.7	1.15	1.11	1.46	1.45	0.57	0.08	2.61	1.78	0.81	0.48	0.69	1.95	1.71
P_2O_5	0.09	0.05	0.09	0.09	0.05	0.22	0.16	0.18	0.16	0.13	0.16	0.12	0.13	0.02	0.21	0.17	0.66	0.6	0.68	0.18	0.17
LOI	1.8	1.9	2.7	1.5	1.5	1.5	1.1	1.5	2.8	6.6	6.1	4	11.4	2.7	2.4	5.6	10	7.4	9	5.8	6.6
S	1.14	0.54	1.66	1.9	2.55	0.2	0	0.04	0.03	0.57	0.06	0	0.01	0.8	0.11	0.88	0	0.09	0.77	0.99	1.02
TOTAL	99.32	98.85	97.84	99.83	102.11	99.61	99.90	100.56	100.40	99.58	97.93	101.25	99.58	101.14	100.63	100.09	99.69	99.07	99.75	99.88	99.30
CO_2	0.5	0.2	0.4	0	0.3	0.1	0.5	0.9	2.2	5.5	6	3	8.7	2.2	0.8	4.7	9.3	7.3	7.4	4.1	5.7
H_20^+	0.9	1.7	1.9	1.5	1.2	1.4	0.6	0.6	0.6	1.1	0.1	1	2.7	0.5	1.6	0.8	0.7	0.1	1.6	1.7	0.9
H_2O^-	0.4	0	0.4	0	0	0	0	0	0	0	0	0	0	0	0	0.1	0	0	0	0	0
Parts per million unless otherwise indicated																					
Au (ppb)	33	54	3200	160	120	60	6	2	16	34	2	6	9	145	12	50	7	11	150	41	7
Ag	0.6	0.9	0.7	0.7	0.7	0.3	0	0	0	0	0	0	0	0	0	0	0	0	0.2	0	0
Pd (ppb)	0	0	1	0	11	0	0	0	0	0	0	0	0	0	0	0	0	0	0	0	0
Pt (ppb)	0	0	0	0	5	0	0	0	0	0	0	0	0	0	0	0	0	0	0	0	0
Cu	220	62	155	260	260	29	50	31	45	55	50	15	51	71	17	72	30	16	23	40	53
Pb	23	2	2	5	10	7	10	7	10	9	8	7	7	1	13	8	7	7	7	9	5
Zn	180	180	190	175	185	66	125	98	89	56	65	110	135	28	60	59	145	130	135	62	89
Cr	135	115	135	140	240	175	125	130	110	60	105	50	100	20	150	65	85	30	100	55	55
Ni	260	200	300	300	130	62	78	81	76	58	64	35	61	27	56	53	64	47	70	49	70
W	2	0	6	6	2	11	0	0	0	2	2	2	0	0	6	3	4	8	6	4	0
Mo	0.3	0.9	0.4	1.8	0.5	0.7	0.8	1	1.1	0.4	0.6	0.3	2.4	3.2	0.4	0.6	1	0.8	0.7	1.2	0.5
Sn	7	4	4	5	5	5	6	2	7	2	6	19	0	2	2	0	1	1	3	16	2
As	41	0	0	2	2	0	0	0	4	4	3	5	0	3	0	0	4	5	6	9	3
Sb	0.3	0.4	0.7	0.2	11	0.2	0.3	0	0	0	0	0	0	0	0	0	0	0	0	0.2	0
Bi	0	0.1	0.2	0.3	1	0.1	0	0	0.1	0.5	0.1	0	0.1	8	0.2	0.6	0.3	0.2	0.5	0.5	0.2
Cd	0.3	0.4	0.2	0.4	0.5	0.3	0.3	0.2	0.4	0.3	0.4	0.6	0.3	0.1	0.2	0.2	0.2	0.1	0.3	0.6	0.2
Be	1.3	1.5	1.3	1.7	0.9	1.9	1.7	1.3	1.4	1.4	1.5	1.1	1.4	0.3	2.2	1.4	1.5	1.8	1.9	1.4	1.6
Co	83	66	100	79	70	18	30	30	27	28	25	22	29	27	15	26	41	36	40	30	33
Sc	32	28	35	34	39	14	15	17	15	13	16	11	16	2	20	13	16	16	17	13	13
V	260	240	300	280	280	125	115	120	120	100	110	85	120	15	160	105	145	170	150	110	105
Ga	15.5	17.5	20.5	19	19.5	17	17	18	18.5	16	18.5	17	20.5	2	23.5	18	18.5	20	20	19.5	17
Nb	0	0	5.5	0	0	6	8	10.5	8	5.5	7	6	7.5	0	9	6	15	13.5	15	6	6
Zr	90	70	90	85	55	160	150	165	140	125	120	115	145	15	185	125	170	165	180	130	135
Ba	40	95	90	320	190	940	240	125	380	180	280	220	105	0	600	180	175	75	120	240	200
Rb	11.5	64	42	105	67	125	24.5	21.5	40.5	35	73	42.5	21	2	73	50	26	18	25.5	67	51
Sr	240	55	125	145	220	380	260	180	280	260	220	170	165	10	340	300	420	580	480	260	240
Li	34	88	69	78	54	105	6	9.5	10	11.5	13.5	16	13	3	14	10	15	15	15.5	33	34.5
U	0	0	0	0	0	1	1	1	1	1	1	1	1	0	1	1	1	1	1	1	1.5
Th	1	0	0.5	0	0	3	3.5	4	3.5	3.5	2.5	3.5	3	0.5	3.5	3	3.5	4.5	4	3	3.5
La	5	4	6	5	3	25	24	25	25	17	17	17	17	2	24	21	53	56	57	24	24
Ce	13	11	15	12	7	54	41	46	42	29	30	29	33	3	43	38	110	115	120	40	41
Y	30	26	30	28	23	16	16	17	16	13	16	9	18	3	18	13	22	22	23	13	17
Se	2	4	4	5	4	2	0	0	0	0	0	0	0	0	0	0	1	2	1	0	0

Appendix 5 (continued)

	Patricia					*Linden*		*Red October*							
	130758	*130764*	*130763*	*130768*	*130742*	*121667*	*121668*	*132946*	*132947*	*132948*	*132949*	*132950*	*132951*	*132952*	*132953*
							Percentage								
SiO_2	62.8	53	51.8	49.5	36.6	69.6	70	51.8	51.9	49	34.9	67.5	54	44.9	53.7
TiO_2	0.72	0.81	0.72	0.94	0.89	0.32	0.22	0.76	0.74	0.72	0.71	0.08	0.08	1.18	1.13
Al_2O_3	15.1	16.8	15.3	16.1	10.7	15.6	15.2	10	10	9.37	9.58	1.77	3.6	12	11.6
Fe_2O_3	2.18	2.48	3.62	2.43	0.81	2.4	0.412	1.35	2.12	3.31	4.9	7.32	9.9	3.87	2.04
FeO	3.8	4.7	2.8	4.2	7	0	1.4	10.1	9.6	9.4	5.4	3.6	6.2	5.6	9.8
MnO	0.09	0.15	0.12	0.09	0.18	0.03	0.02	0.17	0.19	0.23	0.21	0.09	0.09	0.17	0.19
MgO	3	5.79	6.12	5.53	9.95	1.06	0.75	9.25	8.78	9.92	6.08	1.96	2.73	5.12	5.69
CaO	3.96	6	4.53	5.87	11	3.13	2.36	9.63	10.9	10.7	12.2	5.71	6.3	10	8.3
Na_2O	4.1	4.27	0.51	6.85	3.83	5.13	5.32	3.28	2.48	1.36	0.76	0.07	0.06	1.12	3.11
K_2O	1.08	0.38	3.31	1.34	2.65	1.67	1.77	0.12	0.15	0.26	2.92	0.14	1.08	2.56	0.24
P_2O_5	0.21	0.18	0.15	0.4	0.72	0.09	0.06	0.04	0.04	0.04	0.04	0.17	0.01	0.12	0.1
LOI	2.2	6.5	7	6.3	16.9	0.9	1.6	2.3	3.3	6.4	16.5	7.1	8.7	10.1	2.9
S	0.04	0.03	2.55	0.12	0.1	0	0.12	0.03	0.21	0	3.72	6.86	8.82	1.32	1.2
TOTAL	99.28	101.09	98.53	99.67	101.33	99.93	99.23	98.83	100.41	100.71	97.92	102.37	101.57	98.06	100.00
CO_2	1.2	3.6	4.7	4.6	16.3	0	0.7	0.7	1.9	3.5	14.5	5	7.1	7.2	1.7
H_20^+	1	2.9	2.3	1.7	0.6	0.9	0.9	1.5	1.2	2.8	1.9	1.8	1.3	2.6	0.8
H_2O^-	0	0	0	0	0	0	0	0.1	0.2	0.1	0.1	0.3	0.3	0.3	0.4
							Parts per million unless otherwise indicated								
Au (ppb)	0	0	3	0	15	1	1	3	2	3	3000	4800	7600	1200	66
Ag	0.3	0.3	0.4	0.4	0.8	0	0	0.6	0.6	0.6	0.7	0.7	3.3	0.9	1
Pd (ppb)	0	0	0	0	0	0	0	14	14	12	16	0	2	3	3
Pt (ppb)	0	0	0	0	0	0	0	0	0	0	0	0	0	0	0
Cu	48	49	46	25	79	84	15	155	125	18	145	100	2000	120	1400
Pb	4	4	7	7	10	6	6	1	3	2	6	4	7	10	4
Zn	77	90	97	95	100	52	34	64	90	120	320	41	70	145	110
Cr	55	145	85	140	200	25	20	580	620	740	900	65	50	300	260
Ni	61	130	96	125	240	14	12	125	135	170	185	70	135	135	100
W	0	0	4	0	0	0	0	0	0	0	9	260	50	42	2
Mo	0.9	0.5	0.5	0.2	0.2	0.9	1.6	0.3	0.4	0.2	0.2	1.3	1.8	0.5	0.9
Sn	5	4	7	6	4	3	1	4	12	24	23	24	9	29	6
As	3	24	4	0	20	3	0	0	13	14	5500	4300	4000	1800	84
Sb	0.6	1.2	1.5	0.6	0.9	0	0	0	0.6	1	41.5	4.5	4.4	2.4	0.5
Bi	0	0	0	0	0	0	0.4	0	0	0	0	0.8	1	0.1	0
Cd	0.2	0.2	0.6	0.2	0.3	0.1	0.1	0.3	0.5	0.7	2.2	0.7	0.6	0.8	0.6
Be	0.8	0.7	0.6	1.2	1.9	1.9	1.7	0.9	1.1	1	1.2	0.9	0.8	1.6	1.5
Co	20	36	30	30	49	6	4	55	56	51	24	42	90	48	51
Sc	12	20	17	12	15	4	2	39	39	38	37	4	2	35	34
V	85	140	125	110	125	35	20	260	260	240	260	35	30	280	280
Ga	15	15.5	15	17.5	11.5	18	16	12	12.5	12	15	4	8	17	15.5
Nb	8.5	6	5	7.5	7.5	0	0	0	0	0	2	0.5	0	0	0
Zr	195	140	110	180	145	120	100	45	35	50	55	15	25	95	85
Ba	175	130	480	340	360	500	600	40	45	55	340	0	80	300	65
Rb	30.5	9.5	65	39.5	115	40.5	38	6.5	6	12.5	99	13	35	105	7.5
Sr	140	145	50	420	660	460	420	35	75	40	50	25	25	55	65
Li	9	17.5	15.5	18	7.5	13	4	5.5	4.5	7.5	12.5	7.5	10.5	37	6
U	1	1	1.5	2.5	5.5	1.5	2	0	0	0	0	0	0	0.5	0.5
Th	4	2.5	2.5	7.5	7.5	4.5	4	1	0.5	0.5	0	0	0.5	1.5	1.5
La	21	12	13	47	105	19	17	3	3	3	3	2	1	7	8
Ce	43	28	28	105	220	30	27	6	7	6	6	5	2	15	17
Y	23	19	16	15	22	4	3	15	14	15	12	6	7	24	26
Se	0	1	0	0	1	0	0	1	1	2	2	5	5	2	2

Appendix 6
Quality control data from whole-rock geochemical analyses

	Batch 1						Batch 2					Batch 3				
	LLD	*Method*	*BLK*	*STD SY3*	*STD MRG1*	*STDUM1*	*LLD*	*Method*	*BLK*	*STD NIM-N*	*STD NIM-G*	*LLD*	*Method*	*BLK*	*STD NIM-N*	*STD NIM-G*
Weight percent																
SiO_2	0.01	IC4E	0	59.6	39.7	37.8	0.01	IC4E	0	52.6	75.9	0.01	IC4E	0.08	51.6	75.2
TiO_2	0.01	IC4E	0	0.15	3.87	0.07	0.01	IC4E	0	0.19	0.09	0.01	IC4E	-0.01	0.2	0.1
Al_2O_3	0.01	IC4E	0	11.5	8.45	0.91	0.01	IC4E	0	16.7	12.1	0.01	IC4E	-0.01	16.3	12.1
Fe_2O_3	0	IC4E	0.013	2.67	8.63	0.55	0	IC4E	–	–	–	0.01	IC4E	-0.01	1.13	–
FeO	0.1	VOL1A	0	3.5	8.6	17.4	0.1	VOL1A	0	7.5	–	0.1	VOL1A	-0.1	7.1	–
MnO	0.01	IC4E	0	0.33	0.17	0.15	0.01	IC4E	0	0.19	0.02	0.01	IC4E	-0.01	0.18	0.02
MgO	0.01	IC4E	0	2.6	13.5	37	0.01	IC4E	0	7.51	0.04	0.01	IC4E	-0.01	7.58	0.04
CaO	0.01	IC4E	0	8.24	14.7	2.16	0.01	IC4E	0	11.7	0.72	0.01	IC4E	-0.01	11.9	0.75
Na_2O	0.01	IC4E	0	4.17	0.74	0.05	0.01	IC4E	0	2.48	3.34	0.01	IC4E	-0.01	2.5	3.27
K_2O	0.01	IC4E	0	4.34	0.17	0	0.01	IC4E	0	0.25	4.99	0.01	IC4E	-0.01	0.25	5.03
P_2O_5	0.01	IC4E	0	0.53	0.06	0	0.01	IC4E	0	0.02	0	0.01	IC4E	-0.01	-0.01	-0.01
LOI	–	GRAV7	0	0	0	0	0.01	GRAV7	–	–	–	0.01	GRAV7	–	0.32	1.02
S	0.01	VOL2	0	0.05	0.05	3.6	0.05	VOL2	0	–	–	0.05	VOL2	-0.05	–	–
TOTAL	–	–	–	97.68	98.64	99.69	–	–	–	99.14	97.2	–	–	–	99.05	97.52
CO_2	0.1	GRAV4A	0	0.4	1.1	0.2	0.05	GRAV4A	–	–	–	0.05	GRAV4A	-0.05	–	–
Parts per million unless otherwise indicated																
Au (ppb)	1	FA3	0	460	6	30	1	FA3	0	5	5900	1	FA3	<1	–	–
Ag	0.2	IC3M	0	0.7	0.7	1.2	0.2	IC3M	0	0.2	14.5	0.2	IC3M	0.4	0.4	-0.2
Pd (ppb)	1	FA3	0	60	0	20	1	FA3	0	0	0	1	FA3	<1	–	–
Pt (ppb)	5	FA3	0	10	0	5	5	FA3	0	0	0	5	FA3	<5	–	–
Cu	1	IC3E	0	18	150	4300	1	IC3E	0	12	330	1	IC3E	-1	5	8
Pb	1	IC3M	0	91	7	11	1	IC3M	5	3	680	1	IC3M	-1	3	36
Zn	2	IC3E	5	260	220	79	2	IC3E	0	88	600	2	IC3E	-2	61	54
Cr	5	IC4E	5	10	480	2900	5	IC4E	0	40	20	5	IC4E	20	80	35
Ni	2	IC3E	0	6	200	8700	2	IC3E	0	125	135	2	IC3E	-2	115	-2
W	1	IC3M	0	2	0	0	1	IC3M	0	0	7	1	IC3M	-1	-1	1
Mo	0.1	IC3M	0	1	1.1	2.7	0.1	IC3M	0	1	27	0.1	IC3M	0.1	1.2	3.2
Sn	1	IC4M	0	5	2	0	1	IC4M	2	2	8	1	IC4M	-1	1	11
As	2	IC3E	0	39	0	3	2	IC3E	0	12	93	2	IC3E	2	-2	20
Sb	0.2	IC3M	0	0.4	0.5	0.5	0.2	IC3M	0	0	4	0.2	IC3M	-0.2	0.2	1
Bi	0.1	IC3M	0	0.3	0.1	0.4	0.1	IC3M	0.6	0	72	0.1	IC3M	-0.1	-0.1	0.3
Cd	0.1	IC3M	0	0.4	0.4	0.3	0.1	IC3M	0.4	0.1	36	0.1	IC3M	0.1	0.3	0.4
Be	0.1	IC4M	0	24	0.8	0.6	0.5	IC3M	0	0	6	0.5	IC3M	-0.5	-0.5	5.5
Co	1	IC3E	0	9	100	540	1	IC3E	0	60	69	1	IC3E	-1	55	-1
Sc	1	IC4E	0	7	55	10	1	IC4E	0	40	0	1	IC4E	-1	28	-1
V	5	IC4E	0	50	540	50	5	IC4E	0	230	0	5	IC4E	-5	220	-5
Ga	0.5	IC3M	0	47	21	4.5	0.5	IC3M	0	17.5	13	1	IC4M	-1	17	28
Nb	0.5	IC3M	0	220	28	2	0.5	IC3M	0	1	8	0.5	IC3M	-0.5	0.5	46
Zr	5	IC4E	0	340	100	15	5	IC4E	0	25	300	5	IC4E	5	10	300
Ba	10	IC4E	0	440	50	15	10	IC4E	0	85	100	10	IC4E	-10	70	100
Rb	0.5	IC3M	0	165	9	1.5	0.5	IC3M	1	3.5	95	0.5	IC4M	0.5	3	290
Sr	5	IC4E	0	300	240	0	5	IC4E	0	240	10	5	IC4E	-5	230	10
Li	0.5	IC3E	0	75	3.5	2	0.5	IC3E	0	4	33	0.5	IC3E	-0.5	4.5	10.5
U	0.5	IC4M	0	680	1	0	0.5	IC4M	0	0.5	16	0.02	IC3M	-0.02	0.35	17
Th	0.5	IC4M	0	960	1.5	6	0.5	IC4M	1	1.5	54	0.2	IC3M	-0.02	0.49	53
La	1	IC4M	0	1300	10	0	1	IC4M	3	4	110	1	IC4M	1	3	105
Ce	1	IC4M	0	2000	25	0	1	IC4M	3	7	220	1	IC4M	2	6	185
Y	2	IC4E	0	680	12	0	2	IC4E	0	7	135	2	IC3E	-2	6	115
Se	1	IC3M	0	22	4	12	–	–	–	–	–	–	–	–	–	–

NOTES:

–: not determined
LLD: lower level of detection (negative values mean analysis is less than LLD)
LOI: loss on ignition
BLK: blank
STD: International standard reference sample

Samples from:

Batch 1: Randalls, Kurnalpi, Mulgabbie, Yerilla, Yilgangi, Porphyry, Yarri, Pennyweight Point, Yundamindera, Butcher Well, Safari Bore, Karonie, Pinjin, and Linden
Batch 2: Gordon, Bulong, Majestic, and Mount Monger
Batch 3: Lindsays Find and Kanowna

Analytical methods:

IC3E: Inductively coupled plasma optical emission spectroscopy; multi-acid sample digestion
IC3M: Inductively coupled plasma mass spectroscopy; multi-acid sample digestion
IC4E Inductively coupled plasma optical emission spectroscopy; borate fusion of sample
IC4M: Inductively coupled plasma mass spectroscopy; borate fusion of sample
FA3: Fire say/Gravimetric thermal analysis/Mass spectroscopy
GRAV4A: Gravimetric method for determining CO_2 (weight %)
GRAV7: Gravimetric method for LOI
VOL2: Sulfur by LECO sulfur determinator
VOL1A: Volumetric analysis

Certified reference materials:

SY-3: Syenite
MRG-1: Gabbro
UM-1: Ultramafic rock
NIM-N: Norite
NIM-G: Granite

Appendix 7

Analytical conditions for mineral analyses

The mineral phases were analysed on a JEOL 6400 scanning electron microscope (SEM) at the Centre for Electron Microscopy, University of Western Australia (UWA). Analytical conditions were 15 kV and 3×10^{-9}Å. Analytical spectra were collected for 60 seconds. A copy of the analytical file, SIL15H.ZAF, is reproduced in Table A7.1.

Table A7.1. Analytical file SIL15H.ZAF used for mineral microanalysis at the Centre for Electron Microscopy, UWA

		FWHM		Range-1		Range-2		C/s/nÅ	Brem	ZAF	Standard
Si	Kα	84	90	55	115	0	0	1313.54	1.8594	2.9285	Wollastonite
Ti	Kα	222	229	205	263	0	0	727.22	0.6649	5.0171	Pure Ti
Al	Kα	71	77	45	95	0	0	1107.11	1.8302	2.6555	CAAL
Cr	Kα	267	274	250	316	0	0	520.09	0.5200	5.3813	Pure Cr
Fe	Kα	316	324	299	371	13	49	375.37	0.3976	5.7541	Pure Fe
Ni	Kα	369	378	352	433	23	57	255.07	0.3119	6.0608	Pure Ni
Mn	Kα	291	299	274	343	0	0	441.40	0.4652	5.6652	Pure Mn
Mg	Kα	60	66	35	84	0	0	872.84	1.7587	2.5141	Periclase
Ca	Kα	181	188	165	218	0	0	877.36	0.9374	3.9616	Wollastonite
Na	Kα	49	55	28	72	0	0	397.98	1.4950	1.7659	Albite
K	Kα	162	169	146	198	0	0	904.50	1.0137	3.6597	Orthoclase
C	Kα	128	134	110	161	0	0	1045.03	1.2041	3.4072	Apatite

Notes: FWHM: full width at half maximum
C/s/nÅ: counts per second per nanoampere
Brem: Bremsstrahlung background
ZAF: matrix correction, based on absorption correction, and corrections for fluorescence and atomic number effect

The Edjudina–Kanowna region covers more than 50 000 km^2 within the Eastern Goldfields Granite–Greenstone Terrane of the Archaean Yilgarn Craton in Western Australia. This Report summarizes the characteristics and features of gold deposits in the Edjudina–Kanowna region and includes information on host rock, structure, and alteration. Gold was discovered in this region in the late 1890s and early 1900s, and there was intermittent production of small quantities of gold until the discovery of deposits such as Kanowna Belle and Carosue Dam in the mid-1980s to late 1990s. Gold mineralization is widespread, hosted in a variety of rock types, and mostly of structurally hosted lode style, typically developed within shear zones. There is good potential for further discoveries of gold in the region.

This Report is published in digital format (PDF), as part of a digital dataset on CD, and is available online at: www.doir.wa.gov.au/gswa.
This copy is provided for reference only. Laser-printed copies can be ordered from the Information Centre for the cost of printing and binding.

Further details of geological publications and maps produced by the Geological Survey of Western Australia can be obtained by contacting:

Information Centre
Department of Industry and Resources
100 Plain Street
East Perth WA 6004
Phone: (08) 9222 3459 Fax: (08) 9222 3444
www.doir.wa.gov.au/gswa

ROBERTS et al. Gold mineralization in the Edjudina–Kanowna region, Eastern Goldfields, Western Australia REPORT 90